UNIVERSITY OF
KWAZULU-NATAL
INYUVESI
YAKWAZULU-NATALI

OXIDATIVE DEGRADATION OF TEXTILE DYES WITH HYPOCHLORITE AND CHLORINE DIOXIDE

By

SRINIVASU NADUPALLI

Submitted in fulfillment of the academic requirements for the degree of Doctor of Philosophy in the School of Chemistry, University of KwaZulu-Natal, Durban

11 October 2010

DECLARATION

The experimental work described in this thesis was carried out in the School of Chemistry, University of KwaZulu-Natal, Durban, under the supervision of Professor SB Jonnalagadda and co-supervisor Dr N Koorbanally.

These studies represent original work by the author and have not otherwise been submitted in any form for any degree or diploma to any tertiary institution. Where use has been made of the work of others it is duly acknowledged in the text.

Signed: _____ Name: _____ Date: _____

As the candidate's supervisor I have/have not approved this thesis/dissertation for submission.

Signed: _____ Name: _____ Date: _____

DECLARATION - PLAGIARISM

I, ……S. Nadupalli……. declare that

1. The research reported in this thesis, except where otherwise indicated, and is my original research.

2. This thesis has not been submitted for any degree or examination at any other university.

3. This thesis does not contain other persons' data, pictures, graphs or other information, unless specifically acknowledged as being sourced from other persons.

4. This thesis does not contain other persons' writing, unless specifically acknowledged as being sourced from other researchers. Where other written sources have been quoted, then:
   a. Their words have been re-written but the general information attributed to them has been referenced
   b. Where their exact words have been used, then their writing has been placed in italics and inside quotation marks, and referenced.

5. This thesis does not contain text, graphics or tables copied and pasted from the Internet, unless specifically acknowledged, and the source being detailed in the thesis and in the References sections.

Signed: ……

ACKNOWLEDGEMENTS

First and foremost I want to express my sincere gratitude to my supervisor Professor S.B. Jonnalagadda and Co-supervisor Dr. N. Koorbanally for their guidance, time, encouragement of ideas and their collaborative involvement through their helpful discussions to make my Ph.D experience productive and stimulating.

I would like to acknowledge National Research Foundation for the financial support through their Doctoral scholarship programme.

My parents Mr. N. Ramakrishna Rao and Mrs. Nagamani, who instilled in me the values of faith and hard work and afforded me every opportunity to further myself with their love and support throughout this period of study.

I would like to thank Dr. A. Ramakrishna, Dr. C.S. Vasam, and Dr. R. Pullabhotla for the numerous discussions that substantially improved the quality of my research and their encouragement.

I would like to thank my wife Madhuri., and Mr. V. Dasireddy for their enthusiasm, patience and help.

Mr. Mark Pritchard, TGK Scientific Ltd, UK for his prompt replies even at late nights for my emails regarding issues with Stopped Flow system.

I would like to express my gratitude to my fellow researchers, colleagues and lab technicians at School of Chemistry for their help in promoting a stimulating and welcoming academic and social environment.

Not to be forgotten Ms. L. Govender and my colleagues at Corporate Relations, for the inspiration and support during my endeavors.

PUBLICATIONS

S. B. Jonnalagadda and S. Nadupalli, Effluent treatment using electrochemically bleached seawater-oxidative degradation of pollutants, *Talanta*, 2004, **64(1)**, p. 18-22.

CONFERENCE CONTRIBUTIONS: ORAL/POSTER PRESENTATIONS

Oral Presentations

35th Convention of South African Chemical Institute (SACI), June 2001, University of Natal, Durban, entitled "Oxidative degradation of Industrial effluents using Hypochlorite and Chlorine Dioxide".

36th Convention of South African Chemical Institute (SACI), July 2002, University of Port Elizabeth, entitled "Oxidation of Amaranth with Hypochlorite".

Poster Presentations

Local

SACI annual postgraduate colloquium, University of Durban Westville, 2001, October, Durban entitled, "Oxidative degradation of industrial effluents using Hypochlorite".

Convention of South African Chemical Institute (SACI)/ CATSA, 2001, November, Pilanesburg, entitled "Oxidation of Brilliant blue-R with Hypochlorite"

International

CHEMCON, December, 2002, Osmania University, Hyderabad, India, entitled, "Oxidative Degradation of Industrial Effluent with Hypochlorite".

TABLE OF CONTENTS

ABSTRACT

The oxidation reaction mechanisms of water soluble textile dyes amaranth (an azo dye), brilliant blue-R (a triaryl dye) and safranine-O (an azine dye) with oxidants- hypochlorite and chlorine dioxide, were investigated. The detailed kinetics of the reactions of the three dyes was studied under excess concentrations of the oxidant and other reagents. The depletion of concentration of the chosen dye, taken at low concentration was monitored using a Hi-Tech SF-61 DX2 double mixing micro volume stopped-flow apparatus.

The hypochlorite initiated oxidations were investigated as function of varying concentration of oxidant and hydrogen ion, ionic strength and temperature. For the chosen dyes and reaction conditions, the depletion of dye followed *pseudo* first-order kinetics and the rate constants were estimated using KinetAsyst^{TM} software. All the three reactions had first-order dependence on the oxidant concentration, and the reaction rates increased by varied extent with increase in $[H^+]_0$. The role of acid in their reaction mechanisms was established. The kinetic data was analysed to evaluate the rate constants for the competitive pathways initiated by hypochlorite ion and hypochlorous acid. The overall second-order rate coefficients for the OCl^- and HOCl initiated reactions were estimated for all the three reactions. Major oxidation products for the reactions were separated and characterized by ^1H NMR and ^{13}C NMR and GC-MS techniques and the stoichiometry was established. The energy parameters inclusive of Arrhenius factor, enthalpy, entropy and energy of activations for the oxidation of three dyes both by OCl^- and HOCl species were estimated. Based on the experimental findings, the probable rate laws, mechanisms and reaction schemes were described. Simulations studies were conducted to validate the proposed

mechanisms using SIMKINE2 computer programme. The rate of oxidation of safranine-O is greater than that of amaranth and brilliant blue-R with OCl^- / HOCl reaction.

Following similar protocol, the oxidations of the chosen dyes with chlorine dioxide were investigated by monitoring the depletion kinetics of dye as function of varying concentration of ClO_2 and OH^- ion, ionic strength and temperature. All the three dyes, exhibited *pseudo* first-order kinetics and the rate constants were estimated using KinetAsyst^{TM} software. All the three reactions had first-order dependence on the oxidant concentration at pH conditions 7.0, 8.0 and 9.0 suggesting that reaction mechanism remains unaltered with pH variation. The effect of hydroxide ion on the reaction rate revealed that it acts as catalyst. All the three reactions had first-order dependence on $[OH^-]_0$, when its concentration was low; but the order with respect to $[OH^-]$ decreased as $[OH^-]$ increased stoichiometry proportion to reactants. The catalytic constant for hydroxide catalysed reaction was estimated for all the three reactions. Kinetic salt effect experiments were conducted to identify the possible reaction species involved in the reactions.

The major reaction products were characterized by ^1H NMR, ^{13}C NMR and GC-MS techniques. The stoichiometry ratios were established and energy parameters were estimated. The rate laws and probable reaction mechanisms were proposed and appropriate reaction schemes for all the reactions were described. The elucidated mechanisms were confirmed by simulation studies using SIMKINE2 software. At neutral pH the rate of oxidation of amaranth is greater than safranine-O and brilliant blue-R, and brilliant blue R being the slowest.

LIST OF FIGURES

LIST OF TABLES

SYMBOLS AND ABBREVIATIONS

R^2	correlation coefficient
ε	molar absorbtivity coefficient
$^{\circ}C$	degrees centigrade
I	ionic strength
μM	micro molar concentration
^{13}C NMR	carbon thirteen nuclear magnetic resonance
^{1}H NMR	proton nuclear magnetic resonance
A	Debye-Hűckel constant
AM^-	amaranth
A h dm^{-3}	amperes in hour per volume
BB^+	brilliant blue-R
ClO_2	chlorine dioxide
ClO_2^-	chlorite
ClO_3^-	chlorate
cm	centimetre
$\Delta H^{\ddagger}$	activation enthalpy
$\Delta\Sigma^{\ddagger}$	activation entropy
e^-	electron
E_a	activation energy
Exp	exponential
g	gram
g/L	gram per litre
GC	gas chromatography
GC-MS	gas chromatography-mass Spectrometry
HOCl	hypochlorite
K	Kelvin
k'	*pseudo* first-order rate constant
k	second or third-order rate constant
K J mol^{-1}	Kilo Joule per mol
k_1, k_2	rate constants
k_{obs}	observed *pseudo* first-order rate constant
L	litre
M	molar concentration (mol/L)
M^{-1} s^{-1}	mol/ L sec
mg	milligrams
mL	millilitre
MS	mass spectrometry
ng	nano gram
nm	nano metre

NMR	nuclear magnetic resonance
pH	potential hydrogen
ppm	parts per million
R	Universal gas constant; 8.3145 J K^{-1} mol^{-1}
RSD	relative standard deviation
s	second
SO^{+}	safranine-O dye
t	time
TLC	thin layer chromatography
TM	trade mark
UV	ultraviolet
V	volt
z	ionic charge
γ	activity coefficients

CHAPTER 1

1.1 Introduction

With the phenomenal decline in water quality resulting from indiscriminate anthropogenic activities, access to potable water is at the forefront of the global agenda.

Virtually all human activities require clean water. Water is a renewable resource, yet the world's supply of clean and drinkable water is steadily decreasing. Half of the world's population and most of the world's economic output is located in urban areas. Water demand already exceeds supply in many parts of the world.[1] Today, 41 percent of the world's population lives in river basins that are under water stress. The control of water pollution has become increasing importance in recent years. The textile industry, in particular, faces a severe pollution problem. The World Bank estimates that 17 to 20 percent of industrial water pollution comes from textile dyeing and treatment. Many of the dye chemical substances which are produced are toxic.[2]

Treatment of highly-coloured dye effluent streams has attracted the attention of environmentalists, technologists, and entrepreneurs because of its socio-economic and political dimensions. Water consumption in the textile dye house is very high. Water as a utility is becoming more and more costly, and its availability is becoming increasingly scarce.[3] The nature of the pollution that accompanies the dyeing industry is primarily due to the non-biodegradable nature of the dyes along with the strong presence of toxic metals/acid/alkali/carcinogenic aromatic amines traceable in the effluents.[4]

Wastewater generated by the dye production industry and many other industries which use dyes and pigments is high in both color and organic content. There are more than 100 000

commercially available dyes with over 7 x 10^5 tons of dye materials produced annually.[5] It has been estimated that 10-15% of these dyes are released as effluent during the dyeing process.[6] The discharge of highly colored waste is not only aesthetically displeasing, but also impedes light penetration, thus upsetting biological processes within a stream. In addition, many dyes are toxic to some organisms and may cause direct destruction of aquatic life. The removal of dyes from such wastewaters is therefore a major environmental problem and is extremely necessary because dyes are visible even at low concentrations.[7]

Dye pollutants produced from the textile industries are becoming a major source of environmental contamination.[8,9] It is estimated that more than 60% of the world's dye production is consumed by the textile industry, 15% of the total world production of dyes is lost during the dyeing and finishing operations,[10] and more than half of this is discharged into receiving water bodies more or less without proper treatment, thus hampering the functioning of the ecological process.[11] The treatment of spent dye wastewater effluent is a growing concern for the textile industry because of aesthetic conditions, as well as eco-toxicological issues regarding colored rinsing and processing wastewater and the impact of that wastewater on the receiving streams. As regulations become more stringent, the effectiveness and cost of the treatment processes have become more significant. Conventional biological treatment can be ineffective for color removal, but chemical oxidative processes seem to provide an opportunity for future use in industrial wastewater.[12] Examples of such potentially effective chemical oxidants for oxidative processes include hydrogen peroxide (H_2O_2), ozone (O_3), chlorine dioxide (ClO_2), ultraviolet irradiation following ClO_2 (UV/ClO_2), and H_2O_2/ultrasonication and Advanced oxidation processes (AOPs) include UV/H_2O_2, UV/O_3, O_3/H_2O_2, Fenton's reagent, and the wet-air oxidation processes.[13]

Wastewaters that are generated at various stages of dyeing differ in strength and temperature. The high pollution load is caused mainly by spent dyeing baths. Their constituents are: untraced dyeing compounds, dispersing agents (surfactants), and salts and organics washed out of the material which undergoes dyeing.[14] The wastewaters are characterized by high color and high chemical oxygen demand content and pH varying from 2.0 to 12.0.[15,16] Liquid pollutants of the dyeing industries include effluents discharged from batch operations as the equipment is cleaned and they usually contain toxic organic residues, which affect the parameters such as pH, Biological Oxidation Demand (BOD), and Chemical Oxygen Demand (COD).[17,18] Direct dyes will have pollutants such as salt, unfixed dyes, copper salts, and cationic fixing agents. Reactive dyes will have salts, unfixed dyes, and alkalis. Vat dyes will have alkalis, oxidising agents, and reducing agents. Sulfur dyes will have alkalis, oxidising agents, reducing agents, and unfixed dyes. Acid dyes will have unfixed dyes, and organic dyes and disperse dyes will have carriers, reducing agents, and organic acids.[19]

Several methods are used to decolorise textile wastewater but they cannot be effectively applied for all dyes.[20] Synthetic dyes often receive considerable attention from researchers interested in textile wastewater treatment processes. Initial environmental efforts with dyes dealt with color pollution, which has a strong psychological effect. More recently interest has shifted to the potential toxicity of dyes, dye precursors (e.g. certain aromatic amines used in the production of azo dyes), and their degradation products, especially the suspected carcinogenicity of potential intermediate products. As toxicity standards are becoming more common and stringent, the development of technological systems for minimizing the concentration of dyes and their breakdown products in wastewater is now necessary.[21]

In the textile industries the chemical reagents used are very diverse in their chemical composition, which include inorganic compounds, polymers and organic products.[22] Due to their chemical structure, dyes are resistant to fading on exposure to light, water and many chemicals.[23] Many dyes are difficult to decolorise due to their complex structure and synthetic origin. There are many structural varieties such as acidic, basic, disperse, azo, diazo, anthroquinone-based and metal complex dyes. Decolorisation of textile dye effluent does not occur when treated aerobically by municipal sewerage systems.[24] Currently the main method of textile wastewater treatment is by physical and chemical means with research concentrating on cheaper and effective alternatives.

1.2 Water pollution and treatment methods

The causes of water pollution are located at municipal, industrial and agricultural level. Municipal causes are related to waste water from homes and commercial establishments. Industrial causes vary as per the biochemical demand, suspended solids, inorganic and organic substances. Agricultural causes include commercial livestock and poultry farming. These lead to organic and inorganic pollutants in surface waters and groundwater.[25] Water pollution is caused by the emission of domestic or urban sewage, agricultural waste, pollutants and industrial effluents into water bodies.

One of the main sources of water pollution is the waste material discharged by industrial units known as industrial water pollution, it produces pollutants that are extremely harmful to people and the environment.[26] Many industrial facilities use freshwater to carry waste away from the plant and into rivers, lakes and oceans. Pollutants from industrial sources include waste materials such as acids, alkalis, toxic metals, oil, grease, dyes, pesticides and even radioactive materials that are poured into the water bodies.[27] Other important pollutants

include polychlorinated biphenyl (PCB) compounds, lubricants and hot water discharged by power plants. The pollutants unloaded into the water bodies usually dissolve or remain suspended in water. Sometimes, they also accumulate on the bottom of the water bodies.[28]

Wastewater treatment consists of applying known technology to improve or upgrade the quality of wastewater. Usually wastewater treatment will involve collecting the wastewater in a central, segregated location (Wastewater Treatment Plant) and subjecting the wastewater to various treatment processes. Most municipal wastewater treatment plants have primary and secondary treatment facilities followed by a tertiary processing plant.[29]

Wastewater treatment, however, can also be organised or categorised by the nature of the treatment process being used. Primary treatment involves physical separation of floatable and settleable solids. Secondary treatment involves biological removal of dissolved solids. Tertiary treatment involves physical, chemical, and biological treatment.[30]

1.2.1 Ozonation

Advanced oxidation is one of the potential alternatives to decolorise and reduce recalcitrant wastewater loads from textile dyeing and finishing effluents. This process implies generation and subsequent reaction of hydroxyl radicals, which are the most powerful oxidising species after fluorine. Advanced oxidation processes including ozonation, UV/H_2O_2, TiO_2/UV, Fenton's reagent, photo-Fenton and photo-electrocatalytic oxidation have been used for the purification of water and wastewater. Among these methods ozonation is very popular. An easy-operated oxidation technology, it is very effective in treating wastewaters containing harmful compounds.[31]

Ozone and hydroxyl radicals generated by ozone in the aqueous solution are able to break aromatic rings of dyes.[32] Ozonation provides no germicidal or disinfection residual to inhibit or prevent regrowth.[33] Some disadvantages of ozone include higher equipment and operational costs and the fact that it may be more difficult to find professionals proficient in ozone treatment and system maintenance. Ozonation by-products are still being evaluated and it is possible that some by-products may be carcinogenic. These may include brominated byproducts, aldehydes, ketones, and carboxylic acids.[34] This is one reason that the post-filtration system may include an activate carbon filter in the ozonation process.

Ozonation of water treatment may require pre-treatment for hardness reduction or the addition of polyphosphate, preventing the formation of carbonate scale. Ozone is less soluble in water compared to chlorine, and therefore special mixing techniques are needed. Potential fire hazards and toxicity issues are associated with ozone generation. Typically, ozonation of dye effluents rarely leads to the complete mineralization, but the partial oxidation of dyes to organic acids, aldehydes, and ketones.[35] It is quite efficient in decolorising solutions, but considerably less efficient in terms of total organic carbon (TOC) removal.

Ozonation is fairly effective in water treatment. However, the technology is relatively expensive. Another disadvantage of ozonation is its short half-life, typically being 20 min. This time can be further shortened if dyes are present, with stability being affected by the presence of salts, pH, and temperature.[36] In alkaline conditions, ozone decomposition is accelerated, and so careful monitoring of the effluent pH is required,[37] and in general ozone has to be generated *in-situ*, which restricts its wider use to use it in remote locations.[38]

1.2.2 Chlorination

The most commonly used chemical process in water treatment is chlorination. This is a very effective technology. Its effectiveness depends on the quality of the water that is being chlorinated and the method of chlorination used. Normally gas chlorination is a more efficient method of disinfection, although a system based on the use of hypochlorite tablets is easier to operate and maintain and is preferred by individual users.[39] The advantages of chlorination systems include the fact that these systems are extremely reliable. The hypochlorite system is easier to operate than the gas system because the operators need not be as skilled or as cautious. Chlorination is also less costly than other disinfection systems and is generally easier to implement. Chlorine (Cl_2) can be made easily *in-situ* and safety considerations for its production, transportation, and uses are well-known.[40]

1.2.3 Hypochlorination: history of hypochlorite

Sodium hypochlorite is one of the most versatile chemicals, to which humankind is constantly exposed. It is a powerful oxidising agent, bleaching agent, disinfectant and deodorizer.[41] It's low cost and versatility makes it very desirable in industry and households alike.[42] In 1774, Scheele first reported that chlorine water was able to bleach vegetable colors.[43] In 1785, Berthelot, a French chemist suggested that this property could be useful commercially. He noted that solutions of chlorine in potash lye proved more concentrated and powerful bleaches. In addition, this particular combination did not have the deleterious effects on workers and materials caused by excess chlorine. The high cost of alkalis prompted Tennant, in 1789 to develop bleaching solutions by dissolving chlorine in aqueous suspensions of lime [$Ca(OH)_2$], strontia [$Sr(OH)_2$] and baryta [$Ba(OH)_2$]. In 1789 he patented a process for the manufacture of "bleaching powder" by saturating dry calcium hydroxide with chlorine gas.[44]

By the end of the nineteenth century, Louis Pasteur had discovered sodium hypochlorite's potent effectiveness against disease-causing bacteria which led to it being widely used as a disinfectant. To this day, sodium hypochlorite remains one of the most effective bleaches around. Daily, millions of households worldwide rely on sodium hypochlorite for their disinfection, deodorizing and cleaning needs. The world consumer market for sodium hypochlorite bleach is in excess of 4 million tons. This does not include the large quantities used for industrial purposes such as waste water treatment and drinking water disinfection.[45]

In the light of the above, the current study focus on dye chemical treatments using two commonly-used oxidants - hypochlorite[46,47] and chlorine dioxide. [48]

1.3 Methods for the preparation of hypochlorite

The literature survey shows that various methods have been adopted for the preparation of aqueous sodium hypochlorite. A few of the important methods are outlined here. Cl_2 may be reacted directly with sodium hydroxide and water.[49] The presence of excess base stabilizes the solutions to some extent. A small excess of sodium hydroxide is allowed as residue to maintain the pH between 11.0 and 13.0 and minimize the decomposition of hypochlorite formed.

$$2\ NaOH + Cl_2 \rightarrow NaCl + NaOCl + H_2O \qquad (1.1)$$

Electrolysis of a cold sodium chloride solution is another method, in which the brine solution in an iron cell is electrolyzed, with iron serving as the cathode. The anode and cathode products are allowed to mix at low temperatures to minimize the decomposition caused by a temperature increase.[50]

Sodium hypochlorite can be obtained in solution by passing chlorine into a cold, dilute solution of sodium carbonate.[51]

$$Na_2CO_3 + Cl_2 \rightarrow NaCl + NaOCl + CO_2 \quad (1.2)$$

Hypochlorite solutions are prepared by the neutralization of hypochlorous acid or dichlorine monoxide.[52] With alkalis, hypochlorous acid forms salts, which are largely hydrolysed:

$$HOCl + OH^- \rightarrow H_2O + OCl^- \quad (1.3)$$

Gaseous chlorine is bubbled through aqueous slurry of yellow HgO at room temperature.[53] For every mol of chlorine dissolved in the slurry, 3.0 mol HgO is added to provide an adequate excess. The slurry is mixed for 45 min at which time all of the Cl_2 is converted to HOCl and all the chloride ion is precipitated as $HgCl_2$. This HOCl/$HgCl_2$/HgO slurry is distilled under a reduced-pressure nitrogen atmosphere into a 0.10 M NaOH solution, and the HOCl is collected as NaOCl. The nitrogen atmosphere is utilized so that no CO_2 is present to form carbonate ion as a contaminant in the final NaOCl solution.[54]

1.4 Advantages and uses of hypochlorination

Sodium hypochlorite has long been recognized as having outstanding disinfection properties. Hypochlorite compounds are non-flammable. It does not present the same hazards as gaseous chlorine and is therefore safer to handle. It can be easily stored and transported when it is produced on-site.

Hypochlorite spills can be cleaned up with large volumes of water. Sodium hypochlorite effectively destroys disease-causing bacteria and is thus a major contributor to efforts to stem the debilitating consequences of cholera, dysentery, typhoid and other waterborne biotic diseases. In hospitals and health care facilities, bleach is used to disinfect surfaces against fatal viruses like Human Immunodeficiency Virus (HIV) and Hepatitis-B. It is used extensively in the area of water treatment to disinfect municipal drinking water and drinking water from wells.[55] It is widely used for swimming pool water disinfection, both as a daily

regimen and as a shock treatment. It is a bactericidal and has good solvent properties for vital necrotic and fixed tissues.[56]

Hypochlorite is used for industrial and institutional applications. It is used for the treatment of sewage to reduce odours and to increase digesting efficiency, as an irrigating solution for endodontic treatment[57] as well as in the treatment of the cyanide effluent in gold mining and in cyanide waste treatment in metal finishing. In food processing it is used for sanitizing dairy equipment, fruit and vegetable processing, mushroom production, hog, beef and poultry production, maple syrup production, fish processing, and to effectively control algae in open reservoirs. Hypochlorite is used in cooling water and boiler water treatment to prevent fouling.[58] It is used for the oxidative degradation of residual dyes present in waste water streams.[59,60]

It can be safely used on many washable, color fast fabrics including cotton, polyester, nylon, acetate, linen, rayon and permanent press. It is highly effective in removing a wide range of stains and soils which are not totally removed by laundry detergents, e.g. blood, body soiling, coffee, grass, mustard, red wine, etc. Hypochlorite can provide a significant boost to the whitening and cleaning power of laundry detergents even in cold or hard water. Hypochlorite's unique disinfecting properties assure sanitization, which is of particular importance in hospital linens to reduce the possible transmission of disease.[61,62]

1.5 Limitations of hypochlorination

The use of chlorine in gaseous form or as a solution can cause safety hazards. All operating personnel should be made aware of these hazards and trained in handling. Chlorine is reactive and interacts with certain chemicals present in the product water, depending on pH and water

temperature; resulting in the depletion of the chlorine concentration, leaving only residual amounts of chlorine for disinfection (over-chlorination may result in the formation of chlorinated hydrocarbons, such as trihalomethanes, which are known to be carcinogenic).[63]

Chlorine will also oxidise ammonia, hydrogen sulfide, and metals present in the product water to their reduced states. Chlorine gas is heavier than air, and is extremely toxic and corrosive in moist atmospheres. Dry chlorine can be safely handled in steel containers and piping, but where moisture is present (as it is in most treatment plants), corrosion-resistant materials such as silver, glass, pressurized gas Teflon, and certain other plastics must be used.[64] Hypochlorite may cause damage to the eyes and skin upon contact, because it is a powerful oxidant, and may cause fires if it comes into contact with organic or other easily oxidisable substances.[65]

1.6 History of chlorine dioxide

Among the different chemical agents that can be used as chlorine alternatives for water potabilisation, chlorine dioxide has attracted considerable attention.[66] The discovery of ClO_2 has largely been credited to Sir Humphrey Davy, who in the 1800s created the compound by mixing sulfuric acid with potassium chlorate.[67] Since its discovery, researchers have found that ClO_2 shares some common characteristics with chlorine. Specifically, ClO_2 is a greenish-yellowish gas with a chlorine-like odor that is irritating to the eyes, nose, and throat. Apart from these very limited similarities, however, it has been learned that ClO_2 exhibits physical and chemical properties that are dramatically different from those of chlorine, even though it contains a chlorine atom in its molecular structure.

ClO_2 is unstable as a gas and will undergo decomposition into chlorine gas (Cl_2), and oxygen gas (O_2) and produces heat. However, ClO_2 is stable and soluble in an aqueous solution. For example, solutions of approximately one percent ClO_2 (10 g/L) may be safely stored if the solution is protected from light and kept chilled. In solution form, ClO_2 exists as a true gas.

Chlorine dioxide is commonly used as a pre-oxidant and primary disinfectant during treatment of drinking water. As a pre-oxidant, it is used mainly as an alternative to chlorine, for tri-halomethane (THM) control.[68,69] It is also used for taste-and-odor control, manganese and iron oxidation, and color removal. In the United States, over 500 water treatment plants use ClO_2 full time and as many as 900 use it either part time or seasonally.[70]

1.6.1 Methods of preparation of chlorine dioxide

Chlorine dioxide is a highly endothermic compound that can decompose when separated from diluting substances. As a result preparation methods that involve producing solutions of it without going through a gas phase stage are often preferred.

Most commercial generators use sodium chlorite ($NaClO_2$) as the common feedstock chemical to generate chlorine dioxide for drinking water application. Recently, production of chlorine dioxide from sodium chlorate ($NaClO_3$) has been introduced as a generation method wherein $NaClO_3$ is reduced by a mixture of concentrated hydrogen peroxide (H_2O_2) and concentrated sulfuric acid (H_2SO_4). More than 95% of the sodium chlorate produced today is used in the pulp and paper industry where it is a primary raw material for the production of chlorine dioxide. Chlorine dioxide is a strong and selective oxidiser and is used in the pulp bleaching process.[71,72]

The most common methods for the generation of ClO_2 for water treatment involve sodium chlorite ($NaClO_2$), either as a solid or in solution.[73] Sodium chlorite is reacted with either chlorine gas (Cl_2), hypochlorous acid (HOCl), or hydrochloric acid (HCl) in the following reactions. [74] This method was used to generate the chlorine dioxide in the current study.

$$2NaClO_2 + Cl_2(g) \rightarrow 2ClO_{2(g)} + 2NaCl \quad (1.4)$$

$$2NaClO_2 + HOCl \rightarrow NaCl + NaOH + 2ClO_2(g) \quad (1.5)$$

$$5NaClO_2 + 4HCl \rightarrow 4ClO_{2(g)} + 2H_2O + 5NaCl \quad (1.6)$$

In the first two reactions, an unstable intermediate, Cl_2O_2, is formed if the reactants are in high concentrations. When chlorite ion (ClO_2^-) concentrations are low, the intermediate decays to chlorate ion (ClO_3^-). The chlorate ion production can also occur, when initial reactant concentrations are low or when chlorine (or hypochlorous acid) is in excess. When initial reactant concentrations are high or when ClO_2^- concentrations are in excess, the intermediate decays to ClO_2.[75]

During the generation of ClO_2, it is desirable to minimize or eliminate unwanted by-products such as ClO_2^- and ClO_3^- as well as excess chlorine. The production of unwanted by-products can occur when there is feedstock contamination, improper generator control, or excess chlorine.[76,77] In reaction 1.5, only 80 percent conversion of $NaClO_2$ to ClO_2 is possible and, therefore, this method is not popular. Pure chlorine dioxide can also be produced by electrolysis of a chlorite solution:

$$2NaClO_2 + 2H_2O \rightarrow 2ClO_{2(g)} + 2NaOH + H_2 \quad (1.7)$$

High purity chlorine dioxide gas (7.7 percent in air or nitrogen atmosphere) can be produced by the Gas: Solid method, which reacts dilute chlorine gas with solid sodium chlorite:

$$2NaClO_2 + Cl_2 \rightarrow 2ClO_{2(g)} + 2NaCl \quad (1.8)$$

Another method for generating high-purity ClO_2 by reaction of solid $NaClO_2$ with chlorine gas has become available.[75] The chlorine gas is first mixed with humidified air and then passed through a series of drums containing solid $NaClO_2$. No unreacted $NaClO_2$ enters the system because the generated ClO_2 is in the gas phase, and ClO_3^- is not produced.

1.6.2 Advantages and uses of chlorine dioxide

Chlorine dioxide is less expensive than other disinfection methods, such as ozone. Chlorine dioxide is used primarily (>95%) for bleaching of wood pulp, as an oxidiser chlorine dioxide is very selective. It has this ability due to unique one-electron exchange mechanisms. Chlorine dioxide attacks the electron-rich centers of organic molecules. By comparing the oxidation strength and oxidation capacity of different disinfectants, chlorine dioxide is effective at low concentrations; It can be effectively used when a large amount of organic matter is present in the effluents. It is also used for the bleaching of flour, and for the disinfection of municipal drinking water.

New York's water treatment plant first used chlorine dioxide for drinking water treatment in 1944 for phenol destruction. It's most common use in water treatment is as a pre-oxidant prior to chlorination of drinking water to destroy natural water impurities that produce trihalomethanes to free chlorine.[78,79] Chlorine dioxide is also superior to chlorine when operated above pH 7.0, in the presence of ammonia and amines and/or for the control of biofilms in water distribution systems. Chlorine dioxide is used in many industrial water treatment applications as a biocide including cooling towers, process water and food processing. Chlorine dioxide is less corrosive than chlorine and superior for the control of

legionella bacteria. It is more effective as a disinfectant in most circumstances than chlorine against waterborne pathogenic microbes such as viruses, bacteria and protozoa.[80] At a low concentration level chlorine dioxide gas can be used as a precaution against Influenza A virus infection.[81] It can also be used for air disinfection, and was the principal agent used in the decontamination of buildings in the United States after the 2001 anthrax attacks.[82] After the disaster of Hurricane Katrina in New Orleans, Louisiana and the surrounding Gulf Coast, chlorine dioxide has been used to eradicate dangerous mold from houses inundated by water from massive flooding.[83] Chlorine dioxide is used as an oxidant for phenol destruction in waste water streams, control of zebra and quagga mussels in water intakes and for odor control in the air scrubbers of animal by-product plants. Stabilized chlorine dioxide can also be used in an oral rinse to treat oral disease and malodor.[84]

1.6.3 Limitations of chlorine dioxide

When using chlorine dioxide with sodium chlorite and chlorine gas, safety measures must be taken both during its transportation and usage. Sufficient ventilation and gas masks are required for handling. Chlorine dioxide is a very unstable substance, and it decomposes when exposed to sunlight. During chlorine dioxide production processes, a large amount of chlorine is formed,[85] Free chlorine reacts with organic matter to form halogenated disinfection by-products. Chlorine dioxide and its disinfection by-products chlorite and chlorate, if present in water can create health problems for dialysis patients. To control pathogenic micro-organisms, chlorine dioxide is generally effective, but it is less effective for the deactivation of rota viruses and *E. coli* bacteria. Chlorine dioxide is about 5 to 10 times more expensive than chlorine.[86] Chlorine dioxide is usually made on site. The costs depend upon the price of the chemicals that are used to produce it.

1.7 Dyes and classification of dyes

A wide range of dyes exists to meet the demands of industry. An aromatic ring structure coupled with a side chain is usually required for resonance and to impart its color. The color is usually given by the chromophore group, such as azo (–N=N–); carbonyl (>C=O); carbon (–C–C–); carbon-nitrogen (>C=NH or –CH=N–); nitroso (–NO or N–OH); nitro (–NO_2 or =NO–OH); and sulfur (>C=S, and other carbon-sulfur groups), which also form a basis for the chemical classification of dyes.[87] All commercial textile dyes are classified by their generic name and chemical constitution. They are assigned a Color Index classification number by Color Index (C.I.),[88] a journal published by the Society of Dyers and Colorists (United Kingdom) in association with the American Association of Textile Chemists and Colorists (AATC). Every commercial dye and pigment in it is given a C.I. Generic Name, which includes its application class, its hue and a number which indicates its chronological discovery. Most of the dyes and pigments in the Color Index are placed in one of the 25 structural classes according to their chemical type. Azo dyes, the largest class, are subdivided into four sections.[89] However, if we take color index as one of the basis for classification, the typical dyes most used widely in the textile industry include acid dyes, basic dyes, direct dyes, disperse dyes, sulfur dyes, reactive dyes, oxidation dyes, and vat dyes.[90,91]

1.7.1 Acid dyes

Acid dyes are typically used to dye acrylics, wool, nylon, and nylon/cotton blends, and are also used in the paper and leather industries. They are called acid dyes because they are normally applied to the nitrogenous fibers of fabrics in organic or inorganic acid solutions. The three most commercially important acid dyes are azo, anthraquinone, and triarylmethane. These dyes are generally applied as a liquid at elevated temperatures of greater than 39 $^{\circ}$C.

In general, these dyes have poor wet fastness and their molecular weights range from 200 to 900 g mol^{-1}. The structure of typical acid dye, brilliant blue-R is illustrated in Figure 1.1.1.[92]

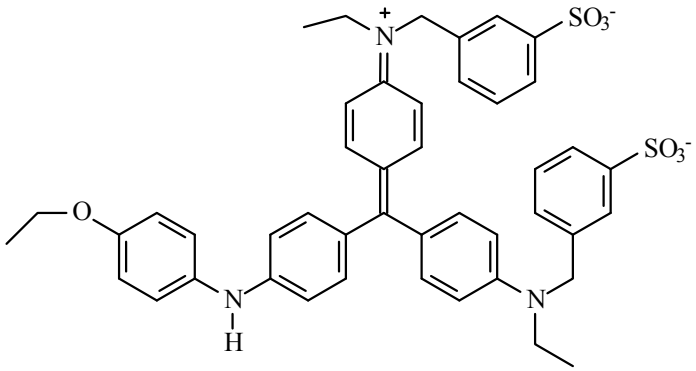

Figure 1.1.1 Structure of acid dye-brilliant blue R.

1.7.2 Direct dyes

Direct dyes are commonly used on cotton fibers. These dyes are mixed with all purpose dyes along with the acid dyes. The color of direct dyes on cotton fibers is not bright in comparison with other dyes. These dyes are normally used to dye cotton and other cellulosic fibers; they bond to fibers by electrostatic forces. Direct dyes are applied in an aqueous bath containing ionic salts and electrolytes; these can be also used to stain silk and wool. Few direct dyes, like direct orange 39 and direct blue 86 are considered as having very high light fastness capacity. The structure of typical acid dye, direct fast red 8B, is illustrated in Figure 1.1.2.[93]

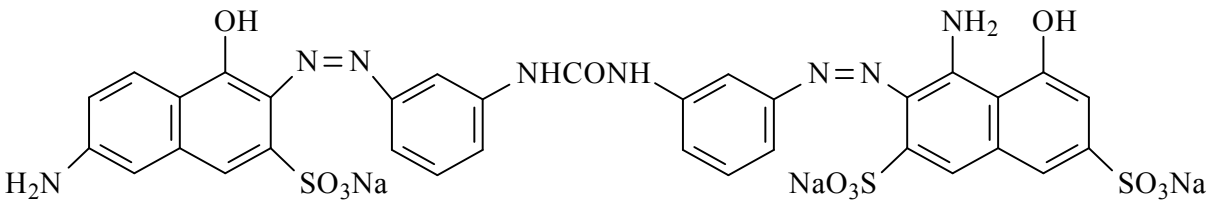

Figure 1.1.2 Structure of direct dye-direct fast red 8B.

1.7.3 Disperse dyes

Disperse dyes are colloidal and have very low water solubility. These dyes were originally developed for the dyeing of cellulose acetate, and are substantially water insoluble. They are finely grounded in the presence of a dispersing agent and then sold as a paste, or spray-dried and sold as powder. Most of these dyes are used for polyester, nylon, acetate, and triacetate fibers and surface dyeing of plastics. They are usually applied from a dye bath as dispersions by direct colloidal absorption. Dye bath conditions (temperature, use of carrier) are varied based on the degree of difficulty encountered by the dyes in penetrating the fiber being dyed. They are sometimes applied dry at high temperatures by means of a sublimation process followed by colloidal absorption. A typical disperse dye, reactive orange 4 is shown in Figure 1.1.3.[94]

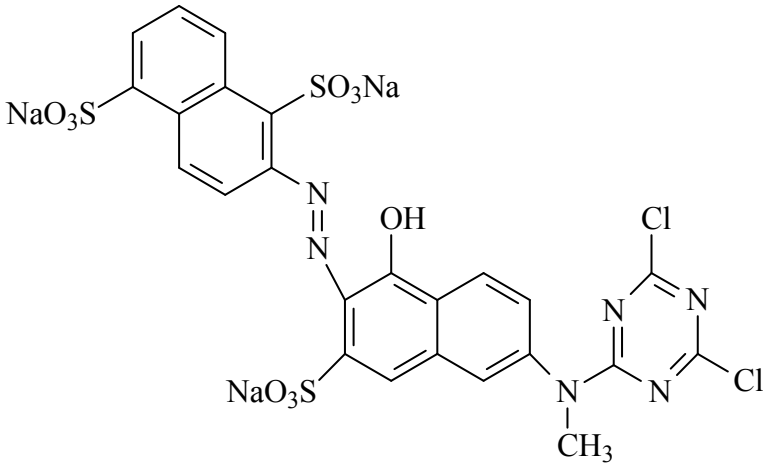

Figure 1.1.3 Structure of disperse dye-reactive orange 4.

1.7.4 Sulfur dyes

Sulfur dyes are used primarily for cotton and rayon. The main characteristics of sulfur dyes are that they have lustrous grains, and make a complete black shade with a slight reddish or greenish impact. These dyes are used for jigger, cotton and viscose rayon. From the name it is clear that these dyes contain a small amount of sulfuric acid. The fibers that can be dyed by these dyes are viscous, staple fibers, yarn, any materials which give a resin finish, silk etc.

These dyes have excellent light fastness properties. The structure of typical sulfur dye, soluble sulfur black is illustrated in Figure 1.1.4.[95]

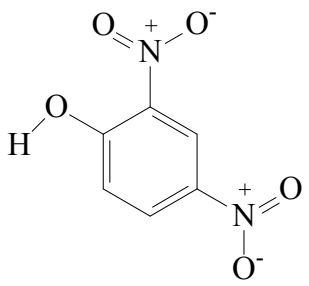

Figure 1.1.4 Structure of sulfur dye-soluble sulfur black .

1.7.5 Reactive dyes

Reactive dyes or fiber reactive dyes are basically a class of highly colored organic substances. Reactive dye uses a chromophore that contains a substituent that is quite capable of a direct reaction with a fiber substrate. Fiber reactive dyes derive their name from the fact that they form covalent bonds with the fiber molecules to be dyed. Cold reactive dyes, like cibacron F, procion MX, and drimarene K, are very easy to use as they can be applied at room temperature. Reactive dyes are very good for dyeing cotton and other cellulose fibers. They are primarily used for tinting textiles. These dyes also have outstanding wet fastness. An example of a reactive dye reactive red 22 is shown in Figure 1.1.5. [96]

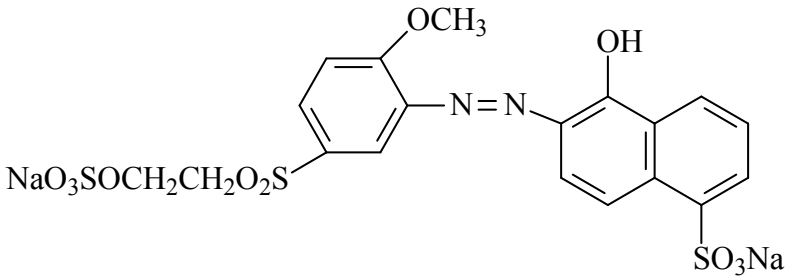

Figure 1.1.5 Structure of reactive dye-reactive red 22.

1.7.6 Basic dyes

Basic dyes are the class of dyes that are most commonly synthetic. Their primary nature is to act as bases, and they are actually aniline dyes. Initially their color base prevents them from being water soluble. They can be made with the base being converted into a salt. At the chemical level, basic dyes are typically cationic or positively charged. Basic dyes display cationic functional groups like $-NR_3^+$ or $=NR_2^+$. Basic dye is a stain that is cationic or positively charged and this is the reason that it reacts well with material that is anionic or negatively charged. Basic dyes consist of amino groups, or alkyl amino groups, as their auxochromes. Some prominent examples of basic dyes are methylene blue, crystal violet, basic fuchsin and safranin etc. The structure of typical basic dye, safranine-O is illustrated in Figure 1.1.6.[97]

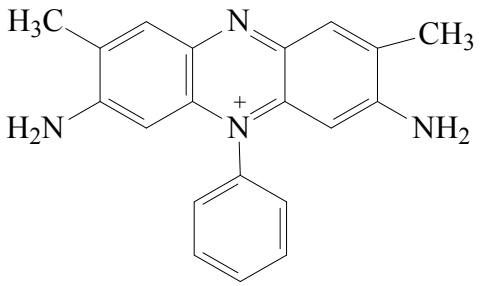

Figure 1.1.6 Structure of basic dye-safranine-O.

1.7.7 Vat dyes

Vat dyes are based on an original Indigo dye that is a kind of natural dye. Vat dyes are an ancient class of dye. Indigo dyes (parent of vat dyes) are manufactured synthetically. Various kinds of fibers can be washed by using vat dyes and the main categories of fibers are cotton and wool. In the dyeing process the vat dyes are not directly used. The major application is the dyeing and printing of cotton. Such are the outstanding fastness properties of this group that special methods for the dyeing and printing of substrates other than cotton e.g. wool, silk

and cellulose acetate have been developed. The structure of typical vat dye, vat brown 1 is illustrated in Figure 1.1.7.[98]

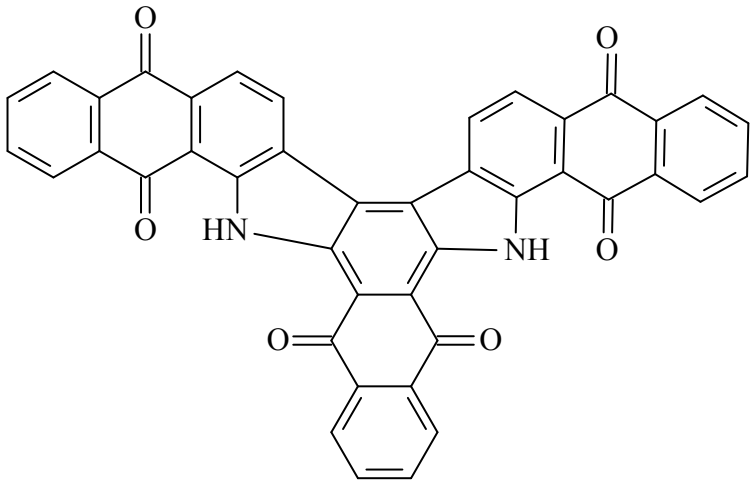

Figure 1.1.7 Structure of vat dye-vat brown 1.

1.7.8 Literature survey

Effluent from most textile dyeing operations generally has a dark reddish-brown hue that is aesthetically unpleasing when discharged in receiving waters. In typical dyeing and printing processes, 50 to 100 percent of the color is discarded in the form of spent dye-baths or in wastewater from washing operations. In recent years the oxidation of dyes has attracted much attention. Many methods of color removal exists using different oxidants. Because of the difficulties and expense in treating color, due to the large variability of the composition of textile wastewater, most of the traditional methods are becoming inadequate.[89-99] There is a need to investigate the best approach for minimizing colour discharges as a measure of pollution prevention.

The literature survey suggests that some azo and anthraquinone dyes were non-degradable by the conventional activated sludge process.[100] Muruganandham *et al*. studied the

photochemical oxidation of reactive orange 4 in the presence of H_2O_2 and UV-light and concluded that the dye follows *pseudo* first-order kinetics with the UV-H_2O_2 and solar-H_2O_2 processes and efficient at pH 3.0.[101] Oakes *et al*. studied the kinetics of the heterogeneous oxidation (by hypochlorite) of an azo dye (Remazol Red RB) reactively bound to cotton,[102] and reported that the physical state of bound dye (e.g. its pKa and tautomeric form) and its oxidation profile with pH are similar to those of dye in a homogeneous solution. The analysis presented suggested that the mechanism of oxidation in the two environments is similar. The oxidation of azo dyes of pyrazolone and pyridone types occurred at similar rates to arylazonaphthol dyes and oxidation kinetics were independent of groups attached to either side of the azo linkage, confirming that the site of attack is the more nucleophilic nitrogen atom of the azo group of the common anion.

Oakes and Gratton investigated the oxidation of orange I, and orange II,[103] and also a series of substituted azo dyes with hypochlorite, peracids and hydrogen peroxide in aqueous media. They concluded that the observed second-order rate constants exhibit maxima in alkaline media at a pH equal to the midpoint of the pKa values of dye and oxidant. They also reported that substituents upon the aryl ring ortho to the azo group suppress dye reactivity towards hypochlorite and peracids. In contrast, oxidation by hydrogen peroxide is enhanced by ortho substituents, suggesting that it functions *via* a different mechanism. The dye common anion has been identified as the form of the dye most susceptible to oxidation by peracids and hypochlorite, with the undissociated oxidant molecules acting as electrophiles. In contrast, dye oxidation by hydrogen peroxide proceeds *via* the perhydroxyl anion and the hydrazone tautomeric form of the dye. The main function of ortho substituents was to increase the dye pKa, thereby influencing observed rates by changing the equilibrium concentration of reactive species. Reactive oxygen species, e.g. singlet oxygen, superoxide or hydroxyl

radicals, were not implicated in the rate-controlling step of their reaction.

Rauf *et al*. studied the photolytic degradation of Amaranth azo dye,[104] Coomassie brilliant blue,[105] and safranine-O using H_2O_2 and UV light.[106] They observed the first-order kinetics with the respective dyes and concluded that the reaction of the dye is due to the hydroxyl radicals generated in solution and UV oxidation degradation of the dye was less in the presence of bromide, chloride, acetate, sulfite, silver and bicarbonate ions. The results showed that mere UV light or H_2O_2 alone were not sufficient for degradation of this dye.

Szpyrkowicz *et al*. studied the oxidation of pollutants in synthetic textile wastewater containing partially soluble disperse dyes. In their study the removal of pollutants was mediated by active chlorine generated by electro-oxidation of chloride ions or by other mediators generated *in situ* and not by a direct discharge of pollutants at the anode. They achieved 39 percent removal of chemical oxygen demand after 40 min of electrolysis. They reported that the apparent *pseudo* first-order rate constant for the removal of color was equal to 2.54×10^{-4} s^{-1} and it increased to 8.23×10^{-4} s^{-1} under pH control at the value of 4.5, resulting in 90 percent removal of color after the passage of 1.9A h dm^3. They reported that in comparative studies on the chemical oxidation of pollutants by hypochlorite far lower efficiency was obtained.[107]

Hastie *et al*. studied the electrochemical methods for degradation of orange II.[108] They concluded that in divided flow-through cells, reductive electrolysis of orange II was first-order in both substrate and applied current and gave the products reductive cleavage at the azo linkage in essentially quantitative yield. Oxidative electrolysis was also *pseudo* first-order and led to mineralization. At a boron-doped diamond anode, the rate of disappearance of dye

is closely tracked through the loss of total organic carbon from solution. In undivided cells oxidation and reduction occurred simultaneously; under acidic conditions the reduction products (anilines) were rather persistent because they were present as ammonium ions, but under alkaline conditions the anilines were mineralized along with the starting material. When chloride ion was present in the supporting electrolyte, electrochemical oxidation afforded hypochlorite, and the disappearance of dye proceeded by way of hypochlorination.

Sergio *et al*. studied the chlorine dioxide reaction with selected amino acids in water and reported that chlorine dioxide can attack the electron-rich aromatic moieties as well as the nitrogen atom lone electron pair[109]. However very little is known about the chlorine dioxide reactivity with dyes.

Any type of chlorine that is added to water during the treatment process will result in the formation of hypochlorous acid (HOCl) and hypochlorite ions (OCl^-), which are the main disinfecting species in chlorinated water. The literature survey revealed that little is known about the role of HOCl and OCl^- and their speciation behavior towards the oxidation of the dyes. There are only a few studies of the reaction of chlorine dioxide with organic compounds especially with dyes. It is a strong oxidant, and surface waters exhibit a chlorine dioxide demand similar to that for chlorine.[110] Chlorine dioxide destroys phenolic compounds when the oxidant is used for taste and odor control in water supplies.[111] Höigne *et al.* demonstrated the reactivity of ClO_2 with inorganic and organic compounds and established first-order kinetics with respect to ClO_2 and also first-order with respect to the compound.[112]

In the current study, the oxidation of three selected dyes i.e. amaranth (azo dye), brilliant blue-R (triarylmethane dye) and safranine-O (azine dye) with hypochlorite and chlorine

dioxide were carried out by kinetic approach. The outline is further supported by other spectroscopic studies. A brief summary of these dyes based on their chemical class and uses is given below.

1.8 Classes of the dyes studied

1.8.1 Azo dyes

The azo dyes are also broadly used in the textile, color solvent, ink, paint, varnish, paper, plastic, food, drug and cosmetic industries. More than two thousand azo dyes are known to exist, and over half of commercial dyestuffs are azo dyes, with some of them, and azo precursors and their degraded products (like aromatic amines), being carcinogens.[113] It is for this reason that amaranth was chosen as the representative dye. It is also commonly referred to as red no. 2, food red 9, acid red 27 and azorubin S. Amaranth is an anionic dye.

Azoic dyes are also called azoic or napthol dyes. These azo dyes consist of a group called the azo group which has two nitrogen atoms. This group (covalent bond) connects atomic ring compounds. The two Nitrogen atoms are bonded with each other and forms -N=N- as part of their molecular structure. Azoic dyes are found mainly in three colors - red, brown and yellow. They are manufactured from aromatic amines. Azoic dyes are applied by combining two soluble components impregnated in the fiber to form an insoluble colour molecule. These dye components, sold as paste-like dispersions and powders, are used chiefly for cellulosics, especially cotton, giving shades of a high standard of fastness to light and wet processing. They give bright, intense hues particularly in the yellow, orange, and red ranges.[114]

Amaranth is made from amaranth plants. Its leaves range from purple and red to gold. There are about sixty *Amaranthus* species. Several of them are cultivated as leaf vegetables, cereals,

or ornamental plants. It is a dark red to purple azo dye used in many countries as a food dye and to color cosmetics. It usually comes as a trisodium salt. It has the appearance of reddish-brown, dark red to purple and is water-soluble. Its water-based solution has absorption maximum at about 520 nm. It is banned in some countries such as the United States by the Food and Drug Administration (FDA) as it is a suspected carcinogen[115]

1.8.2 Triarylmethane dyes

Tri aryl dyes are the derivatives of triphenylmethane. They have poor resistance to light and to chemical bleaches and are used extensively in the textile, paper, leather and plastic industry and also in large applications in food and beverages. Brilliant blue - R was selected for the study as it is often found in ice cream, tinned processed peas, dairy products, sweets, and drinks. It is also used in soaps, shampoos, syrups and other hygiene and cosmetics applications. It is one of the colorants that has been suggested should be eliminated from the diet of children.[116] It is commonly referred as basic red 2, cotton red, gossypimine.

1.8.3 Azine dyes

Azine dyes are widely used in the textile industry and also in combination with other dyes as color additives. Safranin (also safranin-O or basic red 2) (3,8-diamino-4,7-dimethylphenyl phenazinium chloride) was selected as the model compound for this study because of its wide application in various textile industries either on its own or in combination with other dyes as color additives.[117,118] Safranin is used as a counter stain in some staining protocols, coloring all cell nuclei red. Safranin is also used as redox indicator in analytical chemistry.

1.9 Chemistry of hypochlorite ion

1.9.1 Hypochlorite decomposition

Commercially produced bleach is normally kept at a pH between 11.0 and 13.0 as it contains between 0.001 M and 0.100 M hydroxide ion (OH^-) to minimize its decomposition.[119] Hypochlorite ion decomposition in basic solution is a slow second order process[120] in the 40 - 60 °C range with the following stoichiometry and rate law:

$$3\ OCl^- = ClO_3^- + 2\ Cl^- \quad (1.9)$$

$$\frac{-d[OCl]^-}{3dt} = k_{obs}\,[OCl^-]^2 \quad (1.10)$$

The decomposition of OCl^- reported involves its disproportionation and chlorite ion (ClO_2^-) as an intermediate leading to formation of chlorite and chloride ions.[18,121,122]

$$OCl^- + OCl^- \rightarrow ClO_2^- + Cl^- \quad \text{(slow)} \quad (1.11)$$

$$OCl^- + ClO_2^- \rightarrow ClO_3^- + Cl^- \quad \text{(fast)} \quad (1.12)$$

Because reaction (1.12) is the fast process, the concentration of ClO_2^- remains relatively low.[123] Chlorate ion, often present in drinking water that has been treated with OCl^-, is foundin three possible sources.[124,125] The first is from the raw (untreated) water itself and the second source of ClO_3^- is the decomposition of residual hypochlorous acid (HOCl) during the the disinfection process. It has been shown that in the dark, decomposition of HOCl at mg per litre level between pH 5.0 and pH 8.0 is relatively slow. In the presence of UV light (sunlight), HOCl decomposes with a photolysis half life[126] of 12 mins at pH 8.0 and increases as the ratio of OCl^- to HOCl increases. The third possible source of ClO_3^- is the decomposition of OCl^- in liquid bleach during storage prior to application. The formation of oxygen from the decomposition of OCl^- is a very slow side reaction[127] in solutions of pure OCl^- and is considered to be only a minor decomposition pathway (< 10%).

$$OCl^- + OCl^- \rightarrow O_2 + 2\ Cl^- \quad \text{(very slow)} \qquad (1.13)$$

The liquid bleach stored with a pH between 12.0 and 13.0 is the most stable. As the pH of the bleach stock solution is lowered, the pH of the OCl^- stock solution will continue to decrease over time because of a competing acid-producing decomposition pathway with the following stoichiometry:[128]

$$2\ HOCl + OCl^- \rightarrow ClO_3^- + 2\ H^+ + 2\ Cl^- \qquad (1.14)$$

This could be a serious problem because the high HOCl in the stored liquid bleach will lead to a large ClO_3^- residual in the storage tank and eventually in the finished water. Dilution of the stock bleach can be an effective strategy for minimizing OCl^- decomposition and concomitant ClO_3^- formation. To minimize ClO_3^- formation, the pH of the liquid bleach should be adjusted and maintained at a pH $\geq$ 11.0.[129] Commercial bleach contains enough caustic soda to maintain a pH $\geq$ 12.0 even after 50 percent dilution. It has also been shown that increasing the temperature of liquid bleach increases its rate of decomposition. Thus in summer months and in unventilated storage sheds, the decomposition of liquid bleach will be rapid.[130] The rate constants for the decomposition pathways are affected not only by temperature, but also by the ionic strength, ionic media present and the presence of UV light.

1.9.2 Bleaching action of hypochlorite ion

Bleach is a chemical that removes color or whitens, often *via* oxidation. Color in most dyes and pigments is produced by molecules, such as beta carotene, which contain chromophores. Chemical bleaches work in one of two ways: an oxidising bleach works by breaking the chemical bonds that make up the chromophore; this changes the molecule into a different substance that either does not contain a chromophore, or contains a chromophore that does

not absorb visible light. A reducing bleach works by converting double bonds in the chromophore into single bonds. This eliminates the ability of the chromophore to absorb visible light.[131,132]

The bleaching action of hypochlorite ion depends on three main reactions,[133] i.e. disruptive oxidation of colored molecules, addition of halogen oxides across olefinic functions and halogenations of saturated compounds.

1.9.3 Oxidising action of hypochlorite ion

The oxidation reaction with hypochlorite normally involves two electron oxidations both under basic and acidic pH conditions.

The oxidising action of hypochlorite may be expressed by the ion electron equations:[134]

In alkali:

$$OCl^- + H_2O + 2e^- \rightarrow Cl^- + 2OH^- \quad (1.15)$$

In acid:

$$OCl^- + 2H^+ + 2e^- \rightarrow Cl^- + H_2O \quad (1.16)$$

1.9.4 Hypochlorite and hypochlorous acid distribution

The decomposition of hypochlorite (HOCl and $OC1^-$) has been studied initially by Chapin *et al.* in the pH range 1.0 to 13.0.[135] The pKa value of hypochlorite is 7.4.[6,136] He further reported that maximum decomposition rate of hypochlorite is in the neutral pH range. Based on its pKa value the speciation of hypochlorite and hypochlorous acid as function of pH is calculated and the data is summarized in Table1.1.1

Table 1.1.1 Percentage distribution of OCl^- and HOCl*

pH	$[OCl^-]$%	[HOCl]%
2.0	0.45	99.55
3.0	1.21	98.79
4.0	3.23	96.77
5.0	8.32	91.68
6.0	19.78	80.22
7.0	40.13	59.87
8.0	64.57	35.43
9.0	83.20	16.80
10.0	93.09	6.91

*calculated values using pKa 7.4 up to four significant figures.

1.10 Chemistry of chlorine dioxide

Chlorine dioxide (ClO_2) exists as a volatile, energetic free radical and is quite reactive. Due to its explosive nature, ClO_2 cannot be compressed or stored and must be generated on-site. Solutions with concentrations greater than 10.0 g/L can poses an explosive hazard[137] and its ignition temperature is about 130 °C. Chlorine dioxide concentrations used in the water treatment are generally in the range of 0.1 mg/L to 5.0 mg/L.

One of the most important physical properties of chlorine dioxide is its high solubility in water, particularly in chilled water. Chlorine dioxide does not hydrolyze in water but remains a highly soluble gas above 11°C over a broad range of pH (2.0 to 10.0). Solutions are greenish-yellow and smell strongly chlorinous.[75] Aqueous solutions must be protected from light, as chlorine dioxide is subject to photolysis by ultraviolet light,[138] and even fluorescent lights.

The main reaction product of ClO_2 in water is the chlorite ion. Its reduction occurs by an electron transfer, forming ClO_2^- as shown in this half-reaction.[74,139]

$$ClO_2 + e^- \rightarrow ClO_2^- \quad (1.17)$$

Masschelein[140] reported, "In aqueous solution, chlorination by chlorine dioxide is not a direct reaction. However, indirect chlorination by dioxide having undergone a previous reaction may not necessary be excluded." He attributed reports of chlorinated organic by-products produced to the presence of chlorine in the ClO_2 solution that was used. Chlorine, on the other hand, reacts with organic compounds to form chlorinated organic by-products.[141,142]

Chlorite ion, which also is an oxidant, reacts at a much slower rate than ClO_2 under conditions generally encountered in water treatment. Chlorite ion is reduced to chloride ion (Cl^-) by the following reaction[74,137,140] :

$$ClO_2 + 4H^+ + 4e^- \rightarrow Cl^- + 2H_2O \quad (1.18)$$

This reaction does not occur, however, unless reduced compounds such as ferrous ion (Fe_2^+), phenol, or humic materials are present.[143] Typically, from 50 to 70 percent of the reacted ClO_2 appears as ClO_2^- with the balance forming either Cl^- or ClO_3^-.[144,145]

In basic solutions, ClO_2 disproportionates to form $ClO_2^-$and ClO_3^- [137] :

$$2ClO_2 + 2OH^- \rightarrow ClO_2^- + ClO_3^- + H_2O \quad (1.19)$$

Under certain conditions chlorine and ClO_2 can react to form ClO_3^-

$$2ClO_2 + HOCl + H_2O \rightarrow 2\ ClO_3^- + 2H^+ + HCl \quad (1.20)$$

When chlorine dioxide is subject to photochemical decomposition through a series of reactions to Cl^- and ClO_3^- [146,147] there was significant formation of ClO_3^- (0.36 to 0.97 mg/L) when water containing from 3.56 mg/L to 3.99 mg/L of ClO_2 was exposed to fluorescent

light. In controlled experiments, when water was treated with ClO_2 and kept in the dark it did not contain ClO_3^-.

Chlorite ion reacts with chlorine in treated water to reform ClO_2, in the same manner that ClO_2 is generated (Reaction 1.5). This reaction, however, depends heavily on pH and relative reactant concentrations. In basic solutions when the hypochlorite ion (OCl^-) is present, greater amounts of ClO_3^- are formed by the following reaction.[144,148]

$$ClO_2^- + HOCl + OH^- \rightarrow H_2O + Cl^- + ClO_3^- \quad (1.21)$$

In acidic conditions more ClO_2 than ClO_3^- is formed.

$$2ClO_2^- + HOCl + H^+ \rightarrow 2\ ClO_2 + Cl^- + H_2O \quad (1.22)$$

In neutral solutions also chlorine and ClO_2 react to form $ClO_3^-$and Cl^-

$$2ClO_2 + HOCl + H_2O \rightarrow 2ClO_3- + Cl^- + 3H^+ \quad (1.23)$$

1.11 Chemical kinetics

The chemical kinetics is the study of rates of chemical processes as a function of time. Chemical kinetics includes investigations of how different experimental conditions can influence the speed of a chemical reaction and yield information about the reaction's mechanism and transition states, as well as the construction of mathematical models that can describe the characteristics of a chemical reaction.[149,150]

The reaction kinetics can be applied to the optimization of process conditions, as in organic synthesis, analytical reactions, and chemical manufacturing. The chemical kinetics is used for the determination and control of the stability of commercial products such as pharmaceutical dosage forms, foods, paints, and metals. Further uses of kinetics, less sweeping in their scope than the preceding application, are for the testing of rate theories; the measurement of

equilibrium constants; the analysis of solutions, including mixtures of solutes; and the measurement of solvent properties that depend upon rates.[151]

1.11.1 Classification of reaction rates

The rates of chemical reactions are found to be a function of the extent to which the reaction has proceeded.[152] Some reactions are roughly classified as fast reactions and the rest are slow reactions. But in general a 'fast' reaction is one which is over in one second or less.

A very rough general classification of rates can also be given in terms of the time taken for reaction to appear to be virtually complete, or in terms of half-lives. These will include very fast reaction, fast rate, moderate rate, slow rate and very slow rate reactions. Typically the reactions in the current study can be classified into moderate (1 to 10^3 s) and fast rate reactions (10^{-6} to 1 s). Hence to monitor the reaction rates for such reactions a Hi-Tech stopped flow instrument was used.

The study of the reaction rates can be explained in terms of the reaction mechanism involving elementary reactions.[153] A complete reaction mechanism would involve knowledge of all molecular details of the reaction, including the energetic and stereochemistry, e.g. interatomic distances and angles throughout the course of the reaction of individual molecular stems involved in a mechanism.[154]

1.11.2 Factors influencing reaction rates

A number of variables are recognized that influence the rate of a reaction. The major factors are concentrations of reactants, products, and possibly catalysts, physical conditions such as

temperature and pressure, the intensity of absorbed radiation, for reactions in solution, properties of the solvent such as viscosity, dielectric constant, and ionic strength.[155]

Each of the variables will be considered in turn, and emphasis will be placed particularly on the concentration variables. They are the variables which provide the most direct connection between chemical kinetics and reaction mechanism. The minimum goal of a kinetic study is to establish a possible mechanism for the reaction in the sense in which the term was used earlier to learn whether it proceeds by a single pathway, whether a sequence of reactions occurs, whether equilibria precede the rate-limiting step, and whether one or more reaction intermediates is involved.

Variation of temperature and pressure can provide additional information, particularly about the energetic and volume relations of reaction steps in the mechanism. The quantities deduced from the variations are collectively termed "activation parameters," and they include such values as entropy of activation $\Delta S^{\ddagger}$ and the volume of activation $\Delta V^{\ddagger}$.[156]

1.11.3 First-order reactions

Most reactions are either first-order or are carried out under conditions that approximate first-order. For a first-order reaction of the type,

$$A \overset{k_1}{\rightarrow} C \tag{1.24}$$

where k_1 is rate of the reaction

the rate of the reaction is as follows

$$Rate = k_1 [A] = \frac{-d[A]}{dt} \tag{1.25}$$

where $[A]$, $[A]_t$ are the concentrations of A initial and at time t = t respectively

It can be rearranged as,

$$\frac{-d[A]}{[A]} = k_1\, dt \tag{1.26}$$

Integrating from t = 0, $[A]_0$ to t = $[A]_t$ gives

$$\int_{[A]_0}^{[A]_t} \frac{d[A]}{[A]_t} = -\int_0^t k_1\, dt \tag{1.27}$$

here, $[A]_0, [A]_t$ rations of A at time t = 0 and t = t respectively which

$$\ln\frac{[A]}{[A]_0} = -k_1 t \tag{1.28}$$

Equivalent forms of the integrated first-order rate Equation (1.28) are shown below (Equation 1.29 to 1.30)

$$\ln[A]_t = -k_1 t + \ln[A]_0 \tag{1.29}$$

or

$$[A]_t = [A]_0\, e^{-k_1 t} \tag{1.30}$$

Thus for a first-order reaction, a plot of ln $[A]_t$ versus t should be linear, with the first-order rate constant being represented by the slope. The dimension of a first-order rate constant is time^{-1}, usually represented as s^{-1}.

1.11.4 Reversible first-order reactions

In principle, all reactions are reversible and although simple considerations suggest ways of driving many reactions in one direction only, there are systems where reversibility cannot be ignored. The simplest of these is the reversible, first-order reaction.

$$A \underset{k_b}{\overset{k_f}{\rightleftarrows}} B \tag{1.31}$$

Where k_f and k_b are that the rate constants for forward and back reactions.

Recognizing that the loss of a reagent corresponds to a negative rate and that the gain of a reagent corresponds to a positive rate the rate law applicable to this system is:

$$Rate = -\frac{d[A]}{dt} \tag{1.32}$$

$$= k_f[A]_t - k_b[B]_t \tag{1.33}$$

where [A] and [B] express the concentration of the species A and B, and

$[A]_0$, $[A]_t$ and $[B]_t$ are the concentrations of A and B at time t = 0 and t = t respectively

At time t = 0, $[B]_{t=0} = 0$, and $[A]_{t=0} = [A]_0$, consequently at any given time:

$$[B]_t = [A]_0 - [A]_t \tag{1.34}$$

Substitution of (1.34) into (1.33) gives:

$$-\frac{d[A]}{dt} = k_f[A]_t - k_b([A]_0 - [A]_t) \tag{1.35}$$

No net reaction occurs at equilibrium, and hence:

$$-\frac{d[A]}{dt} = 0 \tag{1.36}$$

Applying equation (1.36) to (1.35) and (1.33) affords the following equilibrium expression:

$$k_f[A]_{eq} = k_b[B]_{eq} = k_b([A]_0 - [A]_{eq}) \tag{1.37}$$

where $[A]_{eq}$ and $[B]_{eq}$ are equilibrium concentrations of A and B

which implies that:

$$[A]_0 = \frac{k_f + k_b}{k_b}[A]_{eq} \tag{1.38}$$

Substitution of (1.38) into (1.34) affords the following term:

$$-\frac{d[A]}{dt} = (k_f + k_b)[A]_t - (k_f + k_b)[A]_{eq} \quad (1.39)$$

Subsequent separation of variables:

$$\frac{d[A]}{([A]_t - [A]_{eq})} = -(k_f + k_b)\, dt \quad (1.40)$$

Integration of (1.40) gives:

$$\int_{[A]_0}^{[A]_t} \frac{d[A]}{([A]_t - [A]_{eq})} = -(k_f + k_b) \int_0^t dt \quad (1.41)$$

which affords:

$$ln\left[\frac{[A]_t - [A]_{eq}}{[A]_o - [A]_{eq}}\right] = -(k_f + k_b)\, t \quad (1.42)$$

An equivalent form of equation (1.41) is shown in equation (1.42):

$$\ln([A]_t - [A]_{eq}) = -(k_f + k_b)\, t + \ln([A]_0 - [A]_{eq}) \quad (1.43)$$

A plot of ln ($[A]_t - [A]_{eq}$) *versus* time should give a straight slope that corresponds to $-(k_f + k_b)$.

Evaluation of the equilibrium constants allows one to determine the individual rate constants k_f and k_b respectively.

$$K_{eq} = \frac{[B]_{eq}}{[A]_{eq}} = \frac{k_f}{k_b} \quad (1.44)$$

With the observed rate constant, k_{obs},

$$K_{obs} = (k_f + k_b) \quad (1.45)$$

The most difficult problem encountered in treating reversible first-order reactions is in accurately measuring $[A]_{eq}$.[157]

1.11.5 Second-order reactions

Second-order reactions can be divided into two types. The first type is when the rate is second-order with respect to one of the reactants and zero-order with respect to the second reactant. The second type that will be analyzed in further detail is when the second-order reaction is first-order with respect to each reagent.

For the reaction:

$$A + B \xrightarrow{k_2} X \tag{1.46}$$

where k_2 is rate constant upon the rate equation can be written as:

$$\frac{d[X]}{dt} = -\frac{d[A]}{dt} = -\frac{d[B]}{dt} = k_2[A]_t[B]_t \tag{1.47}$$

Upon separation of the variables, equation (1.47) can be written as (where [A] and [B], and $[A]_t$ and $[B]_t$ express the concentrations of A and B at time t = 0 and t = t respectively)

Separation of the two leads to:

$$\frac{d[X]}{[A]_t\,[B]_t} = -k_2 dt \tag{1.48}$$

In order to integrate Equation 1.48, one must first relate the concentration of B to that of A. If then, the initial concentrations of A and B are $[A]_0$ and $[B]_0$ respectively, it follows from the reaction Stoichiometry that when the concentrations of A have fallen to $[A]_0$–x, the concentration of B has fallen into $[B]_0$– x.

Equation 1.48 can be written as

$$-\frac{d[x]}{dt} = k_2\,\{[A]_0 - \mathrm{x}\}\,\{[B]_0 - \mathrm{x}\} \tag{1.49}$$

Since $[A]_t = [A]_0 - \mathrm{x}$, it follows that $-\frac{d[A]}{dt} = \frac{dx}{dt}$ and thus Equation 1.49 can be written as

$$\frac{d\mathrm{x}}{dt} = k_2\,\{[A]_0 - \mathrm{x}\}\,\{[B]_0 - \mathrm{x}\} \tag{1.50}$$

Separation of the variables results in an alternate version of Equation 1.48

$$\frac{dx}{\{[A]_0 - x\}\{[B]_0 - x\}} = k_2 dt \tag{1.51}$$

Integrating Equation 1.51 under the condition that x=0 when t=0 gives

$$\int_0^x \frac{dx}{\{[A]_0 - x\}\{[B]_0 - x\}} = k_2 \int_0^t dt \tag{1.52}$$

Which affords Equation 1.52 in the form of y=mx

$$\frac{1}{[A]_0 - [B]_0} \ln \frac{[B]_0\{[A]_0 - x\}}{[A]_0\{[B]_0 - x\}} = k_2 t \tag{1.53}$$

$$\frac{1}{[A]_0 - [B]_0} \ln \frac{[B]_0[A]_t}{[A]_0[B]_t} = k_2 t \tag{1.54}$$

In order to evaluate the second-order rate constant k_2 (M^{-1} s^{-1}) for the reaction, one needs to know the concentrations of both *A* and *B*, both initially and at any time *t*, i.e. $[A]_0$, $[B]_0$, $[A]_t$ and $[B]_t$. However, this represents a complicated and time-consuming process for most kinetic experiments. As a result of this, these experiments are often conducted with either reactant A or B in large excess, i.e. $[B]_0 >> [A]_0$ (at least 10-fold excess). Under these conditions the concentration of B remains constant throughout the course of the reaction, and the reaction may be treated as a first-order reaction. These conditions whereby one reactant is present in a large excess over the other are commonly referred to as *pseudo* first-order conditions.

Therefore Equation 1.47 may be written as:

$$-\frac{d[x]}{dt} = k_2[A]_t[B]_t = \{k_2[B]_0\}[A]_t$$

$$= k_{obs}[A]_t \tag{1.55}$$

where k_{obs} is the observed rate constant with units s^{-1}.

A plot of ln [A] *versus* time will result in a straight line with a slope equal to $k_{obs.}$ Monitoring the reactions for several concentrations of B, whilst simultaneously ensuring that B is in a large excess over A, generates a series of k_{obs} for different [B]. With reference to Equation (1.55), a plot of k_{obs} *vs* $[B]_0$ will be linear with a slope of k_2 having units of $M^{-1} s^{-1}$.

1.11.6 Reversible second-order reactions

Reactions may not go to completion at times. Instead equilibrium between the reactants may be reached. These types of reactions may be represented as follows:

$$A + B \underset{k_b}{\overset{k_f}{\rightleftarrows}} C \tag{1.56}$$

This assumes that the reverse reaction is first-order, whilst the forward reaction is second-order. Due to this the reaction in general exhibits a mixed-order behavior. To eliminate the complexity of the problem, *pseudo* first-order conditions are often selected for the forward reaction, i.e. $[B]_0 >> [A]_0$,. This result is in the equation now being treated as if it were a reversible first-order reaction.

The rate of formation of C can be written as:

$$-\frac{d[A]}{dt} = -\frac{d[B]}{dt} = \frac{d[C]}{dt} = k_f\,[A]_t[B]_t = k_b[C]_t \tag{1.57}$$

(where [A] and [B] and $[A]_t$and $[B]_t$ express the concentration of the species A and B at time t = 0 and t = t respectively)

for the given stoichiometry of 1:1:1, applying t mass balance at any time *t* gives:

$$[A]_t = [A]_0 - [C]_t \tag{1.58}$$

and

$$[B]_t = [B]_0 - [C]_t \tag{1.59}$$

At equilibrium:

$$[A]_{eq} = [A]_0 - [C]_{eq} \; and \; [B]_{eq} = [B]_0 - [C]_{eq} \tag{1.60}$$

The rates of the two opposing reactions at equilibrium are equal, i.e.

$$-\frac{d[A]}{dt} = k_f [A]_{eq}[B]_{eq} - k_b[C]_{eq} = 0 \tag{1.61}$$

This implies that:

$$k_f [A]_{eq}[B]_{eq} = k_b[C]_{eq} \tag{1.62}$$

However, $[C]_t = [A]_0 - [A]_t$ and $[C]_{eq} = [A]_0 - [A]_{eq}$ and equation (1.57) may now be written as:

$$k_f [A]_{eq}[B]_{eq} = k_b([A]_0 - [A]_{eq}) \tag{1.63}$$

Resulting in:

$$k_b [A]_0 = k_f [A]_{eq}[B]_{eq} + k_b[A]_{eq} \tag{1.64}$$

Substituting $[C]_t = [A]_0 - [A]_t$ and Equation (1.64) into (1.57) results in:

$$-\frac{d[A]}{dt} = k_f [A]_t[B]_t - k_b [A]_{eq}[B]_{eq} - k_b [A]_{eq} + k_b [A]_t \tag{1.65}$$

Since $[B]_0 >> [A]_0$, Equation (1.65) can be expressed as:

$$\begin{aligned} -\frac{d[A]}{dt} &= k_f [A]_t[B]_0 - k_f [A]_{eq}[B]_0 - k_b [A]_{eq} + k_b [A]_t \\ &= (k_f [B]_0 + k_b)([A]_t - [A]_{eq}) \end{aligned} \tag{1.66}$$

Separation of variables and integration gives:

$$\int_{[A]_0}^{[A]_t} \frac{d[A]}{([A]_t - [A]_{eq})} = -(k_f [B]_0 + k_b) \int_0^t dt \tag{1.67}$$

Which results in:

$$\ln\left(\frac{[A]_t - [A]_{eq}}{[A]_0 - [A]_{eq}}\right) = -(k_f [B]_0 + k_b)\, t$$

$$with \quad k_{obs} = k_f[B]_0 + k_b \tag{1.68}$$

For a second-order reversible reaction a plot of k_{obs} *versus* $[B]_0$ will be linear with a slope equal to k_f and an intercept equal to k_b. The equilibrium constant K can be obtained from the ratio of k_f/k_b and may also be determined thermodynamically.

1.11.7 Consecutive first-order reactions

Frequently a product of one reaction becomes a reactant in a subsequent reaction. This is true in multi-step reaction mechanisms. A simple case involving two consecutive irreversible first-order reactions is represented by equation (1.69)

$$A \xrightarrow{k_1} B \xrightarrow{k_2} C \tag{1.69}$$

The rates of change of at time t; [A], [B] and [C] are as follows:

$$\frac{d[A]}{dt} = -k_1[A]_t \tag{1.70}$$

$$\frac{d[B]}{dt} = k_1[A]_t - k_2[B]_t \tag{1.71}$$

$$\frac{d[C]}{dt} = -k_2[B]_t \tag{1.72}$$

Since B is formed by the first reaction and is destroyed by the second reaction, the expression for $\frac{d[B]}{dt}$ has two terms.

Let only A be present in the system at t = 0:

$$[A] \neq [A]_0,\ [B]_0 = 0,\ [C]_0 = 0 \tag{1.73}$$

and at any time t

$$[A]_0 = [A]_t + [B]_t + [C]_t \tag{1.74}$$

subsequent integration of Equation (1.70) yields:

$$[A]_t = [A]_0 e^{-k_1 t} \tag{1.75}$$

Equation 1.75 is substituted into Equation (1.71) thus

$$\frac{d[B]}{dt} = k_1[A]_0 e^{-k_1 t} - k_2[B]_t \tag{1.76}$$

Equation 1.76 can be integrated using the integrating factor method

Noting that at time t = 0, $[B]_0 = 0$, application of product rule and subsequent integration of (1.76) yields:

$$[B]_t = \frac{k_1[A]_0}{k_2 - k_1}\left(e^{-k_1 t} - e^{-k_2 t}\right) \tag{1.77}$$

Using conservation of matter enables one to determine [C]. The total number of moles present is constant with time, so $[A] + [B] + [C] = [A]_0$. Substituting Equations (1.75) and (1.77) into Equation (1.74) yields:

$$[C]_t = [A]_0\left(1 - \frac{k_2}{k_2 - k_1}\ e^{-k_1 t} + \frac{k_1}{k_2 - k_1}\ e^{-k_2 t}\right) \tag{1.78}$$

1.12 Kinetic salt effect

In aqueous solutions, ionic strength plays an important role in the rates of the reaction. The effect of primary salt can be studied by varying the ionic strength of the reaction by employing an inert electrolyte solution. The kinetic salt effect gives an insight into the charges and nature of the reacting species involved in the rate-limiting step.

The Bronsted equation predicts the influence of the concentration of ions and their charges on the rate constant k when the reaction occurs between two charged species A and B. The rate constant *k* of a bimolecular reaction is defined by the following equation:

$$k = k_o \gamma_A \gamma_B / \gamma^{\ddagger} \tag{1.79}$$

where k_o is the limiting value of the rate constant for zero value of all ion concentrations in the mixture. γ_A, γ_B and $\gamma^{\ddagger}$ the activity coefficients of A, B and the activated complex respectively.[7] The Debye-Huckel theory states that "electrolytes in solution as fully dissociated, assuming that each ion is surrounded by an ionic atmosphere of opposite charges. The behavior of this atmosphere is assumed to retard the motion of ions moving through it". Combining the Bronsted equation and Debye-Huckel limiting law, a relationship between the rate constant and ionic strength can be established.[158]

$$\log k = \log k_o - A\{Z_A^2 Z_B^2 - (Z_A+Z_B)^2\} I^{1/2} \tag{1.80}$$

$$\log k = \log k_o + 2AZ_A Z_B I^{1/2} \tag{1.81}$$

where Z_A and Z_B are the valences and I is the ionic strength

If the Bronsted equation holds good, in dilute solutions a plot of log k versus $I^{1/2}$ should be linear, with slope equal to 1.02 $Z_A Z_B$ and intercept equal to log k_o.[8] In aqueous solutions the gradient indicates the product of charges on the species involved in rate-limiting step. If both the reactive species are like charges, a positive slope is expected and a negative slope is expected, if they are oppositely charged.

1.13 Kinetic simulations

Kinetic simulations are a good tool to provide insight into complex chemical reactions. They give information, which is often inaccessible experimentally, such as details of unstable species (transition rates and reaction intermediates).[159] Kinetic simulations are the initiation of experimental behavior with respect to time, and they also involve determination and investigation of various species with respect to time.

1.13.1 Simulations

Simulation is the imitation of real world processes over time. Simulation involves the generation of a system with the properties that draw inferences concerning the operation characteristics of the real system. The simulation model is developed to study the behavior of the system over time based on a set of assumptions that are expressed mathematically, logically and symbolically.[160] The simulation model can be used to investigate the performance of a system by simulating the potential changes to it. It can be used as an analytic tool for predicting the effect of changes to the existing system. It can also be used to as a design tool to predict the performance of new systems under varying sets of circumstances.[161]

In some instances a model can be developed which is simple enough to be solved by mathematical methods. Such a solution may be reached by the use of differential calculus, probability theory, algebraic methods or other mathematical techniques. The solution usually consists of one or more numerical measures of performance of the system. Many real world systems are so complex that their models are virtually impossible to solve mathematically.[162] In these instances numerical computer-based simulation can be used to imitate the behavior

of the system over time. Simulation data is collected as if a real system is observed. The simulated data is used to estimate the measures of performance of the system.

1.13.2 Importance of simulation as a tool

Simulation enables the study of complex reaction mechanisms, and experimentation with the internal action of a complex system or of a subsystem within a complex one. Informational, organizational and environmental changes can be simulated and the effect of these alterations on the behavior of the model can be observed. The knowledge gained in designing a simulation model may be of great value towards suggesting improvement in the system under investigation. By changing simulation inputs and observing the resulting outputs valuable insight may be obtained into which variables are most important and how they interact. Simulation can be used to experiment with new designs or policies prior to implementation so as to prepare for what may happen. Simulation can be used to verify analytic solutions. It can help in understanding how the system operates rather than how individuals think the system operates. Time can be compressed or expanded to allow for a speeded-up or slow-down of the phenomena under investigation.[163,164] Simulation can provide hypothesis about how or why certain phenomena occur and these can be tested for feasibility. Simulation and modeling have been used in the motor industry, controlling of traffic during peak hours, in the army, in the designing and testing of new weapons and biological processes, and in the building industry to mention a few.

1.13.3 Requirements for kinetics simulation

The requirements for kinetic simulation are: proposed mechanisms for a reaction, rate constants for each reaction step involved in a proposed mechanism and initial concentrations of the starting species. There are different kinds of software available for kinetics simulation.

The most frequently used is the FitAll software developed by MTR Software,[165] Easy-Fit developed by Schittkowski,[166] the Kaps and Rentrop program,[167] and Simkine 2 software.[168]

To simulate the kinetic profile of reactants, a proposed mechanism is essential. To propose the mechanism, the reaction kinetics and other aspects needs to be studied experimentally. In any mechanism there is a slowest step and a reaction cannot progress slower than its slowest reaction step. The slowest reaction step is thus the rate-determining step. Practical experiments involve determination of an average rate of reaction of a large number of molecules for the rate-determining step.[169]

1.14 Kinetic measurements-fast reactions

Kinetic studies are accomplished by studying the time dependence of some variable that is proportional to the concentration of reactant or product. Subsequent fitting of the concentration-time data to an appropriate model allows for the determination of the rate constant.

Flow methods are the best way of following fast reactions in which the reagents cannot be prematurely mixed. All fast flow methods are based on the pioneering work of Hartridge and Roughton.[170,171] Flow methods involve the fast together of separate solutions of the reactants. The rapid mixing of reactants is usually coupled to a rapid-response method for monitoring the progress of the reaction flowing. With such methods one can determine the rate constants in the order of 5×10^2 s^{-1} (i.e. $t_{1/2} > 1$ ms). The advantage of these methods over conventional techniques is the ability of mixing the reactants rapidly.

The continuous flow method operates on the principle whereby solutions of two reactants are forced by pistons into a mixing chamber, whose design contributes to rapid mixing. The mixed solutions then flows into an observation tube, where detection by spectroscopy takes place at a specific distance downstream from the mixer. A schematic representation of the continuous flow method is given in Figure 1.1.8.

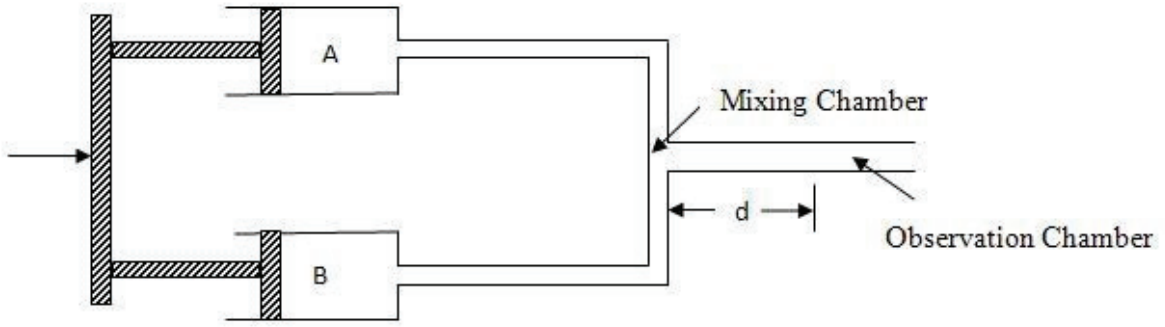

Figure 1.1.8 Schematic diagram of a continuous flow kinetic system. (where d is the distance from the mixer to the point of observation.)

The stopped flow technique operates on the same principles as the continuous flow method and is very popular in studying reactions having a half-life range of 10^0-10^3 s. The apparatus, whose schematic diagram is illustrated in Figure 2.1.11, consists of the four drive syringes, which are reagent filled through separate valves from the reagent reservoir syringes, containing the individual reactants. The drive syringes are usually maintained at a specific temperature by immersion in a water bath with a thermostated jacket. Once filled, the solutions are allowed to equilibrate at the specified temperature. The drive mechanism, which is usually piston driven, either mechanically or by a compressed gas, drives the reactant solutions into a mixing chamber in such a manner that the solutions impinge on one another and give very rapid mixing within 0.001 s. The mixed solution then flows into a reaction cuvette or, alternately, the two solutions may be combined in the reaction chamber, which in

turn triggers the recording device, which might be an oscilloscope, a transient scope, or a digital sensitizer. The solution is now stationary, and this marks the beginning of the collection of kinetic data.[163]

The usual method of detection is UV-Visible spectrophotometry and once the recording device is triggered, the amount of light at a predetermined wavelength setting of the monochromator is transmitted through the mixed solution in the cuvette, will change as the reaction proceeds in the static mixed solution. A photomultiplier then converts this transmitted light into the electric current and a signal is fed through to a computer acquisition system over an appropriate time interval. The kinetic data is then processed and the rate constant evaluated.[172,173,174]

1.14.1 Analysis of kinetic data

KinetAsyst^{TM} software package (Hi-Tech Ltd.) was used for data collection. Figure 1.1.9 represents the analysis of the data accomplished using the KinetAsyst^{TM} Fit Asystant software for a typical kinetic curve obtained from the stopped-flow instrument. Data were fit with models including a single or sum of exponential phases, as appropriate. In each case, the residuals indicate the best fit assigned as the simplest one giving the smallest deviation in a least-squares fit analysis and random residuals over the whole time course.[175] The upper region indicates the fit between the fitted and experimental curves obtained whilst the lower portion indicates the residuals (deviation between the two curves)

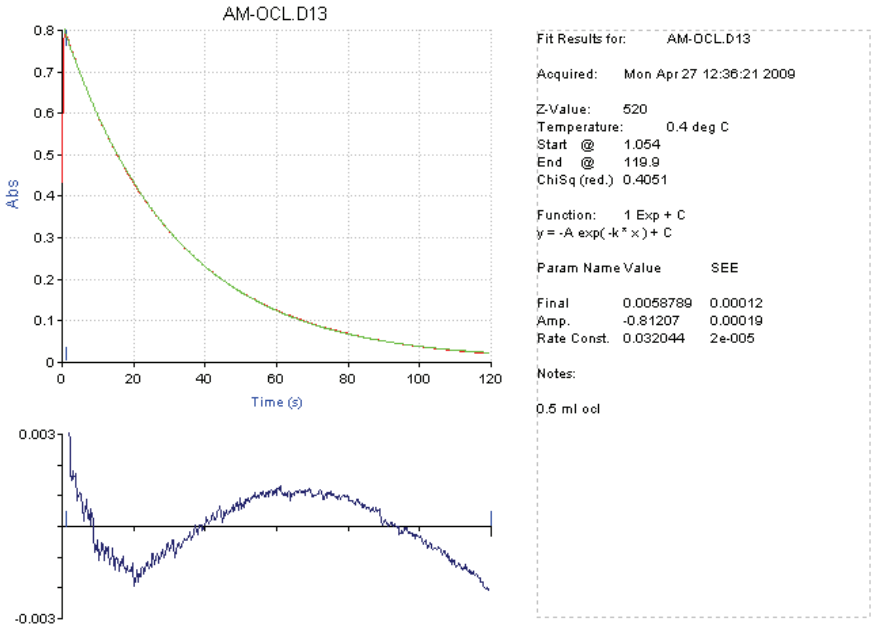

Figure 1.1.9 KinetAsyst™ single-exponential equation fit (green) and the experimental curve (red) with residuals (lower curve) and the rate parameters for the reaction of $[AM^-]_0$ (7.0×10^{-5} M) with $[OCl^-]_t$ (1.5×10^{-3} M).

1.15 Scope and objectives of the study

Although the literature survey shows that considerable attention has been paid to understand the chemistry of dyes; not much is known about their reactions with various materials and chemical reagents, and their reaction mechanisms with bleaching agents, which are commonly used in industry and in water treatment processes. The literature review indicates that little information is available about the kinetics of degradation of the dyes and the mechanisms of their oxidation by hypochlorite and chlorine dioxide. The role of acid in such reactions and possible intermediates are still not completely understood.

The objective of the current study is to investigate the oxidation reaction mechanisms of selected three water soluble dyes from three different classes amaranth (Azo dye), brilliant blue-R (Triarylmethane dye), safranine-O (Azine dye) by hypochlorite and chlorine dioxide

which are the most widely used oxidants in the water treatment under varied reaction conditions. The study focuses on the reaction rates with emphasis on their decolorisation kinetics. Different factors influencing the reactive rates will be examined and the elucidated mechanisms and proposed rate laws for the chosen dyes will be described.

CHAPTER 2

2.1 Experimental

All the solutions were prepared with double distilled water using 'A' grade glassware. All the reagents were of analytical grade or of high purity. All acid and base stock solutions were standardized by the prescribed methods.

Absorbance measurements:

Absorbance readings were recorded using a Cary II-Varian double beam spectrophotometer. The instrument is equipped with a thermostated cuvette holder and data capturing facilities interfaced with a computer. Quartz cuvettes were used for absorbance measurements so as to extend measurements into the ultraviolet region of the electromagnetic spectrum.

2.1.1 Three dyes-amaranth, brilliant blue-R, safranine-O

Amaranth (Sigma-Aldrich, USA 95% purity) was used with no further purification. Since the dye was sparingly soluble in water, a stock solution of 1 x 10^{-2} M was prepared by dissolving 0.604 g of amaranth dye in distilled water and making up to the mark in a 1 L standard volumetric flask. The stock solution was further diluted requisite to the need of experiments. The structure of azo dye amaranth is presented in Figure 2.1.1.

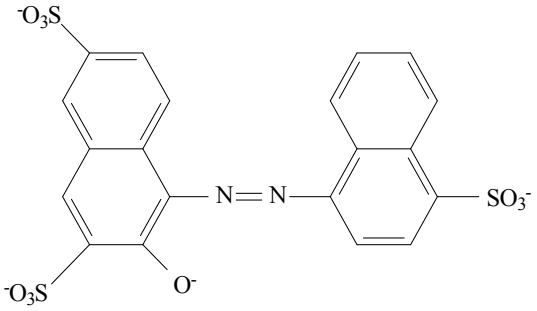

Figure 2.1.1 Structure of amaranth

A typical spectrum obtained in the visible range and using UV-Visible Cary 100 double beam spectrophotometer with data interval of 1 nm and average time interval of 0.1 s showed maxima absorbance at 520 nm (Figure 2.1.2).

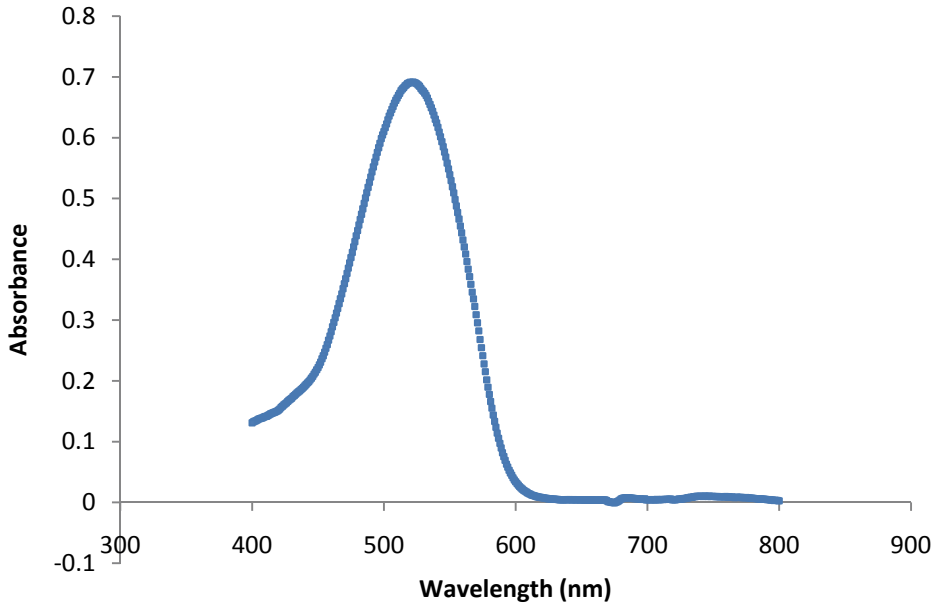

Figure 2.1.2 UV-Visible spectrum of amaranth, $[AM^-]_0$ (1 x 10^{-6} M).

From five replicate measurements the absorption coefficient at the absorption maxima for this dye was estimated to be (1.98 ± 0.02) x 10^4 dm^3 mol^{-1} cm^{-1} (Figure 2.1.2). No peak shift was registered due to changes in pH.

Brilliant blue-R (Aldrich, USA 95% purity) was used with no further purification. Since the dye was sparingly soluble in water, a stock solution of 1 x 10^{-2} M was prepared by dissolving 0.802 g of brilliant blue - R in water and making up to the mark in a 1 L standard volumetric flask. The stock solution was further diluted requisite to the need of experiments. The structure of the dye is shown in Figure 2.1.3.

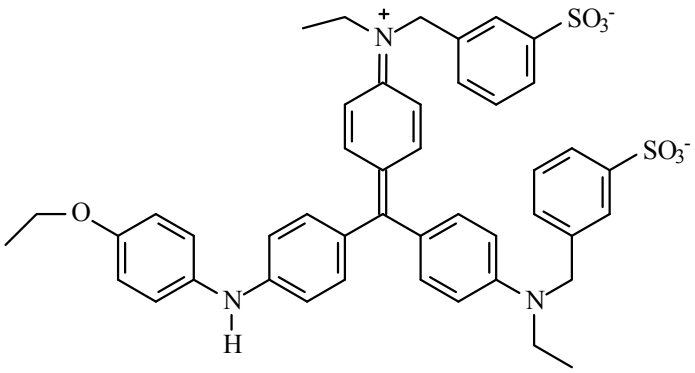

Figure 2.1.3 Structure of brilliant blue-R.

A typical spectrum obtained in the visible range obtained using UV-Visible Cary 100 Double beam Spectrophotometer with data interval of 1 nm average time interval 0.1 s showed maxima absorbance at 555 nm.

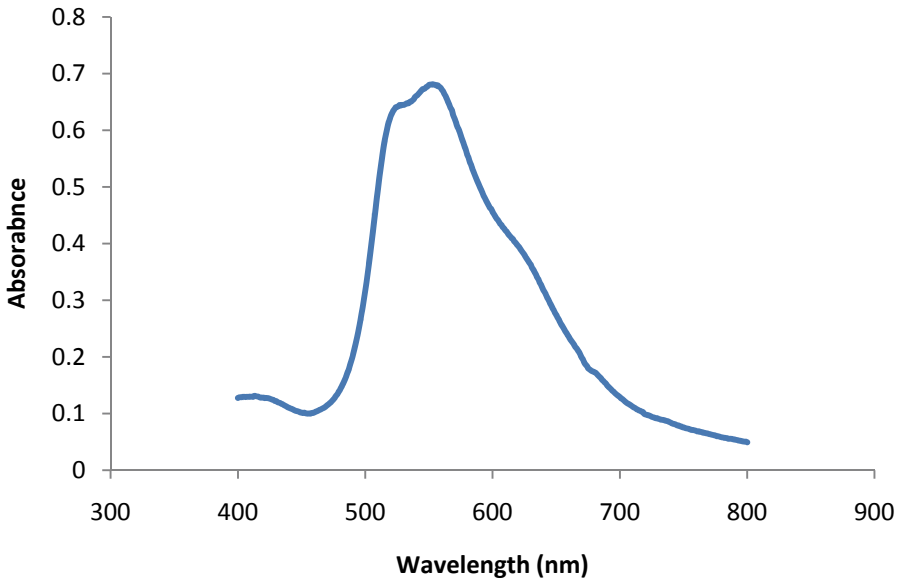

Figure 2.1.4 UV- Visible spectrum of brilliant blue-R, $[BB^+]_0$ (1 x 10^{-6} M).

From five replicate measurements the absorption coefficient at the absorption maxima for this dye was estimated to be (1.78 ± 0.02) x 10^4 dm^3 mol^{-1} cm^{-1} (Figure 2.1.4). No peak shift was registered due to changes in pH.

Safranine-O (Aldrich, USA 95% purity) was used with no further purification since the dye was sparingly soluble in water, a stock solution of 1 x 10^{-2} M was prepared by weighing out 0.315 g/L of the dye in distilled water into a standard volumetric flask. The stock solution was further diluted requisite to the need of experiments.[176] Figure 2.1.5 represents the structure of the dye.

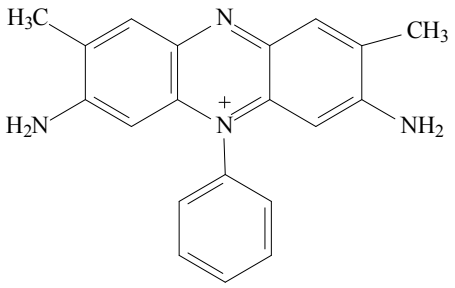

Figure 2.1.5 Structure of safranine-O

A typical spectrum obtained in the visible range obtained using UV-Visible Cary 100 Double beam Spectrophotometer with data interval of 1 nm average time interval 0.1 s showed maxima absorbance at 519 nm.

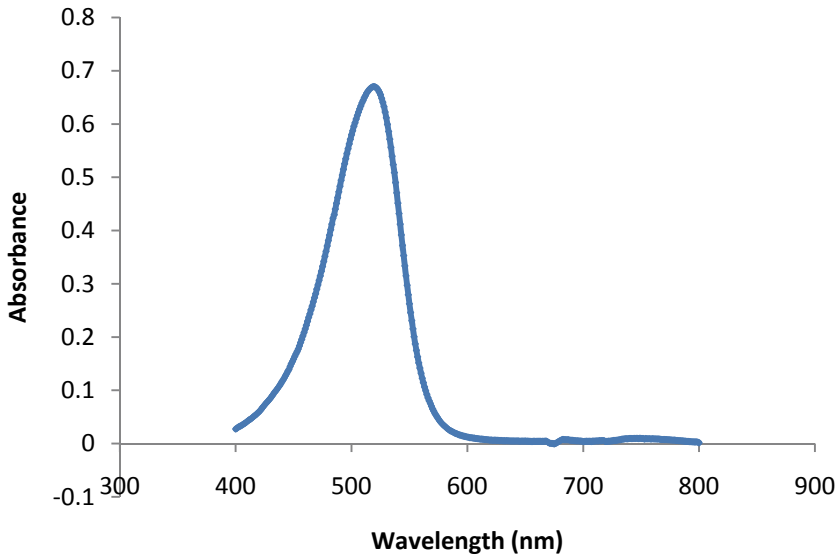

Figure 2.1.6 UV- Visible spectrum of safranine-O, $[SO]_0$ (1 x 10^{-6} M)

From five replicate measurements the absorption coefficient at the absorption maxima for this dye was estimated to be (2.98 ± 0.02) x 10^4 dm^3 mol^{-1} cm^{-1} (Figure 2.1.6). No peak shift was registered due to changes in pH.

2.1.2 Hypochlorite solution

Sodium hypochlorite solutions were prepared by electrolysis of sodium chloride solutions. The instrument used to generate these solutions was the Baird & Tatlock electrolytic analysis apparatus. (Figure 2.1.7)

2.1.4.1 Preparation method

The instrument comprises a single compact unit containing its own low voltage D.C. (direct current) supply unit capable of giving an output of 0 to 10 amperes (A) at up to 12 V. The electrodes consists of "unimesh" inner and outer platinum electrodes. The inner platinum electrode has a cylinder height and diameter of 32 mm with its overall height measuring 145 mm. The outer platinum electrode has a cylinder height and diameter of 45 mm with an overall height of 130 mm. The polarity of the central electrode can be changed to positive or negative by means of a "polarity change" switch. (Figure 2.1.7).

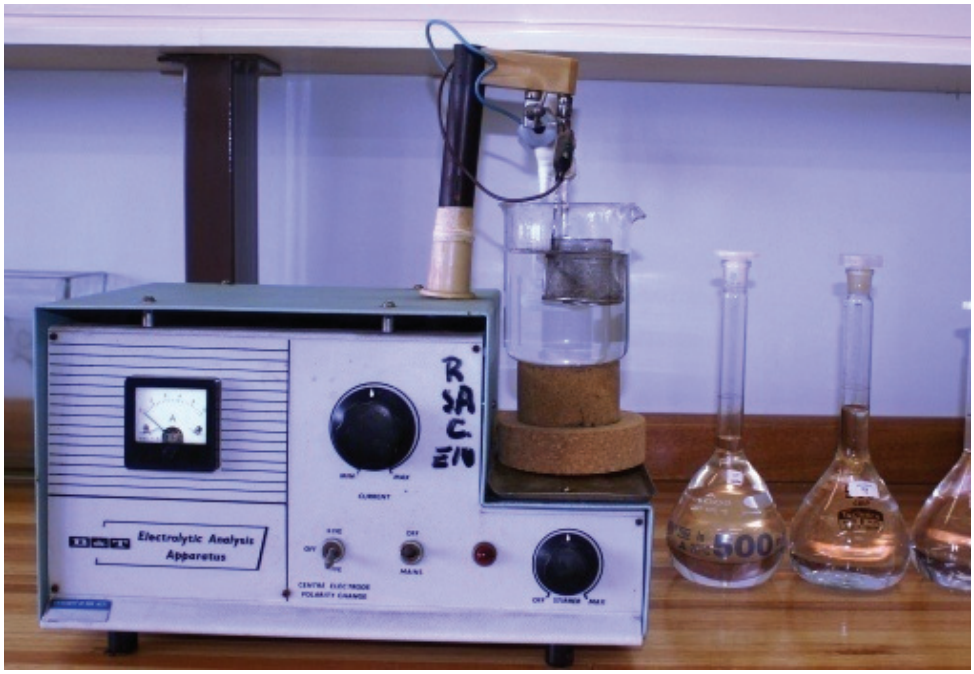

Figure 2.1.7 Baird & Tatlock hypochlorite generator.

100 mL of a 5% (w/v) NaCl solution was refrigerated for an hour prior to electrolysis to avoid sodium hypochlorite decomposition caused by a temperature increase during the electrolytic process. The chilled NaCl solution was then electrolyzed at 2 amperes (A) for a period of 45 minutes. The operating conditions for the generation of OCl^- are discussed at the end of this chapter. A number of researchers have used the Baird & Tatlock apparatus for the generation of sodium hypochlorite solutions. The generated hypochlorite solutions were stored in brown bottles left away from light to minimize decomposition caused by light and air.

The reactions involved in the electrolysis of NaCl are:

$$\text{Anode:} \quad 2Cl^-(aq) \rightarrow Cl_2(g) + 2e^- \qquad (2.1)$$

$$\text{Cathode:} \quad 2H_2O(l) + 2e^- \rightarrow H_2(g) + 2OH^-(aq) \qquad (2.2)$$

$$\text{Overall:} \quad 2H_2O(l) + 2Cl^-(aq) \rightarrow H_2(g) + Cl_2(g) + 2OH^-(aq) \qquad (2.3)$$

The Cl_2 (g) thereafter reacts with the H_2O (l) to form hypochlorite.

$$Cl_2(g) + H_2O(l) \rightarrow 2\ H^+(aq) + OCl^-(aq) + Cl^-(aq) \qquad (2.4)$$

In order to minimize Cl_2 (g) escaping into the atmosphere, the vessel containing the sodium chloride solution is sealed with parafilm during the electrolytic procedure. The hypochlorite ion generation conditions were optimized by establishing suitable reaction conditions such as % (w/v) of NaCl, duration of electrolysis and temperature.

After electrolysis, the solution was neutralized with 1.0 M sulfuric acid to prevent the further disproportionation of hypochlorite to the corresponding chlorate ions. The solution was then standardized by the arsenite method. In the arsenite method, the sample is titrated against standard sodium arsenite solution. An external indicator, potassium iodide-starch paper, is employed. The neutralization with acid also facilitates the effective oxidation of arsenite, since optimum conditions for its oxidation lie between pH 4.0 and 9.0, the best value being 6.5.[177] Since NaOCl is degraded by light and air, normally solutions were kept in diffused light in air tight flasks and fresh stock solutions were prepared, whenever required.

2.1.4.2 Calculation of molarity of the hypochlorite-arsenite method

Two methods for OCl^- ion determination, commonly employed in the laboratories are the arsenite and iodometric methods. Of the two methods, the arsenite method is preferred because it is more accurate. The reagents involved in the iodometric method include KIO_3, KI and starch, which have to be freshly prepared and standardized. Solid As_2O_3 on the other hand, is stable and readily available in a high degree of purity.

Preparation of As_2O_3 solution

Arsenic trioxide (As_2O_3) is a colorless crystalline solid, formed when arsenic or a sulfide of arsenic burns in air. Arsenic trioxide sublimes on heating. Up to 800 °C, the molecules are As_4O_6 but by 1800 °C, dissociation to As_2O_3 is complete. Sublimation gives a very pure product, which is used as a primary standard in volumetric analysis 0.025 M As_2O_3 solution was prepared by dissolving 2.473 g finely powdered arsenious oxide in a 10% (w/v) sodium hydroxide (NaOH) solution.[178] The solution was then diluted to 200 mL and neutralized with 1 M HCl using litmus paper as indicator. The neutralized solution was then quantitatively transferred to a 500 mL volumetric flask. 2.0 g of pure $NaHCO_3$ was added, and when all the salt was dissolved, the solution as made up to the mark.

A volume of the generated OCl^- solution was titrated with 0.025 M As_2O_3 solution and the end point was determined using KI-starch paper which serves as an external indicator. As long as OCl^- is present, the sample solution turns the KI-starch paper blue. At the end point, the sample solution no longer produces a blue stain on the starch paper.

$$2\ OCl^- + As_2O_3 \rightarrow As_2O_5 + 2\ Cl^- \qquad (2.5)$$

Thus $2 \times (\text{Volume of } As_2O_3) \times (0.025\ M) = (\text{Molarity } OCl^-) \times (\text{Volume of } OCl^-)$

$(\text{Molarity of } OCl^-) = 2 \times (0.025) \times (\text{Volume of } As_2O_3) / (\text{Volume of } OCl^-)$

2.1.3 Chlorine dioxide

2.1.5.1 Chlorine dioxide preparation

A pure solution of chlorine dioxide is prepared by slowly adding dilute sulfuric acid to a sodium chlorite solution, removing any contaminants such as chlorine by means of a sodium chlorite scrubber, and passing the gas into distilled water by means of a steady stream of air.

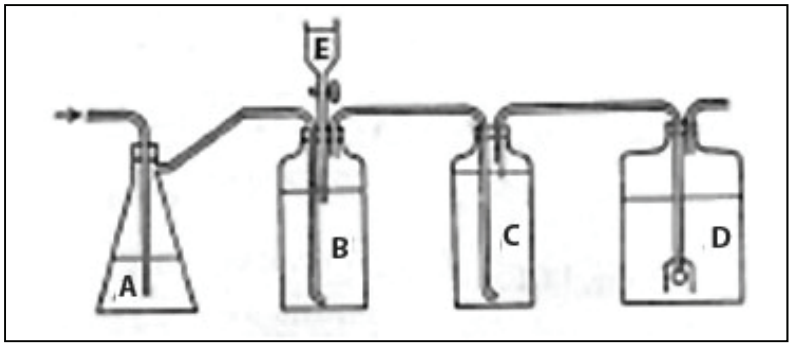

Figure 2.1.8 Chlorine dioxide generation and absorption system.[179]

The experimental setup to generate the chlorine dioxide is described below. An aspirator flask A of 500 mL capacity as illustrated in Figure 2.1.8 was attached by means of rubber tubing to a source of compressed air. The air was bubbled through a layer of 300 mL of distilled water and then passed over and down through a glass tube to within 5 mm of the bottom of the 1-1 gas-generating bottle B. The evolved gas passed *via* glass tubing through a scrubber into bottle C containing saturated sodium chlorite solution or a tower packed with flaked sodium chlorite, and finally, *via* glass tubing, into a 2-1 Pyrex collecting bottle D, where the gas is absorbed in 1500 mL distilled water. An air outlet tube on bottle D provided for escape of the moving air. A bottle was selected for gas generation which was constructed of strong Pyrex glass and having a mouth wide enough to permit the insertion of three separate glass tubes: the first leading almost to the bottom for admitting air, the second reaching below the liquid surface for the gradual introduction of the H_2SO_4, and the third near the top for exit of the evolved gas and air. A graduated cylinder, E, containing H_2SO_4 was fitted to the second tube.

10.0 g sodium chlorite, $NaClO_2$ was dissolved in 740 mL distilled water and a smooth current of air through the system, as evidenced by the bubbling rate in all bottles. A 5 mL increments

of sulfuric acid from cylinder E into bottle B at 5 min interval was introduced. The generated chlorine dioxide which was absorbed was kept in a refrigerator.

2.1.5.2 Calculation of molarity of the chlorine dioxide - iodometric method

Chlorine dioxide releases free iodine from a potassium iodide solution acidified with acetic or sulfuric acid. Chlorine dioxide solution was allowed prior to the titration to react in the dark with the acid and the potassium iodide for 5 minutes. The liberated iodine is titrated with a standard solution of sodium thiosulfate, with starch as the indicator. The required volume of stock chlorine dioxide solution was diluted to the desired strength with chlorine-demand-free water prepared. The stock solution is standardized by titrating with standard 0.010 M or 0.025 M sodium thiosulfate solution in the presence of KI, acid and starch indicator.

Chlorine dioxide concentrations were expressed in terms of chlorine dioxide alone or available chlorine content. The available chlorine is defined as the total oxidising power of the chlorine dioxide measured by titrating the iodine released by the chlorine dioxide from an acidic solution of KI. The following expressions were used for standardizing chlorine dioxide stock solution:

$$\text{mg/mL } ClO_2 = \frac{(A \pm B) \times N \times 13.49}{\text{mL sample titrated}} \quad (2.6)$$

$$\text{mg/mL Cl} = \frac{(A \pm B) \times N \times 35.45}{\text{mL sample titrated}} \quad (2.7)$$

For determining chlorine dioxide in temporary standards:

$$\text{mg/L } ClO_2 = \frac{(A \pm B) \times N \times 13{,}490}{\text{mL sample}} \quad (2.8)$$

$$\text{mg/L Cl} = \frac{(\text{A} \pm \text{B}) \times \text{N} \times 35{,}450}{\text{mL sample}} \qquad (2.9)$$

Where A represents the sample volume in mL, B is the volume of the blank in mL obtained from titration for blank (positive or negative), and N is normality of $Na_2S_2O_3$.

2.1.4 General reagents

1.000 M stock solutions of sulfuric acid, sodium hydroxide, and sodium chloride were prepared by dissolving AR grade (Merck) in triple distilled water as per standard methods of preparations. The solutions were further diluted to suitable concentration. The strength of these solutions was determined by standard procedures.

2.1.5 Kinetic measurements

All the kinetic measurements for the consumption of the organic dyes were conducted with low concentration of dye and excess concentrations of all the other reagents. The kinetic measurements for all the reactions were conducted under *pseudo* first-order conditions and the reactions were completed in few milliseconds at certain given conditions. Therefore, they were monitored using the stopped-flow spectrophotometer, which is designed to follow the fast signal changes with a rapid mixing system.

All kinetic measurements for amaranth-hypochlorite, brilliant blue-R-hypochlorite or safranine-O-hypochlorite reactions, as well as amaranth-chlorine dioxide, brilliant blue-R-chlorine dioxide and safranine-O-chlorine dioxide reactions were conducted using the HI-TECH (SF-61DX2) stopped-flow apparatus. The high performance stopped-flow spectrometer has a double mixing facility. Flow circuit diagram Figure 2.1.9, Bench Setup (Figure 2.1.10), Sample handling unit (Figure 2.1.11) and optical setup (Figure 2.1.12) are

shown respectively. To prepare the reagent mixtures for the reactions, the requisite volumes of reagents were added to bring the final volume to 10 mL. The experiments were performed by using conventional single mixing. Only drive 2 (Figure 2.1.9), was used so that reagents C and D are delivered to mixer 2 and the A and B reagent pathway was filled with water and not used. The rapid mixing initiated the study reaction. The flow displaced aged solutions (from previous runs) as the reaction mixture was driven into the observation cell. A stop syringe, used to set the driven volume, stops the flow. The stop syringe plunger travel was set by a rigid stop block causing rapid cessation of flow of the solution and thus triggering the data acquisition system. It should be noted at this point that the concentrations of the reagents in the mixing chamber are half that of the reagent in the syringe.

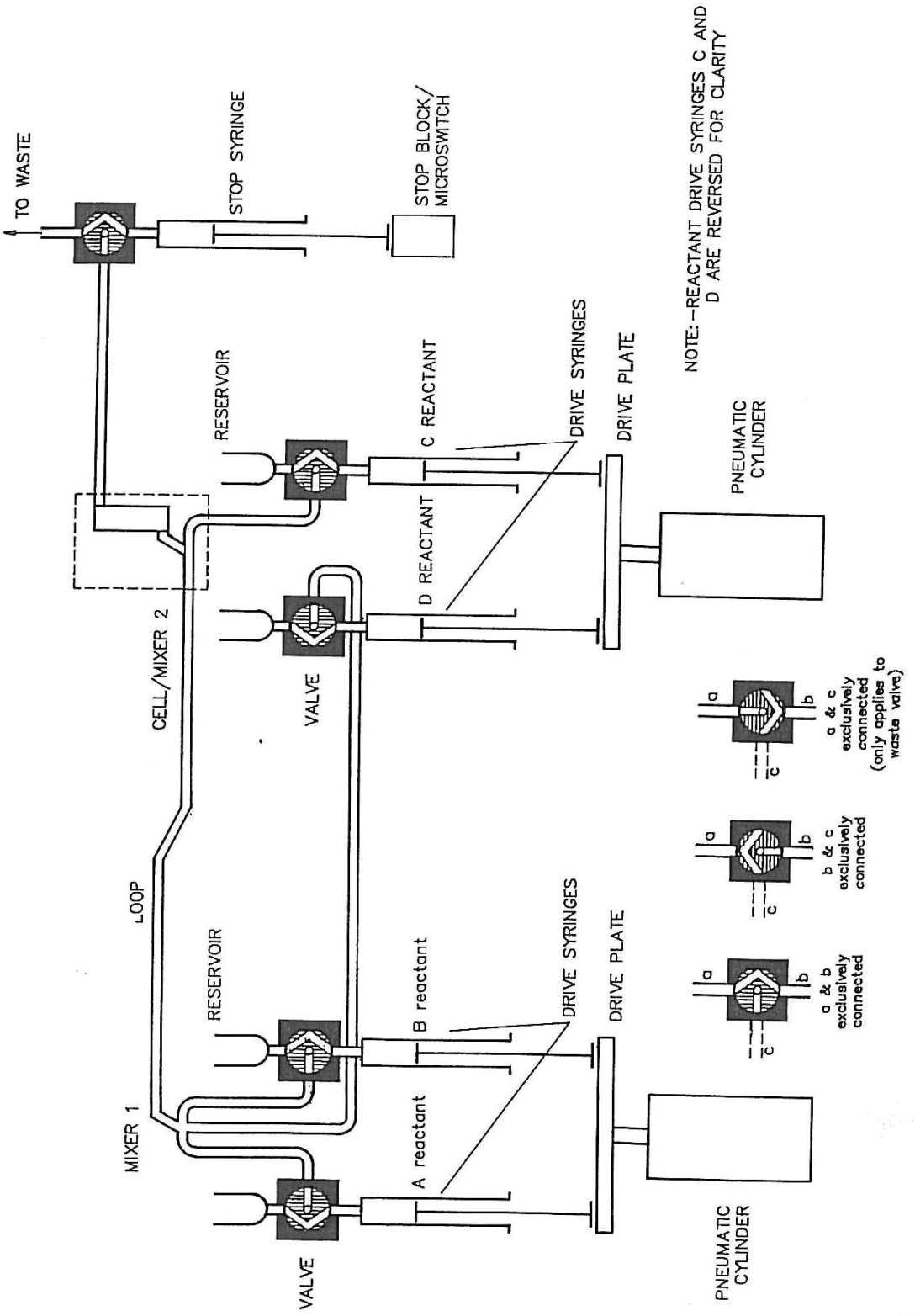

Figure 2.1.9 Hi-Tech Stopped flow apparatus - Flow circuit diagram.[180]

.

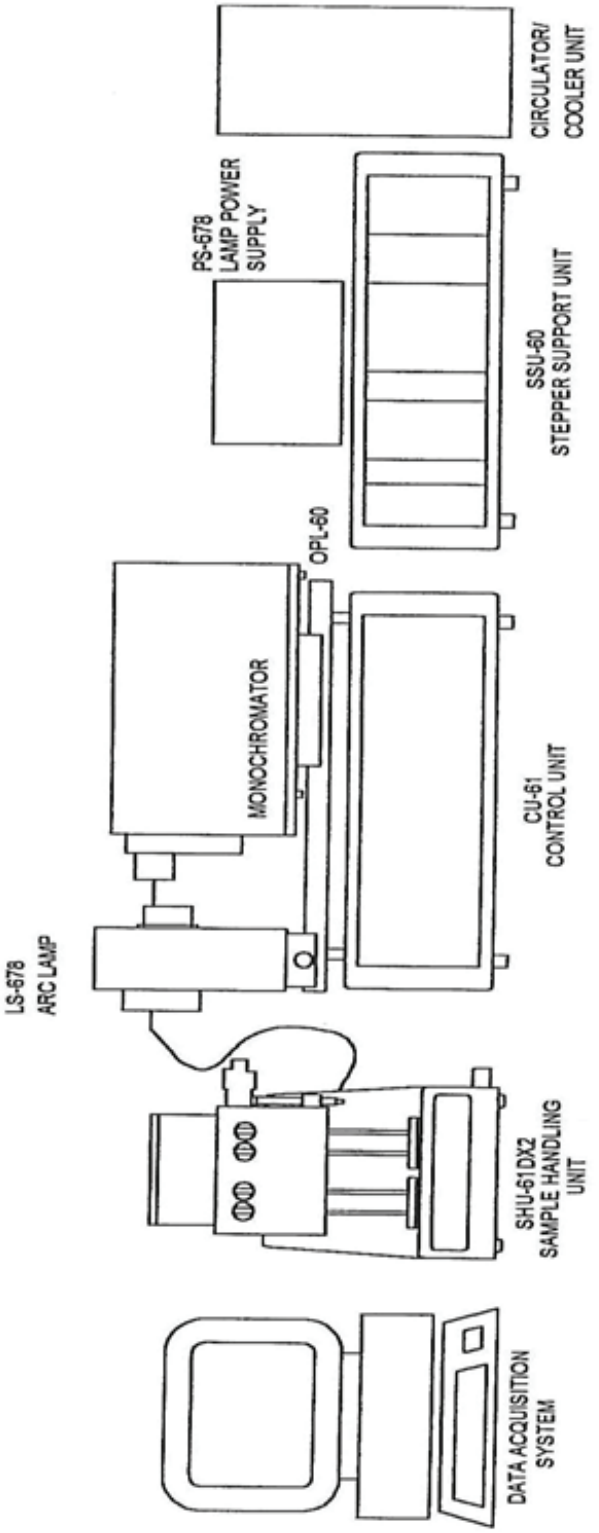

Figure 2.1.10 Hi-Tech Stopped flow apparatus-Typical bench setup. [174]

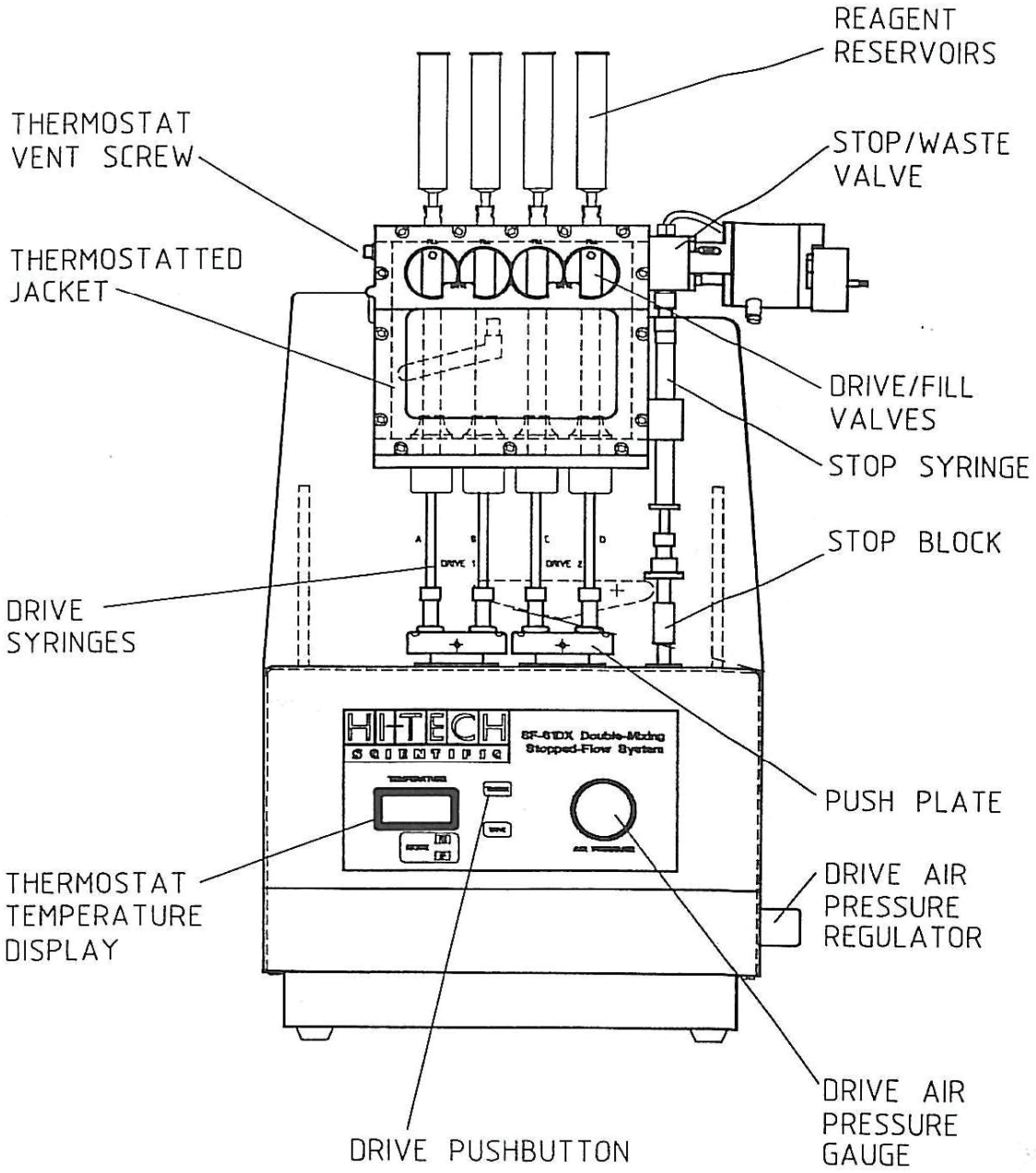

Figure 2.1.11 Hi-Tech Stopped flow apparatus-Sample Handling Unit. [174]

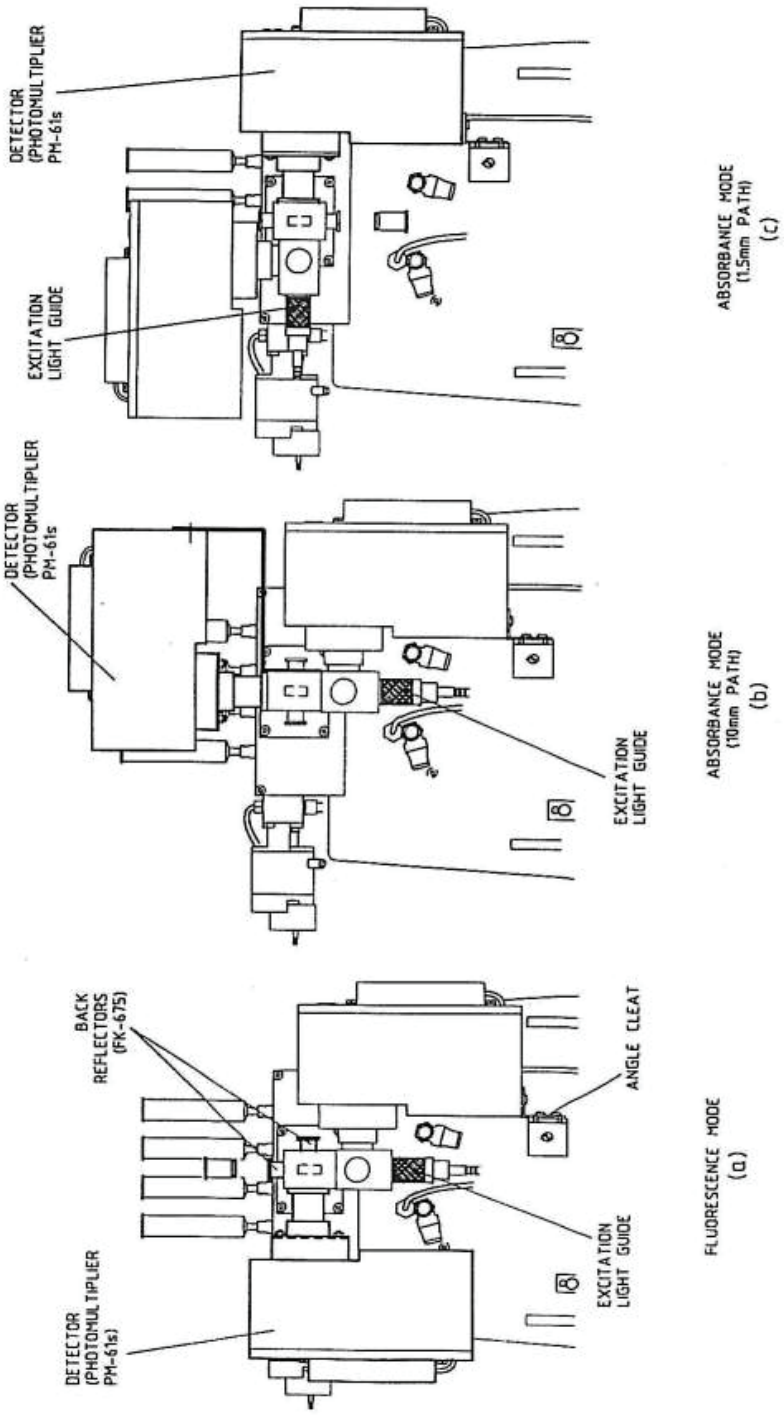

Figure 2.1.12 Hi-Tech Stopped flow apparatus-Optical setup.[181]

The rapid scanning single mixing mode technique was used to acquire multi-wavelength data for reactions in the current study.

2.1.6 Simulations and software used

In the current study "Simkine2" software was used due to its advantages of being efficient, less time consuming, and it can handle most of the errors, its flexibility and the fact that it provides more options. Simkine2 was an improved version of the original software developed called Simkine.[182] Simkine2 software was rewritten using Delphi professional 5 that met the needs of the various operating systems. The advantage of using Delphi was that the software could be operated at a good speed.

The available softwares only plots the generated data and experimental data separately, and gives a plot for comparison at a later stage. Simkine2 has the ability to plot the generated data as it gets is generated. The Simkine2 gives the user an option to plot the generated and experimental data simultaneously and separately.[183] While doing simulations it is useful to see how close the experimental and generated data agrees[184], and also in order to see how the generated and experimental data matches both plots need to be in the same set of axis.

2.1.7 Product analysis

The characterisation of the reaction products is esesential postulating probable reaction mechanism. To obtain sufficient quantities of the reaction products, reactants were taken in large quantities but approximately in relative proportions to that used in the kinetic experiments. Then an attempt is made to isolate and characterize the products of each reaction. The products were characterized using ^{1}H NMR and ^{13}C NMR with Bruker Avance III 400 MHz and 600 MHz NMR instruments with Probe BBO-2 gradient and the

'Top spin 2.1' software was used to analyse the spectras. Thermo Finnigan Trace GC coupled to a Polaris Q- MS was used for GC-MS analysis with column size 3.0 m x 0.2 mm internal diameter with 0.25 μm 5% phenyl(equivalent)/ 95% methyl polysilphenylene /siloxane stationary phase film with mobile phase helium gas.

Hypochlorite initiated reactions

The products of the reaction are analysed to propose the plausible reaction mechanism and the rate law. To commence the reaction 0.60 g of amaranth, 0.80 g of brilliant blue, 0.40 g of safranine-O was dissolved in 100 mL of water, and 400 mL of 0.010 M hypochlorite was added. The mixture was allowed to stand for 24 hours with constant stirring at room temperature. The reaction mixture was extracted with dichloromethane using batch separation technique. The extracted filtrate was evaporated using rotavapor. The filtrate was allowed to evaporate and dissolved in ethyl acetate. The separation of compounds was carried out using column chromatography and thin layer chromatography (TLC) techniques using the procedure outlined below.

Chlorine dioxide initiated reactions

To initiate the reaction 0.60 g of amaranth, 0.80 g of brilliant blue, 0.40 g of safranine-O were dissolved in 100 mL of water, to which 400 mL of 0.012 M chlorine dioxide was added. The mixture was allowed to stand for 24 h with constant stirring at room temperature. The reaction mixture was extracted and evaporated in the same manner as mentioned above. The filtrate was allowed to evaporate and dissolved in ethyl acetate. A silica gel column was used for the separation of the compounds. The products were characterised using ^{1}H NMR and ^{13}C spectroscopy on Varian 400 MHz NMR and the GC-MS spectrometer.

Column and thin layer chromatography

The separation, isolation and purification of compounds were carried out by gravity column chromatography and monitored by thin layer chromatography (TLC). For column chromatography, all crude extracts were dry packed onto a 4.5 cm crude column and fractions of 10 mL were collected. Merck silica gel 60 (0.040-0.063 mm) was used for column chromatography and Merck 20 × 20 cm silica gel 60 F254 aluminum sheets were used for thin-layer chromatography. The TLC plates were analysed under UV (254 nm and 366 nm) before being sprayed with reagent (spray reagent is developed with a [1:2:97] anisaldehyde: concentrated sulfuric acid: methanol) and the plates are subjected to heat. Varying ratios of hexane, dichloromethane and ethyl acetate were used for both column chromatography and thin layer chromatography.

2.1.8 Precision calculations

It is seldom easy to estimate the precision and accuracy of experimental data. Attempts must be made however, to satisfy such estimates because data of unknown precision and accuracy are worthless. A tenfold increase in accuracy may take hours, days or even weeks of added labor. Time to generate such accurate results is generally not available, thus most chemists usually carry out two to five replicates of an entire analytical procedure.

Most of the experiments in this project were performed in triplicate and the data generated were subjected to precision calculations. Precision may be defined as the concordance of a series of measurements of the same quantity. Generally, the precision of a measurement is determined by simply repeating the measurement. Three terms are used to describe the precision of a set of replicate data: standard deviation (s), variance (s^2), relative standard deviation (RSD) and coefficient of variation (CV).

2.1.9 Standard deviation (s)

In analytical chemistry, one of the most common statistical terms employed, is the standard deviation of a population of observations.

If we consider a series of n observations arranged in ascending order of magnitude:

$$x_1, x_2, x_3, \ldots, x_{n-1}, x_n,$$

The arithmetic mean is given by:

$$\bar{a} = \frac{x_1 + x_2 + x_3 \ldots + \ldots + x_{n-1} + x_n}{n} \qquad (2.10)$$

The spread of the values is measured most efficiently by the standard deviation defined by:

$$s = \left[\frac{(x_1 - \bar{a})^2 + (x_2 - \bar{a})^2 + \ldots (x_n - \bar{a})^2}{n - 1} \right]^{1/2} \qquad (2.11)$$

In this equation the denominator is (n – 1) rather than n when the number of values is small.

The equation 2.11 may also be written as :

$$s = \left[\frac{\Sigma (x - \bar{a})^2}{n - 1} \right]^{1/2}$$

The equation for computing a pooled standard deviation from several sets of data takes the form :

$$s_p = \left[\frac{\sum_{i=1}^{N_1} (x_i - \bar{a}_1)^2 + \sum_{j=1}^{N_2} (x_j - \bar{a}_2)^2 + \sum_{k=1}^{N_3} (x_k - \bar{a}_3)^2 + \ldots}{N_1 + N_2 + N_3 + \ldots - N_s} \right]^{1/2} \qquad (2.12)$$

where s_p represents pooled standard deviation, N_1 is the number of data in set1, N_2 is the number in set 2, and so forth. The term N_s is the number of data sets that are pooled.

2.1.10 Variance (s^2)

The variance is the square of the standard deviation. The standard deviation has the same units as the data whereas the variance has the units of the data squared. Scientists tend to use standard deviation rather than variance as a measure of precision. It is easier to relate the precision of a measurement to the measurement itself if they both have the same units. The advantage of using variance is that variances are additive.

Standard deviations are frequently quoted in relative rather than absolute terms. The relative standard deviation multiplied by 100 % is called the coefficient of variation (CV).

$$CV = (s / \bar{a}) \times 100\ \%$$

Relative standard deviations often give a clearer picture of data quality than do absolute standard deviations. The relative standard deviation (s) and coefficient of variation (CV) will serve as measures of precision for all data obtained in this project.

Kinetic data acquisition is done by KinetAsyst^{TM} 2 which allows single wave length-single shot or single wave length- multishot to give the most meaningful data. A series of shots were conducted automatically for each experiment in three replicates. The observed coefficient of variation is always less than 4% unless otherwise specified.

CHAPTER 3
OXIDATION OF DYES WITH HYPOCHLORITE

The sodium hypochlorite is a strong oxidising agent. Its bleaching reaction typically is one of oxidative cleavage of a double bond, breaking the delocalization and hence the molecule's ability to absorb light in the visible region, resulting in a colorless solution. The kinetics of oxidation of amaranth, brilliant blue-R and safranine-O dyes with hypochlorite in an aqueous solution was investigated as a function of pH. Speciation profiles of the oxidant were utilized to estimate the rate constants of the dyes over a wide pH range. The kinetic investigations were complemented by product analysis, energy parameters and simulations, to propose plausible reaction mechanisms for the reactions.

3.1 Reaction between amaranth and hypochlorite

3.1.1 Order with respect to amaranth

The kinetics and mechanism of oxidation of amaranth (AM^-), an anionic azo dye by hypochlorite was studied under diverse reaction conditions. All the experimental runs were conducted with low concentrations of dye and excess concentrations of the other reagents. Unless otherwise stated all the experiments were carried out at (25 ± 0.1) °C. The rate of depletion of AM^- was monitored at 520 nm corresponding to the absorption maximum of the dye. At 520 nm, no interferences from the products or intermediates were observed. The reaction was monitored using the Hi-Tech SF-61 DX2 double mixing micro volume stopped-flow equipment. Figure 3.1.1 shows the typical depletion curve of amaranth as a function of time. A perusal of the curve shows that depletion of the dye is completed in less than 100 s.

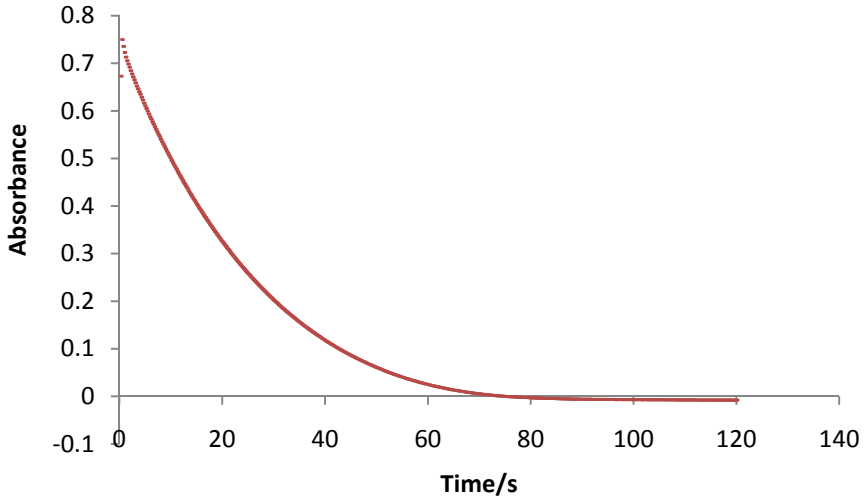

Figure 3.1.1 Typical kinetic curve absorbance *versus* time plot for the reaction of $[AM^-]_0$ (7.0 x 10^{-5} M) with $[OCl^-]_t$ (1.5 x 10^{-3} M) at pH = 9.0 and 520 nm.

The kinetic data acquired at single wavelength was analysed using the KinetAsyst^{TM} software which allows the matching of experimental results with different rate equations and to estimate the rate constants by choosing appropriate integrated rate equations.

3.1.2 Analysis of kinetic data using KinetAsyst^{TM} Fit software

The analysis of the data was accomplished using the KinetAsyst^{TM} Fit Asystant software. The data traces were selected to analyse with the KinetAsyst^{TM} Fit Asystant, for the first-order reaction using the rate equation {1 Exp + C, y = -A exp (-k * x) + C} and the matching simulated curve was generated. Figure 3.1.2 represents the illustration of the typical experimental curve with the fitted simulated curve. The upper curve shows the fit between the theoretical and experimental curves, whilst the lower plot indicates the residuals illustrating the agreement or variation between the two curves.

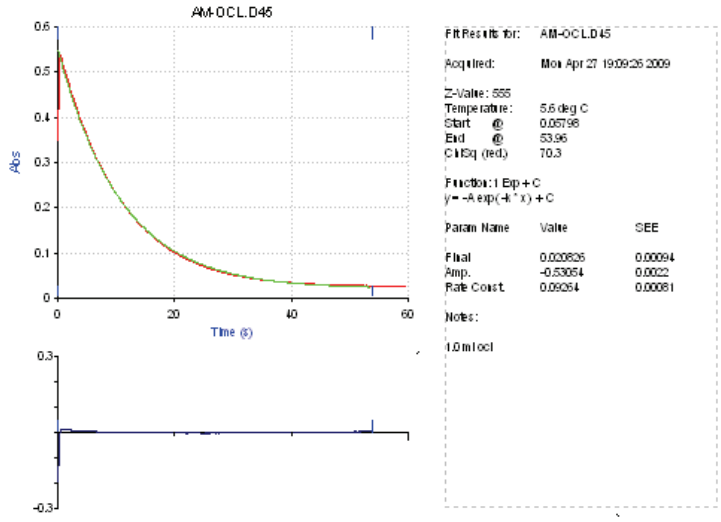

Figure 3.1.2 KinetAsyst^{TM} single-exponential equation fit (green) and the experimental curve (red) with residuals shown in the (lower curve) and the rate parameters in the adjacent box for the reaction of $[AM^-]_0$ (7.0×10^{-5} M) with $[OCl^-]_t$ (1.5×10^{-3} M).

An observation of Figure 3.1.2 shows that using a first-order rate equation, {1 Exp + C, y = - A exp (-k * x) + C}, a fair agreement occurred between the experimental and computed curves, with small residuals. The software fit analysis results for the curve displayed in the box show that the rate constant is ($3.20 \pm 0.02 \times 10^{-3}$) s^{-1} showing small standard deviation. The curve and data also suggest that for the chosen conditions, the reaction follows *pseudo* first-order kinetics and reaction order with respect to AM^- is unity.

3.1.3 Order with respect to hypochlorite

To establish the reaction order with respect to oxidant, a series of experiments were conducted with different initial concentrations of hypochlorite at pH 9.0 and fixed ionic strength, using sodium sulfate as a neutral salt. Typical curves showing depletion of AM^- as function of time monitored at different initial concentrations of hypochlorite are shown in Figure 3.1.3. In presence of varying initial excess concentrations of hypochlorite, the absorbance of dye decreased exponentially.

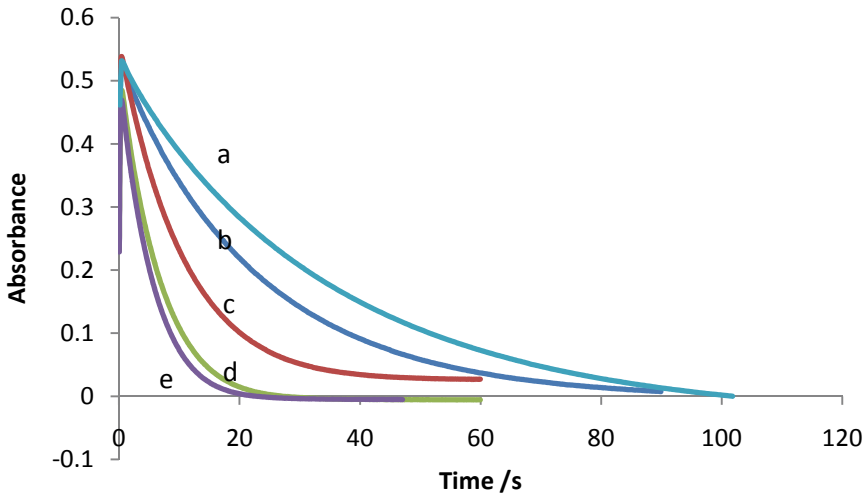

Figure 3.1.3 Depletion of amaranth with various hypochlorite concentrations for the reaction of $[AM^-]_0$ (7.0 x 10^{-5} M) with $[OCl^-]_t$ x 10^{-3}/M (a = 0.085, b = 1.70, c = 2.55, d = 3.40 and e = 5.10) at pH = 9.0.

The typical plots of absorbance *versus* time, showing the effect of variation of hypochlorite concentration are shown in Figure 3.1.3, while the traces obtained using KinetAsyst^{TM} software and the respective obtained *pseudo* first-order rate coefficients, k'(s^{-1}) values are illustrated in Figure 3.1.4.

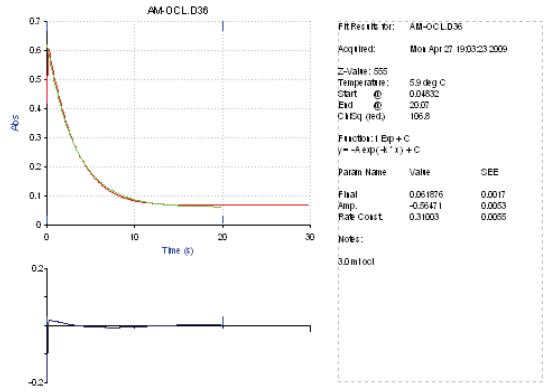

(a)

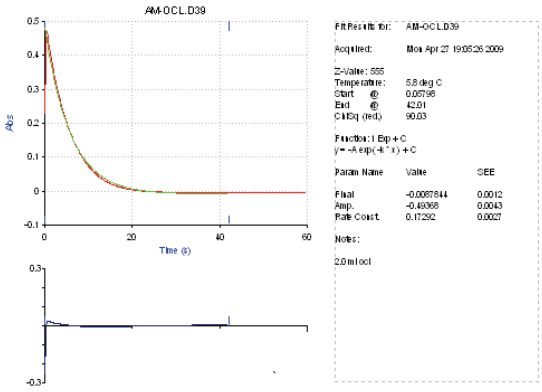

(b)

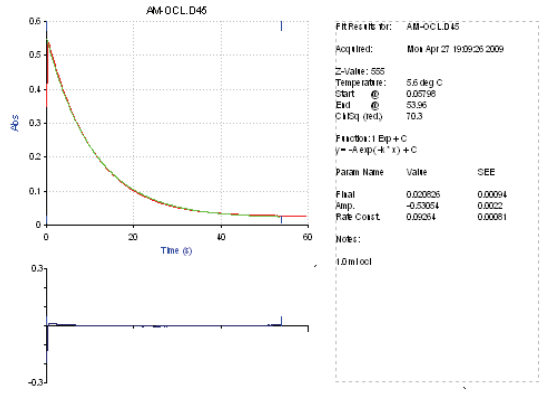

(c)

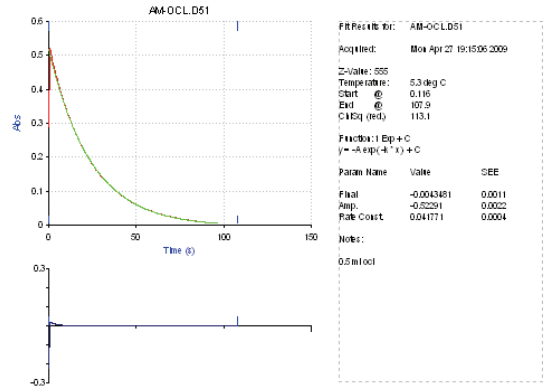

(d)

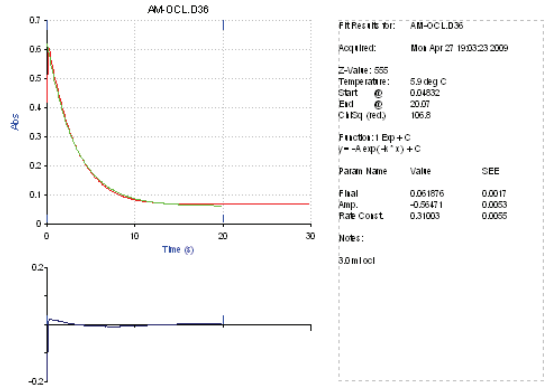

(e)

Figure 3.1.4 Fits using KinetAsyst^{TM} single-exponential equation, and rate equation {1 Exp + C, y = -A exp (-k * x) + C} (where k'/s^{-1} a = 0.041, b = 0.093, c = 0.145, d = 0.175 and e = 0.322).

The k' values obtained by analyzing the respective experimental kinetic curves for different initial hypochlorite concentrations are also shown in Table 3.1.1 at constant ionic strength and pH equals to 9.0.

Table 3.1.1 Reaction between amaranth and hypochlorite at constant ionic strength $[AM^-]_0$ (7.0×10^{-5} M), $[OCl^-]_t$ (0.85×10^{-4} – 5.1×10^{-3} M), pH = 9.0 and ionic strength (I = 0.128 M).

$[OCl^-]_t / 10^{-3}$ M	k'/s^{-1}*
0.50	0.041
1.70	0.093
2.55	0.145
3.40	0.175
5.10	0.322

* Mean of four replicate experiments with relative standard deviation < 4%

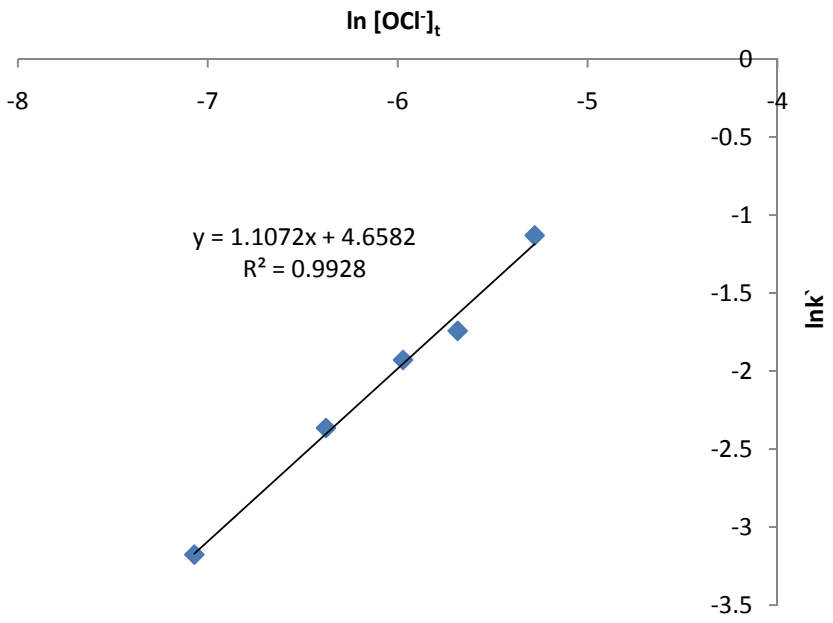

Figure 3.1.5 Plot of ln $[OCl^-]_t$ *versus* ln k' for the reaction of $[AM^-]_0$ (7.0×10^{-5} M) with $[OCl^-]_t$ (0.85×10^{-4} – 5.1×10^{-3} M) at pH = 9.00 and I = 0.128 M.

From Figure 3.1.5 the plot of ln k' *versus* ln $[OCl^-]_t$, which is a straight line with slope equals to 1.1 (R^2 = 0.99) suggesting that order with respect to hypochlorite at pH 9.0 is one.

3.1.4 Effect of pH on the reaction rate

One important parameter that normally influences the reaction dynamics is pH. To assess the role of acid in the oxidation process, the kinetics of the reaction as a function of pH was investigated. The effect of added acid on reaction was probed by the initial addition of varied amounts of sulfuric acid solution, maintaining the total ionic strength constant and the initial pH values were simultaneously recorded. The kinetic data obtained for different experiments was analysed for k' values using 'KinetAsyst^{TM} Fit Asystant'. The initial pH and k' values obtained after analysis for different runs are summarized in Table 3.1.2. Figure 3.1.6 illustrates the plot of the obtained k' versus pH values. A perusal of Figure 3.1.6 shows that the increase in k' values was small at low acid concentrations and the rise was bigger at higher acid concentrations indicating the profound effect of pH on the reaction.

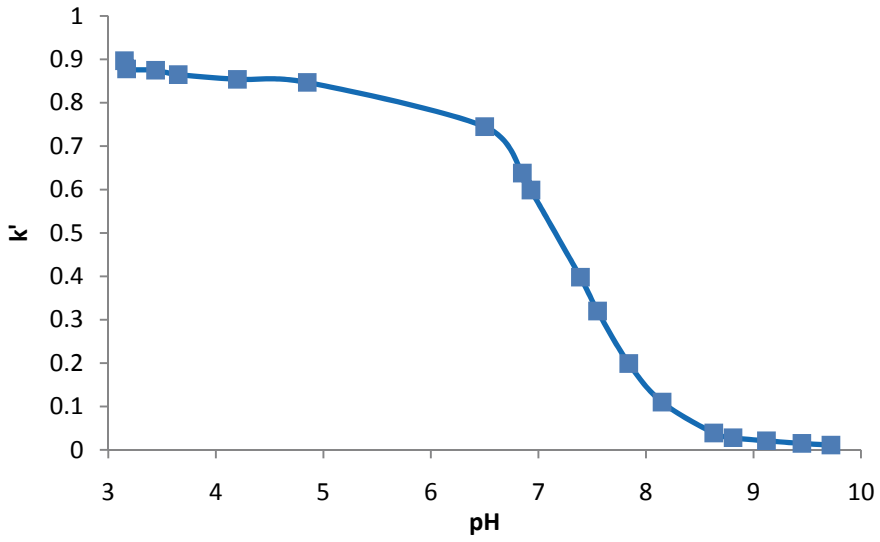

Figure 3.1.6 Plot of k' *versus* pH for the reaction of $[AM^-]_0$ (7.0 x 10^{-5} M) with $[OCl^-]_t$ (1.45 x 10^{-3} M), $[H^+]_{eq}$ (1.99x10^{-9}- 7.752 x 10^{-4} M).

Table 3.1.2 Effect of pH on reaction rate for the reaction of $[AM^-]_0$ (7.0×10^{-5} M) with $[OCl^-]_t$ (1.45×10^{-3} M).

pH	k'/s^{-1} *
9.89	0.005
9.72	0.011
9.45	0.015
9.12	0.021
8.81	0.028
8.63	0.039
8.15	0.110
7.84	0.199
7.55	0.320
7.39	0.398
6.93	0.599
6.85	0.638
6.50	0.745
4.85	0.847
4.20	0.854
3.65	0.865
3.44	0.875
3.17	0.878
3.15	0.897

* Mean of four replicate experiments with relative standard deviation < 4%

Further, to establish the order with respect to acid, the ln k' versus ln $[H^+]$ values were plotted (Figure 3.1.7), which gave a slope of 0.27 ($R^2 = 0.96$). The observed partial reaction order with respect to acid clearly suggests that the reaction mechanism is intricate and acid is directly involved in the rate-limiting step.

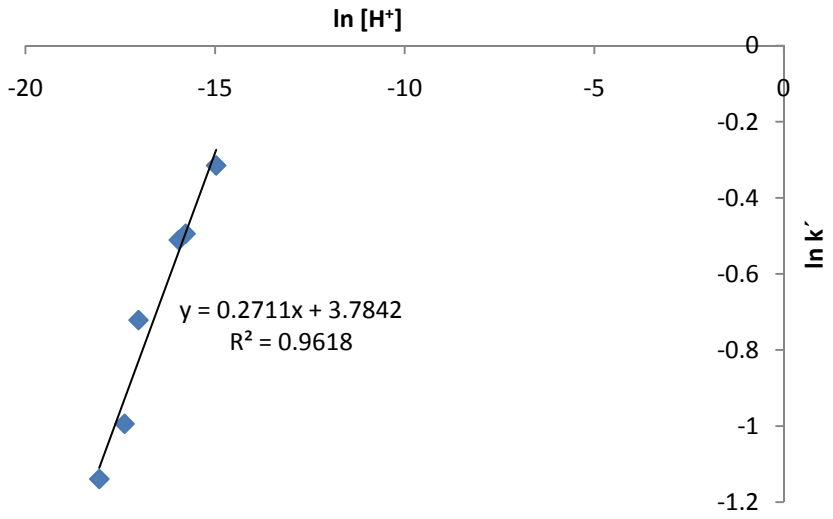

Figure 3.1.7 Plot of ln k' *versus* ln $[H^+]$ for the reaction of $[AM^-]_0$ (7.0×10^{-5} M) with $[OCl^-]_t$ (1.45×10^{-3} M), $[H^+]_{eq}$ (1.99×10^{-9} - 7.752×10^{-4} M).

The observed partial order with respect to H^+ can be viewed in terms of its role in speciation of hypochlorite by protonation to hypochlorous acid, and the existing equilibrium between the two species i.e., $OCl^- + H^+ \rightleftharpoons HOCl$. With $pK_a = 7.4$ for protonation of OCl^-, the addition of acid will shift the equilibrium to the right. Thus the oxidation of dye possibly occurs simultaneously through its reaction with OCl^- and HOCl species.[185]

The observed increase in k' values with increasing acid concentration suggests that the rate of oxidation by HOCl is faster than with OCl^-. It can also be predictable based on the oxidation potentials of the two species. Of the chlorine-containing disinfecting agents, hypochlorous acid has the higher oxidation potential (E^o =1.44 V), compared to 1.39 V for Cl_2 and 1.12 V for OCl^- ion. The kinetic data obtained for acid variation studies was scrutinized again for the likelihood of the occurrence of two competitive reactions. Based on that assumption, the kinetic curves were analysed using fit for the two competitive first-order

reactions, i.e. by using the equation {y = -A exp (-R1 * x) + -A exp (-R2 * x) + C}. The simulated curve fitted quite well with negligible residuals. Typical curves are illustrated of the Figures 3.1.8 and 3.1.9 and the obtained k_1' and k_2' values were summarised in Table 3.1.3.

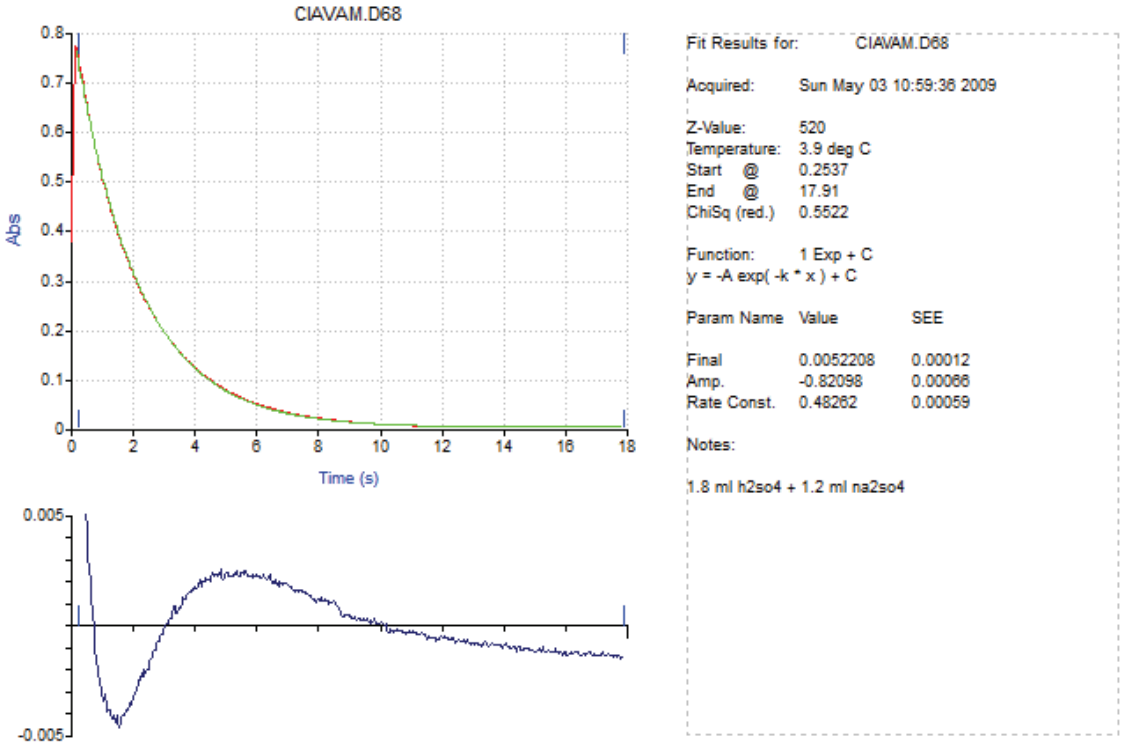

Figure 3.1.8 KinetAsyst™ single-exponential equation fit of two curves and residuals (lower sketch) using the first-order equation for the reaction of $[AM^-]_0$ (7.0 x 10^{-5} M) with $[OCl^-]_t$ (1.45 x 10^{-3} M) $[H^+]_0$ (9.96 x 10^{-9} M) and I (0.12 M).

Figure 3.1.8 illustrates the typical KinetAsyst™ fit of the two curves and the residual (lower part of Figure 3.1.8) for the reaction of OCl^- with amaranth using the first-order rate equation Eqn. {y = -A exp (-k * x) + C} displaying the residuals, where as Figure 3.1.9 illustrates the same curve with fit obtained employing Eqn. {y = -A exp (-R_1 * x) + -A exp (-R_2 * x) + C.

The residual (lower part) for the reaction of OCl^- with later fit were much smaller suggesting later is a better fit.

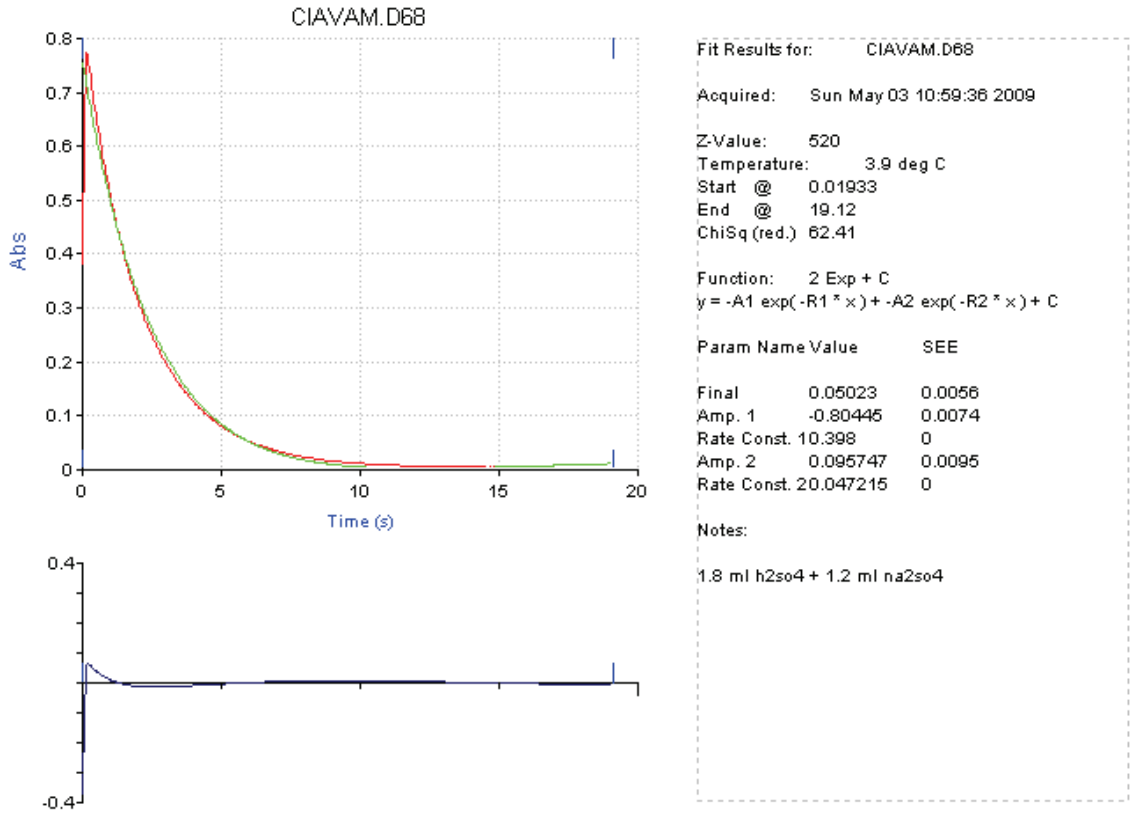

Figure 3.1.9 KinetAsyst™ double-exponential equation fit of two curves and residuals (lower sketch) for the two competitive first-order reactions for the reaction of $[AM^-]_0$ (7.0×10^{-5} M) with $[OCl^-]_t$ (1.45×10^{-3} M), $[H^+]_0$ (9.96×10^{-9} M) and I (0.12 M)

The absorbance versus time data for different acidic conditions were analysed on the basis of the occurrence of two simultaneous reactions and the corresponding *pseudo* first-order rate constants obtained are summarized in Table 3.1.3, together with the estimated initial concentrations of H^+, OCl^- and HOCl in equilibrium, corresponding to different pH values. While k_1' represents the *pseudo* first-order rate constant for the OCl^- initiated oxidation, k_2' represents the corresponding value for the reaction by HOCl. Further, k_1 and k_2 are the

calculated second-order reaction constants for the competitive reactions by OCl^- and HOCl respectively.

Table 3.1.3 Effect of acid on the speciation of hypochlorite, and observed reaction rates.

pH	H^+	$[OCl^-]_{eq}$	$[HOCl]_{eq}$	k_1'/s^{-1} *	k_2'/s^{-1} *	$k_1/M^{-1}s^{-1}$	$k_2/M^{-1}s^{-1}$
8.63	2.34×10^{-9}	3.40×10^{-3}	1.94×10^{-3}	8.0×10^{-2}	0.039	2.34	19.90
8.15	7.06×10^{-9}	3.07×10^{-3}	5.30×10^{-3}	7.1×10^{-2}	0.110	2.32	20.77
7.84	1.44×10^{-8}	2.66×10^{-3}	9.38×10^{-3}	6.5×10^{-2}	0.199	2.47	21.32
7.55	2.81×10^{-8}	2.13×10^{-3}	1.47×10^{-2}	5.2×10^{-2}	0.320	2.45	21.83
7.39	4.06×10^{-8}	1.80×10^{-3}	1.79×10^{-2}	4.7×10^{-2}	0.398	2.61	22.19
6.93	1.17×10^{-7}	9.30×10^{-4}	2.67×10^{-2}	2.5×10^{-2}	0.599	2.73	22.44
6.85	1.41×10^{-7}	8.10×10^{-4}	2.79×10^{-2}	1.7×10^{-2}	0.638	2.16	22.88
6.50	3.15×10^{-7}	4.10×10^{-4}	3.19×10^{-2}	8.0×10^{-3}	0.745	1.99	23.38
4.85	1.41×10^{-5}	1.00×10^{-5}	3.59×10^{-2}	2.0×10^{-5}	0.847	1.76	23.60
4.20	6.30×10^{-5}	2.34×10^{-5}	3.60×10^{-2}	3.9×10^{-5}	0.854	1.68	23.75
3.65	2.24×10^{-5}	6.59×10^{-6}	3.60×10^{-2}	1.0×10^{-5}	0.864	1.59	24.02
3.44	3.63×10^{-5}	4.06×10^{-6}	3.60×10^{-2}	5.7×10^{-6}	0.875	1.43	24.31
3.17	6.75×10^{-5}	2.18×10^{-6}	3.60×10^{-2}	2.6×10^{-6}	0.878	1.23	24.39
3.15	7.07×10^{-5}	2.08×10^{-6}	3.60×10^{-2}	2.5×10^{-6}	0.897	1.22	24.93
3.14	7.23×10^{-5}	2.04×10^{-6}	3.60×10^{-2}	2.4×10^{-6}	0.912	1.19	25.35
2.89	12.87×10^{-5}	1.14×10^{-6}	3.60×10^{-2}	1.1×10^{-6}	0.958	1.02	26.61
Mean k_1 and k_2 with standard deviation						1.9 ± 0.6	23.2 ± 1.8

* Mean of four replicate experiments with relative standard deviation < 4%

where k_1' and k_2' *pseudo* first-order rate constants with respect to OCl^- and HOCl,

where $k_1 = k_1'/ [OCl^-]_{eq}$ and $k_2 = k_2'/ [HOCl]_{eq}$ where k_1 and k_2 represents the second order reaction rates for OCl^- and HOCl competitive reactions.

The equilibrium concentrations of acid, the OCl^- and HOCl were calculated based on the initial pH values and the protonation constant of hypochlorite. An examination of the data in the table shows that with increasing initial acid concentration, a decreasing trend is registered for k_1' values, while the k_2' values showed an increasing trend. The ln-ln plots of k_1' and $[OCl^-]_{eq}$ and k_2' and $[HOCl]_{eq}$ gave straight lines, which are shown in Figures 3.1.10 and 3.1.11.

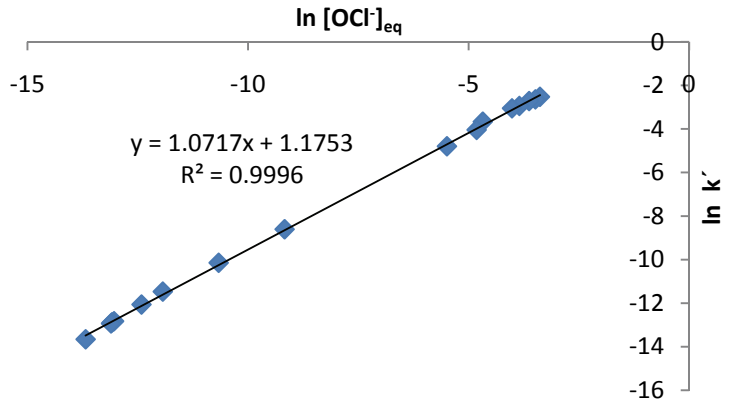

Figure 3.1.10 Plot of ln k' *versus* ln $[OCl^-]_{eq}$ for the reaction of $[AM^-]_0$ (7.0×10^{-5} M) with $[OCl^-]_t$ (1.45×10^{-3} M) at $[H^+]_{eq}$ (3.97×10^{-6} - 7.75×10^{-3} M), $[OCl^-]_{eq}$ (1.14×10^{-3} – 1.53×10^{-6} M).

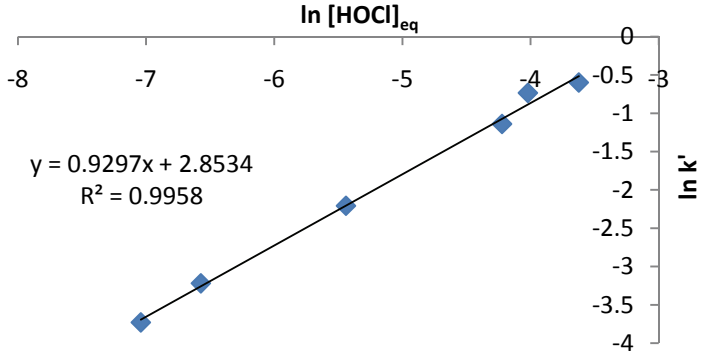

Figure 3.1.11 Plot of ln k' *versus* ln $[HOCl]_{eq}$ for the reaction of $[AM^-]_0$ (7.0×10^{-5} M) with $[OCl^-]_t$ (1.45×10^{-3} M) at $[H^+]_{eq}$ (1.99×10^{-9} - 9.98×10^{-7} M), $[OCl^-]_{eq}$ (2.76×10^{-2} – 3.3×10^{-6} M).

In Figure 3.1.10, the values of $[OCl^-]_{eq}$ at very low pH were not considered, as $[OCl^-]_{eq}$ was small, and hence *pseudo* first-order conditions will not be obeyed under those conditions. The

mean values (1.9 ± 0.6) $M^{-1} s^{-1}$, (23.2 ± 1.8) $M^{-1} s^{-1}$ shown in Table 3.1.3 represent the k_1 and k_2 values respectively, which are the second-order coefficients for the OCl^- and HOCl initiated oxidations, respectively. The obtained results confirm that acid is not directly involved in the rate limiting reaction as suggested earlier (page 79), but it influences the equilibrium of OCl^- to HOCl. Increase in HOCl concentration results in a higher rate constant indicating an increase in the rate of oxidation of the dye. This explains the partial order observed with respect to acid. The observed decrease in reaction order with increasing $[H^+]$ confirms that the observed reaction rate is a resultant effect of the reactions of AM^- with hypochlorite and hypochlorous acid, but with a minor contribution of hypochlorite at lower pH. Interestingly, the increase in acid concentration at pH < 3 does not enhance the rate constant significantly (Table 3.1.3). Under these conditions all the hypochlorite exists in HOCl form, thus the increase in $[H^+]$ will have no further applicable effect on the reaction rate.

3.1.5 Primary salt effect

The kinetic salt effect provides insight into the nature of the reacting species involved in the rate-limiting step. To identify the probable species involved in the rate limiting step, the reaction between hypochlorite and AM^- was investigated as a function of varying ionic strength (I), between 0.01 and 0.04 M with fixed initial concentrations of hypochlorite and amaranth supplemented by sodium sulfate. At pH 9.0, 15% of total hypochlorite exists in the form of HOCl. Hence, the curves were analysed for two consecutive reactions in the same manner as it was done previously and results obtained are summarised in Table 3.1.4. For the reaction between amaranth and hypochlorite the plot of log k' *versus* $I^{1/2}$ gave a linear curve with a positive slope = 1.216 and $R^2 = 0.98$ (Figure 3.1.12). The positive salt effect indicates

that the rate-limiting step involves species of like charges, possibly AM^- and OCl^- ions. The reaction between AM^- and HOCl slope was of fractional value (0.793) (Figure 3.1.12).

Table 3.1.4 Effect of ionic strength on the reaction rate $[OCl^-]_t$ (1.45×10^{-3} M), $[AM^-]_0$ (7.0×10^{-5} M), pH = 9.0.

.

Ionic strength/M	k_1'/s^{-1} *	k_2'/s^{-1}
0.0092	0.043	0.047
0.0167	0.050	0.048
0.0242	0.052	0.048
0.0317	0.054	0.050
0.0392	0.059	0.051

* Mean of four replicate experiments with relative standard deviation < 4 %

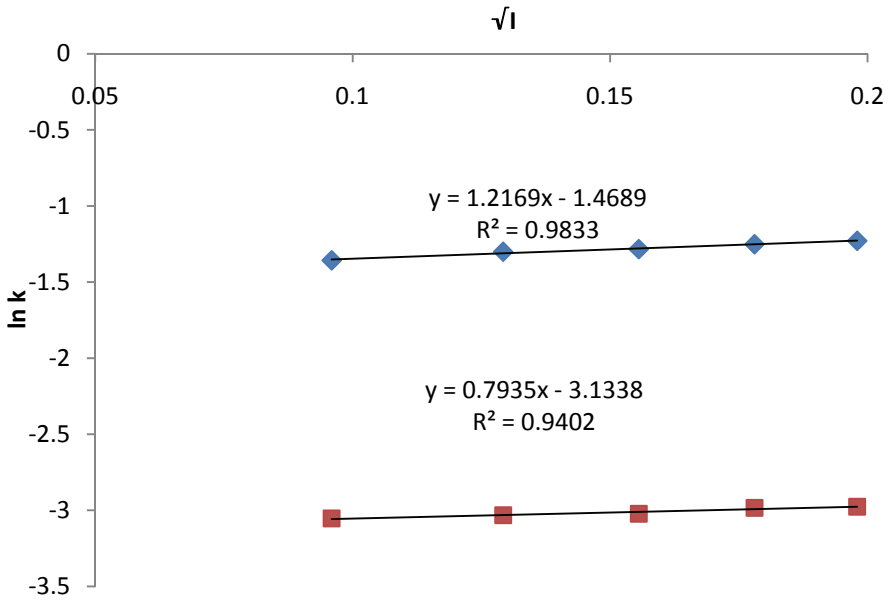

Figure 3.1.12 Plot of log k_1' *versus* $\sqrt{I}$ (ionic strength) for the reaction of $[AM^-]_0$ (7.0×10^{-5} M) with $[OCl^-]_t$ (1.45×10^{-3} M)), at pH 9.00, ionic strength (I = 0.009-0.039 M).

3.1.6 Kinetic salt effect at acidic pH

Under acidic conditions, as 99 % of the oxidant will be in the form of HOCl, a neutral species, the kinetic salt effect should theoretically be nil. Considering the reaction is between cationic dye and a strongly polar HOCl, a linear relationship is anticipated between rate constant and ionic strength species and so the expected salt effect should be between the protonated dye and HOCl. The rate constant should therefore have linear dependence on ionic strength. Table 3.1.5 and Figure 3.1.13 summaries the results of k' values obtained as function of ionic strength at low acid conditions.

Table 3.1.5 Effect of ionic strength on the reaction rate for the reaction of $[AM^-]_0$ (7.0×10^{-5} M), $[OCl^-]_t$ (1.45×10^{-3} M), pH = 3.10.

Ionic strength/M	k'/s^{-1} *
0.0092	0.047
0.0167	0.048
0.0242	0.048
0.0317	0.050
0.0392	0.051

* Mean of four replicate experiments with relative standard deviation < 4 %

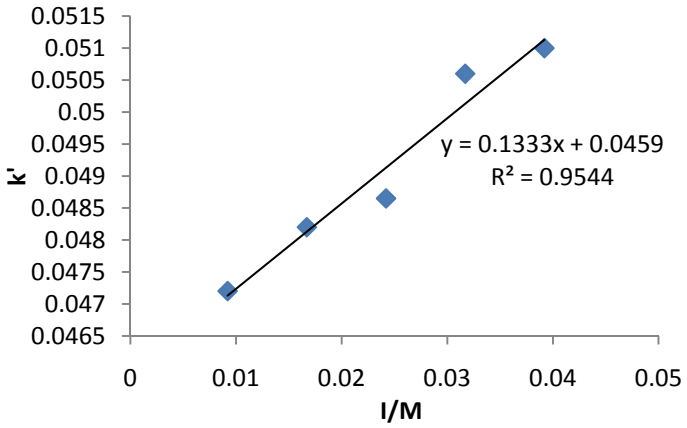

Figure 3.1.13 Plot of k' *versus* $\sqrt{I}$ (ionic strength) for the reaction of $[AM^-]_0$ (7×10^{-4} M) with $[OCl^-]_t$ (1.45×10^{-3} M) at varying ionic strength, I(0.009-0.039 M) at fixed acid $[H^+]_0$ (4.5×10^{-3} M) and pH 4.0.

The k' *versus* respective I values were plotted and shown in Figure 3.1.13. A good linear curve with R^2 = 0.95 confirms such anticipated relationship. The fractional slope indicates that the rate limiting step does not involve two charged species under acidic pH. Thus, possibly the rate limiting reaction involves one charged species AM^- and a neutral species, HOCl as anticipated.

3.1.7 Effect of chloride on the reaction rate

The influence of the added chloride was also studied. In reality, effluents from textile and dyeing industries would contain a high concentration of salts which may affect the removal of dye.[186] Considering chloride is one of the species associated with hypochlorite generation and product of the oxidation reaction, the effect of chloride on the reaction was investigated. Although, initial chloride concentrations in the reaction mixture are less than 2 x 10^{-3} M, the effect of higher amounts of initial chloride is studied and results obtained are summarised in Table 3.1.6.

Table 3.1.6 Effect of addition of chloride ions for the reaction of $[AM^-]_0$ (7.0 x 10^{-5} M) with $[OCl^-]_t$ (1.45 x 10^{-3} M), $[Cl^-]$ (1 x 10^{-1} M).

$[Cl^-]$/M	k'/s^{-1} *
0.100	0.107
0.148	0.109
0.298	0.107
0.447	0.104
0.597	0.104
0.725	0.104

* Mean of four replicate experiments with relative standard deviation < 4%

A perusal of the results in Table 3.1.6 suggests that presence of chloride ion has marginal effect on the reaction rate.

3.1.8 Activation parameters

The activation parameters of the chemical reaction provide valuable information about the nature of the transition state and the reaction mechanism. A huge enthalpy of activation ($\Delta H^{\ddagger}$) indicates that a large amount of stretching or breaking of chemical bonds is necessary for the formation of the transition state. The entropy of activation gives a measure of the inherent probability of the transition state, apart from energetic considerations.[187,188] If $\Delta S^{\ddagger}$ is large and negative, the formation of the transition state requires the reacting molecules to orient into conformations and approach each other at a precise configuration.[189]

The energy parameters for the dye with HOCl and OCl^- reactions were studied by measuring the rate constants over the range of 15 to 35^o C temperature by using the Arrhenius and Eyring's equations.[190]

Table 3.1.7 Varied temperature and observed rate constants for the reaction of $[AM^-]_0$ (7.0×10^{-5} M) with $[OCl^-]_t$ (1.45×10^{-3} M).

Temp. / K	k_1'/s^{-1} *	$k/M^{-2} s^{-1}$	k_2'/s^{-1} *	$k/M^{-2} s^{-1}$
283	0.015	1.30	0.033	2.87
288	0.016	1.39	0.052	4.52
293	0.017	1.39	0.060	5.22
298	0.025	2.17	0.072	6.26
303	0.031	2.69	0.091	7.91

* Mean of four replicate experiments with relative standard deviation < 4%

where $k = k'/[OCl^-] [H^+]$.

The Arrhenius plot was used to determine the E_a, the activation energy of the reaction. The data were fitted by linear regression using the following equation, $\ln k = -E_a/RT + \ln A$ (Figure 3.1.14).

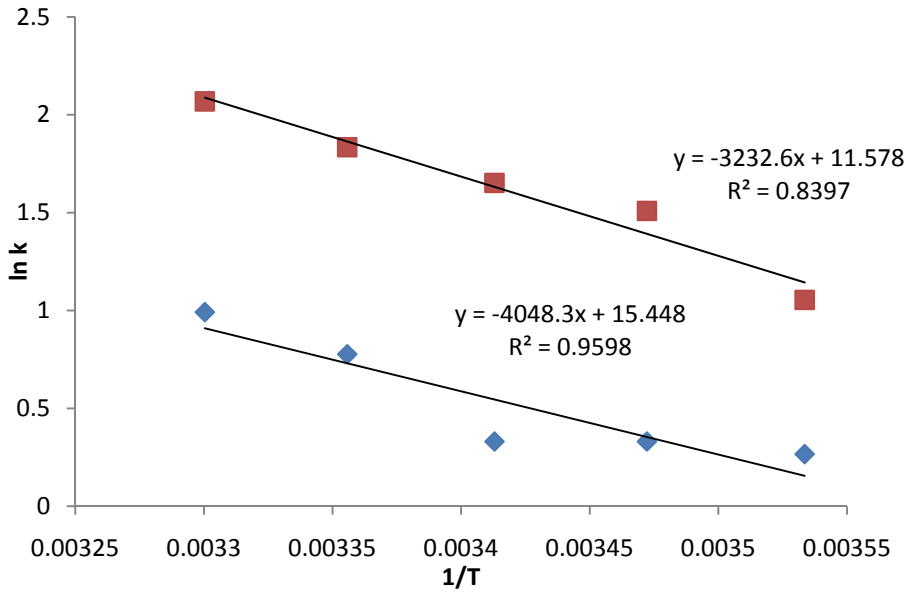

Figure 3.1.14 Plot of ln k' *versus* 1/T for the reaction of $[AM^-]_0$ (7.0×10^{-5} M) with $[OCl^-]_t$ (1.45×10^{-3} M) at different temperatures (T/K= 283-303).

Table 3.1.8 summarises the calculated values of four energy parameters, namely the energies of activation, enthalpy and entropy for both the reactions.

Table 3.1.8 Energy parameters.

Reaction pathway	Enthalpy of reaction, $\Delta H^{\ddagger}$/k J mol^{-1}	Entropy of activation, $\Delta S^{\ddagger}$/J K^{-1} mol^{-1}	Energy of activation E_a/k J mol^{-1}
AM^- with OCl^-	31.2	-190.6	33.65 ± 0.09
AM^- with HOCl	24.3	-222.8	26.87 ± 0.09

The enthalpy of activation, $\Delta H^{\ddagger}$ for the reaction was calculated using the equation,

$\Delta H^{\ddagger} = (E_a - mRT)$. The letters m, R and T represent respectively the total-order of reaction, gas constant and temperature. The $\Delta H^{\ddagger}$ value at 25 °C was found to be 31.2 kJ mol^{-1} for the OCl^- ion initiated reaction and 24.3 kJ mol^{-1} for the reaction with HOCl. Theoretically HOCl reaction needed slightly lower energy of activation (26.87 ± 0.09 kJ mol^{-1}) compared to (33.65 ± 0.09 kJ mol^{-1}) for the OCl^- ion initiated reaction. Both the reactions had large negative entropies of activation, suggesting the formation of a compact activated complex.

3.1.9 Product identification and characterization

The reaction products from the aqueous reaction mixtures were extracted with diethyl ether and the organic extract was further used for product separation and identification as explained in the experimental section. The main oxidation product separated using column chromatography which was found to be 3,4-dihydroxy naphthalene-2,7-disulfonic sodium salt (product P_1, Table 3.1.9). The ^1H NMR and ^{13}C NMR are provided in (Appendix 1, Figure 1.1.3 and Figure 1.1.4). The ^1H NMR showed the resonances that could be attributed to the structure of Product P_1, in particular four proton carbons can be seen in ^1H NMR, and ^{13}C spectra showed the resonances between δ120 and δ145 that could be attributed to aromatic portion of the P_1. The resonance at δ 166 could be carbonyl group and the resonance at δ106 could be due to the carbon atoms at the juncture between the two rings. The same extract was again analysed using the GC-MS. The gas chromatograph (GC) of the oxidation products (extract) showed two major peaks and no amaranth was present.

GC-MS spectrum of product P_2 (dichloro-1, 4-naphthoquione, Table 3.1.9) had molecular ion peak at 274, which corresponds to the molecular formula of $C_{10}H_6Cl_2O_2$. The m/z value 226, could be due to the loss of one chlorine atom, and m/z 191 corresponds to the loss of the

remaining chlorine atom. The mass spectrum of the product P_3 identified to be naphtha (2, 3) oxirene-2, 3-dione (P_3, Table 3.1.9) based on NIST library exhibited m/z at 174, and the loss of two oxygen atoms lead to m/z 164. Further loss of the oxygen atom peak could be seen at m/z 130.(M^{-2}).

Both the products matched well (95%) with the known compounds from the NIST library database. The GC-MS spectra are provided in (Appendix 1, Figure 1.1.1 and Figure 1.1.2).

Table 3.1.9 Plausible oxidation products.

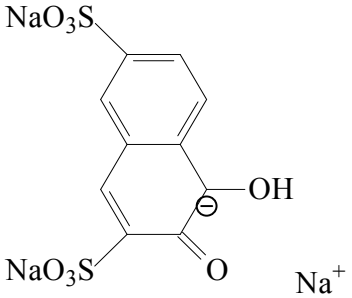 (P_1)	3,4-dihydroxy naphthalene-2,7-disulfonic sodium salt
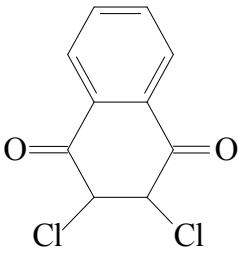 (P_2)	dichloro-1,4-naphthoquione
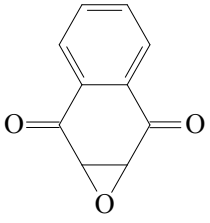 (P_3)	naphtha (2,3) oxirene-2,3-dione

Literature reports show that little is known with certainty about effect of hypochlorite on azo dyes and involved reaction mechanisms, especially in alkaline media.[191,192] In particular about the certainty of the reactions with three oxidant species, HOCl, OCl^- and Cl_2 as they coexist in equilibrium in aqueous solution. Omura *et al.* suggested that upon oxidation of azo dyes isolation of products at low pH revealed the formation of naphthalene and 1,2-naphthoquinone.[193] Elodie *et al*. studied the oxidation of azo dyes such as azo-benzene, methyl orange and *p*-methyl red using electro-fenton process in acidic medium. They demonstrated that the degradation mechanism begins with azo bond cleavage and is followed by the hydroxylation of aromatic rings. The identified products were hydroquinone, 1,4-benzo-quinone, pyrocatechol, nitrocatechol, 1,3,5-trihydroxynitrobenzene, *p*-nitrophenol.[194] As reported in number of articles in literature, the isolation and characterization of reaction products of dyes is complicated by limitations in extraction and separation of products and it's a major challenge as the reaction intermediates are tend to further react or the dye concentrations are too low with the hypochlorite.[195] Oakes *et al.* studied the oxidation of azo dyes by a range of oxidants[196] and they investigated the reactive species responsible for initiating oxidation in alkaline media, and the effect of substituent's on both dye and oxidant using hypochlorite. It was demonstrated that the relevant equilibrium has been shown that HOCl is the active species towards the dye common anion in neutral to alkaline media.[197,198] However they concluded that in acid medium equilibrium results in formation of aqueous chlorine, a powerful electrophile, and acid solutions of hypochlorite generates chlorine and thereby forming chlorinated organic molecules.[199]

Oakes *et.al* also studied the oxidation of azo dye methyl orange I and benzene is reported to be one of the main reaction product with peroxo sulfate which was found to be benzene, by

GC-MS analysis. They suggested that the formation of benzene is probable by hydrogen atom abstraction by phenyl radicals, formed from decomposition of a diazene intermediate. [200]

3.1.10 Stoichiometric equation

All the stoichiometry experiments were carried out using stock hypochlorite concentration of 0.0015 M. The stoichiometry of the reaction was established with 1:1 and 1:5 ratios of amaranth and hypochlorite respectively and the amount of dye and hypochlorite reacted were estimated from the initial and residual amounts. The stoichiometry was found to be approximately 1:3 (± 10%) of AM^- and HOCl. Thus considering the major products identified stoichiometric equation for the overall reaction can be written as,

$$AM^- + 3HOCl + 2H_2O \rightarrow P_1 + P_2 / P_3 + SO_3^{2-} + Na^+ + N_2 + H_3O^+ + 3HCl \qquad (3.1)$$

where P_1 (3,4-dihydroxy naphthalene-2,7-disulfonic sodium salt), P_2 (dichloro-1,4 naphthoquione) and P_3 (naphtha (2,3) oxirene-2,3-dione) products.

3.1.11 Reaction scheme

Based on the identified oxidation products and estimated stoichiometry of reactants the probable mechanistic scheme is illustrated in the Figure 3.1.15.

When hypochlorite or HOCl reacts with amaranth, hydroxy proton on the aromatic ring is lost, leaving negatively charged oxygen, which delocalises onto the aromatic ring and ultimately the nitrogen atom of the azo bond linking the two aromatic rings together. This molecule with negative charge acts as a nucleophile and attacks the oxygen atom of the HOCl resulting in intermediate (I_1). This in turn reacts with H^+ to form another intermediate (I_2).

A water molecule then attacks the electrophilic carbon of the (I_2) resulting in the elimination of water from the nitrogen atom of the azo bond producing (I_3). Cleavage of the C-N bond then occurs, yielding (I_4), with the other negatively charged species picking up proton to yield P_1. A further nucleophilic attack by water on the electrophilic carbon to which the sulfite group is attached, results in loss of a proton and replacement of the sulfite group by a hydroxy group (I_5). The nucleophilic attack of the hypochlorite ion on intermediate (I_5) leads to the formation of another intermediate (I_6) and the release of N_2. The electron rearrangement further yields the quinone intermediate (I_7) and loss of hydrogen chloride. The electrophilic attack of chlorine or HOCl on (I_7), respectively produces either P_2 or P_3.

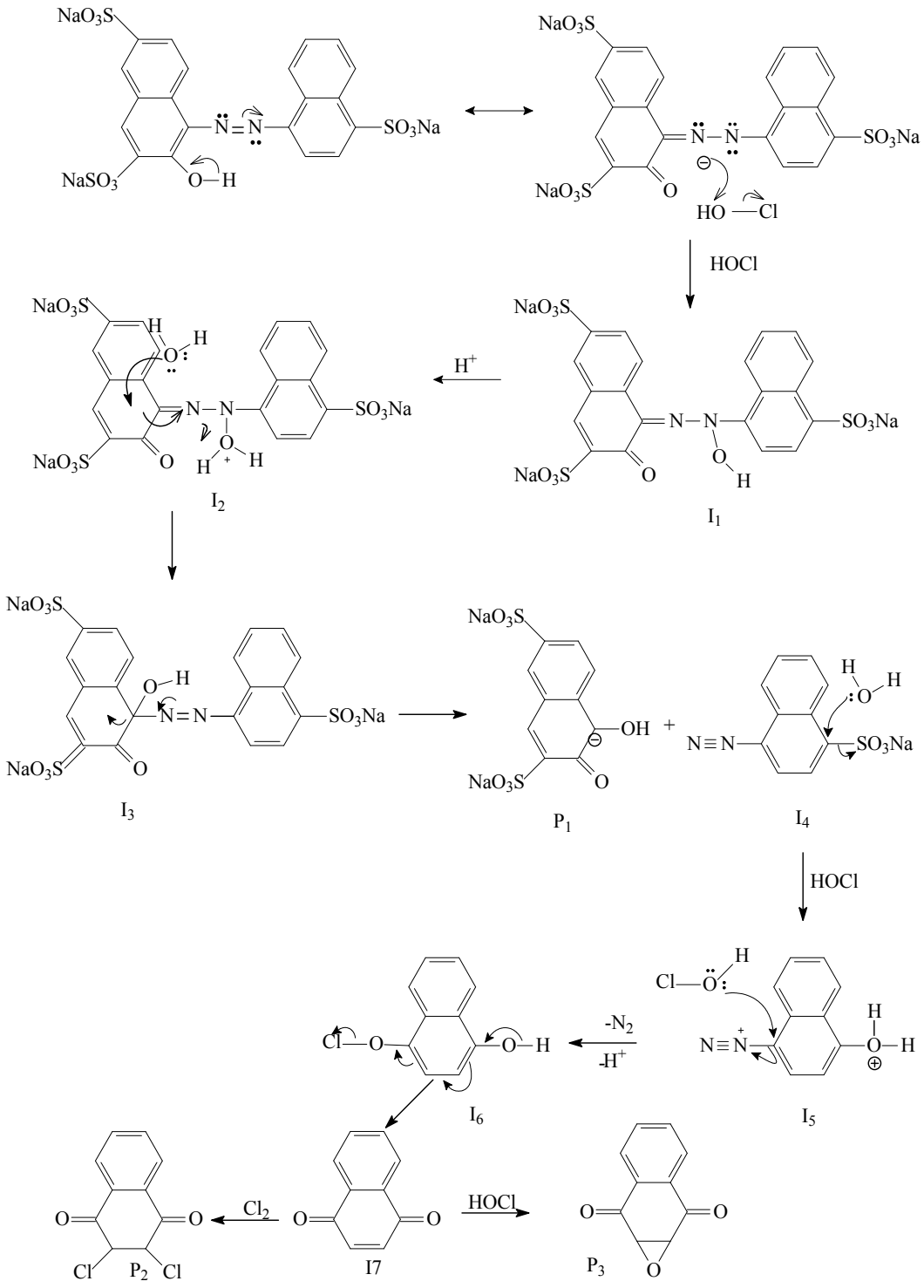

Figure 3.1.15 Mechanistic scheme for the oxidation of amaranth with hypochlorite

3.1.12 Proposed mechanism

Based on reaction stoichiometry estimated, and the major products identified, in agreement with probable reaction scheme for the reaction of amaranth with hypochlorite the reaction mechanism can be expressed in the following steps.

$$H^+ + OCl^- \rightleftharpoons HOCl$$

$$HOCl + Cl^- + H^+ \rightleftharpoons Cl_2 \qquad R1$$

$$AM^- + HOCl \rightarrow I_1 + Cl^- \qquad R2$$

$$I_1 + H^+ \rightarrow I_2^+ \qquad R3$$

$$I_2^+ + H_2O \rightarrow I_3 + H_3O^+ \qquad R4$$

$$I_3 + H_2O + H^+ \rightarrow P_1 + I_4^+ \qquad R5$$

$$I_4^+ + H_2O \rightarrow I_5^+ + Na^+ + SO_3^{2-} + H^+ \qquad R6$$

$$I_5^+ + HOCl \rightarrow I_6 + N_2 + H^+ \qquad R7$$

$$I_6 \rightarrow I_7 + HCl \qquad R8$$

$$I_7 + Cl_2 \rightarrow P_2 \qquad R9$$

$$I_7 + HOCl \rightarrow P_3 + HCl$$

The overall reaction with HOCl is proposed as

$$AM^- + 3HOCl + 2H_2O \rightarrow P_1 + P_2/P_3 + SO_3^{2-} + Na^+ + N_2 + 3HCl \qquad (3.2)$$

3.1.13 Rate law

The rate law expresses the relationship of the reaction rate and the concentrations of the reactions raised to the same power, i.e. the order of the reaction with respect to the respective reactants or products. The kinetic salt effect indicates the possible species involved in the slowest step of the reaction scheme. Thus the proposed reaction scheme should agree with the

experimentally observed reaction orders with respect to the reactants. The first-order dependence of the reaction rate on the reactants and the observed salt effect at pH 9.0 suggests that the rate limiting step involves one each of AM^- and OCl^- ions. Thus the major pathways of the reaction involve HOCl or OCl^- forming possibly an activated complex, which undergoes decomposition, to form the intermediates and products. The intermediates further undergo oxidation to give stable products.

The reactions were studied under *pseudo* first-order conditions. Thus the reaction involves two pathways involving HOCl (fast and major pathway) and OCl^-(slow and minor pathway) Based on this assumption the rate law may be proposed as

$$Rate = k_1[OCl^-][AM^-] + k_2[HOCl]\,[AM^-]$$

$$r = \{k_1[OCl^-] + k_2[HOCl]\}[AM^-] = k'[AM^-] \quad (3.3)$$

Where the *pseudo* first-order const, k' equals to

$$k' = k_1[OCl^-]_o + k_2[HOCl]_o = k'_1 + k'_2 \quad (3.4)$$

where $k_1'$and k_2'were the *pseudo* first-order rate constants corresponding to hypochlorite and hypochlorous acid reactions of the dye. Thus

$$k_1 = \frac{k_1'}{[OCl^-]};\quad k_2 = \frac{k_2'}{[HOCl]} \quad (3.5)$$

3.1.14 Simulations

The simulations were done to establish the probability of the reaction mechanism and to prove that it is the more plausible one. The Simkine 2 was used to simulate the curves using the proposed mechanism and the experimental kinetic data generated in the current studies. The estimated rate constants were optimised to match the simulated curves with the experimental curves. The rate constants were adjusted to manually to test the sensitivity and

importance of the elementary reactions. Table 3.1.10 summarises the elementary steps and rate coefficients finally used for the simulations. Rate constants determined in the present studies employed for C3 and C4. Literature values were used for reactions C1 and C2[201,202] and values C5 to C10 represent the optimised rate constants.

Table 3.1.10 Forward and reverse rate constants obtained from literature and simulations.

Reaction	Reaction Mechanism	Forward rate	Reverse rate
C1	$H^+ + OCl^- \rightleftharpoons HOCl$	$3.97 \times 10^{-4}\ M^{-1}s^{-1}$	$1.0 \times 10^{-4}\ s^{-1}$
C2	$HOCl + Cl^- + H^+ \rightleftharpoons Cl_2$	$3.63 \times 10^{-3}\ M^{-1}s^{-1}$	$1.1\ s^{-1}$
C3	$AM^- + HOCl \rightarrow I_1 + Cl^-$	$2.3 \times 10^{1}\ M^{-1}s^{-1}$	--
C4	$AM^- + OCl^- \rightarrow I_1^- + Cl^-$	$1.88 \times 10^{1}\ M^{-1}s^{-1}$	--
C5	$I_1 + H^+ \rightarrow I_2^+$	$4.30 \times 10^{9}\ M^{-1}s^{-1}$	--
C6	$I_1^- + 2H^+ \rightarrow I_2^+$	$4.15 \times 10^{9}\ M^{-2}s^{-1}$	--
C7	$I_2^+ \rightarrow P_1 + I_5^+ + Na^+ + SO_3^{2-} + H^+$	$3.01 \times 10^{8}\ s^{-1}$	--
C8	$I_5^+ + HOCl \rightarrow I_7 + N_2 + H^+$	$6.49 \times 10^{9}\ M^{-1}s^{-1}$	--
C9	$I_7 + Cl_2 \rightarrow P_2$	$4.35 \times 10^{8}\ M^{-1}s^{-1}$	--
C10	$I_7 + HOCl \rightarrow P_3 + HCl$	$3.17 \times 10^{8}\ M^{-1}s^{-1}$	--

The speciation of OCl^- in presence of acid is shown by the equation C1. The rate limiting step of the oxidation mechanism involves the steps initiated by OCl^- or HOCl on AM^- leading to the formation of the reactive intermediate. (Reactions C3 and C4 are the rate-determining steps for amaranth oxidation). Reactions C5 to C10 show the consecutive steps for further oxidation of the reactive intermediates by different species and C7, C9 and C10 representing the reactions leading to different probable products.

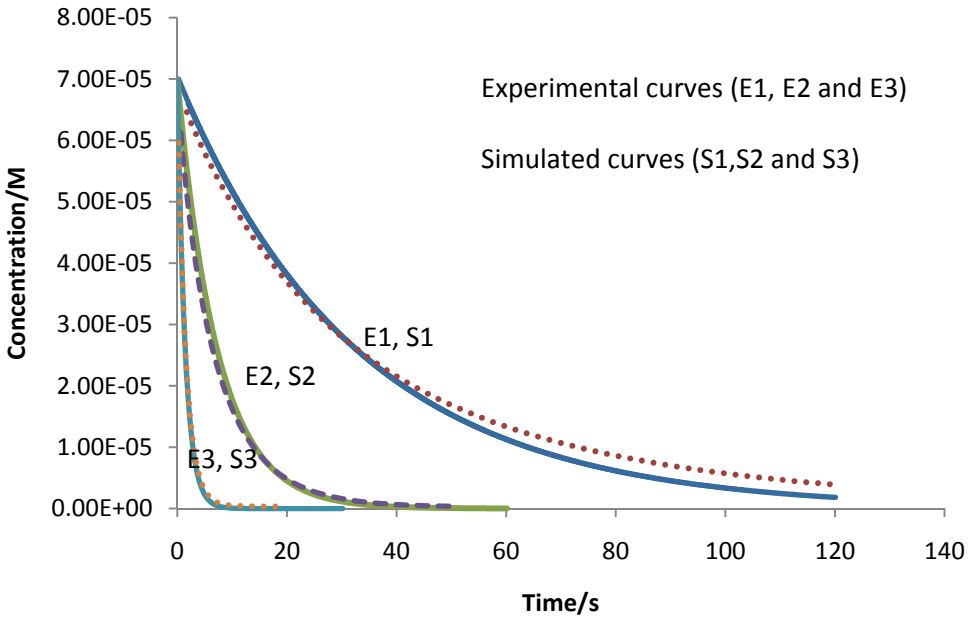

Figure 3.1.16 Experimental curves *versus* simulated curves for reaction of $[AM^-]_0$ (7.0 x 10^{-5} M) with $[OCl^-]_t$ (1.45x10^{-3} M).

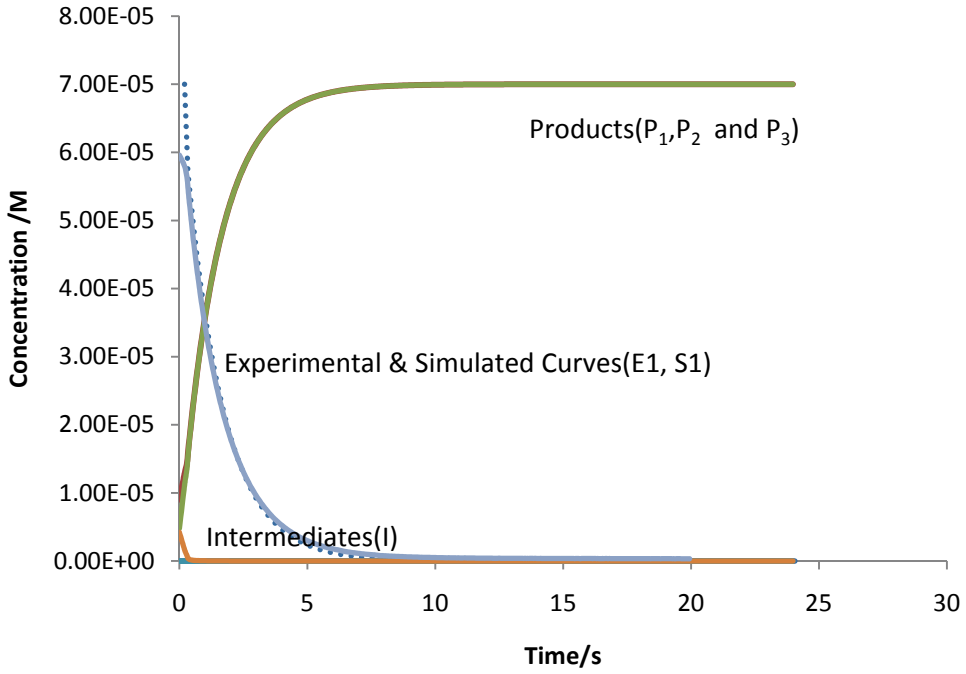

Figure 3.1.17 Intermediates and product formation for the reaction of amaranth with hypochlorite.

Figure 3.1.17 (conditions similar to curves in Figure 3.1.16), curves E1 and S1 shows the experimental and simulated curves for the reaction of AM^- with OCl^-. P_1, P_2 and P_3 show the product formation and I indicate the intermediates formed during the process. A fair agreement between the experimental and corresponding simulated curves, (Figure 3.1.16) strongly support the proposed reaction scheme as most probable to explain the intricate reaction mechanism between amaranth and hypochlorite. The simulations also support the assumption that under low pH conditions, HOCl is the crucial reactive intermediate to drive the rapid kinetics, rather than OCl^-. The concentration versus time data for all the reactants, and products and selected reaction intermediates for the experimental and simulated curves tabulated (Appendix 1, Table 1.1, and Table 1.2).

3.2 Reaction between brilliant blue and hypochlorite

3.2.1 Order with respect to brilliant blue-R

The kinetic measurements for the consumption of brilliant blue-R (BB^+) were conducted with low concentrations of dye and excess of all other reagents and the progress of depletion was monitored at 555 nm the maximum absorption corresponding to dye using stopped flow technique. At the absorption maxima, no interference from products or intermediates was observed. Figure 3.2.1 shows the typical depletion curve of brilliant blue. Perusal of the curve shows that a typical reaction is completed in 80 seconds.

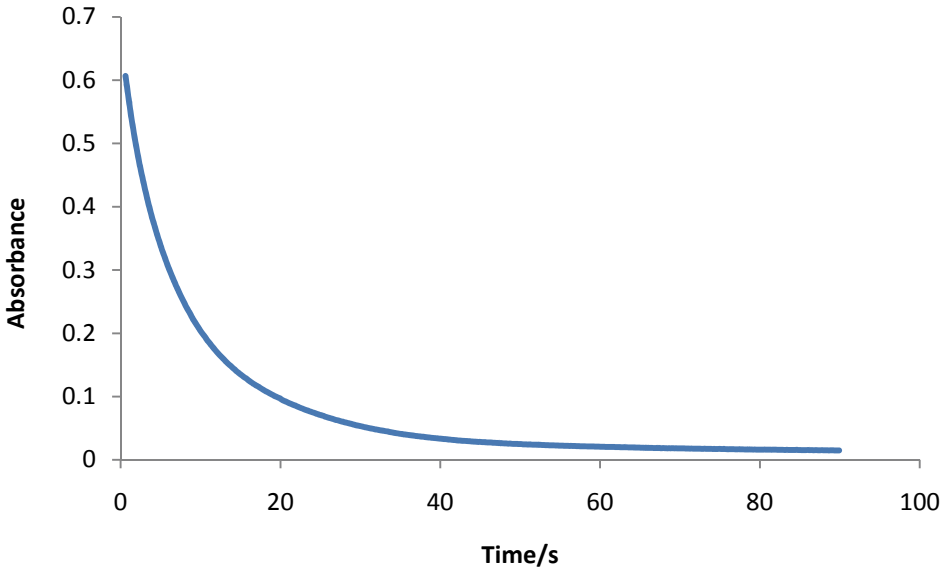

Figure 3.2.1 Typical kinetic curve - absorbance *versus* time plot for the reaction of $[BB^+]_0$ (7.0×10^{-5} M) with $[OCl^-]_t$ (1.5×10^{-3}) at pH = 9.0 and 555 nm.

The kinetic data acquired at single wavelength was analysed by employing the KinetAsyst^{TM} software using the first-order rate equation to estimate the *pseudo* first-order rate constants.

3.2.2 Analysis of kinetic data using KinetAsyst^{TM} Fit software

A KinetAsyst^{TM} fit for the first-order reaction using the rate equation was run and the generated curve fits quite well along with the experimental curve. Figure 3.2.2 illustrates

both experimental and generated curves and the absorbance *versus* time data. While the upper curve shows the fit between the theoretical and experimental curves, the lower plot indicates the residuals illustrating good agreement between the two curves.

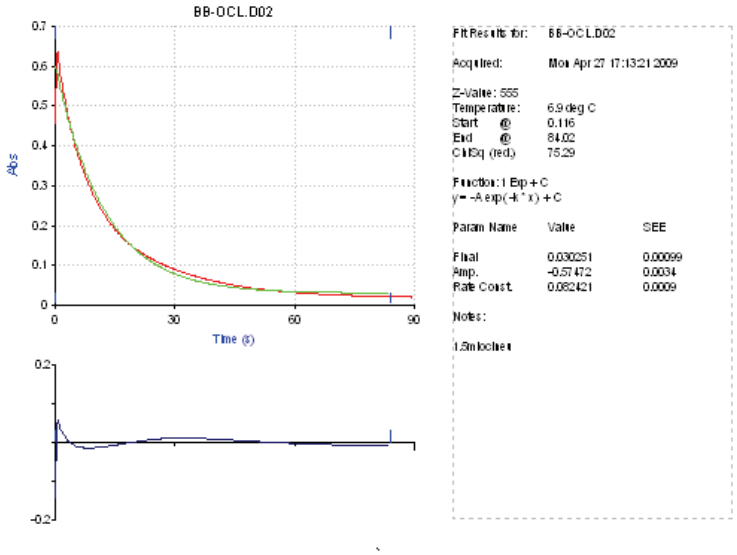

Figure 3.2.2 KinetAsyst^{TM} single -exponential equation fit (green) and the experimental curve (red) with residuals shown in the (lower curve) and the rate parameters in the adjacent box for the reaction of $[BB^{+}]_0$ (7.0×10^{-5} M) with $[OCl^{-}]_t$ (1.5×10^{-3} M).

The fit results for the above curve shows that the rate constant obtained using first-order rate equation is ($0.082 \pm 9.0 \times 10^{-5}$) s^{-1}, illustrates that the reaction follows *pseudo* first-order kinetics, and the order with respect to dye is unity.

3.2.3 Order with respect to hypochlorite

To establish the order with respect to oxidant, experiments were done using different initial concentrations of hypochlorite at constant ionic strength (pH 9.0). As the initial concentration of hypochlorite increased, the rate of depletion of dye also increased significantly. Figure 3.2.3 represents the typical curves of depletion of BB^{+} as function of time monitored at

555 nm for different initial concentrations of hypochlorite. The absorbance *versus* time plots is illustrated in Figure 3.2.3.

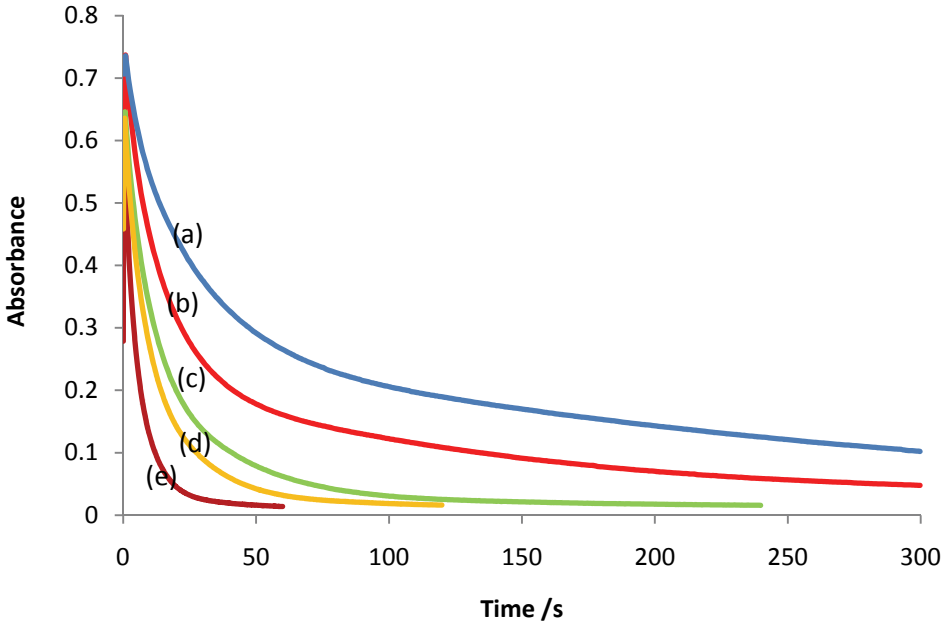

Figure 3.2.3 Depletion of brilliant blue with various hypochlorite concentrations for the reaction of $[BB^{+}]_0$ (7.0 x 10^{-5} M) with $[OCl^{-}]_t$ x 10^{-3}/M (a = 0.73 b = 1.45, c = 2.18 , d = 2.90 and e = 4.35) at pH 9.0.

Different concentrations of hypochlorite reactions with the substrate with their theoretical curves and residues are shown in Figure 3.2.4, a perusal of the curves from a to e in Figure 3.2.4 indicates that experimental and theoretical curves match well with small residues and the k' values were obtained by analysing the respective kinetic curves are also summarised.

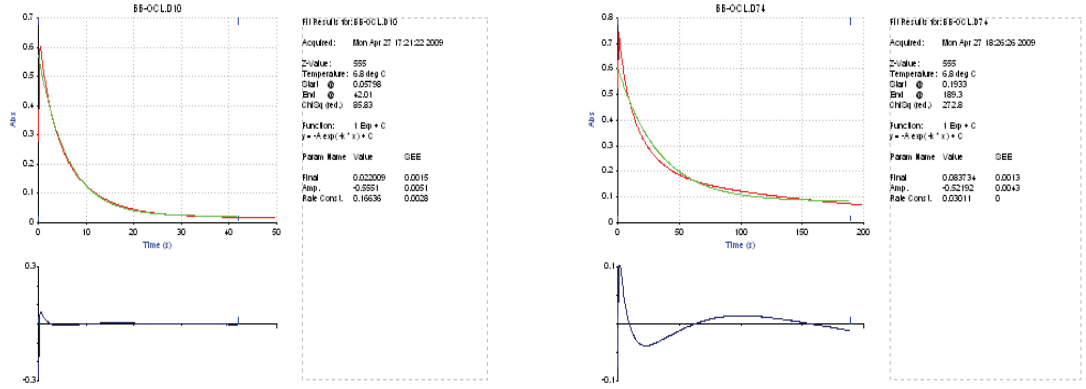

(a) (b)

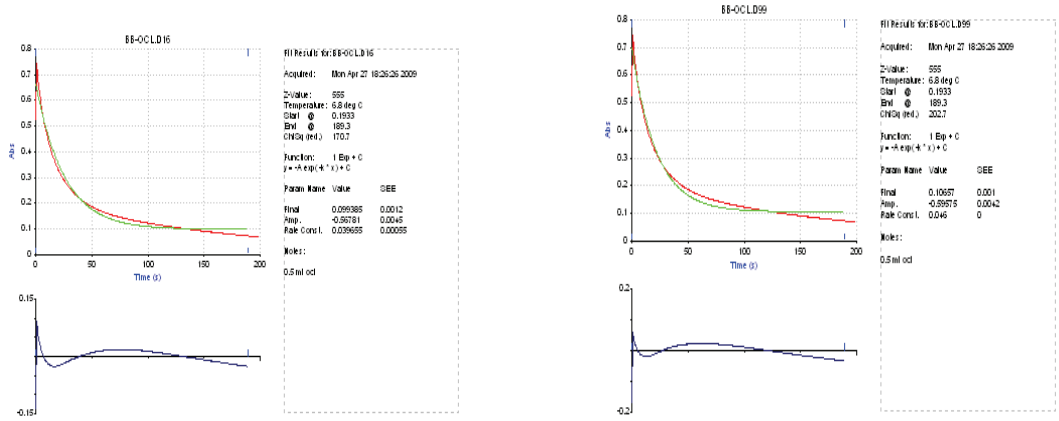

(c) (d)

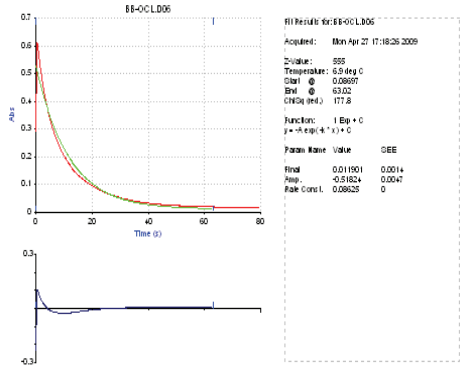

(e)

Figure 3.2.4 Fits using KinetAsyst^{TM} single-exponential equation, and rate equation {1 Exp + C, y = -A exp (-k * x) + C} (where k'/s^{-1} a = 0.12, b= 0.030, c = 0.037, d = 0.046 and e = 0.086).

Table 3.2.1 shows the corresponding *pseudo* first-order rate coefficients, k' for different hypochlorite concentrations.

Table 3.2.1 The reaction between brilliant blue and hypochlorite at constant ionic $[BB^+]_0$ (7.0×10^{-5} M), $[OCl^-]_t$ ($0.725 \times 10^{-3} - 4.35 \times 10^{-3}$ M), pH = 9.0 (I = 0.128 M).

$[OCl^-]_t / 10^{-3}$ M	k'/s^{-1*}
0.73	0.012
1.45	0.030
2.18	0.037
2.90	0.046
4.35	0.086

* Mean of four replicate experiments with relative standard deviation < 4%

A perusal of the data in table 3.2.1 shows that the first-order rate increased proportionately to the increase in hypochlorite concentration. To establish the order with respect to the hypochlorite, ln $[OCl^-]_t$ *versus* ln k' values obtained were plotted in Figure 3.2.5, which resulted in a straight-line with slope 1.03 (R^2 = 0.97) suggesting that order with respect to hypochlorite at pH 9.0 is one.

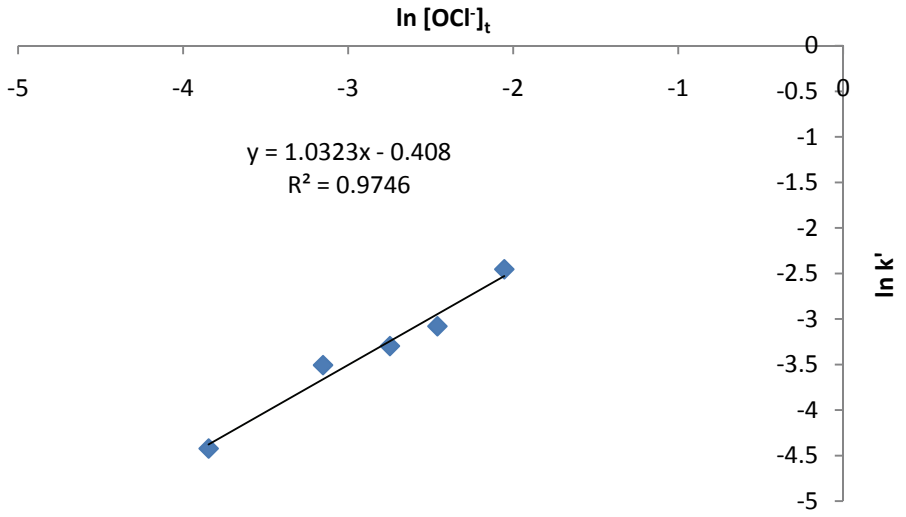

Figure 3.2.5 Plot of ln $[OCl^-]_t$ *versus* ln k' for the reaction of $[BB^+]_0$ (7.0×10^{-5} M) with $[OCl^-]_t$ ($0.725 \times 10^{-3} - 4.35 \times 10^{-3}$ M) at pH = 9.0 and I = 0.128 M.

3.2.4 Effect of pH on the reaction rate

The pH has significant influence on the relative formation of OCl^- and HOCl species. The shift in the equilibrium is greatly influenced by acid concentration. To assess the role of acid in the oxidation process, the kinetics of the reaction as function of pH was investigated. Figure 3.2.6 illustrates the plot of the k' *versus* corresponding pH values.

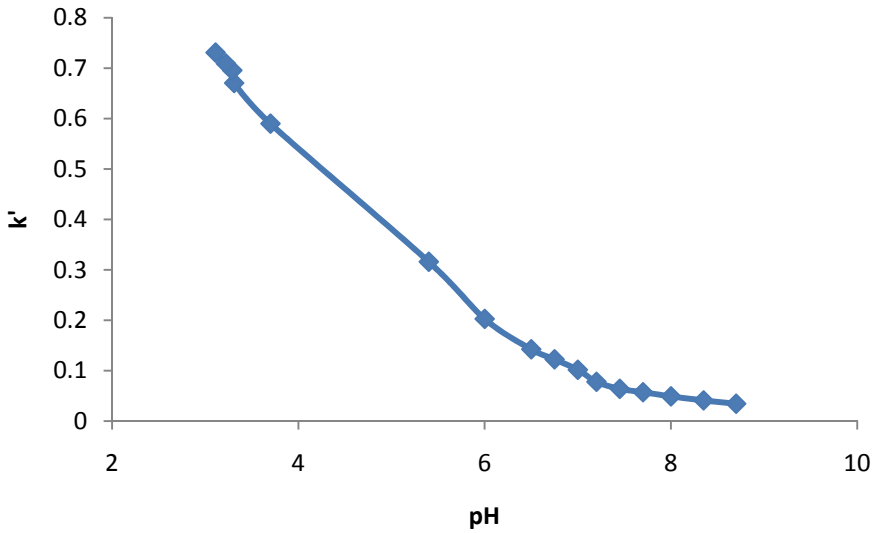

Figure 3.2.6 Plot of k' *versus* pH for the reaction of $[BB^+]_0$ (7.0×10^{-5} M) with $[OCl^-]_t$ (1.45×10^{-3} M) with $[H^+]_e$ (1.99×10^{-9} - 7.752×10^{-4} M)

A perusal of the Figure 3.2.6 shows that the increase in k' values was small at low acid concentrations and while the increase was higher at higher acid concentrations pH below 7.0 onwards indicating the profound effect of pH on the reaction.

The *pseudo* first-order rate constants obtained for different pH values were shown in Table 3.2.2.

Table 3.2.2 Effect of pH on the reaction rate.

pH	k'/s^{-1} *
9.00	0.0347
8.70	0.0345
8.35	0.0411
8.00	0.0491
7.70	0.0574
7.45	0.0640
7.20	0.0780
7.00	0.1018
6.75	0.1226
6.50	0.1425
6.00	0.2027
5.40	0.3160
3.70	0.5900
3.31	0.6704
3.29	0.6955
3.22	0.7093
3.11	0.7309

* Mean of four replicate experiments with relative standard deviation < 4%

Further, to establish the order with respect to acid, the ln k' *versus* ln $[H^+]$ values were plotted (Figure 3.2.7), which gave a slope 0.24 ($R^2 = 0.98$). The observed partial reaction order with respect to acid clearly suggests that reaction mechanism is intricate and acid is indirectly involved in the rate limiting step.

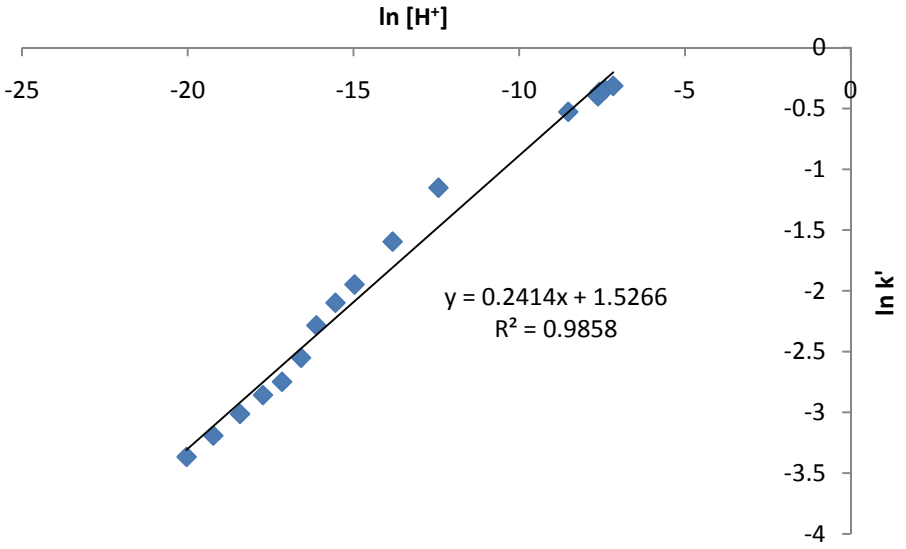

Figure 3.2.7 Plot of ln k' *versus* ln $[H^+]$ for the reaction of $[OCl^-]_t$ (1.45×10^{-3} M) with $[BB^+]_0$ (7.0×10^{-5} M) at $[H^+]_{eq}$ (1.99×10^{-9}- 7.752×10^{-3} M).

From Figure 3.2.7 the observed order with respect to H^+ is small suggesting that the reaction rate observed is the resultant effect of the acid in the concentrations of hypochlorite and hypochlorous acid. The kinetic data was further analysed to estimate the *pseudo* first-order rate constants for the two competitive reactions that are facilitated by hypochlorite ion and hypochlorous acid respectively, using two simultaneous first-order reactions using KinetAsyst^{TM} analysis.

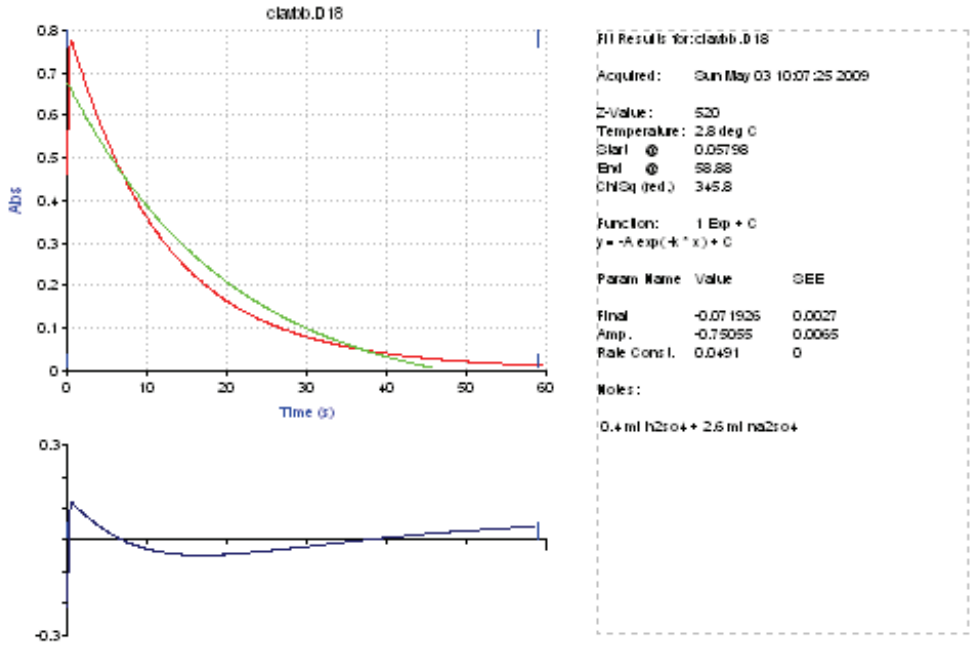

Figure 3.2.8 KinetAsyst^{TM} single-exponential equation fit of two curves and residuals (lower sketch) for the reaction of $[BB^{+}]_0$ (7.0 x 10^{-5} M) with $[OCl^{-}]_t$ (1.45 x 10^{-3} M) $[H^{+}]_0$ (9.96 x 10^{-9} M) and I (0.13 M).

For comparison, the theoretical fits for occurrence of single first-order reaction and two simultaneous first-order reactions are shown in Figure 3.2.8 and Figure 3.2.9 respectively. An examination of the curves shows that Figure 3.2.9 has lower residuals compared to Figure 3.2.8, confirming the occurrence of two simultaneous reactions.

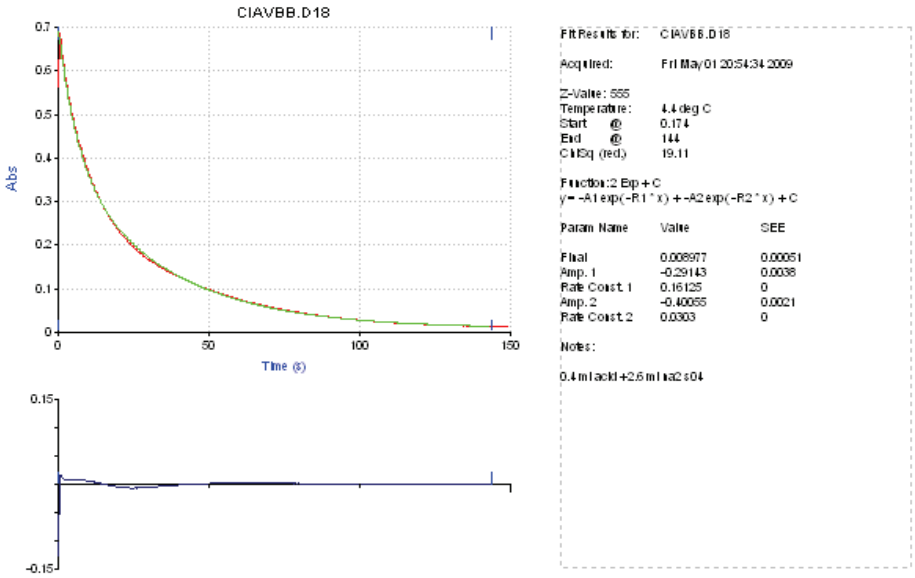

Figure 3.2.9 KinetAsyst^{TM} double-exponential equation fit of two curves and residuals for two competitive first-order reactions (lower sketch) for the reaction of $[BB^{+}]_0$ (7.0 x 10^{-5} M) with $[OCl^{-}]_t$ (1.45 x 10^{-3} M), $[H^{+}]_0$ (9.96 x 10^{-9} M) and I (0.12 M).

The calculated equilibrium concentrations for H^{+}, OCl^{-} and HOCl, and the *pseudo* first-order rate constants for hypochlorite k_1' and hypochlorous acid k_2' at different pH values are summerised in Table 3.2.3.

A perusal of Table 3.2.3 shows that k_1' is much smaller in magnitude than k_2'. While k_1' values had a decreasing trend, k_2' recorded an increasing trend. This is predictable considering the changes i.e. decrease in $[OCl^{-}]$ and increase in [HOCl] with increasing acid concentration. The mean values of second order rate constants, 1.2 ± 0.2 M^{-1} s^{-1}, 22.0 ± 1.2 M^{-1} s^{-1} shown in Table 3.2.3 represent the k_1 and k_2 values respectively, which are the respective second-order coefficients for the OCl^{-} and HOCl initiated oxidations.

Table 3.2.3 Effect of acid on the speciation of hypochlorite and reaction rate.

pH	$[H^+]$	$[OCl^-]_{eq}$	$[HOCl]_{eq}$	k_1'/s^{-1} *	k_2'/s^{-1} *	$k_1/M^{-1}s^{-1}$	$k_2/M^{-1}s^{-1}$
8.70	1.99×10^{-9}	2.76×10^{-2}	1.34×10^{-3}	0.0390	0.0270	1.41	20.08
8.35	4.45×10^{-9}	2.61×10^{-2}	2.85×10^{-3}	0.0360	0.0610	1.37	21.43
8.00	9.97×10^{-9}	2.33×10^{-2}	5.68×10^{-3}	0.0303	0.1400	1.29	24.64
7.70	1.99×10^{-8}	1.95×10^{-2}	9.49×10^{-3}	0.0250	0.2050	1.28	21.61
7.45	3.54×10^{-8}	1.55×10^{-2}	1.34×10^{-2}	0.0190	0.2799	1.22	20.81
7.20	6.29×10^{-8}	1.14×10^{-2}	1.76×10^{-2}	0.0135	0.3670	1.18	20.88
7.00	9.97×10^{-8}	8.43×10^{-3}	2.06×10^{-2}	0.0094	0.4275	1.12	20.79
6.75	1.77×10^{-7}	5.43×10^{-3}	2.36×10^{-2}	0.0060	0.4930	1.10	20.92
6.50	3.15×10^{-7}	3.32×10^{-3}	2.57×10^{-2}	0.0035	0.5390	1.05	21.00
6.00	9.98×10^{-7}	1.14×10^{-3}	2.79×10^{-2}	0.0011	0.5880	1.00	21.11
5.40	3.97×10^{-6}	2.94×10^{-4}	2.87×10^{-2}	0.0002	0.6459	0.84	22.50
3.70	1.99×10^{-4}	5.95×10^{-6}	2.90×10^{-2}	--	0.6582	--	22.70
3.31	4.89×10^{-4}	2.42×10^{-6}	2.90×10^{-2}	--	0.6652	--	22.94
3.29	5.12×10^{-4}	2.32×10^{-6}	2.90×10^{-2}	--	0.6725	--	23.19
3.22	6.02×10^{-4}	1.97×10^{-6}	2.90×10^{-2}	--	0.6842	--	23.59
3.11	7.75×10^{-4}	1.53×10^{-6}	2.90×10^{-2}	--	0.6910	--	23.83
Mean and standard deviation						1.2 ± 0.2	22.0± 1.2

* Mean of four replicate experiments with relative standard deviation < 4%

where k_1' and k_2' *pseudo* first-order rate constants with respect to OCl^- and HOCl respectively. $k_1 = k_1'/[OCl^-]_{eq}$ and $k_2 = k_2'/[HOCl]_{eq}$, where k_1 and k_2 represents the second-order reaction rates for OCl^- and HOCl competitive reactions.

At pH below 3, no significant increase in rate constant was observed with increase in acid concentration which anticipated at that pH as all OCl^- will be in the form of HOCl, a further increase in the acid concentration does not increase the HOCl concentration. Figure 3.2.10

and Figure 3.2.11 represents the order with respect to OCl^- and HOCl in the pH range from 3.0 to 9.0

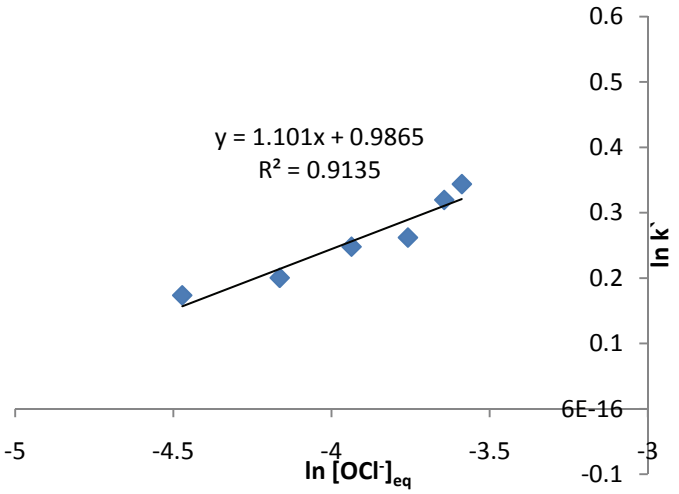

Figure 3.2.10 Plot of ln k' *versus* ln $[OCl^-]_{eq}$ for the reaction of $[BB^+]_0$ (7.0×10^{-5} M) with $[OCl^-]_t$ (1.45×10^{-3} M) at $[H^+]_{eq}$ (3.97×10^{-6} - 7.75×10^{-3} M), $[OCl^-]_{eq}$ (1.14×10^{-3} – 1.53×10^{-6} M).

The ln-ln plot of k_1' *versus* $[OCl^-]_{eq}$, a fair straight line with gradient equal to 1.1 (Figure 3.2.10) suggests that order with respect to hypochlorite is one. At low pH, the concentration of hypochlorite reduces to small values, where the *pseudo* first-order conditions with respect to dye are no more valid. Hence for such conditions, k_1' values were not estimated or that data was not taken into consideration.

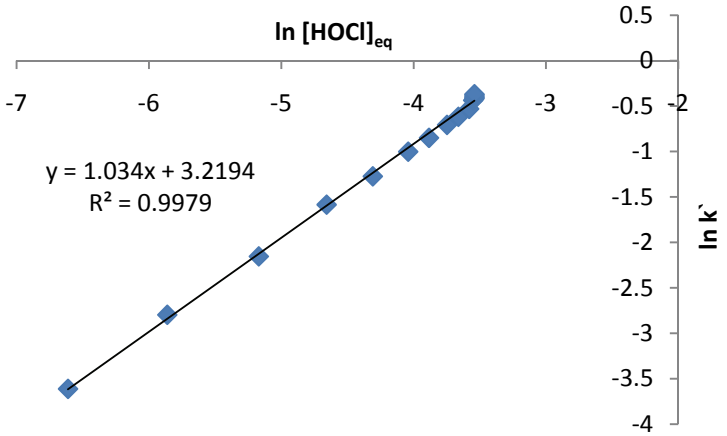

Figure 3.2.11 Plot of ln k' *versus* ln $[HOCl]_{eq}$ for the reaction of $[BB^+]_0$ (7.0×10^{-5} M) with $[OCl^-]_t$ (1.45×10^{-3} M) at $[H^+]_{eq}$ (1.99×10^{-9}- 9.98×10^{-7} M), $[HOCl]_{eq}$ (2.76×10^{-2} – 3.3×10^{-6} M).

Figure 3.2.11, a plot of ln $[HOCl]_{eq}$ *versus* ln k' gave a linear curve with slope 1.034, suggesting that reaction is predominantly between the HOCl and dye and the reaction has first-order dependence on HOCl concentration.

Although at alkaline pH the reaction order with respect to OCl^- is one, an observation of Figure 3.2.11 indicates that at neutral pH, the change in rate constant is negligible due to low concentration of OCl^- at that pH. Thus, its contribution to overall reaction remains small.

The obtained results confirm that acid is not directly involved in the rate limiting reaction for the oxidation of brilliant blue, but it influences the speciation and equilibrium of OCl^- to HOCl. The observed decrease in reaction order with increasing $[H^+]$ confirms that observed reaction rate is resultant effect of the reactions of BB^+ with hypochlorite and hypochlorous acid, but with minor contribution of hypochlorite at lower pH.

3.2.5 Primary salt effect

The influence of added salt on the reaction was studied and the results are summerised in Table 3.2.4. An observation of results show an increasing ionic strength had negative salt effect on both OCl^- and HOCl initiated reactions. The plot of log k' *versus* $I^{1/2}$ of the data obtained gave a linear curve (A) with negative slope = 1.03 and R^2 = 0.99 (Figure 3.2.12) Suggesting a negative salt effect with reacting species of opposite charges, possibly BB^+ and OCl^- ions. The slope corresponds to linear curve B (0.745; R^2 = 0.99) corresponds to that of the reaction between HOCl and BB^+.

Table 3.2.4 Effect of ionic strength on the reaction rate $[OCl^-]_t$ (1.45 x 10^{-3} M), $[BB^+]_0$ (7.0 x 10^{-5} M), pH = 9.0.

Ionic strength/M	k_1'/s^{-1}*	k_2'/s^{-1} *
0.0099	0.035	0.0452
0.0188	0.035	0.0459
0.0225	0.037	0.0471
0.0263	0.038	0.0485
0.0338	0.040	0.0499

* Mean of four replicate experiments with relative standard deviation < 4%

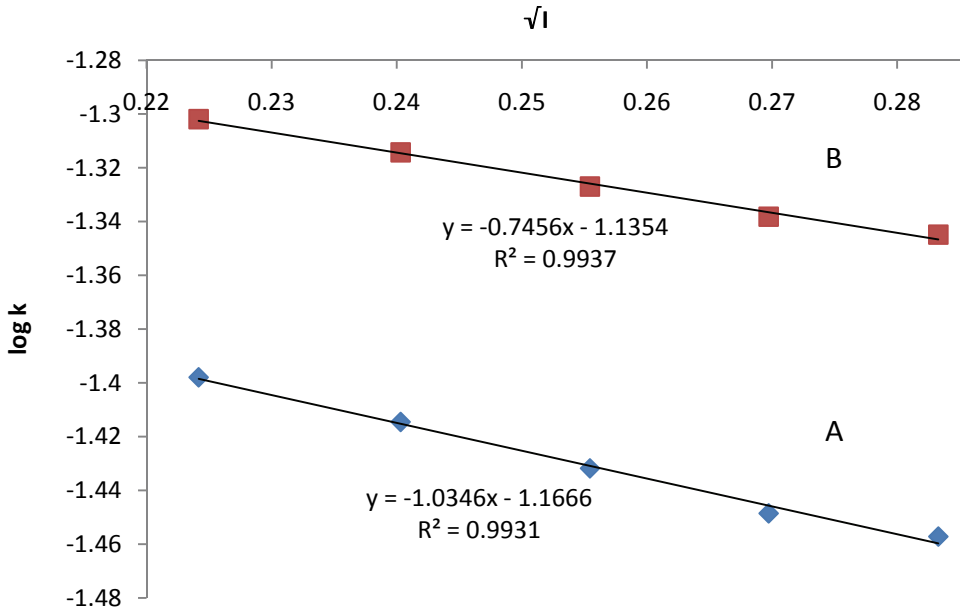

Figure 3.2.12 Plot of log k' *versus* ionic strength for the reaction of $[OCl^-]_t$ (1.45 x 10^{-3} M), with $[BB^+]_0$ (7.0 x 10^{-5} M) at pH = 9, ionic strength (I = 0.01-0.03 M). (A- OCl initiated, B- HOCl initiated reaction)

3.2.6 Kinetic salt effect at acidic pH

Experiments were conducted to investigate the salt effect under acidic conditions. At pH 3.1 with negligible amount of hypochlorite, main reaction is anticipated between the protonated

dye and HOCl if it is true, salt effect will be less pronounced. The k' values obtained are shown in Table 3.2.5.

Table 3.2.5 Effect of Ionic Strength on the reaction rate for the reaction of $[BB^+]_0$ (7.0 x 10^{-5} M), $[OCl^-]_t$ (1.45 x 10^{-3} M), pH = 3.1.

Ionic strength/M	k'/s^{-1} *
0.0510	1.61
0.0547	1.57
0.0585	1.55
0.0622	1.53
0.0697	1.50

* Mean of four replicate experiments with relative standard deviation < 4%

If the reaction is between neutral species (HOCl) and BB^+ there should be linear relationship between log k' and I but plot of log k' *versus* √I from Table 3.2.5 did not give a good straight line as anticipated and the obtained slope is -0.77, therefore the k' *versus* respective ionic strength values were plotted, which is a linear curve suggesting that the rate limiting step possible involves a neutral species (Figure. 3.2.13).

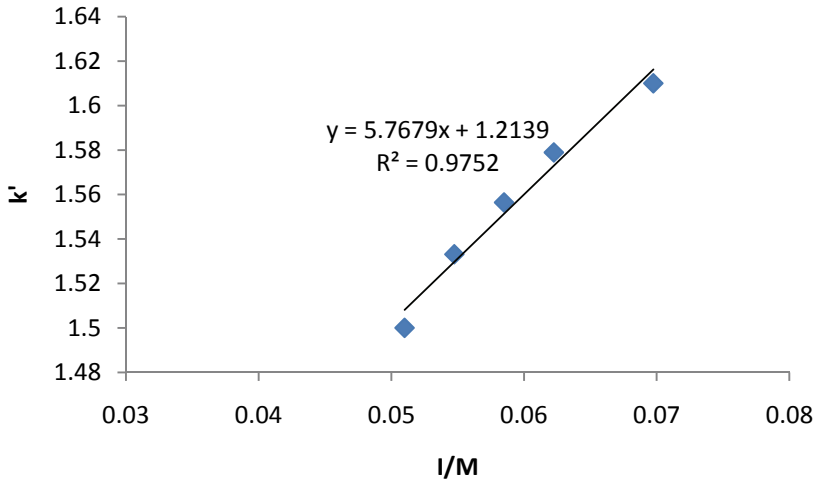

Figure 3.2.13 Plot of k *versus* I (Ionic strength) for the reaction of $[BB^+]_0$ (7.0 x 10^{-5} M) with $[OCl^-]_t$ (1.45 x 10^{-3} M) at varying ionic strength, I (0.051-0.069 M) at fixed acid $[H^+]$ (4.5 x 10^{-3} M) at pH 4.0.

3.2.7 Effect of chloride on reaction rate

To investigate the effect of chloride on the reaction, rates were measured with different amounts of initially added chloride in the reaction, while other conditions maintained the same. The observed rate constants suggest that chloride is not involved in any possible reaction.

Table 3.2.6 Effect of addition of chloride ions on the reaction. $[BB^+]_0$ (7.0×10^{-5} M), $[OCl^-]_t$ (1.45×10^{-3} M) $[Cl^-]$ (1×10^{-1} M).

$[Cl^-]$/M	k'/s^{-1} *
0.000	0.125
0.148	0.126
0.298	0.126
0.447	0.126
0.597	0.127
0.725	0.127

* Mean of four replicate experiments with relative standard deviation < 4%

A perusal of the results in Table 3.2.6 suggests that presence of chloride ion has marginal effect on the reaction rate.

3.2.8 Activation parameters

The energy parameters for the reactions of dye with HOCl and OCl^- were estimated by measuring the rate constants over the temperature range of 15 °C to 35 °C. Table 3.2.7 summarises the calculated values of four energy parameters, namely the energies of activation, enthalpy and entropy for both the reactions (Table 3.2.8). A typical Arrhenius plot shown in Figure 3.2.14, suggests that effect of temperature on the two reactions was not the same.

Table 3.2.7 Rate constants for the BB^+ oxidation as function of temperature for the reaction of $[BB^+]_0$ (7.0×10^{-5} M), $[OCl^-]_t$ (1.45×10^{-3} M) at pH 9.0.

Temp. / K	k_1'/s^{-1} *	$k/M^{-2}\,s^{-1}$	k_2'/s^{-1} *	$k/M^{-2}\,s^{-1}$
283	0.014	1.21	0.041	3.56
288	0.019	1.65	0.058	5.04
293	0.028	1.65	0.064	5.56
298	0.033	2.86	0.079	6.86
303	0.037	3.21	0.098	8.52

* Mean of four replicate experiments with relative standard deviation < 4%

and $k = k'/[OCl^-]\,[H^+]$

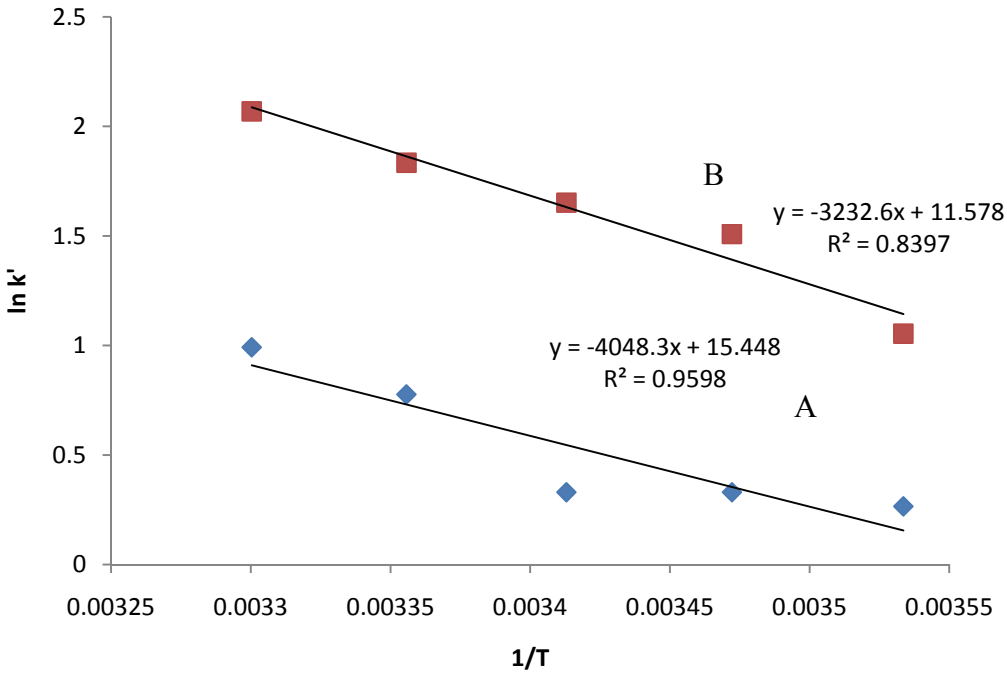

Figure 3.2.14 Plot of ln k' *versus* 1/T for the reaction of with $[BB^+]_0$ (7.0×10^{-5} M) with $[OCl^-]_t$ (1.45×10^{-3} M) at varying temperature conditions. (A-OCl initiated, B-HOCl initiated reaction)

Table 3.2.8 Energy parameters.

Reaction pathway	Enthalpy of reaction, $\Delta H^{\ddagger}$/kJ mol^{-1}	Entropy of activation, $\Delta S^{\ddagger}$/JK^{-1} mol^{-1}	Energy of activation E_a/kJ mol^{-1}
BB^+ with OCl^-	33.05	-191.93	35.53 ± 0.09
BB^+ with HOCl	26.80	-204.57	29.28 ± 0.09

The $\Delta H^{\ddagger}$ values are found to be 33.05 kJ mol^{-1} and 26.80 kJ mol^{-1} for the OCl^- and HOCl initiated reactions respectively. The HOCl initiated reaction had slightly lower energy of activation (29.28 ± 0.09 kJ mol^{-1}) compared to (35.53 ± 0.09 kJ mol^{-1}) the OCl^- initiated reaction. The observed entropy of activation $\Delta S^{\ddagger}$ -191.93 for OCl ion initiated reaction and -204.57 for HOCl initiated reaction suggest that the formed activated complex is relatively of compact nature.

3.2.9 Product identification and characterization

BB-OCl reaction product obtained after dichloromethane extraction (0.64 g) was chromatographed using silica gel (Merck 9385) as the stationary phase on a 4 cm diameter column. The mobile phase consisted of hexane: dichloromethane step gradient (100% hexane (fractions 1-10), 10% dichloromethane in hexane (fractions 11-20), 30% dichloromethane in hexane (fractions 21- 38), 50% dichloromethane in hexane (fraction 40-57) and 80% dichloromethane (fraction 58-64). Fractions of 10 mL were collected in each step. From these fractions total of four major compounds were separated namely products (P_1 = 4-ethoxy-phenylamine, P_2 = 3-ethylaminomethyl-benzenesulfonic acid, P_3 = 3- ethylamino chloro methyl-benzene sulfonic acid and P_4 = 4-[bis-(4-hydroxy-phenyl)-methylene]-cyclohexa-2,5-hydroxide). The products P_2, P_3 and P_4 were identified in the current study. Plausible oxidation products are shown Table 3.2.9.

Proton NMR of product P_2 (3-ethylaminomethyl-benzenesulfonicacid) showed appearance of aromatic protons between δ 7.50 and δ 8.01 which integrates to the three protons of the aromatic ring, and methyl and methylene protons at δ 3.83 and δ 4.12 respectively (Appendix 1, Figure 1.1.5). In the ^{13}C spectrum, the aromatic peaks are found in between δ 116 -168. The aromatic carbons in the ^{13}C spectra can be seen between δ 130 and 150. The ethyl group can be seen at δ 2.15 and triplet methyl at δ 0.9 (Appendix 1, Figure 1.1.6). From GC-MS spectrum corresponding molecular ion peak with retention time 13.99 min could be found at m/z 216 (M^{+1}) representing the molecular formula of $C_9H_{13}NO_3S$ (Appendix 1, Figure 1.1.7) From the product, loss of sulfonyl and ethyl group leads to the fragment with a molecular mass of m/z 107 which accounts to the molecular formula (C_7H_9N).

Proton NMR of the identified product P_3 revealed that appearance of triplet and quartet for methyl and methylene group at lower δ 0.92 and higher δ 2.29 respectively. The protons of the methylene group which serves as bridge between phenyl ring and tertiary nitrogen is seen at higher δ 3.81 due to deshielding effect of substitutions. All aromatic protons are seen between δ 7.0-7.65 (Appendix 1, Figure 1.1.8). The ^{13}C-NMR exhibited appearance of methyl and methylene carbons at δ 13.71 and δ 37.37 respectively. Higher δ 64.7 value for methylene carbon is observed due to deshielding effect between phenyl and tertiary nitrogen. Aromatic carbons are observed between δ 130.96 – 144.63 (Appendix 1, Figure 1.1.9). The GC-MS of product P_3 showed m/z at 249 (M^{+1}) at 14.2 min, which is in good agreement with molecular formula of the identified product P_3 ($C_9H_{12}NO_3ClS$). The other significant peaks at m/z = 215 corresponds to loss of chlorine from product. Molecular mass of m/z 107.2

corresponds to the loss of ethyl and sulfonyl groups which accounts to the molecular formula (C_7H_9N) (Appendix 1, Figure 1.1.10).

The proton NMR spectra of product P_4 exhibits the resonances at δ 7.4 - 8.04 can be assigned to the ortho-coupled protons of the two aromatic rings. The integration is twice that of other pair of the doublets because of the symmetry in the molecule. The other pair of doublets can be seen at δ 6.7 and δ 7.45 and can be assigned to the double bonds in the remaining ring. (Appendix 1, Figure 1.1.11). The aromatic carbons in the ^{13}C spectra can be found in the range of δ 110 - 140.3 (Appendix 1, Figure 1.1.12). The GC-MS of product, P_4 revealed the molecular mass of 292 (M^+) at retention time 15.19 min (Appendix 1, Figure 1.1.13) which is in good agreement with molecular formula $C_{19}H_{16}O_3$. Loss of *para* hydroxy phenyl group from product P_4 led to the formation of the fragment with molecular mass 200 ($C_{13}H_{12}O_2$) followed by loss of the hydroxy group from the fragment to arrive at another fragment with molecular mass 185.1 (M^{+1}) $C_{13}H_{12}O$.

Table 3.2.9 Plausible oxidation products.

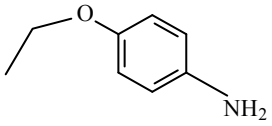 (P_1)	4-ethoxy-phenylamine
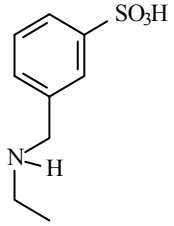 (P_2)	3-ethylamino methyl-benzene sulfonic acid

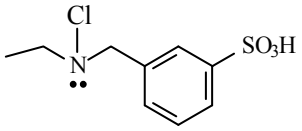 (P_3)	3-ethylamino chloro methylbenzene sulfonic acid
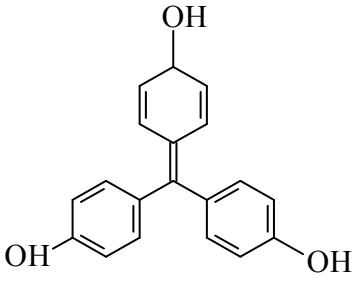 (P_4)	4-[bis-(4-hydroxy-phenyl)-methylene]-cyclohexa-2,5-hydroxide

3.2.10 Stoichiometric equation

The stoichiometry of the reaction between brilliant blue and hypochlorite was established with 1:1 and 1:10 ratio of the oxidant and the substrate. The amount of brilliant blue-R reacted was calculated from the initial and residual amounts. The stoichiometry was found to be approximately 1:4 (± 10%). The stoichiometry for the reaction can be expressed as

$$BB^{+} + 4HOCl + 3H_2O \rightarrow P_1 + P_2 + P_3 + P_4^{+} + 3HCl + OH^{-} + H^{+} \qquad (3.6)$$

3.2.11 Reaction scheme

Brilliant blue upon treatment with HOCl results in the formation of an intermediate I_1 with the loss of para ethoxy aniline as product P_1. The intermediate I_1 is attacked by OCl^- ion to form intermediate I_2 which looses *meta* substituted benzyl ethyl amine as product P_2 and forms I_3. Intermediate I_3 is further attacked by HOCl ending up with the formation of product

P_3 and intermediate I_4. The latter is further attacked by three hydroxy ions and leads to the formation of P_4.

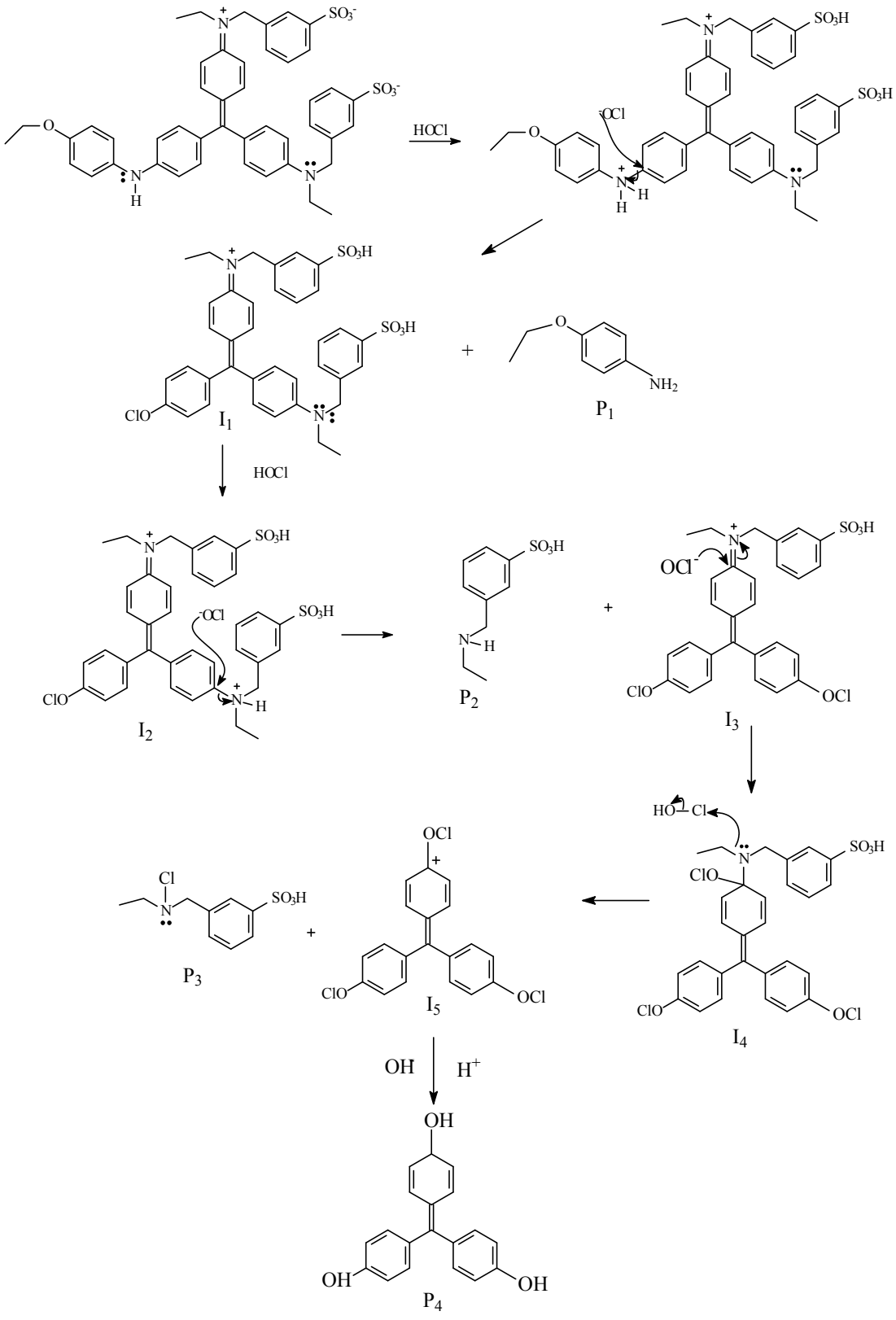

Figure 3.2.15 Mechanistic scheme for the oxidation of brilliant blue-R with hypochlorite.

3.2.12 Proposed reaction mechanism

The probable reaction mechanism is proposed based on the known chemistry of hypochlorite decomposition as discussed. The reaction mechanism is represented as,

$$H^+ + OCl^- \rightleftharpoons HOCl$$

$$HOCl + Cl^- + H^+ \rightleftharpoons Cl_2$$

$$BB^+ + HOCl \rightarrow I_1^+ + P_1 \qquad \text{R1}$$

$$I_1^+ + HOCl \rightarrow I_1^{2+} + OCl^- \qquad \text{R2}$$

$$I_2^{2+} + OCl^- \rightarrow I_3^+ + P_2 \qquad \text{R3}$$

$$I_3^+ + HOCl \rightarrow I_4 + H^+ \qquad \text{R4}$$

$$I_4 + HOCl \rightarrow I_3^+ + OH^- + P_3 \qquad \text{R5}$$

$$I_3^+ + 3H_2O \rightarrow P_4^+ + 3HCl \qquad \text{R6}$$

The overall reaction mechanism is proposed as

$$BB^+ + 4HOCl + 3H_2O \rightarrow P_1 + P_2 + P_3 + P_4^+ + 3HCl + OH^- + H^+ \qquad (3.7)$$

3.2.13 Rate law

Based on the first-order dependence of the reaction rate on the reactants and observed negative salt effect, the rate law may be proposed as

$$Rate = k_1[OCl^-][BB^+] + k_2[HOCl][BB^+] \qquad (3.8)$$

Where k_1 and k_2 represents the rate constants.

$$r = \{k_1[OCl^-] + k_2[HOCl]\}[BB^+] = k'[BB^+] \qquad (3.9)$$

Where the *pseudo* first-order constant, k' equals to

$$k' = k_1[OCl^-]_o + k_2[HOCl]_o \quad (3.10)$$

and where (3.11)

$$k_1 = \frac{k_1'}{[OCl^-]} \; ; \quad k_2 = \frac{k_2'}{[HOCl]} \quad (3.12)$$

3.2.14 Simulations

Based on the comprehensive scheme (Figure 3.2.15) and the subsequent proposed reaction mechanism, the reaction scheme in the product analysis detailed the structures of the probable intermediates. For the simulations only steps involving the formation of intermediates which undergo consecutive reactions with other intermediates or reactive species are considered. In each elementary step, while the overall charge and mass balances are strictly accounted for, the concentration of water which is the solvent is not simulated.

The Table 3.2.10 summarises the elementary steps and rate coefficients used for the simulations. Estimated rate coefficients were used for the remainder of the reactions. Rate constants determined in the present studies were employed for C3 and C4. Estimated rate coefficients were adjusted such that the simulated curves agreed with the experimental curves.[203]

Table 3.2.10 Forward and reverse rate constants obtained from literature and simulations.

Reaction No	Reaction Mechanism	Forward rate	Reverse rate
C1	$H^+ + OCl^- \rightleftharpoons HOCl$	$3.97 \times 10^{-4}\ M^{-1}\ s^{-1}$	$1.0 \times 10^{-4}\ s^{-1}$
C2	$HOCl + Cl^- + H^+ \rightleftharpoons Cl_2$	$3.63 \times 10^{-3}\ M^{-2}\ s^{-1}$	$1.1\ s^{-1}$
C3	$BB^+ + HOCl \rightarrow I_1^+ + P_1$	$2.2 \times 10^{1}\ M^{-1}\ s^{-1}$	--

Table 3.2.10 contd.

Reaction No	Reaction Mechanism	Forward rate	Reverse rate
C5	$BB^+ + OCl^- \rightarrow I_1$	1.22 $M^{-1} s^{-1}$	--
C6	$I_1 + H^+ \rightarrow I_1^+ + P_1$	$3.30 \times 10^9 M^{-1} s^{-1}$	--
C7	$I_1^+ + HOCl \rightarrow I_1^{2+} + OCl^-$	$2.30 \times 10^9 M^{-1} s^{-1}$	--
C8	$I_2^{2+} + OCl^- \rightarrow I_3^+ + P_2$	$4.30 \times 10^9 M^{-1} s^{-1}$	--
C9	$I_3^+ + HOCl \rightarrow I_4 + H^+$	$3.41 \times 10^9 M^{-1} s^{-1}$	--
C10	$I_4 + HOCl \rightarrow I_3^+ + OH^- + P_3$	$3.01 \times 10^8 M^{-1} s^{-1}$	--
C11	$I_3^+ \rightarrow P_4^+ + 3HCl$	$4.17 \times 10^8 s^{-1}$	--

The speciation of OCl^- in the presence of acid is shown by the equation C1. The rate limiting step of the oxidation mechanism involves steps initiated by OCl^- or HOCl on BB^+ leading to the formation of the reactive intermediates. Reactions C3 and C4 are the rate-determining steps for brilliant blue-R oxidation. Reactions C5-C8 shows the consecutive steps for further oxidation of the reactive intermediates leading to different probable products.

Three experimental curves were analyzed using Simkine 2 software and the generated simulated curves are shown in Figure 3.2.16

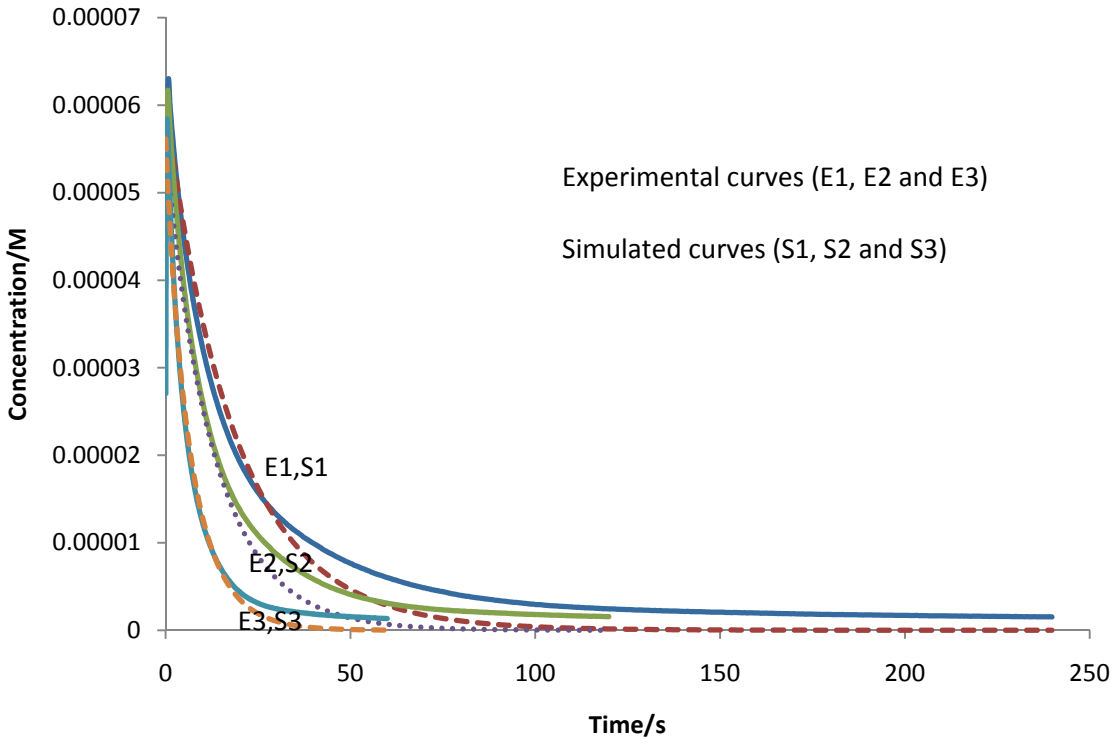

Figure 3.2.16 Experimental curves *versus* simulated curves for reaction of $[BB^+]_0$ (7.0×10^{-5} M) with $[OCl^-]_t$ (1.45×10^{-3} M).

From Figure 3.2.16 the experimental E1, E2 and E3 and corresponding simulated curves S1, S2 and S3 (dotted) are in agreement with each other confirming that the proposed reaction scheme as most reasonable and estimated rate constants are fairly acceptable.

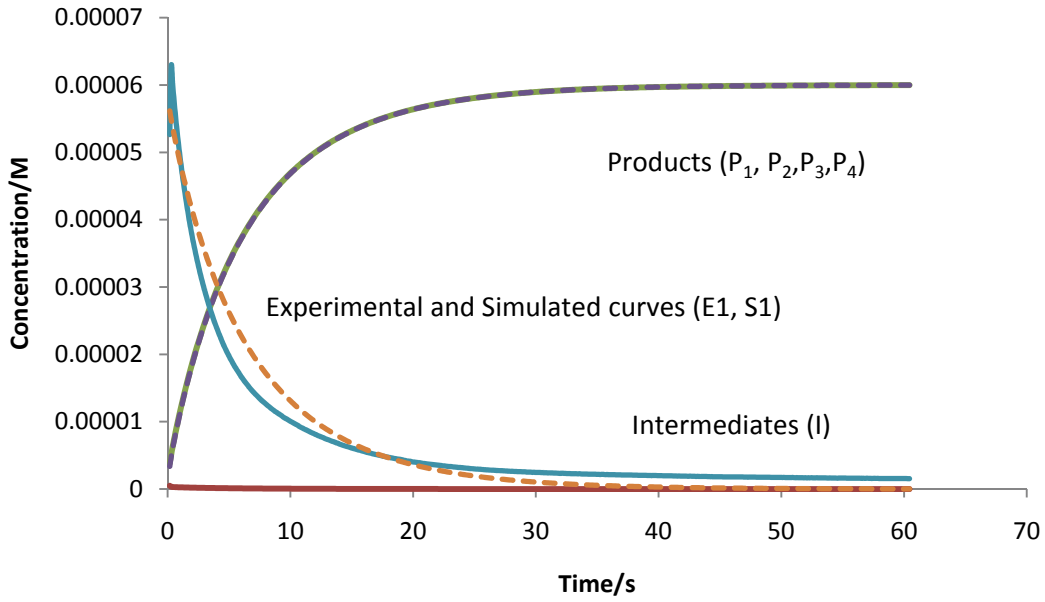

Figure 3.2.17 Intermediates and product formation for the reaction of brilliant blue with hypochlorite.

By maintaining the similar reaction conditions, in Figure 3.2.17 curves E1 and S1 indicates the experimental and simulated curves for the reaction. P_1, P_2, P_3 and P_4 show the product formation and I is the intermediate formed during the process and also indicates that the dye is completely transformed in to the products. The data of the simulated *versus* experimental curves and the concentrations of the other reactants, intermediates and products are compiled in (Appendix 1, Table 1.3, and Table 1.4).

3.3 Reaction of hypochlorite with safranine-O

3.3.1 Order with respect to safranine-O

To elucidate the mechanism of the reaction between this anthraquinone dye with hypochlorite, the kinetics of the reaction was studied under varied reaction conditions. The dye had absorption maximum at 519 nm with no peak shift due to pH variation. In all the cases, the kinetic runs were conducted with excess concentrations of all the reagents except safranine-O (SO^+), which was taken at low concentration. The reaction was monitored at 519 nm, where interferences were observed during the reaction. All the experiments were carried out at (25 ± 0.1) $^{\circ}$C. Figure 3.3.1 shows the typical kinetic trace of $[SO^+]$.

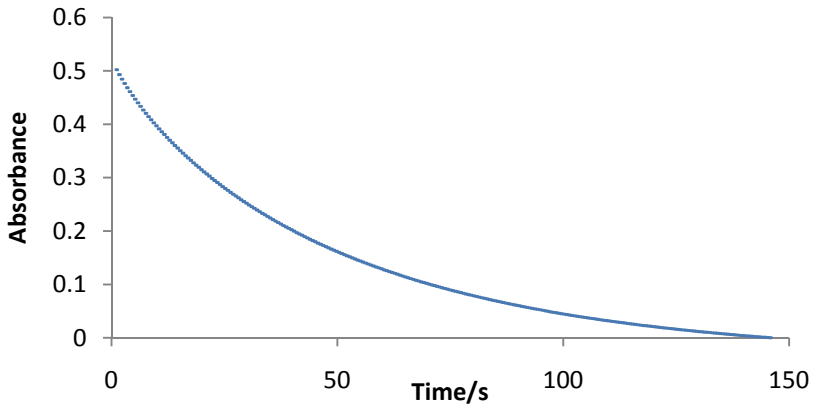

Figure 3.3.1 Typical kinetic curve- absorbance *versus* time plot for the reaction of $[SO^+]_0$ (3.0 x 10^{-5} M) with $[OCl^-]_t$ (1.5 x 10^{-3} M) at pH = 9.0, wavelength 519 nm.

3.3.2 Analysis of kinetic data

The kinetic data acquired at single wavelength measurements was analysed using the kinetic software and the first-order rate equation as described earlier. Figure 3.3.2 represents the typical experimental curve with the fitted curve and the residuals. A fair agreement between the curves with small residuals suggests that reaction follows *pseudo* first-order kinetics for the chosen conditions and order with respect to the dye is one.

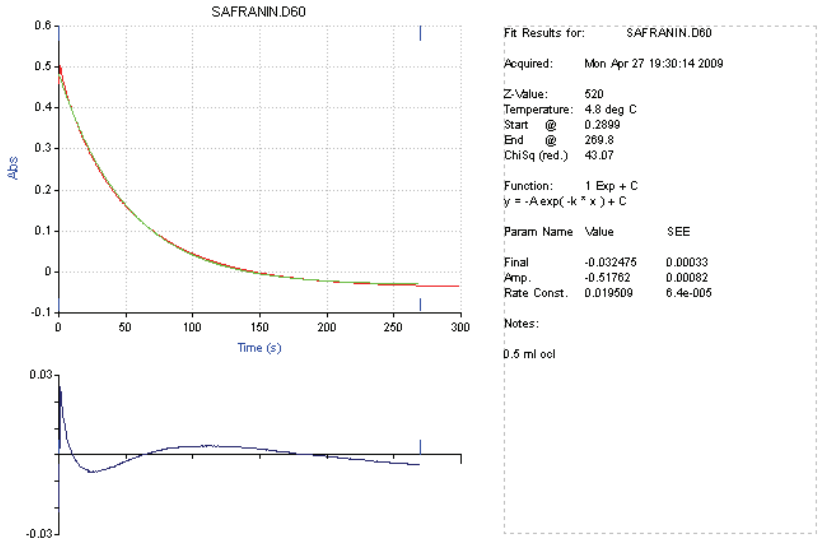

Figure 3.3.2 KinetAsyst^{TM} single-exponential equation fit (green) and the experimental curve (red) with residuals shown in the (lower curve) and the rate parameters box for the reaction of $[SO^{+}]_0$ (3.0 x 10^{-5} M) with $[OCl^{-}]_t$ (1.5 x 10^{-3} M).

Perusal of Figure 3.3.2 indicates that by employing first-order equation a good agreement between experimental and theoretical curve is observed. The kinetic data analysis results for the curve displayed in the box shows that the rate constant obtained is (0.019 ± 6. 4 x 10^{-5}) s^{-1} with small standard deviation and the reaction follows first-order kinetics with safranine-O.

3.3.3 Order with respect to hypochlorite

To establish the reaction order with respect to oxidant, a series of experiments were conducted with different initial concentrations of hypochlorite at pH 9.0 and fixed ionic strength using sodium sulfate as a neutral salt. Typical curves showing depletion of SO^{+} as function of time at different initial concentrations of hypochlorite are shown in Figure 3.3.3.

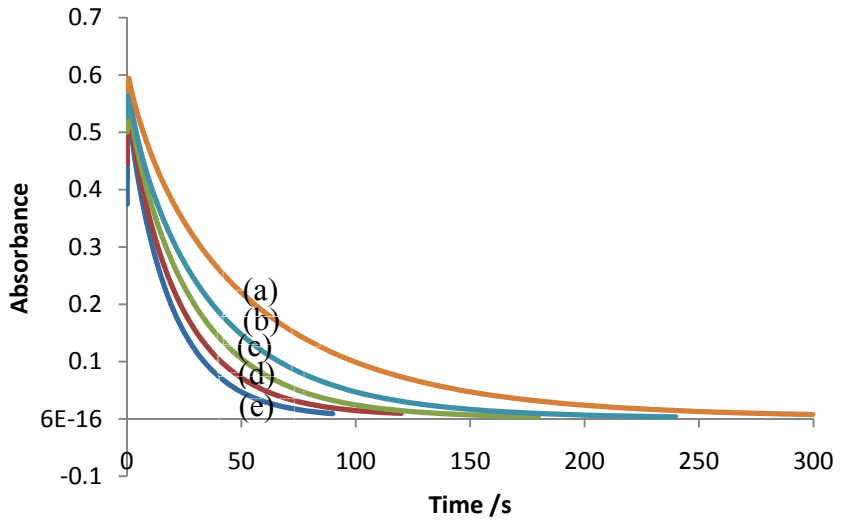

Figure 3.3.3 Depletion of safranine-O with various hypochlorite concentrations for the reaction of $[SO^{+}]_0$ (3.0×10^{-5} M) with $[OCl^{-}]_t$ x 10^{-3} M (a = 0.85, b = 1.70, c = 2.55, d = 3.40 and e = 5.10) at pH = 9.0.

With increasing initial concentration of hypochlorite from (0.85-5.10) x 10^{-3} M, the rate of depletion of dye is increased proportionately. The representative absorbances *versus* time plots are shown in Figure 3.3.3. The *pseudo* first-order rate coefficients, k' for different hypochlorite concentrations are shown in Table 3.3.1.

The thumbnail impressions given in Figure 3.3.4, illustrates the depletion of the dye and respective kinetic traces with residuals for the chosen conditions.

.

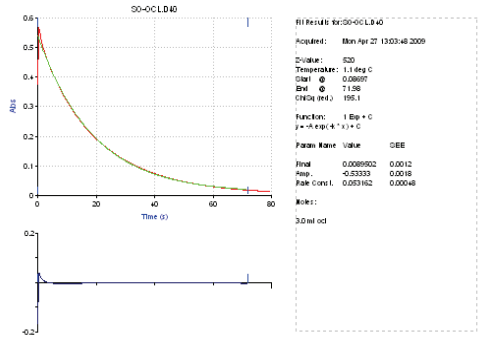

(a)

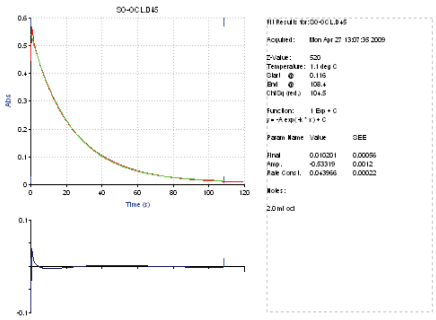

(b)

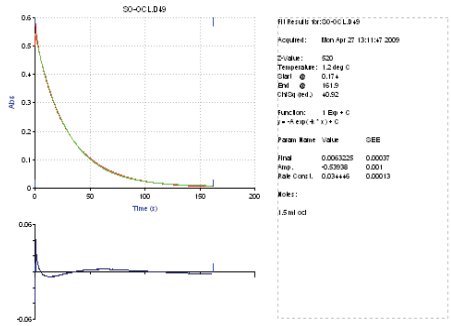

(c)

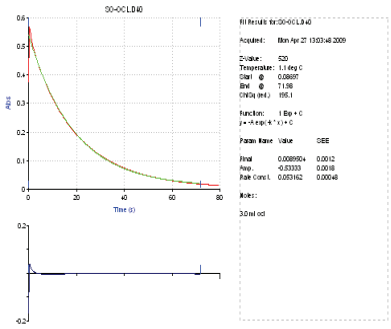

(d)

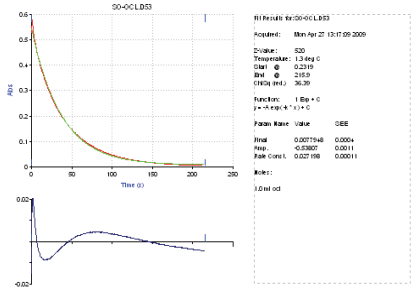

(e)

Figure 3.3.4 Fits using KinetAsyst^{TM} single-exponential equation, and rate equation {1 Exp + C, y = -A exp (-k * x) + C where k' /s-1 (a= 0.0100, b = 0.0271, c = 0.0346, d = 0.0439 and e = 0.0520).

The observed k'/s^{-1} values are shown in Table 3.3.1 for different initial concentrations of total hypochlorite for the curves analysed in Figure 3.3.4 and Figure 3.3.5 illustrates the ln k' *versus* ln [OCl^-] for the same.

Table 3.3.1 The reaction between safranine-O and hypochlorite at constant ionic strength $[SO^+]_0$ (3.0 x 10^{-5} M), $[OCl^-]_t$ (0.85 x 10^{-4} – 5.1 x 10^{-3} M), pH = 9.0, (I = 0.128 M).

$[OCl^-]_t$ / 10^{-3} M	k'/s^{-1}*
0.085	0.010
1.70	0.026
2.55	0.034
3.40	0.043
5.10	0.052

* Mean of four replicate experiments with relative standard deviation < 4%

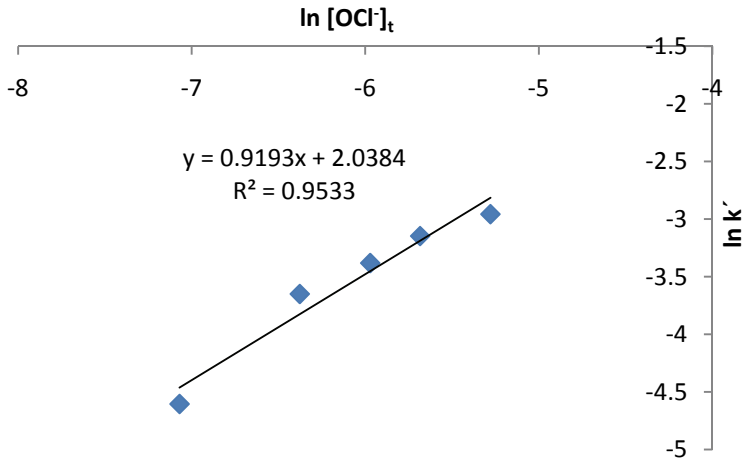

Figure 3.3.5 Plot of ln $[OCl^-]_t$ *versus* ln k' for the reaction of $[OCl^-]_t$ (0.85 x 10^{-4} - 5.1 x 10^{-3} M) with $[SO^+]_0$ (3.0 x 10^{-5} M) at pH = 9.00 and I = 0.128 M.

While the *pseudo* first-order rate constants increased proportionately with the increase in the initial concentration of hypochlorite, from Figure 3.3.5 the plot of ln k' *versus* ln $[OCl^-]$ gave good straight line with slope = 0.91 suggesting that the order with respect to oxidant is one.

3.3.4 Effect of acid concentration on the reaction rate

To establish the role of acid in the reaction dynamics, kinetic experiments were repeated with fixed excess concentration of oxidant and low amount of dye and varied initial pH conditions

from basic to acidic pH. The obtained k' values are summarized in Table 3.2.2 and Figure 3.3.6 illustrates the plot of *pseudo* first-order rate constant as function of pH. With increase in pH, the change had different impact on the rate depending on the pH range. The increase in rate constant was small at neutral pH range while steep increase in the lower pH ranges.

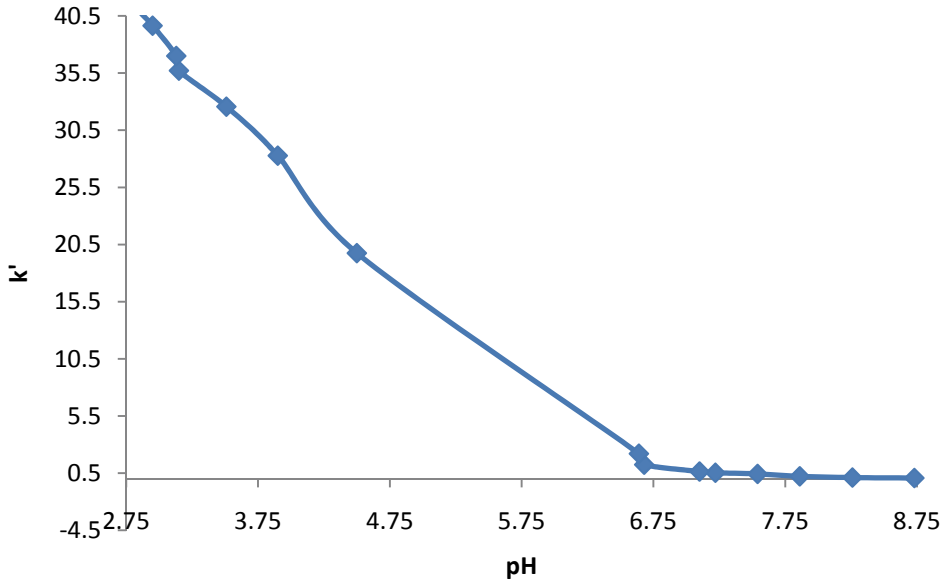

Figure 3.3.6 Plot of k' *versus* pH for the reaction of $[SO^{+}]_0$ (3.0 x 10^{-5} M) with $[OCl^{-}]_t$ (1.45 x 10^{-3} M), $[H^{+}]_{eq}$ (1.99 x 10^{-9}- 7.752 x 10^{-4} M).

Table 3.3.2 Effect of pH on reaction rate for the reaction of $[SO^{+}]_0$ (3.0 x 10^{-5} M), $[OCl^{-}]_t$ (1.45 x 10^{-3} M).

pH	k'/s^{-1} *
8.73	0.08
8.26	0.12
7.86	0.23
7.54	0.44
7.22	0.54
7.10	0.82
6.68	1.25
6.64	2.21
4.50	19.75

Table 3.3.2 contd.

pH	k'/s^{-1} *
3.90	28.27
3.51	32.56
3.61	33.47
3.15	35.71
3.13	36.99
2.95	39.64
2.85	40.87

* Mean of four replicate experiments with relative standard deviation < 4%

The increase in k' values with increasing acid concentration suggests that oxidation with formed HOCl is faster than with OCl^-. This can be possibly explained taking into consideration the occurrences of simultaneous reactions, initiated by OCl^- and HOCl. Further, to assess the order with respect to acid, the ln k' *versus* ln $[H^+]$ values were plotted (Figure 3.3.7).

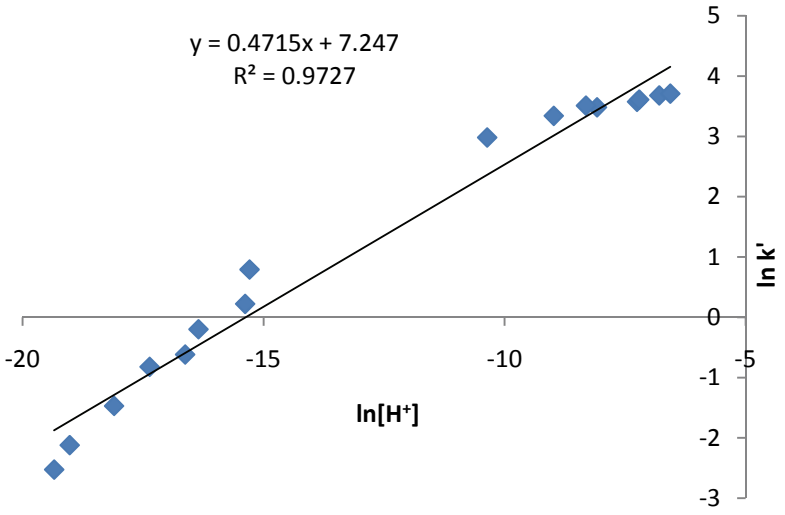

Figure 3.3.7 Plot of ln k' *versus* ln $[H^+]$ for the reaction of $[SO^+]_0$ (3 x 10^{-5} M), with $[OCl^-]_t$ (1.45 x 10^{-3} M) $[H^+]_{eq}$ (1.99 x 10^{-9}- 7.752 x 10^{-4} M).

The plot of ln k' *versus* ln [H^+] gave a plot with positive slope = 0.471 and R^2 = 0.97, and two distinct ranges observable, one slow increase in k' at high pH and another fast increase at low pH. The observed partial order with respect to H^+ can be anticipated in view of the conversion of hypochlorite to hypochlorous acid influenced by the acid concentrations through protonation. The rate of the oxidation of the substrate will depend on the reactivity's of hypochlorite and hypochlorous acid towards the dye. The competitive oxidation of dye occurs with OCl^- and HOCl species and can be further established by re-analysing the curves with two competitive reactions equations in the same manner as was done previously.

Hence, the kinetic data obtained with varied initial amounts of added acid was analysed carefully to estimate the rate coefficient values for the occurrence of two competitive reactions. Assuming the incidence of two competitive reactions the kinetic data in the pH range 6.0 to 2.0 was processed using the fit for two competitive first-order reactions. The generated and experimental curves fitted quite well with minimum residuals.

Figure 3.3.8 and 3.3.9 respectively show the fitting of theoretical curves and residuals, with assumption of occurrence of either one *pseudo* first-order reaction or two *pseudo* first-order reactions simultaneously.

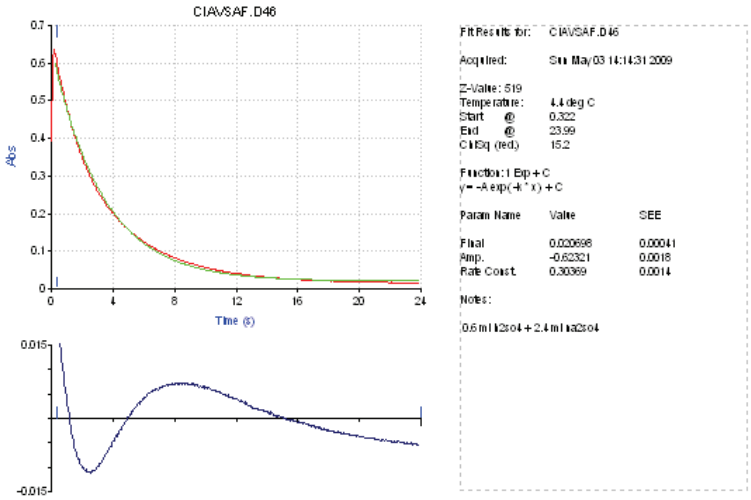

Figure 3.3.8 KinetAsyst™ single-exponential equation fit of two curves and residuals (lower sketch) for the reaction of $[SO^{+}]_0$ (3.0 x 10^{-5} M) with $[OCl^{-}]_t$ (1.45 x 10^{-3}M), $[H^{+}]$ (9.96 x 10^{-9} M) and I (0.128 M).

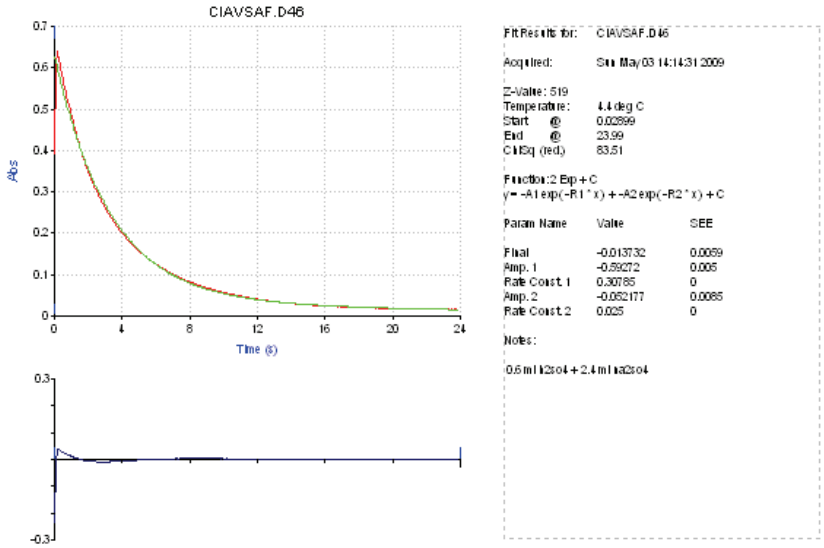

Figure 3.3.9 KinetAsyst™ double-exponential equation fit of two curves and residuals (lower part) for the reaction of $[SO^{+}]_0$ (3.0 x 10^{-5} M) with $[OCl^{-}]_t$ (1.45 x 10^{-3} M), $[H^{+}]$ (9.96 x 10^{-9} M) and I (0.128M).

The values of the two *pseudo* first-order rate constants obtained from the analysis are summarized, together with the initial equilibrium concentrations of acid, hypochlorite and hypochlorous acid indicated as $[H^{+}]_{eq}$, $[OCl^{-}]_{eq}$ and $[HOCl]_{eq}$ at different pH values

(Table 3.3.3). k_1' represents the *pseudo* first-order rate constant for the OCl^- initiated oxidation and k_2' represents the corresponding value for the reaction by HOCl. Further k_1 and k_2 are the calculated second-order rate constants for OCl^- and HOCl facilitated reactions respectively. The ln-ln plots of k_1' and $[OCl^-]_{eq}$ and k_2' and $[HOCl]_{eq}$ are illustrated in Figures 3.3.10 and 3.3.11 which were straight lines with decreasing order at different pH ranges.

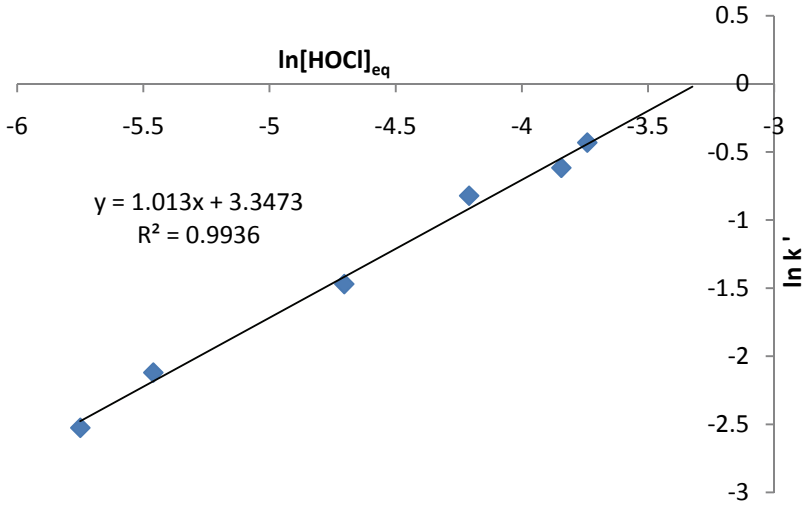

Figure 3.3.10 Plot of ln k' *versus* ln $[HOCl]_{eq}$ for the reaction $[SO^+]_0$ (7×10^{-5} M) with $[OCl^-]_t$ (1.45×10^{-3} M) at $[H^+]_{eq}$ (1.86×10^{-9} - 1.41×10^{-5} M).

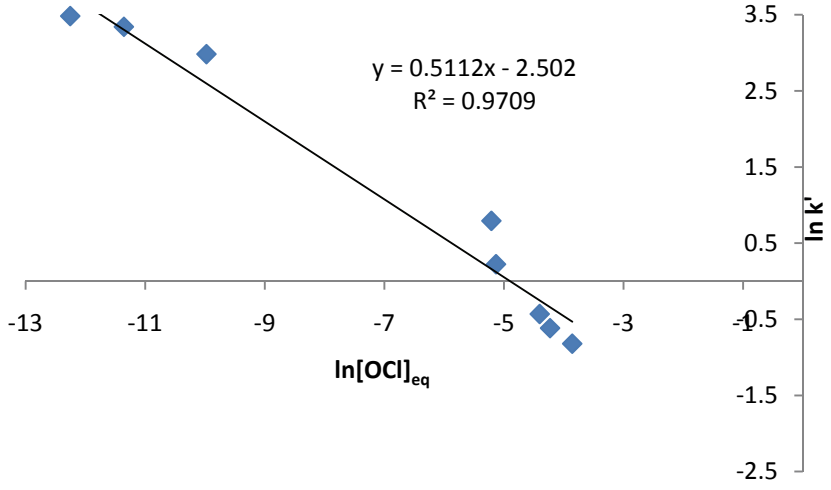

Figure 3.3.11 Plot of ln k' *versus* ln $[OCl^-]_{eq}$ for the reaction of $[SO^+]_0$ (3.0×10^{-5} M) with $[OCl^-]_t$ (1.45×10^{-3} M) at $[H^+]_{eq}$ (1.86×10^{-9} - 1.41×10^{-5} M).

Table 3.3.3 Effect of acid on the speciation of hypochlorite and reaction rates.

pH	H^+	$[HOCl]_{eq}$	$[OCl^-]_{eq}$	k_1'/s^{-1} *	k_2'/s^{-1} *	$k_1/M^{-1}\ s^{-1}$	$k_2/M^{-1}\ s^{-1}$
8.73	1.86×10^{-9}	1.56×10^{-3}	3.40×10^{-2}	0.064	0.093	1.95	29.22
8.26	5.48×10^{-9}	4.40×10^{-3}	3.10×10^{-2}	0.066	0.127	2.09	29.99
7.86	1.38×10^{-8}	9.21×10^{-3}	2.60×10^{-2}	0.058	0.276	2.17	30.48
7.54	2.88×10^{-8}	1.50×10^{-2}	2.10×10^{-2}	0.053	0.458	2.54	30.87
7.22	6.01×10^{-8}	2.15×10^{-2}	1.40×10^{-2}	0.040	0.676	2.79	31.57
7.10	7.92×10^{-8}	2.39×10^{-2}	1.20×10^{-2}	0.035	0.761	2.91	32.09
6.68	2.08×10^{-8}	3.01×10^{-2}	5.90×10^{-2}	0.018	0.985	3.18	32.74
6.64	2.28×10^{-8}	3.06×10^{-2}	5.45×10^{-2}	--	1.07	--	35.28
4.05	8.90×10^{-5}	3.60×10^{-2}	1.64×10^{-5}	--	1.29	--	35.96
3.90	1.26×10^{-4}	3.60×10^{-2}	1.20×10^{-5}	--	1.30	--	36.24
3.51	3.09×10^{-4}	3.60×10^{-2}	4.55×10^{-6}	--	1.33	--	37.13
3.61	2.45×10^{-4}	3.60×10^{-2}	5.89×10^{-6}	--	1.36	--	37.80
3.15	7.07×10^{-4}	3.60×10^{-2}	2.03×10^{-6}	--	1.38	--	38.31
3.13	7.40×10^{-4}	3.60×10^{-2}	1.98×10^{-6}	--	1.41	--	39.22
2.95	1.12×10^{-3}	3.60×10^{-2}	1.34×10^{-6}	--	1.43	--	39.74
2.85	1.41×10^{-3}	3.60×10^{-2}	1.07×10^{-6}	--	1.44	--	40.05
Mean k_1 and k_2 with standard deviation						3.0 ± 0.5	34.8 ± 2.8

* Mean of four replicate experiments with relative standard deviation < 4%

$k_1 = k_1'/[OCl^-]_{eq}$ and $k_2 = k_2'/[HOCl]_{eq}$ where k_1 and k_2 represents the second-order reaction rates for OCl^- and HOCl competitive reactions. The equilibrium concentrations of acid, OCl^- and HOCl were calculated based on the measured initial pH values and the protonation constant of hypochlorite. From Table 3.3.3, the mean second-order rate coefficients for the OCl^- and HOCl initiated oxidations respectively are k_1 (3.0 ± 0.5) $M^{-1}\ s^{-1}$ and k_2 (34.8 ± 2.8) $M^{-1}\ s^{-1}$. An examination of the data in Table 3.3.3 shows that with increasing initial acid concentration, the k_2' values increased, a decreasing trend is registered for k_1' values.

Interestingly at pH below 4.0 the overall rate constants observed, tend to increase where there is no further increase in [HOCl] is possible. This suggests that unlike the other dyes investigated, possibly the protonated substrate gets oxidized much faster than the unprotonated species. In such a case the HOCl oxidizes the unprotonated and protonated safranine-O at different rates.

Considering the complexity of the reaction dynamics of oxidation of safranine-O under varied pH conditions, a generalized rate law accommodating the oxidation of SO^+ by OCl^- and HOCl, in competitive reactions at high and medium pH (> 4) and the simultaneous oxidation of unprotonated and protonated safranine-O at lower pH by HOCl can be expressed as follows:

$$r = \{k_1[OCl^-][SO^+] + k_2[HOCl][SO^+]\} + k_3\,[HOCl][SOH^{2+}] \quad (3.13)$$

At pH conditions above 4, where no protonated SOH^{2+} possibly exists, the third term in the above eqn. [3.11] disappears, and rate can be expressed as

$$r = \{k_1[OCl^-][SO^+] + k_2[HOCl][SO^+]\} \quad (3.14)$$

Thus, $r = k'[SO^+]$, (3.15)

where the *pseudo* first-order constant, k' equals to

$$k' = \{k_1[OCl^-]_o + k_2[HOCl]_o\} \quad (3.16)$$

$= k'_1 + k'_2$, *where* k_1' and k_2' were analyzed using KinetAsyst specfit analysis and k_1 and k_2 are the second order rate constants estimated from k_1' and k_2'

$$k_1 = \frac{k_1'}{[OCl^-]} \;\; ; \;\; k_2 = \frac{k_2'}{[HOCl]} \quad (3.17)$$

Under pH conditions below 4.0, where all the hypochlorite is in the form of HOCl or the concentration of $[OCl^-]_{eq}$ is negligible, it is expected the further increase in acid concentration should result in no enhancement in k' values. At low pH, interestingly the observed increase in the overall *pseudo* first-order rate constant with an increase in acid concentration suggests that acid has a diverse role to play in this mechanism. This can only be explained based on the possible protonation of the dye, which in turn may get oxidised more easily than the unprotonated species. With further increase in the pH, evidently with no peak shift from 520 nm absorption maximum is observed. Thus, obviously both the unprotonated and protonated dye absorb at the same wavelength, but possibly get oxidized by HOCl at different rates. Under these conditions the direct estimation of the *pseudo* first-order constants for these reactions is not feasible, due to lack of appropriate equations with software. The assumption can only be verified indirectly.

As such at pH conditions below pH 4, where protonated SO^+ may exist, the first term in the above equation 3.11, (i.e. $k_1[OCl^-][SO^+]$) may be neglected and rate may expressed as

$$r = k_2[HOCl][SO^+] + k_3[HOCl][SOH^{2+}] \tag{3.18}$$

$where\ [SO^+] + [H^+] \rightleftharpoons [SOH^{2+}]$

$$K = \frac{[SOH^{2+}]}{[SO^+][H^+]}$$

$$r = \{k_2[HOCl] + k_3k[HOCl][H^+]\}[SO^+] \tag{3.19}$$

$$k'' = \{k_2' + k_3'[H^+]\} \tag{3.20}$$

$where\ k_3' = k_3k[HOCl]$ and $k_3 = \frac{k_3'}{k[HOCl]}$

If the assumption is correct, and the rate equation holds good, the plot of the overall rate constant k' in the pH range (9.0 to 6.0) *versus* $[H^+]_{eq}$ should be a straight line, with slope

equivalent to k_3 and intercept equivalent to k_2. k_3 can be estimated knowing the value of K, the protonation constant for the dye. The estimation of k_3 value is limited due to the lack of information on the protonation constant of safranine-O.

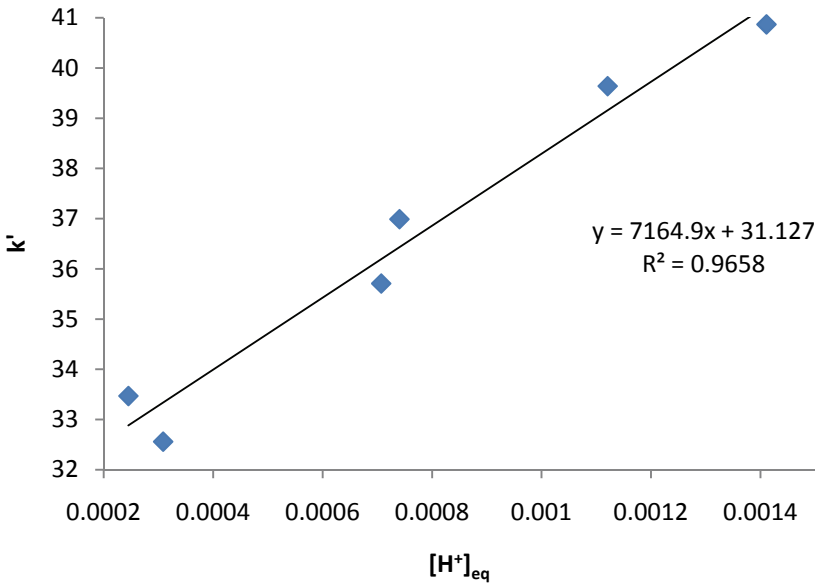

Figure 3.3.12 Plot of k' *versus* $[H^+]_{eq}$ below pH = 6.0.

The fair agreements of the intercept value, 31.12 (Figure 3.3.12) with the estimated value of k_2 = 34.79 (Table 3.3.3) supports the approximation reasonable.

3.3.5 Primary salt effect

At pH 9.0 HOCl exists in equilibrium to 15% together with OCl^-, so the curves were analysed for two consecutive reactions in the same manner as it was done previously. The results obtained are summarized in Table 3.3.4.

Table 3.3.4 Effect of ionic strength on the reaction rate $[SO^{+}]_0$ = (3x 10^{-5} M), $[OCl^{-}]_t$ (1.45 x 10^{-3} M), pH =9.

Ionic strength/M	k_1'/s^{-1} *	k_2'/s^{-1} *
0.0092	0.047	0.63
0.0167	0.042	0.62
0.0242	0.039	0.60
0.0317	0.037	0.56
0.0392	0.034	0.54

* Mean of four replicate experiments with relative standard deviation < 4%

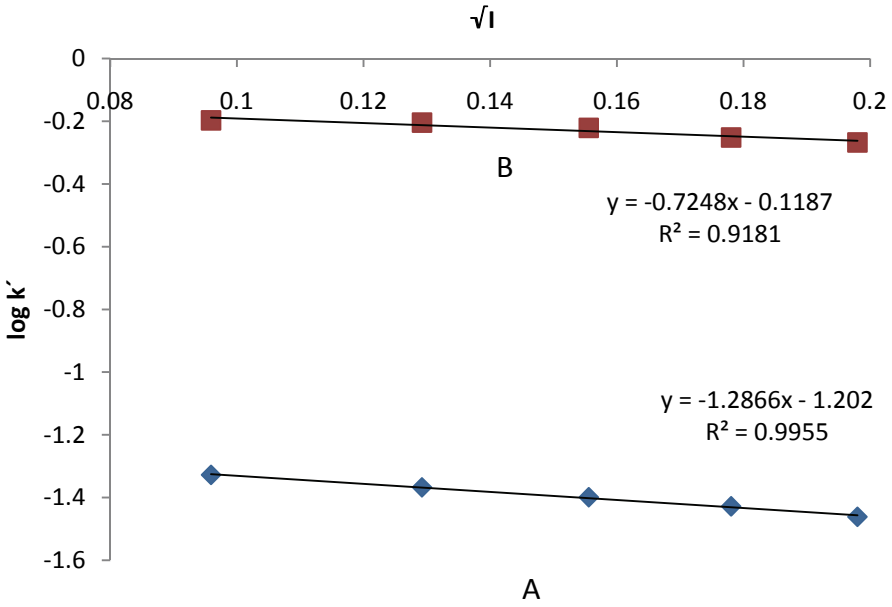

Figure 3.3.13 Plot of log k_1' and log k_2' *versus* √I for the reaction of $[SO^{+}]_0$ (3.0 x 10^{-5} M) with $[OCl^{-}]_t$ (1.45 x 10^{-3}M) at pH = 9, Ionic Strength (I = 0.009 to 0.039 M).

The plot of log k' *versus* $I^{1/2}$ of the data obtained gave a linear plot (A) with negative slope = 1.28 and R^2 = 0.99 (Figure 3.3.13). The negative salt effect indicates that the rate-limiting step involves species of opposite charges, possibly SO^{+} and OCl^{-} ions. The slope = 0.72, less than unity represented by plot B, Figure 3.3.13 corresponds to the reaction between HOCl and SO^{+}.

3.3.6 Kinetic salt effect at acidic pH

The effect of added chloride was investigated to establish the rate constants and its dependence on the ionic strength. The k' *versus* respective I values were plotted and are shown in Figure 3.3.14. Table 3.3.5 summarises the k' values obtained as function of ionic strength at low acid conditions. The log k' *versus* √I did not show such dependence, hence the values of k' *versus* I were plotted directly.

Table 3.3.5 Effect of ionic strength on the reaction rate $[SO^{+}]_0$ (3.0 x 10^{-5} M) with $[OCl^{-}]_{t\ t}$ (1.45 x 10^{-3}M), pH = 4.0.

Ionic strength/M	k'/s^{-1} *
0.0092	0.63
0.0167	0.62
0.0242	0.60
0.0317	0.56
0.0392	0.54

* Mean of four replicate experiments with relative standard deviation < 4%

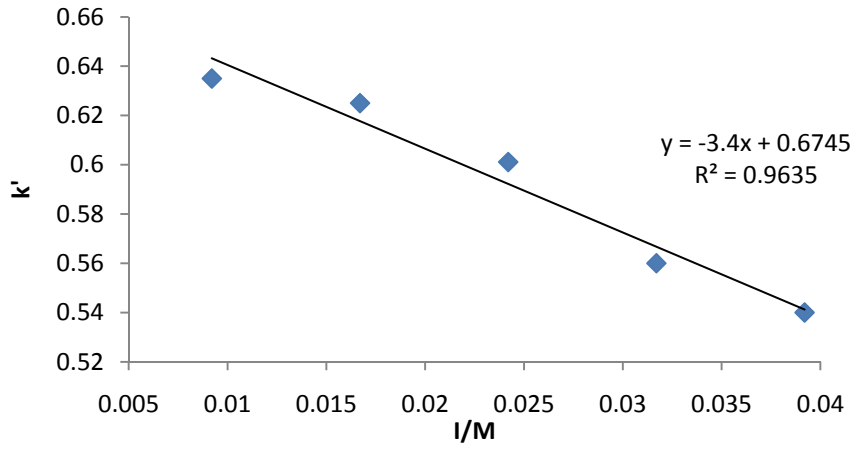

Figure 3.3.14 Plot of k' *versus* I (Ionic strength) for the reaction of $[SO^{+}]_0$ (3.0 x 10^{-5} M) with $[OCl^{-}]_t$ (1.45 x 10^{-3} M) at varying ionic strength, I (0.0092 - 0.0392 M) at fixed acid $[H^{+}]$ (4.5 x 10^{-3} M).

Figure 3.3.14 shows the good linear curve which indicates the linear dependence on the ionic strength with R^2 values equals to 0.96 confirming that the reaction is between the cationic dye and the hypochlorous acid which is neutral species.

3.3.7 Effect of chloride on reaction rate

Considering chloride is one of the species associated with hypochlorite generation and product of reaction, the effect of chloride on the reaction was investigated by adding varying amounts of chloride. The increase in added chloride registered a negligible effect on the k' value (Table 3.3.6).

Table 3.3.6 Effect of addition of chloride ions for the reaction of $[SO^+]_0$ (3.0×10^{-5} M)with $[OCl^-]_t$ (1.45×10^{-3} M).

$[Cl^-]$/M	k'/s^{-1} *
0.000	0.901
0.148	0.901
0.298	0.902
0.447	0.902
0.597	0.902
0.725	0.903

* Mean of four replicate experiments with relative standard deviation < 4%

3.3.8 Activation parameters

Table 3.3.7 summarises the *pseudo* first-order and overall second order rate coefficients of the hypochlorite and hypochlorous acid initiated oxidation of safranine-O at pH 9.0 investigated at five different temperatures unless otherwise identical conditions. Using the Eyring's equation and the kinetic data as a function of temperature, energy parameters namely, energy of activation, enthalpy and entropies of activation were estimated

(Table 3.3.8). Figure 3.3.15 shows the plot of ln rate coefficient *versus* reciprocal temperature plots which were straight lines.

Table 3.3.7 Varied temperature and observed rate constants for the reaction of $[SO^{+}]_0$ (3.0 x 10^{-5} M) with $[OCl^{-}]_t$ (1.45 x 10^{-3} M).

Temp./K	k_1'/s^{-1} *	$k/M^{-2}\,s^{-1}$	k_2'/s^{-1} *	$k/M^{-2}\,s^{-1}$
283	0.019	1.72	0.049	4.26
288	0.022	2.00	0.062	5.39
293	0.037	3.36	0.075	6.52
298	0.041	3.72	0.082	7.13
303	0.051	4.63	0.098	8.52

* Mean of four replicate experiments with relative standard deviation < 4%

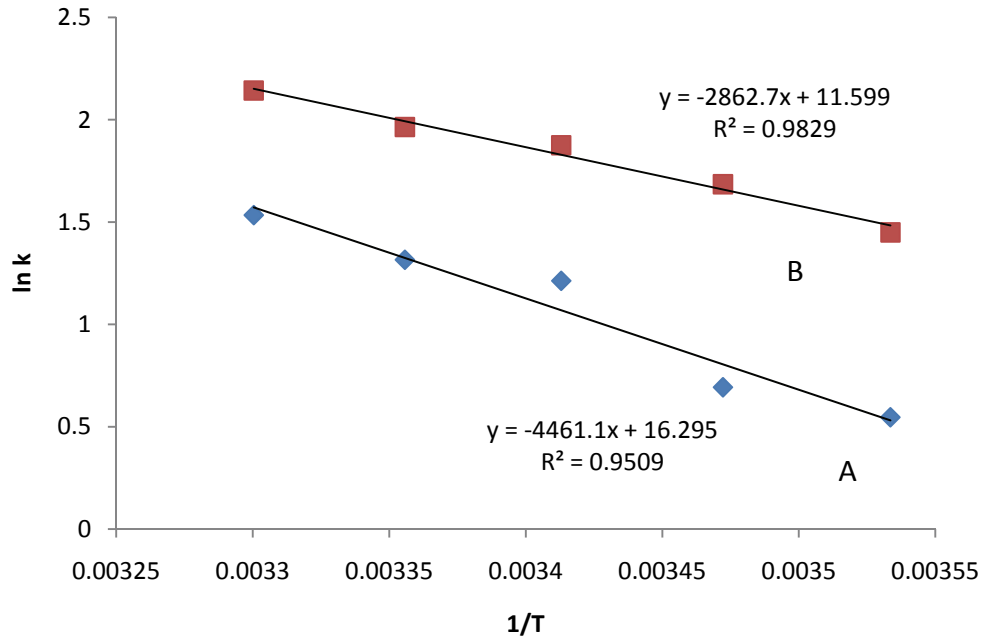

Figure 3.3.15 Plot of ln k' *versus* 1/T for the reaction of $[SO^{+}]_0$ (3.0 x 10^{-5} M) with $[OCl^{-}]_t$ (1.45 x 10^{-3} M) at different temperatures (T/K = 283-303). (A = OCl^{-} reaction and B = HOCl reaction)

Table 3.3.8 Energy parameters.

	Enthalpy of reaction, $\Delta H^{\ddagger}$/kJ mol^{-1}	Entropy of activation, $\Delta S^{\ddagger}$/J K^{-1} mol^{-1}	Energy of activation E_a/kJ mol^{-1}
SO^{+} with OCl^{-}	34.6	-183.53	37.09 ± 0.09
SO^{+} with HOCl	21.3	-222.62	23.04 ± 0.09

From the gradient value of Figure 3.3.15, the energy of activation, enthalpy and entropies of activation for the reactions were estimated. The enthalpy values were found to be 34.6 kJ mol^{-1} for OCl^{-} and 21.3 kJ mol^{-1} for the HOCl initiated reactions. The HOCl initiated oxidation, which is relatively a fast reaction, had lower energy of activation of (23.04 ± 0.09 kJ mol^{-1}) compared to (37.09 ± 0.09 kJ mol^{-1}) for the OCl^{-} reaction. Large negative entropies of activation values -183.53 with OCl^{-} and -222.62 with HOCl initiated reactions observed experimentally reflect the possible formation of compact activated complex.

3.3.9 Product identification and characterization

The product obtained from SO-OCl reaction (0.5g) was separated by column chromatography, using silica gel (Merck 9385) as the stationary phase on 4 cm diameter column. The mobile phase consisted of a hexane: dichloromethane: ethyl acetate with step gradient (100% hexane (fractions 1-10), increased by 10% dichloromethane (fractions 11-18) 20% dichloromethane (fractions 19-29), 40% dichloromethane (fractions 30-38) and 60% dichloromethane (fractions 39-47), Fractions of 10 mL were collected in each step. Two compounds were obtained from this dye; they were from fractions 12-16 and 52-60. The plausible products from the above fractions are P_1 (4-amino-5-methylbenzene-1,2-dichloride) and P_2 (4-amino-6-(2-chloro-6-hydroxyphenyl amino) 3-methyl-cyclohexa-2,4-dienone oxime). Product P_2 is identified in the current study. Plausible oxidation products were shown in Table 3.3.9.

Table 3.3.9 Plausible oxidation products.

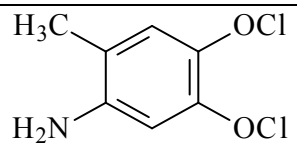 (P_1)	4-amino-5-methylbenzene-1,2-dichloride
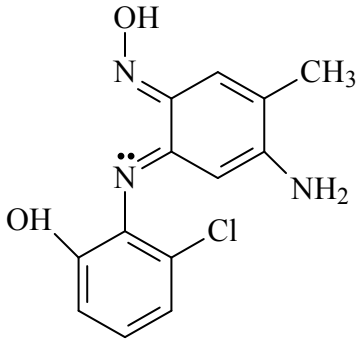 (P_2)	4-amino-6-(2-chloro-6-hydroxy-phenylimino)-3-methyl-cyclohexa-2,4-dienone oxime

3.3.10 Stoichiometry equation

Stoichiometry of the safranine oxidation with hypochlorite was carried out using stock hypochlorite concentration of 0.0015 M. The stoichiometry of the reaction was established with 1:1 and 1:5 ratios of Safranine-O and hypochlorite respectively using Beer-Lamberts law the ratio of dye consumed to the oxidant was determined. The stoichiometry was found to be approximately 1:4 (± 10%) of SO^+ and HOCl. Thus the stoichiometric equation for the overall reaction can be written as,

$$SO^+ + 4HOCl \rightarrow P_1 + P_2 + 2H^+ + Cl^- \qquad (3.21)$$

where P_1 is (4-amino-5-methyl-benzene-1,2-dichloride) and P_2 is (4-amino-6-(2-chloro-6-hydroxy-phenylimino)-3-methyl-cyclohexa-2,4-dienone oxime).

3.3.11 Reaction scheme

When the dye molecule reacts with the oxidant, the hypochlorite ion attacks on the quaternary carbon adjacent to quaternary nitrogen which bears a bulky phenyl ring and the proton is transferred on to the other tertiary nitrogen. The OCl^- ion attaches to the carbon and will result in cleavage of the bond between quaternary carbon and quaternary nitrogen, which forms an intermediate I_1. The intermediate I_1 further gets attacked by the OCl^- or HOCl at quaternary carbon, which is connected to quaternary nitrogen which results in the formation of intermediate I_2 and product P_1. The intermediate I_2 is further attacked by HOCl and hydroxyl ion is transferred on to the secondary nitrogen on the ring system. That leads the nitrogen to its quaternary state resulting in the formation of I_3.

The OCl^- abstracts a proton from quaternary nitrogen of intermediate I_3 to form HOCl, which in turn further oxidises the intermediate I_3 and leads to the formation of product P_2. The formation of product P_2 is confirmed with ^1H NMR, ^{13}C NMR and mass spectrum. The proton NMR spectra revealed that the singlet peak at δ 2.13 for methyl protons, the primary amino group is seen at δ 5.27 and three aromatic protons are found at the range of δ 6.4 to 7.6 (Appendix 1, Figure 1.1.14). In ^{13}C NMR the alkyl carbon is observed at δ 14.12. Aromatic carbons are found at δ 124-129. The carbons which bear substituted nitrogen's can be seen at higher δ 179 and δ 182 values (Appendix, 1 Figure 1.1.15). From the GC-MS spectrum the molecular ion peak M^+ is found at 277 which is observed at retention time 20.64 min and corresponds to the molecular formula ($C_{13}H_{12}N_3O_2Cl$) of the product P_2 (Appendix 1, Figure 1.1.16).

The plausible oxidation products can be explained by the mechanistic scheme illustrated in Figure 3.3.16.

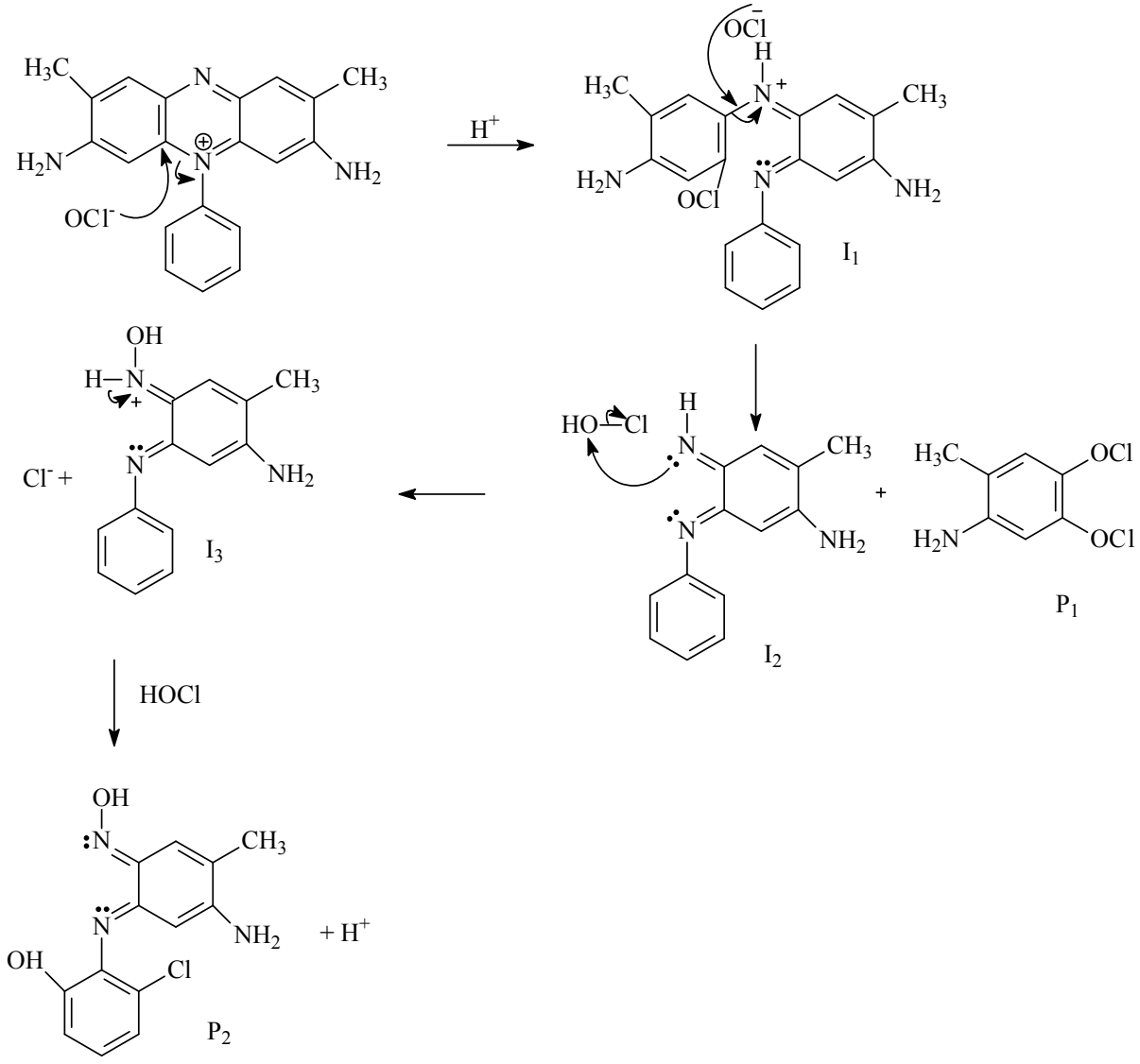

Figure 3.3.16 Possible reaction pathway for the oxidation of safranine-O.

3.3.12 Proposed reaction mechanism

The reaction mechanism for the oxidation of safranine-O can be proposed as

$$H^+ + OCl^- \rightleftharpoons HOCl$$

$$HOCl + Cl^- + H^+ \rightleftharpoons Cl_2$$

$$SO^+ + HOCl \rightarrow I_1^+ \qquad R1$$

$$I_1^+ + HOCl \rightarrow I_2 + P1 + H^+ \qquad R2$$

$$I_2 + HOCl \rightarrow I_3 + Cl^- \qquad R3$$

$$I_3 + HOCl \rightarrow P_2 + H^+ \qquad R4$$

The overall reaction mechanism is proposed as

$$SO^{+} + 4HOCl \rightarrow P_1 + P_2 + 2H^{+} + Cl^{-} \quad (3.22)$$

where P1 is (4-amino-5-methyl-benzene-1,2,dichloride) and P_2 is (4-amino-6-(2-chloro-6-hydroxy-phenylimino)-3-methyl-cyclohexa-2,4-dienone oxime) products.

3.3.13 Rate law

The rate law expresses the order of reaction with respect to the respective reactants. The observed first-order dependence of the reactants and the observed salt effect suggests that the rate limiting step involves one ion each of SO^{+} and OCl^{-}. Thus the major pathway of the reaction may involve both HOCl and OCl^{-} to give an activated complex which decomposes completely to form the intermediates and products.

The reaction fulfils *pseudo* first-order conditions, based on this assumption the rate law may be proposed as

$$Rate = k_1[OCl^{-}][SO^{+}] + k_2[HOCl][SO^{+}] \quad (3.23)$$

3.3.14 Simulations

Simulation studies were conducted based on the proposed mechanistic scheme (Figure 3.1.16). The reaction scheme detailed the structures of the probable intermediates and the products identified. The proposed mechanism and the mechanism used for the simulations represent the steps involving the formation of intermediates, which undergo consecutive reactions with other intermediates or the reactive species. The estimated rate constants were adjusted automatically with Simkine 2 software. Table 3.3.10 summarises the elementary steps and rate coefficients used for the simulations and estimated rate coefficients. Rate

constants obtained from the experiments in the present studies were employed for C3 and C4. Estimated rate coefficients were adjusted such that the simulated curves agreed with the experimental curves (C5- C8).

Table 3.3.10 Forward and reverse rate constants obtained from literature and simulations.

Reaction No.	Reaction Mechanism	Forward rate	Reverse rate
C1	$H^+ + OCl^- \rightleftharpoons HOCl$	$3.97 \times 10^{-4}\ M^{-1}\ s^{-1}$	$1.0 \times 10^{-4}\ s^{-1}$
C2	$HOCl + Cl^- + H^+ \rightleftharpoons Cl_2$	$3.63 \times 10^{-3}\ M^{-1}\ s^{-1}$	$1.1\ s^{-1}$
C3	$SO^+ + HOCl \rightarrow I_1^+$	$3.47 \times 10^{2}\ M^{-1}\ s^{-1}$	--
C4	$SO^+ + OCl^- \rightarrow I_1$	$3.02\ M^{-1}\ s^{-1}$	--
C5	$I_1 + H^+ \rightarrow I_1^+$	$2.3 \times 10^{9}\ M^{-1}\ s^{-1}$	--
C6	$I_1^+ + HOCl \rightarrow I_2 + P1 + H^+$	$4.75 \times 10^{6}\ M^{-1}\ s^{-1}$	--
C7	$I_2 + HOCl \rightarrow I_3 + Cl^-$	$6.03 \times 10^{9}\ M^{-1}\ s^{-1}$	--
C8	$I_3 + HOCl \rightarrow P_2 + H^+$	$5.78 \times 10^{9}\ M^{-2}\ s^{-1}$	--

The rate limiting step of the oxidation mechanism involves steps initiated by OCl^- or HOCl on SO^+ leading to the formation of the reactive intermediates. (Reactions C3 and C4 are the rate-determining steps for safranine oxidation). Consecutive steps for further oxidation of the reactive intermediates were shown from C5-C8. C6 and C8 representing the reactions leading to different probable products.

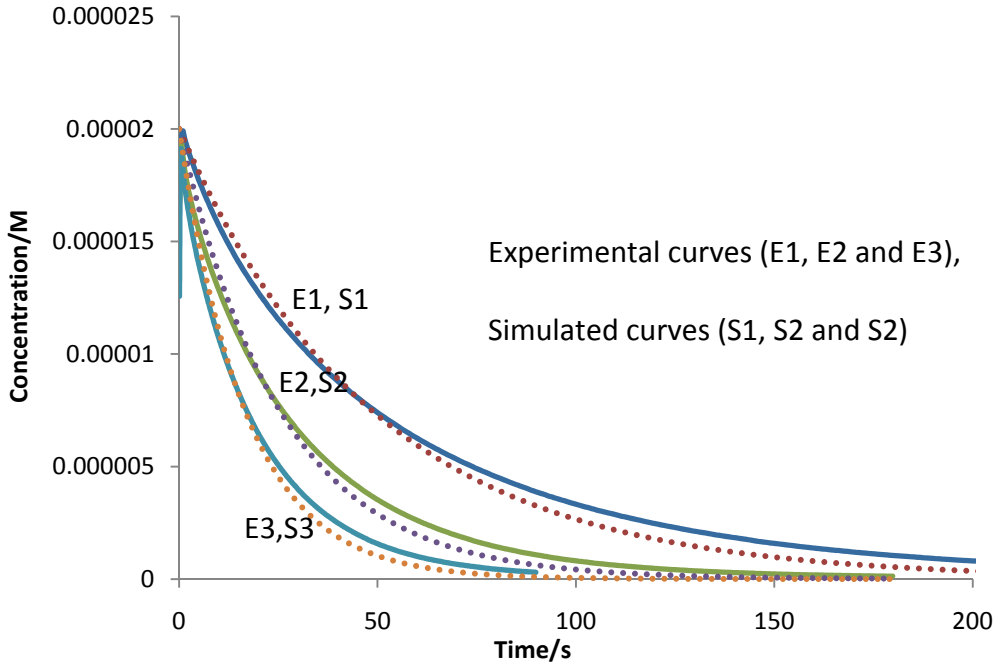

Figure 3.3.17 Experimental curves *versus* simulated curves for reaction of $[SO^{+}]_0$ (3.0×10^{-5}M) with $[OCl^{-}]_t$ (1.45×10^{-3} M).

A fair agreement between the experimental and corresponding simulated curves (Figure 3.3.17), strongly supports that the proposed reaction scheme is most probable. The estimated rate constants are fairly acceptable and also substantiate that HOCl is the crucial species that drives the rapid reaction kinetics under low pH conditions.

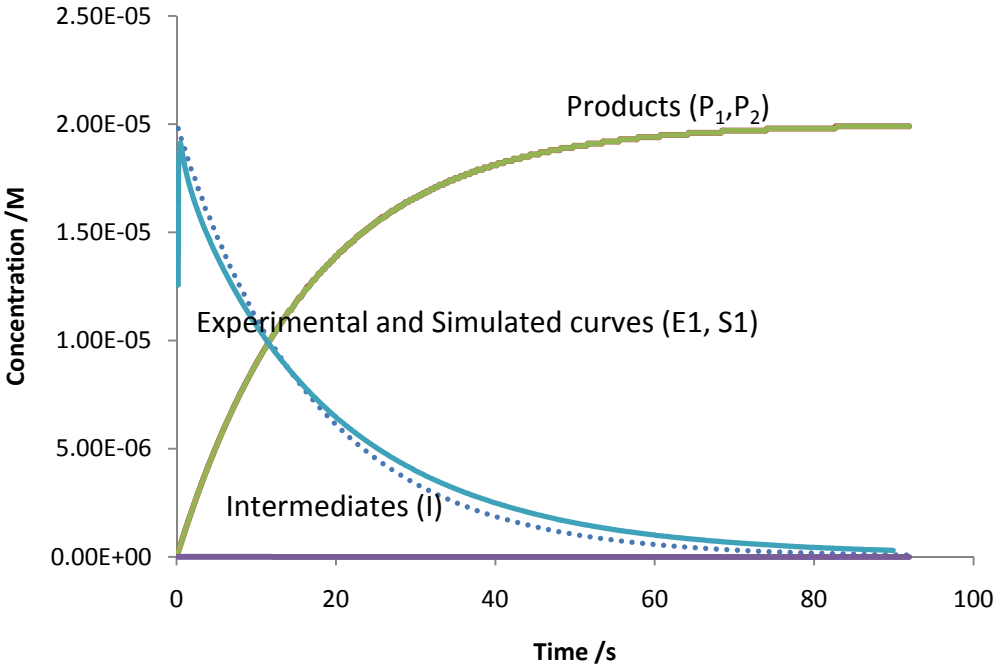

Figure 3.3.18 Product and intermediate formation for the reaction of safranine-O with hypochlorite.

A typical curve is analysed for product and intermediates formation and the analysis isshown in Figure 3.3.18 (conditions similar to curves in Figure 3.3.17). Curves E1 and S1 shows the experimental and simulated curves for the reaction. P_1 and P_2 represent the product formation while the substrate depletion (E1) and I represent the intermediates formed during the process. The compiled data of simulated *versus* experimental curves and the concentrations of the other reactants intermediate and products are presented (Appendix 1, Table 1.5 and 1.6).

CHAPTER 4
OXIDATION OF DYES WITH CHLORINE DIOXIDE

Chlorine dioxide is a strong oxidising agent with capability to oxidise both organic and inorganic pollutants and biotical properties for disinfection of water. Over 95% of the chlorine dioxide produced in the world today is made from sodium chlorite. Chlorine dioxide (ClO_2) has become the most significant bleaching agent in the pulp and paper industry and is currently accepted as most prominent technology for water treatment. In this chapter the results of detailed kinetic and spectroscopic investigations carried out on the reactions of three selected dyes, i.e. amaranth, brilliant blue-R and safranine-O with chlorine dioxide solution as a function of pH are elaborated. The interpretations from the kinetic studies were further supported by measuring the energy parameters for the reactions, product characterisation, and simulations. Plausible mechanisms for all three reactions were proposed.

4.1 Oxidation of amaranth and chlorine dioxide

4.1.1 Order with respect to amaranth

The kinetics of reaction between amaranth and chlorine dioxide were studied under varied reaction conditions with large excess concentration of chlorine dioxide relative to the dye. All the experiments were carried out at 25 ºC (± 0.1) except the runs for estimation of the energy parameters. Figure 4.1.1 shows a typical curve with 0.0115 M initial concentration of ClO_2 and (7×10^{-5} M) of dye at pH 9.0. A perusal of Figure 4.1.1 shows that the reaction had an exponential decay and reaction was completed in less than two seconds, indicating that the reaction is very fast under alkaline conditions.

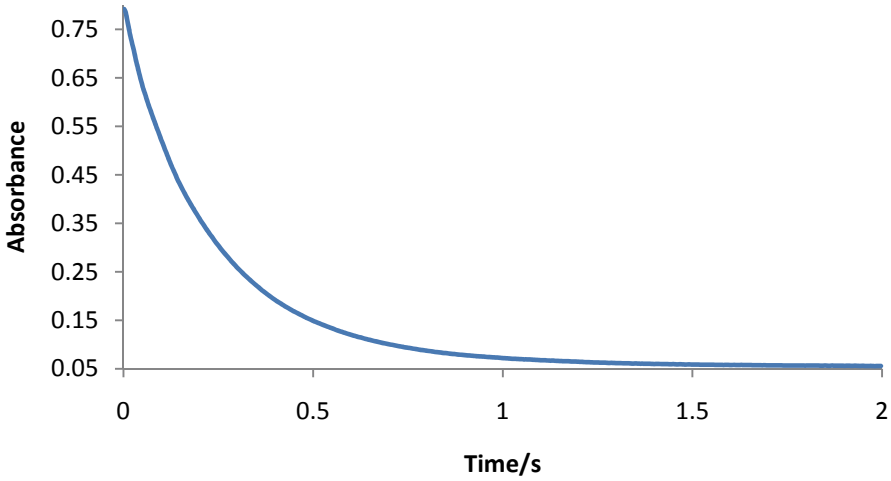

Figure 4.1.1 Typical kinetic curve absorbance *versus* time plot for the reaction of $[AM]_0$ ($7x\ 10^{-5}$ M) with $[ClO_2]_t$ (1.15×10^{-3} M) at pH = 9.0.

4.1.2 Analysis of kinetic data using KinetAsyst™ Fit software

The kinetic data was analysed using the KinetAsyst™ Fit Asystant and the first-order equation as described in detail earlier. Figure 4.1.2 represents the typical experimental curve with the fitted curve.

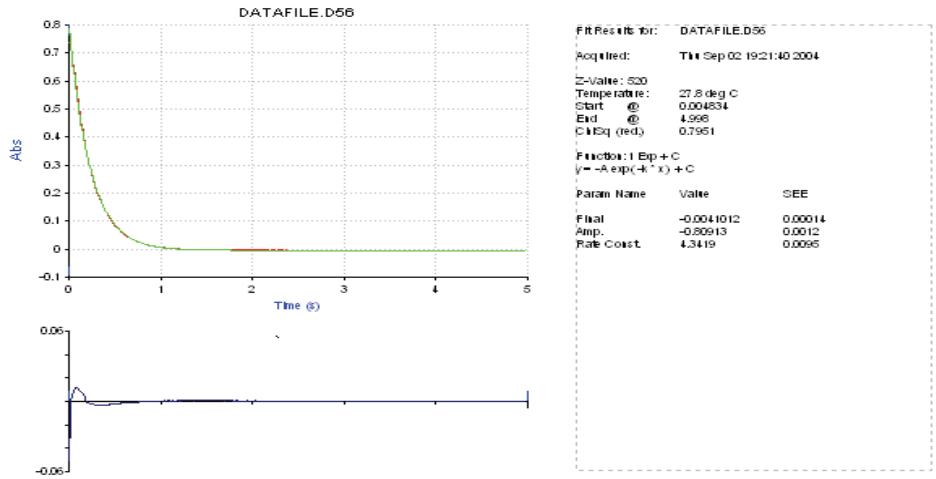

Figure 4.1.2 KinetAsyst™ single-exponential equation fit of two curves and residuals (lower sketch) for the reaction of $[AM]_0$ (7.0×10^{-5} M) with $[ClO_2]_t$ (1.15×10^{-3} M) using the first-order equation {1 Exp + C, y = -A exp (-k * x) + C}.

An observation of Figure 4.1.2 shows that the software fit results for the above curve is a fair agreement that occurs between the experimental and computed curves, with small residuals and the rate constant obtained using first-order rate equation, shows that the *pseudo* first-order rate constant is 4.34 ± 0.01 s^{-1} and further indicates that for the chosen conditions the reaction follows first-order kinetics with respect to the dye.

4.1.3 Order with respect to chlorine dioxide

To establish the reaction order with respect to oxidant, the experiments were carried out at various initial concentrations of chlorine dioxide to monitor the rate of reaction. The reaction was fast and all the reactions exhibited exponential decay characteristics. The reaction rate increased with the increase in the initial concentration of chlorine dioxide and reaction was almost completed in less than two seconds. (Figure 4.1.3)

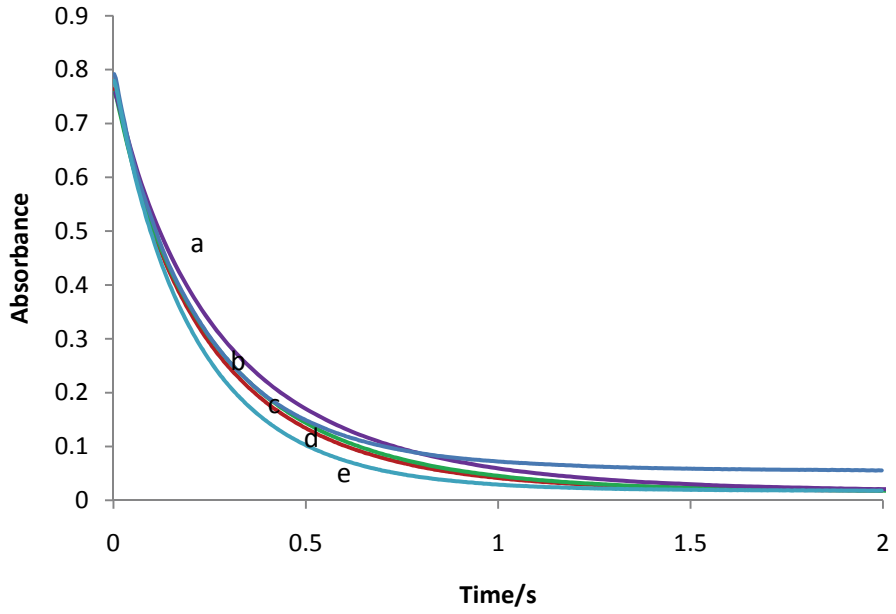

Figure 4.1.3 Depletion of amaranth with various chlorine dioxide concentrations for the reaction of $[AM]_0$ (7.0 x 10^{-5} M) with $[ClO_2]_t$ /10^{-3} M (a = 2.52, b = 3.79, c = 5.05, d = 6.31 and e = 7.57) at pH = 9.0.

The absorbance *versus* time plots and the corresponding k' (s^{-1}) values are illustrated in Figure 4.1.3, corresponding fitted curves are shown in Figure 4.1.4 The k' values were obtained by analysing the respective kinetic curves.

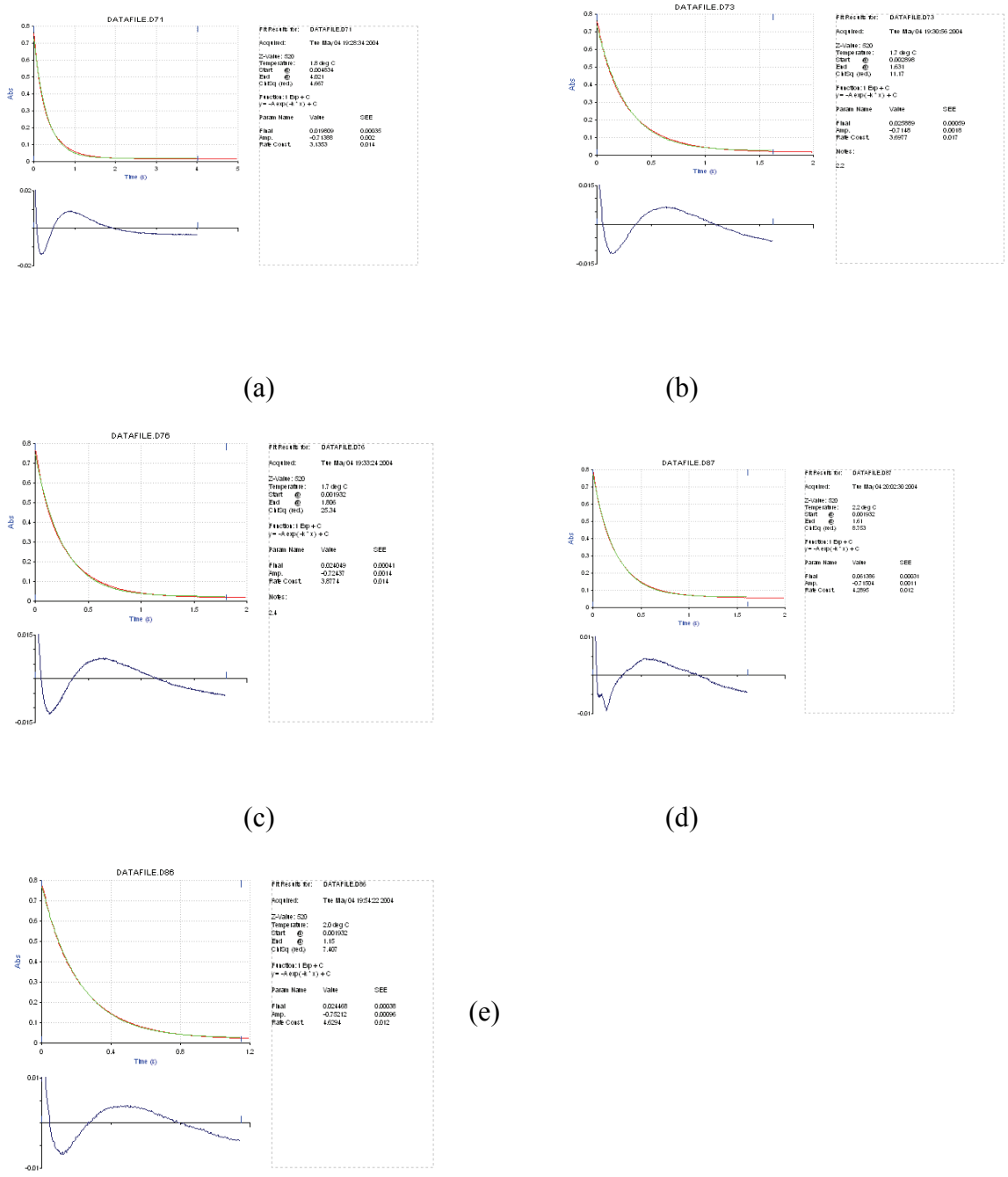

Figure 4.1.4 Fits using KinetAsyst™ single-exponential equation, and rate equation {1 Exp + C, y = -A exp (-k * x) + C} for the reaction for amaranth with chlorine dioxide where k' /s^{-1} (a = 3.32, b = 3.74 , c = 3.99 , d = 4.22 and e = 4.80)

Table 4.1.1 summarises the values of *pseudo* first-order rate coefficients, k' obtained for different chlorine dioxide initial concentrations at fixed ionic strength, and Figure 4.1.5 illustrates the ln $[ClO_2]$ *versus* ln k' plot.

Table 4.1.1. Reaction between amaranth and chlorine dioxide at constant ionic strength $[ClO_2]_t$ ($2.5 \times 10^{-3} - 7.5 \times 10^{-3}$ M) with $[AM]_0$ (7.0×10^{-5} M), pH = 9.0 and ionic strength (I = 0.128).

$[ClO_2] / 10^{-3}$ M	k'/s^{-1}*
2.52	3.320
3.79	3.740
5.05	3.990
6.31	4.340
7.57	4.800

* Mean of four replicate experiments with relative standard deviation < 4%

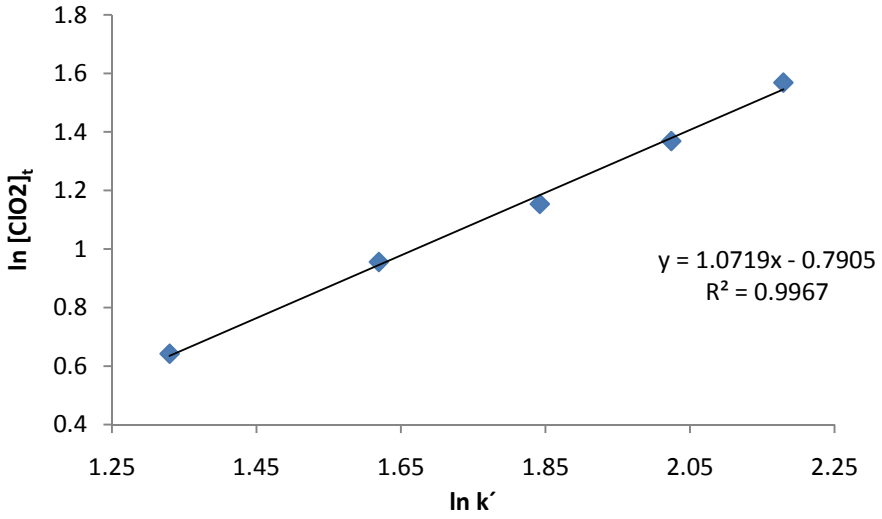

Figure 4.1.5 Plot of ln $[ClO_2]_t$ *versus* ln k' for the reaction of $[AM]_0$ (7.0×10^{-5} M) with $[ClO_2]_t$ ($2.5 \times 10^{-3} - 7.5 \times 10^{-3}$ M) at pH = 9.0 and I = 0.128 M.

The plot of ln [ClO_2] *versus* ln k' (Figure 4.1.5) gave a linear curve with a slope (1.07) and correction coefficient (0.99) suggesting that the reaction rate has first-order dependence on $[ClO_2]_0$.

4.1.4 Effect of pH on reaction rate and reaction order with respect to OH^- ion

The literature survey of the chlorine dioxide chemistry shows that predominant oxidation reaction mechanism for chlorine dioxide proceeds through a process known as free radical electrophilic abstraction rather than by oxidative substitution or addition (as in chlorinating agents such as chlorine or hypochlorite). Chlorine dioxide functions as a highly selective oxidant due to its unique one-electron abstraction mechanism, whereby it is reduced to chlorite (ClO_2^-). Unlike the oxidants Cl_2 and HOCl, which are more effective under acidic conditions, chlorine dioxide is more reactive at higher pH. [203]

Chlorine dioxide is relatively inert and stable under acidic pH and it becomes unstable with increasing pH.[204] Hence, the influence of pH, on the oxidation rate of the substrate by chlorine dioxide was investigated under wide range of pH conditions. The *pseudo* first-order rate constants obtained at different pH conditions were plotted. The plot of k' *versus* pH (Figure 4.1.6) suggests that the rate of oxidation of substrate increased with increasing pH from 6.0 to 9.0.

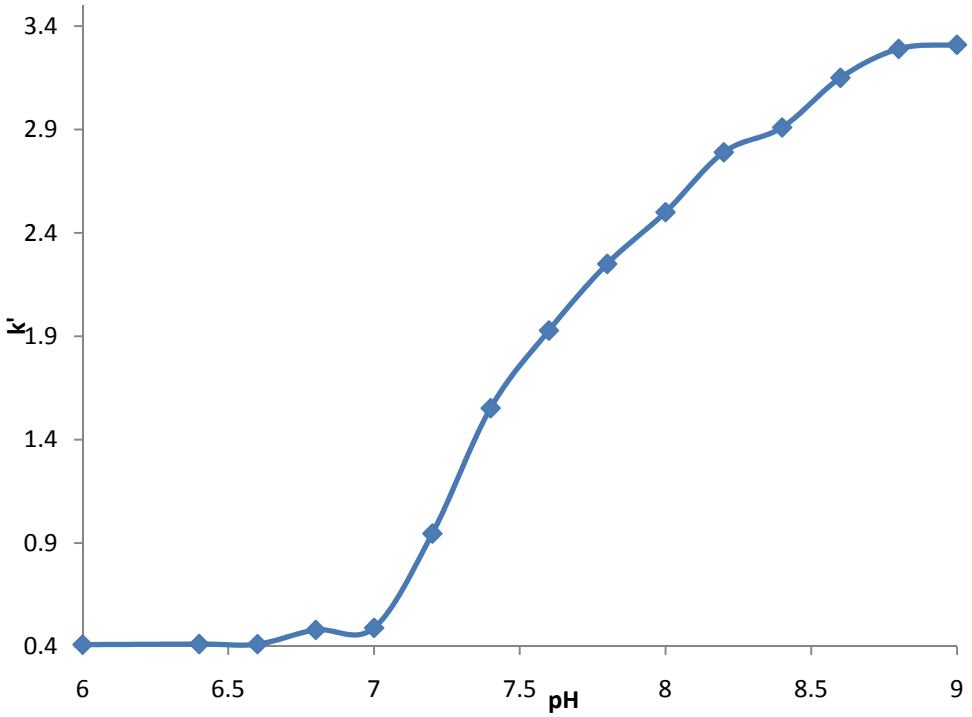

Figure 4.1.6 Plot of k' *versus* pH for the reaction of $[AM]_0$ (7.0×10^{-5} M) with $[ClO_2]_t$ (1.15×10^{-3} M), $[H^+]_{eq}$ (1.99×10^{-9}- 7.752×10^{-4} M).

Table 4.1.2. Effect of pH on reaction rate for the reaction.

pH	k'/s^{-1}
6.0	0.409
6.4	0.411
6.6	0.411
6.8	0.480
7.0	0.490
7.2	0.946
7.4	1.552
7.6	1.928
7.8	2.250
8.0	2.500

Table 4.1.2 contd….

8.2	2.790
8.4	2.910
8.6	3.150
8.8	3.290
9.0	3.310

* Mean of four replicate experiments with relative standard deviation < 4%

To establish the role of hydroxide ion in the reaction mechanism, the order with respect to hydroxide ion was estimated by plotting the ln k' *versus* ln [OH^-] (Figure 4.1.7). The slope of the plot was equal to 0.83 suggesting that reaction rate is close to first-order dependence on the hydroxide concentration.

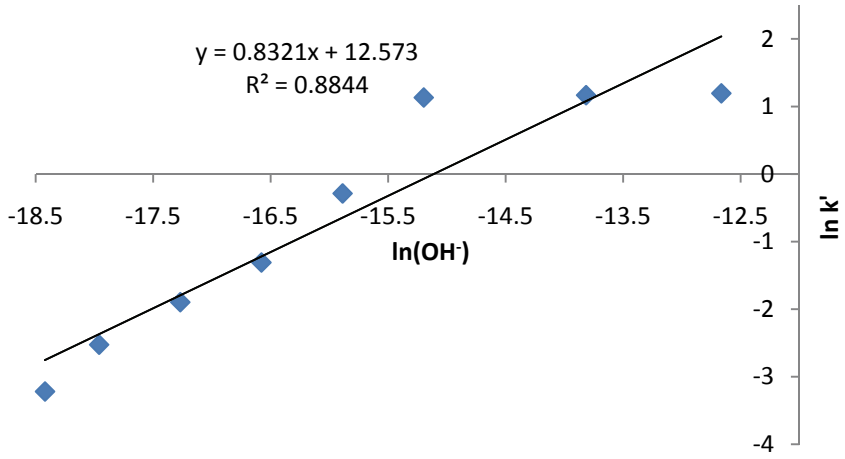

Figure 4.1.7 Plot of ln [OH^-] *versus* ln k' for the reaction of $[AM]_0$ (7.0×10^{-5} M) with $[ClO_2]_t$ (1.15×10^{-3} M),$[OH^-]_{eq}$ ($1 \times 10^{-8} - 1.95 \times 10^{-7}$ M).

The [OH^-] variation experiments were repeated with increased number of runs in each of the pH ranges, the log k' *versus* log [OH^-] were plotted in three different pH ranges (Figure 4.1.8). The reaction order with respect to [OH^-] is observed to decrease with increasing pH.

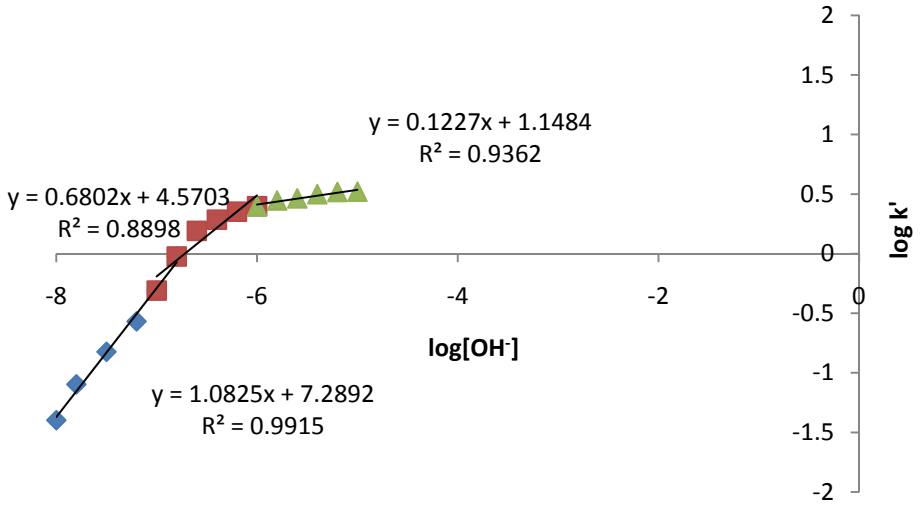

Figure 4.1.8 Plot of log [OH^-] *versus* log k' at different pH conditions.

The observed order with respect to hydroxide ion under near neutral conditions was near unity and its decrease with increasing pH (Figure 4.1.8), can be possibly explained in terms of the likely occurrence of competitive reactions involving chlorine dioxide, with and without the involvement of hydroxide ion. The probable rate of reaction contributed by the two competitive reactions may be expressed as

(4.1)

$$r = k_1 [ClO_2] [AM^-] + k_{OH^-} [ClO_2] [OH^-] [AM^-]$$

$$= \{k_1 + k_{OH^-} [OH^-]\}[ClO_2] [AM^-] = k [ClO_2] [AM^-] = k' [AM^-]$$

Where k' is the observed *pseudo* first-order rate constant in the presence of excess concentration of chlorine dioxide. The second-order rate constant, k is equal to k'/[ClO_2] and for fixed [ClO_2] it can be expressed as $k = k'/[ClO_2] = \{k_1 + k_{OH^-} [OH^-]\}$, where k_1 is the second-order rate constant for the reaction between chlorine dioxide and dye, and k_{OH^-} is the third-order rate constant for the reaction between chlorine dioxide and dye, which is catalysed by [OH^-]. If the assumption is valid, then in presence of [OH^-] conditions, the plot of k'/[ClO_2]

versus $[OH^-]$ should give a straight line Such a linear curve should have intercept equal to k_1 and slope equal to k_{OH^-}. Most likely, such a linear relationship may not be observed at high concentrations of hydroxide, when it reaches stoichiometric proportions of the reductant. The plot of second order rate constant k *versus* $[OH^-]$ is illustrated in Figure.4.1.9. Table 4.1.3 summarises the calculated values of the second-order rate constant.

Table 4.1.3. Calculated $[OH^-]_{eq}$ values and corresponding second order constants for the reaction of $[AM]_0$ (7.0×10^{-5} M) with $[ClO_2]_t$ (1.15×10^{-3} M).

$[OH^-]_{eq}$/M	k'/s^{-1*}	$k/ 10^2 M^{-1}s^{-1}$
7.94×10^{-9}	0.08	0.3
1.58×10^{-8}	0.12	0.5
2.51×10^{-8}	0.15	1.0
6.31×10^{-8}	0.17	1.8
1.78×10^{-7}	0.49	3.3
6.31×10^{-7}	1.30	6.3
3.16×10^{-6}	4.30	10.4
7.94×10^{-6}	5.80	12.9

* Mean of four replicate experiments with relative standard deviation < 4%

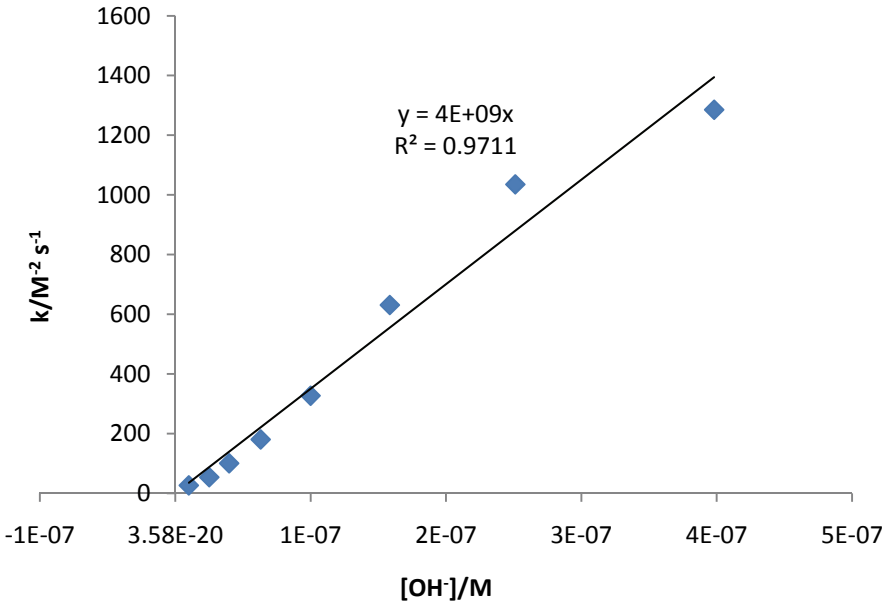

Figure 4.1.9 Plot of $[OH^-]$ *versus* $k'/[ClO_2]$ for the reaction $[AM]_0$ (7.0×10^{-5} M) with $[ClO_2]_t$ (1.15×10^{-3} M), $[OH^-]_{eq}$ (1.0×10^{-8}- 6.31×10^{-7} M).

An observation of the Figure 4.1.9 shows that y-intercept value (k_1) is of very small value, suggesting that in the absence of hydroxide ion, the reaction is very slow and almost nil, which can be predicted from the reported inert behavior of chlorine dioxide at acidic pH. From the plot (Figure 4.1.9), the catalytic constant for the hydroxide catalysed reaction was estimated to be 4.0×10^9 M^{-2} s^{-1} in the pH range of 6.0 - 7.5.

Although a number of literature reports describe the increased decomposition of chlorine dioxide at higher pH conditions, very few studies explain the chemistry involved in the increased oxidative activity of chlorine dioxide. With many reactants, the reaction of chlorine dioxide undergoing one electron reduction forming chlorite ion is fast ($ClO_{2(aq)} + e^- \rightarrow ClO_2^-$, $E° = 0.954$ V)[205,206] during such reactions, chlorite is reported as the reaction product. At alkaline pH conditions, even in the absence of reducing substrates, the chlorine dioxide is known to disproportionate forming chlorite and chlorate ions, various reactions leading to

disproportionation of chlorine dioxide under alkaline conditions result only in formation of less reactive species such as chlorite and chlorate.[207]

$$ClO_2 + AM^- \rightarrow ClO_2^- + AM \quad (4.2)$$

$$2ClO_2 + 2OH^- \rightarrow ClO_2^- + ClO_3^- + H_2O \quad (4.3)$$

Under alkaline conditions, relative to ClO_2 both chlorite and chlorate ions are less reactive species. The reactions of chlorite ion are relatively slow under acidic conditions and much slower with alkaline pH. Chlorate is almost inert under alkaline conditions. The species that possibly could attack the substrates at a significant rate are $HClO_2$, Cl_2O_4, HOCl and peroxide ion. Their concentrations under alkaline pH play a significant role in estimating their contribution towards higher reactivity. The concentrations of reactive species such as $HClO_2$ and HOCl under alkaline conditions will be very small, contributing negligibility towards the oxidation of the substrate. The formation of a dimer of ClO_2, i.e. Cl_2O_4 is not pH dependent. Hydroxide ion with two molecules of ClO_2 could lead to the formation of peroxide ion, but in small concentrations.[208,209]

$$ClO_2 + OH^- \rightleftharpoons (OClOOH)^- \quad (4.4)$$

$$(OClOOH)^- + ClO_2 \rightleftharpoons OClOOH + ClO_2^- \quad (4.5)$$

$$OClOOH + OH^- \rightleftharpoons HOClO + HOO^- \quad (4.6)$$

$$HOO^- + 2ClO_2 + OH^- \rightleftharpoons 2ClO_2^- + H_2O \quad (4.7)$$

Thus the increased reactivity under alkaline pH is certainly not due to such less reactive species. Hence higher reaction rates with increasing hydroxide concentration observed need to

be explained from a different point of view. This probably happens through OH^- ion facilitated generation of much reactive species. Possibly, such species could form a transient complex involving OH^- ion, ClO_2 and substrate. Considering the almost first-order dependence of the reaction rate on hydroxide ion near neutral conditions, its direct role in the rate limiting step through probable formation of a reactive intermediate involving oxidant, reductant and hydroxide can be envisaged.

$$ClO_2 + AM + OH^- \rightarrow [ClO_2\ AM\ OH^-] \qquad (4.8)$$

Margerum *et al*.[210] in their studies on the oxidation of nitrogen dioxide with chlorine dioxide under alkaline conditions suggested the role of hydroxide ion with a preferential binding to NO_2 yielding ClO_2^- and NO_3^- as products. If, the nucleophile associated with ClO_2 instead, as was reported previously, ClO_2^- and ClO_3^- would be the products. Margerum *et al*., indicated in the mechanism that NO_3^- is formed preferentially over ClO_3^- with small amounts of chlorate.

4.1.5 Effect on pH on the order with respect to chlorine dioxide

To assess the role of pH on the reaction order with respect to chlorine dioxide, experiments were conducted with varied initial concentrations of chlorine dioxide at three pH values (7.0, 8.0 and 9.0). The values of first-order rate coefficients, k' for different $[ClO_2]$ are shown in Table 4.1.4 at different pH values.

Table 4.1.4. Observed rate constants at pH 7.0, 8.0 and 9.0 regions for the reaction of $[AM]_0$ (7.0×10^{-5} M) with $[ClO_2]_t$ (1.15×10^{-3} M).

pH = 7.0			
$[ClO_2] \times 10^{-3}$ /M	k'/ s^{-1}*	$k_2/M^{-1}s^{-1}$	k
2.52	0.49	19.44	1.94×10^8
2.77	0.78	20.58	2.06×10^8
3.03	0.93	18.41	1.84×10^8
3.28	1.30	20.60	2.06×10^8
3.53	1.50	19.81	1.98×10^8
	Mean k_2 with std.dev.	19.8 ± 0.9	
pH = 8.0			
$[ClO_2] \times 10^{-3}$ /M	k' /s^{-1}	$k_2/M^{-1}s^{-1}$	k
2.52	2.50	99.20	9.9×10^7
2.77	2.60	93.86	9.4×10^7
3.03	2.90	95.70	9.6×10^7
3.28	3.20	97.56	9.8×10^7
3.53	3.50	99.15	9.9×10^7
	Mean k_2 with std.dev.	97.1 ± 2.3	
pH = 9.0			
$[ClO_2] \times 10^{-3}$ /M	k' /s^{-1}	$k_2/M^{-1}s^{-1}$	k
2.52	3.32	131.74	1.3×10^7
2.78	3.74	134.53	1.3×10^7
3.03	3.99	131.68	1.3×10^7
3.28	4.22	128.65	1.3×10^7
3.53	4.80	135.97	1.4×10^7
	Mean k_2 with std.dev.	132.5 ± 2.8	

where $k_2 = k' / [ClO_2^-]$, $k = k' / \{[ClO_2][OH^-]\}$ * four replicate experiments with RSD < 4%

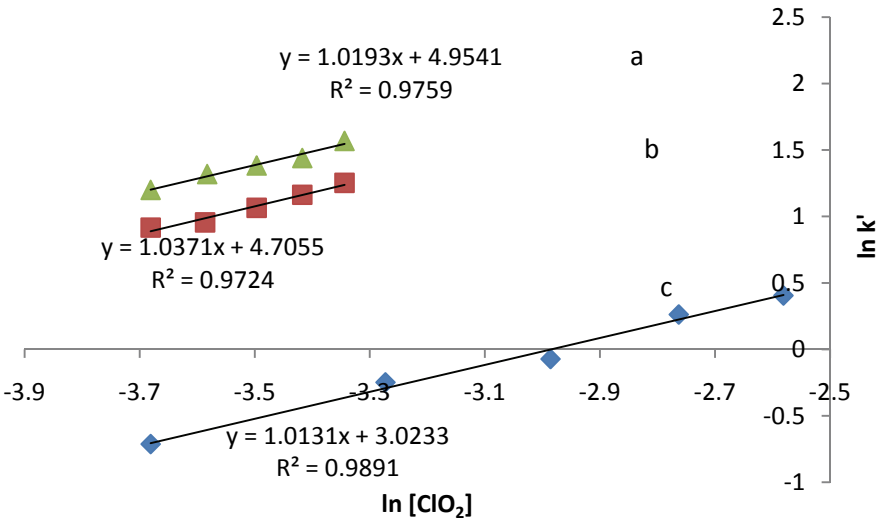

Figure 4.1.10 Plot of ln k' *versus* ln $[ClO_2]$ for the reaction of $[AM]_0$ (7.0×10^{-5} M) with $[ClO_2]_t$ (1.15×10^{-3} M), a (pH = 9.0), b (pH = 8.0), c (pH = 7.0).

Figure 4.1.10 shows the linear plots of ln k' *versus* ln $[ClO_2]$ at pH 7.0, 8.0 and 9.0 with slopes equal to 1.01, 1.04 and 1.01 respectively. The experimental results confirm that the change in pH doesn't have influence on the order with respect to ClO_2 or the overall reaction mechanism.

4.1.6 Kinetic salt effect

From the pH studies, it is evident that the reaction pathway involves $[OH^-]$ at both neutral and alkaline conditions. To confirm this assumption, the kinetic salt effect on the reaction was investigated, by measuring the reaction rates at varied ionic strengths and fixed concentrations of amaranth and chlorine dioxide. A perusal of Table 4.1.5 indicates that the increase in I resulted in increase in k' values resulting in positive salt effect. The log k' *versus* square root of ionic strength is plotted in Figure 4.1.11.

Table 4.1.5. Effect of ionic strength on the reaction rate, $[AM]_0$ (7.0×10^{-5}M) with $[ClO_2]_t$ (1.15×10^{-3} M), pH = 8.0.

Ionic Strength, I/M	k'/s^{-1}*
0.0096	3.11
0.0174	3.41
0.0262	3.57
0.0354	3.75
0.0397	3.95

*Mean of four replicate experiments with relative standard deviation < 4%

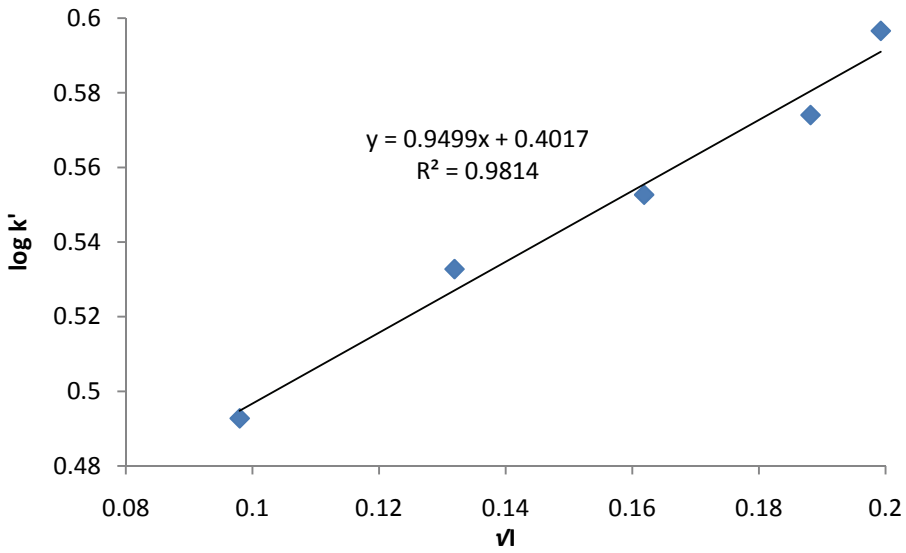

Figure 4.1.11 Plot of log k' *versus* √I for the reaction of $[AM]_0$ (7×10^{-5} M) with $[ClO_2]t$ (1.15×10^{-3} M) at varying ionic strength, I (0.0096 - 0.03) .

The positive slope obtained (0.94) with correlation coefficient R^2 = 0.98 (Figure 4.1.11) indicates the rate-limiting step involves similar like charged species possibly i.e. $[OH^-]$ and AM^-.

4.1.7 Effect of chloride on reaction rate

The reaction rate can be affected by the presence of other species. The presence of the other ions may interfere with the reaction being investigated. The effect of chloride taken at varied concentrations was investigated by adding small amounts of sodium chloride salt.

Table 4.1.6. Varied chloride concentration and observed rate constants for the reaction of $[AM]_0$ (7.0×10^{-5} M) with $[ClO_2]_t$ (1.15×10^{-3} M) .

$[Cl^-]$/M	k'/s^{-1}*
0.148	0.486
0.298	0.496
0.447	0.502
0.597	0.512
0.725	0.530

*Mean of four replicate experiments with relative standard deviation < 4%

From Table 4.1.6 the added chloride shows a small increase in rate of oxidation. Unfortunately the literature survey did not provide any adequate explanation of such behavior. Some chloride and other species might have formed a weak oxidant hypochlorite that may have contributed towards the increase in the rate.

4.1.8 Activation parameters

The enthalpy and entropy of activation of a chemical reaction provide valuable information about the nature of the transition state, and hence about the reaction mechanism. The temperature dependence of the rate constant k, was studied by performing experiments at different temperature ranges 10 ºC to 30 ºC. A typical Eyring's plot is shown in Figure 4.1.12. Assuming that the main path way of oxidation is OH^- facilitated, and taking the reaction order

with respect to OH^- as unity the overall third order reaction coefficients calculated in Table 4.1.7.

Table 4.1.7. Varied temperature in presence of chlorine dioxide and observed rate constant for the reaction of $[AM^-]_0$ (7.0×10^{-5} M) with $[ClO_2]_t$ (1.15×10^{-3} M).

T/K	k'/s^{-1}*	$k_3/ M^{-2} s^{-1}$
283	0.050	3.33×10^6
288	0.090	6.00×10^6
293	0.120	8.00×10^6
298	0.170	1.10×10^7
303	0.210	1.40×10^7

*Mean of four replicate experiments with relative standard deviation < 4%

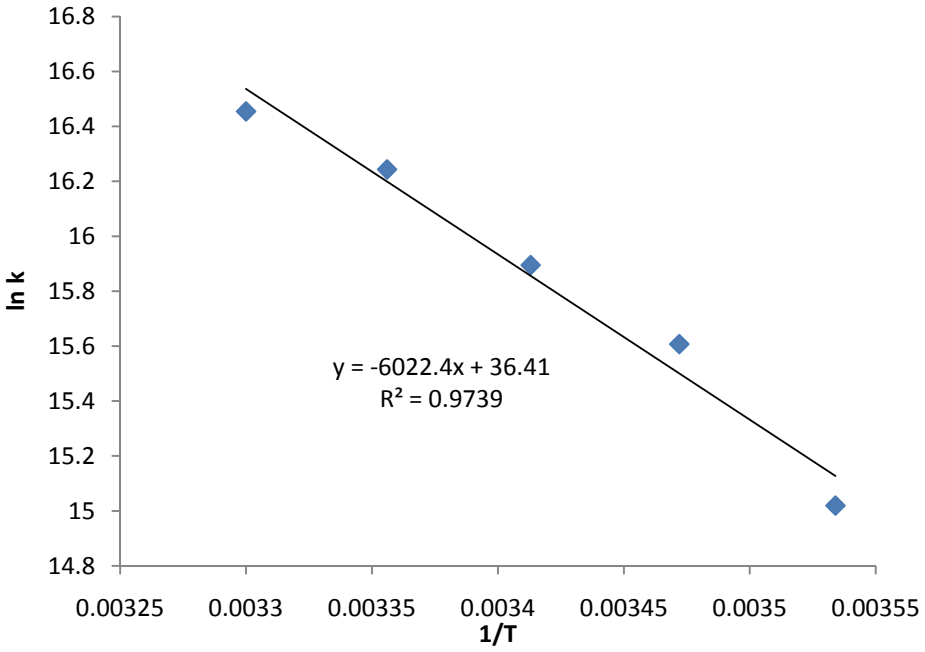

Figure 4.1.12 Plot of ln k *versus* 1/T for the reaction of amaranth with ClO_2 at different temperatures.

From Figure 4.1.12 the value of the slope obtained is equals to -Ea/R, and the calculated energy of activation for this reaction is found to be 50.06 kJ mol^{-1}.

Table 4.1.8. Energy parameters.

Reaction	Enthalpy of reaction, $\Delta H^{\ddagger}$/kJ mol^{-1}	Entropy of activation, $\Delta S^{\ddagger}$/J K^{-1} mol^{-1}	Energy of activation E_a/kJ mol^{-1}
AM^- with ClO_2	47.58	-658.73	50.06

The enthalpy of activation, $\Delta H^{\ddagger}$ for the reaction was found to be 47.58 kJ mol^{-1}, while the entropy of activation was equal to -658.73 J K^{-1} mol^{-1}, suggesting that entropy of activated complex was much lower than that of reactants (Table 4.1.8) of large and negative, and suggests that the formation of the transition state requires the reacting molecules to orient into small conformations and approach each other at a precise angle.

4.1.9 Products identification and characterization

AM-ClO_2 crude product (0.54 g) was chromatographed using silica gel as the stationary phase on a 4 cm diameter column. The mobile phase consisted of hexane: ethyl acetate step gradient 100% hexane (fractions 1-20), 10% dichloromethane in hexane (fractions 20-30) 30% dichloromethane in hexane (fractions 30- 40). Fractions of 10 mL were collected in each step. (fractions 20-30) Elution with 40% ethyl acetate afforded compound 2 (5 mg). The plausible products identified as (P_1 = 1,2 dioxy-3-hyposufite-8-sodiumsufite, P_2 = 1,4 napthalenedione) (Table 4.1.9). Product P_2 is identified in this study.

Table 4.1.9. Possible major oxidation products

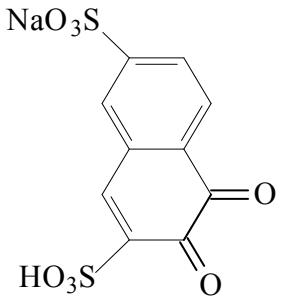 (P_1)	1,2 dioxy-3-hyposulfite-8-sodium sulfite
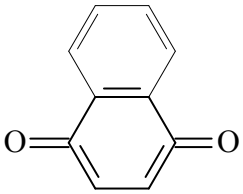 (P_2)	1,4-napthalenedione or 1,4-napthaqunione

4.1.10 Stoichiometric equation

Using 1.5 x 10^{-3} M ClO_2 the stoichiometry of the reaction mixture was maintained with 1:1 and 1:5 ratios of amaranth and chlorine dioxide respectively. After a 30 min reaction, the residual reacted was determined and the amounts reacted were estimated. The stoichiometry was found to be approximately 1:4 (± 10%) of AM^- and ClO_2. Thus, the stoichiometric equation for the overall reaction can be written as

$$AM^- + 4ClO_2 + OH^- + H_2O \rightarrow P_1 + P_2 + 4ClO_2^- + 3H^+ + N_2 + SO_3^{2-} + Na^+ \quad (4.9)$$

Stoichiometry and reaction products varied with longer reaction times

4.1.11 Reaction scheme

One electron abstraction by ClO_2 molecule from nitrogen atom will result in intermediate I_1. I_1 resonates between the two structures. Loss of a hydroxyl proton with subsequent attack by a hydroxyl ion on the carbon atom bearing the nitrogen results in I_2. Three further electron abstractions from I_2 (two electrons from nitrogen yielding N^+ and one electron from the carbon atom in between the two rings) results in I_3. Loss of a proton and rearrangement of the electrons results in product (P_1) and the ring bearing the nitrogen is further attacked by two hydroxyl ions resulting in I_4 which undergoes oxidation to the product napthaquinone (P_2).

The structure of the napthaquionone was verified by the GC-MS and ^1H and ^{13}C NMR spectroscopy (Appendix 2, Figure 2.1.1 and Figure 2.1.2). The singlet peak at δ 6.9 are due to the olefinic proton and the resonances at δ 7.7 - δ 8.2 are due to the protons on the aromatic ring. In the ^{13}C NMR spectrum the carbonyl carbon is seen at δ 185 and the olefinic carbon is seen at δ 126. The aromatic carbons are seen at δ 131, δ 133 and δ 138. The GC-MS shows a molecular ion peak at 158 (product, P_2) at retention time 12.65 min. The loss of the carbonyl group shows a peak at 130 (which is intermediate) and the loss of the double bond can be seen at peak 104 (Appendix 2, Figure 2.1.3)

These identified oxidation products can be explained by the mechanistic scheme illustrated in Figure 4.1.13.

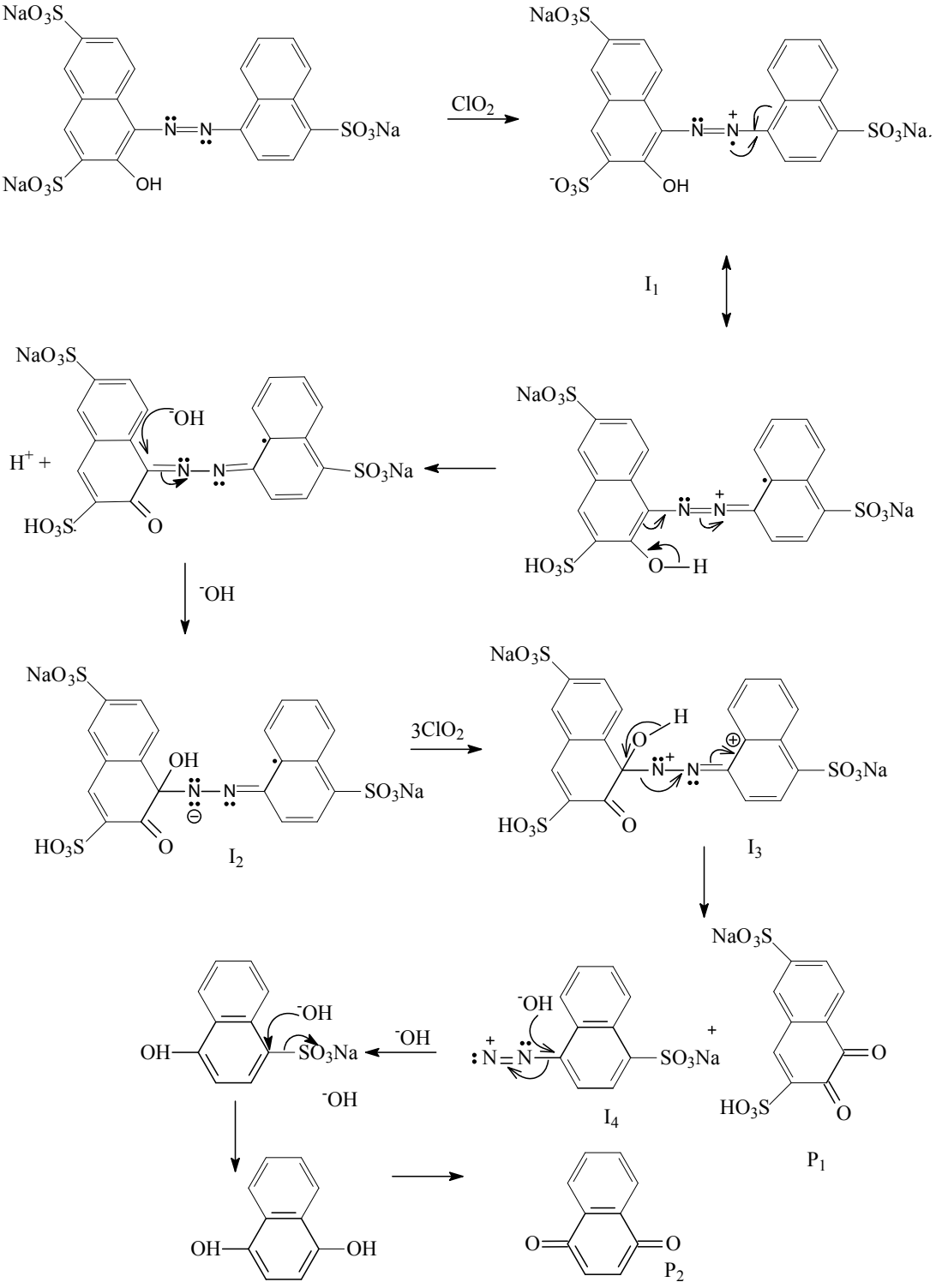

Figure 4.1.13 Plausablie mechanistic scheme for the oxidation of amaranth with chlorine dioxide.

4.1.12 Proposed mechanism

Based on the reaction scheme provided (Figure 4.1.13), and the stoichiometric results obtained the mechanism can be proposed as follows.

$ClO_2 + AM^- \rightarrow ClO_2^- + AM$ (very slow)

$AM^- + ClO_2 + OH^- \rightarrow \{HO\ AM\ ClO_2\}^{2-}$ (slow and rate limiting step)

$\{HO\ AM\ ClO_2\}^{2-} \rightarrow ClO_2^- + \{HO\ AM\}^-$ (fast)

$AM^- + ClO_2 + OH^- \rightarrow I_1^- + ClO_2^-$ R1

$I_1^- + ClO_2 \rightarrow I_2 + ClO_2^-$ R2

$I_2 + ClO_2 \rightarrow I_3^+ + ClO_2^-$ R3

$I_3^+ + ClO_2 \rightarrow I_4^{2+} + ClO_2^-$ R4

$I_4^{2+} \rightarrow P_1 + I_5^+ + H^+ + N_2$ R5

$I_5^+ + H_2O \rightarrow P_2 + 2H^+ + SO_3^{2-} + Na^+$ R6

The overall reaction can be expressed as

$$AM^- + 4ClO_2 + OH^- + H_2O \rightarrow P_1 + P_2 + 4ClO_2^- + 3H^+ + N_2 + SO_3^{2-} + Na^+ \quad (4.10)$$

4.1.13 Rate law

While the overall order was three on chlorine dioxide, reductant and hydroxide ion, all the three reactants registered order of one each. Further the observed positive salt effect on the reaction rate suggests that the rate limiting step involves one each i.e. AM^- and OH^-. Thus, the rate limiting step may involves both AM^-, OH^- and ClO_2 to form the activated complex. The activated complex further undergoes fast consecutive steps.

$$Rate = k_1 [ClO_2][AM^-] + k_2 [ClO_2][OH^-][AM^-] \quad (4.11)$$

As the reaction conditions, fulfill *pseudo* first-order conditions, the rate law may be proposed as

$$= k_1 [ClO_2][AM^-] + k_{OH^-} [ClO_2][OH^-][AM^-] \quad (4.12)$$

where $k_{OH^-} = \frac{k_2}{[OH^-]}$

$$r = \{ k_1 + k_{OH^-} [OH^-]\}[ClO_2][AM^-] \quad (4.13)$$

when $[ClO_2]$ is in large excess then

$Rate = k'[AM^-]$

where the *pseudo* first-order constant, k' equals

$$k' = \{ k_1 + k_{OH^-} [OH^-]\}[ClO_2] \quad (4.14)$$

4.1.14 Simulations

The computer simulations were done using the proposed mechanism using simkine software. The estimated rate constants were adjusted using the software until better fitting was obtained. The rate coefficients used for final simulations were optimized, and matching of the computed curves with experimental profiles under varied reaction conditions obtained are shown in Figure 4.1.14 and Table 4.1.10. C1 is experimentally determined values in the current study. Coefficients used for reactions C3 – C6 are the estimated rate constants. The simulated curves exhibit the behavior of the experimental curves. The graphs showing the simulated and experimental curves are illustrated in Figure 4.1.14.

Table 4.1.10. Forward and reverse rate constants obtained from literature and simulations.

Reaction No	Reaction	Forward rate
C1	$AM^- + ClO_2 + OH^- \rightarrow I_1^- + ClO_2$	$1.0 \times 10^{-7}\ M^{-2}s^{-1}$
C2	$I_1^- + ClO_2 \rightarrow I_2 + ClO_2^-$	$4.0 \times 10^{9}\ M^{-1}s^{-1}$
C3	$I_2 + ClO_2 \rightarrow I_3^+ + ClO_2^-$	$5.34 \times 10^{9}\ M^{-1}\ s^{-1}$
C4	$I_3^+ + ClO_2 \rightarrow I_4^{2+} + ClO_2^-$	$4.97 \times 10^{9}\ M^{-1}s^{-1}$
C5	$I_4^{2+} \rightarrow P_1 + I_5^+ + H^+ + N_2$	$4.54 \times 10^{9}\ s^{-1}$
C6	$I_5^+ + H_2O \rightarrow P_2 + 2H^+ + SO_3^{2-} + Na^+$	$5.17 \times 10^{9}\ M^{-1}s^{-1}$

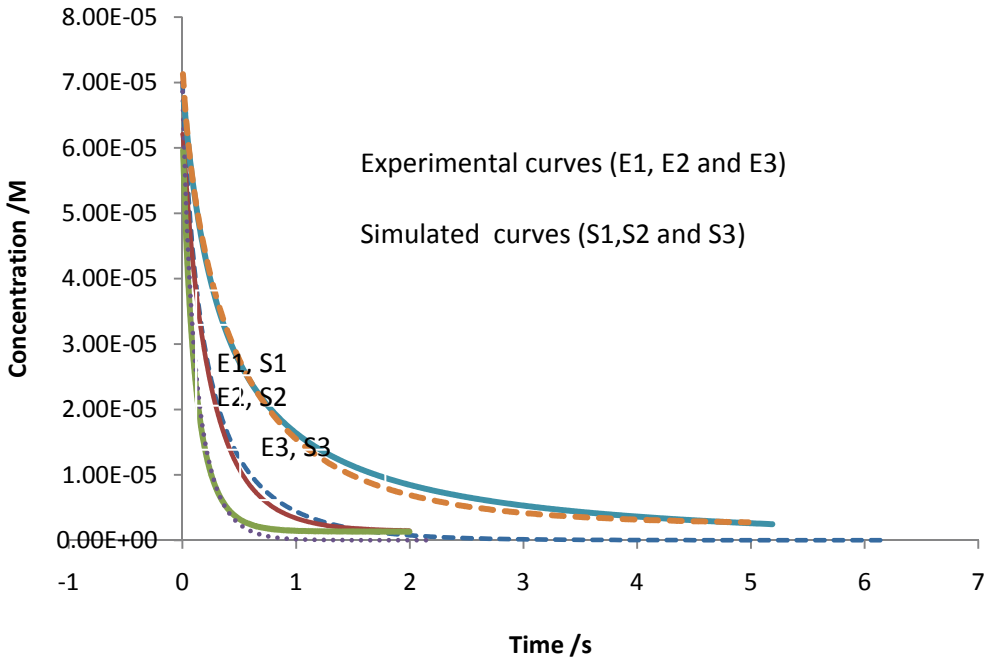

Figure 4.1.14 Experimental curves *versus* simulated curves for reaction of $[AM^-]_0$ (7.0 x 10^{-5} M) with $[ClO_2]_t$ (1.15x10^{-3} M).

From Figure 4.1.14 the generated simulated curves which were indicated by dashed lines matched with experimental curves, fair agreement between the experimental and corresponding simulated curves, strongly support that proposed reaction scheme as most probable and estimated rate constants are fairly acceptable.

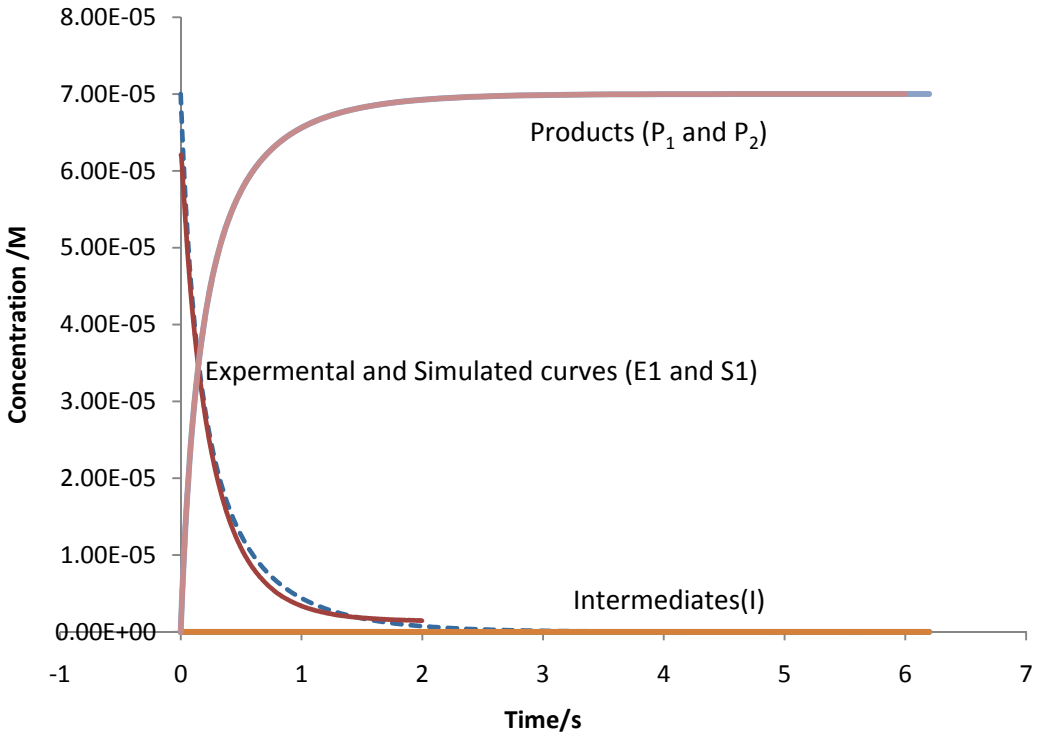

Figure 4.1.15 Intermediates and product formation for the reaction of amaranth with chlorine dioxide.

Figure 4.1.15 (conditions similar to curves in Figure 4.1.14), curves E1 and S1 shows the experimental and simulated curves for the reaction. The kinetic profiles of P_1, P_2 show their formation and I is the intermediate formed during the process. The data of simulated *versus* experimental curves and the concentrations of the other reactants, intermediates and products are compiled and provided (Appendix 2, Table 2.1, Table 2.2).

4.2 Reaction of brilliant blue and chlorine dioxide

4.2.1 Order with respect to brilliant blue-R

Using low concentrations of dye and about hundred-fold excess of other reactants the kinetics of oxidation of brilliant blue by chlorine dioxide was studied as a function of oxidant concentration, pH, ionic strength and temperature. The reaction progress was monitored by measuring the change in concentration of the dye at 555 nm, which is its absorption maximum. At pH 9.0, the depletion of dye was fast and the reaction completed in less than four seconds, with $[BB^+]_0$ 7.0 x 10^{-5} M and with $[ClO_2]_t$ 1.15 x 10^{-3} M (Figure 4.2.1).

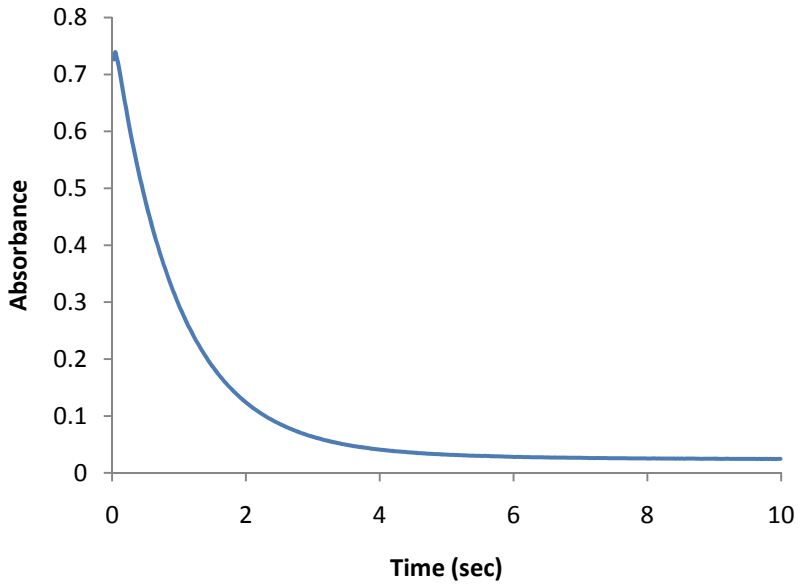

Figure 4.2.1 Typical kinetic curve absorbance *versus* time plot for the reaction of $[BB^+]_0$ (7.0 x 10^{-5} M) with $[ClO_2]_t$ (1.15 x 10^{-3} M) at pH = 9.0 .

4.2.2 Analysis of kinetic data

The analysis of the kinetic data was accomplished using the KinetAsyst^{TM} Fit software as described earlier. All kinetic profiles fitted well with the single exponential equation, confirming the reaction follows first-order kinetics and the order with respect to the dye is one. Figure 4.2.2 represents the typical experimental curve with the fitted curve.

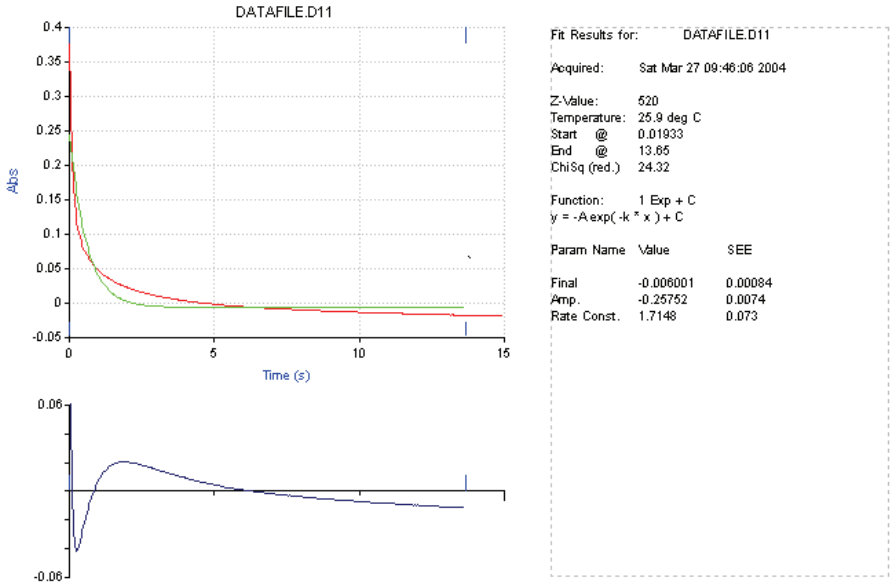

Figure 4.2.2 KinetAsyst^{TM} single-exponential equation fit of two curves and residuals (lower sketch) for the reaction of $[BB^{+}]_0$ (7.0×10^{-5} M) with $[ClO_2]_t$ (1.15×10^{-3} M) using the first-order equation.

An observation of Figure 4.2.2 shows that software fit results for the above curve shows a fair agreement between the experimental and computed curves, with small residuals, and the *pseudo* first-order rate constant obtained is 1.715 s^{-1} with standard deviation of 0.073.

4.2.3 Order with respect to chlorine dioxide

The reaction order with respect to oxidant was investigated by measuring the reaction rates with different initial concentrations of oxidant at constant initial ionic strength and pH. Typical kinetic traces obtained for different initial concentrations of chlorine dioxide are illustrated in Figure 4.2.3.

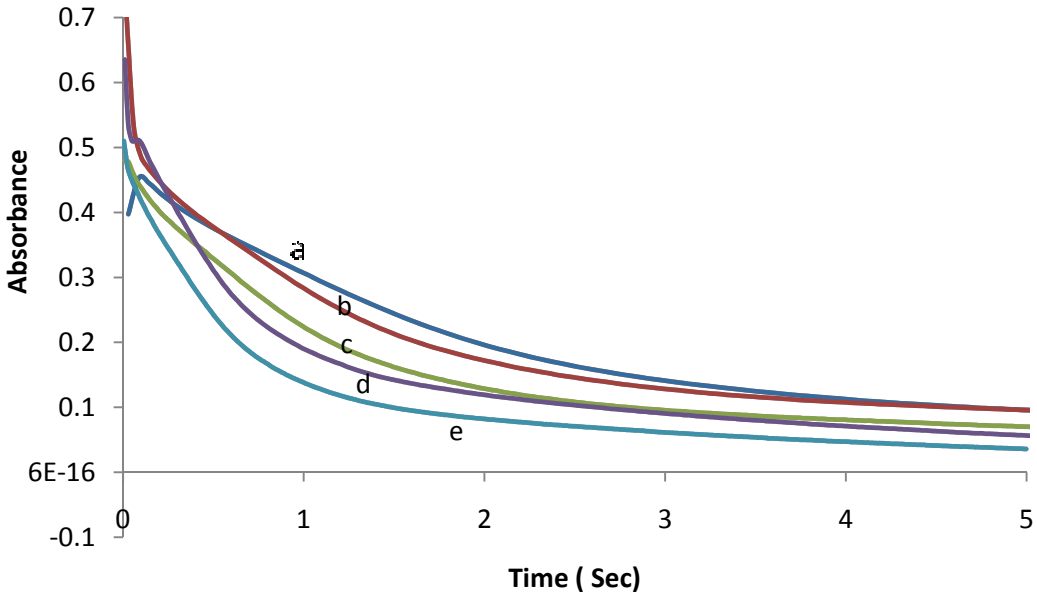

Figure 4.2.3 Depletion of brilliant blue-R with various chlorine dioxide concentrations for the reaction of $[BB^{+}]_0$ (7.0 x 10^{-5} M) with $[ClO_2]_t$ /10^{-3} M at pH = 9.00, I (0.128 M) with $[ClO_2]_t$ / 10^{-3} M (a = 2.52 , b = 2.78 , c = 3.03, d = 3.28 and e = 3.53)

Figure 4.2.4 shows curves illustrated together with fitted curves and corresponding residuals using a first-order expression.

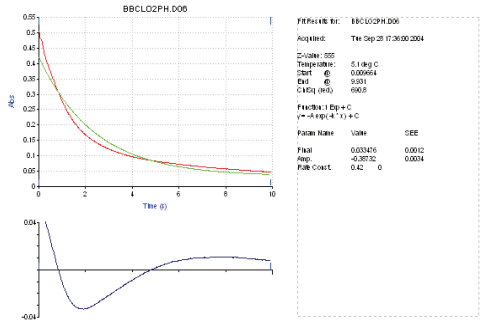

(a)

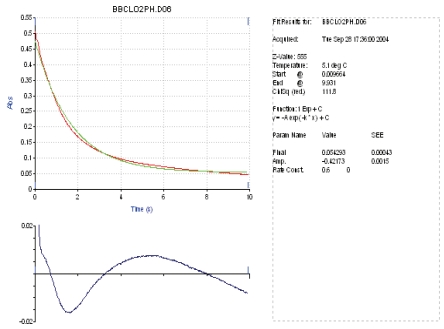

(b)

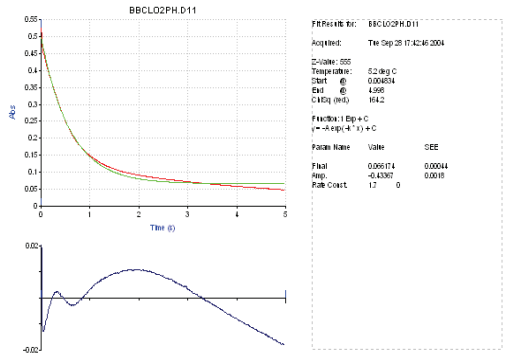

(c)

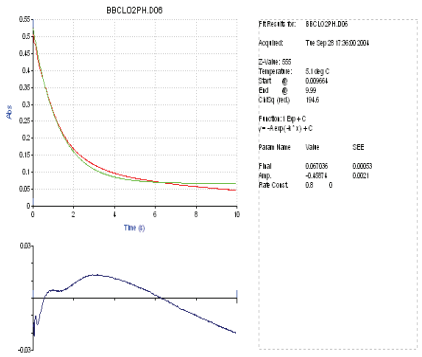

(d)

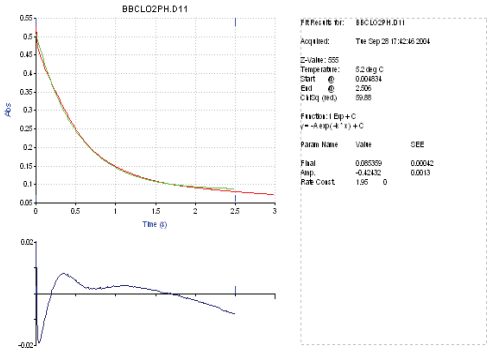

(e)

Figure 4.2.4 Fits using Kinet Asyst ^{TM} single-exponential equation, and rate equation {y = - A exp (-k * x) + C} for the reaction of $[BB^{+}]_0$ (7.0 x 10^{-5} M) where k' /s (a = 3.32, b = 3.74, c= 3.99, d = 4.22 and e = 4.67)

The values of the *pseudo* first-order rate coefficients, k' increased with increasing initial chlorine dioxide concentration and results obtained from the above depicted curves are listed in the Table 4.2.1.

Table 4.2.1 Reaction between brilliant blue and chlorine dioxide at constant ionic strength $[ClO_2]_t$ (2.5×10^{-3} – 3.5×10^{-3} M) with $[BB^+]_0$ (7.0×10^{-5} M), pH = 9.0 and Ionic Strength (I = 0.128).

$[ClO_2]_t$ / 10^{-3} M	k'/s^{-1}*
2.52	3.32
2.78	3.74
3.03	3.99
3.28	4.22
3.53	4.67

*Mean of four replicate experiments with relative standard deviation < 4%

The ln $[ClO_2]_t$ *versus* ln k' plot of the data summarised in Table 4.2.1 is shown in Figure 4.2.5, which had slope value equal to 1.03 ($R^2 = 0.98$). A linear relation with gradient equal to unity confirms reaction has first-order dependence on the oxidant concentration.

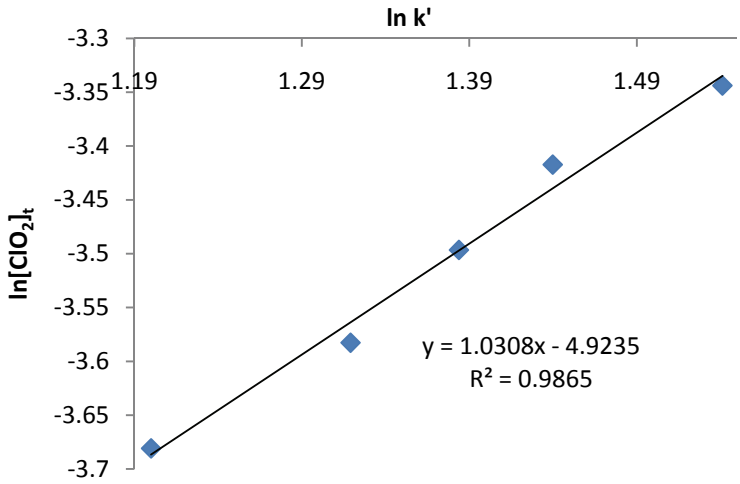

Figure 4.2.5 Plot of ln $[ClO_2]_t$ *versus* ln k' for the reaction of $[BB^+]_0$ (7.0×10^{-5} M) with $[ClO_2]_t$ (2.5×10^{-3} – 3.5×10^{-3} M) at pH = 9.0 and I = 0.128 M.

4.2.4 Effect of pH on reaction rate and reaction order with respect to hydroxide ion.

The dependence of the rate constant on pH was examined under wide range of pH conditions. The values of observed *pseudo* first-order rate constants at different pH conditions are summarised in Table 4.2.2.

Table 4.2.2 Effect of pH on reaction rate for the reaction of $[BB^+]_0$ (7.0×10^{-5} M) with $[ClO_2]_t$ (2.5×10^{-3} – 3.5×10^{-3} M)

pH	k'/s^{-1*}
6.0	0.29
6.3	0.32
6.7	0.38
6.9	0.47
7.2	0.82
7.4	0.96
7.9	1.34
8.1	1.60
8.2	1.69
8.4	1.71
8.6	1.79
8.8	1.75
9.0	1.86

*Mean of four replicate experiments with relative standard deviation < 4%

Figure 4.2.6 shows the plot of k' *versus* pH. Although, chlorine dioxide is known to have a fast reaction at alkaline pH, a perusal of Figure 4.2.6 shows that the rate of oxidation of substrate increases with increasing pH, but the increases registered were not uniform.

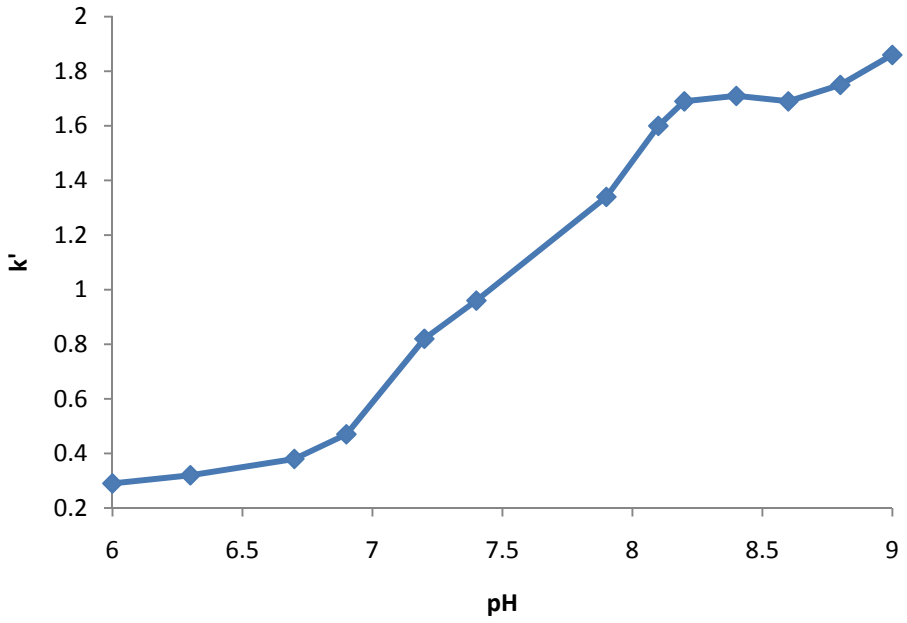

Figure 4.2.6 Plot of k' *versus* pH for the reaction of $[BB^+]_0$ (7.0×10^{-5} M) with $[ClO_2]_t$ (1.15×10^{-3} M), $[H^+]_{eq}$ (1.99×10^{-9}- 7.75×10^{-4} M).

Therefore, to further establish the role of hydroxide ion in the reaction mechanism, the order with respect to it, ln k' values were plotted against their corresponding ln $[OH^-]$ values in the pH range 8.0 - 9.0 (Figure 4.2.7). The slope of the plot was equal to 0.80, and suggests that reaction rate has approximately first-order dependence on the hydroxide ion concentration.

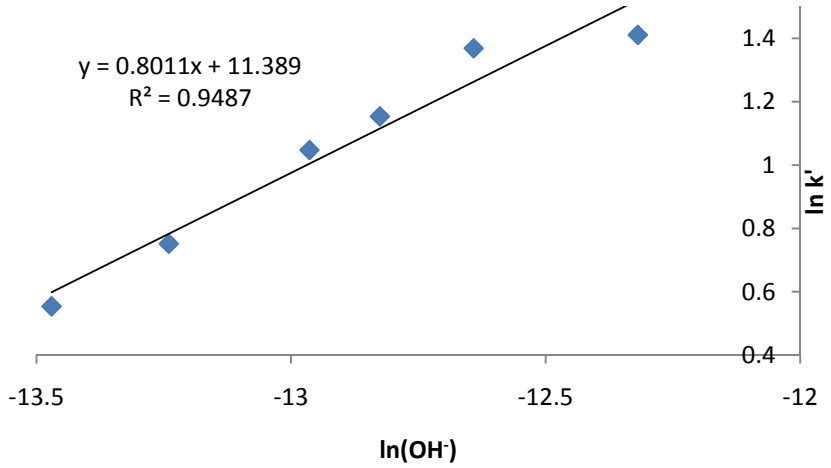

Figure 4.2.7 Plot of ln $[OH^-]$ *versus* ln k' $[BB^+]_0$ (7.0 x 10^{-5} M) with $[ClO_2]_t$ (1.15 x 10^{-3} M).

Figure 4.2.7 illustrates the figure depicting the ln $[OH^-]$ *versus* ln k' graph over the pH range 5.0-9.0 is not a linear curve. Representative linear curves obtained the three different pH ranges were shown in Figure 4.2.8 and suggests that the observed reaction order with respect to $[OH^-]$ is decreased with decreasing pH.

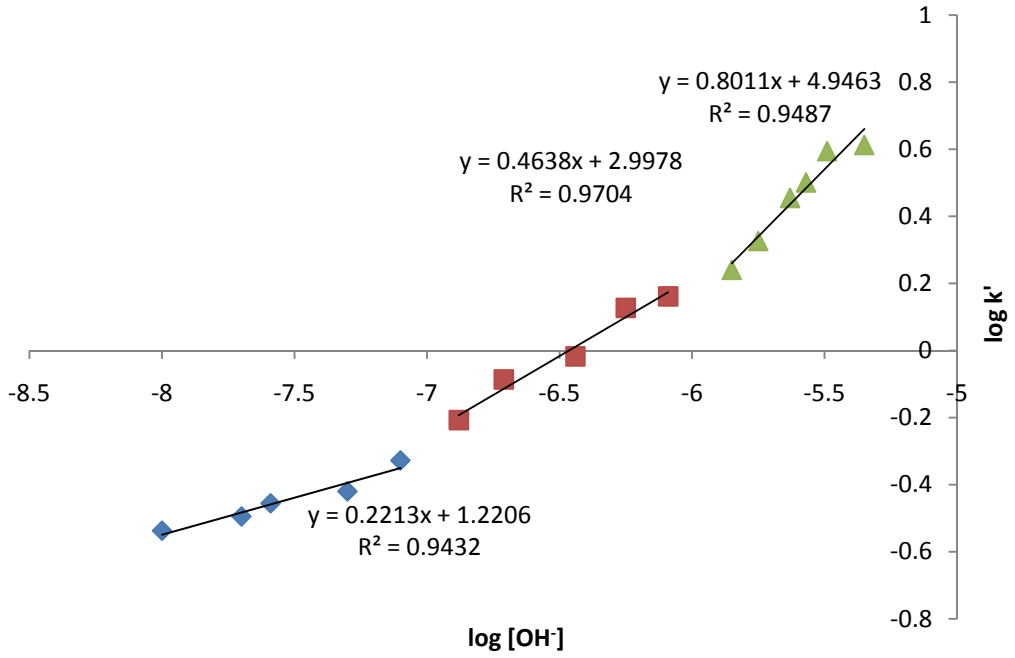

Figure 4.2.8 Plot of log $[OH^-]$ *versus* log k' at different pH conditions.

While the order with respect to hydroxide ion was close to one at neutral conditions, it tends to decrease with decreasing pH, This could be due to likely occurrence of oxidation through two competitive pathways, i.e. one by direct reaction of chlorine dioxide with the cationic dye and the other involving chlorine dioxide, dye and hydroxyl ions at the same given time. At high pH with excess concentration of OH^-, the later reaction which is fast will be predominant and at very low hydroxyl ion concentration, only the former slow reaction will occur. Thus, the probable rate of reaction contributed by the two competitive reactions may be expressed as

$$r = k_1 [ClO_2] [BB^+] + K_{OH^-} [ClO_2] [OH^-] [BB^+] \quad (4.15)$$

$$= \{k_1 + K_{OH^-} [OH^-]\}[ClO_2] [BB^+] = k' [ClO_2] [BB^+] \quad (4.16)$$

where k' is the observed *pseudo* first-order rate constant in presence of excess of chlorine dioxide. The second-order constant, k is equal to $k'/[ClO_2]$ and for fixed $[ClO_2]$ it can be expressed as $k = \{k_1 + k_{OH^-} [OH^-]\}$, where k_1 is the second-order rate constant for the reaction between chlorine dioxide and dye, while k_{OH^-} is the third-order rate constant for the OH^- catalysed reaction between chlorine dioxide and dye.

If the assumption is valid, then with varied initial $[OH^-]$ conditions, a plot of $k'/[ClO_2]$ against $[OH^-]$ should give a straight line. That linear curve should have an intercept equal to k_1 and gradient equal to k_{OH^-}. Such linear relationship may not be observed at high concentrations of hydroxide, when it reaches stoichiometric proportions with the reductant. The calculated values of k at varied hydroxide concentrations are listed in Table 4.2.3 and the plot of second-order constant, k *versus* $[OH^-]$ is illustrated in Figure 4.2.9.

Table 4.2.3 Calculated $[OH]_{eq}$ values and corresponding second-order constants for the reaction of $[BB^+]_0$ (7.0×10^{-5} M) with $[ClO_2]_t$ (1.15×10^{-3} M).

$[OH^-]_0$/M	k'/s^{-1}*	k/ 10^2 $M^{-1}s^{-1}$
1.00×10^{-8}	0.29	1.93
2.00×10^{-8}	0.32	2.13
2.57×10^{-8}	0.35	2.37
5.01×10^{-8}	0.38	2.53
7.94×10^{-8}	0.47	3.14
1.32×10^{-7}	0.62	4.13
1.95×10^{-7}	0.82	5.46

*Mean of four replicate experiments with relative standard deviation < 4%

An observation of the Figure 4.2.9 shows that y-intercept value k_1 is small value, suggesting that in the absence of hydroxide ion, the reaction is about 1.93, which can be anticipated based on the known inert behavior of chlorine dioxide under acidic pH. From the plot (Figure 4.2.9), the catalytic constant for the hydroxide catalysed reaction in the pH range of 6.0-7.5 was estimated to be 2.0×10^9 M^{-2} s^{-1}.

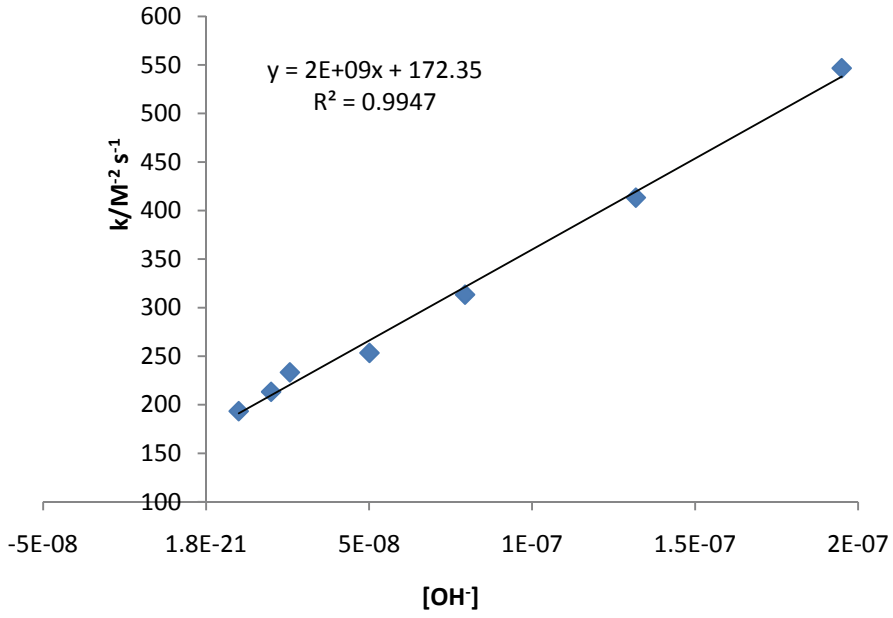

Figure 4.2.9 Plot of $[OH^-]$ *versus* $k/[ClO_2]$ for the reaction $[BB^+]_0$ (7.0×10^{-5} M) with $[ClO_2]_t$ (1.15×10^{-3} M), $[OH^-]_{eq}$(1.0×10^{-8} M - 1.95×10^{-7} M).

As discussed in detail for the reaction of ClO_2 with amaranth, considering almost first-order dependence of the reaction rate on hydroxide ion near neutral conditions, a rate limiting step involving chlorine dioxide, BB^+ and hydroxide may be proposed, with formation an activated complex as intermediate, which decomposes in a fast reaction to form the intermediates or products.

$$ClO_2 + BB^+ + OH^- \rightarrow [ClO_2\ BB^+\ OH^-] \qquad (4.17)$$

4.2.5 Effect of pH on the order with respect to chlorine dioxide

Rates of reaction of chlorine dioxide at three different pH conditions of oxidation of brilliant blue-R was studied. The values of first-order rate coefficients, k and the calculated second-order rate constants, k_2 for different $[ClO_2]$ under varied pH conditions and third-order rate constants k_3 are summarised in Table 4.2.4.

Table 4.2.4 Observed rate constants at pH 7.0, 8.0 and 9.0 regions for the reaction of $[BB^+]_0$ (7.0×10^{-5} M) with $[ClO_2]_t$ (1.15×10^{-3} M).

pH = 7.0			
$[ClO_2] \times 10^{-3}$/M	k'/s^{-1}*	$k_2/M^{-1}s^{-1}$	$k_3//M^{-2}s^{-1}$
2.52	0.29	11.50	1.15×10^8
2.77	0.44	11.60	1.16×10^8
3.03	0.59	11.68	1.17×10^8
3.28	0.75	11.88	1.19×10^8
3.53	0.91	12.02	1.20×10^8
	Mean k_2 with std.dev.	11.7 ± 0.2	
pH = 8.0			
$[ClO_2] \times 10^{-3}$/M	k'/s^{-1}	$k_2/M^{-1}s^{-1}$	$k_3//M^{-2}s^{-1}$
2.52	1.08	42.85	4.30×10^7
2.77	1.15	41.51	4.20×10^7
3.03	1.24	40.92	4.10×10^7
3.28	1.38	42.07	4.20×10^7
3.53	1.41	39.94	4.00×10^7
	Mean k_2 with std.dev.	41.4 ± 1.1	
pH = 9.0			
$[ClO_2]/x \times 10^{-3}$/M	k'/s^{-1}	$k_2/M^{-1}s^{-1}$	$k_3//M^{-2}s^{-1}$
2.52	2.98	118.25	1.18×10^7
2.78	3.24	115.10	1.15×10^7
3.03	3.52	115.51	1.15×10^7
3.28	3.81	115.85	1.15×10^7
3.53	4.25	118.98	1.18×10^7
	Mean k_2 with std.dev.	116.7 ± 1.7	

where $k_2 = k' / [ClO_2]$, $k = k' / \{[ClO_2][OH^-]\}$

*Mean of four replicate experiments with relative standard deviation < 4%

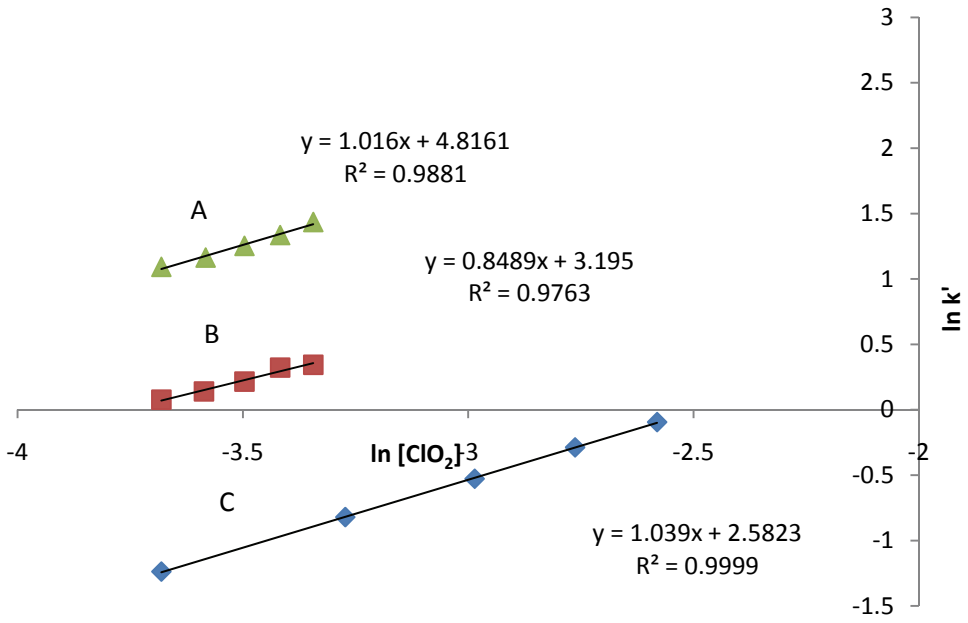

Figure 4.2.10 Plot of ln k' *versus* ln [ClO_2] for the reaction of [BB^+]$_0$ (7.0 x 10^{-5} M) with [ClO_2]$_t$ (1.15 x 10^{-3} M), A (pH = 9.0), B (pH = 8.0), C (pH = 7.0).

Figure 4.2.10 illustrates the plots of ln k' *versus* ln [ClO_2] at pH 7.0, 8.0 and 9.0 obtained were linear with the slopes equal to 1.04, 0.84, 1.03 respectively. The reaction order unity with respect to ClO_2 under different pH conditions confirms that the change in pH doesn't have influence on the order with respect to ClO_2 or on the overall reaction mechanism.

4.2.6 Kinetic salt effect

The effect of added salt on the reaction of the dye with the oxidant were investigated by adding different concentrations of neutral salt and by measuring the reaction rates with fixed concentrations of brilliant blue and chlorine dioxide The obtained k' values are summarised in Table 4.2.5.

Table 4.2.5 Effect of ionic strength on the reaction rate, $[BB^+]_0$ (7.0×10^{-5} M) with $[ClO_2]_t$ (1.15×10^{-3} M), pH = 9.0.

Ionic strength, I/M	k'/s^{-1}*
0.0096	0.091
0.0174	0.095
0.0262	0.105
0.0354	0.109
0.0397	0.111

*Mean of four replicate experiments with relative standard deviation < 4%

The log k' *versus* square root of ionic strength values are plotted in Figure 4.2.11, which indicates a good straight line with positive slope value with $R^2 = 0.97$.

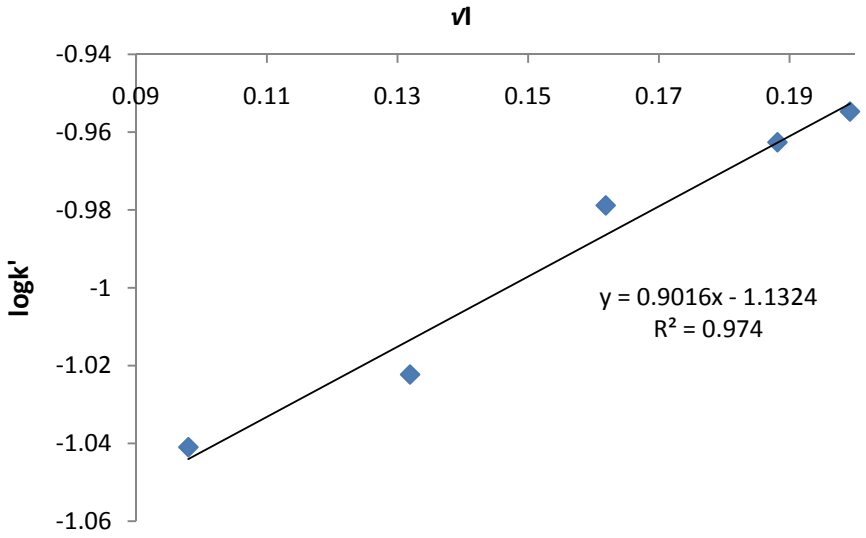

Figure 4.2.11 Plot of log k' *versus* $\sqrt{I}$ for the reaction of $[BB^+]_0$ (7.0×10^{-5} M) with $[ClO_2]_t$ (1.15×10^{-3} M) at varying ionic strength, I (0.0050 - 0.056).

From Figure 4.2.11 the observed positive slope indicates the positive salt effect confirming the rate-limiting step involves oppositely charged species, i.e. possibly $[OH^-]$ and BB^+ ions.

4.2.7 Effect of chloride on reaction rate

The activity of the reaction rate can be affected by the presence of other species. The presence of the other ions may interfere with the reaction being investigated. The effect of chloride taken at varied concentrations was investigated by adding small amounts of sodium chloride salt.

Table 4.2.6 Varied chloride concentration and observed rate constants for the reaction of $[BB^{+}]_0$ (7.0×10^{-5} M) with $[ClO_2]_t$ (1.15×10^{-3} M).

$[Cl^{-}]$/M	k'/s^{-1}*
0.148	0.720
0.298	0.730
0.447	0.710
0.597	0.710
0.725	0.720

*Mean of four replicate experiments with relative standard deviation < 4%

From Table 4.2.6 the added chloride indicate a little/no change in the rate of the reaction nor its participation in any important reaction

4.2.8 Effect of temperature on rate of reaction

In order to study the effect of reaction temperature on the degradation of brilliant blue-R a series of experiments were conducted at different temperature ranges 10 ºC to 30 ºC. The third-order rate constants at different temperatures were obtained from the kinetic curves. The results are tabulated in Table 4.2.7.

Table 4.2.7 Varied temperature in presence of chlorine dioxide and observed rate constant for the reaction of $[BB^{+}]_0$ (7.0×10^{-5} M) with $[ClO_2]_t$ (1.15×10^{-3} M).

T/K	k'/s^{-1}*	$k_3/ M^{-2}s^{-1}$
283	0.100	7.0×10^6
288	0.136	9.0×10^6
293	0.172	1.1×10^7
298	0.260	1.7×10^7
303	0.329	2.2×10^7

*Mean of four replicate experiments with relative standard deviation < 4%

The ln k_2 values were plotted against the corresponding reciprocal temperature values and the linear plot is illustrated in the Figure 4.2.12. From the plot, the activation energy, E_a and the other energy parameters were estimated (Table 4.2.8).

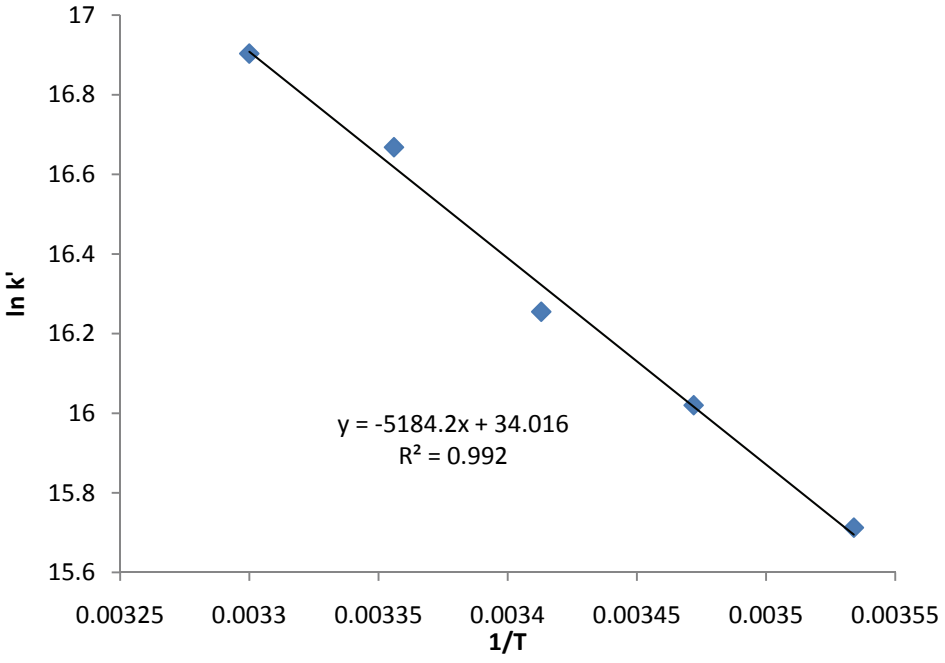

Figure 4.2.12 Plot of ln k' *versus* 1/T for the reaction of brilliant blue with ClO_2 at different temperatures.

Table 4.2.8 Energy parameters.

Reaction	Enthalpy of activation, $\Delta H^{\ddagger}$/kJ mol^{-1}	Entropy of activation, $\Delta S^{\ddagger}$/J K^{-1} mol^{-1}	Energy of activation E_a/kJ mol^{-1}
BB^{+} with ClO_2	47.58	-676.36	50.06

The enthalpy of activation, $\Delta H^{\ddagger}$ for the reaction was calculated using the equation, $\Delta H^{\ddagger} = (E_a - mRT)$, where m is the total order of reaction, and R and T are the gas constant and temperature respectively. The activation energy obtained were (E_a = 50.06 kJ mol^{-1}), $\Delta H^{\ddagger}$ value at 25° C was found to be 47.58 kJ mol^{-1}, and the reaction had large negative entropy of activation (-676.36 J K^{-1} mol^{-1}), suggesting the formation of an tightly packed activated complex resulting in decrease in entropy.

4.2.9 Products identification and characterization

The extraction of the oxidation product of brilliant blue with chlorine dioxide was done as explained in the experimental chapter (Section 2.1.7, page no 69). Separation of BB-ClO_2 (44 mg) afforded two compounds, compound 1 (8 mg) and compound 2 (5 mg). These were from fraction 41-46 eluted with 50% dichloromethane in hexane, compound 1 was from fraction 54-56 eluted by 70% dichloromethane. The fraction 57-64 yielded compound 2 when eluted with 80% dichloromethane. The identified products were (P_1 = 4-(4-ethoxy-phenylamino)-benzoic acid, and P_2 = *N*-(4-ethoxy-phenyl)-hydroxylamine) (Table 4.2.9).

The proton NMR spectrum of the product (P_1) exhibited triplet for methyl protons at δ 0.83 and 1.46 quartet for methylene proton at δ 4.12 and eight aromatic protons are in the range of

δ 6.20 - δ 7.40. (Appendix 2, Figure 2.1.4). ^{13}C NMR reveals that carbonyl carbon is observed at δ 169.72, and aromatic carbons are in the range of δ 116.18 - 149.47. The alkyl carbons are observed at δ 60.37 and δ 14.08 for $-CH_2$ and $-CH_3$ respectively (Appendix 2, Figure 2.1.5). The GC-MS of product P_1 showed molecular ion peak at m/z 257 (M^+) this corresponds to molecular formula of $C_{15}H_{15}NO_3$. The observed prominent peak at m/z 229 (M^+) was due to loss of ethyl group, and the m/z 110 (M^{+1}) corresponds to loss of *p*-aminophenol. (Appendix 2, Figure 2.1.6).

The ^1H-NMR spectrum of product P_2 displayed ethyl protons at δ 1.49 and δ 4.17 - 4.19 as triplet and quartet for methyl and methylene protons respectively. Methylene protons are observed at δ 5.29 and aromatic protons are observed as multiplet in the range of δ 6.71 - δ 8.08. (Appendix 2 , Figure 2.1.7). The ^{13}C NMR spectrum exhibited two alkyl carbon at lower δ 11.2 and δ 60.37 for $-CH_3$ and $-CH_2$ respectively. The methylene carbon is observed at higher δ 63.83 due to deshielding effect from aromatic ring. Aromatic carbons are observed at δ 118.80 -149.47 and two aromatic carbons are observed at higher δ 140.32 and δ 149.47 due to more deshielding effect from the substituent's on the carbon (Appendix 2, Figure 2.1.8). Mass spectrum of P_2 exhibited molecular ion peak at 578 (M^+) which was in agreement with molecular mass of P_2. Another significant peak was observed at 249 (M^{-1}) due to the loss of two moles of *meta*-substituted benzyl group (Appendix 2, Figure 2.1.9).

Table 4.2.9 Plausible major oxidation products.

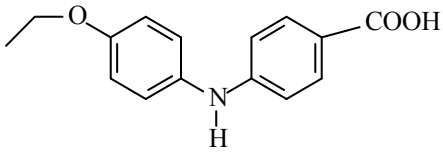 (P_1)	4-(4-ethoxy-phenylamino)-benzoic acid
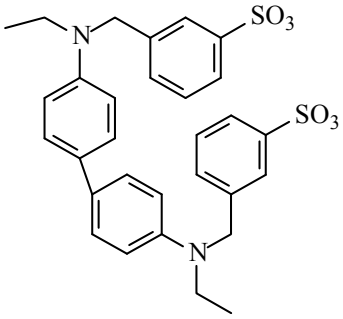 (P_2)	*N*-(4-ethoxy-phenyl)-hydroxylamine

4.2.10 Stoichiometric equation

The stoichiometry experiments were carried out using 0.0015 M chlorine dioxide concentration. The stoichiometry is established with 1:1 and 1:5 ratios of the dye and oxidant. Residual amounts of dye and chlorine dioxide reacted were estimated from the initial and final concentrations. The stoichiometry was found to be roughly 1:2 (± 10%) of BB^+ and ClO_2. Thus the stoichiometric equation for the overall reaction can be represented as

$$BB^+ + 2\ ClO_2 + 3OH^- \rightarrow P_1 + P_2 + 2\ ClO_2^- + H_2O \qquad (4.18)$$

where P_1 {-(4-Ethoxy-phenylamino)-benzoic Acid} and P_2 {*N*-(4-Ethoxy-phenyl)-hydroxylamine}.

4.2.11 Reaction scheme

When brilliant blue is made to contact with the oxidant chlorine dioxide, the hydroxy radical attacks the carbon radical and forms a hydroxyl intermediate, I_1. The intermediate I_1 is again attacked by hydroxyl ion and forms ether type of intermediate, I_2 and the it gets oxidized by hydroxyl ion which to yield product substituted biphenyl analog P_1 and substituted biphenyl amine analog P_2.

The identified oxidation products can be explained by the mechanistic scheme shown in Figure 4.2.13.

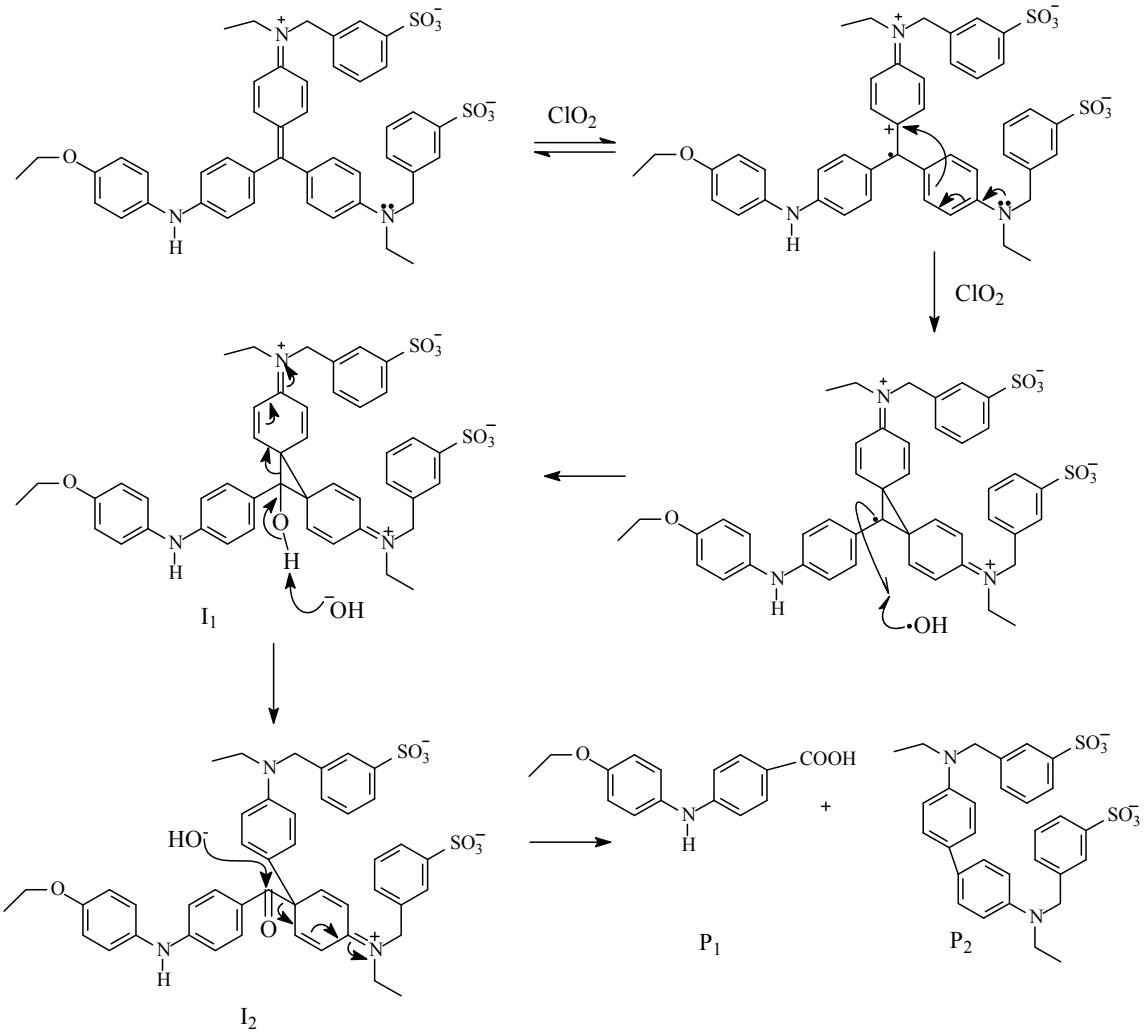

Figure 4.2.13 Mechanistic scheme for oxidation of brilliant blue-R with chlorine dioxide.

4.2.12 Proposed mechanism

The reaction mechanism and the rate law can be proposed based on the known chemistry of chlorine dioxide decomposition as discussed.

$$ClO_2 + BB^+ \rightarrow ClO_2^- + BB^{2+} \qquad \text{Very slow} \tag{4.19}$$

$$BB^+ + ClO_2 + OH^- \rightarrow \{HO\ BB\ ClO_2\} \rightarrow ClO_2^- + \{HO\ BB\}^+ \tag{4.20}$$

Rate limiting step

$$\{HO\ BB\}^{+} + H_2O \rightarrow BB^{2+} + OH^{-} \quad \text{fast} \tag{4.21}$$

$$BB^{+} + ClO_2 + OH^{-} \rightarrow I_1^{+} + ClO_2^{-} \quad \text{R1}$$

$$I_1^{+} + OH^{-} \rightarrow I_2 + H_2O \quad \text{R2}$$

$$I_2 + ClO_2 + OH^{-} \rightarrow P_1 + P_2 + ClO_2^{-} \quad \text{R3}$$

Overall equation can be represented as :

$$BB^{+} + 2ClO_2 + 3OH^{-} \rightarrow P_1 + P_2 + 2ClO_2^{-} + H_2O \tag{4.22}$$

4.2.13 Rate law

The rate law for the oxidation of brilliant blue has been thoroughly examined. The first-order dependence of the reaction rate on the reactants and the observed salt effect suggests that the rate limiting step involves one each of like charges possibly the BB^{+} and hydroxide ions and ClO_2. Thus, the major pathway of the reaction may involve both chlorine dioxide and $[OH^{-}]$ ion to give an activated complex which decomposes to form the intermediates and products.

$$Rate = k_1[ClO_2][BB^{+}] + k_2\,[ClO_2][OH^{-}]\,[BB^{+}] \tag{4.23}$$

As the reaction conditions fulfill *pseudo* first-order conditions, the rate law may be proposed as

$$= k_1[ClO_2][BB^{+}] + k_{OH^{-}}\,[ClO_2][OH^{-}][BB^{+}] \tag{4.24}$$

where $k_{OH^-} = \frac{k_2}{[OH^-]}$

$$r = \{ k_1 + k_{OH^-} [OH^-]\}[ClO_2] [BB^+] \quad (4.25)$$

when $[ClO_2]$ is in large excess then

$$Rate = k' [BB^+] \quad (4.26)$$

where the *pseudo* first-order const, k' equals

$$k' = k_1 + k_{OH^-} [OH^-]\}[ClO_2] \quad (4.27)$$

4.2.14 Simulations

Simulations were done to validate the proposed mechanisms and prove that it is the more probable one. The estimated rate constant were optimized and adjusted until the simulated curves matched well with the experimental curves (Table 4.2.10). The simulated curves exhibit the behavior of the experimental curves. The graphs showing the simulated and experimental curves are illustrated in Figure 4.2.14.

Table 4.2.10 Forward and reverse rate constants obtained from literature and simulations.

Reaction No	Reaction	Forward rate
C1	$BB^+ + ClO_2 + OH^- \rightarrow I_1^+ + ClO_2^-$	$1.72 \times 10^2 M^{-1} s^{-1}$
C2	$I_1^+ + OH^- \rightarrow I_2 + H_2O$	$2.00 \times 10^9 M^{-2} s^{-1}$
C3	$I_2 + ClO_2 + OH^- \rightarrow P_1 + P_2 + ClO_2^-$	$3.21 \times 10^9 M^{-2} s^{-1}$

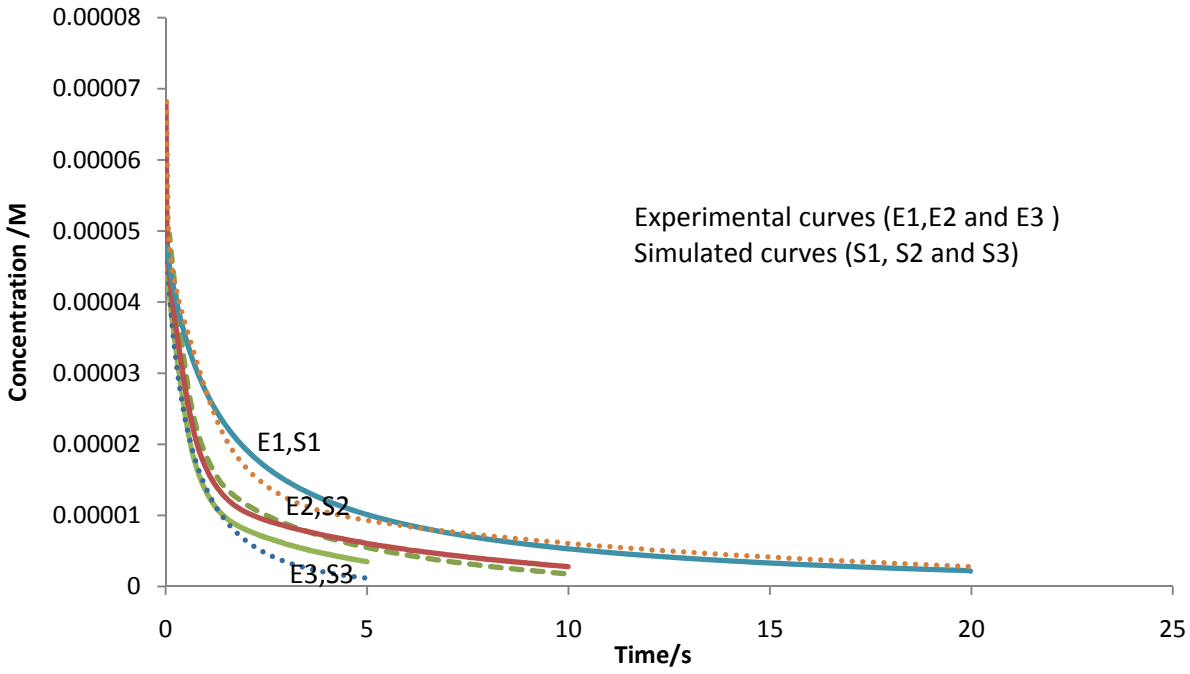

Figure 4.2.14 Experimental curves *versus* simulated curves for reaction of $[BB^+]_0$ (7.0 x 10^{-5} M) with $[ClO_2]_t$ (1.15 x 10^{-3} M).

The simulations were based on the proposed comprehensive mechanism. The reaction scheme in the product analysis gives details for the intermediate structures. The simulated curves matched with experimental curves, confirming the suggested mechanism to be probable. Rate constants from C1 and C2 are experimental values and C3 is the estimated rate constant.

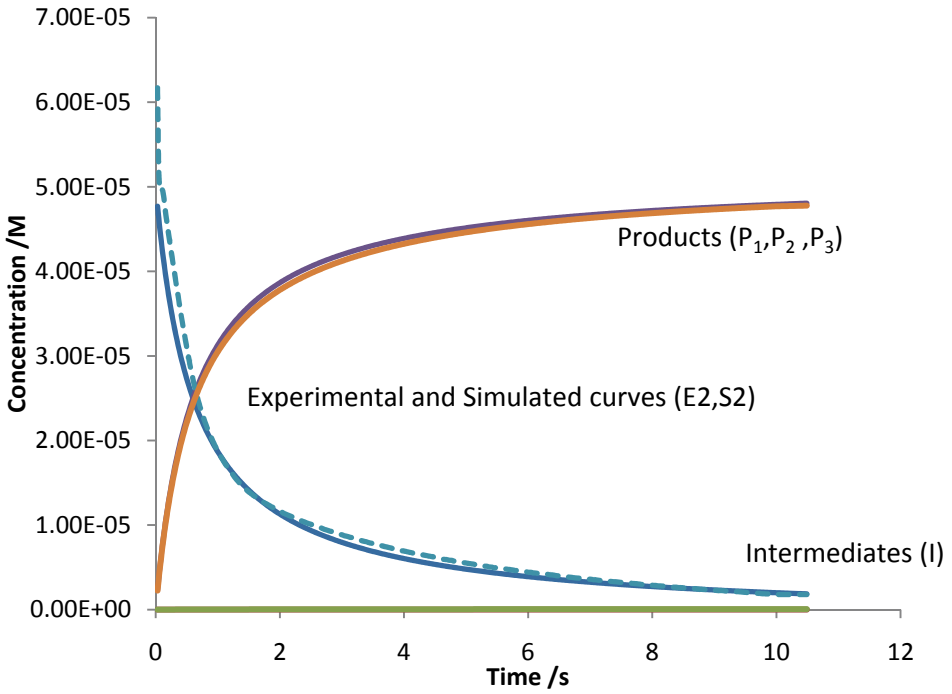

Figure 4.2.15 Intermediates and product formation for selected typical kinetic curves (E2, S2).

Figure 4.2.15 illustrates reaction conditions similar to curves in Figure 4.2.14. Curves E2 and S2 shows the experimental and simulated curves for the reaction. The curves P_1, P_2 and P_3 show the products formation and I is the intermediate formed during the process.

A fair agreement between the experimental and corresponding simulated curves, strongly support that the proposed reaction scheme as most probable and estimated rate constants are fairly acceptable. The data of simulated *versus* experimental curves and the concentrations of the other reactants, intermediates and products are compiled (Appendix 2, Table 2.3, Table 2.4).

4.3 Oxidation of safranine-O with chlorine dioxide

4.3.1 Reaction of safranine-O and chlorine dioxide

The reaction of safranine-O with chlorine dioxide was studied by kinetic approach. The reaction rate was measured by monitoring the change in absorbance at its λ_{max} (519 nm) as a function of time. Figure 4.3.1 illustrates the absorbance *versus* time plot for the reaction of safranine-O (3.0×10^{-5} M) with $[ClO_2]_t = 1.15 \times 10^{-3}$ M at pH 9.00. The depletion of safranine was completed in less than ten seconds indicating that the reaction is fast (Figure 4.3.1).

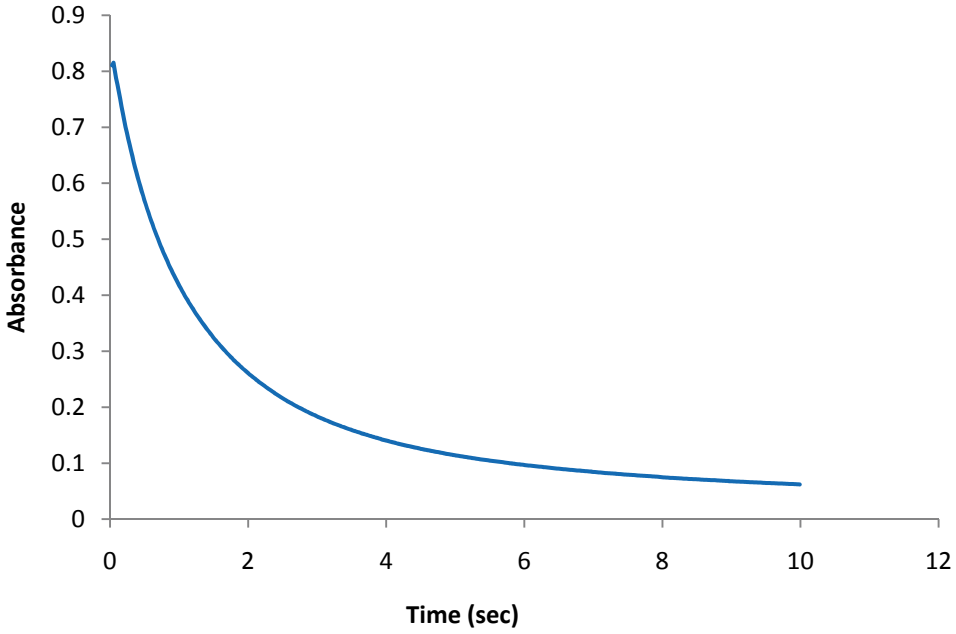

Figure 4.3.1 Typical absorbance *versus* time plot for the reaction of $[SO^+]_0$ (3.0×10^{-5} M) with $[ClO_2]_t$ (1.15×10^{-3} M) at pH = 9.00.

4.3.2 Analysis of kinetic data using KinetAsyst™ Fit software

The obtained curve from Figure 4.3.2 represents the experimental curve and matching this curve generated by asystant software using a first-order rate equation.

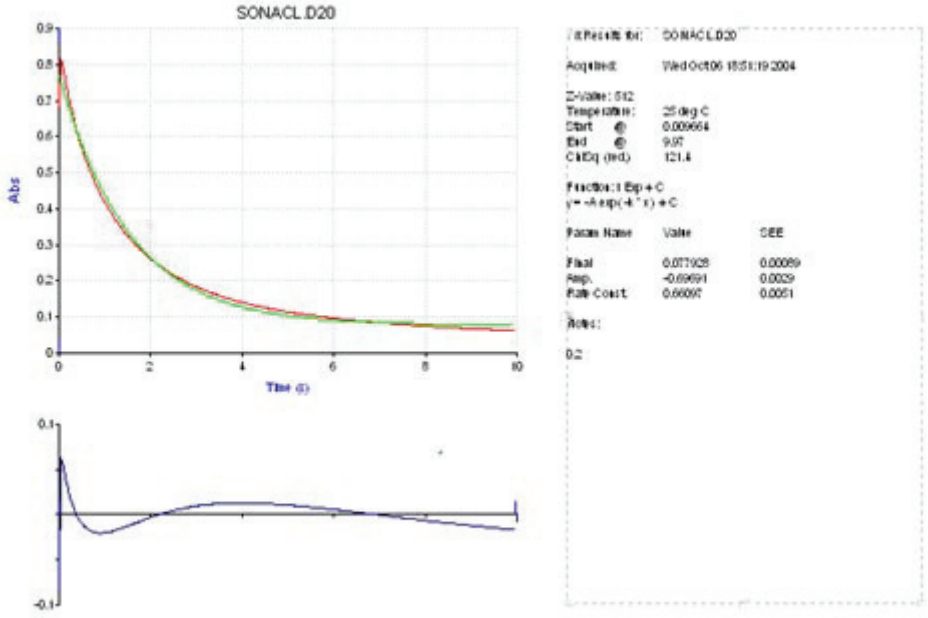

Figure 4.3.2 KinetAsyst™ single-exponential equation fit of two curves and residuals (lower sketch) for the reaction of $[SO^{+}]_0$ (3.0 x 10^{-5} M) with $[ClO_2]_t$ (1.15 x 10^{-3} M) using the first-order equation.

An observation of Figure 4.3.2 shows fair agreement between the experimental (red) and computed (green) curves with small residue (bottom blue curve). The estimated *pseudo* first-order rate constant had a value of 0.6609 s^{-1} with standard deviation of 0.0051 indicating that for the chosen conditions the reaction follows the first-order kinetics with respect to the dye.

4.3.3 Order with respect to chlorine dioxide

To establish the reaction order with respect to the oxidant, kinetic runs were carried out by varying initial concentrations of chlorine dioxide, at constant pH and ionic strength. All the reactions exhibited exponential decay and the reaction rate increased with the increase in the initial concentration of chlorine dioxide.

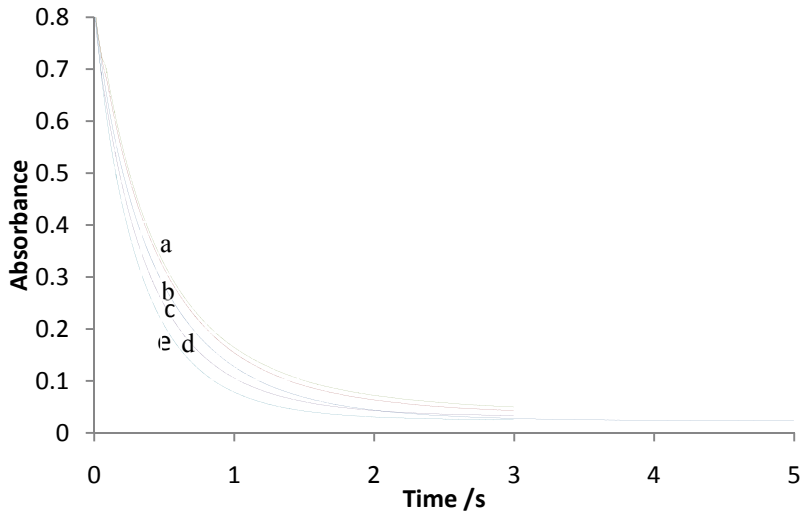

Figure 4.3.3 Depletion of safranine-O with various chlorine dioxide concentrations for the reaction of $[SO^{+}]_0$ (3.0 x 10^{-5} M) with $[ClO_2]_t$ / 10^{-3} M (a = 2.52, b = 2.78, c = 3.03, d = 3.28 and e = 3.53).

Figure 4.3.3 illustrates the kinetic runs for different initial concentrations of chlorine dioxide.and the software fit analysis and corresponding estimated *pseudo* first-order rate constants are shown in Figure 4.3.4 (curves a to e).

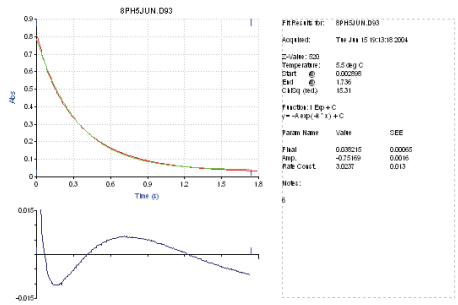

(a)

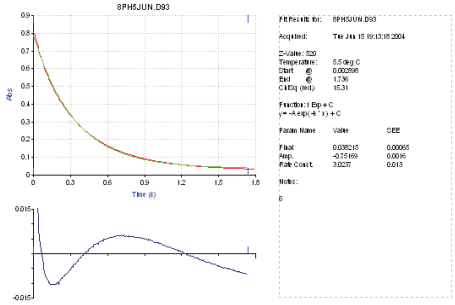

(b)

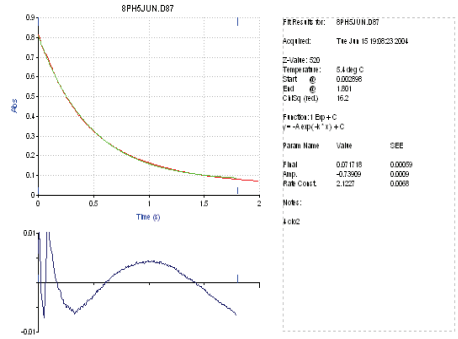

(c)

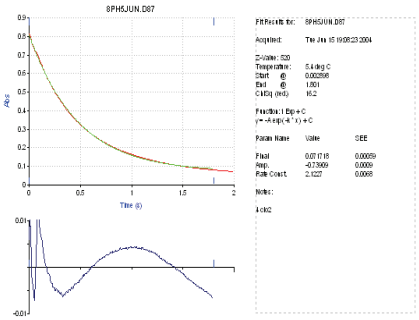

(d)

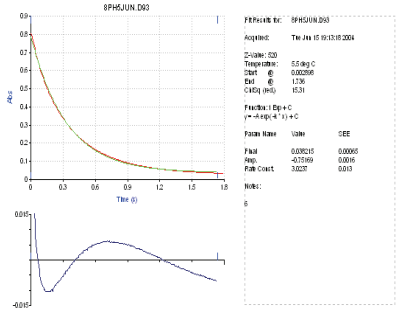

(e)

Figure 4.3.4 Experimental and computed fits using KinetAsyst™ single- exponential equation, for the reaction of $[SO^{+}]_0$ (3.0 x 10^{-5} M) with $[ClO_2]_t$ / 10^{-3} M (a = 2.52, b = 2.78, c = 3.03, d = 3.28 and e = 3.53)

The values of the estimated *pseudo* first-order rate coefficients, k' for different initial chlorine dioxide concentrations are listed in the Table 4.3.1.

Table 4.3.1 Reaction between safranine-O and chlorine dioxide at constant ionic strength $[SO^+]_0$ (3.0×10^{-5} M) with $[ClO_2]_t$ ($2.5 \times 10^{-3} - 7.5 \times 10^{-3}$ M), pH = 9.0 and Ionic Strength (I = 0.128).

$[ClO_2]_t / 10^{-3}$ M	k'/s^{-1}*
2.52	2.100
2.78	2.310
3.03	2.610
3.28	2.820
3.53	3.010

* Mean of four replicate experiments with relative standard deviation < 4%

Further, the plot of ln k' *versus* ln $[ClO_2]$ gave a linear curve with a slope 1.09 and correction coefficient 0.99 (Figure 4.3.5) suggesting that the reaction rate has first-order dependence on $[ClO_2]_0$.

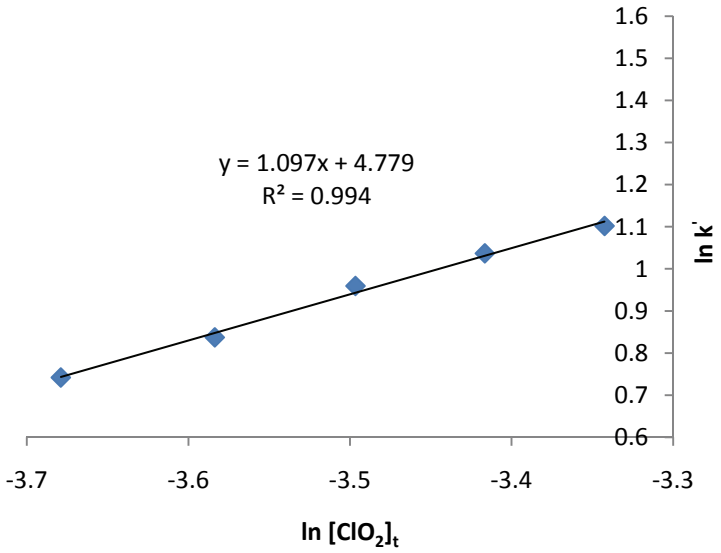

Figure 4.3.5 Plot of ln $[ClO_2]_t$ *versus* ln k' for the reaction of $[SO^+]_0$ (3.0×10^{-5} M) with $[ClO_2]_t$ ($2.5 \times 10^{-3} - 7.5 \times 10^{-3}$ M) at pH = 9.00 and I = 0.128 M.

4.3.4 Effect of pH

The effect of variation of initial pH on the oxidation of safranine–O was studied using fixed concentration of substrate and oxidant, and by adding various initial concentrations of acid. Table 4.3.2 represents the obtained *pseudo* first-order rate constants.

Table 4.3.2 Effect of pH on reaction rate

pH	k'/s^{-1}*
6.0	0.405
6.3	0.41
6.6	0.421
6.8	0.475
7.0	0.499
7.2	0.956
7.4	1.752
7.6	1.828
7.8	2.11
8.0	2.45
8.2	2.69
8.4	2.81
8.6	3.25
8.8	3.49
9.0	3.61

*Mean of four replicate experiments with relative standard deviation < 4%

The plot of k' *versus* pH is illustrated in (Figure 4.3.6). A perusal of the curve suggests that the rate of oxidation of substrate increased with increasing pH and increase was significant at higher pH range.

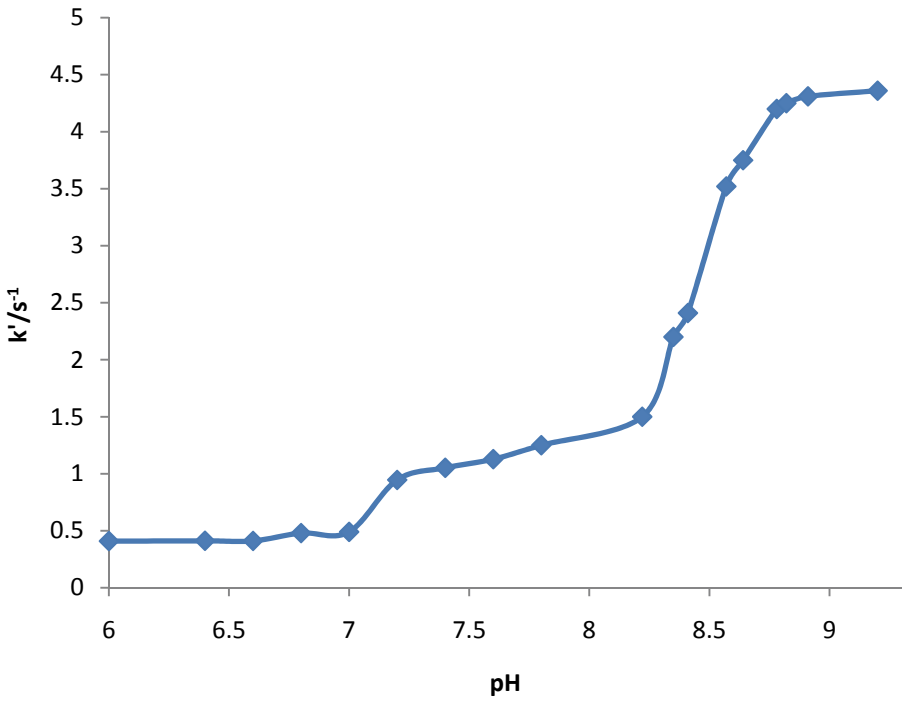

Figure 4.3.6 Plot of k' *versus* pH for the reaction of $[SO^{+}]_0$ (3.0×10^{-5} M) with $[ClO_2]_t$ (1.15×10^{-3} M), $[H^{+}]_{eq}$ (1.99×10^{-9}- 7.752×10^{-4} M).

Between the pH range 6.0 and 7.0 there is very marginal increase in the rate constants. This could be explained due to the slow reactivity of chlorine dioxide under acidic conditions, and the latter increase is due to the high reactivity of chlorine dioxide at alkaline pH range.

To have a close look at the role of OH^- ions in the reaction, the kinetic data for the pH range (6.0 – 9.0) in Table 4.3.2 was plotted as ln k' *versus* ln $[OH^-]$ plot (Figure 4.3.7), which gave a straight line with slope = 0.81 an gradient $R^2 = 0.95$. It shows that in the alkaline pH range reaction order with respect to hydroxyl ion is about unity.

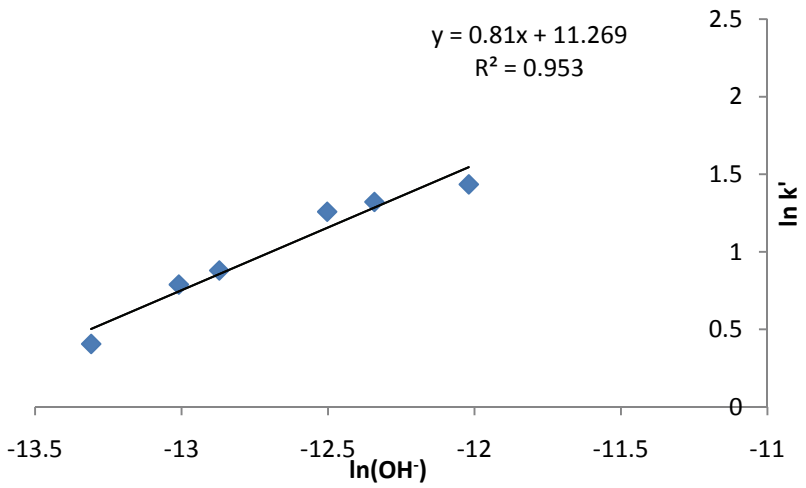

Figure 4.3.7 Plot of ln $[OH^-]$ *versus* ln k' for the reaction of $[SO^+]_0$ (3.0×10^{-5}M) with $[ClO_2]_t$ (1.15×10^{-3} M).

When all the kinetic data over the pH range 3.0 to 9.0 was plotted (Figure 4.3.7) the slope of curve registered a continuous decrease with decrease in pH. The data can be approximately divided into three ranges where somewhat linear relationship can be established. The slope of those curves clearly shows the order with respect to hydroxyl ion decrease from 0.81 (in the pH range 9.0 - 8.0) to 0.019 (in the pH range 7.0 - 3.0).

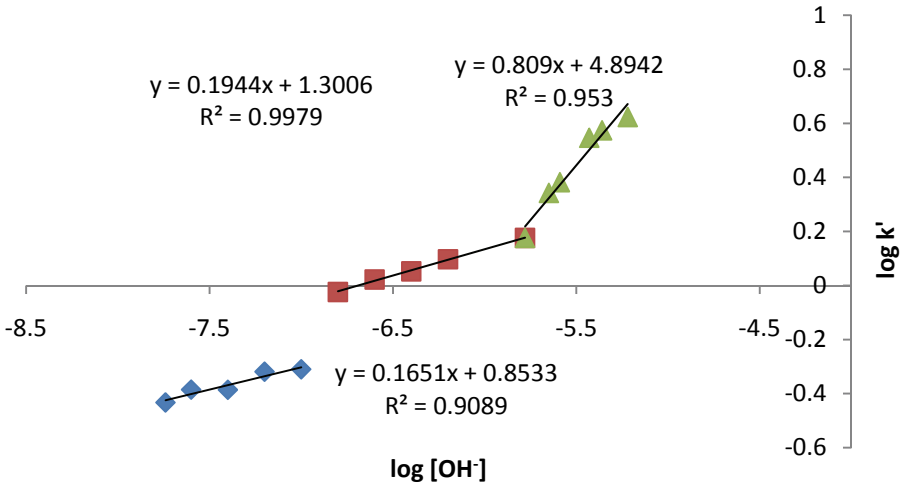

Figure 4.3.8 Plot of log $[OH^-]$ *versus* log k' at different pH conditions.

Initially the observed order with respect to hydroxide ion under near neutral conditions is less than one and further decreased to 0.16 at pH 6.0. This observed decrease in order with respect to hydroxide ion could possibly be explained by assuming the two competitive reactions contributing toward the overall oxidation of substrate, namely reaction one; the direct reaction between substrate and chlorine dioxide and the other involving substrate, ClO_2 and hydroxide ion. The rate law for competitive oxidation of substrate can be written as

$$r = k_1 [ClO_2] [SO^+] + K_{OH^-} [ClO_2] [OH^-] [SO^+] \quad (4.28)$$

$$= \{k_1 + Kk_{OH^-} [OH^-]\} [ClO_2] [SO^+] \quad (4.29)$$

$$= k [ClO_2] [SO^+] \quad (4.30)$$

$$= k' [SO^+] \quad (4.31)$$

where k' represents the observed *pseudo* first-order rate constant in presence of excess concentration of chlorine dioxide. For fixed excess concentration of ClO_2, $k = \{k_1 + k_{OH^-} [OH^-]\}$, where the second-order constant, k will be equal to $\ln k'/[ClO_2]$ and k_1 and k_{OH^-} respectively represent the second-order rate constant for the reaction between chlorine dioxide and dye, and the third-order rate constant for the reaction between chlorine dioxide and dye, involving OH^- ion. For this assumption to be correct, a plot of $k'/[ClO_2]$ *versus* $[OH^-]$ should give a straight line. That linear curve should have intercept = k_1 and slope = k_{OH^-}. Possibly, at high concentrations of hydroxide such linear relationship may not be observed due to stoichiometric magnitude of the dye.

Table 4.3.3 summarises the values of equilibrium concentrations of hydroxide ion for the given pH, its corresponding k' and calculated k values.

Table 4.3.3 Calculated $[OH^-]_{eq}$ values and corresponding second-order constants for their reaction of $[SO^+]_0$ (3.0 x 10^{-5} M) with $[ClO_2]_t$ (1.15 x 10^{-3} M).

$[OH^-]_{eq}$	k'^*	k/ $10^2 M^{-1}s^{-1}$
1.82 x 10^{-8}	0.369	2.46
2.51 x 10^{-8}	0.411	2.74
3.98 x 10^{-8}	0.411	2.74
6.31 x 10^{-8}	0.480	3.20
1.00 x 10^{-7}	0.490	3.26
1.58 x 10^{-7}	0.946	6.30
2.51 x 10^{-7}	1.052	7.01

*Mean of four replicate experiments with relative standard deviation < 4%

Figure 4.3.9 illustrates the plot of k *versus* $[OH^-]$ (data from Table 4.3.2).

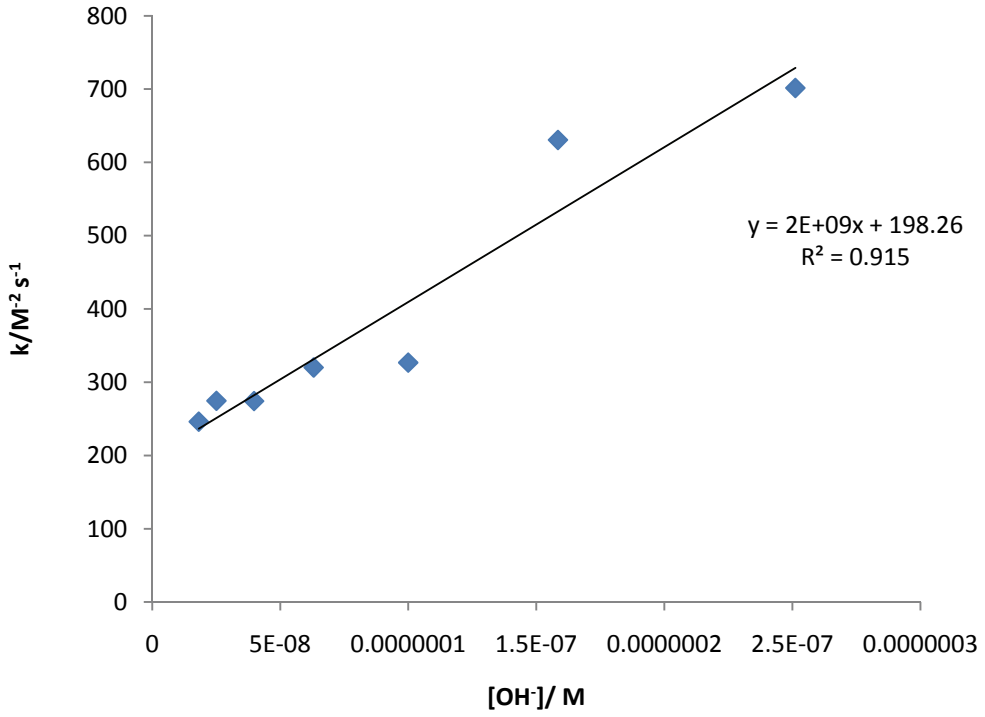

Figure 4.3.9 Plot of $[OH^-]$ *versus* k/$[ClO_2]$ for the reaction $[SO^+]_0$ (3.0 x 10^{-5} M) with $[ClO_2]_t$ (1.15 x 10^{-3} M), $[OH^-]_{eq}$ (1.8 x 10^{-8} - 2.51 x 10^{-7} M).

An observation of Figure 4.3.9 indicates that k_1 value (y-intercept) is small, that suggests that in the absence of hydroxide ion, the reaction rate is small, which can be predicted from the reported inert behavior of chlorine dioxide at acidic pH. From the plot (Figure 4.3.9), the catalytic constant for the hydroxide catalysed reaction was estimated to be 2.0 x 10^9 M^{-2} s^{-1} in the pH range of 6.0 – 7.5. Considering almost first-order dependence of the reaction rate on hydroxide ion near neutral conditions, a rate limiting step involving chlorine dioxide, SO^+ and hydroxide is proposed in section 4.3.12.

4.3.5 Effect of pH on the order with respect to chlorine dioxide

The kinetic runs further carried out to determine the effect of pH on reaction order with respect to oxidant. Experiments were conducted in three different pH range (7.0, 8.0 and 9.0) with varied initial concentrations of chlorine dioxide. The values of first-order rate coefficients, k' and corresponding calculated second-order rate constants k_2 are shown in the Table 4.3.4.

Table 4.3.4 Observed rate constants at pH 7.0, 8.0 and 9.0 regions for the reaction of $[SO^+]_0$ (3.0 x 10^{-5} M) with $[ClO_2]_t$ (1.15 x10^{-3} M).

pH = 7.0			
$[ClO_2]_t$ x 10^{-3}/M	k'/s^{-1}*	$k_2/M^{-1}s^{-1}$	$k_3/M^{-2}s^{-1}$
2.52	0.49	19.44	1.94 x 10^8
2.78	0.59	21.22	2.12 x 10^8
3.03	0.65	21.45	2.15 x 10^8
3.28	0.69	21.04	2.1 0x 10^8
3.53	0.74	20.96	2.1 0x 10^8
Mean k_2 with std.dev.		20.8 ± 0.8	

Table 4.3.4 contd.

pH = 8.0			
$[ClO_2]_t$ x 10^{-3}/M	k'/s^{-1}	$k_2/M^{-1}s^{-1}$	$k_3/M^{-2}s^{-1}$
2.52	1.15	45.63	4.56 x 10^8
2.78	1.35	48.56	4.86 x 10^8
3.03	1.45	47.85	4.79 x 10^8
3.28	1.60	48.78	4.88 x 10^8
3.53	1.75	49.72	4.97 x 10^8
	Mean k_2 with std.dev.	48.1 ± 1.5	
pH = 9.0			
$[ClO_2]_t$ x 10^{-3}/M	k'/s^{-1}	$k_2/M^{-1}s^{-1}$	$k_3/M^{-2}s^{-1}$
2.52	1.90	75.40	7.54 x 10^8
2.78	2.08	74.82	7.48 x 10^8
3.03	2.22	73.27	7.33 x 10^8
3.28	2.50	76.22	7.62 x 10^8
3.53	2.80	79.32	7.93 x 10^8
	Mean k_2 with std.dev.	75.8 ± 2.2	

where $k_2 = k' / [ClO_2]$, $k = k' / \{[ClO_2][OH^-]\}$

*Mean of four replicate experiments with relative standard deviation < 4%

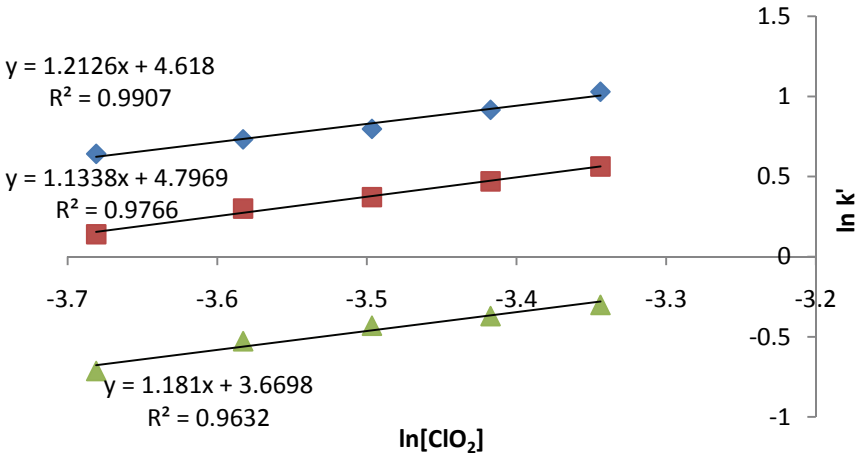

Figure 4.3.10 Plot of ln k' *versus* ln $[ClO_2]$ for the reaction of $[SO^+]_0$ (3.0 x 10^{-5} M) with $[ClO_2]_t$ (1.15 x 10^{-3} M), a (pH=9.0), b (pH=8.0), c (pH=7.0).

The reaction orders with respect to oxidant at pH 7.0,8.0 and 9.0 were 1.21, 1.15 and 1.18 respectively and all the values were of approximately of unity. The reaction orders obtained confirm that the change in pH does not have any influence on the order with respect to ClO_2 implying that reaction pathway remains unchanged.

4.3.6 Kinetic salt effect

Experiments were conducted to establish the reacting species involved in the rate limiting step, by measuring the rate coefficients for the same reaction conditions at varied initial ionic strengths. Sodium sulfate was used as neutral salt to adjust the ionic strength. The obtained results summarised in Table 4.3.5 indicate that the k' values tend to decrease with increasing ionic strength.

Table 4.3.5 Effect of ionic strength on the reaction rate , $[SO^{+}]_0$ (3.0×10^{-5} M) $[ClO_2]_t$ (1.15×10^{-3} M) at pH = 8.0.

Ionic Strength, I/M	k'/s^{-1}*
0.0096	0.126
0.0174	0.109
0.0262	0.105
0.0354	0.096
0.0397	0.093

*Mean of four replicate experiments with relative standard deviation < 4%

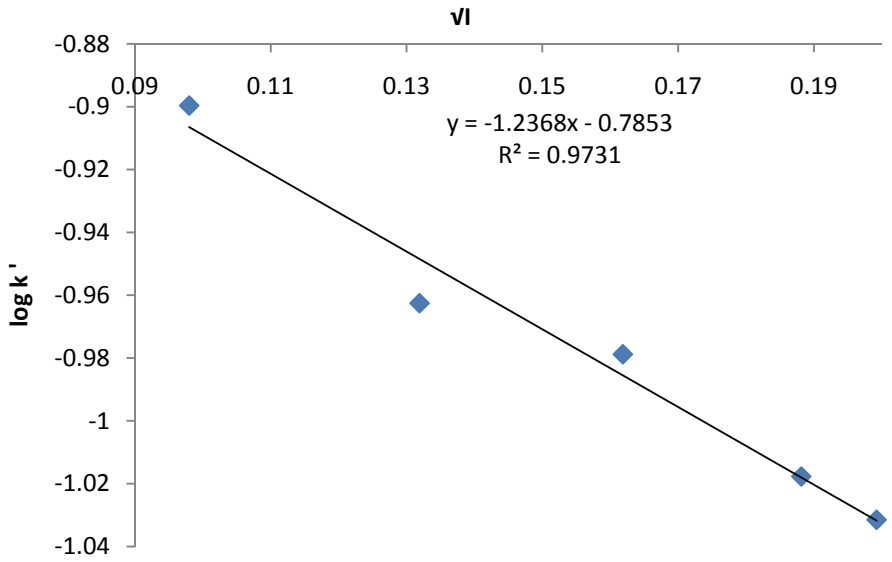

Figure 4.3.11 Plot of log k' *versus* √I for the reaction of $[SO^{+}]_0$ (3.0 x 10^{-5} M) with $[ClO_2]_t$ (1.15 x 10^{-3} M) at varying ionic strength, I (0.009 - 0.04 M).

Figure 4.3.11 shows the plot of log k *versus* square root of ionic strength and the observed slope = -1.26, with negative primary salt effect suggests that reactive species in the rate-determining step are of opposite nature and possibly the OH^{-} and SO^{+} ions.

4.3.7 Effect of chloride on rate of reaction

Similar to the studies with other substrates, the impact of chloride on the reaction was examined. The results in Table 4.3.6 show that addition of initial chloride ion caused some increase in the rate constant. No explanation was found in the literature, but this increase may be due to the possible formation of other weak reactive oxidising species such as HOCl.

Table 4.3.6 Varied chloride concentration and observed rate constants for the reaction of $[SO^+]_0$ (3.0 x10^{-5} M) with $[ClO_2]_t$ (1.15x 10^{-3} M).

I/M	k'/s^{-1}*
0.060	0.153
0.061	0.155
0.062	0.160
0.063	0.175
0.064	0.176

*Mean of four replicate experiments with relative standard deviation < 4%

4.3.8 Effect of temperature

The temperature dependence of the rate constant k, was studied by performing experiments at different temperatures ranges from 10 ^oC to 30 ^oC. From the values of k third order rate constants with respect to OH^- were calculated and summrised in Table 4.3.7. A typical Eyring's plot is shown in Figure 4.3.12.

Table 4.3.7 Varied temperature in presence of chlorine dioxide and observed rate constant for the reaction of $[ClO_2]_t$ (1.15x 10^{-3} M) with $[SO^+]_0$ (3.0 x10^{-5} M) at pH 9.0.

T/K	k'/s^{-1}*	k_3/ $M^{-2}s^{-1}$
283	1.25	8.3 x 10^7
288	1.52	1.0 x 10^8
293	1.79	1.2 x 10^8
298	1.93	1.3 x 10^8
303	2.05	1.4 x 10^8

*Mean of four replicate experiments with relative standard deviation < 4%

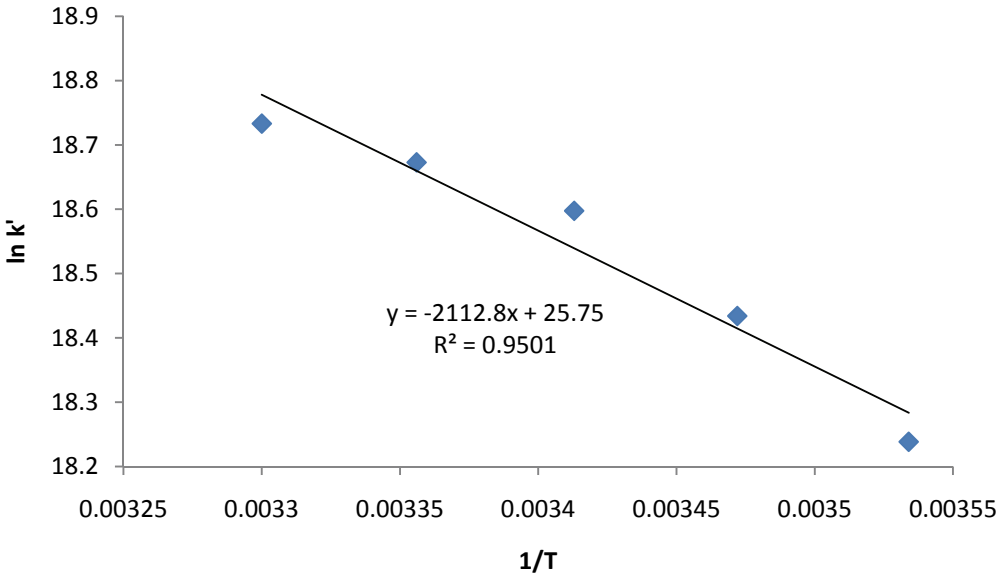

Figure 4.3.12 Plot of ln k' *versus* 1/T for the reaction of $[SO^{+}]_0$ (3 x 10^{-5} M) with $[ClO_2]_t$ (1.15 x 10^{-3} M).

Table 4.3.8 Energy parameters.

Reaction pathway	Enthalpy of reaction, $\Delta H^{\ddagger}$/kJ mol^{-1}	Entropy of activation, $\Delta S^{\ddagger}$/J K^{-1} mol^{-1}	Energy of activation E_a/kJ mol^{-1}
SO^{+} with ClO_2	15.08	-748.36	17.55

Using the slope and intercept of Figure 4.3.12, the calculated activation energy obtained (Table 4.3.8) were (E_a = 17.55 kJ mol^{-1}), $\Delta H^{\ddagger}$ value at 25 °C was found to be 15.08 kJ mol^{-1}, and the reaction had large negative entropy of activation (-748.36 J K^{-1} mol^{-1}), suggesting the formation of an activated complex resulting in a decrease in entropy.

4.3.9 Products identification and characterization

The product extracted from the reaction of SO-ClO_2 (0.35 g) was separated by column chromatography using silica gel (Merck 9385) as the stationary phase on 4 cm diameter column. The mobile phase consisted of a hexane: dichloromethane: ethyl acetate step gradient 100% hexane (fractions 1-15), increasing by 10% dichloromethane (fraction 15-18) 20% dichloromethane (fraction 19-29), 40% dichloromethane (fraction 30-38) Fractions of 10 mL were collected in each step. Two compounds were obtained from this dye; they were from fractions 12-16 and 52-60. Product P_1(phenol) and P_2 (3,7-dimethyl-phenazine-2-8-diol) (Table 4.3.9). Product P_2 is identified in the current study.

The proton NMR spectrum of product P_2 exhibits olefinic methyl groups at lower δ 2.1 aromatic protons in the range of δ 6.57 to δ 6.7 (Appendix 2, Figure 2.1.10), due to symmetry in the molecule one half of the product can be seen. The ^{13}C NMR spectrum revealed the appearance of aromatic carbons that were observed in the rage of δ 116 to δ 149. Two methyl groups corresponds to the δ 29.68 and δ 16.95 (Appendix 2, Figure 2.1.11). The mass spectrum of the product P_2 showed molecular ion peak at m/z 239.1 (M^-) at retention time 13.97 min that accounts to the molecular formula of $C_{14}H_{14}N_2O_2$. (Appendix 2, Figure 2.1.12) The observed peak at m/z212 (M^+) may be due the loss of two methyl groups from the product P_2.

Table 4.3.9 Major oxidation products.

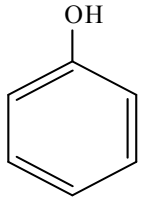 (P_1)	phenol
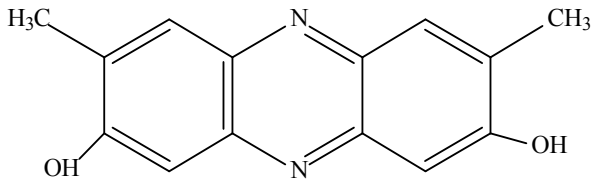 (P_2)	3,7-dimethyl-phenazine-2-8-diol

4.3.10 Stoichiometric equation

The stoichiometry experiments were conducted in a similar manner as it was described earlier. The stoichiometry was found to be approximately 1:5 (± 10%) of SO^+ to ClO_2. The stoichiometric equation for the overall reaction can be written as,

$$SO^+ + 4\ ClO_2 + 5OH^- \rightarrow P_1 + P_2 + 4ClO_2^- + 2NH_2OH \qquad (4.32)$$

where (P_1 = phenol) and (P_2 =3,7-dimethyl-phenazine-2-8-diol) .

4.3.11 Reaction scheme

When chlorine dioxide comes in contact with the dye safranine-O the hydroxyl ion attacks the quarternary carbon of phenyl group which is a substituent on nitrogen atom forming an

intermediate I_1 together with possible product phenol (P_1). The intermediate I_1 further undergoes oxidation with chlorine dioxide to yield product, P_2 which is confirmed by NMR and GC-MS spectrum.

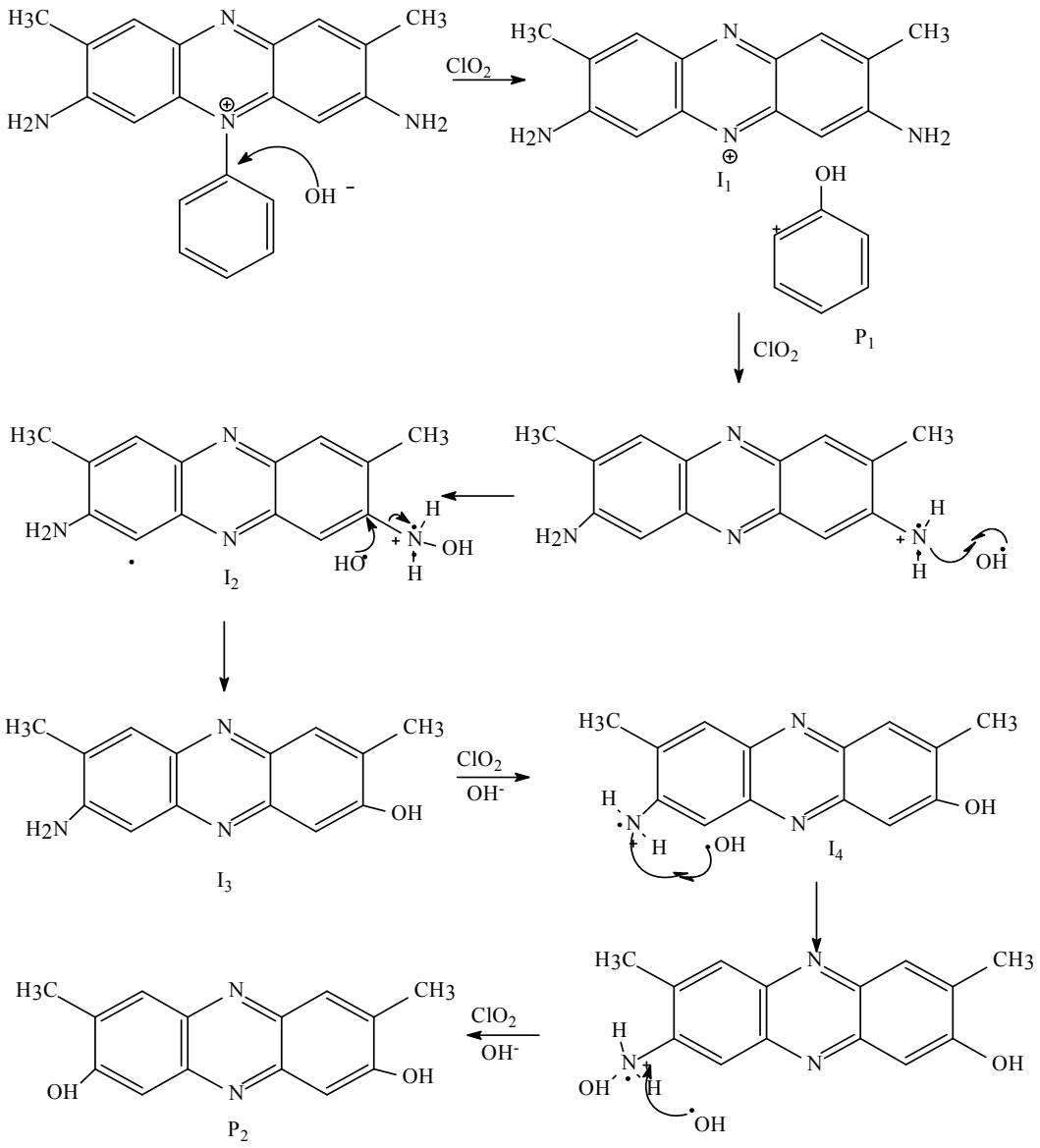

Figure 4.3.13 Mechanistic scheme for the oxidation of safrainine-O with chlorine dioxide.

4.3.12 Proposed mechanism

The overall reaction scheme for safranine oxidation with chlorine dioxide can be proposed as,

$$ClO_2 + SO^+ \rightarrow ClO_2^- + SO^{2+} \quad \text{Very slow} \qquad (4.33)$$

$$SO^+ + ClO_2 + OH^- \rightarrow \{HO\ SO\ ClO_2\} \rightarrow ClO_2^- + \{HO\ SO\}^+ \quad \text{Rate limiting} \qquad (4.34)$$

$$\{HO\ SO\}^+ + H_2O \rightarrow SO^{2+} + OH^- \quad \text{fast}$$

$$SO^+ + ClO_2 + OH^- \rightarrow P_1 + I_1^+ + ClO_2^- \qquad R1$$

$$I_1^+ + ClO_2 + OH^- \rightarrow I_2^+ + ClO_2^- \qquad R2$$

$$I_2^+ + OH^- \rightarrow I_3 + NH_2OH \qquad R3$$

$$I_3 + ClO_2 + OH^- \rightarrow I_4 + ClO_2^- \qquad R4$$

$$I_4 + ClO_2 + OH^- \rightarrow P_2 + NH_2OH + ClO_2^- \qquad R5$$

The overall equation can be represented as :

$$SO^+ + 4\ ClO_2 + 5OH^- \rightarrow P_1 + P_2 + 4ClO_2^- + 2NH_2OH \qquad (4.35)$$

4.3.13 Rate law

The first-order dependence of the reaction rate on the reactants and from the salt effect experiments, the major pathway of the reaction may involve both chlorine dioxide and [OH^-] ion to give an activated complex which decomposes to form the intermediates and products. Under such circumstances the rate law can be proposed as

$$Rate = k_1 [ClO_2][SO^+] + k_2 [ClO_2][OH^-] [SO^+] \quad (4.36)$$

As the reaction conditions fulfill *pseudo* first-order conditions, the rate law may be proposed as

$$= k_1 [ClO_2][SO^+] + k_{OH^-} [ClO_2][OH^-] [SO^+] \quad (4.37)$$

where $k_{OH^-} = \frac{k_2}{[OH^-]}$

$$r = \{ k_1 + k_{OH^-} [OH^-]\}[ClO_2] [SO^+] \quad (4.38)$$

when $[ClO_2]$ is in large excess then

$$Rate = k' [SO^+] \quad (4.39)$$

where the *pseudo* first-order const, k' equals

$$k' = \{k_1 + k_{OH^-} [OH^-]\}[ClO_2] \quad (4.40)$$

4.3.14 Simulations

The reaction scheme from product analysis gives insight for the intermediate structures. To support the mechanism is probable one, the simulations were done based on the comprehensive mechanism explained in Figure 4.3.13. The rate constants obtained from experimental data were employed, and for the other steps estimated rate constants were calculated and provided for simulation programme (Table 4.3.10). Rate constants from C1 and C2 are experimental values. C3- C5 are the estimated rate constants.

Table 4.3.10 Forward and reverse rate constants obtained from literature and simulations.

Reaction No	Reaction	Forward rate
C1	$SO^+ + ClO_2 + OH^- \rightarrow P_1 + I_1^+ + ClO_2^-$	$1.98 \times 10^2\ M^{-1}\ s^{-1}$
C2	$I_1^+ + ClO_2 + OH^- \rightarrow I_2^+ + ClO_2^-$	$2.00 \times 10^9\ M^{-2}s^{-1}$
C3	$I_2^+ + OH^- \rightarrow I_3 + NH_2OH$	$4.56 \times 10^9\ M^{-2}s^{-1}$
C4	$I_3 + ClO_2 + OH^- \rightarrow I_4 + ClO_2^-$	$5.90 \times 10^9\ M^{-2}s^{-1}$
C5	$I_4 + ClO_2 + OH^- \rightarrow P_2 + NH_2OH + ClO_2^-$	$6.75 \times 10^9\ M^{-2}s^{-1}$

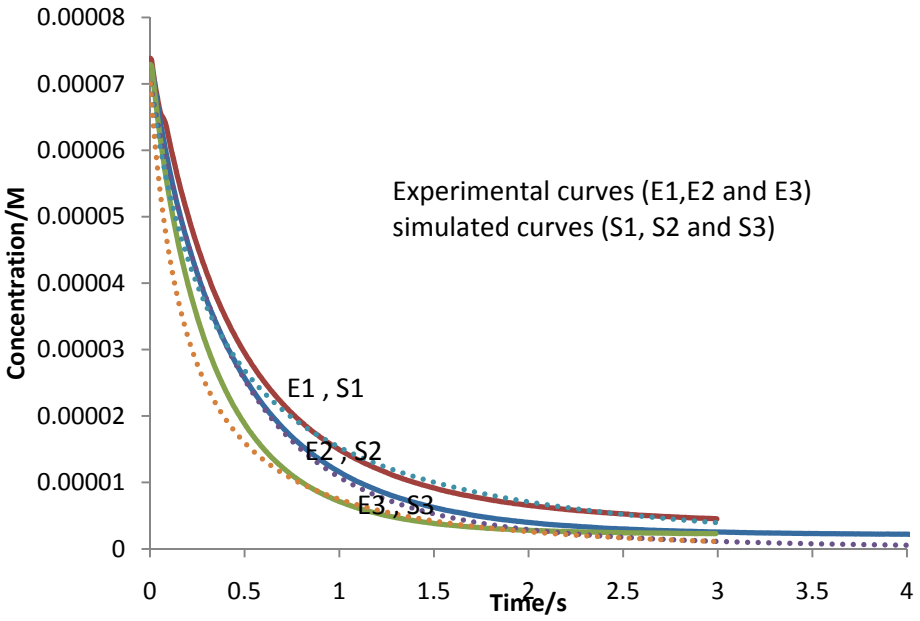

Figure 4.3.14 Experimental curves *versus* simulated curves for reaction of $[SO^+]_0$ (7.0×10^{-5} M) with $[ClO_2]_t$ (1.45×10^{-3} M) intermediates and product formation.

The graphs showing the simulated and experimental curves are illustrated in Figure 4.3.14. The estimated rate constants are optimized to obtain the better fits using the Simkine 2 programme. The simulated curves matched with experimental curves, confirming the suggested mechanism to be probable.

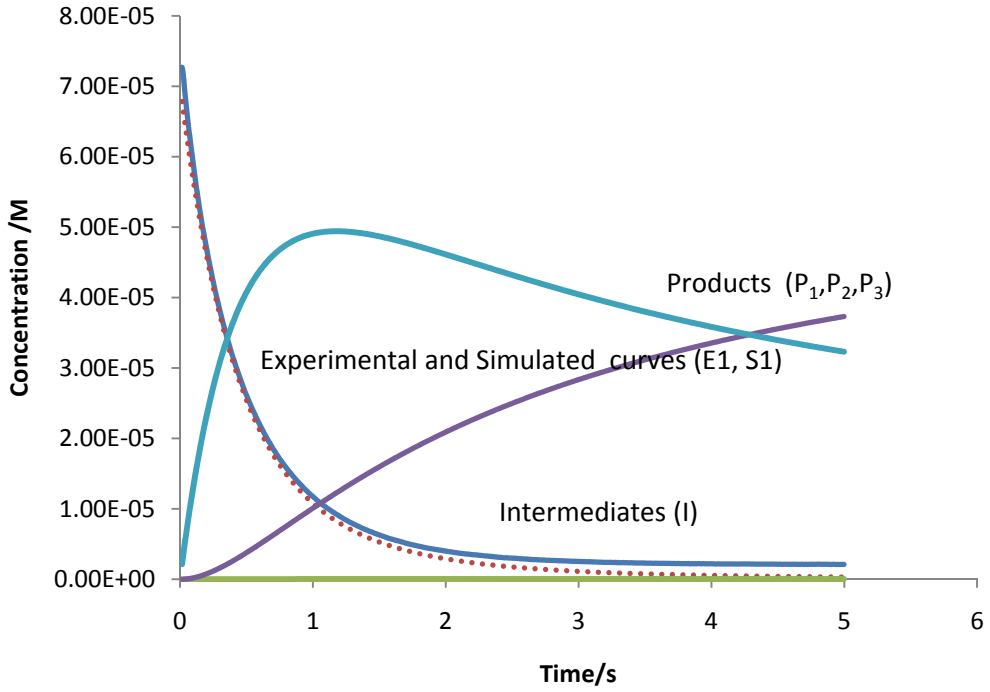

Figure 4.3.15 Product and intermediate formation for the reaction of safranine-O with chlorine dioxide.

Figure 4.3.15, for the similar experimental conditions E1 and S1 represents experimental and simulated curves for the reaction. P_1, P_2, P_3 show the product formation and I is the intermediates formed during the process. The data of simulated *versus* experimental curves and the concentrations of the other reactants, intermediates and products are compiled in (Appendix 2, Table 2.5, and Table 2.6).

CHAPTER 5
CONCLUSIONS

5.1 Reactions with hypochlorite

The oxidation reaction mechanisms of three water soluble textile dyes, amaranth (azo dye), brilliant blue-R (triaryl dye) and safranine-O (azine dye) with hypochlorite were investigated by kinetic approach. The kinetics of all the reactions were studied under low dye concentration conditions and with excess concentrations of all the other reagents. Under those conditions all the reactions followed *pseudo* first-order kinetics confirming the first-order dependence of the reaction rate on the organic substrate concentration. Although, reaction rates had first-order dependence on the oxidising agent, for the three reactions, pH played an important role. With increasing acid concentration, the reaction order with respect to acid decreased from unity to fractional value. For all the three reactions, it was found that acid was not directly involved in the rate limiting step, but it influenced the equilibrium concentrations of hypochlorite and hypochlorous acid. The oxidation of all the three organic substrates occurred through competitive pathways, one facilitated by hypochlorite ion and the other by hypochlorous acid. The oxidation by hypochlorous acid reaction was found to be the faster and major pathway. The major oxidation products were identified and the stoichiometric ratios, for all the reactions were established. Based on the major oxidation products and the partial orders with respect to the reactants, probable reaction mechanisms were elucidated. The proposed mechanisms were validated by the simulation of the kinetic profiles. The energy parameters inclusive of Arrhenius factor, enthalpy, entropy and energy of activations for both pathways of the three reactions were estimated.

For the amaranth oxidation reaction the second-order rate constants for OCl^- and HOCl facilitated oxidations were (k_1 = 1.9 ± 0.6) M^{-1} s^{-1} and (k_2 = 23.2 ± 1.8) M^{-1} s^{-1} respectively. The rate limiting steps involved reaction between AM^- and OCl^- ions and AM^- and HOCl, which was confirmed by the positive salt effect (log k' *versus* $I^{1/2}$) for the former reaction and a linear relation between k and the ionic strength in the latter. At high pH conditions, reaction was slow and reached a plateau with increasing acid concentrations. The energy parameters namely, the energy and entropy of activations were (33.65 kJ mol^{-1} and -190.6 J K^{-1} mol^{-1}) for OCl^- initiated reaction and (26.87 k J mol^{-1} and -222.8 J K^{-1} mol^{-1}) for the reaction with HOCl. The main plausible oxidation products were 3,4-dihydroxy naphthalene-2,7 disulfonic sodium salt, dichloro-1,4-naphthoquione and naphtha (2,3) oxirene-2,3-dione. The stoichiometric ratio of dye to hypochlorite was found to be 1:3.

For the brilliant blue oxidation reaction the second-order rate constants for OCl^- and HOCl initiated oxidations were (k_1 = 1.2 ± 0.2) M^{-1} s^{-1} and (k_2 = 22.0 ± 1.2) M^{-1} s^{-1} respectively. The species that are involved in the rate determining steps for the two paths were BB^+ and OCl^- ions; and BB^+ and HOCl. This was supported by the observed negative salt effect (log k' *versus* $I^{1/2}$) for the hypochlorite driven reaction and the linear relation between k and I in the later case. At high pH, reaction was slow and reached a maximum at increased $[H^+]$. The values of energy and entropy of activations were (35.53 kJ mol^{-1} and -191.93 J K^{-1} mol^{-1}) for OCl^- initiated reaction and (29.28 kJ mol^{-1} and -204.57 J K^{-1} mol^{-1}) for the reaction with HOCl. The main oxidation products were 4-ethoxy-phenylamine, 3-ethylaminomethyl-benzenesulfonicacid anion, 3- ethylamino chloro methyl-benzene sulfonic acid anion and 4-[bis-(4-hydroxy-phenyl)-methylene]-cyclohexa-2,5-hydroxide. For the safranine-O oxidation reaction the second-order rate constants for OCl^- and HOCl driven oxidations were (k_1 = 3.0 ± 0.5) M^{-1} s^{-1} and (k_2 = 34.8 ± 2.8) M^{-1} s^{-1} respectively. The rate limiting steps involved

reactions between SO^+ and OCl^- ions and SO^+ and HOCl, which again were supported by the observed negative salt effect (log k versus $I^{1/2}$) for the former reaction and a linear relation between k and I for the SO^+/HOCl as it involved reaction between charged species, SO^+ and neutral polar species, HOCl. At alkaline pH, the reaction was slow and the reaction rate recorded continued rise with increasing acid concentration. This suggests that at low pH, possibly the protonated substrate gets oxidized faster than the unprotonated entity. The energy parameters namely, energy and entropy of activations (37.09 kJ mol^{-1} and -183.53 J K^{-1} mol^{-1}) for the OCl^- initiated reaction and (23.04 kJ mol^{-1} and -222.62 J K^{-1} mol^{-1}) for the reaction with HOCl. The main oxidation products were 4-amino-5-methyl-benzene-1, 2, dichloride and amino-6-(2-chloro-6-hydroxy-phenylimino)-3-methyl-cyclohexa-2,4-dienone oxime.

A comparison of the rate constants suggests that the oxidation of the two textile dyes, amaranth and brilliant blue-R had second-order rate constants of similar magnitude for both the hypochlorite and HOCl initiated oxidations, but the rate constant for safranine-O was observed to much higher than the other two dyes.

While the amaranth/hypochlorite reaction needed three moles of HOCl (six electron oxidation), brilliant blue-R consumed four moles of HOCl (eight electron oxidation) and safranine-O oxidations consumed four moles of HOCl. A longer exposure of the dyes to oxidants resulted in increased consumption of the reactant, resulting in further oxidation of the reaction products. A comparison of energy parameters reveals that the safranine-O required slightly higher activation energy to that of amaranth and brilliant blue-R. The entropy values obtained indicates that amaranth and brilliant blue-R had same activation energies where as safranine-O recorded slightly lower values with hypochlorite initiated

reactions, and safranine-O and amaranth recorded similar entropy values compared to brilliant blue-R which had slightly lower values.

5.2 Reactions with chlorine dioxide

The kinetics and mechanisms of the of oxidation of three water soluble textile dyes, amaranth (azo dye), brilliant blue-R (triaryl dye) and safranine-O (azine dye) with chlorine dioxide were investigated in detail. The decolorisation kinetics of the dyes was studied with excess concentrations of all the other reagents except the dye, which was taken at low concentration. Under the chosen conditions all the reactions followed *pseudo* first-order kinetics with respect to organic substrate. Under all conditions the reaction rate had first-order dependence on the chlorine dioxide concentration while the concentration of hydroxide ion played an important role as catalyst hence the *pseudo* first-order rate constants registered an increasing trend with increase in $[OH^-]$. The reaction rate had first-order dependence on hydroxide ion when its concentration was low, but order with respect to $[OH^-]$ decreased when $[OH^-]$ was in stoichiometric proportion to reactants. The experimental data suggested that the predominant oxidation reaction mechanism for chlorine dioxide proceeds through free radical electrophilic (i.e. electron-attracting) abstraction rather than by oxidative substitution or addition (as in chlorinating agents such as chlorine or hypochlorite). The rate limiting step involved the formation of an activated complex involving one each of ClO_2, dye and OH^- ions. That complex possibly had both chlorine dioxide and hydroxide ion directly attached to organic substrate.

For the amaranth oxidation by chlorine dioxide, the second-order rate constants are k_2 = (19.8 ± 0.9) M^{-1} s^{-1} at pH 7.0, (97.1 ± 2.3) M^{-1} s^{-1} pH 8.0 and pH 9.0 (132.5 ± 2.8) M^{-1} s^{-1} respectively. The elementary rate limiting step involved reaction between similar charged

ions, AM^- and $[OH^-]$ which was confirmed by the positive salt effect (log k' *versus* $I^{1/2}$). The catalytic constant for hydroxyl ion was estimated to be 4.0 x 10^9 M^{-2} s^{-1} in the pH range of 6.0-7.5. The energy parameters namely, energy and entropy of activations were 50.06 kJ mol^{-1} and -658.73 J K^{-1} mol^{-1} respectively. The main oxidation products were 1,2-dioxy-3 hyposulfite- 8 sodium sulfite and 1,4-napthalenedione.

For the chlorine dioxide-brilliant blue-R reaction the second-order rate constants were k_2 = (11.7 ± 0.2 M^{-1} s^{-1}) at pH 7.0; (41.4 ± 1.1 M^{-1} s^{-1}) at pH 8.0 and (116.7 ± 1.7 M^{-1} s^{-1}) at pH 9.0. The rate limiting step involved reaction between BB^+ and OH^- ions in addition to ClO_2. The involvement of oppositely charged species was validated by the positive salt effect (log k' *versus* $I^{1/2}$) observed. The catalytic constant for $[OH^-]$ catalysed reaction was estimated to be 2.0 x 10^9 M^{-2} s^{-1} in the pH range 6.0 -7.5. The values of energy and entropy of activations were 50.06 kJ mol^{-1} and -676.36 J K^{-1} mol^{-1} respectively. The main oxidation products were identified as 4-(4-ethoxy-phenylamino)-benzoic acid, *N*-(4-ethoxy-phenyl)-hydroxylamine.

For the safranine-O oxidation with chlorine dioxide values of the second-order rate constants k_2 were (20.8 ± 0.8 M^{-1} s^{-1}), (48.1 ± 1.5 M^{-1} s^{-1}) and (75.80 ± 2.2 M^{-1} s^{-1}) at pH 7.0, 8.0 and pH 9.0 respectively. The rate limiting steps involved reactions between SO^+ and OH^- ions, which are supported by the exerted negative kinetic salt effect. The energy and entropy of activation values were 17.55 kJ mol^{-1} and -748.36 J K^{-1} mol^{-1} respectively. The main oxidation products identified were phenol, 3,7-dimethyl-phenazine-2,8-diol (P_2) as identified in the current study.

In relative terms under identical conditions, comparing the values at pH 7.0, amaranth and safranin-O had *pseudo* first-order rate constants of similar magnitudes, while brilliant blue-R had a lower value. At pH 9.0 high k' values were observed for Amaranth reaction followed by brilliant blue-R and safranine-O reactions had lower rate coefficient values.

Amaranth-chlorine dioxide reaction had a 1:4 stoichiometric ratio showing a four electron abstraction, where as brilliant blue consumed two moles of chlorine dioxide with two electron abstraction and safranine-O consumed four moles of chlorine dioxide suggesting four electron abstraction.

Scope for future work:

This work has potential for further investigations to evaluate the effect of longer exposure of dyes to oxidants and the scope of various recyclable heterogeneous catalyst materials, to achieve complete mineralization of the organic substrates with better efficiencies and in shorter durations.

REFERENCES

1 M. FalkenMark and J. Rockstrom, *Balancing water for humans and nature-the new approach in ecohydrology*, Earth scan Publishers, 2004, p.21-24

2 B. K. Korbahti and A. Tanyolac¸ *J. Hazard. Mater.,* 2008, **151,** 422-431.

3 A. D. Dhale and V.V. Mahajani, *Ind. Eng. Chem. Res.*, 1999, **38(5)**, 2058-2064.

4 M. M. Karim, A. K. Dasa and S. H. Lee, *Analytica Chimica Acta*, 2006, **576,** 37-42.

5 H. Zollinger, *Colour chemistry-synthesis, properties of organic dyes and pigments*, VCH Publishers, New York, 1987, p.92-100.

6 V. Gómez, M. S. Larrechi and M. P. Callao, *Chemosphere*, 2007, **69**, 1151-1158.

7 G. Crini, *Bioresource Technology*, 2006, **97**, 1061-1085.

8 E.J. Weber and R. L. Adams. *Environ. Sci. Technol.,* 1995, **29**, 1163-1170.

9 T. Robinson, G. McMullan, R. Marchant, P. Nigam, *Bioresource Technology*. 2001, **77,** 247-255.

10 H. Zollinger, *Color Chemistry: Synthesis, Properties and Applications of Organic Dye and Pigments*, VCH Publishers, New York, 1983, p.161-365.

11 M. Khadhraoui, H. Trabelsi, M. Ksibi, S. Bouguerra and B. Elleuch, *J. Hazard. Mater.,* 2009, **161**, 974-981.

12 C. P. L. Grady, *Hazardous Wastes Hazardous Mater.*, 1986, **3(4)**, 333-365.

13 A. A. Liwensky, *Hazardous materials and Waste water: treatment, removal and analysis*, Chapter 5, Nova Science Publishers Inc., 2007, p.149.

14 L. Szpyrkowicz, C. Juzzolino, *Ind. Eng. Chem. Res*., 2000, **39(9)**, 3241-3248.

15 S. H. Lin and C. M. Lin, *Water Res.,* 1993, **27,** 1743-1748.

16 L. Szpyrkowicz and G. F. Zilio, *Toxicol Environ Chem.,* 1996, **56(2)**, 23-34.

17 R. Anliker, *Ecotoxicol. Environ. Safety,* 1979, **3**, 59-74.

18 L. Szpyrkowicz, J. Naumczyk and F. Zilio-Grandi, *Water Res.,* 1995, **29**, 517-524.

19 J. R. Aspland , *Textile dyeing and coloration*, American Association of Textile Chemists and Colorists, Research Triangle Park, NC, 199, p. 63.

20 S. K. Bhattacharya, *Treatment of textile wastes in Handbook of industrial waste treatment,* L.K.Wang, M.H.S. Wang, 1st Edition, NY, 1992, p. 201-206.

21 G. Crini, *Bioresour. Technol.,* 2006, **97**, 1061-1085.

22 G. Mishra, and M. Tripathy, *Colourage,* 1993, **40**, 35-38.

23 V. J. P. Poots, G. McKay and J. J. Healy, *Water Res.,* 1976, **10**, 1061-1066.

24 N. Willmott, J. Guthrie and G. Nelson, *J. Soc Dyers. Color.,* 1998, **114**, 38-41.

25 N. Geopaul, *Agri. Wastes,* 1980*,* **2**, 313-318.

26 V. M. Correia, T.Stephenson, S.J Judd., *Environmental technology*, 1994, **15(10),** 917-929.

27 N. L. Nemerow, *Industrial waste treatment: contemporary practice and vision for the future*, Elsevier Inc., 2007, 53-77.

28 H. G. Coskun, A. Tanik, U. Alganci and H. K. Cigizoglu, *Water Air Soil Pollut*, 2008, **194**, 275-285.

29 G. Tchobanoglous, F. L. Burton, H. D. Stensel, Metcalf and Eddy, *Wastewater engineering: treatment and reuse*, 4th Edition, McGraw-Hill, 2003, p.333-344

30 M. A. Shannon, P. W. Bohn, M. Elimelech, J. G. Georgiadis, B. J. Marinas and A. M. Mayes, *Nature Reviews*, 2008, **452**, 301-310.

31 A. M. Talarposhti, T. Donnelly and G. K. Anderson, *Water Res.,* 2001, **35**, 425-432.

32 W. Chu and M.H. Ching, *Water Res.,* 2003, **37**, 39-46.

33 F. Zuma, J. Lin and S.B. Jonnalagadda. *J. Environ. Science and Health.*, 2009, **44(1)**, 48-56.

34 U.V Gunten, *Water Research* , 2003, **37***,* 1469-1487.

35 J. Staehelin and J. Hoigné, *Environ. Sci. Technol.,* 1985, **19**, 1206-1213.

36 V.S.R. Pullabhotla, C. Southway and S.B. Jonnalagadda, *Reaction Kinetics and Catalysis letters,* 2008, **94(2)**, 289-299.

37 Y. M. Slokar, A. M. Le Marechal, *Dyes Pigments* 1997, **37**, 335-356.

38 K. Arihara, C. Terashima, and A .Fujishima, *J. Electrochem. Soc*., 2007, **154(4),** 71-75.

39 R.W. Fullerton, *Proceedings of the Water Environment Federation, WEFTEC 2007: Session 61 through Session 70,* **15,** 4801-4815.

40 G. W. Marshall Jr, Dr. M. R. Wirthlin, *J. of Periodontology,* 2001, **72(3)**, 401-410.

41 J. W. Mellor, G. D. Parkes, *Modern Inorganic Chemistry*, 5th Edition, Longman, Green & Co., London, 1961, p.548.

42 A. Harriram, and S. B. Jonnalagadda, *Pakistan Journal of Applied Sciences*, 2001, **1(2)**, 203 -206.

43 Henry M. Leicester, Herbert S. Klickstein, A Source Book in Chemistry, 1400-1900, (1969). Harvard University Press, p.111.

44 W. B. Hugo, *Int. Biodeter. Biodegr.,* 1995, **36 3/4**, 197-217.

45 D. M. Coons, *J. American Oil Chemists' Society*, 1978, **55(1)**, 104-108.

46 J. Oakes and P. Gratton, *J. Chem. Soc. Perkin Trans.,* 1998, **1,** 2201-2206.

47 J. Oakes and P. Gratton, *J. Chem. Soc. Perkin Trans.,* 1998, **2,** 1857-1864.

48 C Xiangyu, H. Junli, C. Chongwei and L. Shaofeng, *J. Soc. Leather Technologists and Chemists*, 2007, **91 (4)**, 145-148.

49 J. W. Mellor, *Comprehensive Treatise on Inorganic and Theoretical Chemistry*, Longman, Green & Co., London, 1946, Vol 4, p.911.

50 J. W. Mellor, *Comprehensive Treatise on Inorganic and Theoretical Chemistry*, Longman, Green & Co., London, 1922, **2**, 240-418.

51 J. W. Mellor and G. D. Parkes, *Mellor's Modern Inorganic Chemistry*, 6th Edition, Longman, p. Green & Co., London, 1967, Vol III, p. 692-696.

52 G. H. Caddy, *Inorganic Synthesis*, Moeller, McGraw - Hill Co., New York, 1957, 5th Edition, p.156-165.

53 I. Nagypal, G. Peintler, and I.R. Epstein, *J. Phys. Chem.*, 1990, **94**, 2954-2958.

54 L. C. Adam, K. Suzuki, I. Fabian, and G. Gordon, *Inorg. Chem.*, 1992, **31**, 3534-3541.

55 G. C. White, *Handbook of Chlorination*, 2nd Edition, Van Nostrand Reinhold Company Inc., New York, 1986, p.150-213.

56 R. E. Hand, M. L. Smith and J. W. Harrison, *J. Endodontics*, 1987, **4**, 60-64.

57 E. C. Penick and E. M. Ostek, *Dent Clin North Am.*, 1970, **14(4)**, 743-756.

58 T. Omura, Y. Kabjane and Y. Tezuka, *Dyes & Pigments*, 1992, **20**, 227-246.

59 J. T. Spadaro, L. Isabell and V. Renganathan, *Environ. Sci. & Tech.*, 1994, **28**, 1389-1393.

60 D. Phillips, M. Duncan, E. Jenkins, G. Bevan, J. Lloyd, and J. Hoffmeister, *J. Soc. Dyers & Color*, 1996, **112**, 287-293.

61 M.H. Wilcox, W.N. Fawley, N. Wigglesworth, P. Parnell, P. Verity, J. Freeman. *J. Hospital Infection,* 2003, **54**, 109-114.

62 R. Singla, A. Ganguli, M. Gosh and S.Shoal, *Int. J. Food sci. Nutr.,* 2009, **60(7)**, 297-307.

63 N. Suzuki and J. Nakanishi, *J. Water Pollution Control Federation*, 1987, **59(8)**, 767-773.

64 J. B. Barhorst and R. Kubiak, *Environ. Sci. Pollut. Res.,* 2009, 16(5), 582-589.

65 M. Rosenbloom, J. B. Leikin, N. S. Vogel and A. Z. Chaudry, *Am. J.Therapeutics*, 2002 , **9(1)**, 5-14.

66 S. Sussman and W. J. Ward, *Water & Sewage Works,* 1979, 120-121.

67 H. Davy, *Philosophical Transactions of the Royal Society,* 1811, **101**,155-162.

68 A. M. Dietrich, M. P. Orr, D. L. Gallagher and R. C. Hoehn, *J. Am. Wat. Wks. Assoc.,* 1992, **92(6)**, 82-88.

69 B. W. Lykins and H. G. Griese, *J. Am. Wat. Wks. Assoc.,* 1986, **71(6)**, 88-93.

70 R. C. Hoehn, A. M. Dietrich, W. S. Farmer, M. P. Orr, R. G. Lee, M. Aieta, D. W. Wood, and G. Gordon, *J. Am. Wat. Wks. Assoc.*, 1990, **81(4)**, 166-172.

71 G. Thompson, J. Swain, M. Kay and C. F. Forster, *Bioresource Technology*, 2001, **77,** 275-286.

72 K. R. Solomon, *Pure & Appl. Chem.,* 1996, **68(9),** 1721-1730.

73 E. M. Aieta and J. D. Berg, *J. Am. Wat. Wks, Assoc.,* 1986, **78**, 62-72.

74 G. Gordon, R. G. Kieffer and D. H. Rosenblatt, *The Chemistry of Chlorine Dioxide In Progress in Inorganic Chemistry,* Wiley-Interscience Publishers, New York, **15**, 1972. p.230-256.

75 G. Gordon and A. A. Rosenblatt*, Gaseous Chlorine-Free Chlorine Dioxide for Drinking Water.* Proceedings of the 1995 Water Quality Technology Conference. Denver, CO: AWWA, 1996.

76 D. J. Gates, *The Chlorine Dioxide Handbook*, Denver, CO: AWWA*,* 1998.

77 B. W. Long, R. F. Miller and A. A. Rosenblatt, *Proceedings of the 6th International Symposium on Chemical Oxidation: Technology for the Nineties,* Vanderbilt University, Nashville, TN, April 15-17, 1996.

78 G. C. White, *The Handbook of Chlorination and Alternative Disinfectants*, 3rd Edition,Van Nostrand Reinhold, New York, 1992, p.150-151.

79 A. G. Myer, *J. Am. Wat. Wks. Assoc.,* 1990, **82**, 77-84.

80 N. Narkis, A. Katz, F. Orshansky, Y. Kott, Y. Friedland, *Wat. Sci. Tech.,* 1995, **31**, 105-114.

81 N. Ogata and T. Shibata, *J.Gen. Virol.,* 2008, 89, 60-67.

82 J. Patrick Fitch, E. Raber, D.R. Imbro., *Science*, 2003, **302(21)**, 1350-1354.

83 A. Adhikari, Y. Iossifova, S. A. Grinshpun, and T.Reponen, *J. Air & Waste Manage. Assoc*. 2008, **58**, 647-656.

84 J. Frascella, R. D Gilbert, P. Fernandez and J. Hendler., *Compend Contin Educ Dent.* 2000, **21(3)**, 241-248.

85 G Gordon, B Slootmaekers, S Tachiyashiki, *J. Am. Wat. Wks. Assoc.,* 1990, **82(4),** 160-165.

86 J.F Malpas, *Water Treatment and Examination,* 1973, **22(3)**, 209-221.

87 P. Gregory, *Dye stuffs in The Chemical Industry,* C. A. Heaton , 2nd Edition, Blackie Academic & Professional, 1994, p. 143-188.

88 J. Shore, *Society of Dyers and Colourists. Colorants and Auxiliaries Volume 1,* Manchester, England, 1990, p. 331-332.

89 K. Turhan and Z. Turgut, *Desalination*, 2009, **242**, 256-263.

90 E. N. Abrahart, *Dyes and their Intermediates,* 1st Edition*,* 1968, p.15-40.

91 H. L. Needles, Handbook of Textile Fibers: Dyes and Finishes, Garland: New York, 1981, p. 144.

92 V.K. Gupta, A. Mittal, L. Krishnan and J. Mittal, *J. of Colloid and Interface Science*, 2006, **293**, 16-26.

93 A. H. Konsawa, *Desalination*, 2003, **158**, 233-240.

94 A.I.Del Río, J. Molina, J. Bonastre and F. Cases, *J. Hazard. Mater.,* 2009, **172**, 187-195.

95 S. M. Burkinshaw, F. E. Chaccour and A. Gotsopoulos, *Dyes and Pigments,* 1997, 34(3), 227-241.

96 D. Brodnjak Voncina, A. L. Majcen-Le-Marechal, *Dyes and Pigments*, 2003, **59**, 173-179.

97 F. H. Abdullah, M.A. Rauf and S. S. Ashraf, *Dyes and Pigments,* 2007, **72**, 349-352.

98 M. A Kulandainathan, A. Muthukumaran, K. Patil, R.B. Chavan, *Dyes and Pigments,* 2007, **73**, 47-54.

99 O. J. Hao, H. Kim and P.C. Chiang, *Environ. Sci. Technol.,* 2000, **30(4)**, 449-505.

100 D. L. Michelsen, *AATCC Book of Papers*, 1992, 165-170.

101 M. Muruganandham and M. Swaminathan, *Dyes and Pigments*, 2004, **62**, 269-275.

102 J. Oakes, P. Gratton and T. Gordon-Smith, *Dyes and pigments*, 2000, **46**, 169-180.

103 J. Oakes and P. Gratton, *J. Chem. Soc., Perkin Trans.,* 1998, **2**,1857-1864.

104 P. M. Paradis, *J. Chem. Research (S)*, 1999, 340-341.

105 M. A. Rauf, S. Ashraf and S.N. Alhadrami, *Dyes and Pigments*, 2005, **66(3)**, 197-200.

106 F. H. Abdullaha, M. A. Rauf, and S. S. Ashrafa , *Dyes and Pigments*, 2007, **72(3)**, 349-352.

107 L. Szpyrkowicz, C. Juzzolino, S. N. Kaul, S. Daniele and M. D. De Faveri, *Ind. Eng. Chem. Res.*, 2000, **39(9)**, 3241-3248.

108 J. Hastie, D. Bejan, M. Teutli-León and N. J. Bunce, *Ind. Eng. Chem. Res.*, 2006, **45(14)**, 4898-4904.

109 S. Navalon, M. Alvaro and H. Garcia, *J. Hazard. Mater.*, 2009, **164**, 1089-1097.

110 J. M. Symons, A. A. Stevens, R. M. Clark, E. E. Geldreich, O. T. Love and J. DeMarco Jr, *Treatment Techniques for Controlling Trihalomethanes in Drinking Water.* USEPA, Cincinnati, 1981, EPA-600/2-81-156.

111 G. C. White, *Handbook of Chlorination*, Van Nostrand, Reinhold Co., New York, 1972, p. 604.

112 J. Hoigne and H. Bader, *Water Research*., 1994, **28**, 45-55.

113 Y. S. Hung, *Chemosphere*, 1994, **29**, 2597-2607.

114 M.A.Metwally E. Abdel-Latif, A. M. Khalil, F. A. Amer, G. Kaupp, *Dyes and pigments*, 2004, **62(2)**, 181-195.

115 M.A. Jabar and A. Mossawi, *Env. International,* 1983, **9(2)**, 145-148.

116 W. H. Hansen, O. G. Fitzhugh, A. A. Nelson and K. J. Davis, *Toxicology and Applied Pharmacology*, 1996, **8(1)**, 29-36.

117 R. Jain, N. Sharma, N. Jadon and K. Radhapyari, *Internat. J. Environ. and Pollution*, 2006, **27(1-3)**, 121-134.

118 F. H. Abdallah, M. A. Rauf and S. S. Ashraf, *J. Dyes and Pigments*., 2007, **72**, 349-352.

119 G. Gordon, L.C. Adam and B. P. Bubnis, *J. Am. Water Works Assoc.*, 1997, **89(4)**, 142-149.

120 M. W. Lister, *Can. J. Chem.*, 1956, **34(4)**, 479-488.

121 G. Gordon, *The Formation of Chlorate Ion in Drinking Water Treated with Free Available Chlorine*. Presented to the D / DBP TAW in session at the Water Quality Technology Conference, Orlando, November, 1991.

122 M. Bolyard, P. S. Fair and D. P. Hautman, *Environ. Sci. Technol.*, 1992, **26**, 1663-1665.

123 G. Gordon, L. C. Adam, B. P. Bubnis, B. Hoyt, S.J. Gillette, and A. Wilczac, *J. Am. Water Works Assoc*., 1993, **86(9)**, 89-97.

124 M. Bolyard, P. S. Fair and D. P. Hautman, *J. Am. Water Works Assoc.*, 1993, **85(9)**, 81-88.

125 G. Gordon, L. C. Adam and B. P. Bubnis, *Minimizing Chlorate Ion Formation in Drinking Water When Hypochlorite Ion is the Chlorinating Agent.* AWWA Research Foundation, Denver CO, Contract 83392, 1994.

126 L. Nowell and J. Hoigne, *Water Res*., 1992, **26**, 593-598.

127 M. W. Lister and R. C. Petterson, *Can. J. Chem.*, 1962, **40**, 729-733.

128 R. M. Chapin, *J. Am. Chem. Soc.*, 1934, **56**, 2211-2215.

129 L. C. Adam and G. Gordon, *Inorg. Chemistry*, 1999, **38**, 1299-1304.

130 *Sodium Hypochlorite Safety & Handling*, Pamphlet 96, 1st Edition., Chlorine Institute, Washington, DC, 1992, p.17. Accessed on 30th March, 2009.

131 G. Holst, *Chem. Reviews.,* 1954, **54**, 169-194.

132 R. L. Feller, *Bulletin of the American Group. International Institute for Conservation of Historic and Artistic Works*, 1971, **11(2)**, 39-57.

133 J. C. Bailar, H. J. Emeleus and A. F. Trotman - Dickenson, *Comprehensive Inorganic Chemistry*, Pergamon Press Ltd., New York, 2nd Edition, 1973, p. 1024.

134 B. Moody, *Comparative Inorganic Chemistry*, 2nd Edition., Edward Arnold Ltd., 1965, p.245-267.

135 R. M. Chapin, *J. Am. Chem. Soc.,* 1934, **56**, 2211.

136 J. C. Morris, *J. Phys. Chem.,* 1966, **70,** 3798-3802.

137 E. M. Aieta and J. D. Berg, *J. Am. Water Works Assoc*, 1986, **78(6)**, 62-72.

138 R. G. Zika, C. A. Moore, L. T. Gidel and W. J. Cooper, *Water Chlorination: Environmental Impact and Health Effects*. Lewis Publishers, 5th Edition**,** 1985, p.207-220.

139 G. C. White, *Handbook of chlorination*, 4th Edition, John Wiley & Sons, 1999, p.363-397.

140 W. J. Masschelein, *Chlorine Dioxide: Chemistry and Environmental Impact of Oxychlorine Compounds,* Ann Arbor Science Publishers, 1979, p.172.

141 J. J. Rook, *J. Society for Water Treatment Exam.,* 1974, **23(2)**, 234-243.

142 T. A. Bellar, J. J. Lichtenberg and R.C. Kroner, *J. Am. Water Works Assoc*.,1974, **66(11)**, 703-706.

143 B. Limoni, E. C. Goldstein and C. Rav-Acha, *J. Environ. Sci. Health.*, 1984, **19(8)**, 943-957.

144 K. S. Werdehoff and P. C. Singer, *J. Am. Water Works Assoc.*, 1987, **79(9)**, 107-113.

145 P. C. Singer and W. K. O Neil, *J. Am. Water Works Assoc.*, 1987, **79(11)**, 75-76.

146 R. G. Zika, C. A. Moore, L. T. Gidel and W. J. Cooper in *Water Chlorination: Environmental Impact and Health Effects*, Lewis Publishers, 1985, **5**, 1041-1053.

147 M. H. Griese, J. J. Kaczur and G. Gordon, *J. Am. Water Works Assoc*., 1992, **84(11)**, 69-77.

148 R. C. Hoehn, A. M. Dietrich, W. S. Farmer, M. P. Orr, R. G. Lee, E. M. Aieta, D. M. Wood III and G. Gordon, *J. Am. Water Works Assoc.*, 1990, **82(4)**, 166-172.

149 M. P. McCann, *J. Chem. Education.,* 2000, **77**, 1562-1564.

150 O. N. Temkin, A. V. Zeigarnik and D. Bonchev, *Chemical reaction networks: A graph-theoretical approach,* CRC Press Inc, 1996. p.7-12

151 K. A. Connors, *Chemical kinetics: the study of reaction rates in solution,* VCH Publishers Inc, 1990, p 2-30.

152 SR Logan, *Fundamentals of chemical kinetics*, Longman group Ltd, 1996, p.2-5.

153 M. G. Evans, M. Polanyi, *Trans. Faraday Soc.,* 1935, **34**, 874-894,

154 K J. Laidler and M. C Klng, *J. Chem. Phys.,* 1983, **87**, 2657-2664.

155 J. H. Rdpenson, *Chemical kinetics and reaction mechanisms in Advanced Chemistry* McGraw-Hill Series, 1981, p.81-94.

156 M. R. Wright, in *An Introduction to Chemical Kinetics*, John Wiley and Sons Ltd, 2004, p.140-144, 268 -280.

157 R. B. Jordan, Reaction Mechanisms of Inorganic and Organometallic Systems, Oxford University Press, New York, 1991, p.1-16.

158 E. A. Moelwyn-Hughes, *The Kinetics of Reactions in Solution,* 2nd Edition, Oxford at the Clarendon Press, 1947, p.93-97.

159 K. Y. Tam and F. T. Chau, *Chemom. Intell. Lab. Syst.*, 1994, **25**, 25-42.

160 F. R. Giordno, M. D. Wier and W. P. Fox in *A First course in Mathematical Modelling,* 2nd Edition*,* Brooks/Cole publishing Co., Pacific Grove, 1997, p.97-216.

161 J. Banks, J. S. Carson II, B. L. Nelson, *Discrete-Event System Simulation,* 2nd Edition*,* Prentice Hall International Inc., New Jersy, 1996, p.1-70.

162 K.J. Molloy, M. Maeder, M. M. Schumacher, *Chemom. Intell. Lab. Syst.*, 1999, **46**, 221-230.

163 F. R Giordano, M. D. Weir, W. P. Fox, *A First Course in Mathematical Modelling,* 2nd Edition, Brooks/Cole Publishing Co, Pacific Grove, 1997, p.97-216.

164 J. Banks, J. S. Carson II, B. L. Nelson, *Discrete-Event System Simulation*, 2nd Edition, Prentice Hall International Inc, New Jersey, 1996, p.1-70.

165 *Fitall a general purpose, non linear regression (curve-fitting) program,* by MTR Software, Canada, 1998, http://www.fitall.com/ Accessed on 30th March, 2009.

166 K. Schittkowski, EASY-FIT: *A software system for data fitting in dynamic systems*, *Structural and Multidisciplinary Optimization*, 2002, **23(2)**, 153-169.

167 P. Kaps, P. Rentrop, *Numer. Math.,* 1979, **33**, 55-68.

168 M. N. Shezi and S.B. Jonnalagadda, *South African Journal of Chemistry*, 2006, ***59*****,** 82-85.

169 D. Kaufman, C. Sterner, B. Masek, R. Svenningsen and G. Samuelson, *J. Chem. Educ.,* 1982, **12**, 885-886.

170 J. W. Moore and R. G Pearson, *Kinetics and Mechanism*, 3rd Edition, W.H. Freeman & Co., New York, 1995, p.480.

171 H. Hartridge and F.J. W. Roughton, *Proc.R.Soc.,* London,1923, **A104,** 376-394.

172 K. A. Connors, *Chemical Kinetics: The Study Of Reaction Rates In A Solution,* Wiley-VCH, New York, 1990, p.1-22, 57-68, 177-180.

173 P. Atkins and J. de Paula, Atkins' Physical Chemistry, 8th Edition., Oxford University Press, Oxford, 2006, p.791-829.

174 K.J. Laidler and J.H. Meiser, Physical Chemistry, 3rd Edition., Houghton Mifflin, Boston, 1999, p.365-385, 598.

175 J. Buckman and S. M. Miller, *Biochemistry*, 2000, **39**, 10521-10531.

176 S. Gokturk, M. Tuncay, *Spectrochimica Acta Part A,* 2003, **59**, 1857-/1866.

177 R. E. Hand, M. L. Smith and J. W. Harrison, J. Endodontics, 1987, **4**, 60-64.

178 A. I. Vogel, *Textbook of Quantitative Chemistry*, 5th Edition, Longman Group, UK, 1989. p.340-359.

179 Greenberg, E. Arnold, *Standard Methods for the Examination of Water and Wastewater,* 14th Edition, 1975, p.350-351.

180 Hi - TECH Scientific, *Operator's Manual for the SF-61DX2 Double-Mixing Stopped-Flow*, 1997, Issue 2, p.3.1-3.17.

181 Hi - TECH Scientific, *Operator's Manual for the SF-61DX2 Double-Mixing Stopped-Flow*, 1996, Issue 1.

182 S.B. Jonnalagadda, N. Parumasur and M.N. Shezi, *Computational Biology and Chemistry*, 2003, **27**, 147-152.

183 M.N Shezi, S.B Jonnalagadda, *South African Journal of Chemistry,* 2006*,* **59**, 82-85.

184 F.T. Chau, K.W. Mok, *Comput. Chem.,* 1992, **16**, 239-242.

185 N. Mohan, N. Balasubramanian, C. Ahmed Basha, *J. Hazard. Mater.,* 2007, **147**, 644-651.

186 N. Zaghbani, A. Hafiane and M. Dhahbi, *Desalination, 2008,* **222,** 348-356.

187 M. Al-Ghouti, M.A.M. Khraisheh , M.N.M. Ahmad and S. Allen, *Journal of Colloid and Interface Science,* 2005, **287**, 6-13.

188 M. Dogan, M. Alkan, *Chemosphere,* 2003, **50**, 517-528.

189 A. Cornish-Bowden in *Fundamentals of enzyme kinetics,* 2nd Edition, Portland Press, London, 1995, p.14-16.

190 H. Eyring, *Chem. Rev.*, 1935, **17(1)**, 65-77.

191 P.Gregory and C.V.Stead, *J.Soc Dyers Colour*, 1978, **94**, 187-202.

192 T.Omura, *Dyes and Pigm,* 1993, **23**, 1994, **24**, 26-33.

193 T.Omura, Y.kayane and Y.Tezuka, *Dyes and Pigm*, 1992, **20**, 227-246.

194 E. Guivarch, S. Trevin, C. Lahitte and M. A.Oturan, *Environ Chem.Letters*, 2003, **1,** 38-44.

195 J. Oakes and P. Gratton, *J.Phem.Soc, Perkin Trans.,* 1998, **2**, 2201-2206.

196 J. Oakes and P.L.Gratton, *J.Chem.Soc, Perkin Trans.,* 1998, **2**, 1857-1864.

197 R. C. Weast, in *Hand Book of chemistry and physics*, RC Press, 1987, p.381-400.

198 J. Oakes, *Coloration Technology*, 2002, **32(1)**, 63-79.

199 J. March in *Advances in Organic Chemistry,* 6th Edition*,* John Wiley and Sons, 2007, 1703-1731

200 J. Oakes and P. Gratton, *J. Chem. Soc., Perkin Trans.* 1998, **2**, 2563-2568

201 J. Oakes and P. Gratton, *J. Chem. Soc., Perkin Trans.* 1998, **2,**2201-2206.

202 L. K. Adam, I.Fabian, K. Suzuki, and G. Gordon, *Inorg. Chem,* 1992, **31**, 3534-3541.

203 V. Csorda, B. Bubnis, Istva´n Fa´bia´n, and G. Gordon, *Inorg. Chem.,* 2001, **40**, 1833-1836.

204 B. R. Deshwal and H. Lee, *Ind. Eng. Chem.,* 2004, **10(4)**, 667-673.

205 HDR Engineering Inc*, Hand book of public water systems,* 2nd Edition, John Wiley & Sons, 2001, p.526-528.

206 L. M. Babcock, T. Pentecost and W. H. Koppeno1, *J. Phys. Chem.*, 1983, **93**, 8126-8127.

207 E. M. Aieta and J. D. Berg, *J. Am. Water Works Assoc.,* 1986, **78**, 62-70.

208 I. N. Odeh, J. S. Francisco and D.W. Margerum, *Inorg. Chem.,* 2002, **41**, 6500-6506.

209 J. Hoigne, H. Bader, *Water Res.*, 1994, **28**, 45-55.

210 R.H. Becker, J.S. Nicoson and D.W. Margerum, *Inorg. Chem.,* 2003, **42**, 7938-7944.

APPENDIX 1-CHAPTER 3

1.1 Amaranth oxidation products with hypochlorite.

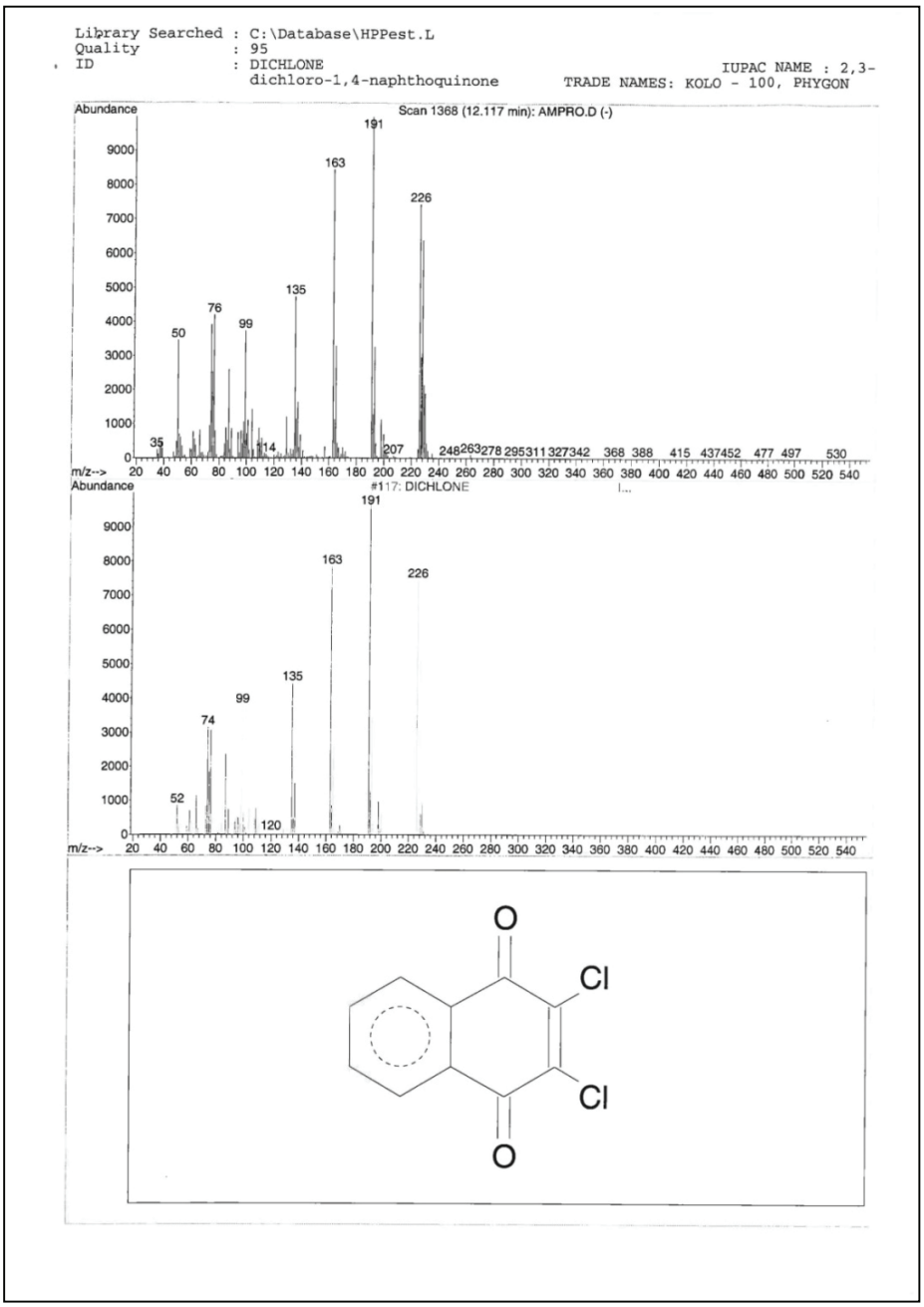

Figure 1.1.1 GC-MS spectrum of amaranth oxidation product P_2 dichloro-1,4-naphthoquione (m/z = 228) with hypochlorite.

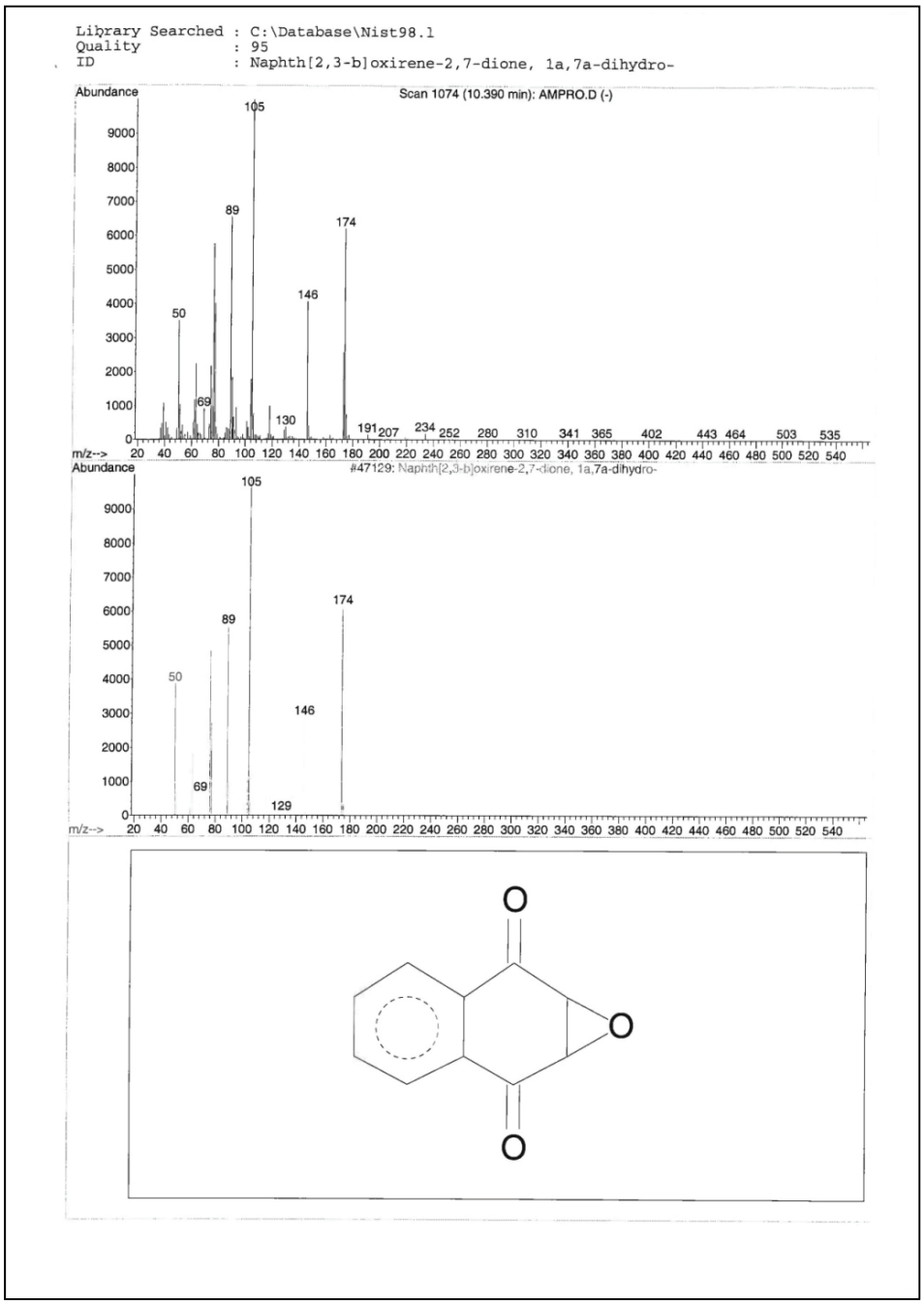

Figure 1.1.2 GC-MS spectrum of amaranth oxidation product P_3 naphtha (2, 3) Oxirene-2,7-dione (m/z = 174) with hypochlorite.

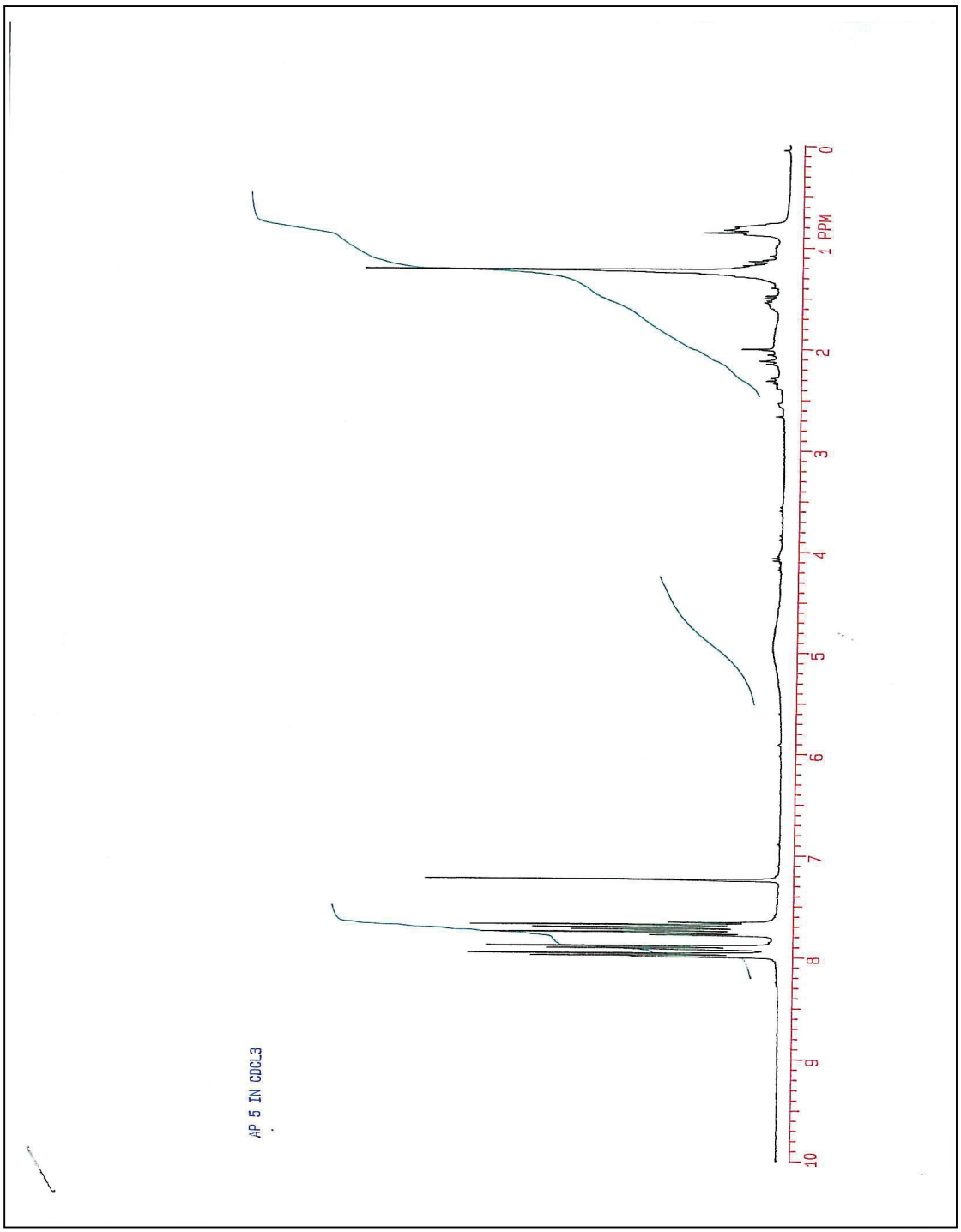

Figure 1.1.3 ^{1}H NMR spectrum of amaranth product P_1 (3,4-dihydroxy naphthalene-2,7 di sulphonic sodium salt) with hypochlorite.

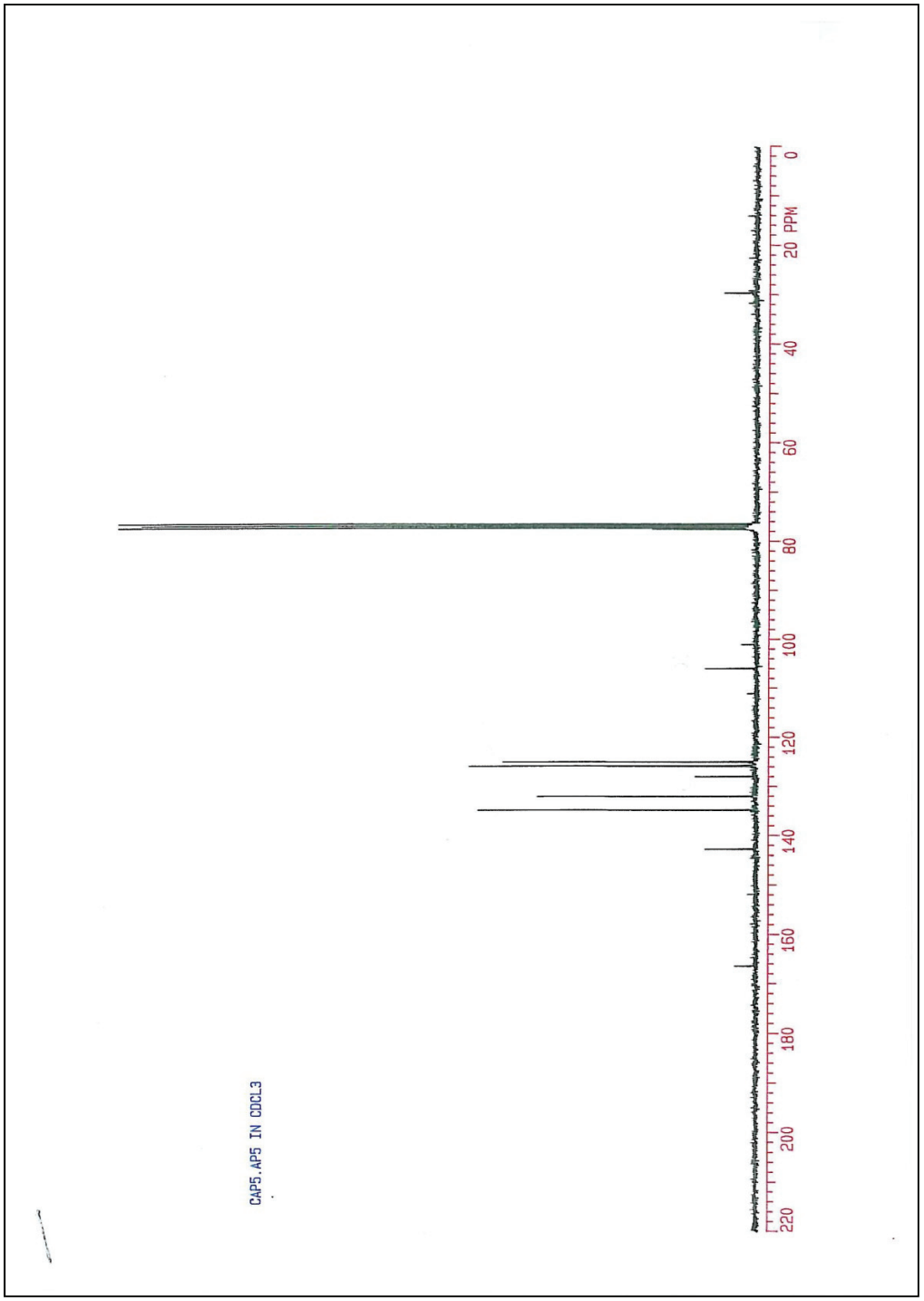

Figure 1.1.4 ^{13}C NMR spectrum of amaranth oxidation product P_1 (3,4-dihydroxy naphthalene- 2,7 di sulphonic sodium salt) with hypochlorite.

Table 1.1 Amaranth - hypochlorite experimental and simulated curves-compiled data.

Time	E1	Time	S1	Time	E2	Time	S2	Time	E3	Time	S3
0.2	7.00E-05	1.757	6.46E-05	0	7.00E-05	0.63	6.12E-05	0	7.00E-05	0.254	5.96E-05
0.4	6.96E-05	1.991	6.40E-05	0.2	6.81E-05	0.73	6.01E-05	0.2	6.10E-05	0.293	5.80E-05
0.6	6.92E-05	2.225	6.35E-05	0.4	6.63E-05	0.83	5.92E-05	0.293	5.73E-05	0.332	5.64E-05
0.8	6.87E-05	2.46	6.30E-05	0.6	6.45E-05	0.93	5.82E-05	0.332	5.57E-05	0.371	5.49E-05
1	6.83E-05	2.694	6.25E-05	0.732	6.33E-05	1.02	5.73E-05	0.371	5.43E-05	0.41	5.33E-05
1.2	6.79E-05	2.929	6.20E-05	0.83	6.25E-05	1.12	5.63E-05	0.41	5.28E-05	0.449	5.19E-05
1.4	6.75E-05	3.163	6.15E-05	0.927	6.17E-05	1.22	5.54E-05	0.449	5.14E-05	0.488	5.05E-05
1.6	6.71E-05	3.397	6.11E-05	1.025	6.08E-05	1.32	5.46E-05	0.488	5.00E-05	0.527	4.92E-05
1.76	6.67E-05	3.632	6.05E-05	1.123	6.00E-05	1.42	5.37E-05	0.527	4.87E-05	0.566	4.78E-05
1.96	6.63E-05	3.866	6E-05	1.22	5.92E-05	1.51	5.29E-05	0.566	4.74E-05	0.605	4.65E-05
1.99	6.59E-05	4.1	5.96E-05	1.318	5.85E-05	1.61	5.21E-05	0.605	4.62E-05	0.644	4.53E-05
2.69	6.45E-05	5.507	5.70E-05	1.904	5.39E-05	2.2	4.75E-05	0.84	3.93E-05	0.879	3.86E-05
3.13	6.40E-05	6.21	5.58E-05	2.197	5.18E-05	2.49	4.54E-05	0.957	3.62E-05	0.996	3.56E-05
3.16	6.36E-05	6.444	5.54E-05	2.294	5.11E-05	2.59	4.47E-05	0.996	3.53E-05	1.035	3.47E-05
3.36	6.35E-05	6.679	5.50E-05	2.392	5.04E-05	2.69	4.40E-05	1.035	3.43E-05	1.074	3.38E-05
3.4	6.32E-05	6.913	5.46E-05	2.49	4.98E-05	2.78	4.34E-05	1.074	3.34E-05	1.113	3.29E-05
3.87	6.23E-05	7.851	5.30E-05	2.88	4.72E-05	3.17	4.1E-05	1.23	3.00E-05	1.269	2.97E-05
4.07	6.22E-05	8.085	5.26E-05	2.978	4.66E-05	3.27	4.04E-05	1.269	2.92E-05	1.308	2.89E-05
4.1	6.18E-05	8.319	5.23E-05	3.076	4.59E-05	3.37	3.98E-05	1.308	2.85E-05	1.347	2.82E-05
4.3	6.18E-05	8.554	5.19E-05	3.173	4.53E-05	3.47	3.92E-05	1.347	2.77E-05	1.387	2.74E-05
4.8	6.05E-05	9.726	5.01E-05	3.662	4.24E-05	3.95	3.65E-05	1.543	2.42E-05	1.582	2.41E-05
5	6.04E-05	9.96	4.97E-05	3.759	4.18E-05	4.05	3.60E-05	1.582	2.36E-05	1.621	2.35E-05
5.04	6.01E-05	10.19	4.94E-05	3.857	4.13E-05	4.15	3.55E-05	1.621	2.30E-05	1.66	2.30E-05
5.24	6.00E-05	10.43	4.90E-05	3.955	4.07E-05	4.25	3.51E-05	1.66	2.23E-05	1.699	2.24E-05
5.27	5.96E-05	10.66	4.86E-05	4.052	4.02E-05	4.35	3.46E-05	1.699	2.18E-05	1.738	2.18E-05
5.74	5.88E-05	11.6	4.73E-05	4.443	3.81E-05	4.74	3.27E-05	1.855	1.95E-05	1.894	1.97E-05
5.94	5.87E-05	11.84	4.69E-05	4.54	3.76E-05	4.83	3.22E-05	1.894	1.90E-05	1.933	1.92E-05
5.98	5.84E-05	12.07	4.66E-05	4.638	3.71E-05	4.93	3.18E-05	1.933	1.85E-05	1.972	1.87E-05
6.18	5.83E-05	12.3	4.63E-05	4.736	3.66E-05	5.03	3.14E-05	1.972	1.80E-05	2.012	1.83E-05
6.21	5.80E-05	12.54	4.6E-05	4.833	3.61E-05	5.13	3.10E-05	2.012	1.76E-05	2.051	1.78E-05
6.41	5.79E-05	12.77	4.56E-05	4.931	3.56E-05	5.22	3.06E-05	2.051	1.71E-05	2.09	1.74E-05
6.88	5.71E-05	13.71	4.44E-05	5.322	3.38E-05	5.61	2.90E-05	2.207	1.53E-05	2.246	1.57E-05
6.91	5.67E-05	13.94	4.41E-05	5.419	3.33E-05	5.71	2.85E-05	2.246	1.49E-05	2.285	1.54E-05
7.38	5.59E-05	14.88	4.29E-05	5.81	3.16E-05	6.1	2.71E-05	2.402	1.34E-05	2.441	1.39E-05
7.58	5.59E-05	15.12	4.26E-05	5.908	3.12E-05	6.2	2.67E-05	2.441	1.31E-05	2.48	1.36E-05
7.62	5.55E-05	15.35	4.23E-05	6.005	3.07E-05	6.3	2.64E-05	2.48	1.27E-05	2.519	1.32E-05
7.82	5.55E-05	15.59	4.20E-05	6.103	3.03E-05	6.4	2.60E-05	2.519	1.24E-05	2.558	1.29E-05
7.85	5.51E-05	15.82	4.17E-05	6.201	2.99E-05	6.49	2.57E-05	2.558	1.21E-05	2.597	1.26E-05

8.05	5.51E-05	16.05	4.14E-05	6.298	2.95E-05	6.59	2.54E-05	2.597	1.17E-05	2.636	1.23E-05
9.02	5.32E-05	18.16	3.90E-05	7.177	2.62E-05	7.47	2.26E-05	2.949	9.22E-06	2.988	9.89E-06
9.96	5.17E-05	20.04	3.69E-05	7.958	2.35E-05	8.25	2.03E-05	3.261	7.44E-06	3.301	8.18E-06
10.2	5.16E-05	20.27	3.67E-05	8.056	2.32E-05	8.35	2.01E-05	3.301	7.25E-06	3.34	7.98E-06
10.2	5.13E-05	20.51	3.64E-05	8.154	2.29E-05	8.45	1.98E-05	3.34	7.05E-06	3.379	7.78E-06
10.4	5.13E-05	20.74	3.62E-05	8.251	2.26E-05	8.54	1.96E-05	3.379	6.87E-06	3.418	7.61E-06
10.4	5.09E-05	20.98	3.59E-05	8.349	2.23E-05	8.64	1.93E-05	3.418	6.69E-06	3.457	7.43E-06
10.6	5.09E-05	21.21	3.57E-05	8.447	2.20E-05	8.74	1.91E-05	3.457	6.51E-06	3.496	7.26E-06
10.7	5.06E-05	21.44	3.55E-05	8.544	2.17E-05	8.84	1.88E-05	3.496	6.34E-06	3.535	7.08E-06
10.9	5.05E-05	21.68	3.52E-05	8.642	2.14E-05	8.93	1.86E-05	3.535	6.17E-06	3.574	6.91E-06
10.9	5.02E-05	21.91	3.5E-05	8.74	2.11E-05	9.03	1.84E-05	3.574	6.01E-06	3.613	6.75E-06
11.8	4.88E-05	23.79	3.31E-05	9.521	1.90E-05	9.81	1.66E-05	3.886	4.85E-06	3.926	5.6E-06
12	4.88E-05	24.02	3.29E-05	9.618	1.87E-05	9.91	1.64E-05	3.926	4.72E-06	3.965	5.48E-06
12.1	4.85E-05	24.26	3.27E-05	9.716	1.85E-05	10	1.62E-05	3.965	4.59E-06	4.004	5.35E-06
12.3	4.84E-05	24.49	3.25E-05	9.814	1.82E-05	10.1	1.60E-05	4.004	4.47E-06	4.043	5.24E-06
12.3	4.81E-05	24.73	3.23E-05	9.911	1.80E-05	10.2	1.58E-05	4.043	4.35E-06	4.082	5.12E-06
12.5	4.81E-05	24.96	3.21E-05	10.01	1.78E-05	10.3	1.56E-05	4.082	4.24E-06	4.121	5.00E-06
13	4.74E-05	25.9	3.13E-05	10.4	1.68E-05	10.7	1.49E-05	4.238	3.81E-06	4.277	4.57E-06
13	4.71E-05	26.13	3.11E-05	10.5	1.66E-05	10.8	1.47E-05	4.277	3.71E-06	4.316	4.46E-06
13.2	4.70E-05	26.37	3.09E-05	10.6	1.64E-05	10.9	1.45E-05	4.316	3.61E-06	4.355	4.37E-06
13.7	4.61E-05	27.54	2.99E-05	11.08	1.53E-05	11.4	1.36E-05	4.511	3.16E-06	4.55	3.90E-06
14.8	4.47E-05	29.65	2.82E-05	11.96	1.36E-05	12.3	1.22E-05	4.863	2.48E-06	4.902	3.20E-06
14.9	4.45E-05	29.88	2.81E-05	12.06	1.34E-05	12.4	1.21E-05	4.902	2.42E-06	4.941	3.14E-06
15.1	4.44E-05	30.12	2.79E-05	12.16	1.32E-05	12.5	1.19E-05	4.941	2.35E-06	4.98	3.07E-06
15.1	4.42E-05	30.35	2.77E-05	12.26	1.31E-05	12.5	1.18E-05	4.98	2.29E-06	5.019	3.01E-06
15.3	4.41E-05	30.59	2.75E-05	12.35	1.29E-05	12.6	1.16E-05	5.019	2.23E-06	5.058	2.95E-06
15.8	4.32E-05	31.76	2.67E-05	12.84	1.21E-05	13.1	1.09E-05	5.215	1.95E-06	5.254	2.65E-06
16	4.32E-05	31.99	2.65E-05	12.94	1.19E-05	13.2	1.08E-05	5.254	1.90E-06	5.293	2.59E-06
16.1	4.29E-05	32.23	2.64E-05	13.04	1.17E-05	13.3	1.07E-05	5.293	1.85E-06	5.332	2.53E-06
16.3	4.29E-05	32.46	2.62E-05	13.13	1.16E-05	13.4	1.06E-05	5.332	1.80E-06	5.371	2.49E-06
16.3	4.26E-05	32.7	2.60E-05	13.23	1.14E-05	13.5	1.04E-05	5.371	1.75E-06	5.41	2.43E-06
16.8	4.20E-05	33.63	2.54E-05	13.62	1.08E-05	13.9	9.96E-06	5.527	1.57E-06	5.566	2.25E-06
17	4.20E-05	33.87	2.53E-05	13.72	1.07E-05	14	9.84E-06	5.566	1.53E-06	5.605	2.19E-06
17	4.17E-05	34.1	2.51E-05	13.82	1.05E-05	14.1	9.73E-06	5.605	1.49E-06	5.644	2.16E-06
17.7	4.08E-05	35.51	2.42E-05	14.4	9.73E-06	14.7	9.06E-06	5.84	1.27E-06	5.879	1.91E-06
17.9	4.08E-05	35.74	2.41E-05	14.5	9.60E-06	14.8	8.94E-06	5.879	1.24E-06	5.918	1.87E-06
17.9	4.05E-05	35.98	2.39E-05	14.6	9.48E-06	14.9	8.84E-06	5.918	1.20E-06	5.957	1.84E-06
18.1	4.05E-05	36.21	2.37E-05	14.7	9.35E-06	15	8.72E-06	5.957	1.17E-06	5.996	1.81E-06
18.8	3.96E-05	37.62	2.29E-05	15.28	8.63E-06	15.6	8.15E-06	6.191	9.98E-07	6.23	1.63E-06
18.9	3.94E-05	37.85	2.28E-05	15.38	8.51E-06	15.7	8.04E-06	6.23	9.72E-07	6.269	1.59E-06
19.1	3.93E-05	38.09	2.27E-05	15.48	8.40E-06	15.8	7.94E-06	6.269	9.46E-07	6.308	1.56E-06

19.1	3.91E-05	38.32	2.25E-05	15.58	8.29E-06	15.9	7.84E-06	6.308	9.21E-07	6.347	1.53E-06
19.8	3.85E-05	39.49	2.18E-05	16.06	7.75E-06	16.4	7.42E-06	6.504	8.06E-07	6.543	1.38E-06
19.8	3.83E-05	39.73	2.17E-05	16.16	7.65E-06	16.5	7.33E-06	6.543	7.84E-07	6.582	1.35E-06
20	3.82E-05	39.96	2.16E-05	16.26	7.55E-06	16.6	7.23E-06	6.582	7.64E-07	6.621	1.33E-06
20	3.80E-05	40.2	2.14E-05	16.36	7.45E-06	16.6	7.16E-06	6.621	7.43E-07	6.66	1.30E-06
20.7	3.72E-05	41.6	2.07E-05	16.94	6.88E-06	17.2	6.66E-06	6.855	6.33E-07	6.894	1.18E-06
20.9	3.72E-05	41.84	2.06E-05	17.04	6.78E-06	17.3	6.58E-06	6.894	6.16E-07	6.933	1.16E-06
21	3.69E-05	42.07	2.05E-05	17.14	6.69E-06	17.4	6.50E-06	6.933	6.00E-07	6.972	1.15E-06
21.2	3.69E-05	42.3	2.03E-05	17.24	6.60E-06	17.5	6.42E-06	6.972	5.84E-07	7.011	1.12E-06
21.2	3.67E-05	42.54	2.02E-05	17.33	6.52E-06	17.6	6.35E-06	7.011	5.69E-07	7.05	1.11E-06
27	3.09E-05	54.02	1.53E-05	22.12	3.38E-06	22.4	3.69E-06	8.925	1.53E-07	8.964	6.05E-07
27.1	3.07E-05	54.26	1.52E-05	22.22	3.34E-06	22.5	3.64E-06	8.964	1.49E-07	9.003	6.05E-07
27.7	3.02E-05	55.43	1.48E-05	22.7	3.12E-06	23	3.44E-06	9.16	1.30E-07	9.199	5.74E-07
27.8	3.00E-05	55.66	1.48E-05	22.8	3.08E-06	23.1	3.41E-06	9.199	1.27E-07	9.238	5.66E-07
28	3.00E-05	55.9	1.47E-05	22.9	3.04E-06	23.2	3.37E-06	9.238	1.24E-07	9.277	5.70E-07
28	2.98E-05	56.13	1.46E-05	23	3.00E-06	23.3	3.33E-06	9.277	1.20E-07	9.316	5.65E-07
28.2	2.98E-05	56.37	1.45E-05	23.1	2.96E-06	23.4	3.29E-06	9.316	1.17E-07	9.355	5.63E-07
31.3	2.71E-05	62.46	1.26E-05	25.63	2.09E-06	25.9	2.50E-06	10.33	5.84E-08	10.37	4.67E-07
32.2	2.64E-05	64.34	1.21E-05	26.42	1.88E-06	26.7	2.29E-06	10.64	4.71E-08	10.68	4.54E-07
32.7	2.58E-05	65.51	1.18E-05	26.9	1.76E-06	27.2	2.17E-06	10.84	4.12E-08	10.88	4.37E-07
32.9	2.58E-05	65.74	1.17E-05	27	1.73E-06	27.3	2.15E-06	10.88	4.01E-08	10.92	4.50E-07
32.9	2.57E-05	65.98	1.17E-05	27.1	1.71E-06	27.4	2.13E-06	10.92	3.91E-08	10.96	4.46E-07
33.1	2.56E-05	66.21	1.16E-05	27.2	1.69E-06	27.5	2.11E-06	10.96	3.80E-08	11	4.42E-07
33.2	2.55E-05	66.45	1.15E-05	27.29	1.67E-06	27.6	2.09E-06	11	3.70E-08	11.04	4.30E-07
33.9	2.49E-05	67.85	1.12E-05	27.88	1.54E-06	28.2	1.96E-06	11.23	3.15E-08	11.27	4.42E-07
34.6	2.44E-05	69.26	1.09E-05	28.47	1.42E-06	28.8	1.85E-06	11.46	2.69E-08	11.5	4.26E-07
34.8	2.44E-05	69.49	1.08E-05	28.56	1.40E-06	28.9	1.85E-06	11.5	2.62E-08	11.54	4.23E-07
34.8	2.42E-05	69.73	1.07E-05	28.66	1.38E-06	29	1.82E-06	11.54	2.55E-08	11.58	4.22E-07
35	2.42E-05	69.96	1.07E-05	28.76	1.36E-06	29.1	1.80E-06	11.58	2.48E-08	11.62	4.12E-07
36	2.34E-05	72.07	1.02E-05	29.64	1.21E-06	29.9	1.66E-06	11.93	1.95E-08	11.97	4.19E-07
36.2	2.34E-05	72.31	1.02E-05	29.74	1.19E-06	30	1.64E-06	11.97	1.90E-08	12.01	4.04E-07
36.2	2.32E-05	72.54	1.01E-05	29.83	1.18E-06	30.1	1.61E-06	12.01	1.85E-08	12.05	4.10E-07
36.4	2.32E-05	72.77	1.01E-05	29.93	1.16E-06	30.2	1.60E-06	12.05	1.80E-08	12.09	4.15E-07
36.9	2.29E-05	73.71	9.85E-06	30.32	1.10E-06	30.6	1.53E-06	12.21	1.62E-08	12.25	4.08E-07
36.9	2.27E-05	73.95	9.81E-06	30.42	1.09E-06	30.7	1.50E-06	12.25	1.57E-08	12.29	3.95E-07
37.8	2.22E-05	75.59	9.47E-06	31.1	9.89E-07	31.4	1.39E-06	12.52	1.30E-08	12.56	4.01E-07
37.9	2.21E-05	75.82	9.43E-06	31.2	9.76E-07	31.5	1.38E-06	12.56	1.27E-08	12.6	3.94E-07
38.1	2.21E-05	76.06	9.37E-06	31.3	9.63E-07	31.6	1.36E-06	12.6	1.24E-08	12.64	3.97E-07
38.6	2.16E-05	77.23	9.15E-06	31.79	9.01E-07	32.1	1.31E-06	12.79	1.08E-08	12.83	3.93E-07
38.8	2.16E-05	77.46	9.09E-06	31.88	8.89E-07	32.2	1.3E-06	12.83	1.05E-08	12.87	3.95E-07
38.8	2.15E-05	77.7	9.05E-06	31.98	8.77E-07	32.3	1.29E-06	12.87	1.02E-08	12.91	3.91E-07

39	2.14E-05	77.93	9.00E-06	32.08	8.66E-07	32.4	1.27E-06	12.91	9.97E-09	12.95	3.82E-07
39	2.13E-05	78.16	8.95E-06	32.18	8.54E-07	32.5	1.27E-06	12.95	9.70E-09	12.99	3.79E-07
39.9	2.08E-05	79.81	8.66E-06	32.86	7.78E-07	33.2	1.20E-06	13.22	8.05E-09	13.26	3.84E-07
40	2.07E-05	80.04	8.62E-06	32.96	7.68E-07	33.3	1.18E-06	13.26	7.84E-09	13.3	3.81E-07
40.2	2.07E-05	80.27	8.58E-06	33.06	7.57E-07	33.3	1.17E-06	13.3	7.63E-09	13.34	3.87E-07
43.2	1.88E-05	86.6	7.52E-06	35.69	5.28E-07	36	9.03E-07	14.36	3.70E-09	14.39	3.59E-07
45.1	1.78E-05	90.12	6.97E-06	37.16	4.32E-07	37.5	8.11E-07	14.94	2.48E-09	14.98	3.68E-07
45.1	1.77E-05	90.35	6.94E-06	37.25	4.26E-07	37.5	8.11E-07	14.98	2.41E-09	15.02	3.65E-07
45.8	1.73E-05	91.76	6.73E-06	37.84	3.93E-07	38.1	7.75E-07	15.21	2.05E-09	15.25	3.65E-07
46	1.73E-05	91.99	6.70E-06	37.94	3.88E-07	38.2	7.58E-07	15.25	2.00E-09	15.29	3.62E-07
46.1	1.72E-05	92.23	6.66E-06	38.04	3.83E-07	38.3	7.57E-07	15.29	1.95E-09	15.33	3.65E-07
46.3	1.72E-05	92.46	6.65E-06	38.13	3.78E-07	38.4	7.52E-07	15.33	1.90E-09	15.37	3.56E-07
47	1.67E-05	94.1	6.42E-06	38.82	3.44E-07	39.1	7.15E-07	15.61	1.57E-09	15.64	3.56E-07
47.2	1.67E-05	94.34	6.39E-06	38.91	3.40E-07	39.2	7.11E-07	15.64	1.53E-09	15.68	3.49E-07
48.1	1.62E-05	96.21	6.18E-06	39.7	3.05E-07	40	6.63E-07	15.96	1.24E-09	16	3.58E-07
49.5	1.56E-05	99.02	5.82E-06	40.87	2.60E-07	41.2	6.15E-07	16.43	8.95E-10	16.46	3.47E-07
49.6	1.55E-05	99.26	5.79E-06	40.97	2.56E-07	41.3	6.13E-07	16.46	8.72E-10	16.5	3.46E-07
49.8	1.55E-05	99.49	5.77E-06	41.06	2.53E-07	41.4	6.10E-07	16.5	8.49E-10	16.54	3.41E-07
49.8	1.54E-05	99.73	5.75E-06	41.16	2.50E-07	41.5	5.99E-07	16.54	8.26E-10	16.58	3.53E-07
50	1.53E-05	99.96	5.72E-06	41.26	2.46E-07	41.6	5.90E-07	16.58	8.05E-10	16.62	3.41E-07
50	1.53E-05	100.2	5.69E-06	41.36	2.43E-07	41.6	5.90E-07	16.62	7.83E-10	16.66	3.52E-07
50.2	1.52E-05	100.4	5.67E-06	41.45	2.40E-07	41.7	5.93E-07	16.66	7.63E-10	16.7	3.51E-07
50.3	1.51E-05	100.7	5.65E-06	41.55	2.37E-07	41.8	5.85E-07	16.7	7.42E-10	16.74	3.52E-07
51	1.48E-05	102.1	5.49E-06	42.14	2.18E-07	42.4	5.65E-07	16.93	6.32E-10	16.97	3.49E-07
54	1.36E-05	107.9	4.89E-06	44.58	1.56E-07	44.9	4.83E-07	17.91	3.24E-10	17.95	3.30E-07
54.9	1.32E-05	109.8	4.72E-06	45.36	1.41E-07	45.7	4.68E-07	18.22	2.61E-10	18.26	3.40E-07
55	1.31E-05	110	4.70E-06	45.46	1.39E-07	45.8	4.67E-07	18.26	2.54E-10	18.3	3.33E-07
55.2	1.31E-05	110.3	4.69E-06	45.56	1.37E-07	45.8	4.57E-07	18.3	2.48E-10	18.34	3.42E-07
55.2	1.30E-05	110.5	4.66E-06	45.65	1.35E-07	45.9	4.58E-07	18.34	2.41E-10	18.38	3.34E-07
56.1	1.27E-05	112.2	4.51E-06	46.34	1.23E-07	46.6	4.33E-07	18.61	2.00E-10	18.65	3.39E-07
56.8	1.24E-05	113.8	4.37E-06	47.02	1.12E-07	47.3	4.27E-07	18.89	1.66E-10	18.93	3.30E-07
57	1.24E-05	114	4.35E-06	47.12	1.10E-07	47.4	4.31E-07	18.93	1.61E-10	18.96	3.31E-07
57.1	1.23E-05	114.3	4.33E-06	47.22	1.09E-07	47.5	4.19E-07	18.96	1.57E-10	19	3.30E-07
57.3	1.23E-05	114.5	4.32E-06	47.31	1.08E-07	47.6	4.24E-07	19	1.53E-10	19.04	3.38E-07
57.3	1.22E-05	114.7	4.3E-06	47.41	1.06E-07	47.7	4.23E-07	19.04	1.49E-10	19.08	3.28E-07
58	1.20E-05	115.9	4.21E-06	47.9	9.93E-08	48.2	4.07E-07	19.24	1.30E-10	19.28	3.30E-07
58	1.20E-05	116.1	4.19E-06	48	9.79E-08	48.3	4.10E-07	19.28	1.27E-10	19.32	3.26E-07
58.9	1.16E-05	118	4.04E-06	48.78	8.80E-08	49.1	3.98E-07	19.59	1.02E-10	19.63	3.28E-07
59.1	1.16E-05	118.2	4.03E-06	48.88	8.68E-08	49.2	3.98E-07	19.63	9.97E-11	19.67	3.26E-07
59.8	1.14E-05	119.7	3.92E-06	49.46	8.01E-08	49.8	3.69E-07	19.86	8.49E-11	19.9	3.18E-07
59.9	1.13E-05	119.9	3.90E-06	49.56	7.91E-08	49.9	3.73E-07	19.9	8.26E-11	19.94	3.21E-07

Table 1.2 Amaranth -hypochlorite intermediate and product formation-compiled data.

TIME	AM-	I7	P1	P2	P3
0.41	5.28E-05	2.76E-07	1.72E-05	1.70E-05	1.70E-05
0.49	5.00E-05	1.64E-07	2.00E-05	1.98E-05	1.98E-05
0.53	4.87E-05	1.36E-07	2.13E-05	2.12E-05	2.12E-05
0.57	4.74E-05	1.16E-07	2.26E-05	2.25E-05	2.25E-05
0.61	4.61E-05	1.01E-07	2.39E-05	2.38E-05	2.38E-05
0.64	4.49E-05	8.91E-08	2.51E-05	2.50E-05	2.50E-05
0.68	4.37E-05	7.95E-08	2.63E-05	2.62E-05	2.62E-05
0.72	4.26E-05	7.17E-08	2.74E-05	2.74E-05	2.74E-05
0.76	4.14E-05	6.51E-08	2.86E-05	2.85E-05	2.85E-05
0.8	4.03E-05	5.95E-08	2.97E-05	2.96E-05	2.96E-05
0.84	3.93E-05	5.47E-08	3.07E-05	3.07E-05	3.07E-05
0.88	3.82E-05	5.05E-08	3.18E-05	3.17E-05	3.17E-05
0.92	3.72E-05	4.68E-08	3.28E-05	3.27E-05	3.27E-05
0.96	3.62E-05	4.36E-08	3.38E-05	3.37E-05	3.37E-05
1	3.53E-05	4.07E-08	3.47E-05	3.47E-05	3.47E-05
1.03	3.44E-05	3.81E-08	3.56E-05	3.56E-05	3.56E-05
1.07	3.34E-05	3.57E-08	3.66E-05	3.65E-05	3.65E-05
1.11	3.26E-05	3.36E-08	3.74E-05	3.74E-05	3.74E-05
1.15	3.17E-05	3.17E-08	3.83E-05	3.83E-05	3.83E-05
1.19	3.09E-05	2.99E-08	3.91E-05	3.91E-05	3.91E-05
1.23	3.01E-05	2.83E-08	3.99E-05	3.99E-05	3.99E-05
1.27	2.93E-05	2.68E-08	4.07E-05	4.07E-05	4.07E-05
1.86	1.96E-05	1.35E-08	5.04E-05	5.04E-05	5.04E-05
1.89	1.91E-05	1.30E-08	5.09E-05	5.09E-05	5.09E-05
1.93	1.86E-05	1.25E-08	5.14E-05	5.14E-05	5.14E-05
1.97	1.81E-05	1.20E-08	5.19E-05	5.19E-05	5.19E-05
2.01	1.76E-05	1.16E-08	5.24E-05	5.24E-05	5.24E-05
2.05	1.71E-05	1.11E-08	5.29E-05	5.28E-05	5.28E-05
2.09	1.67E-05	1.07E-08	5.33E-05	5.33E-05	5.33E-05
2.13	1.63E-05	1.03E-08	5.37E-05	5.37E-05	5.37E-05
2.48	1.28E-05	7.52E-09	5.72E-05	5.72E-05	5.72E-05
2.52	1.24E-05	7.27E-09	5.76E-05	5.75E-05	5.75E-05
2.56	1.21E-05	7.03E-09	5.79E-05	5.79E-05	5.79E-05
2.6	1.18E-05	6.80E-09	5.82E-05	5.82E-05	5.82E-05
2.64	1.15E-05	6.58E-09	5.85E-05	5.85E-05	5.85E-05
2.68	1.12E-05	6.36E-09	5.88E-05	5.88E-05	5.88E-05
2.71	1.09E-05	6.16E-09	5.91E-05	5.91E-05	5.91E-05
2.75	1.06E-05	5.96E-09	5.94E-05	5.94E-05	5.94E-05
2.79	1.03E-05	5.77E-09	5.97E-05	5.97E-05	5.97E-05
2.83	1.01E-05	5.59E-09	5.99E-05	5.99E-05	5.99E-05
2.87	9.79E-06	5.41E-09	6.02E-05	6.02E-05	6.02E-05
3.03	8.80E-06	4.77E-09	6.12E-05	6.12E-05	6.12E-05
3.07	8.57E-06	4.62E-09	6.14E-05	6.14E-05	6.14E-05
3.11	8.35E-06	4.48E-09	6.17E-05	6.16E-05	6.16E-05
3.14	8.13E-06	4.34E-09	6.19E-05	6.19E-05	6.19E-05
3.18	7.91E-06	4.21E-09	6.21E-05	6.21E-05	6.21E-05
3.22	7.71E-06	4.08E-09	6.23E-05	6.23E-05	6.23E-05
3.26	7.50E-06	3.96E-09	6.25E-05	6.25E-05	6.25E-05
3.3	7.31E-06	3.84E-09	6.27E-05	6.27E-05	6.27E-05
3.53	6.23E-06	3.21E-09	6.38E-05	6.38E-05	6.38E-05
3.57	6.06E-06	3.11E-09	6.39E-05	6.39E-05	6.39E-05
3.61	5.90E-06	3.02E-09	6.41E-05	6.41E-05	6.41E-05
3.65	5.75E-06	2.93E-09	6.43E-05	6.42E-05	6.42E-05
3.69	5.60E-06	2.85E-09	6.44E-05	6.44E-05	6.44E-05
3.73	5.45E-06	2.77E-09	6.45E-05	6.45E-05	6.45E-05
3.77	5.31E-06	2.69E-09	6.47E-05	6.47E-05	6.47E-05
3.81	5.17E-06	2.61E-09	6.48E-05	6.48E-05	6.48E-05
3.85	5.03E-06	2.53E-09	6.50E-05	6.50E-05	6.50E-05
3.89	4.90E-06	2.46E-09	6.51E-05	6.51E-05	6.51E-05
3.93	4.77E-06	2.39E-09	6.52E-05	6.52E-05	6.52E-05
3.96	4.65E-06	2.32E-09	6.54E-05	6.54E-05	6.54E-05
4	4.52E-06	2.26E-09	6.55E-05	6.55E-05	6.55E-05
4.28	3.75E-06	1.85E-09	6.62E-05	6.62E-05	6.62E-05
4.32	3.66E-06	1.80E-09	6.63E-05	6.63E-05	6.63E-05
4.36	3.56E-06	1.75E-09	6.64E-05	6.64E-05	6.64E-05
4.39	3.47E-06	1.70E-09	6.65E-05	6.65E-05	6.65E-05
4.43	3.38E-06	1.65E-09	6.66E-05	6.66E-05	6.66E-05
4.47	3.29E-06	1.60E-09	6.67E-05	6.67E-05	6.67E-05
4.51	3.20E-06	1.56E-09	6.68E-05	6.68E-05	6.68E-05
4.86	2.52E-06	1.21E-09	6.75E-05	6.75E-05	6.75E-05
4.9	2.45E-06	1.18E-09	6.75E-05	6.75E-05	6.75E-05
4.94	2.39E-06	1.15E-09	6.76E-05	6.76E-05	6.76E-05
4.98	2.33E-06	1.12E-09	6.77E-05	6.77E-05	6.77E-05
5.02	2.26E-06	1.08E-09	6.77E-05	6.77E-05	6.77E-05
5.06	2.21E-06	1.06E-09	6.78E-05	6.78E-05	6.78E-05
5.1	2.15E-06	1.03E-09	6.79E-05	6.79E-05	6.79E-05
5.14	2.09E-06	9.98E-10	6.79E-05	6.79E-05	6.79E-05

5.18	2.04E-06	9.71E-10	6.80E-05	6.80E-05	6.80E-05
5.21	1.98E-06	9.45E-10	6.80E-05	6.80E-05	6.80E-05
5.61	1.52E-06	7.18E-10	6.85E-05	6.85E-05	6.85E-05
5.64	1.48E-06	6.99E-10	6.85E-05	6.85E-05	6.85E-05
5.68	1.44E-06	6.80E-10	6.86E-05	6.86E-05	6.86E-05
5.72	1.40E-06	6.62E-10	6.86E-05	6.86E-05	6.86E-05
5.76	1.37E-06	6.44E-10	6.86E-05	6.86E-05	6.86E-05
5.88	1.26E-06	5.94E-10	6.87E-05	6.87E-05	6.87E-05
5.92	1.23E-06	5.78E-10	6.88E-05	6.88E-05	6.88E-05
5.96	1.20E-06	5.62E-10	6.88E-05	6.88E-05	6.88E-05
6	1.16E-06	5.47E-10	6.88E-05	6.88E-05	6.88E-05
6.03	1.13E-06	5.32E-10	6.89E-05	6.89E-05	6.89E-05
6.07	1.10E-06	5.18E-10	6.89E-05	6.89E-05	6.89E-05
6.11	1.08E-06	5.04E-10	6.89E-05	6.89E-05	6.89E-05
6.82	6.66E-07	3.10E-10	6.93E-05	6.93E-05	6.93E-05
6.86	6.49E-07	3.02E-10	6.94E-05	6.94E-05	6.94E-05
6.89	6.32E-07	2.94E-10	6.94E-05	6.94E-05	6.94E-05
6.93	6.15E-07	2.86E-10	6.94E-05	6.94E-05	6.94E-05
6.97	5.99E-07	2.79E-10	6.94E-05	6.94E-05	6.94E-05
7.01	5.83E-07	2.71E-10	6.94E-05	6.94E-05	6.94E-05
7.05	5.68E-07	2.64E-10	6.94E-05	6.94E-05	6.94E-05
7.44	4.35E-07	2.02E-10	6.96E-05	6.96E-05	6.96E-05
7.52	4.13E-07	1.91E-10	6.96E-05	6.96E-05	6.96E-05
7.87	3.25E-07	1.50E-10	6.97E-05	6.97E-05	6.97E-05
7.91	3.16E-07	1.46E-10	6.97E-05	6.97E-05	6.97E-05
7.95	3.08E-07	1.43E-10	6.97E-05	6.97E-05	6.97E-05
7.99	3.00E-07	1.39E-10	6.97E-05	6.97E-05	6.97E-05
8.03	2.92E-07	1.35E-10	6.97E-05	6.97E-05	6.97E-05
8.07	2.84E-07	1.32E-10	6.97E-05	6.97E-05	6.97E-05
8.11	2.77E-07	1.28E-10	6.97E-05	6.97E-05	6.97E-05
8.77	1.76E-07	8.14E-11	6.98E-05	6.98E-05	6.98E-05
9.08	1.42E-07	6.57E-11	6.99E-05	6.99E-05	6.99E-05
9.12	1.39E-07	6.40E-11	6.99E-05	6.99E-05	6.99E-05
9.71	9.31E-08	4.29E-11	6.99E-05	6.99E-05	6.99E-05
9.75	9.06E-08	4.18E-11	6.99E-05	6.99E-05	6.99E-05
9.78	8.82E-08	4.07E-11	6.99E-05	6.99E-05	6.99E-05
9.82	8.59E-08	3.96E-11	6.99E-05	6.99E-05	6.99E-05
9.86	8.37E-08	3.86E-11	6.99E-05	6.99E-05	6.99E-05
9.9	8.15E-08	3.76E-11	6.99E-05	6.99E-05	6.99E-05
9.94	7.93E-08	3.66E-11	6.99E-05	6.99E-05	6.99E-05
9.98	7.72E-08	3.56E-11	6.99E-05	6.99E-05	6.99E-05

10	7.52E-08	3.47E-11	6.99E-05	6.99E-05	6.99E-05
10.7	4.66E-08	2.15E-11	7.00E-05	7.00E-05	7.00E-05
13.3	8.06E-09	3.71E-12	7.00E-05	7.00E-05	7.00E-05
13.3	7.84E-09	3.61E-12	7.00E-05	7.00E-05	7.00E-05
14.1	4.73E-09	2.18E-12	7.00E-05	7.00E-05	7.00E-05
14.1	4.61E-09	2.12E-12	7.00E-05	7.00E-05	7.00E-05
14.2	4.49E-09	2.07E-12	7.00E-05	7.00E-05	7.00E-05
14.2	4.37E-09	2.01E-12	7.00E-05	7.00E-05	7.00E-05
14.2	4.25E-09	1.96E-12	7.00E-05	7.00E-05	7.00E-05
15	2.57E-09	1.18E-12	7.00E-05	7.00E-05	7.00E-05
15	2.50E-09	1.15E-12	7.00E-05	7.00E-05	7.00E-05
15.1	2.43E-09	1.12E-12	7.00E-05	7.00E-05	7.00E-05
15.3	2.02E-09	9.31E-13	7.00E-05	7.00E-05	7.00E-05
15.4	1.97E-09	9.06E-13	7.00E-05	7.00E-05	7.00E-05
15.4	1.92E-09	8.83E-13	7.00E-05	7.00E-05	7.00E-05
15.5	1.82E-09	8.36E-13	7.00E-05	7.00E-05	7.00E-05
15.5	1.77E-09	8.14E-13	7.00E-05	7.00E-05	7.00E-05
15.6	1.72E-09	7.93E-13	7.00E-05	7.00E-05	7.00E-05
15.6	1.68E-09	7.72E-13	7.00E-05	7.00E-05	7.00E-05
15.6	1.63E-09	7.52E-13	7.00E-05	7.00E-05	7.00E-05
15.7	1.59E-09	7.32E-13	7.00E-05	7.00E-05	7.00E-05
15.7	1.55E-09	7.13E-13	7.00E-05	7.00E-05	7.00E-05
15.8	1.51E-09	6.95E-13	7.00E-05	7.00E-05	7.00E-05
15.8	1.47E-09	6.76E-13	7.00E-05	7.00E-05	7.00E-05
16	1.29E-09	5.92E-13	7.00E-05	7.00E-05	7.00E-05
16	1.25E-09	5.77E-13	7.00E-05	7.00E-05	7.00E-05
16.1	1.22E-09	5.61E-13	7.00E-05	7.00E-05	7.00E-05
16.1	1.19E-09	5.47E-13	7.00E-05	7.00E-05	7.00E-05
16.2	1.16E-09	5.32E-13	7.00E-05	7.00E-05	7.00E-05
16.2	1.13E-09	5.18E-13	7.00E-05	7.00E-05	7.00E-05
16.2	1.10E-09	5.05E-13	7.00E-05	7.00E-05	7.00E-05
16.3	1.07E-09	4.91E-13	7.00E-05	7.00E-05	7.00E-05
17.1	6.11E-10	2.81E-13	7.00E-05	7.00E-05	7.00E-05
18	3.31E-10	1.52E-13	7.00E-05	7.00E-05	7.00E-05
18	3.22E-10	1.48E-13	7.00E-05	7.00E-05	7.00E-05
18.1	3.14E-10	1.45E-13	7.00E-05	7.00E-05	7.00E-05
18.1	2.98E-10	1.37E-13	7.00E-05	7.00E-05	7.00E-05
19.6	1.14E-10	5.26E-14	7.00E-05	7.00E-05	7.00E-05
19.6	1.11E-10	5.13E-14	7.00E-05	7.00E-05	7.00E-05
19.9	8.99E-11	4.14E-14	7.00E-05	7.00E-05	7.00E-05
19.9	8.76E-11	4.03E-14	7.00E-05	7.00E-05	7.00E-05

1.2 Brilliant blue-R oxidation products with hypochlorite.

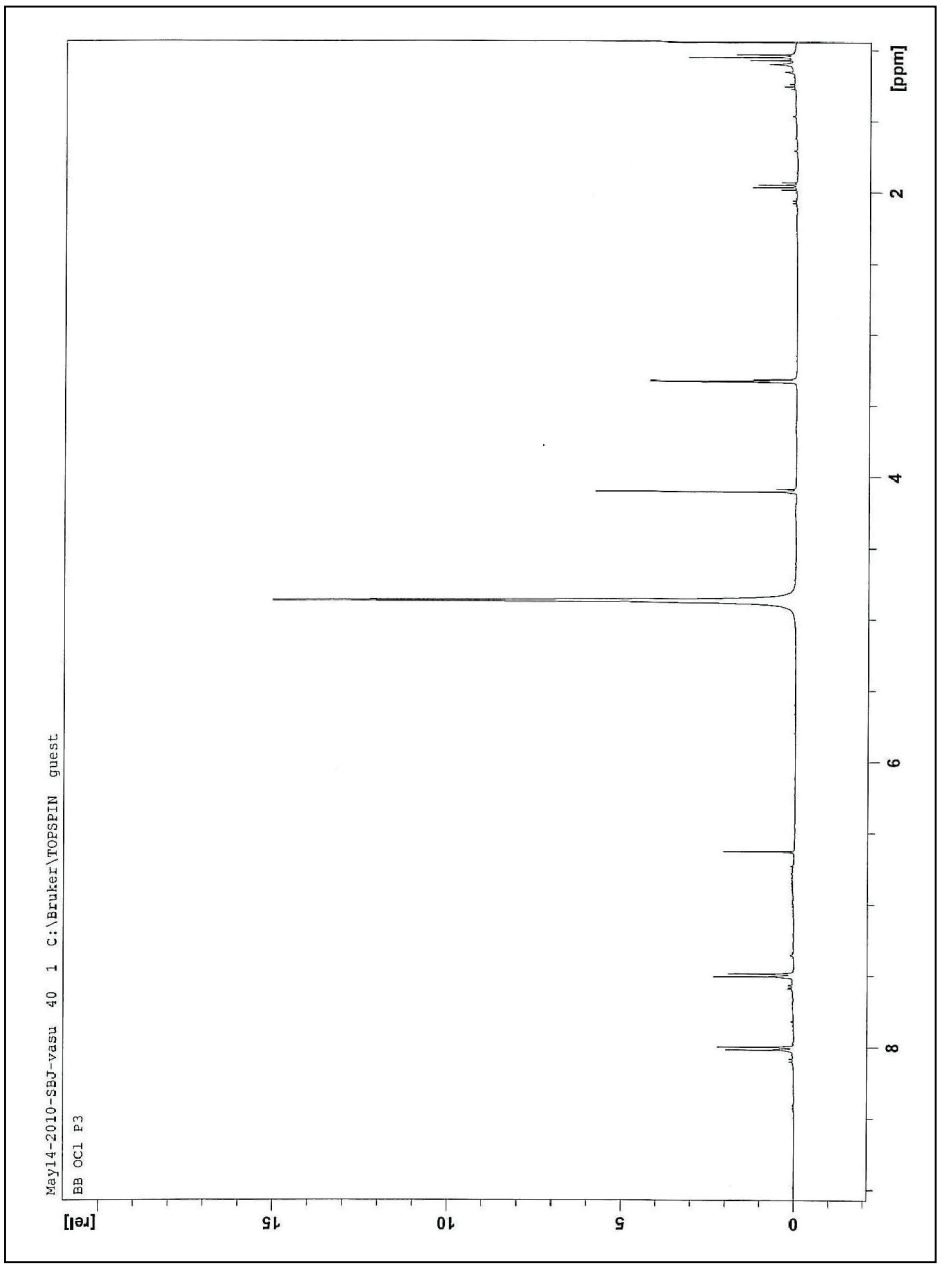

Figure 1.1.5 ^{1}H NMR spectrum for brilliant blue-R major oxidation product P_2 (3- ethyl amino methyl benzene sulphonic acid) with hypochlorite.

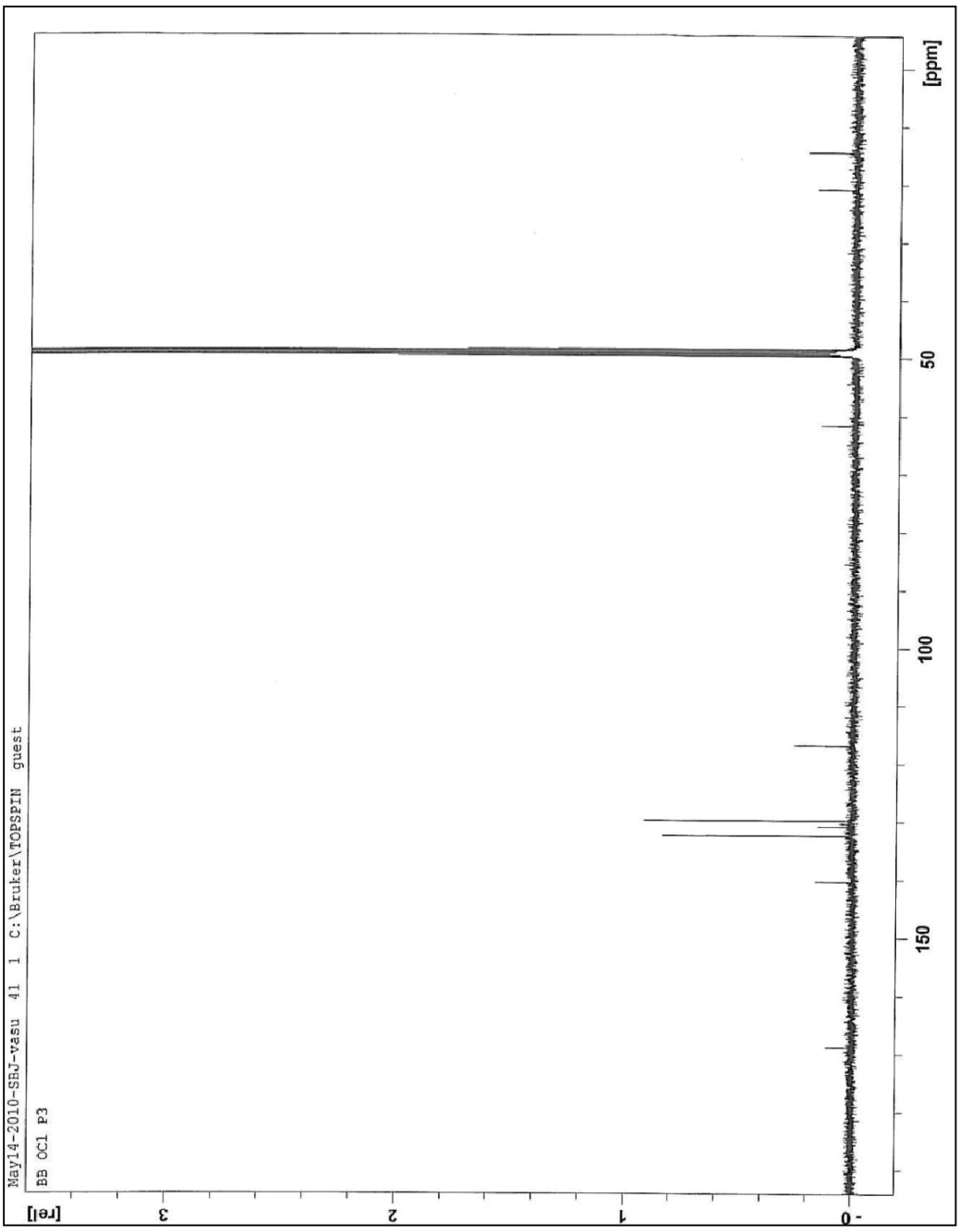

Figure 1.1.6 ^{13}C NMR spectrum for brilliant blue-R major oxidation product P_2 (3- ethyl amino methyl benzene sulphonic acid) with hypochlorite.

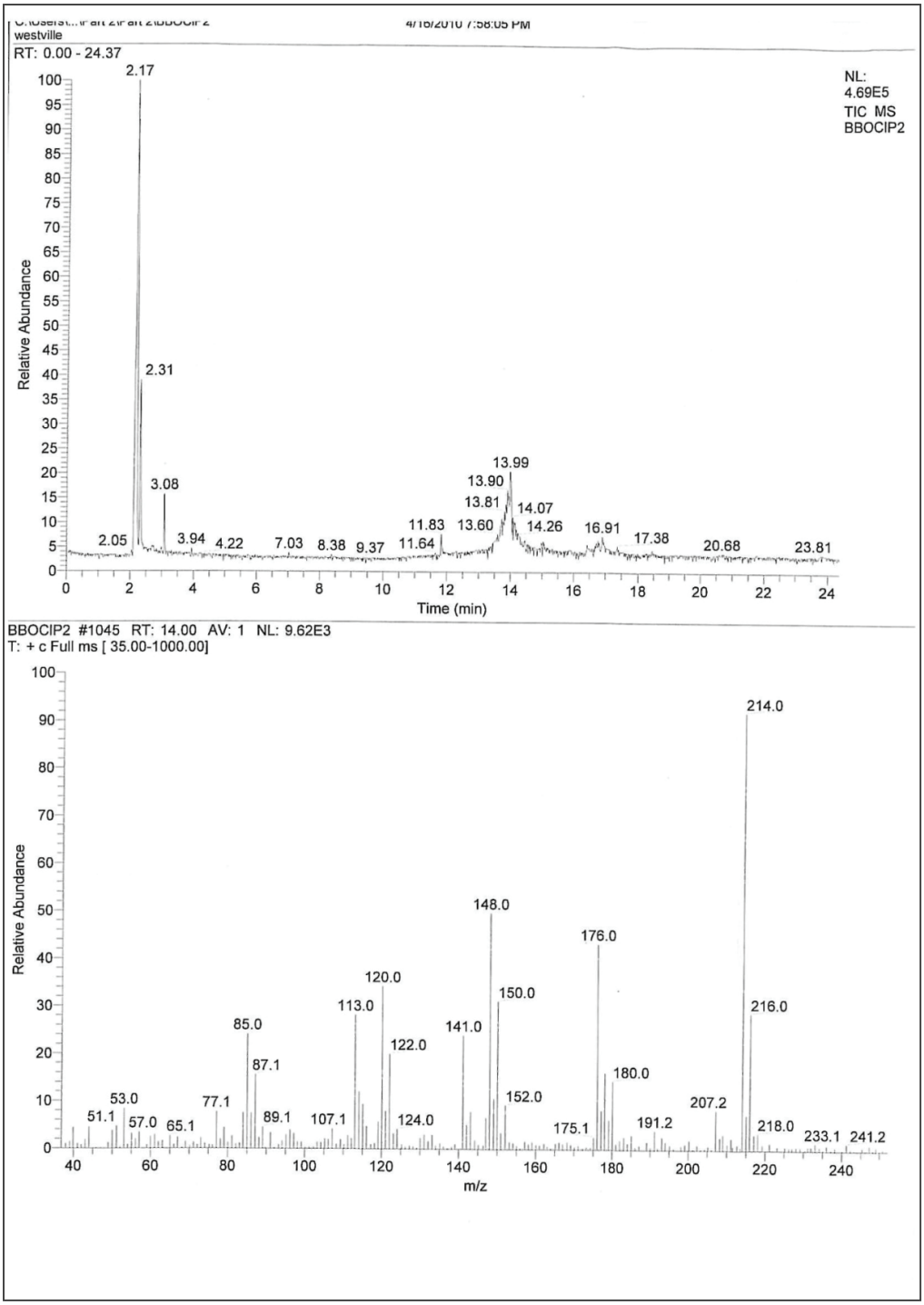

Figure 1.1.7 GC-MS spectrum for brilliant blue-R major oxidation product P_2 (3- ethyl amino methyl benzene sulphonic acid) with hypochlorite.

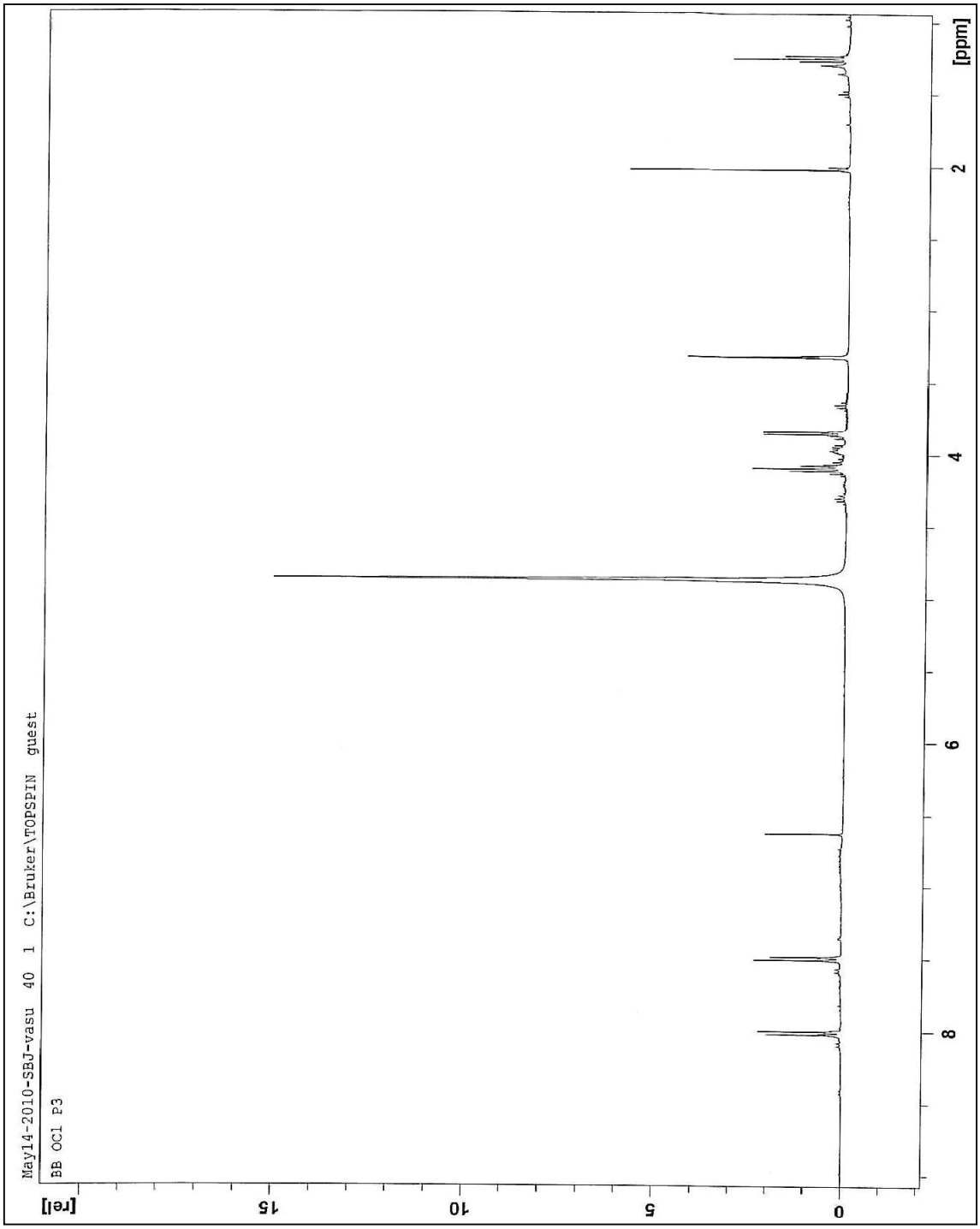

Figure 1.1.8 ^{1}H NMR spectrum for brilliant blue-R major oxidation product P_3 (3- ethyl amino methyl-benzene sulphonic acid) with hypochlorite.

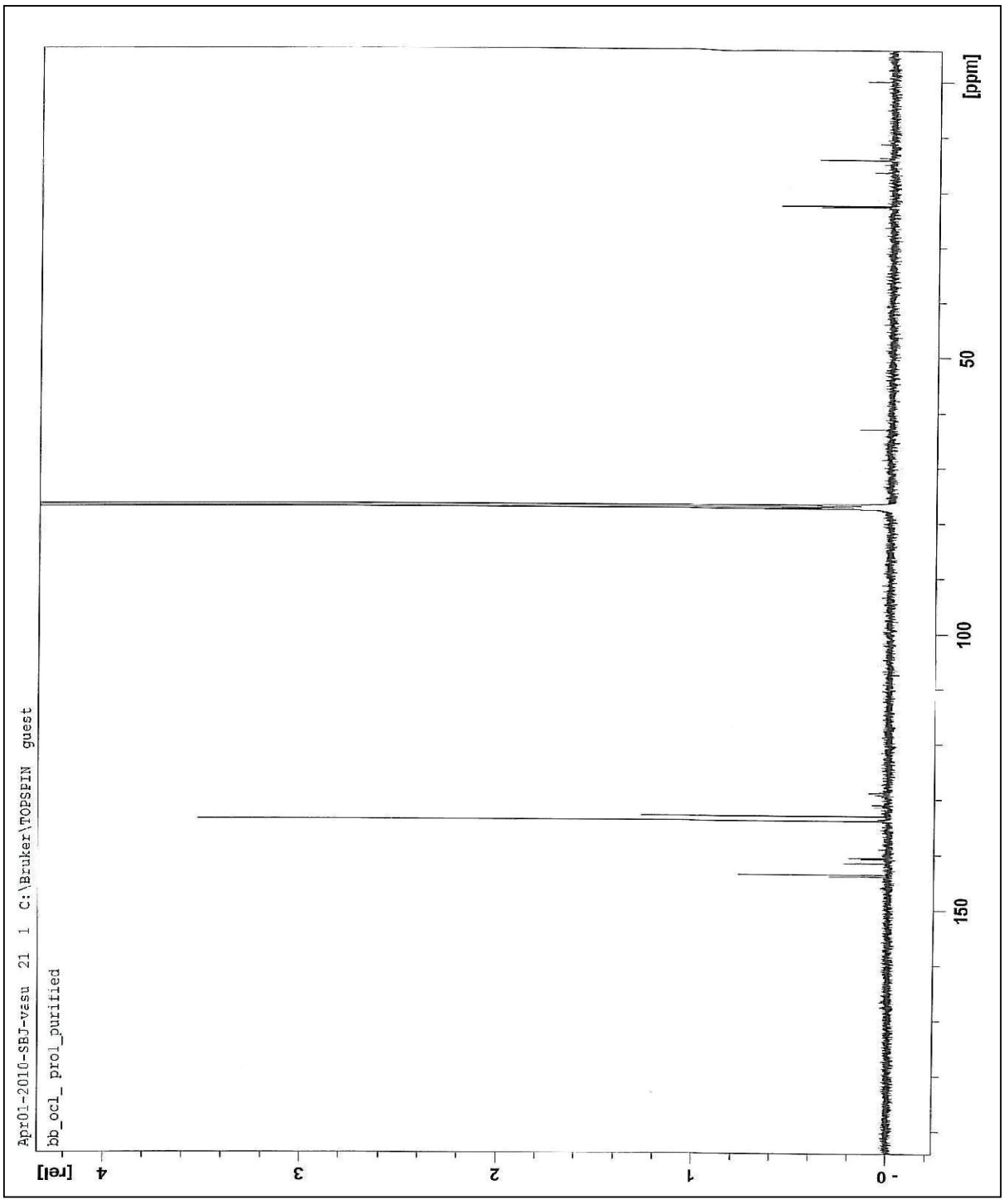

Figure 1.1.9 ^{13}C NMR spectrum for brilliant blue-R major oxidation product P_3 (3-ethyl amino methyl-benzene sulphonic acid) with hypochlorite.

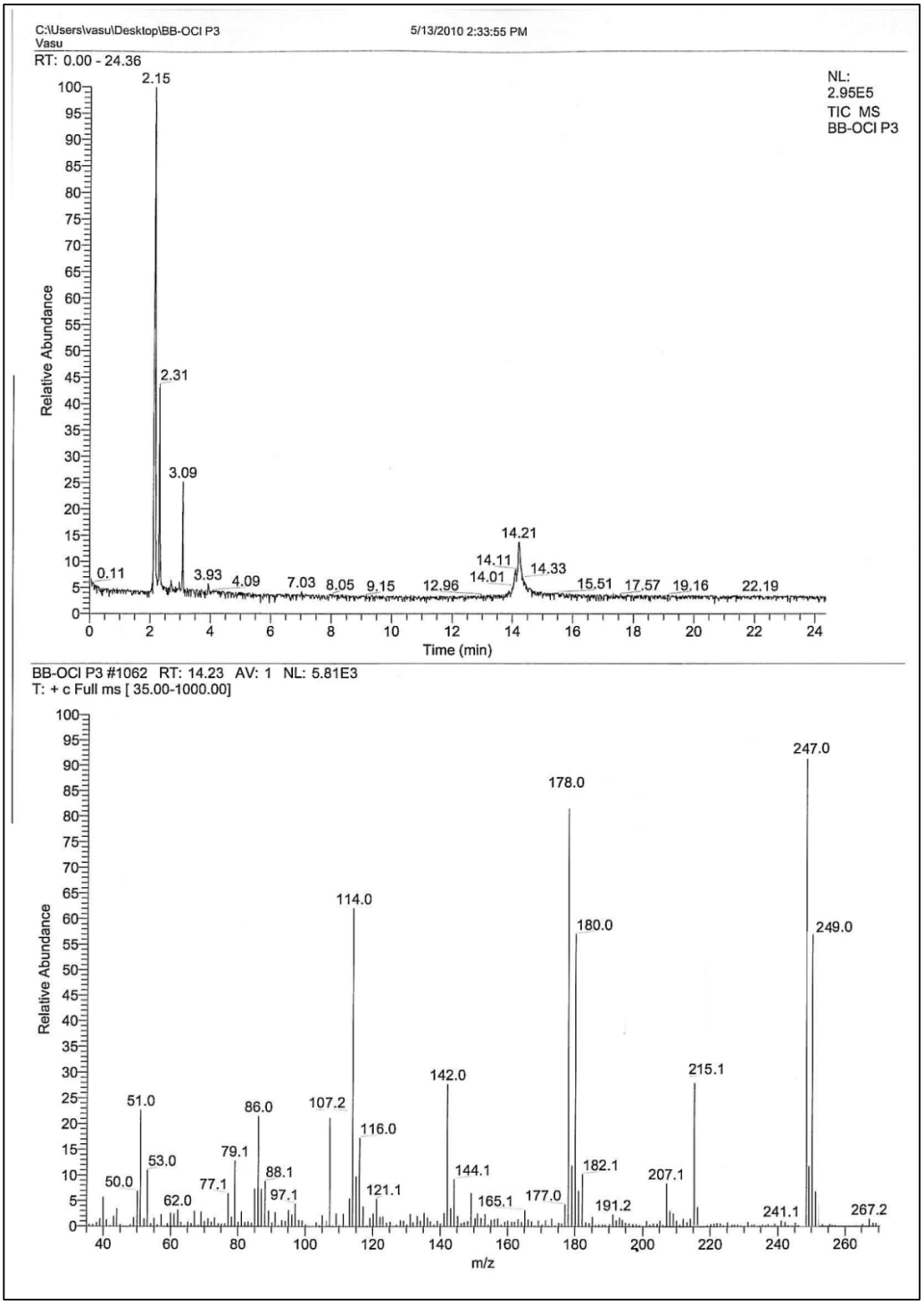

Figure 1.1.10 GC-MS spectrum for brilliant blue-R major oxidation product P_3 (3-ethyl amino methyl benzene sulphonic acid) with hypochlorite.

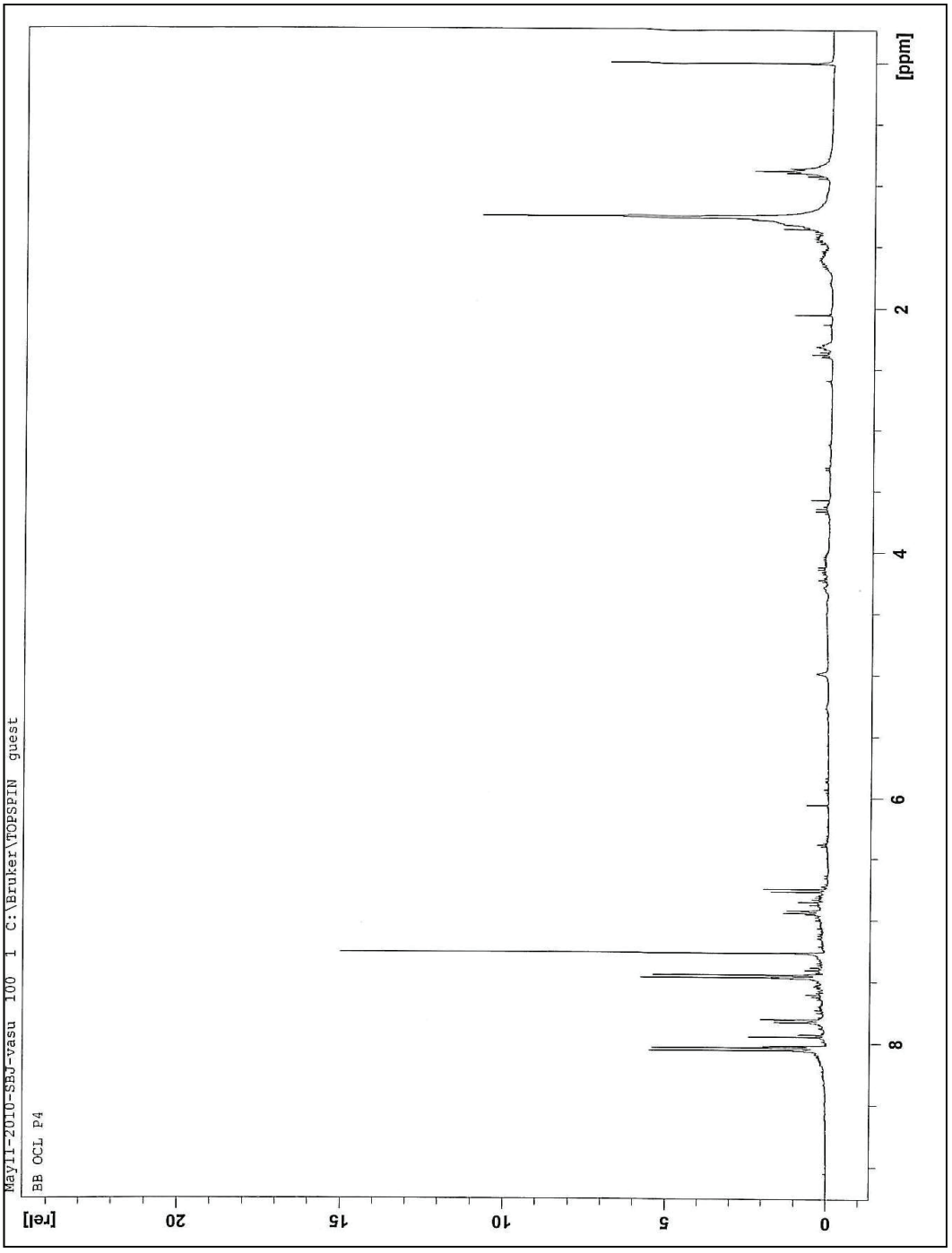

Figure 1.1.11 ^{1}H NMR spectrum of brilliant blue-R major oxidation product P_4 (4-[bis-(4-hydroxy-phenyl)-methylene]-cyclohexa-2,5-hydroxide) with hypochlorite.

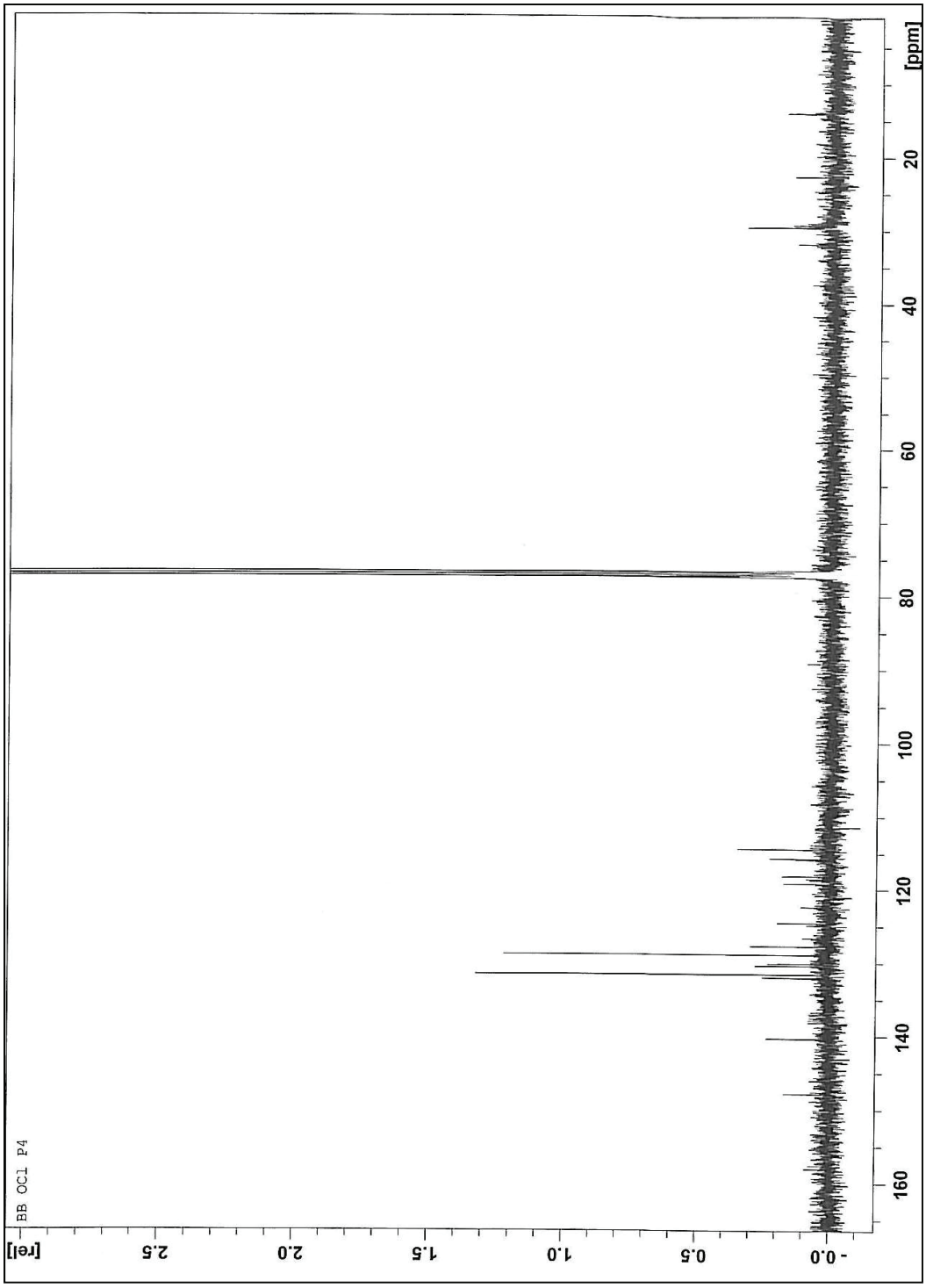

Figure 1.1.12 ^{13}C NMR spectrum of brilliant blue-R major oxidation product P_4 (4-[bis-(4-hydroxy-phenyl)-methylene]-cyclohexa-2,5-hydroxide) with hypochlorite.

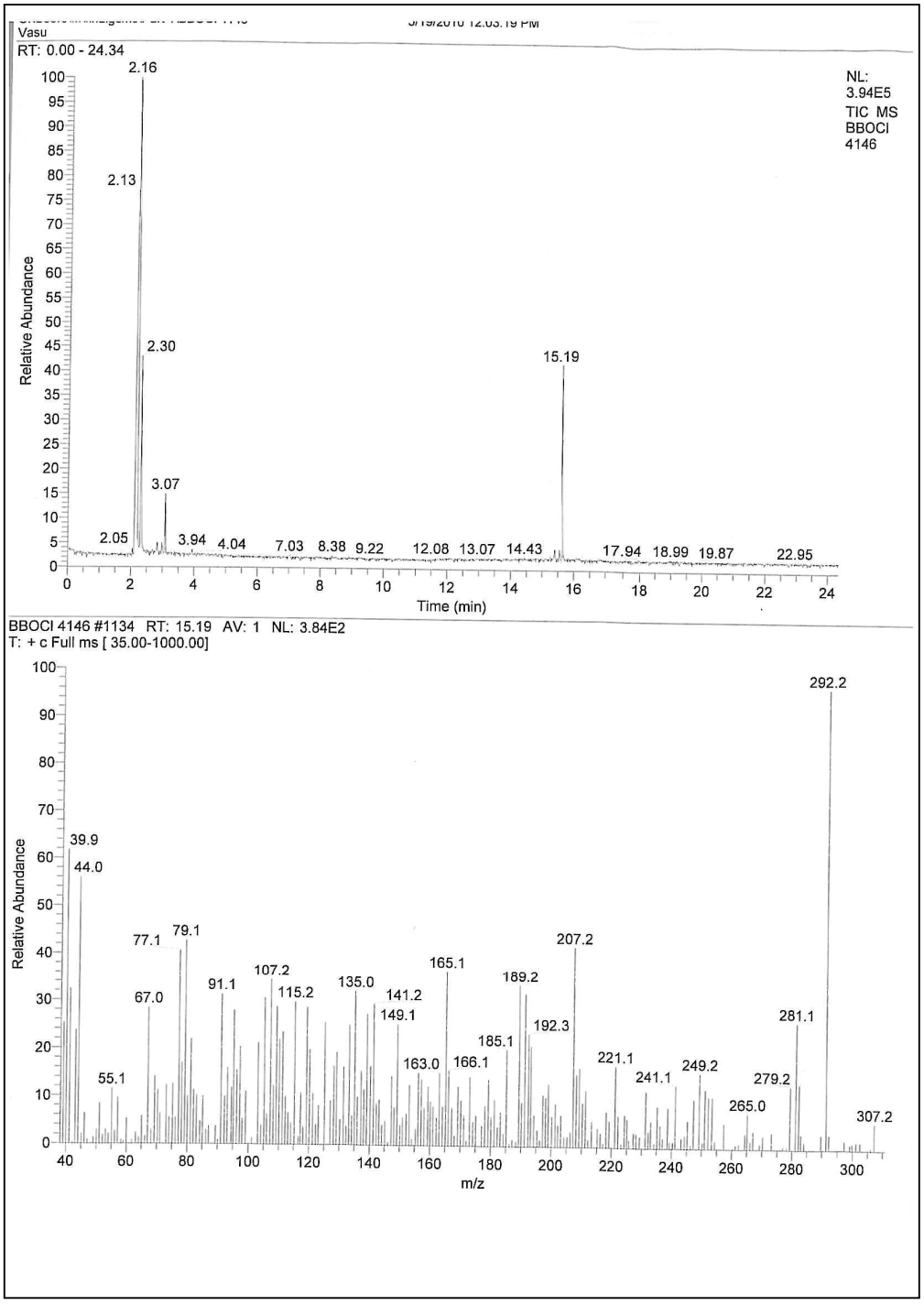

Figure 1.1.13 GC-MS spectrum of brilliant blue-R major oxidation product P_4 (4-[bis-(4-hydroxy-phenyl)-methylene]-cyclohexa-2,5-hydroxide) with hypochlorite.

Table 1.3 Brilliant Blue - hypochlorite experimental and simulated curves-compiled data .

Time	E1	S1	Time	E2	S2	Time	E3	S3
0.23193	5.26E-05	5.86E-05	0.11597	4.45E-05	5.58E-05	0.057982	2.71E-05	5.61E-05
0.70068	6.27E-05	5.80E-05	0.35035	6.14E-05	5.44E-05	0.17517	4.83E-05	5.48E-05
1.1694	6.01E-05	5.65E-05	0.58473	6.17E-05	5.31E-05	0.29235	5.67E-05	5.37E-05
1.6382	5.76E-05	5.51E-05	0.8191	6.01E-05	5.2E-05	0.40953	5.84E-05	5.26E-05
2.1069	5.54E-05	5.37E-05	1.0535	5.84E-05	5.09E-05	0.52672	5.76E-05	5.16E-05
2.5757	5.33E-05	5.24E-05	1.2879	5.67E-05	4.98E-05	0.6439	5.62E-05	5.06E-05
3.0444	5.14E-05	5.11E-05	1.5222	5.52E-05	4.89E-05	0.76109	5.47E-05	4.96E-05
3.5132	4.95E-05	4.98E-05	1.7566	5.38E-05	4.79E-05	0.87827	5.32E-05	4.87E-05
3.9819	4.79E-05	4.86E-05	1.991	5.24E-05	4.7E-05	0.99545	5.17E-05	4.77E-05
4.4507	4.62E-05	4.74E-05	2.2254	5.11E-05	4.61E-05	1.1126	5.04E-05	4.68E-05
4.9194	4.47E-05	4.62E-05	2.4598	4.99E-05	4.52E-05	1.2298	4.91E-05	4.59E-05
5.3881	4.33E-05	4.50E-05	2.6941	4.86E-05	4.44E-05	1.347	4.78E-05	4.51E-05
5.8569	4.19E-05	4.39E-05	2.9285	4.75E-05	4.36E-05	1.4642	4.66E-05	4.42E-05
6.3256	4.06E-05	4.28E-05	3.1629	4.64E-05	4.28E-05	1.5814	4.54E-05	4.34E-05
6.7944	3.93E-05	4.18E-05	3.3973	4.53E-05	4.2E-05	1.6986	4.44E-05	4.26E-05
7.2631	3.82E-05	4.08E-05	3.6316	4.43E-05	4.12E-05	1.8157	4.33E-05	4.18E-05
7.7319	3.7E-05	3.98E-05	3.866	4.34E-05	4.05E-05	1.9329	4.23E-05	4.10E-05
8.2006	3.6E-05	3.88E-05	4.1004	4.24E-05	3.97E-05	2.0501	4.13E-05	4.03E-05
8.6694	3.5E-05	3.78E-05	4.3348	4.15E-05	3.9E-05	2.1673	4.04E-05	3.95E-05
14.294	2.55E-05	2.82E-05	7.1473	3.26E-05	3.15E-05	3.5735	3.12E-05	3.19E-05
14.763	2.49E-05	2.75E-05	7.3817	3.19E-05	3.09E-05	3.6907	3.06E-05	3.13E-05
15.232	2.43E-05	2.68E-05	7.6161	3.14E-05	3.04E-05	3.8079	3E-05	3.08E-05
15.701	2.37E-05	2.62E-05	7.8505	3.08E-05	2.98E-05	3.9251	2.94E-05	3.02E-05
16.169	2.32E-05	2.56E-05	8.0848	3.02E-05	2.93E-05	4.0422	2.88E-05	2.97E-05
16.638	2.26E-05	2.50E-05	8.3192	2.96E-05	2.88E-05	4.1594	2.83E-05	2.92E-05
17.107	2.21E-05	2.44E-05	8.5536	2.92E-05	2.83E-05	4.2766	2.77E-05	2.87E-05
17.576	2.16E-05	2.38E-05	8.788	2.86E-05	2.78E-05	4.3938	2.72E-05	2.82E-05
18.044	2.11E-05	2.32E-05	9.0224	2.81E-05	2.73E-05	4.511	2.67E-05	2.77E-05
18.513	2.07E-05	2.27E-05	9.2567	2.76E-05	2.68E-05	4.6282	2.62E-05	2.72E-05
18.982	2.02E-05	2.21E-05	9.4911	2.71E-05	2.64E-05	4.7453	2.57E-05	2.68E-05
19.451	1.98E-05	2.16E-05	9.7255	2.67E-05	2.59E-05	4.8625	2.52E-05	2.63E-05
19.919	1.94E-05	2.11E-05	9.9599	2.62E-05	2.55E-05	4.9797	2.48E-05	2.59E-05
20.388	1.9E-05	2.06E-05	10.194	2.57E-05	2.5E-05	5.0969	2.43E-05	2.55E-05
20.857	1.86E-05	2.01E-05	10.429	2.53E-05	2.46E-05	5.2141	2.39E-05	2.50E-05
21.326	1.82E-05	1.96E-05	10.663	2.49E-05	2.42E-05	5.3313	2.34E-05	2.46E-05
21.794	1.79E-05	1.92E-05	10.897	2.44E-05	2.37E-05	5.4484	2.3E-05	2.42E-05
22.263	1.76E-05	1.87E-05	11.132	2.4E-05	2.33E-05	5.5656	2.26E-05	2.38E-05
22.732	1.72E-05	1.83E-05	11.366	2.36E-05	2.29E-05	5.6828	2.22E-05	2.34E-05

27.888	1.42E-05	1.41E-05	13.944	1.98E-05	1.89E-05	6.9718	1.83E-05	1.95E-05
28.357	1.4E-05	1.37E-05	14.179	1.95E-05	1.86E-05	7.089	1.8E-05	1.92E-05
28.825	1.38E-05	1.34E-05	14.413	1.92E-05	1.83E-05	7.2062	1.77E-05	1.89E-05
29.294	1.35E-05	1.31E-05	14.647	1.89E-05	1.8E-05	7.3234	1.75E-05	1.86E-05
29.763	1.33E-05	1.28E-05	14.882	1.86E-05	1.77E-05	7.4406	1.72E-05	1.83E-05
30.232	1.31E-05	1.25E-05	15.116	1.83E-05	1.74E-05	7.5578	1.69E-05	1.80E-05
30.7	1.3E-05	1.22E-05	15.351	1.81E-05	1.71E-05	7.6749	1.66E-05	1.77E-05
31.169	1.28E-05	1.19E-05	15.585	1.78E-05	1.68E-05	7.7921	1.63E-05	1.74E-05
31.638	1.26E-05	1.16E-05	15.819	1.75E-05	1.65E-05	7.9093	1.61E-05	1.71E-05
32.107	1.24E-05	1.14E-05	16.054	1.73E-05	1.62E-05	8.0265	1.58E-05	1.69E-05
32.575	1.22E-05	1.11E-05	16.288	1.71E-05	1.59E-05	8.1437	1.56E-05	1.66E-05
48.982	7.85E-06	4.90E-06	24.491	1.11E-05	8.77E-06	12.245	9.49E-06	9.59E-06
49.45	7.76E-06	4.78E-06	24.726	1.1E-05	8.62E-06	12.362	9.36E-06	9.44E-06
49.919	7.67E-06	4.67E-06	24.96	1.09E-05	8.48E-06	12.479	9.19E-06	9.30E-06
50.388	7.6E-06	4.57E-06	25.194	1.07E-05	8.33E-06	12.597	9.07E-06	9.16E-06
50.857	7.48E-06	4.46E-06	25.429	1.06E-05	8.19E-06	12.714	8.96E-06	9.02E-06
51.325	7.4E-06	4.36E-06	25.663	1.05E-05	8.05E-06	12.831	8.84E-06	8.88E-06
56.482	6.52E-06	3.38E-06	28.241	9.46E-06	6.69E-06	14.12	7.71E-06	7.52E-06
56.95	6.45E-06	3.30E-06	28.476	9.34E-06	6.58E-06	14.237	7.61E-06	7.40E-06
72.888	4.58E-06	1.50E-06	36.445	6.7E-06	3.71E-06	18.222	5.15E-06	4.45E-06
77.575	4.17E-06	1.19E-06	38.788	6.11E-06	3.14E-06	19.393	4.64E-06	3.84E-06
78.044	4.14E-06	1.17E-06	39.023	6.06E-06	3.08E-06	19.511	4.59E-06	3.79E-06
78.513	4.12E-06	1.14E-06	39.257	6.01E-06	3.03E-06	19.628	4.54E-06	3.73E-06
99.606	2.99E-06	4.04E-07	49.804	4.11E-06	1.43E-06	24.901	3.13E-06	1.93E-06
100.07	2.95E-06	3.95E-07	50.039	4.09E-06	1.4E-06	25.018	3.11E-06	1.90E-06
100.54	2.95E-06	3.86E-07	50.273	4.06E-06	1.38E-06	25.135	3.09E-06	1.88E-06
101.01	2.94E-06	3.77E-07	50.507	4.02E-06	1.36E-06	25.253	3.06E-06	1.85E-06
101.48	2.93E-06	3.68E-07	50.742	3.99E-06	1.34E-06	25.37	3.03E-06	1.82E-06
101.95	2.9E-06	3.60E-07	50.976	3.98E-06	1.31E-06	25.487	3.02E-06	1.80E-06
102.42	2.88E-06	3.52E-07	51.211	3.92E-06	1.29E-06	25.604	2.99E-06	1.77E-06
102.89	2.87E-06	3.44E-07	51.445	3.93E-06	1.27E-06	25.721	2.98E-06	1.74E-06
103.36	2.84E-06	3.36E-07	51.679	3.87E-06	1.25E-06	25.838	2.96E-06	1.72E-06
129.14	2.31E-06	9.46E-08	64.57	2.78E-06	4.99E-07	32.284	2.27E-06	7.75E-07
129.61	2.3E-06	9.24E-08	64.804	2.76E-06	4.91E-07	32.401	2.25E-06	7.64E-07
130.07	2.3E-06	9.04E-08	65.039	2.77E-06	4.83E-07	32.518	2.25E-06	7.53E-07
130.54	2.29E-06	8.83E-08	65.273	2.75E-06	4.75E-07	32.635	2.24E-06	7.42E-07
131.01	2.28E-06	8.63E-08	65.508	2.74E-06	4.67E-07	32.752	2.24E-06	7.32E-07
131.48	2.27E-06	8.43E-08	65.742	2.73E-06	4.59E-07	32.87	2.22E-06	7.21E-07
135.23	2.23E-06	7.01E-08	67.617	2.64E-06	4.02E-07	33.807	2.18E-06	6.43E-07
151.17	2.06E-06	3.21E-08	75.586	2.31E-06	2.28E-07	37.791	1.97E-06	3.94E-07
151.64	2.05E-06	3.13E-08	75.82	2.31E-06	2.24E-07	37.908	1.96E-06	3.88E-07

152.11	2.05E-06	3.06E-08	76.055	2.3E-06	2.2E-07	38.026	1.97E-06	3.83E-07
164.29	1.94E-06	1.68E-08	82.149	2.15E-06	1.43E-07	41.072	1.81E-06	2.63E-07
164.76	1.94E-06	1.64E-08	82.383	2.14E-06	1.41E-07	41.19	1.81E-06	2.60E-07
165.23	1.93E-06	1.61E-08	82.617	2.15E-06	1.38E-07	41.307	1.8E-06	2.56E-07
165.7	1.92E-06	1.57E-08	82.852	2.14E-06	1.36E-07	41.424	1.81E-06	2.52E-07
166.17	1.93E-06	1.53E-08	83.086	2.14E-06	1.34E-07	41.541	1.79E-06	2.49E-07
166.64	1.92E-06	1.50E-08	83.32	2.13E-06	1.32E-07	41.658	1.79E-06	2.45E-07
167.11	1.92E-06	1.47E-08	83.555	2.12E-06	1.29E-07	41.775	1.8E-06	2.41E-07
185.39	1.79E-06	5.97E-09	92.696	1.93E-06	6.75E-08	46.346	1.64E-06	1.38E-07
185.86	1.78E-06	5.83E-09	92.93	1.93E-06	6.64E-08	46.463	1.65E-06	1.36E-07
186.32	1.78E-06	5.70E-09	93.164	1.92E-06	6.53E-08	46.58	1.63E-06	1.34E-07
186.79	1.8E-06	5.57E-09	93.399	1.92E-06	6.42E-08	46.697	1.64E-06	1.32E-07
187.26	1.78E-06	5.45E-09	93.633	1.91E-06	6.32E-08	46.814	1.63E-06	1.30E-07
187.73	1.77E-06	5.32E-09	93.867	1.92E-06	6.21E-08	46.932	1.63E-06	1.28E-07
188.2	1.78E-06	5.20E-09	94.102	1.89E-06	6.11E-08	47.049	1.62E-06	1.26E-07
188.67	1.75E-06	5.08E-09	94.336	1.9E-06	6.01E-08	47.166	1.63E-06	1.25E-07
189.14	1.77E-06	4.97E-09	94.571	1.89E-06	5.91E-08	47.283	1.62E-06	1.23E-07
189.61	1.78E-06	4.85E-09	94.805	1.89E-06	5.81E-08	47.4	1.62E-06	1.21E-07
190.07	1.76E-06	4.74E-09	95.039	1.88E-06	5.72E-08	47.518	1.62E-06	1.19E-07
190.54	1.77E-06	4.64E-09	95.274	1.88E-06	5.62E-08	47.635	1.62E-06	1.18E-07
191.01	1.76E-06	4.53E-09	95.508	1.87E-06	5.53E-08	47.752	1.61E-06	1.16E-07
191.48	1.75E-06	4.43E-09	95.742	1.88E-06	5.44E-08	47.869	1.6E-06	1.14E-07
191.95	1.75E-06	4.33E-09	95.977	1.87E-06	5.35E-08	47.986	1.6E-06	1.13E-07
192.42	1.75E-06	4.23E-09	96.211	1.86E-06	5.26E-08	48.103	1.6E-06	1.11E-07
192.89	1.75E-06	4.13E-09	96.446	1.86E-06	5.17E-08	48.221	1.61E-06	1.10E-07
193.36	1.75E-06	4.04E-09	96.68	1.85E-06	5.09E-08	48.338	1.6E-06	1.08E-07
193.82	1.74E-06	3.95E-09	96.914	1.84E-06	5E-08	48.455	1.59E-06	1.06E-07
194.29	1.74E-06	3.86E-09	97.149	1.85E-06	4.92E-08	48.572	1.6E-06	1.05E-07
194.76	1.74E-06	3.77E-09	97.383	1.85E-06	4.84E-08	48.689	1.58E-06	1.03E-07
195.23	1.73E-06	3.68E-09	97.617	1.82E-06	4.76E-08	48.807	1.57E-06	1.02E-07
195.7	1.74E-06	3.60E-09	97.852	1.85E-06	4.68E-08	48.924	1.59E-06	1.01E-07
196.17	1.73E-06	3.52E-09	98.086	1.83E-06	4.6E-08	49.041	1.59E-06	9.91E-08
196.64	1.73E-06	3.44E-09	98.321	1.82E-06	4.53E-08	49.158	1.57E-06	9.77E-08
197.11	1.72E-06	3.36E-09	98.555	1.82E-06	4.45E-08	49.275	1.58E-06	9.63E-08
197.57	1.72E-06	3.28E-09	98.789	1.83E-06	4.38E-08	49.392	1.57E-06	9.49E-08
236.95	1.54E-06	4.74E-10	118.48	1.58E-06	1.08E-08	59.236	1.36E-06	2.84E-08
238.36	1.55E-06	4.43E-10	119.18	1.57E-06	1.03E-08	59.587	1.35E-06	2.72E-08
238.82	1.55E-06	4.33E-10	119.41	1.57E-06	1.01E-08	59.705	1.35E-06	2.68E-08
239.29	1.56E-06	4.23E-10	119.65	1.57E-06	9.94E-09	59.822	1.35E-06	2.64E-08

Table 1.4 Brilliant blue - hypochlorite intermediate and product formation -compiled data.

TIME	P4	HOCl	P1	BB+	P2	I_1	P3
0.17517	1.70E-05	1.04E-03	3.85E-06	5.61E-05	3.85E-06	4.86E-07	3.37E-06
0.29235	1.98E-05	1.08E-03	5.15E-06	5.48E-05	5.15E-06	3.48E-07	4.80E-06
0.40953	2.12E-05	1.09E-03	6.30E-06	5.37E-05	6.30E-06	3.08E-07	5.99E-06
0.52672	2.25E-05	1.09E-03	7.38E-06	5.26E-05	7.38E-06	2.90E-07	7.09E-06
0.6439	2.38E-05	1.09E-03	8.41E-06	5.16E-05	8.41E-06	2.79E-07	8.13E-06
0.76109	2.50E-05	1.09E-03	9.42E-06	5.06E-05	9.42E-06	2.71E-07	9.15E-06
0.87827	2.62E-05	1.09E-03	1.04E-05	4.96E-05	1.04E-05	2.64E-07	1.01E-05
2.2845	2.74E-05	1.08E-03	2.05E-05	3.95E-05	2.05E-05	2.01E-07	2.03E-05
2.4017	2.85E-05	1.08E-03	2.12E-05	3.88E-05	2.12E-05	1.96E-07	2.10E-05
2.5188	2.96E-05	1.08E-03	2.19E-05	3.81E-05	2.19E-05	1.92E-07	2.17E-05
2.636	3.07E-05	1.08E-03	2.26E-05	3.74E-05	2.26E-05	1.88E-07	2.24E-05
2.7532	3.17E-05	1.08E-03	2.32E-05	3.68E-05	2.32E-05	1.84E-07	2.31E-05
2.8704	3.27E-05	1.08E-03	2.39E-05	3.61E-05	2.39E-05	1.80E-07	2.37E-05
2.9876	3.37E-05	1.08E-03	2.45E-05	3.55E-05	2.45E-05	1.76E-07	2.44E-05
3.1048	3.47E-05	1.07E-03	2.52E-05	3.48E-05	2.52E-05	1.73E-07	2.50E-05
3.2219	3.56E-05	1.07E-03	2.58E-05	3.42E-05	2.58E-05	1.69E-07	2.56E-05
3.3391	3.65E-05	1.07E-03	2.64E-05	3.36E-05	2.64E-05	1.66E-07	2.62E-05
3.4563	3.74E-05	1.07E-03	2.70E-05	3.30E-05	2.70E-05	1.62E-07	2.68E-05
3.5735	3.83E-05	1.07E-03	2.76E-05	3.24E-05	2.76E-05	1.59E-07	2.74E-05
3.6907	3.91E-05	1.07E-03	2.81E-05	3.19E-05	2.81E-05	1.56E-07	2.80E-05
3.8079	3.99E-05	1.07E-03	2.87E-05	3.13E-05	2.87E-05	1.53E-07	2.85E-05
3.9251	4.07E-05	1.07E-03	2.92E-05	3.08E-05	2.92E-05	1.50E-07	2.91E-05
6.1515	5.04E-05	1.06E-03	3.77E-05	2.23E-05	3.77E-05	1.04E-07	3.76E-05
6.6203	5.24E-05	1.06E-03	3.92E-05	2.08E-05	3.92E-05	9.62E-08	3.91E-05
6.7375	5.28E-05	1.06E-03	3.95E-05	2.05E-05	3.95E-05	9.45E-08	3.94E-05
6.8547	5.33E-05	1.06E-03	3.98E-05	2.02E-05	3.98E-05	9.28E-08	3.98E-05
6.9718	5.37E-05	1.06E-03	4.02E-05	1.98E-05	4.02E-05	9.11E-08	4.01E-05
7.089	5.72E-05	1.06E-03	4.05E-05	1.95E-05	4.05E-05	8.95E-08	4.04E-05
7.2062	5.75E-05	1.06E-03	4.08E-05	1.92E-05	4.08E-05	8.79E-08	4.07E-05
7.3234	5.79E-05	1.06E-03	4.11E-05	1.89E-05	4.11E-05	8.63E-08	4.10E-05
7.4406	5.82E-05	1.06E-03	4.14E-05	1.86E-05	4.14E-05	8.48E-08	4.13E-05
7.5578	5.85E-05	1.06E-03	4.17E-05	1.83E-05	4.17E-05	8.33E-08	4.16E-05
7.6749	5.88E-05	1.06E-03	4.20E-05	1.80E-05	4.20E-05	8.18E-08	4.19E-05
7.7921	5.91E-05	1.06E-03	4.23E-05	1.77E-05	4.23E-05	8.04E-08	4.22E-05
7.9093	5.94E-05	1.06E-03	4.26E-05	1.74E-05	4.26E-05	7.90E-08	4.25E-05
8.0265	5.97E-05	1.06E-03	4.29E-05	1.71E-05	4.29E-05	7.76E-08	4.28E-05
8.1437	5.99E-05	1.06E-03	4.31E-05	1.69E-05	4.31E-05	7.62E-08	4.31E-05
8.2609	6.02E-05	1.06E-03	4.34E-05	1.66E-05	4.34E-05	7.49E-08	4.33E-05

8.378	6.12E-05	1.06E-03	4.37E-05	1.63E-05	4.37E-05	7.36E-08	4.36E-05
8.4952	6.14E-05	1.06E-03	4.39E-05	1.61E-05	4.39E-05	7.23E-08	4.39E-05
8.6124	6.16E-05	1.06E-03	4.42E-05	1.58E-05	4.42E-05	7.11E-08	4.41E-05
8.7296	6.19E-05	1.06E-03	4.44E-05	1.56E-05	4.44E-05	6.99E-08	4.44E-05
8.8468	6.21E-05	1.06E-03	4.47E-05	1.53E-05	4.47E-05	6.87E-08	4.46E-05
8.964	6.23E-05	1.06E-03	4.49E-05	1.51E-05	4.49E-05	6.75E-08	4.49E-05
9.0811	6.25E-05	1.05E-03	4.52E-05	1.48E-05	4.52E-05	6.63E-08	4.51E-05
9.1983	6.27E-05	1.05E-03	4.54E-05	1.46E-05	4.54E-05	6.52E-08	4.53E-05
12.831	6.45E-05	1.05E-03	5.10E-05	9.02E-06	5.10E-05	3.90E-08	5.09E-05
12.948	6.47E-05	1.05E-03	5.11E-05	8.88E-06	5.11E-05	3.84E-08	5.11E-05
13.065	6.48E-05	1.05E-03	5.13E-05	8.75E-06	5.13E-05	3.78E-08	5.12E-05
13.183	6.50E-05	1.05E-03	5.14E-05	8.61E-06	5.14E-05	3.72E-08	5.13E-05
13.3	6.51E-05	1.05E-03	5.15E-05	8.48E-06	5.15E-05	3.66E-08	5.15E-05
13.417	6.52E-05	1.05E-03	5.16E-05	8.36E-06	5.16E-05	3.60E-08	5.16E-05
13.534	6.54E-05	1.05E-03	5.18E-05	8.23E-06	5.18E-05	3.55E-08	5.17E-05
13.651	6.55E-05	1.05E-03	5.19E-05	8.11E-06	5.19E-05	3.49E-08	5.19E-05
15.878	6.62E-05	1.05E-03	5.39E-05	6.09E-06	5.39E-05	2.59E-08	5.39E-05
15.995	6.63E-05	1.05E-03	5.40E-05	6.00E-06	5.40E-05	2.55E-08	5.40E-05
16.112	6.64E-05	1.05E-03	5.41E-05	5.91E-06	5.41E-05	2.51E-08	5.41E-05
16.698	6.65E-05	1.05E-03	5.45E-05	5.48E-06	5.45E-05	2.32E-08	5.45E-05
16.815	6.66E-05	1.05E-03	5.46E-05	5.40E-06	5.46E-05	2.29E-08	5.46E-05
16.932	6.67E-05	1.05E-03	5.47E-05	5.32E-06	5.47E-05	2.25E-08	5.47E-05
17.05	6.68E-05	1.05E-03	5.48E-05	5.24E-06	5.48E-05	2.22E-08	5.47E-05
17.167	6.75E-05	1.05E-03	5.48E-05	5.17E-06	5.48E-05	2.19E-08	5.48E-05
17.987	6.75E-05	1.04E-03	5.53E-05	4.66E-06	5.53E-05	1.96E-08	5.53E-05
20.096	6.76E-05	1.04E-03	5.64E-05	3.57E-06	5.64E-05	1.50E-08	5.64E-05
21.971	6.85E-05	1.04E-03	5.72E-05	2.82E-06	5.72E-05	1.18E-08	5.72E-05
25.135	6.86E-05	1.04E-03	5.81E-05	1.90E-06	5.81E-05	7.89E-09	5.81E-05
25.253	6.86E-05	1.04E-03	5.81E-05	1.88E-06	5.81E-05	7.78E-09	5.81E-05
25.37	6.86E-05	1.04E-03	5.82E-05	1.85E-06	5.82E-05	7.66E-09	5.81E-05
25.487	6.87E-05	1.04E-03	5.82E-05	1.82E-06	5.82E-05	7.55E-09	5.82E-05
25.604	6.88E-05	1.04E-03	5.82E-05	1.80E-06	5.82E-05	7.44E-09	5.82E-05
25.721	6.88E-05	1.04E-03	5.82E-05	1.77E-06	5.82E-05	7.33E-09	5.82E-05
25.838	6.88E-05	1.04E-03	5.83E-05	1.74E-06	5.83E-05	7.23E-09	5.82E-05
25.956	6.89E-05	1.04E-03	5.83E-05	1.72E-06	5.83E-05	7.12E-09	5.83E-05
26.073	6.89E-05	1.04E-03	5.83E-05	1.69E-06	5.83E-05	7.02E-09	5.83E-05
26.19	6.89E-05	1.04E-03	5.83E-05	1.67E-06	5.83E-05	6.91E-09	5.83E-05
26.307	6.93E-05	1.04E-03	5.84E-05	1.65E-06	5.84E-05	6.81E-09	5.83E-05
26.424	6.94E-05	1.04E-03	5.84E-05	1.62E-06	5.84E-05	6.72E-09	5.84E-05
28.182	6.94E-05	1.04E-03	5.87E-05	1.30E-06	5.87E-05	5.39E-09	5.87E-05
29.706	6.94E-05	1.04E-03	5.89E-05	1.08E-06	5.89E-05	4.46E-09	5.89E-05

29.823	6.94E-05	1.04E-03	5.89E-05	1.07E-06	5.89E-05	4.40E-09	5.89E-05
29.94	6.94E-05	1.04E-03	5.89E-05	1.05E-06	5.89E-05	4.33E-09	5.89E-05
30.057	6.94E-05	1.04E-03	5.90E-05	1.04E-06	5.90E-05	4.27E-09	5.90E-05
30.174	6.96E-05	1.04E-03	5.90E-05	1.02E-06	5.90E-05	4.21E-09	5.90E-05
34.627	6.97E-05	1.04E-03	5.94E-05	5.90E-07	5.94E-05	2.43E-09	5.94E-05
41.19	6.98E-05	1.04E-03	5.97E-05	2.63E-07	5.97E-05	1.08E-09	5.97E-05
41.307	6.98E-05	1.04E-03	5.97E-05	2.60E-07	5.97E-05	1.07E-09	5.97E-05
41.424	6.98E-05	1.04E-03	5.97E-05	2.56E-07	5.97E-05	1.05E-09	5.97E-05
41.541	6.99E-05	1.04E-03	5.97E-05	2.52E-07	5.97E-05	1.04E-09	5.97E-05
41.658	6.99E-05	1.04E-03	5.98E-05	2.49E-07	5.98E-05	1.02E-09	5.98E-05
41.775	6.99E-05	1.04E-03	5.98E-05	2.45E-07	5.98E-05	1.01E-09	5.98E-05
41.893	6.99E-05	1.04E-03	5.98E-05	2.41E-07	5.98E-05	9.91E-10	5.98E-05
42.01	6.99E-05	1.04E-03	5.98E-05	2.38E-07	5.98E-05	9.77E-10	5.98E-05
42.947	6.99E-05	1.04E-03	5.98E-05	2.12E-07	5.98E-05	8.71E-10	5.98E-05
43.533	6.99E-05	1.04E-03	5.98E-05	1.97E-07	5.98E-05	8.11E-10	5.98E-05
43.65	6.99E-05	1.04E-03	5.98E-05	1.95E-07	5.98E-05	7.99E-10	5.98E-05
43.768	6.99E-05	1.04E-03	5.98E-05	1.92E-07	5.98E-05	7.87E-10	5.98E-05
45.76	6.99E-05	1.04E-03	5.98E-05	1.50E-07	5.98E-05	6.17E-10	5.98E-05
45.877	6.99E-05	1.04E-03	5.99E-05	1.48E-07	5.99E-05	6.08E-10	5.99E-05
45.994	7.00E-05	1.04E-03	5.99E-05	1.46E-07	5.99E-05	5.99E-10	5.99E-05
46.111	7.00E-05	1.04E-03	5.99E-05	1.44E-07	5.99E-05	5.91E-10	5.99E-05
48.103	7.00E-05	1.04E-03	5.99E-05	1.13E-07	5.99E-05	4.63E-10	5.99E-05
54.783	7.00E-05	1.04E-03	6.00E-05	4.97E-08	6.00E-05	2.04E-10	6.00E-05
54.9	7.00E-05	1.04E-03	6.00E-05	4.90E-08	6.00E-05	2.01E-10	6.00E-05
55.017	7.00E-05	1.04E-03	6.00E-05	4.83E-08	6.00E-05	1.98E-10	6.00E-05
55.134	7.00E-05	1.04E-03	6.00E-05	4.76E-08	6.00E-05	1.95E-10	6.00E-05
56.189	7.00E-05	1.04E-03	6.00E-05	4.19E-08	6.00E-05	1.72E-10	6.00E-05
56.306	7.00E-05	1.04E-03	6.00E-05	4.13E-08	6.00E-05	1.69E-10	6.00E-05
56.423	7.00E-05	1.04E-03	6.00E-05	4.07E-08	6.00E-05	1.67E-10	6.00E-05
58.65	7.00E-05	1.04E-03	6.00E-05	3.10E-08	6.00E-05	1.27E-10	6.00E-05
58.767	7.00E-05	1.04E-03	6.00E-05	3.05E-08	6.00E-05	1.25E-10	6.00E-05
58.884	7.00E-05	1.04E-03	6.00E-05	3.01E-08	6.00E-05	1.23E-10	6.00E-05
59.002	7.00E-05	1.04E-03	6.00E-05	2.97E-08	6.00E-05	1.22E-10	6.00E-05
59.939	7.00E-05	1.04E-03	6.00E-05	2.64E-08	6.00E-05	1.08E-10	6.00E-05
60.439	7.00E-05	1.04E-03	6.00E-05	2.49E-08	6.00E-05	1.02E-10	6.00E-05

1.3 Safranine-O oxidation products with hypochlorite .

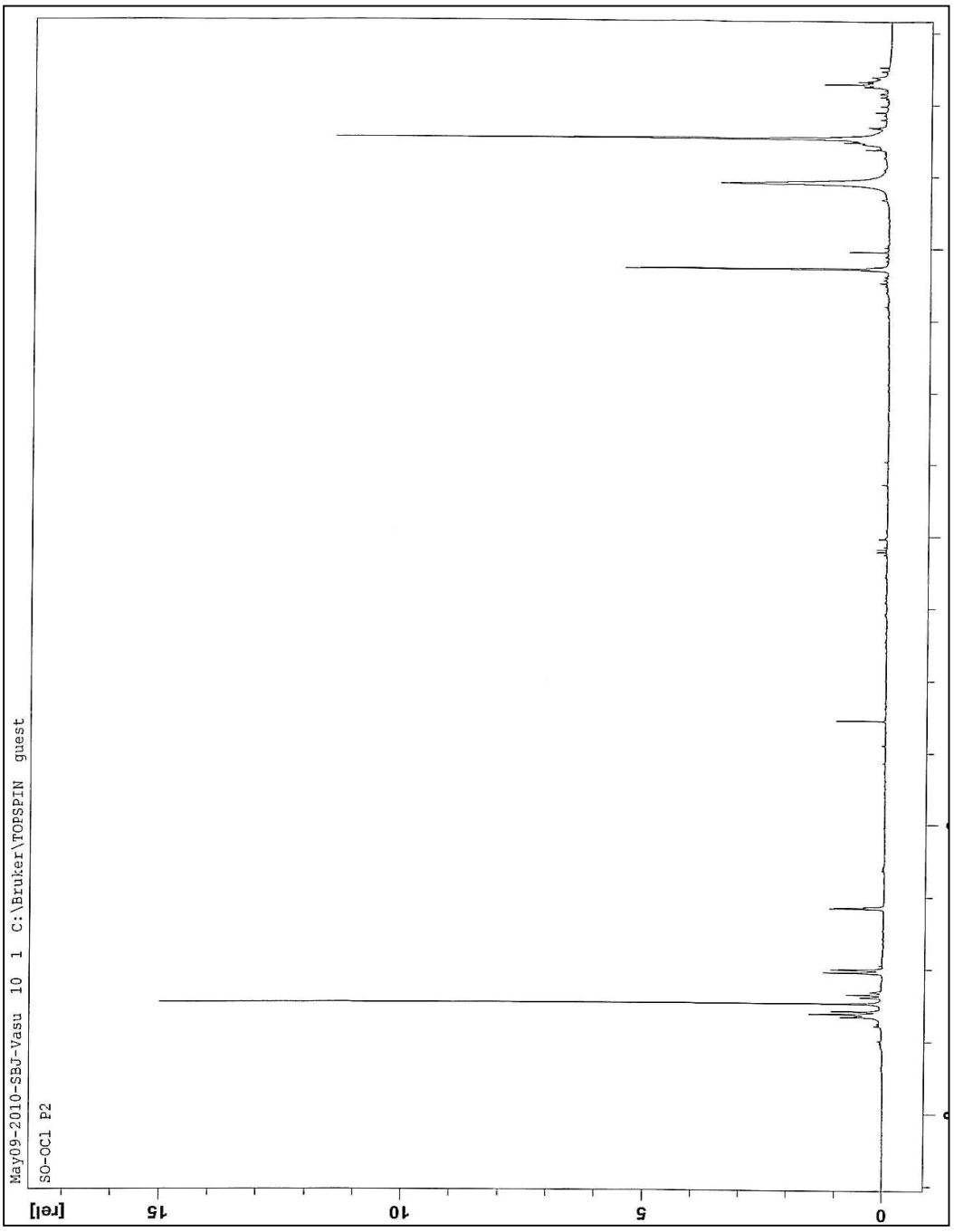

Figure 1.1.14 ^{1}H NMR spectrum of safranine-O major oxidation product P_2 (4-amino-6-(-2-chloro-6-hydroxy-phenylimini)-3-methyl cyclohexa-2,4-dienone oxide) with hypochlorite.

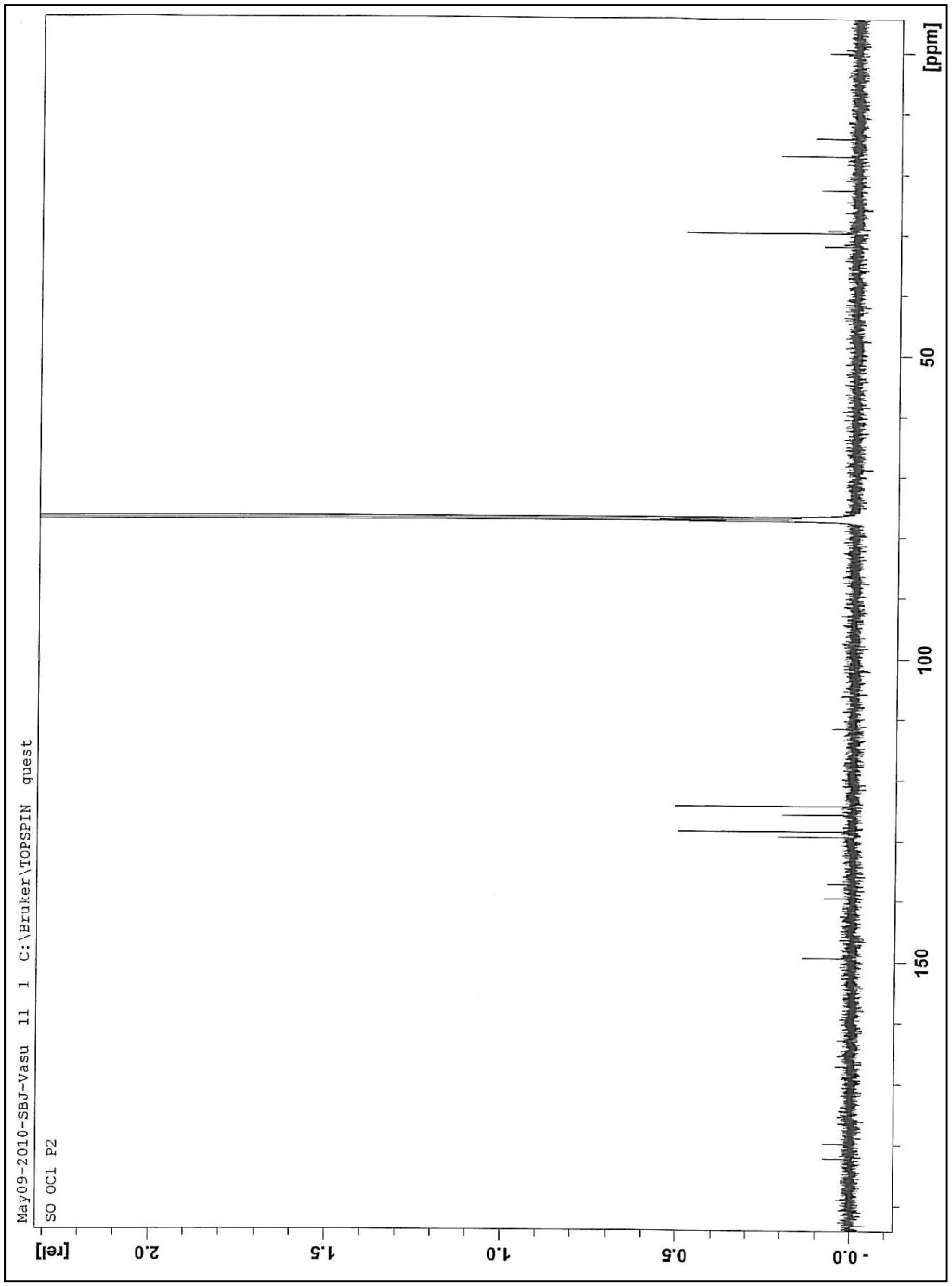

Figure 1.1.15 ^{13}C NMR spectrum of safranine-O major oxidation product P_2 (4-amino-6-(-2-chloro-6-hydroxy-phenylimini)-3-methyl cyclohexa-2,4-dienone oxide) with hypochlorite.

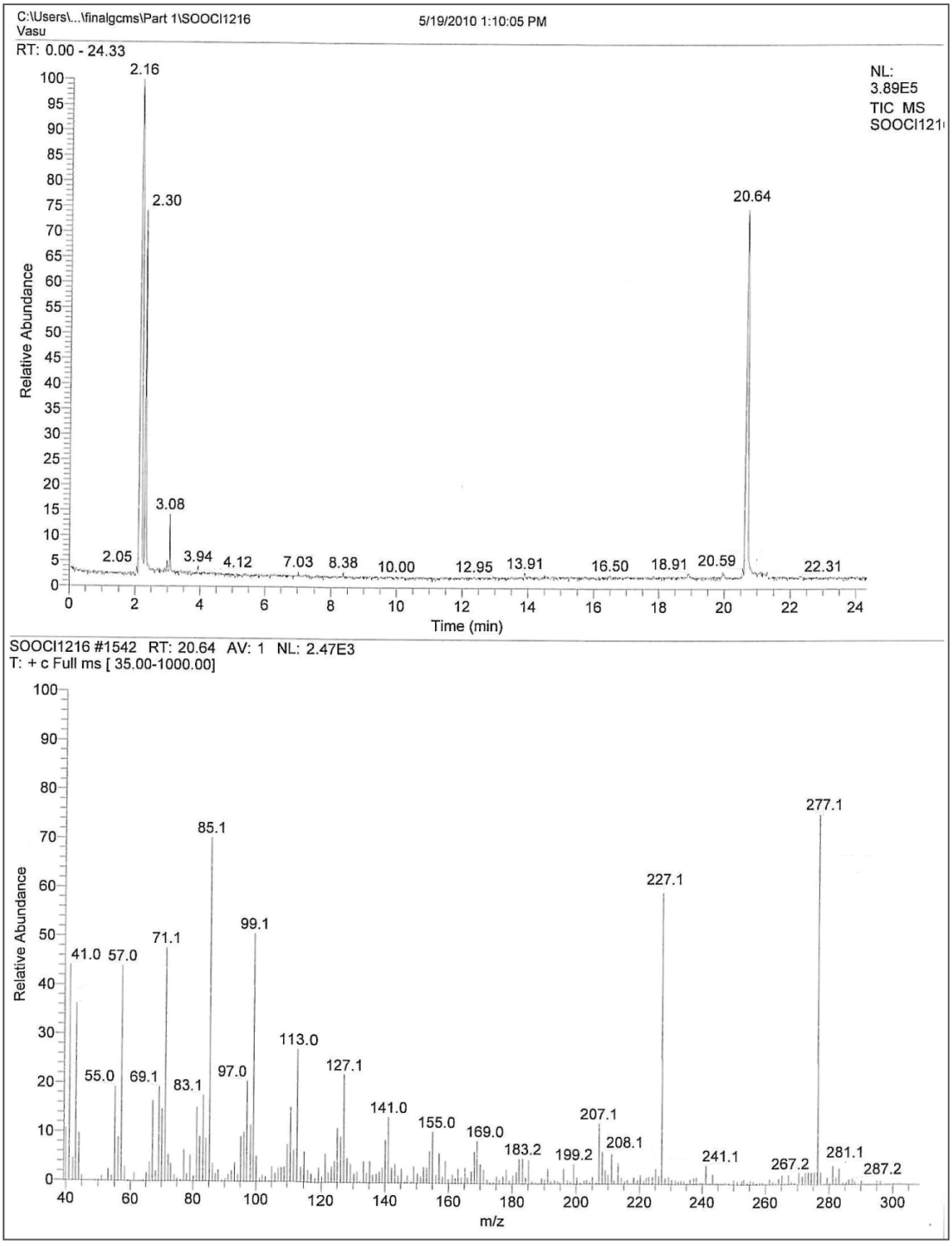

Figure 1.1.16 GC-MS spectrum of safranine-O major oxidation product P_2 (4-amino-6-(-2-chloro-6-hydroxy-phenylimini)-3-methyl cyclohexa-2,4-dienone oxide) with hypochlorite.

Table 1.5 Safranine-O - hypochlorite experimental and simulated curves-compiled data.

Time	E1	Time	S1	Time	E2	Time	S2	Time	E3	Time	S3
0.2899	1.92E-05	0	0.00002	0.17395	1.68E-05	0	0.00002	0.087	1.26E-05	0	0.00002
0.8759	1.99E-05	0.2	1.99E-05	0.52551	1.94E-05	0.2	1.98E-05	0.2628	1.82E-05	0.2	1.98E-05
1.4618	1.95E-05	0.4	1.98E-05	0.87708	1.89E-05	0.4	1.97E-05	0.4385	1.91E-05	0.2628	1.97E-05
2.0477	1.92E-05	0.6	1.98E-05	1.2286	1.84E-05	0.5255	1.96E-05	0.6143	1.89E-05	0.4385	1.95E-05
2.6337	1.88E-05	0.8	1.97E-05	1.5802	1.8E-05	0.7255	1.94E-05	0.7901	1.85E-05	0.6143	1.93E-05
3.2196	1.86E-05	0.876	1.97E-05	1.9318	1.77E-05	0.8771	1.93E-05	0.9659	1.82E-05	0.7901	1.91E-05
3.8056	1.83E-05	1.076	1.96E-05	2.2833	1.73E-05	1.0771	1.92E-05	1.1416	1.79E-05	0.9659	1.89E-05
4.3915	1.8E-05	1.276	1.95E-05	2.6349	1.71E-05	1.2286	1.91E-05	1.3174	1.76E-05	1.1416	1.87E-05
4.9774	1.77E-05	1.462	1.94E-05	2.9865	1.68E-05	1.4286	1.89E-05	1.4932	1.73E-05	1.3174	1.85E-05
5.5634	1.75E-05	1.662	1.93E-05	3.338	1.65E-05	1.5802	1.88E-05	1.669	1.71E-05	1.4932	1.83E-05
6.1493	1.72E-05	1.862	1.93E-05	3.6896	1.63E-05	1.7802	1.87E-05	1.8447	1.69E-05	1.669	1.81E-05
6.7353	1.7E-05	2.048	1.92E-05	4.0411	1.61E-05	1.9318	1.85E-05	2.0205	1.67E-05	1.8447	1.79E-05
7.3212	1.67E-05	2.248	1.91E-05	4.3927	1.58E-05	2.1318	1.84E-05	2.1963	1.65E-05	2.0205	1.77E-05
7.9072	1.65E-05	2.448	1.9E-05	4.7443	1.56E-05	2.2833	1.83E-05	2.3721	1.63E-05	2.1963	1.76E-05
8.4931	1.63E-05	2.634	1.9E-05	5.0958	1.54E-05	2.4833	1.82E-05	2.5478	1.61E-05	2.3721	1.74E-05
9.079	1.61E-05	2.834	1.89E-05	5.4474	1.52E-05	2.6349	1.8E-05	2.7236	1.59E-05	2.5478	1.72E-05
9.665	1.58E-05	3.034	1.88E-05	5.799	1.5E-05	2.8349	1.79E-05	2.8994	1.57E-05	2.7236	1.7E-05
10.251	1.56E-05	3.22	1.87E-05	6.1505	1.48E-05	2.9865	1.78E-05	3.0752	1.56E-05	2.8994	1.68E-05
10.837	1.54E-05	3.42	1.87E-05	6.5021	1.46E-05	3.1865	1.77E-05	3.2509	1.54E-05	3.0752	1.67E-05
11.423	1.52E-05	3.62	1.86E-05	6.8536	1.44E-05	3.338	1.76E-05	3.4267	1.53E-05	3.2509	1.65E-05
12.009	1.5E-05	3.806	1.85E-05	7.2052	1.42E-05	3.538	1.74E-05	3.6025	1.51E-05	3.4267	1.63E-05
12.595	1.48E-05	4.006	1.84E-05	7.5568	1.4E-05	3.6896	1.73E-05	3.7783	1.49E-05	3.6025	1.61E-05
13.181	1.46E-05	4.206	1.84E-05	7.9083	1.38E-05	3.8896	1.72E-05	3.954	1.48E-05	3.7783	1.6E-05
13.767	1.45E-05	4.392	1.83E-05	8.2599	1.37E-05	4.0411	1.71E-05	4.1298	1.47E-05	3.954	1.58E-05
14.353	1.43E-05	4.592	1.82E-05	8.6115	1.35E-05	4.2411	1.7E-05	4.3056	1.45E-05	4.1298	1.57E-05
14.938	1.41E-05	4.792	1.82E-05	8.963	1.33E-05	4.3927	1.69E-05	4.4814	1.43E-05	4.3056	1.55E-05
15.524	1.39E-05	4.977	1.81E-05	9.3146	1.32E-05	4.5927	1.67E-05	4.6571	1.42E-05	4.4814	1.53E-05
16.11	1.38E-05	5.177	1.8E-05	9.6661	1.3E-05	4.7443	1.66E-05	4.8329	1.41E-05	4.6571	1.52E-05
16.696	1.36E-05	5.377	1.79E-05	10.018	1.28E-05	4.9443	1.65E-05	5.0087	1.39E-05	4.8329	1.5E-05
17.282	1.34E-05	5.563	1.79E-05	10.369	1.27E-05	5.0958	1.64E-05	5.1845	1.38E-05	5.0087	1.49E-05
17.868	1.33E-05	5.763	1.78E-05	10.721	1.25E-05	5.2958	1.63E-05	5.3603	1.37E-05	5.1845	1.47E-05
18.454	1.31E-05	5.963	1.77E-05	11.072	1.24E-05	5.4474	1.62E-05	5.536	1.35E-05	5.3603	1.46E-05
19.04	1.3E-05	6.149	1.77E-05	11.424	1.22E-05	5.6474	1.61E-05	5.7118	1.34E-05	5.536	1.44E-05
23.728	1.18E-05	7.721	1.71E-05	14.236	1.11E-05	7.0536	1.52E-05	7.118	1.24E-05	6.9422	1.32E-05
24.314	1.17E-05	7.907	1.7E-05	14.588	1.1E-05	7.2052	1.51E-05	7.2938	1.23E-05	7.118	1.31E-05
24.899	1.16E-05	8.107	1.7E-05	14.94	1.08E-05	7.4052	1.5E-05	7.4696	1.22E-05	7.2938	1.3E-05
25.485	1.14E-05	8.307	1.69E-05	15.291	1.07E-05	7.5568	1.49E-05	7.6453	1.21E-05	7.4696	1.28E-05
26.071	1.13E-05	8.493	1.68E-05	15.643	1.06E-05	7.7568	1.48E-05	7.8211	1.2E-05	7.6453	1.27E-05

26.657	1.12E-05	8.693	1.68E-05	15.994	1.04E-05	7.9083	1.47E-05	7.9969	1.19E-05	7.8211	1.26E-05
30.173	1.05E-05	9.865	1.64E-05	18.104	9.72E-06	8.963	1.41E-05	9.0515	1.12E-05	8.8758	1.18E-05
30.759	1.04E-05	10.07	1.63E-05	18.455	9.6E-06	9.163	1.4E-05	9.2273	1.11E-05	9.0515	1.17E-05
31.345	1.03E-05	10.25	1.62E-05	18.807	9.5E-06	9.3146	1.39E-05	9.4031	1.1E-05	9.2273	1.16E-05
31.931	1.02E-05	10.45	1.62E-05	19.158	9.38E-06	9.5146	1.38E-05	9.5789	1.09E-05	9.4031	1.14E-05
44.236	8.16E-06	14.55	1.49E-05	26.541	7.37E-06	13.182	1.2E-05	13.27	9.04E-06	13.094	9.2E-06
44.821	8.08E-06	14.75	1.48E-05	26.893	7.29E-06	13.382	1.19E-05	13.446	8.96E-06	13.27	9.1E-06
45.407	8E-06	14.94	1.48E-05	27.244	7.21E-06	13.533	1.18E-05	13.622	8.89E-06	13.446	9.01E-06
45.993	7.92E-06	15.14	1.47E-05	27.596	7.12E-06	13.733	1.17E-05	13.798	8.8E-06	13.622	8.92E-06
50.095	7.38E-06	16.51	1.43E-05	30.057	6.57E-06	14.94	1.12E-05	15.028	8.27E-06	14.852	8.29E-06
50.681	7.31E-06	16.7	1.43E-05	30.408	6.51E-06	15.14	1.11E-05	15.204	8.2E-06	15.028	8.2E-06
51.267	7.24E-06	16.9	1.42E-05	30.76	6.43E-06	15.291	1.1E-05	15.379	8.13E-06	15.204	8.12E-06
72.947	5.08E-06	24.13	1.23E-05	43.768	4.28E-06	21.819	8.58E-06	21.883	5.89E-06	21.707	5.52E-06
73.533	5.03E-06	24.31	1.22E-05	44.119	4.24E-06	21.971	8.53E-06	22.059	5.84E-06	21.883	5.47E-06
78.806	4.62E-06	26.07	1.18E-05	47.283	3.84E-06	23.577	8.01E-06	23.641	5.41E-06	23.465	4.98E-06
79.392	4.58E-06	26.27	1.17E-05	47.635	3.8E-06	23.729	7.96E-06	23.817	5.36E-06	23.641	4.93E-06
79.978	4.54E-06	26.47	1.17E-05	47.986	3.76E-06	23.929	7.9E-06	23.993	5.31E-06	23.817	4.88E-06
80.564	4.5E-06	26.66	1.17E-05	48.338	3.71E-06	24.08	7.86E-06	24.168	5.27E-06	23.993	4.83E-06
81.15	4.46E-06	26.86	1.16E-05	48.69	3.67E-06	24.28	7.8E-06	24.344	5.23E-06	24.168	4.78E-06
81.736	4.41E-06	27.06	1.16E-05	49.041	3.63E-06	24.432	7.75E-06	24.52	5.18E-06	24.344	4.73E-06
82.322	4.38E-06	27.24	1.15E-05	49.393	3.6E-06	24.632	7.69E-06	24.696	5.14E-06	24.52	4.68E-06
82.908	4.33E-06	27.44	1.15E-05	49.744	3.56E-06	24.783	7.65E-06	24.871	5.1E-06	24.696	4.63E-06
90.525	3.84E-06	29.99	1.09E-05	54.315	3.1E-06	27.093	6.99E-06	27.156	4.56E-06	26.981	4.04E-06
91.111	3.81E-06	30.17	1.09E-05	54.666	3.07E-06	27.244	6.95E-06	27.332	4.53E-06	27.156	4E-06
91.697	3.78E-06	30.37	1.08E-05	55.018	3.03E-06	27.444	6.9E-06	27.508	4.49E-06	27.332	3.96E-06
95.212	3.58E-06	31.55	1.06E-05	57.127	2.84E-06	28.499	6.62E-06	28.563	4.27E-06	28.387	3.72E-06
95.798	3.54E-06	31.75	1.05E-05	57.479	2.82E-06	28.651	6.59E-06	28.738	4.23E-06	28.563	3.68E-06
96.384	3.51E-06	31.93	1.05E-05	57.83	2.79E-06	28.851	6.53E-06	28.914	4.2E-06	28.738	3.64E-06
96.97	3.48E-06	32.13	1.04E-05	58.182	2.76E-06	29.002	6.5E-06	29.09	4.17E-06	28.914	3.61E-06
107.52	2.97E-06	35.65	9.72E-06	64.51	2.28E-06	32.166	5.75E-06	32.254	3.58E-06	32.078	2.99E-06
108.1	2.94E-06	35.85	9.68E-06	64.861	2.26E-06	32.366	5.71E-06	32.43	3.55E-06	32.254	2.96E-06
108.69	2.92E-06	36.03	9.64E-06	65.213	2.23E-06	32.518	5.67E-06	32.606	3.52E-06	32.43	2.93E-06
109.28	2.89E-06	36.23	9.6E-06	65.565	2.21E-06	32.718	5.63E-06	32.781	3.49E-06	32.606	2.9E-06
109.86	2.87E-06	36.43	9.56E-06	65.916	2.19E-06	32.869	5.6E-06	32.957	3.46E-06	32.781	2.87E-06
110.45	2.84E-06	36.62	9.53E-06	66.268	2.17E-06	33.069	5.55E-06	33.133	3.43E-06	32.957	2.84E-06
111.03	2.81E-06	36.82	9.49E-06	66.619	2.14E-06	33.221	5.52E-06	33.309	3.4E-06	33.133	2.81E-06
111.62	2.79E-06	37.02	9.45E-06	66.971	2.12E-06	33.421	5.48E-06	33.484	3.38E-06	33.309	2.78E-06
112.2	2.77E-06	37.2	9.41E-06	67.322	2.1E-06	33.572	5.45E-06	33.66	3.35E-06	33.484	2.75E-06
112.79	2.74E-06	37.4	9.38E-06	67.674	2.08E-06	33.772	5.4E-06	33.836	3.33E-06	33.66	2.72E-06
113.38	2.72E-06	37.6	9.34E-06	68.026	2.06E-06	33.924	5.37E-06	34.012	3.3E-06	33.836	2.7E-06
113.96	2.69E-06	37.79	9.3E-06	68.377	2.03E-06	34.124	5.33E-06	34.188	3.27E-06	34.012	2.67E-06

138.57	1.87E-06	45.99	7.88E-06	83.143	1.31E-06	41.507	4.01E-06	41.57	2.32E-06	41.394	1.72E-06
139.16	1.86E-06	46.19	7.85E-06	83.494	1.3E-06	41.658	3.99E-06	41.746	2.3E-06	41.57	1.71E-06
139.74	1.84E-06	46.39	7.82E-06	83.846	1.29E-06	41.858	3.96E-06	41.922	2.28E-06	41.746	1.69E-06
140.33	1.83E-06	46.58	7.79E-06	84.197	1.28E-06	42.01	3.93E-06	42.097	2.27E-06	41.922	1.67E-06
140.92	1.82E-06	46.78	7.76E-06	84.549	1.26E-06	42.21	3.9E-06	42.273	2.25E-06	42.097	1.65E-06
141.5	1.8E-06	46.98	7.73E-06	84.901	1.25E-06	42.361	3.88E-06	42.449	2.23E-06	42.273	1.64E-06
142.09	1.78E-06	47.17	7.7E-06	85.252	1.24E-06	42.561	3.85E-06	42.625	2.21E-06	42.449	1.62E-06
142.67	1.77E-06	47.37	7.67E-06	85.604	1.22E-06	42.713	3.83E-06	42.801	2.19E-06	42.625	1.6E-06
147.36	1.64E-06	48.92	7.43E-06	88.416	1.13E-06	44.119	3.63E-06	44.207	2.05E-06	44.031	1.48E-06
147.95	1.63E-06	49.12	7.4E-06	88.768	1.12E-06	44.319	3.6E-06	44.383	2.03E-06	44.207	1.46E-06
148.53	1.62E-06	49.32	7.37E-06	89.119	1.11E-06	44.471	3.58E-06	44.558	2.02E-06	44.383	1.44E-06
149.12	1.6E-06	49.51	7.34E-06	89.471	1.1E-06	44.671	3.55E-06	44.734	2.01E-06	44.558	1.43E-06
162.6	1.33E-06	54.01	6.71E-06	97.557	8.66E-07	48.69	3.04E-06	48.777	1.66E-06	48.601	1.13E-06
163.18	1.32E-06	54.2	6.68E-06	97.908	8.62E-07	48.89	3.02E-06	48.953	1.65E-06	48.777	1.11E-06
163.77	1.31E-06	54.4	6.66E-06	98.26	8.55E-07	49.041	3E-06	49.128	1.64E-06	48.953	1.1E-06
164.35	1.3E-06	54.6	6.63E-06	98.611	8.47E-07	49.241	2.98E-06	49.304	1.62E-06	49.128	1.09E-06
164.94	1.29E-06	54.78	6.6E-06	98.963	8.37E-07	49.393	2.96E-06	49.48	1.61E-06	49.304	1.08E-06
165.53	1.27E-06	54.98	6.58E-06	99.315	8.29E-07	49.593	2.94E-06	49.656	1.6E-06	49.48	1.07E-06
166.11	1.27E-06	55.18	6.55E-06	99.666	8.2E-07	49.744	2.92E-06	49.832	1.58E-06	49.656	1.06E-06
166.7	1.26E-06	55.37	6.53E-06	100.02	8.14E-07	49.944	2.9E-06	50.007	1.57E-06	49.832	1.05E-06
167.28	1.24E-06	55.57	6.5E-06	100.37	8.06E-07	50.096	2.88E-06	50.183	1.56E-06	50.007	1.04E-06
173.73	1.14E-06	57.71	6.23E-06	104.24	7.21E-07	52.054	2.67E-06	52.117	1.43E-06	51.941	9.24E-07
183.1	1.01E-06	60.84	5.85E-06	109.86	6.23E-07	54.866	2.4E-06	54.929	1.26E-06	54.753	7.83E-07
188.38	9.34E-07	62.6	5.64E-06	113.03	5.74E-07	56.424	2.26E-06	56.511	1.17E-06	56.335	7.13E-07
188.96	9.28E-07	62.8	5.62E-06	113.38	5.68E-07	56.624	2.24E-06	56.687	1.17E-06	56.511	7.05E-07
199.51	8.12E-07	66.32	5.24E-06	119.71	4.81E-07	59.788	1.98E-06	59.851	1.02E-06	59.675	5.85E-07
200.1	8.04E-07	66.5	5.22E-06	120.06	4.74E-07	59.94	1.97E-06	60.027	1.01E-06	59.851	5.79E-07
200.68	7.99E-07	66.7	5.19E-06	120.41	4.72E-07	60.14	1.96E-06	60.202	9.95E-07	60.027	5.73E-07
201.27	7.92E-07	66.9	5.17E-06	120.76	4.66E-07	60.291	1.95E-06	60.378	9.89E-07	60.202	5.67E-07
205.37	7.55E-07	68.26	5.03E-06	123.22	4.41E-07	61.546	1.85E-06	61.609	9.42E-07	61.433	5.27E-07
205.96	7.47E-07	68.46	5.01E-06	123.57	4.35E-07	61.697	1.84E-06	61.784	9.35E-07	61.609	5.22E-07
206.54	7.43E-07	68.66	4.99E-06	123.92	4.3E-07	61.897	1.83E-06	61.96	9.26E-07	61.784	5.16E-07
207.13	7.4E-07	68.85	4.98E-06	124.28	4.27E-07	62.049	1.82E-06	62.136	9.21E-07	61.96	5.11E-07
207.71	7.31E-07	69.05	4.96E-06	124.63	4.23E-07	62.249	1.8E-06	62.312	9.11E-07	62.136	5.06E-07
208.3	7.27E-07	69.25	4.94E-06	124.98	4.22E-07	62.401	1.79E-06	62.487	9.04E-07	62.312	5.01E-07
208.89	7.18E-07	69.43	4.92E-06	125.33	4.17E-07	62.601	1.78E-06	62.663	8.99E-07	62.487	4.95E-07
209.47	7.14E-07	69.63	4.9E-06	125.68	4.15E-07	62.752	1.77E-06	62.839	8.9E-07	62.663	4.9E-07
210.06	7.07E-07	69.83	4.88E-06	126.03	4.1E-07	62.952	1.76E-06	63.015	8.85E-07	62.839	4.85E-07
210.64	6.99E-07	70.02	4.86E-06	126.38	4.06E-07	63.104	1.75E-06	63.191	8.82E-07	63.015	4.8E-07
211.23	6.95E-07	70.22	4.84E-06	126.74	4.03E-07	63.304	1.73E-06	63.366	8.77E-07	63.191	4.75E-07
227.05	5.75E-07	75.49	4.35E-06	136.23	3.18E-07	68.026	1.44E-06	68.112	7.14E-07	67.937	3.59E-07

227.64	5.7E-07	75.69	4.33E-06	136.58	3.16E-07	68.226	1.43E-06	68.288	7.07E-07	68.112	3.55E-07
228.22	5.7E-07	75.88	4.32E-06	136.93	3.13E-07	68.377	1.43E-06	68.464	7.02E-07	68.288	3.52E-07
228.81	5.65E-07	76.08	4.3E-06	137.28	3.11E-07	68.577	1.41E-06	68.64	6.95E-07	68.464	3.48E-07
229.39	5.62E-07	76.28	4.28E-06	137.63	3.11E-07	68.729	1.41E-06	68.815	6.93E-07	68.64	3.44E-07
229.98	5.57E-07	76.46	4.27E-06	137.99	3.06E-07	68.929	1.4E-06	68.991	6.86E-07	68.815	3.41E-07
230.56	5.54E-07	76.66	4.25E-06	138.34	3.03E-07	69.08	1.39E-06	69.167	6.81E-07	68.991	3.37E-07
231.15	5.47E-07	76.86	4.23E-06	138.69	3.04E-07	69.28	1.38E-06	69.343	6.8E-07	69.167	3.34E-07
239.94	4.94E-07	79.79	3.99E-06	143.96	2.67E-07	71.893	1.25E-06	71.979	6.07E-07	71.804	2.86E-07
240.53	4.89E-07	79.98	3.98E-06	144.31	2.64E-07	72.093	1.24E-06	72.155	6.06E-07	71.979	2.83E-07
246.97	4.5E-07	82.14	3.81E-06	148.18	2.39E-07	74.002	1.15E-06	74.089	5.62E-07	73.913	2.52E-07
253.42	4.17E-07	84.28	3.65E-06	152.05	2.2E-07	75.96	1.06E-06	76.022	5.13E-07	75.846	2.25E-07
254	4.16E-07	84.48	3.63E-06	152.4	2.17E-07	76.111	1.06E-06	76.198	5.12E-07	76.022	2.23E-07
254.59	4.12E-07	84.67	3.62E-06	152.75	2.17E-07	76.311	1.05E-06	76.374	5.07E-07	76.198	2.2E-07
255.17	4.08E-07	84.87	3.6E-06	153.1	2.16E-07	76.463	1.04E-06	76.55	5.04E-07	76.374	2.18E-07
268.65	3.55E-07	89.35	3.29E-06	161.19	1.86E-07	80.53	8.93E-07	80.592	4.31E-07	80.417	1.72E-07
269.24	3.5E-07	89.55	3.28E-06	161.54	1.81E-07	80.682	8.88E-07	80.768	4.25E-07	80.592	1.7E-07
269.82	3.51E-07	89.75	3.27E-06	161.89	1.82E-07	80.882	8.81E-07	80.944	4.24E-07	80.768	1.68E-07
270.41	3.5E-07	89.94	3.25E-06	162.24	1.83E-07	81.033	8.76E-07	81.12	4.2E-07	80.944	1.66E-07
270.99	3.46E-07	90.14	3.24E-06	162.6	1.78E-07	81.233	8.69E-07	81.295	4.19E-07	81.12	1.65E-07
279.2	3.18E-07	92.87	3.07E-06	167.52	1.63E-07	83.694	7.91E-07	83.756	3.75E-07	83.581	1.42E-07
279.78	3.19E-07	93.07	3.06E-06	167.87	1.6E-07	83.846	7.86E-07	83.932	3.76E-07	83.756	1.41E-07
280.37	3.16E-07	93.27	3.04E-06	168.22	1.6E-07	84.046	7.8E-07	84.108	3.78E-07	83.932	1.39E-07
290.92	2.83E-07	96.78	2.84E-06	174.55	1.43E-07	87.21	6.91E-07	87.272	3.31E-07	87.096	1.16E-07
291.5	2.81E-07	96.97	2.83E-06	174.9	1.45E-07	87.361	6.87E-07	87.448	3.35E-07	87.272	1.14E-07
292.67	2.76E-07	97.37	2.8E-06	175.6	1.41E-07	87.713	6.78E-07	87.799	3.31E-07	87.623	1.12E-07
293.26	2.75E-07	97.56	2.79E-06	175.96	1.36E-07	87.913	6.73E-07	87.975	3.24E-07	87.799	1.11E-07
293.85	2.72E-07	97.76	2.78E-06	176.31	1.38E-07	88.065	6.69E-07	88.151	3.21E-07	87.975	1.1E-07
294.43	2.76E-07	97.96	2.77E-06	176.66	1.4E-07	88.265	6.63E-07	88.327	3.21E-07	88.151	1.09E-07
297.95	2.67E-07	99.13	2.71E-06	178.77	1.33E-07	89.319	6.37E-07	89.381	3.12E-07	89.205	1.02E-07
298.53	2.65E-07	99.31	2.7E-06	179.12	1.32E-07	89.471	6.33E-07	89.557	3.1E-07	89.381	1.01E-07
299.12	2.62E-07	99.51	2.69E-06	179.47	1.33E-07	89.671	6.29E-07	89.733	3.02E-07	89.557	1E-07
299.71	2.62E-07	99.71	2.67E-06	179.82	1.33E-07	89.822	6.25E-07	89.909	3.01E-07	89.733	9.9E-08

Table 1.6 Safranine-O - hypochlorite intermediate and product formation- compiled data.

TIME	SO	P1	I	P2
	2.00E-05	0.00E+00	0.00E+00	0.00E+00
0.2	1.98E-05	2.35E-07	9.10E-09	2.26E-07
0.26275	1.97E-05	3.08E-07	9.07E-09	2.99E-07
0.43852	1.95E-05	5.13E-07	8.98E-09	5.04E-07
0.6143	1.93E-05	7.15E-07	8.88E-09	7.06E-07
0.79008	1.91E-05	9.16E-07	8.79E-09	9.07E-07
0.96585	1.89E-05	1.11E-06	8.70E-09	1.11E-06
1.1416	1.87E-05	1.31E-06	8.61E-09	1.30E-06
1.3174	1.85E-05	1.50E-06	8.52E-09	1.50E-06
1.4932	1.83E-05	1.70E-06	8.43E-09	1.69E-06
1.669	1.81E-05	1.89E-06	8.34E-09	1.88E-06
6.2391	1.38E-05	6.19E-06	6.36E-09	6.18E-06
6.4149	1.37E-05	6.33E-06	6.30E-09	6.33E-06
6.5907	1.35E-05	6.47E-06	6.23E-09	6.47E-06
6.7665	1.34E-05	6.61E-06	6.17E-09	6.61E-06
6.9422	1.32E-05	6.75E-06	6.10E-09	6.75E-06
7.118	1.31E-05	6.89E-06	6.04E-09	6.88E-06
7.2938	1.30E-05	7.03E-06	5.98E-09	7.02E-06
7.4696	1.28E-05	7.16E-06	5.92E-09	7.15E-06
7.6453	1.27E-05	7.29E-06	5.86E-09	7.29E-06
7.8211	1.26E-05	7.43E-06	5.80E-09	7.42E-06
7.9969	1.24E-05	7.56E-06	5.74E-09	7.55E-06
8.1727	1.23E-05	7.68E-06	5.68E-09	7.68E-06
8.3484	1.22E-05	7.81E-06	5.62E-09	7.81E-06
14.852	8.29E-06	1.17E-05	3.82E-09	1.17E-05
15.028	8.20E-06	1.18E-05	3.78E-09	1.18E-05
15.204	8.12E-06	1.19E-05	3.74E-09	1.19E-05
15.379	8.04E-06	1.20E-05	3.70E-09	1.20E-05
15.555	7.95E-06	1.20E-05	3.67E-09	1.20E-05
15.731	7.87E-06	1.21E-05	3.63E-09	1.21E-05
15.907	7.79E-06	1.22E-05	3.59E-09	1.22E-05
16.083	7.71E-06	1.23E-05	3.55E-09	1.23E-05
16.258	7.63E-06	1.24E-05	3.52E-09	1.24E-05
16.434	7.55E-06	1.25E-05	3.48E-09	1.24E-05
16.61	7.47E-06	1.25E-05	3.44E-09	1.25E-05
23.465	4.98E-06	1.50E-05	2.30E-09	1.50E-05
23.641	4.93E-06	1.51E-05	2.27E-09	1.51E-05
26.453	4.17E-06	1.58E-05	1.92E-09	1.58E-05
26.629	4.13E-06	1.59E-05	1.90E-09	1.59E-05
26.805	4.09E-06	1.59E-05	1.88E-09	1.59E-05
26.981	4.04E-06	1.60E-05	1.86E-09	1.60E-05
27.156	4.00E-06	1.60E-05	1.85E-09	1.60E-05
27.332	3.96E-06	1.60E-05	1.83E-09	1.60E-05
27.508	3.92E-06	1.61E-05	1.81E-09	1.61E-05
27.684	3.88E-06	1.61E-05	1.79E-09	1.61E-05
27.86	3.84E-06	1.62E-05	1.77E-09	1.62E-05
28.035	3.80E-06	1.62E-05	1.75E-09	1.62E-05
32.957	2.84E-06	1.72E-05	1.31E-09	1.72E-05
33.133	2.81E-06	1.72E-05	1.30E-09	1.72E-05
33.309	2.78E-06	1.72E-05	1.28E-09	1.72E-05
33.484	2.75E-06	1.72E-05	1.27E-09	1.72E-05
33.66	2.72E-06	1.73E-05	1.26E-09	1.73E-05
33.836	2.70E-06	1.73E-05	1.24E-09	1.73E-05
34.012	2.67E-06	1.73E-05	1.23E-09	1.73E-05
34.188	2.64E-06	1.74E-05	1.22E-09	1.74E-05
34.363	2.61E-06	1.74E-05	1.21E-09	1.74E-05
34.539	2.59E-06	1.74E-05	1.19E-09	1.74E-05
34.715	2.56E-06	1.74E-05	1.18E-09	1.74E-05
34.891	2.53E-06	1.75E-05	1.17E-09	1.75E-05
35.066	2.51E-06	1.75E-05	1.16E-09	1.75E-05
38.055	2.10E-06	1.79E-05	9.69E-10	1.79E-05
38.23	2.08E-06	1.79E-05	9.59E-10	1.79E-05
38.406	2.06E-06	1.79E-05	9.49E-10	1.79E-05
38.582	2.04E-06	1.80E-05	9.39E-10	1.80E-05
38.758	2.01E-06	1.80E-05	9.29E-10	1.80E-05
38.933	1.99E-06	1.80E-05	9.20E-10	1.80E-05
44.734	1.42E-06	1.86E-05	6.53E-10	1.86E-05
44.91	1.40E-06	1.86E-05	6.46E-10	1.86E-05
45.086	1.39E-06	1.86E-05	6.39E-10	1.86E-05
45.261	1.37E-06	1.86E-05	6.33E-10	1.86E-05
45.437	1.36E-06	1.86E-05	6.26E-10	1.86E-05
45.613	1.34E-06	1.87E-05	6.20E-10	1.87E-05
45.789	1.33E-06	1.87E-05	6.13E-10	1.87E-05
45.965	1.32E-06	1.87E-05	6.07E-10	1.87E-05
46.14	1.30E-06	1.87E-05	6.01E-10	1.87E-05
46.316	1.29E-06	1.87E-05	5.95E-10	1.87E-05
46.492	1.28E-06	1.87E-05	5.88E-10	1.87E-05

46.668	1.26E-06	1.87E-05	5.82E-10	1.87E-05
46.843	1.25E-06	1.88E-05	5.76E-10	1.88E-05
47.019	1.24E-06	1.88E-05	5.70E-10	1.88E-05
47.195	1.22E-06	1.88E-05	5.64E-10	1.88E-05
47.371	1.21E-06	1.88E-05	5.59E-10	1.88E-05
52.292	9.05E-07	1.91E-05	4.18E-10	1.91E-05
52.468	8.96E-07	1.91E-05	4.13E-10	1.91E-05
52.644	8.86E-07	1.91E-05	4.09E-10	1.91E-05
52.82	8.77E-07	1.91E-05	4.05E-10	1.91E-05
52.996	8.68E-07	1.91E-05	4.01E-10	1.91E-05
53.171	8.59E-07	1.91E-05	3.96E-10	1.91E-05
53.347	8.50E-07	1.91E-05	3.92E-10	1.91E-05
56.16	7.20E-07	1.93E-05	3.32E-10	1.93E-05
56.335	7.13E-07	1.93E-05	3.29E-10	1.93E-05
56.511	7.05E-07	1.93E-05	3.25E-10	1.93E-05
56.687	6.98E-07	1.93E-05	3.22E-10	1.93E-05
56.863	6.91E-07	1.93E-05	3.19E-10	1.93E-05
57.038	6.84E-07	1.93E-05	3.15E-10	1.93E-05
57.214	6.77E-07	1.93E-05	3.12E-10	1.93E-05
57.39	6.70E-07	1.93E-05	3.09E-10	1.93E-05
57.566	6.63E-07	1.93E-05	3.06E-10	1.93E-05
57.742	6.56E-07	1.93E-05	3.03E-10	1.93E-05
57.917	6.49E-07	1.94E-05	2.99E-10	1.94E-05
58.093	6.42E-07	1.94E-05	2.96E-10	1.94E-05
58.269	6.36E-07	1.94E-05	2.93E-10	1.94E-05
58.445	6.29E-07	1.94E-05	2.90E-10	1.94E-05
58.62	6.23E-07	1.94E-05	2.87E-10	1.94E-05
58.796	6.16E-07	1.94E-05	2.84E-10	1.94E-05
61.784	5.16E-07	1.95E-05	2.38E-10	1.95E-05
61.96	5.11E-07	1.95E-05	2.36E-10	1.95E-05
62.136	5.06E-07	1.95E-05	2.33E-10	1.95E-05
62.312	5.01E-07	1.95E-05	2.31E-10	1.95E-05
62.487	4.95E-07	1.95E-05	2.29E-10	1.95E-05
62.663	4.90E-07	1.95E-05	2.26E-10	1.95E-05
62.839	4.85E-07	1.95E-05	2.24E-10	1.95E-05
63.015	4.80E-07	1.95E-05	2.22E-10	1.95E-05
63.191	4.75E-07	1.95E-05	2.19E-10	1.95E-05
63.366	4.70E-07	1.95E-05	2.17E-10	1.95E-05
63.542	4.65E-07	1.95E-05	2.15E-10	1.95E-05
63.718	4.61E-07	1.95E-05	2.13E-10	1.95E-05
63.894	4.56E-07	1.95E-05	2.10E-10	1.95E-05
64.069	4.51E-07	1.95E-05	2.08E-10	1.95E-05
64.245	4.46E-07	1.96E-05	2.06E-10	1.96E-05
64.421	4.42E-07	1.96E-05	2.04E-10	1.96E-05
64.597	4.37E-07	1.96E-05	2.02E-10	1.96E-05
70.749	3.04E-07	1.97E-05	1.40E-10	1.97E-05
70.925	3.01E-07	1.97E-05	1.39E-10	1.97E-05
71.1	2.98E-07	1.97E-05	1.37E-10	1.97E-05
73.913	2.52E-07	1.97E-05	1.16E-10	1.97E-05
80.065	1.75E-07	1.98E-05	8.09E-11	1.98E-05
80.241	1.73E-07	1.98E-05	8.00E-11	1.98E-05
80.417	1.72E-07	1.98E-05	7.92E-11	1.98E-05
80.592	1.70E-07	1.98E-05	7.84E-11	1.98E-05
80.768	1.68E-07	1.98E-05	7.76E-11	1.98E-05
80.944	1.66E-07	1.98E-05	7.68E-11	1.98E-05
81.12	1.65E-07	1.98E-05	7.60E-11	1.98E-05
81.295	1.63E-07	1.98E-05	7.52E-11	1.98E-05
81.471	1.61E-07	1.98E-05	7.44E-11	1.98E-05
81.647	1.60E-07	1.98E-05	7.36E-11	1.98E-05
81.823	1.58E-07	1.98E-05	7.29E-11	1.98E-05
81.999	1.56E-07	1.98E-05	7.21E-11	1.98E-05
82.174	1.55E-07	1.98E-05	7.14E-11	1.98E-05
82.35	1.53E-07	1.98E-05	7.06E-11	1.98E-05
82.526	1.52E-07	1.98E-05	6.99E-11	1.98E-05
82.702	1.50E-07	1.99E-05	6.92E-11	1.98E-05
82.877	1.48E-07	1.99E-05	6.85E-11	1.99E-05
83.053	1.47E-07	1.99E-05	6.78E-11	1.99E-05
83.229	1.45E-07	1.99E-05	6.71E-11	1.99E-05
86.393	1.21E-07	1.99E-05	5.56E-11	1.99E-05
86.569	1.19E-07	1.99E-05	5.51E-11	1.99E-05
86.745	1.18E-07	1.99E-05	5.45E-11	1.99E-05

APPENDIX 2 – CHAPTER 4

2.1 Amaranth oxidation products with chlorine dioxide .

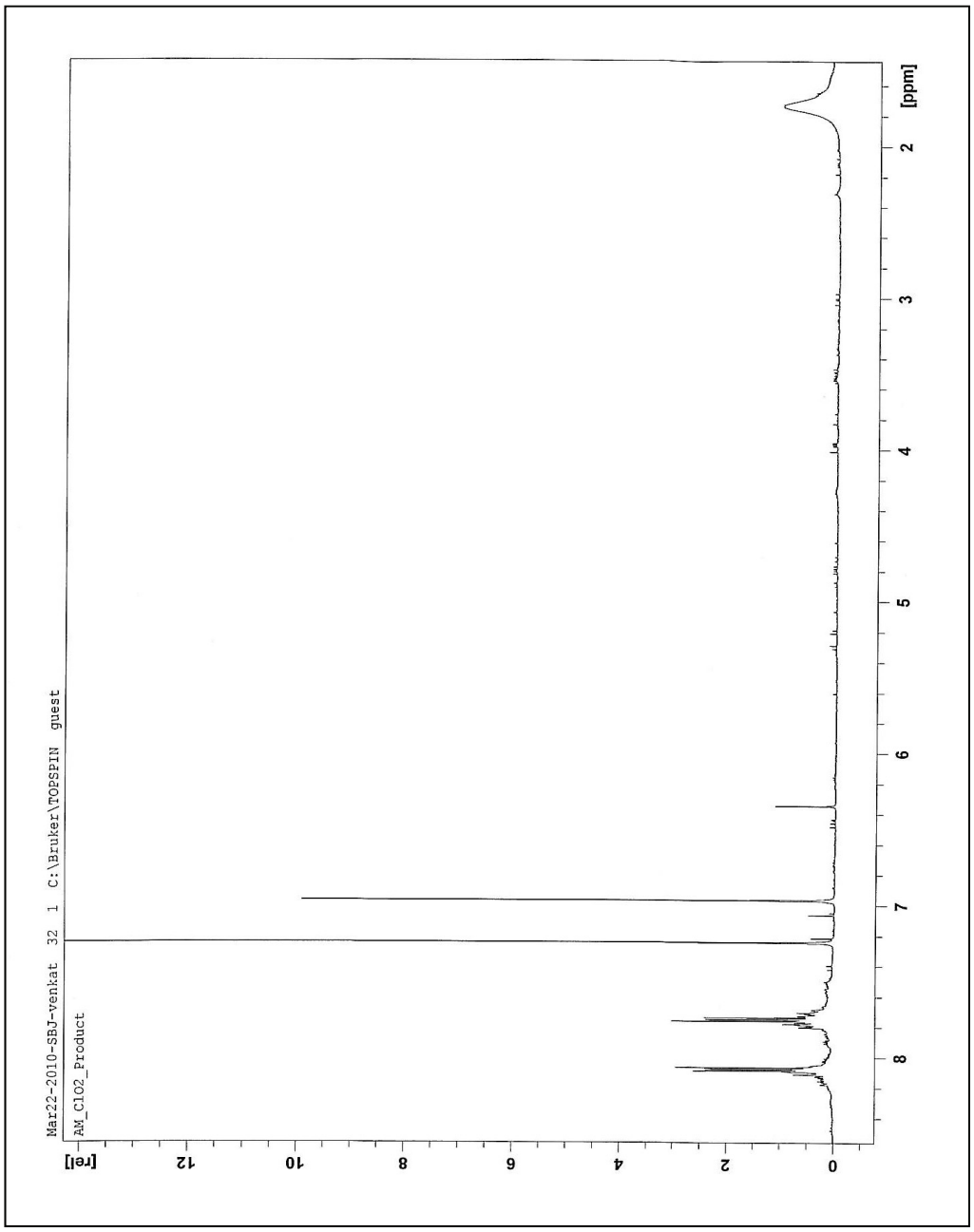

Figure 2.1.1 ^{1}H NMR spectrum of amaranth oxidation product P_2 (1,4 napthalenedione) with chlorine dioxide.

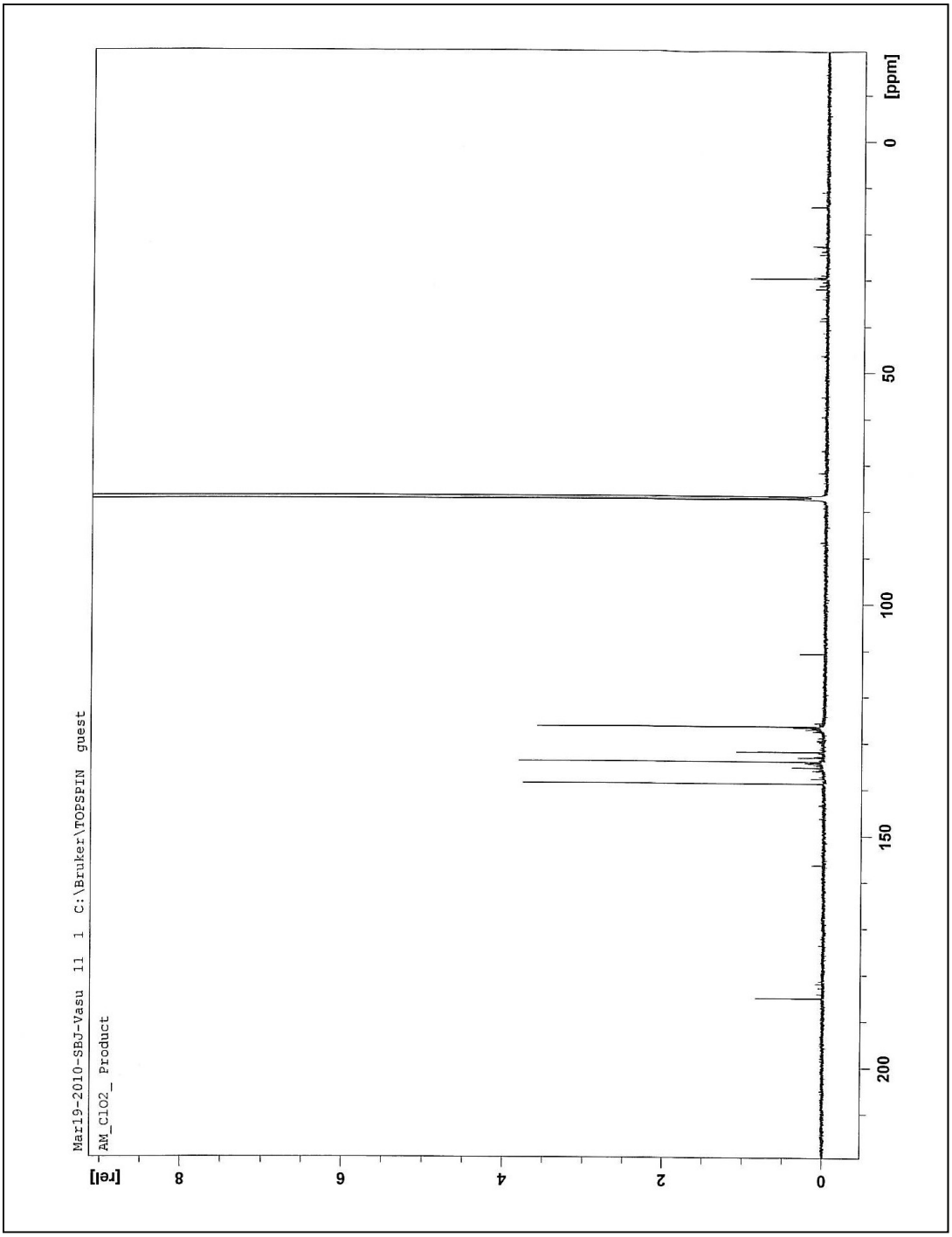

Figure 2.1.2 ^{13}C NMR spectrum of amaranth oxidation product product P_2 **(**1,4 napthalenedione**)** with chlorine dioxide.

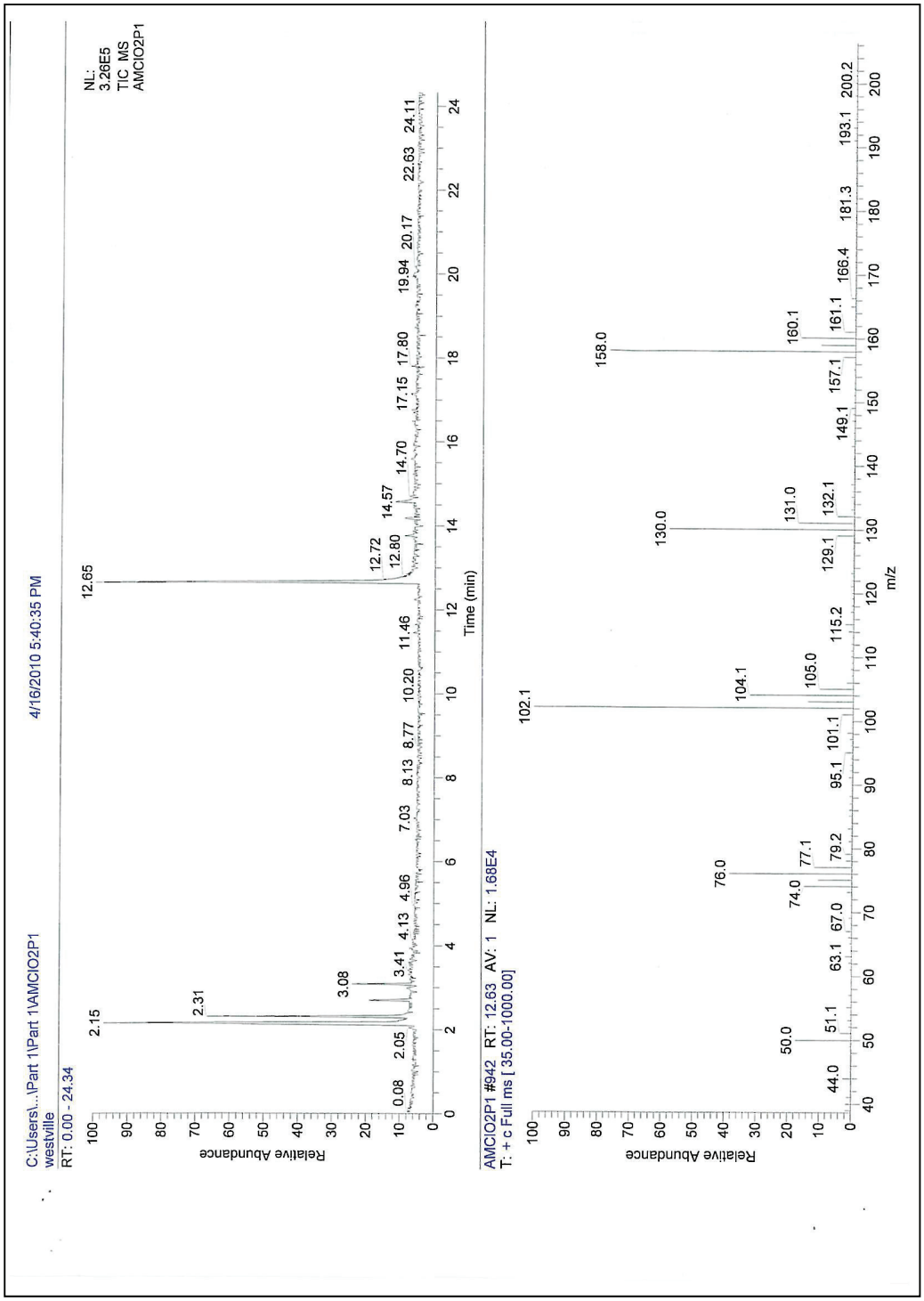

Figure 2.1.3 GC-MS spectrum of amaranth oxidation product P_2 (1,4 napthalenedione) with chlorine dioxide.

Table 2.1 Amaranth - chlorine dioxide experimental and simulated curves-compiled data.

TIME	E1	Time	E2	Time	E3	TIME	S1	Time	S2	Time	S3
0	7.00E-05	0.0019	6.21E-05	0.002	5.96E-05	0	7.00E-05	0.0146	6.70E-05	0.005	7.13E-05
0.018	6.33E-05	0.0215	5.78E-05	0.021	4.95E-05	0.0136	6.12E-05	0.0635	5.87E-05	0.054	6.05E-05
0.021	6.19E-05	0.0254	5.68E-05	0.025	4.78E-05	0.0175	5.89E-05	0.0732	5.72E-05	0.063	5.9E-05
0.025	6.06E-05	0.0293	5.58E-05	0.029	4.62E-05	0.0215	5.68E-05	0.083	5.59E-05	0.073	5.75E-05
0.029	5.94E-05	0.0332	5.48E-05	0.033	4.46E-05	0.0254	5.48E-05	0.0928	5.46E-05	0.083	5.61E-05
0.033	5.82E-05	0.0371	5.38E-05	0.037	4.31E-05	0.0293	5.29E-05	0.1025	5.33E-05	0.093	5.48E-05
0.037	5.70E-05	0.041	5.29E-05	0.041	4.17E-05	0.0332	5.11E-05	0.1123	5.21E-05	0.103	5.37E-05
0.041	5.59E-05	0.0449	5.2E-05	0.045	4.04E-05	0.0371	4.94E-05	0.1221	5.10E-05	0.112	5.25E-05
0.045	5.48E-05	0.0488	5.1E-05	0.049	3.91E-05	0.041	4.77E-05	0.1319	4.99E-05	0.122	5.14E-05
0.049	5.37E-05	0.0527	5.01E-05	0.053	3.79E-05	0.0449	4.61E-05	0.1416	4.89E-05	0.132	5.03E-05
0.053	5.27E-05	0.0566	4.92E-05	0.057	3.67E-05	0.0488	4.46E-05	0.1514	4.79E-05	0.142	4.93E-05
0.057	5.17E-05	0.0605	4.84E-05	0.06	3.55E-05	0.0527	4.32E-05	0.1612	4.69E-05	0.151	4.84E-05
0.06	5.08E-05	0.0644	4.77E-05	0.064	3.45E-05	0.0566	4.18E-05	0.1709	4.60E-05	0.161	4.74E-05
0.092	4.41E-05	0.0956	4.19E-05	0.096	2.72E-05	0.0878	3.26E-05	0.2491	3.97E-05	0.239	4.11E-05
0.096	4.33E-05	0.0995	4.12E-05	0.1	2.64E-05	0.0917	3.17E-05	0.2589	3.90E-05	0.249	4.04E-05
0.1	4.26E-05	0.1034	4.06E-05	0.103	2.56E-05	0.0956	3.07E-05	0.2686	3.83E-05	0.259	3.97E-05
0.103	4.19E-05	0.1073	4E-05	0.107	2.49E-05	0.0995	2.99E-05	0.2784	3.77E-05	0.269	3.91E-05
0.107	4.12E-05	0.1112	3.93E-05	0.111	2.42E-05	0.1034	2.90E-05	0.2882	3.71E-05	0.278	3.84E-05
0.228	2.65E-05	0.2323	2.52E-05	0.232	1.11E-05	0.2245	1.27E-05	0.5911	2.44E-05	0.581	2.48E-05
0.232	2.62E-05	0.2362	2.49E-05	0.236	1.08E-05	0.2284	1.24E-05	0.6009	2.42E-05	0.591	2.45E-05
0.236	2.59E-05	0.2401	2.46E-05	0.24	1.06E-05	0.2323	1.21E-05	0.6106	2.39E-05	0.601	2.42E-05
0.24	2.56E-05	0.244	2.43E-05	0.244	1.04E-05	0.2362	1.18E-05	0.6204	2.36E-05	0.611	2.4E-05
0.244	2.53E-05	0.2479	2.39E-05	0.248	1.01E-05	0.2401	1.15E-05	0.6302	2.34E-05	0.62	2.37E-05
0.248	2.49E-05	0.2518	2.36E-05	0.252	9.92E-06	0.244	1.13E-05	0.6399	2.31E-05	0.63	2.34E-05
0.252	2.46E-05	0.2557	2.33E-05	0.256	9.71E-06	0.2479	1.10E-05	0.6497	2.29E-05	0.64	2.31E-05
0.256	2.43E-05	0.2596	2.3E-05	0.26	9.50E-06	0.2518	1.07E-05	0.6595	2.26E-05	0.65	2.28E-05
0.26	2.41E-05	0.2635	2.27E-05	0.264	9.29E-06	0.2557	1.05E-05	0.6692	2.24E-05	0.659	2.26E-05
0.264	2.38E-05	0.2674	2.24E-05	0.267	9.1E-06	0.2596	1.02E-05	0.679	2.22E-05	0.669	2.23E-05
0.267	2.35E-05	0.2713	2.21E-05	0.271	8.91E-06	0.2635	9.97E-06	0.6888	2.19E-05	0.679	2.2E-05
0.271	2.32E-05	0.2752	2.18E-05	0.275	8.70E-06	0.2674	9.73E-06	0.6986	2.17E-05	0.689	2.18E-05
0.275	2.29E-05	0.2791	2.16E-05	0.279	8.53E-06	0.2713	9.50E-06	0.7083	2.15E-05	0.699	2.15E-05
0.279	2.27E-05	0.283	2.13E-05	0.283	8.36E-06	0.2752	9.27E-06	0.7181	2.13E-05	0.708	2.13E-05
0.435	1.48E-05	0.4392	1.3E-05	0.439	4.03E-06	0.4314	3.67E-06	1.1089	1.50E-05	1.099	1.4E-05
0.439	1.46E-05	0.4431	1.29E-05	0.443	3.96E-06	0.4353	3.59E-06	1.1187	1.49E-05	1.109	1.39E-05
0.611	9.75E-06	0.6149	7.94E-06	0.615	2.32E-06	0.6071	1.35E-06	1.5486	1.10E-05	1.539	9.56E-06
0.701	8.02E-06	0.7047	6.33E-06	0.705	1.93E-06	0.6968	8.14E-07	1.7733	9.60E-06	1.764	8.1E-06
0.705	7.95E-06	0.7086	6.26E-06	0.709	1.92E-06	0.7008	7.96E-07	1.7831	9.55E-06	1.773	8.05E-06
0.752	7.20E-06	0.7554	5.59E-06	0.755	1.77E-06	0.7476	6.13E-07	1.9003	8.94E-06	1.891	7.42E-06

0.755	7.15E-06	0.7593	5.55E-06	0.759	1.77E-06	0.7515	6.00E-07	1.9101	8.89E-06	1.9	7.38E-06
0.759	7.09E-06	0.7632	5.5E-06	0.763	1.76E-06	0.7554	5.87E-07	1.9199	8.84E-06	1.91	7.34E-06
0.763	7.03E-06	0.7671	5.45E-06	0.767	1.76E-06	0.7593	5.74E-07	1.9297	8.79E-06	1.92	7.29E-06
0.841	6.00E-06	0.8452	4.56E-06	0.845	1.61E-06	0.8374	3.71E-07	2.1251	7.93E-06	2.115	6.44E-06
0.845	5.95E-06	0.8491	4.53E-06	0.849	1.62E-06	0.8413	3.63E-07	2.1348	7.89E-06	2.125	6.41E-06
0.935	4.98E-06	0.9389	3.77E-06	0.939	1.50E-06	0.9311	2.21E-07	2.3596	7.05E-06	2.35	5.64E-06
0.939	4.94E-06	0.9428	3.75E-06	0.943	1.51E-06	0.935	2.16E-07	2.3693	7.02E-06	2.36	5.6E-06
1.103	3.62E-06	1.1068	2.82E-06	1.107	1.40E-06	1.099	8.69E-08	2.7797	5.82E-06	2.77	4.58E-06
1.107	3.59E-06	1.1107	2.79E-06	1.111	1.41E-06	1.1029	8.50E-08	2.7895	5.79E-06	2.78	4.55E-06
1.111	3.57E-06	1.1146	2.77E-06	1.115	1.40E-06	1.1068	8.32E-08	2.7992	5.77E-06	2.79	4.55E-06
1.716	1.21E-06	1.7197	1.6E-06	1.72	1.32E-06	1.7119	2.94E-09	4.3137	3.25E-06	4.304	3E-06
1.72	1.21E-06	1.7236	1.61E-06	1.724	1.34E-06	1.7158	2.88E-09	4.3235	3.24E-06	4.314	2.99E-06
1.724	1.20E-06	1.7275	1.6E-06	1.728	1.32E-06	1.7197	2.81E-09	4.3332	3.23E-06	4.324	2.99E-06
1.728	1.19E-06	1.7314	1.59E-06	1.731	1.34E-06	1.7236	2.75E-09	4.343	3.22E-06	4.333	3E-06
1.731	1.18E-06	1.7353	1.59E-06	1.735	1.33E-06	1.7275	2.70E-09	4.3528	3.21E-06	4.343	2.97E-06
1.888	9.04E-07	1.8915	1.52E-06	1.892	1.33E-06	1.8837	1.14E-09	4.7436	2.82E-06	4.734	2.84E-06
1.892	8.98E-07	1.8954	1.51E-06	1.895	1.32E-06	1.8876	1.12E-09	4.7534	2.81E-06	4.744	2.83E-06
1.931	8.40E-07	1.9344	1.48E-06	1.934	1.32E-06	1.9266	9.00E-10	4.8511	2.73E-06	4.841	2.8E-06
1.934	8.35E-07	1.9383	1.48E-06	1.938	1.33E-06	1.9305	8.81E-10	4.8609	2.72E-06	4.851	2.8E-06
1.938	8.29E-07	1.9422	1.48E-06	1.942	1.33E-06	1.9344	8.62E-10	4.8706	2.71E-06	4.861	2.79E-06
1.942	8.24E-07	1.9461	1.49E-06	1.946	1.32E-06	1.9383	8.44E-10	4.8804	2.70E-06	4.871	2.8E-06
1.946	8.18E-07	1.95	1.48E-06	1.95	1.32E-06	1.9422	8.26E-10	4.8902	2.69E-06	4.88	2.79E-06
1.981	7.71E-07	1.9852	1.48E-06	1.985	1.31E-06	1.9774	6.80E-10	4.9781	2.62E-06	4.968	2.76E-06

Table 2.2 Amaranth -chlorine dioxide intermediate and product formation-compiled data.

TIME	**AM-**	P1	I1	P2
0	**7.00E-05**	4.13E-13	2.37E-11	2.42E-11
5.77E-08	**7.00E-05**	2.38E-06	6.75E-10	2.38E-06
5.84E-03	6.76E-05	3.89E-06	6.58E-10	3.89E-06
9.74E-03	6.61E-05	5.34E-06	6.43E-10	5.34E-06
0.013644	6.47E-05	6.74E-06	6.28E-10	6.74E-06
0.017548	6.33E-05	8.09E-06	6.14E-10	8.09E-06
0.021452	6.19E-05	9.39E-06	6.00E-10	9.39E-06
0.025356	6.06E-05	1.06E-05	5.87E-10	1.06E-05
0.02926	5.94E-05	1.18E-05	5.74E-10	1.18E-05
0.033164	5.82E-05	1.30E-05	5.62E-10	1.30E-05
0.037068	5.70E-05	1.41E-05	5.51E-10	1.41E-05
0.040972	5.59E-05	1.52E-05	5.39E-10	1.52E-05
0.044876	5.48E-05	1.63E-05	5.28E-10	1.63E-05
0.04878	5.37E-05	1.73E-05	5.18E-10	1.73E-05
0.052684	5.27E-05	1.83E-05	5.07E-10	1.83E-05
0.056588	5.17E-05	1.92E-05	4.98E-10	1.92E-05
0.060492	5.08E-05	2.02E-05	4.88E-10	2.02E-05
0.064396	4.98E-05	2.11E-05	4.79E-10	2.11E-05
0.0683	4.89E-05	2.19E-05	4.70E-10	2.19E-05
0.072204	4.81E-05	2.28E-05	4.61E-10	2.28E-05
0.076108	4.72E-05	2.36E-05	4.53E-10	2.36E-05
0.080012	4.64E-05	2.44E-05	4.44E-10	2.44E-05
0.083916	4.56E-05	2.52E-05	4.37E-10	2.52E-05
0.08782	4.48E-05	2.59E-05	4.29E-10	2.59E-05
0.091724	4.41E-05	2.67E-05	4.21E-10	2.67E-05
0.095628	4.33E-05	2.74E-05	4.14E-10	2.74E-05
0.099532	4.26E-05	2.81E-05	4.07E-10	2.81E-05
0.10344	4.19E-05	2.88E-05	4.00E-10	2.88E-05
0.10734	4.12E-05	2.94E-05	3.94E-10	2.94E-05
0.11124	4.06E-05	3.01E-05	3.87E-10	3.01E-05
0.11515	3.99E-05	3.07E-05	3.81E-10	3.07E-05
0.11905	3.93E-05	3.13E-05	3.75E-10	3.13E-05
0.12296	3.87E-05	3.19E-05	3.69E-10	3.19E-05
0.12686	3.81E-05	3.25E-05	3.63E-10	3.25E-05
0.13076	3.75E-05	3.30E-05	3.57E-10	3.30E-05
0.13467	3.70E-05	3.36E-05	3.51E-10	3.36E-05
0.162	3.33E-05	3.71E-05	3.16E-10	3.71E-05
0.21275	2.79E-05	4.24E-05	2.64E-10	4.24E-05
0.21665	2.76E-05	4.28E-05	2.60E-10	4.28E-05
0.22056	2.72E-05	4.31E-05	2.57E-10	4.31E-05
0.22446	2.69E-05	4.35E-05	2.53E-10	4.34E-05
0.22836	2.65E-05	4.38E-05	2.50E-10	4.38E-05
0.23227	2.62E-05	4.41E-05	2.47E-10	4.41E-05
0.23617	2.59E-05	4.44E-05	2.44E-10	4.44E-05
0.24008	2.56E-05	4.47E-05	2.41E-10	4.47E-05
0.24398	2.53E-05	4.51E-05	2.38E-10	4.51E-05
0.38452	1.68E-05	5.33E-05	1.57E-10	5.33E-05
0.38843	1.67E-05	5.35E-05	1.56E-10	5.35E-05
0.39233	1.65E-05	5.37E-05	1.54E-10	5.37E-05
0.39624	1.63E-05	5.38E-05	1.52E-10	5.38E-05
0.40014	1.62E-05	5.40E-05	1.51E-10	5.40E-05
0.40404	1.60E-05	5.42E-05	1.49E-10	5.42E-05
0.40795	1.58E-05	5.43E-05	1.48E-10	5.43E-05
0.41185	1.57E-05	5.45E-05	1.46E-10	5.45E-05
0.41576	1.55E-05	5.46E-05	1.45E-10	5.46E-05
0.61486	9.66E-06	6.04E-05	8.96E-11	6.04E-05
0.61876	9.58E-06	6.05E-05	8.88E-11	6.05E-05
0.62267	9.50E-06	6.06E-05	8.80E-11	6.06E-05
0.62657	9.41E-06	6.07E-05	8.72E-11	6.07E-05
0.63048	9.33E-06	6.07E-05	8.65E-11	6.07E-05
0.63438	9.25E-06	6.08E-05	8.57E-11	6.08E-05
0.80616	6.44E-06	6.36E-05	5.94E-11	6.36E-05
0.81006	6.39E-06	6.37E-05	5.90E-11	6.37E-05
0.81396	6.34E-06	6.37E-05	5.85E-11	6.37E-05
0.81787	6.29E-06	6.38E-05	5.80E-11	6.38E-05
0.82177	6.24E-06	6.38E-05	5.76E-11	6.38E-05
0.82568	6.19E-06	6.39E-05	5.71E-11	6.39E-05
0.82958	6.14E-06	6.39E-05	5.67E-11	6.39E-05
0.83348	6.09E-06	6.40E-05	5.62E-11	6.40E-05
0.83739	6.04E-06	6.40E-05	5.58E-11	6.40E-05
0.84129	6.00E-06	6.40E-05	5.53E-11	6.40E-05
0.8452	5.95E-06	6.41E-05	5.49E-11	6.41E-05
0.8491	5.90E-06	6.41E-05	5.45E-11	6.41E-05
0.853	5.86E-06	6.42E-05	5.40E-11	6.42E-05
0.98574	4.52E-06	6.55E-05	4.16E-11	6.55E-05
0.98964	4.48E-06	6.56E-05	4.13E-11	6.55E-05
0.99355	4.45E-06	6.56E-05	4.10E-11	6.56E-05

1.2161	2.94E-06	6.71E-05	2.69E-11	6.71E-05
1.22	2.91E-06	6.71E-05	2.68E-11	6.71E-05
1.2239	2.89E-06	6.71E-05	2.66E-11	6.71E-05
1.2278	2.87E-06	6.71E-05	2.64E-11	6.71E-05
1.2317	2.85E-06	6.72E-05	2.62E-11	6.72E-05
1.2356	2.83E-06	6.72E-05	2.60E-11	6.72E-05
1.2395	2.81E-06	6.72E-05	2.58E-11	6.72E-05
1.2434	2.79E-06	6.72E-05	2.56E-11	6.72E-05
1.2473	2.77E-06	6.72E-05	2.54E-11	6.72E-05
1.2512	2.75E-06	6.73E-05	2.53E-11	6.73E-05
1.2551	2.73E-06	6.73E-05	2.51E-11	6.73E-05
1.259	2.71E-06	6.73E-05	2.49E-11	6.73E-05
1.2903	2.57E-06	6.75E-05	2.35E-11	6.75E-05
1.2942	2.55E-06	6.75E-05	2.34E-11	6.75E-05
1.2981	2.53E-06	6.75E-05	2.32E-11	6.75E-05
1.302	2.51E-06	6.75E-05	2.30E-11	6.75E-05
1.3059	2.49E-06	6.75E-05	2.29E-11	6.75E-05
1.3098	2.48E-06	6.75E-05	2.27E-11	6.75E-05

1.3137	2.46E-06	6.76E-05	2.26E-11	6.76E-05
1.3176	2.44E-06	6.76E-05	2.24E-11	6.76E-05
1.3215	2.43E-06	6.76E-05	2.22E-11	6.76E-05
1.665	1.32E-06	6.87E-05	1.21E-11	6.87E-05
1.6689	1.32E-06	6.87E-05	1.20E-11	6.87E-05
1.6728	1.31E-06	6.87E-05	1.20E-11	6.87E-05
1.6767	1.30E-06	6.87E-05	1.19E-11	6.87E-05
1.6807	1.29E-06	6.87E-05	1.18E-11	6.87E-05
1.7002	1.25E-06	6.88E-05	1.14E-11	6.88E-05
1.7041	1.24E-06	6.88E-05	1.13E-11	6.88E-05
1.7861	1.08E-06	6.89E-05	9.82E-12	6.89E-05
1.79	1.07E-06	6.89E-05	9.76E-12	6.89E-05
1.7939	1.06E-06	6.89E-05	9.69E-12	6.89E-05
1.9774	7.76E-07	6.92E-05	7.08E-12	6.92E-05
1.9813	7.71E-07	6.92E-05	7.03E-12	6.92E-05
1.9852	7.66E-07	6.92E-05	6.99E-12	6.92E-05
1.9891	7.61E-07	6.92E-05	6.94E-12	6.92E-05
1.993	7.56E-07	6.92E-05	6.90E-12	6.92E-05

2.2 Brilliant blue-R oxidation products with chlorine dioxide.

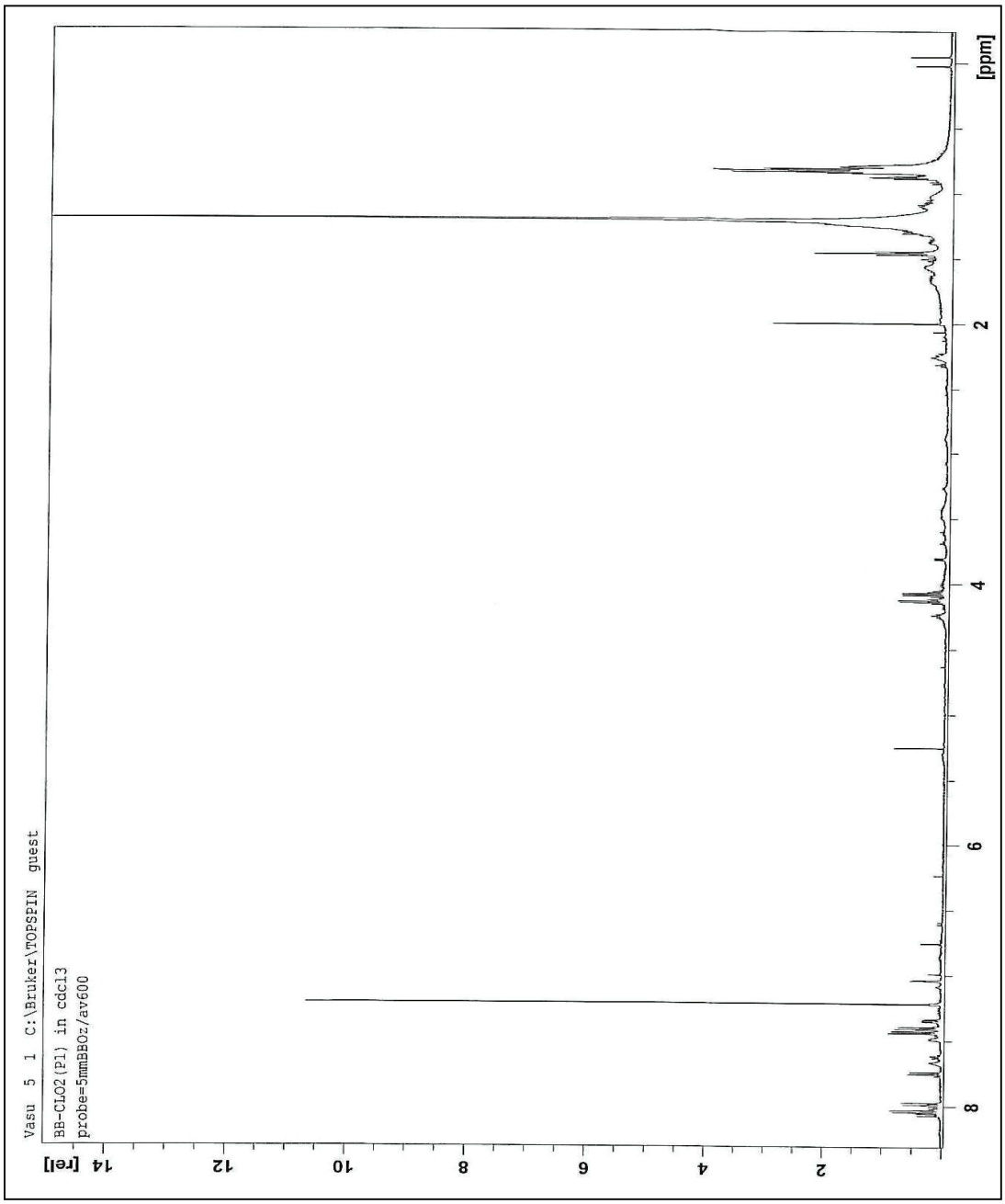

Figure 2.1.4 ^{1}H NMR spectrum of brilliant blue-R major oxidation product P_1 (4-(4- ethoxy-phenyl amino)-benzoic acid) with chlorine oxide

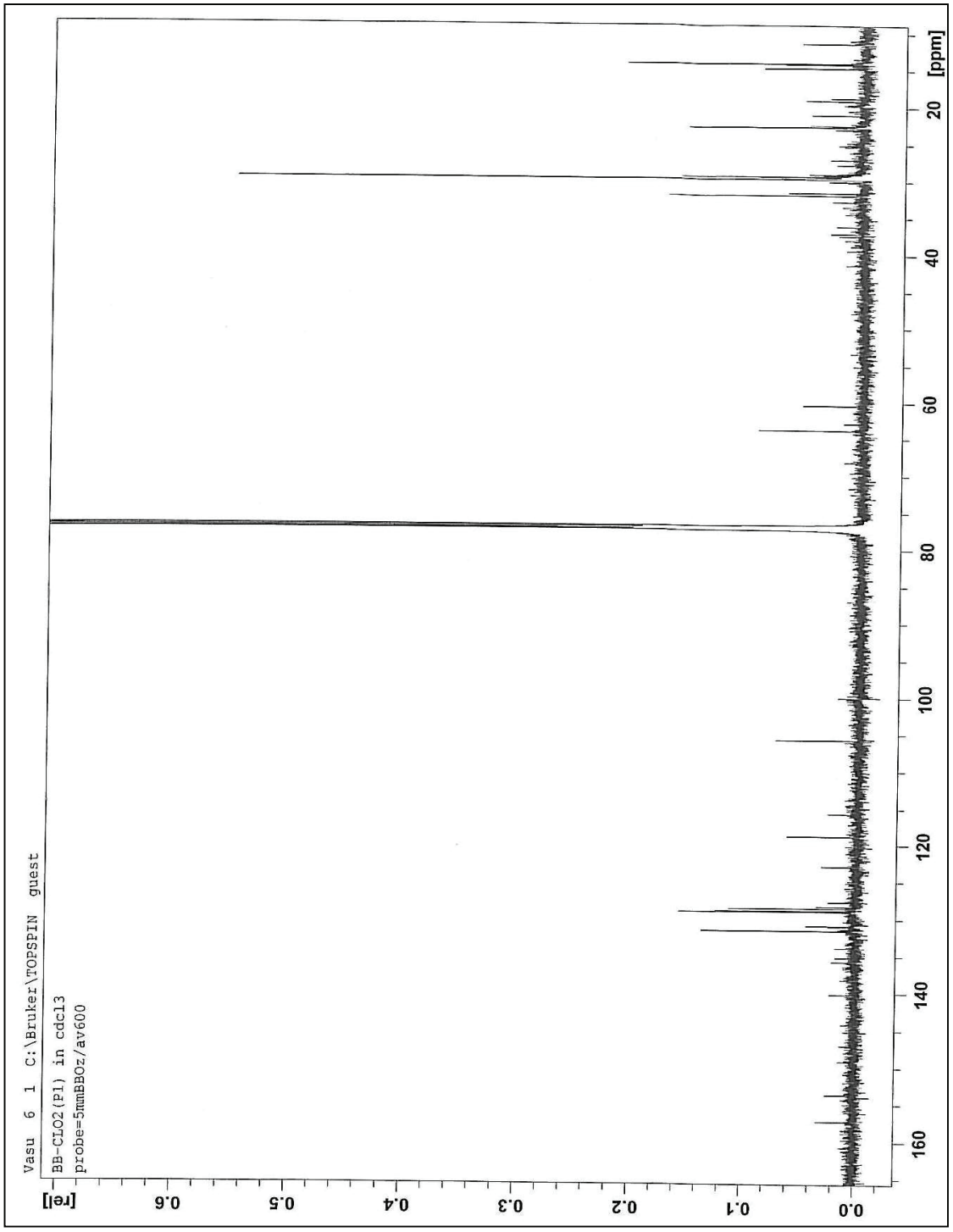

Figure 2.1.5 ^{13}C NMR spectrum of brilliant blue-R major oxidation product P_1 4-(4- ethoxy-phenyl amino)-benzoic acid) with chlorine oxide.

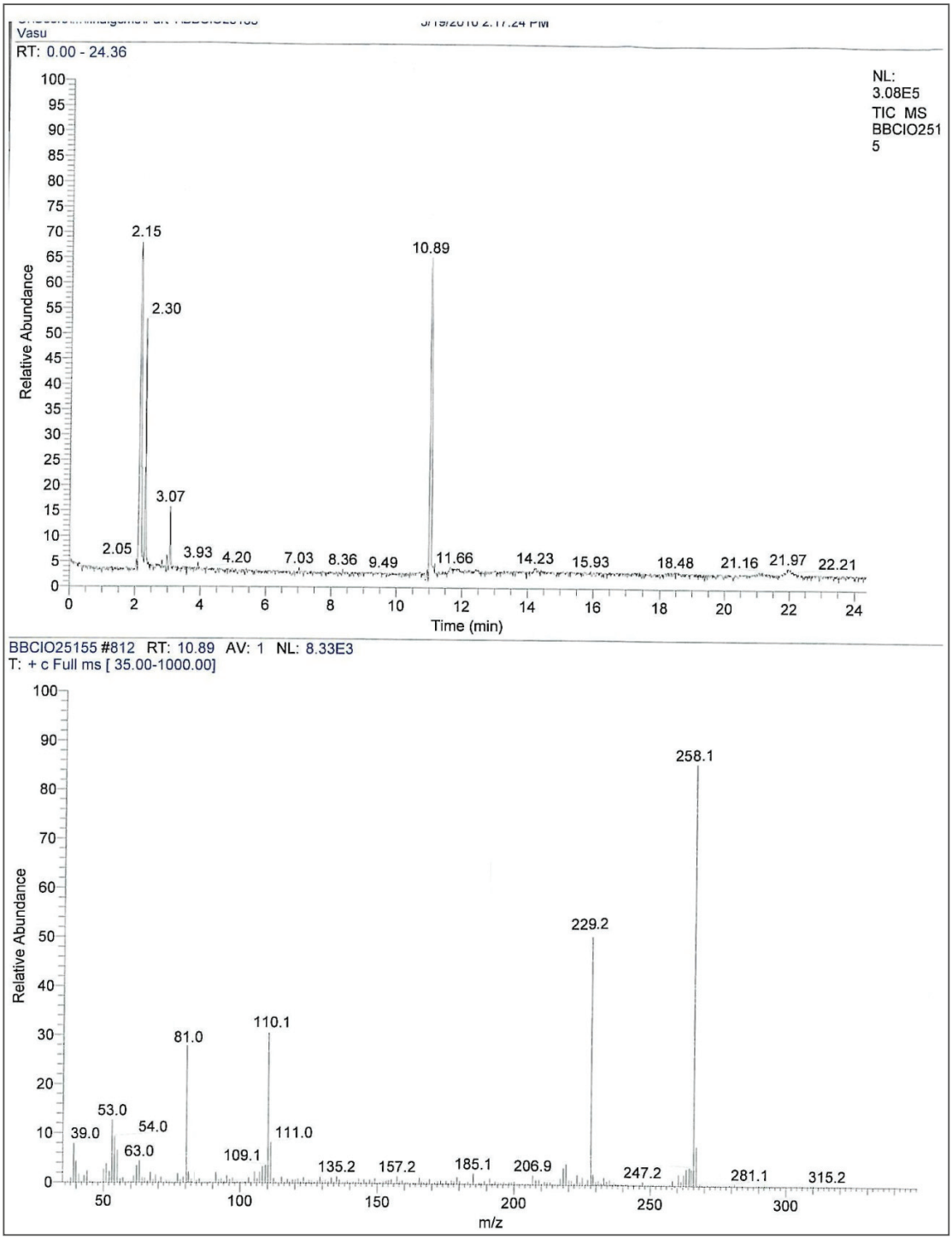

Figure 2.1.6 GC-MS spectrum of brilliant blue-R major oxidation product P_1 4-(4-ethoxy-phenylamino)-benzoic acid) with chlorine oxide.

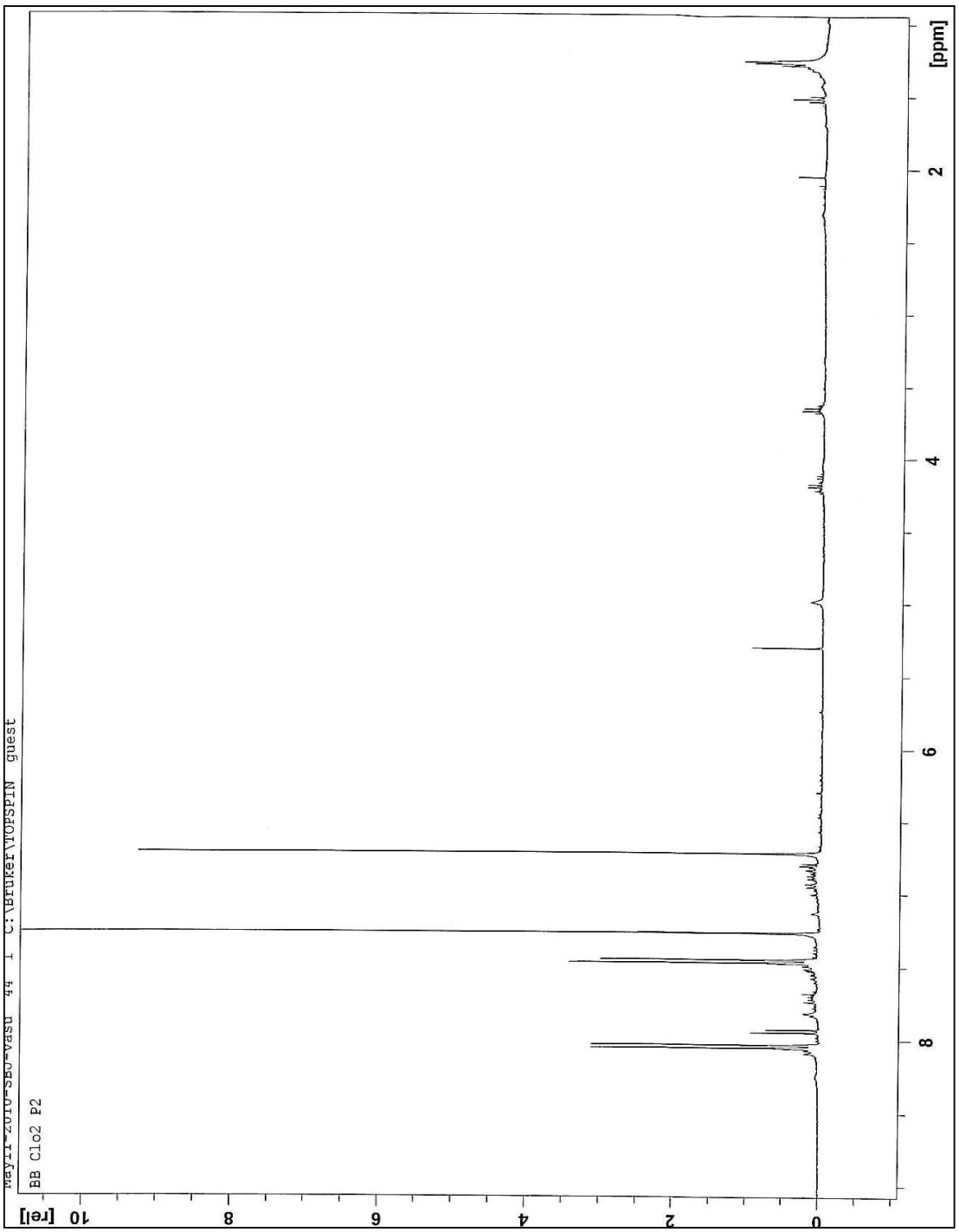

Figure 2.1.7 ^{1}H NMR spectrum of brilliant blue-R major oxidation product P_2 (N-(4- ethoxy-phenyl-hydroxyl amine) with chlorine oxide.

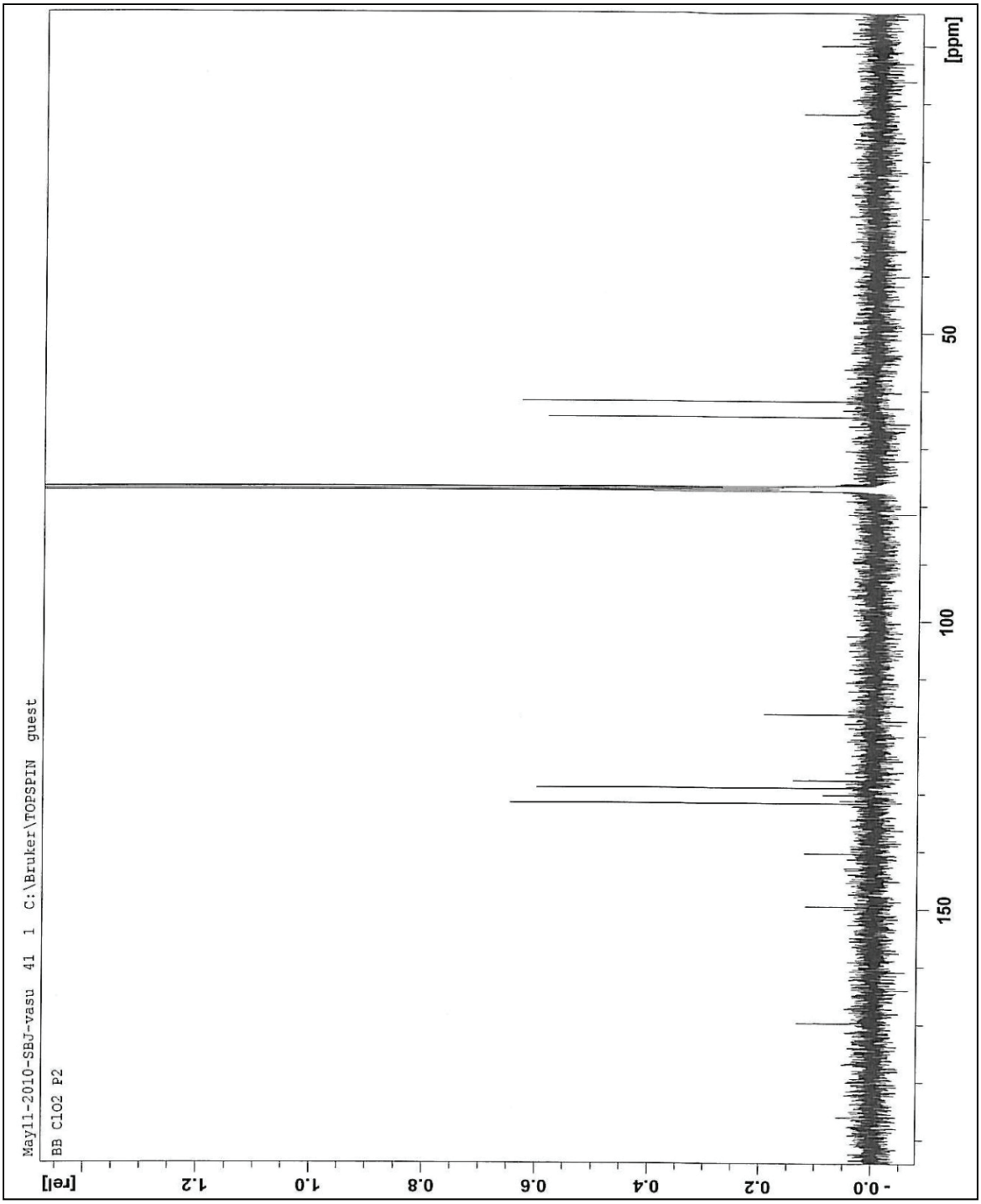

Figure 2.1.8 ^{13}C NMR spectrum of brilliant blue-R major oxidation product P_2 (N-(4- ethoxy-phenyl-hydroxyl amine) with chlorine oxide.

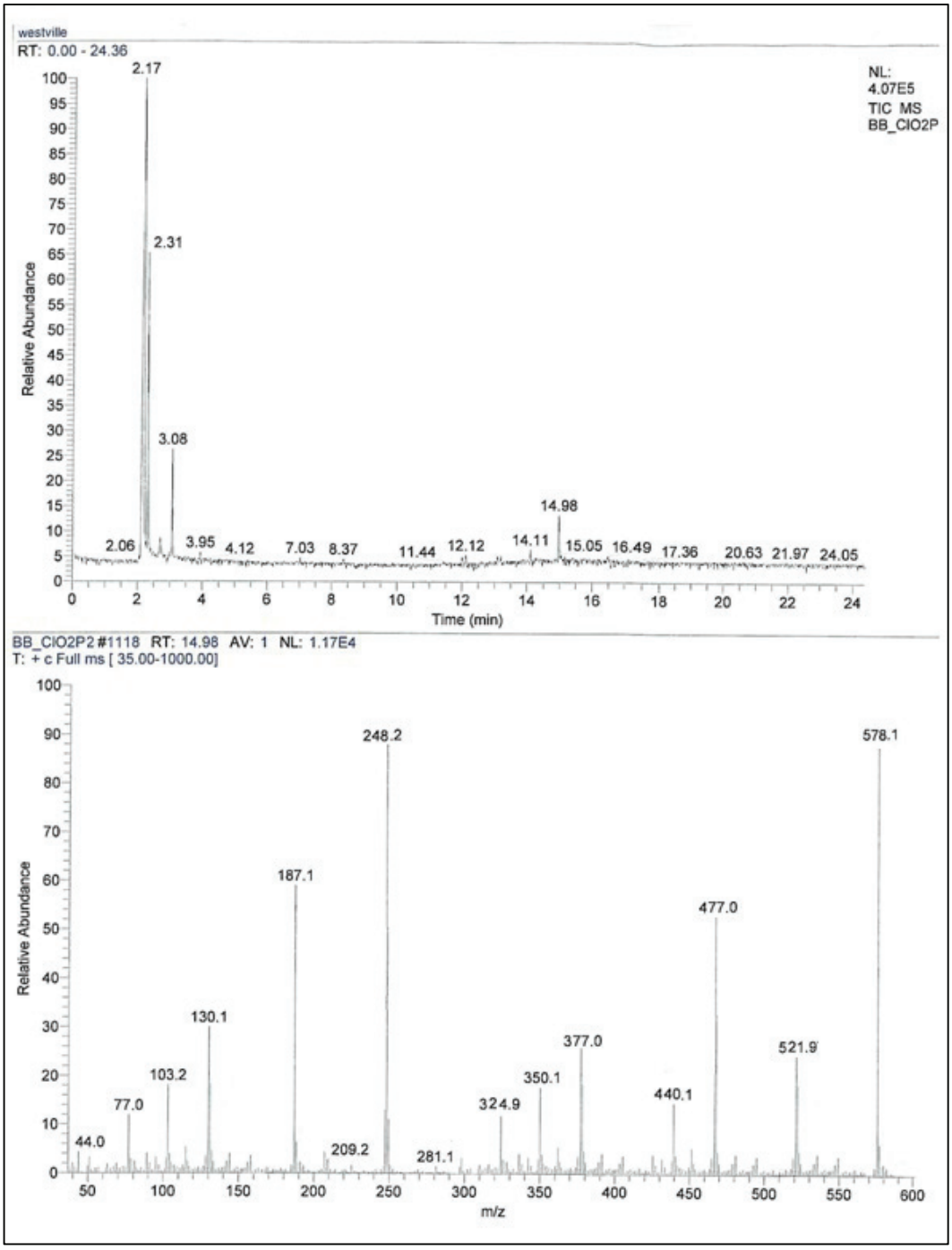

Figure 2.1.9 GC-MS spectrum of brilliant blue-R major oxidation product P_2 (N-(4- ethoxy-phenyl-hydroxyl amine) with chlorine oxide.

Table 2.3 Brilliant blue-R chlorine dioxide experimental and simulated curves- compiled data.

Time	E1	S1	Time	E2	S2	Time	E3	S3
0.004834	4.95E-05	4.86E-05	0.009664	6.17E-05	6.81777E-05	0.019327	4.77357E-05	6.82E-05
0.014605	4.76E-05	4.76E-05	0.029194	5.2E-05	5.18738E-05	0.058389	4.63358E-05	5.19E-05
0.024376	4.57E-05	4.67E-05	0.048725	4.96E-05	4.73146E-05	0.09745	4.50185E-05	4.73E-05
0.034146	4.47E-05	4.59E-05	0.068256	4.96E-05	4.55748E-05	0.13651	4.37765E-05	4.56E-05
0.043917	4.4E-05	4.50E-05	0.087786	4.96E-05	4.42709E-05	0.17557	4.26036E-05	4.43E-05
0.053688	4.33E-05	4.42E-05	0.10732	4.89E-05	4.30699E-05	0.21463	4.14937E-05	4.31E-05
0.063458	4.27E-05	4.34E-05	0.12685	4.78E-05	4.19942E-05	0.2537	4.04425E-05	4.2E-05
0.073229	4.22E-05	4.27E-05	0.14638	4.65E-05	4.10301E-05	0.29276	3.94451E-05	4.1E-05
0.083	4.17E-05	4.19E-05	0.16591	4.56E-05	0.0000401	0.33182	3.84973E-05	4.01E-05
0.09277	4.1E-05	4.12E-05	0.18544	4.46E-05	3.92408E-05	0.37088	3.75956E-05	3.92E-05
0.10254	4.05E-05	4.05E-05	0.20497	4.35E-05	3.83981E-05	0.40994	3.67367E-05	3.84E-05
0.26864	3.28E-05	3.12E-05	0.53699	2.88E-05	2.62757E-05	1.074	2.65557E-05	2.63E-05
0.27841	3.23E-05	3.08E-05	0.55652	2.8E-05	2.56845E-05	1.113	2.61337E-05	2.57E-05
0.36635	2.87E-05	2.73E-05	0.7323	2.31E-05	2.1068E-05	1.4646	2.28778E-05	2.11E-05
0.37612	2.83E-05	2.70E-05	0.75183	2.27E-05	2.06311E-05	1.5037	2.2567E-05	2.06E-05
0.38589	2.79E-05	2.66E-05	0.77136	2.23E-05	2.02184E-05	1.5427	2.22639E-05	2.02E-05
0.39566	2.75E-05	2.63E-05	0.79089	2.19E-05	1.98641E-05	1.5818	2.19698E-05	1.99E-05
0.40543	2.71E-05	2.60E-05	0.81042	2.15E-05	1.95068E-05	1.6208	2.16827E-05	1.95E-05
0.4152	2.67E-05	2.56E-05	0.82995	2.11E-05	1.91573E-05	1.6599	2.14032E-05	1.92E-05
0.42497	2.63E-05	2.53E-05	0.84948	2.08E-05	1.88126E-05	1.699	2.11316E-05	1.88E-05
0.43474	2.6E-05	2.50E-05	0.86901	2.05E-05	0.0000185	1.738	2.08662E-05	1.85E-05
0.44451	2.56E-05	2.47E-05	0.88854	2.01E-05	1.82233E-05	1.7771	2.06082E-05	1.82E-05
0.45429	2.53E-05	2.44E-05	0.90807	1.98E-05	1.79369E-05	1.8161	2.03559E-05	1.79E-05
0.46406	2.49E-05	2.41E-05	0.9276	1.95E-05	1.76583E-05	1.8552	2.01098E-05	1.77E-05
0.47383	2.45E-05	2.39E-05	0.94714	1.92E-05	1.73689E-05	1.8943	1.98702E-05	1.74E-05
0.4836	2.42E-05	2.36E-05	0.96667	1.89E-05	1.71087E-05	1.9333	1.96357E-05	1.71E-05
0.49337	2.38E-05	2.33E-05	0.9862	1.86E-05	1.68544E-05	1.9724	1.94068E-05	1.69E-05
0.6497	1.92E-05	1.95E-05	1.2987	1.52E-05	1.37592E-05	2.5974	1.63591E-05	1.38E-05
0.65947	1.9E-05	1.93E-05	1.3182	1.51E-05	1.36291E-05	2.6364	1.61998E-05	1.36E-05
0.75718	1.69E-05	1.75E-05	1.5135	1.37E-05	1.23689E-05	3.027	1.47607E-05	1.24E-05
0.76695	1.67E-05	1.73E-05	1.5331	1.36E-05	1.22854E-05	3.0661	1.46303E-05	1.23E-05
0.77672	1.66E-05	1.71E-05	1.5526	1.35E-05	1.21641E-05	3.1052	1.45025E-05	1.22E-05
0.78649	1.64E-05	1.70E-05	1.5721	1.34E-05	1.20544E-05	3.1442	1.43764E-05	1.21E-05
0.79626	1.63E-05	1.68E-05	1.5916	1.33E-05	1.19485E-05	3.1833	1.42525E-05	1.19E-05
0.80603	1.61E-05	1.66E-05	1.6112	1.32E-05	1.18612E-05	3.2224	1.41309E-05	1.19E-05
1.0112	1.33E-05	1.37E-05	2.0213	1.15E-05	1.03592E-05	4.0426	1.19668E-05	1.04E-05
1.021	1.32E-05	1.36E-05	2.0409	1.14E-05	1.03184E-05	4.0817	1.18793E-05	1.03E-05
1.0308	1.31E-05	1.35E-05	2.0604	1.13E-05	1.02689E-05	4.1208	1.17931E-05	1.03E-05

1.0405	1.29E-05	1.34E-05	2.0799	1.13E-05	1.02165E-05	4.1598	1.17079E-05	1.02E-05
1.0503	1.28E-05	1.32E-05	2.0994	1.12E-05	1.01563E-05	4.1989	1.16239E-05	1.02E-05
1.0601	1.28E-05	1.31E-05	2.119	1.12E-05	1.01272E-05	4.238	1.15412E-05	1.01E-05
1.0698	1.26E-05	1.30E-05	2.1385	1.11E-05	1.00835E-05	4.277	1.14593E-05	1.01E-05
1.0796	1.26E-05	1.29E-05	2.158	1.1E-05	1.00204E-05	4.3161	1.13788E-05	1E-05
1.0894	1.25E-05	1.28E-05	2.1776	1.1E-05	9.98155E-06	4.3551	1.1299E-05	9.98E-06
1.0991	1.24E-05	1.27E-05	2.1971	1.09E-05	9.94369E-06	4.3942	1.12203E-05	9.94E-06
1.1089	1.23E-05	1.26E-05	2.2166	1.08E-05	0.0000099	4.4333	1.11428E-05	9.9E-06
1.1187	1.22E-05	1.25E-05	2.2362	1.08E-05	9.83883E-06	4.4723	1.10661E-05	9.84E-06
1.1285	1.21E-05	1.24E-05	2.2557	1.07E-05	9.7932E-06	4.5114	1.09905E-05	9.79E-06
1.4216	1.01E-05	9.74E-06	2.8416	9.16E-06	8.71214E-06	5.6832	9.08951E-06	8.71E-06
1.4314	9.98E-06	9.67E-06	2.8611	9.09E-06	8.69524E-06	5.7223	9.03641E-06	8.7E-06
1.5584	9.37E-06	8.78E-06	3.115	8.54E-06	8.2734E-06	6.2301	8.39142E-06	8.27E-06
1.5681	9.34E-06	8.71E-06	3.1346	8.52E-06	8.23903E-06	6.2691	8.34507E-06	8.24E-06
1.7245	8.75E-06	7.77E-06	3.4471	7.87E-06	7.81398E-06	6.8941	7.65966E-06	7.81E-06
1.7342	8.74E-06	7.72E-06	3.4666	7.84E-06	7.79631E-06	6.9332	7.62007E-06	7.8E-06
1.744	8.7E-06	7.66E-06	3.4861	7.79E-06	7.77728E-06	6.9722	7.58072E-06	7.78E-06
1.7538	8.67E-06	7.61E-06	3.5057	7.76E-06	7.75835E-06	7.0113	7.54171E-06	7.76E-06
1.8613	8.33E-06	7.05E-06	3.7205	7.37E-06	7.46932E-06	7.441	7.13428E-06	7.47E-06
1.871	8.3E-06	7.00E-06	3.74	7.33E-06	7.46184E-06	7.48	7.09902E-06	7.46E-06
1.8808	8.28E-06	6.96E-06	3.7596	7.31E-06	7.4301E-06	7.5191	7.06404E-06	7.43E-06
2.0176	7.91E-06	6.34E-06	4.033	6.84E-06	7.08932E-06	8.066	6.60314E-06	7.09E-06
2.0274	7.89E-06	6.29E-06	4.0525	6.8E-06	7.07864E-06	8.105	6.57207E-06	7.08E-06
2.0371	7.86E-06	6.25E-06	4.072	6.77E-06	7.06194E-06	8.1441	6.54132E-06	7.06E-06
2.0469	7.86E-06	6.21E-06	4.0916	6.75E-06	7.02583E-06	8.1831	6.51072E-06	7.03E-06
2.0567	7.84E-06	6.17E-06	4.1111	6.72E-06	6.99786E-06	8.2222	6.48036E-06	7E-06
2.0664	7.8E-06	6.13E-06	4.1306	6.68E-06	6.99029E-06	8.2613	6.45029E-06	6.99E-06
2.0762	7.78E-06	6.09E-06	4.1502	6.65E-06	6.96427E-06	8.3003	6.42038E-06	6.96E-06
2.086	7.77E-06	6.05E-06	4.1697	6.64E-06	6.94243E-06	8.3394	6.39069E-06	6.94E-06
2.0958	7.75E-06	6.01E-06	4.1892	6.62E-06	6.92194E-06	8.3785	6.3613E-06	6.92E-06
2.1055	7.71E-06	5.97E-06	4.2088	6.57E-06	6.89592E-06	8.4175	6.33205E-06	6.9E-06
2.1153	7.7E-06	5.93E-06	4.2283	6.55E-06	6.88728E-06	8.4566	6.30308E-06	6.89E-06
2.1251	7.67E-06	5.90E-06	4.2478	6.53E-06	6.86583E-06	8.4956	6.27426E-06	6.87E-06
2.1348	7.65E-06	5.86E-06	4.2673	6.51E-06	6.83583E-06	8.5347	6.24565E-06	6.84E-06
2.1446	7.62E-06	5.82E-06	4.2869	6.47E-06	6.80806E-06	8.5738	6.21732E-06	6.81E-06
2.1544	7.59E-06	5.78E-06	4.3064	6.45E-06	6.7965E-06	8.6128	6.18912E-06	6.8E-06
2.1642	7.58E-06	5.75E-06	4.3259	6.41E-06	6.78641E-06	8.6519	6.1612E-06	6.79E-06
2.3498	7.15E-06	5.10E-06	4.697	5.86E-06	6.35291E-06	9.394	5.66574E-06	6.35E-06
2.3596	7.16E-06	5.06E-06	4.7166	5.84E-06	6.3368E-06	9.4331	5.64139E-06	6.34E-06
2.467	6.92E-06	4.73E-06	4.9314	5.59E-06	6.12437E-06	9.8628	5.38433E-06	6.12E-06
2.4768	6.91E-06	4.70E-06	4.9509	5.54E-06	6.11058E-06	9.9018	5.36184E-06	6.11E-06

2.4866	6.88E-06	4.67E-06	4.9705	5.53E-06	6.06748E-06	9.9409	5.33949E-06	6.07E-06
2.4964	6.88E-06	4.65E-06	4.99	5.51E-06	6.05126E-06	9.98	5.31735E-06	6.05E-06
2.5061	6.88E-06	4.62E-06	5.0095	5.47E-06	6.02544E-06	10.019	5.29535E-06	6.03E-06
2.5159	6.86E-06	4.59E-06	5.029	5.44E-06	5.99796E-06	10.058	5.27349E-06	6E-06
2.5257	6.82E-06	4.56E-06	5.0486	5.44E-06	5.98806E-06	10.097	5.25176E-06	5.99E-06
2.5354	6.81E-06	4.53E-06	5.0681	5.41E-06	5.97971E-06	10.136	5.23018E-06	5.98E-06
2.8188	6.31E-06	3.82E-06	5.6345	4.79E-06	5.49631E-06	11.269	4.65777E-06	5.5E-06
2.8286	6.27E-06	3.79E-06	5.654	4.76E-06	5.45534E-06	11.308	4.63978E-06	5.46E-06
2.8383	6.27E-06	3.77E-06	5.6736	4.75E-06	5.44553E-06	11.347	4.6219E-06	5.45E-06
2.8481	6.27E-06	3.75E-06	5.6931	4.73E-06	5.42951E-06	11.386	4.60412E-06	5.43E-06
3.7177	4.9E-06	2.29E-06	7.4313	3.27E-06	4.18437E-06	14.863	3.34824E-06	4.18E-06
3.7275	4.91E-06	2.27E-06	7.4508	3.25E-06	4.18573E-06	14.902	3.33709E-06	4.19E-06
3.874	4.72E-06	2.10E-06	7.7438	3.04E-06	3.9634E-06	15.488	3.17572E-06	3.96E-06
3.8838	4.71E-06	2.09E-06	7.7633	3.04E-06	3.95951E-06	15.527	3.16537E-06	3.96E-06
3.962	4.61E-06	2.00E-06	7.9196	2.92E-06	3.88699E-06	15.839	3.08422E-06	3.89E-06
3.9717	4.59E-06	1.99E-06	7.9391	2.9E-06	3.85291E-06	15.878	3.07429E-06	3.85E-06
3.9815	4.58E-06	1.98E-06	7.9586	2.9E-06	3.83272E-06	15.917	3.06439E-06	3.83E-06
3.9913	4.58E-06	1.97E-06	7.9782	2.89E-06	3.81495E-06	15.956	3.05454E-06	3.81E-06
4.001	4.58E-06	1.96E-06	7.9977	2.87E-06	3.80689E-06	15.995	3.04473E-06	3.81E-06
4.0108	4.56E-06	1.95E-06	8.0172	2.86E-06	3.81107E-06	16.034	3.03472E-06	3.81E-06
4.1671	4.37E-06	1.79E-06	8.3297	2.65E-06	3.63777E-06	16.659	2.88398E-06	3.64E-06
4.1769	4.34E-06	1.79E-06	8.3493	2.65E-06	3.62039E-06	16.699	2.87492E-06	3.62E-06
4.1867	4.36E-06	1.78E-06	8.3688	2.65E-06	3.63845E-06	16.738	2.86589E-06	3.64E-06
4.1965	4.35E-06	1.77E-06	8.3883	2.62E-06	3.60757E-06	16.777	2.85691E-06	3.61E-06
4.2062	4.33E-06	1.76E-06	8.4079	2.61E-06	3.60291E-06	16.816	2.84796E-06	3.6E-06
4.558	3.93E-06	1.46E-06	9.111	2.25E-06	3.22903E-06	18.222	2.54927E-06	3.23E-06
4.5677	3.92E-06	1.45E-06	9.1305	2.24E-06	3.22165E-06	18.261	2.5416E-06	3.22E-06
4.5775	3.89E-06	1.45E-06	9.15	2.21E-06	3.22165E-06	18.3	2.53396E-06	3.22E-06
4.8315	3.64E-06	1.27E-06	9.6578	1.94E-06	2.9535E-06	19.316	2.34527E-06	2.95E-06
4.8413	3.64E-06	1.26E-06	9.6773	1.93E-06	2.93796E-06	19.355	2.33841E-06	2.94E-06
4.8511	3.62E-06	1.26E-06	9.6969	1.92E-06	2.93524E-06	19.394	2.33157E-06	2.94E-06
4.8609	3.62E-06	1.25E-06	9.7164	1.93E-06	2.92427E-06	19.433	2.32476E-06	2.92E-06
4.8706	3.61E-06	1.24E-06	9.7359	1.9E-06	2.90796E-06	19.472	2.31797E-06	2.91E-06
4.8804	3.61E-06	1.24E-06	9.7555	1.88E-06	2.90136E-06	19.511	2.31121E-06	2.9E-06
4.8902	3.6E-06	1.23E-06	9.775	1.88E-06	2.89602E-06	19.55	2.30447E-06	2.9E-06
4.8999	3.58E-06	1.23E-06	9.7945	1.87E-06	2.88282E-06	19.589	2.29776E-06	2.88E-06
4.9097	3.57E-06	1.22E-06	9.8141	1.86E-06	2.86951E-06	19.628	2.29108E-06	2.87E-06
4.9781	3.51E-06	1.18E-06	9.9508	1.8E-06	2.80621E-06	19.902	2.24484E-06	2.81E-06
4.9879	3.49E-06	1.17E-06	9.9703	1.79E-06	2.78709E-06	19.941	2.23836E-06	2.79E-06
4.9976	3.48E-06	9.11E-07	9.9898	1.78E-06	2.78019E-06	19.98	2.15738E-06	2.78E-06

Table 2.4 Brilliant blue-R-chlorine dioxide Intermediate and product formation -compiled data .

TIME	OH-	P1	P2
0.029194	5.27E-05	2.30E-06	2.30E-06
0.048725	5.13E-05	3.73E-06	3.73E-06
0.068256	4.99E-05	5.07E-06	5.07E-06
0.087786	4.87E-05	6.34E-06	6.34E-06
0.10732	4.75E-05	7.54E-06	7.54E-06
0.12685	4.63E-05	8.67E-06	8.67E-06
0.14638	4.52E-05	9.75E-06	9.75E-06
0.16591	4.42E-05	1.08E-05	1.08E-05
0.18544	4.33E-05	1.17E-05	1.17E-05
0.20497	4.23E-05	1.27E-05	1.27E-05
0.2245	4.14E-05	1.36E-05	1.36E-05
0.24403	4.06E-05	1.44E-05	1.44E-05
0.26356	3.98E-05	1.52E-05	1.52E-05
0.77136	2.69E-05	1.60E-05	2.81E-05
0.79089	2.66E-05	1.67E-05	2.84E-05
0.81042	2.63E-05	1.74E-05	2.87E-05
0.82995	2.60E-05	1.81E-05	2.90E-05
0.90807	2.49E-05	2.05E-05	3.01E-05
0.9276	2.46E-05	2.11E-05	3.04E-05
0.94714	2.44E-05	2.16E-05	3.06E-05
0.96667	2.41E-05	2.21E-05	3.09E-05
0.9862	2.39E-05	2.26E-05	3.11E-05
1.0057	2.36E-05	2.31E-05	3.14E-05
1.0253	2.34E-05	2.36E-05	3.16E-05
1.0448	2.32E-05	2.40E-05	3.18E-05
1.0643	2.30E-05	2.45E-05	3.20E-05
1.0839	2.28E-05	2.49E-05	3.22E-05
1.1034	2.26E-05	2.53E-05	3.24E-05
1.1229	2.24E-05	2.57E-05	3.26E-05
1.1424	2.22E-05	2.61E-05	3.28E-05
1.162	2.20E-05	2.64E-05	3.30E-05
1.1815	2.18E-05	2.68E-05	3.32E-05
1.201	2.16E-05	2.71E-05	3.34E-05
1.2206	2.14E-05	2.75E-05	3.36E-05
1.2401	2.12E-05	2.78E-05	3.38E-05
1.2596	2.10E-05	2.81E-05	3.40E-05
1.2792	2.09E-05	2.84E-05	3.41E-05
1.2987	2.07E-05	2.87E-05	3.43E-05
1.3182	2.05E-05	2.90E-05	3.45E-05
1.3377	2.04E-05	2.93E-05	3.46E-05
1.4745	1.93E-05	3.11E-05	3.57E-05
1.494	1.92E-05	3.14E-05	3.58E-05
1.5135	1.91E-05	3.16E-05	3.59E-05
1.5331	1.89E-05	3.18E-05	3.61E-05
1.5526	1.88E-05	3.20E-05	3.62E-05
1.5721	1.87E-05	3.22E-05	3.63E-05
1.5916	1.85E-05	3.24E-05	3.64E-05
1.6112	1.84E-05	3.26E-05	3.66E-05
1.6307	1.83E-05	3.28E-05	3.67E-05
1.6502	1.82E-05	3.30E-05	3.68E-05
1.6698	1.81E-05	3.32E-05	3.69E-05
1.6893	1.80E-05	3.34E-05	3.70E-05
1.7088	1.78E-05	3.36E-05	3.72E-05
1.7284	1.77E-05	3.38E-05	3.73E-05
1.7479	1.76E-05	3.40E-05	3.74E-05

2.2166	1.54E-05	3.41E-05	3.96E-05
2.3924	1.48E-05	3.55E-05	4.02E-05
2.4119	1.47E-05	3.57E-05	4.03E-05
2.4315	1.46E-05	3.58E-05	4.04E-05
2.451	1.46E-05	3.59E-05	4.04E-05
2.7049	1.38E-05	3.61E-05	4.12E-05
2.7244	1.37E-05	3.62E-05	4.13E-05
4.4822	1.04E-05	3.72E-05	4.46E-05
4.5017	1.04E-05	3.73E-05	4.46E-05
4.5212	1.04E-05	3.74E-05	4.46E-05
4.5408	1.04E-05	3.75E-05	4.46E-05
4.7361	1.01E-05	3.85E-05	4.49E-05
5.5759	9.29E-06	3.86E-05	4.57E-05
5.5954	9.28E-06	3.87E-05	4.57E-05
5.615	9.26E-06	3.88E-05	4.57E-05
5.7517	9.15E-06	3.93E-05	4.58E-05
5.7712	9.13E-06	3.94E-05	4.59E-05
5.7907	9.11E-06	3.95E-05	4.59E-05
5.8103	9.10E-06	3.96E-05	4.59E-05
5.8298	9.08E-06	3.97E-05	4.59E-05
5.8493	9.07E-06	3.97E-05	4.59E-05
5.8689	9.05E-06	3.98E-05	4.59E-05
5.8884	9.04E-06	3.99E-05	4.59E-05
5.9079	9.02E-06	3.99E-05	4.60E-05
5.9275	9.01E-06	4.00E-05	4.60E-05
5.947	8.99E-06	4.01E-05	4.60E-05
5.9665	8.98E-06	4.02E-05	4.60E-05
5.986	8.96E-06	4.02E-05	4.60E-05

6.0056	8.95E-06	4.03E-05	4.60E-05
6.8845	8.36E-06	4.04E-05	4.66E-05
6.904	8.35E-06	4.04E-05	4.66E-05
7.236	8.16E-06	4.05E-05	4.68E-05
7.2555	8.15E-06	4.06E-05	4.68E-05
7.2751	8.14E-06	4.06E-05	4.68E-05
7.6071	7.97E-06	4.07E-05	4.70E-05
7.6266	7.96E-06	4.07E-05	4.70E-05
7.6462	7.95E-06	4.08E-05	4.70E-05
8.0368	7.77E-06	4.09E-05	4.72E-05
8.0563	7.76E-06	4.09E-05	4.72E-05
8.0954	7.74E-06	4.10E-05	4.72E-05
8.1149	7.73E-06	4.11E-05	4.72E-05
8.9742	7.39E-06	4.12E-05	4.76E-05
9.0133	7.38E-06	4.13E-05	4.76E-05
9.0914	7.35E-06	4.15E-05	4.76E-05
9.111	7.34E-06	4.15E-05	4.76E-05
9.1305	7.33E-06	4.16E-05	4.76E-05
9.15	7.33E-06	4.16E-05	4.77E-05
9.8141	7.11E-06	4.19E-05	4.79E-05
9.8336	7.10E-06	4.19E-05	4.79E-05
9.8531	7.10E-06	4.20E-05	4.79E-05
9.8727	7.09E-06	4.20E-05	4.79E-05
9.8922	7.08E-06	4.21E-05	4.79E-05
9.9117	7.08E-06	4.21E-05	4.79E-05
9.9703	7.06E-06	4.23E-05	4.79E-05
9.9898	7.06E-06	4.23E-05	4.79E-05
10.4898	6.91E-06	4.23E-05	4.81E-05

2.3 Safranine-O oxidation products with chlorine dioxide.

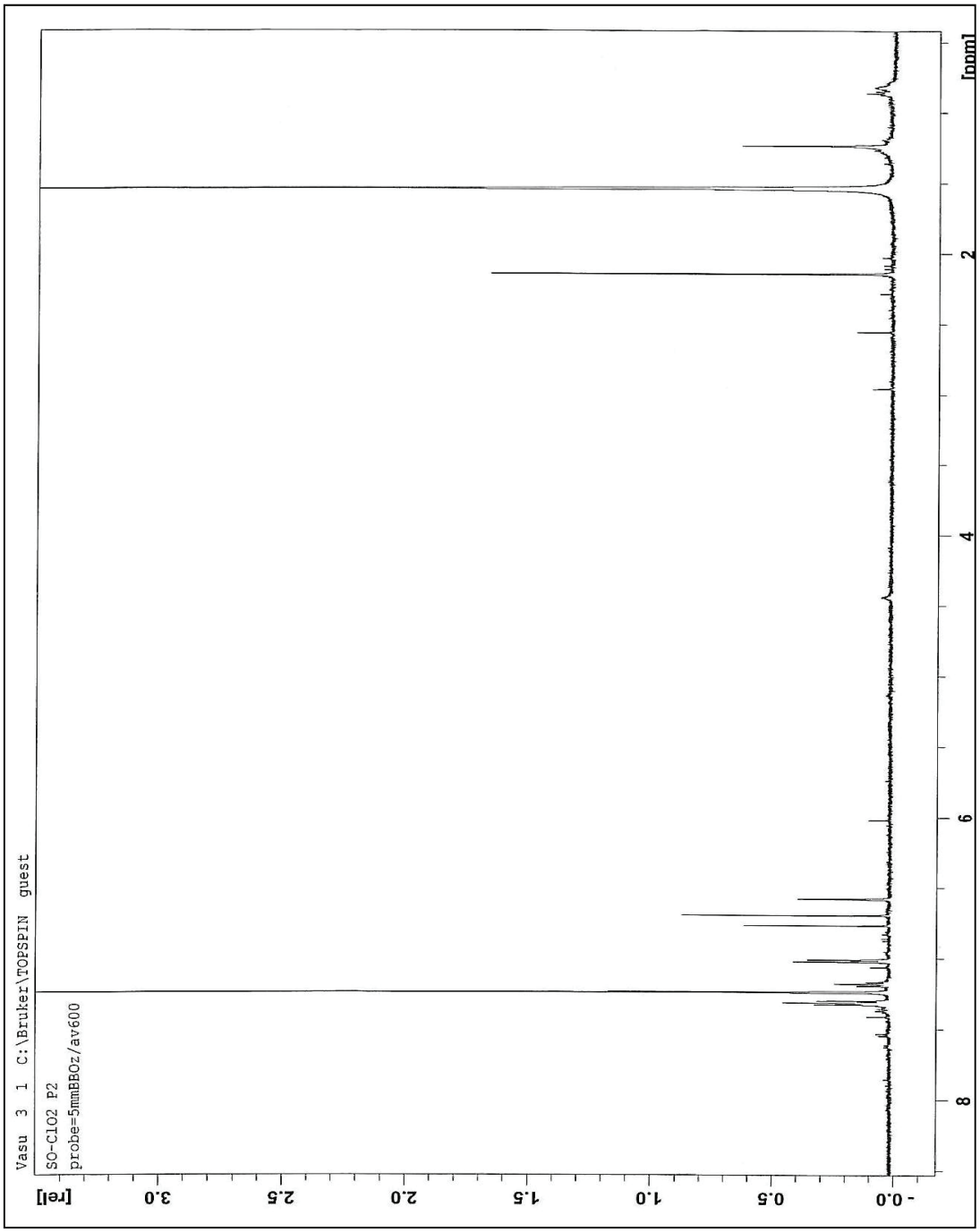

Figure 2.1.10 ^{1}H NMR spectrum of safranine-O major oxidation product P_2 (3,7-dimethyl-phenazine-2,8-diol) with chlorine dioxide

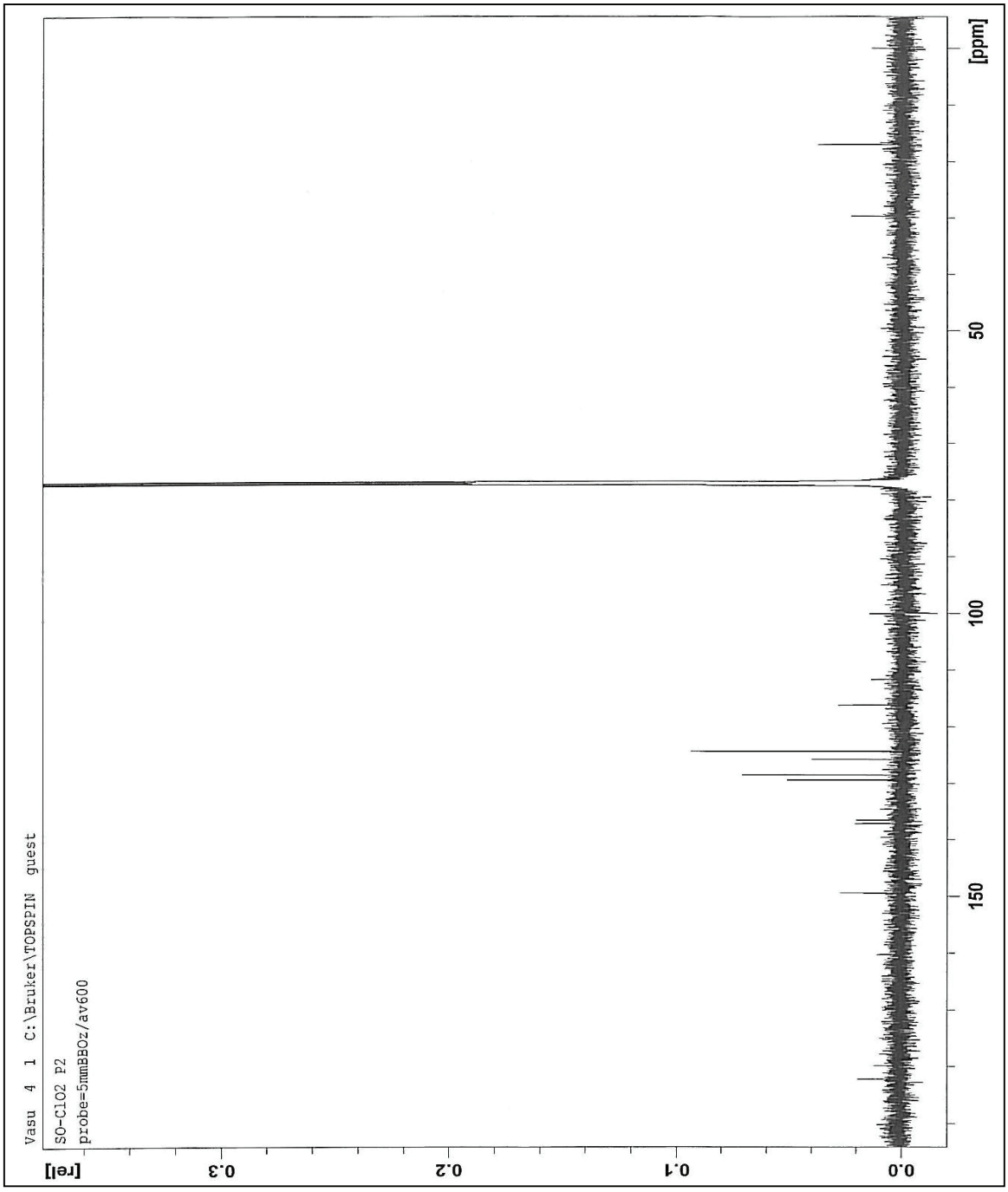

Figure 2.1.11 ^{13} CNMR spectrum of safranine-O major oxidation product P_2 (3,7- dimethyl-phenazine-2,8-diol) with chlorine dioxide

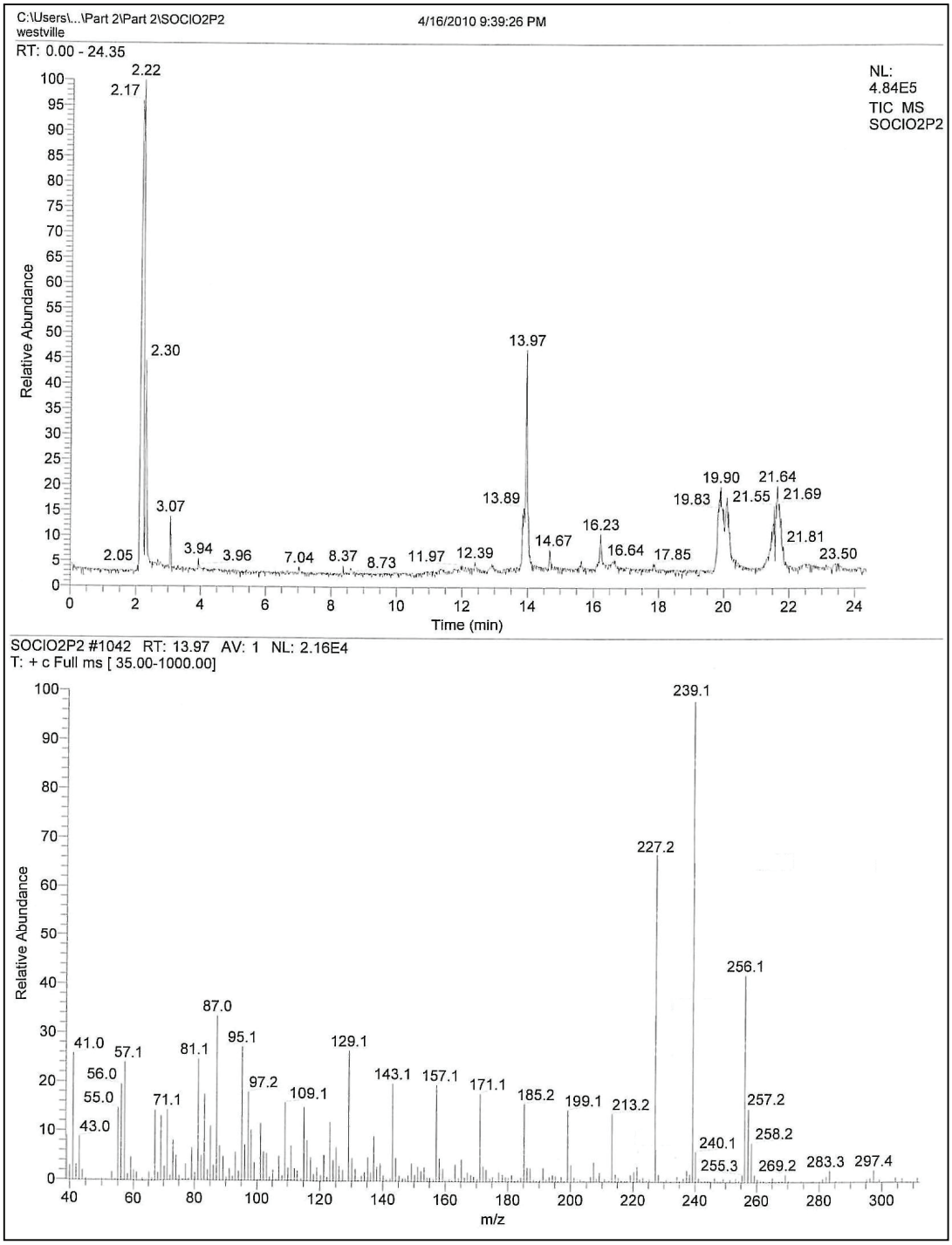

Figure 2.1.12 GC-MS spectrum of safranine-O major oxidation product P_2 (3,7- dimethyl-phenazine-2,8-diol) with chlorine dioxide.

Table 2.5 Safraninee -O chlorine dioxide simulation data experimental and simulated curves- compiled data.

Time	E1	Time	E2	Time	E3	Time	S1	Time	S2	Time	S3
0.0048	7.3E-05	0.0029	7.38E-05	0.0029	7.29E-05	0.0048	0.00007	0.0029	0.00007	0.0029	0.00007
0.0146	7.2E-05	0.0088	7.35E-05	0.0088	7.27E-05	0.0146	6.78E-05	0.0088	6.83E-05	0.00875	6.7E-05
0.0244	7E-05	0.0146	7.23E-05	0.0146	7.13E-05	0.0244	6.64E-05	0.0146	6.71E-05	0.01461	6.5E-05
0.0341	6.8E-05	0.0205	7.1E-05	0.0205	6.97E-05	0.0341	6.51E-05	0.0205	6.61E-05	0.02047	6.3E-05
0.2784	3.9E-05	0.1669	5.37E-05	0.1669	4.38E-05	0.2784	3.92E-05	0.1669	4.67E-05	0.16687	3.5E-05
0.2882	3.8E-05	0.1727	5.31E-05	0.1727	4.31E-05	0.2882	3.84E-05	0.1727	4.61E-05	0.17272	3.5E-05
0.298	3.8E-05	0.1786	5.24E-05	0.1786	4.24E-05	0.298	3.76E-05	0.1786	4.55E-05	0.17858	3.4E-05
0.3077	3.7E-05	0.1844	5.18E-05	0.1844	4.17E-05	0.3077	3.69E-05	0.1844	4.5E-05	0.18443	3.3E-05
0.3175	3.6E-05	0.1903	5.13E-05	0.1903	4.1E-05	0.3175	3.62E-05	0.1903	4.45E-05	0.19029	3.3E-05
0.3273	3.5E-05	0.1962	5.07E-05	0.1962	4.04E-05	0.3273	3.55E-05	0.1962	4.4E-05	0.19615	3.2E-05
0.337	3.5E-05	0.202	5.01E-05	0.202	3.96E-05	0.337	3.48E-05	0.202	4.35E-05	0.202	3.2E-05
0.3468	3.4E-05	0.2079	4.95E-05	0.2079	3.9E-05	0.3468	3.42E-05	0.2079	4.3E-05	0.20786	3.1E-05
0.3566	3.4E-05	0.2137	4.89E-05	0.2137	3.84E-05	0.3566	3.35E-05	0.2137	4.25E-05	0.21371	3.1E-05
0.4738	2.7E-05	0.284	4.28E-05	0.284	3.18E-05	0.4738	2.67E-05	0.284	3.74E-05	0.28399	2.5E-05
0.4836	2.6E-05	0.2898	4.24E-05	0.2898	3.14E-05	0.4836	2.62E-05	0.2898	3.7E-05	0.28984	2.5E-05
0.4934	2.6E-05	0.2957	4.19E-05	0.2957	3.09E-05	0.4934	2.58E-05	0.2957	3.66E-05	0.2957	2.5E-05
0.5031	2.6E-05	0.3016	4.14E-05	0.3016	3.04E-05	0.5031	2.53E-05	0.3016	3.63E-05	0.30155	2.4E-05
0.5129	2.5E-05	0.3074	4.1E-05	0.3074	3E-05	0.5129	2.48E-05	0.3074	3.59E-05	0.30741	2.4E-05
0.5227	2.5E-05	0.3133	4.06E-05	0.3133	2.96E-05	0.5227	2.44E-05	0.3133	3.56E-05	0.31327	2.4E-05
0.5325	2.4E-05	0.3191	4.01E-05	0.3191	2.91E-05	0.5325	2.39E-05	0.3191	3.52E-05	0.31912	2.3E-05
0.5422	2.4E-05	0.325	3.96E-05	0.325	2.87E-05	0.5422	2.35E-05	0.325	3.49E-05	0.32498	2.3E-05
0.552	2.3E-05	0.3308	3.92E-05	0.3308	2.83E-05	0.552	2.31E-05	0.3308	3.46E-05	0.33083	2.3E-05
0.7474	1.7E-05	0.448	3.22E-05	0.448	2.12E-05	0.7474	1.63E-05	0.448	2.89E-05	0.44795	1.8E-05
0.7572	1.7E-05	0.4538	3.18E-05	0.4538	2.1E-05	0.7572	1.6E-05	0.4538	2.86E-05	0.45381	1.7E-05
0.767	1.6E-05	0.4597	3.15E-05	0.4597	2.07E-05	0.767	1.58E-05	0.4597	2.84E-05	0.45967	1.7E-05
0.7767	1.6E-05	0.4655	3.12E-05	0.4655	2.04E-05	0.7767	1.55E-05	0.4655	2.82E-05	0.46552	1.7E-05
0.7865	1.6E-05	0.4714	3.09E-05	0.4714	2.01E-05	0.7865	1.53E-05	0.4714	2.79E-05	0.47138	1.7E-05
0.7963	1.6E-05	0.4772	3.06E-05	0.4772	1.98E-05	0.7963	1.5E-05	0.4772	2.77E-05	0.47723	1.7E-05
0.806	1.5E-05	0.4831	3.03E-05	0.4831	1.96E-05	0.806	1.48E-05	0.4831	2.75E-05	0.48309	1.7E-05
0.8158	1.5E-05	0.489	3E-05	0.489	1.93E-05	0.8158	1.45E-05	0.489	2.73E-05	0.48895	1.6E-05
0.8256	1.5E-05	0.4948	2.98E-05	0.4948	1.91E-05	0.8256	1.43E-05	0.4948	2.71E-05	0.4948	1.6E-05
0.8353	1.5E-05	0.5007	2.95E-05	0.5007	1.88E-05	0.8353	1.41E-05	0.5007	2.68E-05	0.50066	1.6E-05
0.8451	1.5E-05	0.5065	2.92E-05	0.5065	1.85E-05	0.8451	1.38E-05	0.5065	2.66E-05	0.50651	1.6E-05
0.8549	1.4E-05	0.5124	2.89E-05	0.5124	1.83E-05	0.8549	1.36E-05	0.5124	2.64E-05	0.51237	1.6E-05
0.8647	1.4E-05	0.5182	2.87E-05	0.5182	1.81E-05	0.8647	1.34E-05	0.5182	2.62E-05	0.51823	1.5E-05
0.8744	1.4E-05	0.5241	2.84E-05	0.5241	1.78E-05	0.8744	1.32E-05	0.5241	2.6E-05	0.52408	1.5E-05
0.8842	1.4E-05	0.5299	2.82E-05	0.5299	1.76E-05	0.8842	1.3E-05	0.5299	2.58E-05	0.52994	1.5E-05
0.894	1.4E-05	0.5358	2.79E-05	0.5358	1.74E-05	0.894	1.28E-05	0.5358	2.56E-05	0.53579	1.5E-05

0.9037	1.3E-05	0.5417	2.76E-05	0.5417	1.71E-05	0.9037	1.26E-05	0.5417	2.54E-05	0.54165	1.5E-05
0.9135	1.3E-05	0.5475	2.74E-05	0.5475	1.69E-05	0.9135	1.24E-05	0.5475	2.52E-05	0.54751	1.5E-05
0.9233	1.3E-05	0.5534	2.72E-05	0.5534	1.67E-05	0.9233	1.22E-05	0.5534	2.5E-05	0.55336	1.5E-05
0.9331	1.3E-05	0.5592	2.69E-05	0.5592	1.65E-05	0.9331	1.2E-05	0.5592	2.48E-05	0.55922	1.4E-05
0.9428	1.3E-05	0.5651	2.67E-05	0.5651	1.63E-05	0.9428	1.18E-05	0.5651	2.46E-05	0.56507	1.4E-05
1.1187	9.8E-06	0.6705	2.28E-05	0.6705	1.3E-05	1.1187	9E-06	0.6705	2.17E-05	0.67048	1.2E-05
1.1285	9.7E-06	0.6763	2.26E-05	0.6763	1.29E-05	1.1285	8.87E-06	0.6763	2.15E-05	0.67634	1.2E-05
1.1382	9.6E-06	0.6822	2.25E-05	0.6822	1.27E-05	1.1382	8.74E-06	0.6822	2.14E-05	0.68219	1.2E-05
1.5291	6.1E-06	0.9164	1.65E-05	0.9164	8.19E-06	1.5291	5.09E-06	0.9164	1.66E-05	0.91643	8.3E-06
1.5388	6E-06	0.9223	1.64E-05	0.9223	8.09E-06	1.5388	5.03E-06	0.9223	1.65E-05	0.92229	8.3E-06
1.5486	5.9E-06	0.9282	1.63E-05	0.9282	8.03E-06	1.5486	4.97E-06	0.9282	1.64E-05	0.92815	8.2E-06
1.5584	5.8E-06	0.934	1.61E-05	0.934	7.97E-06	1.5584	4.9E-06	0.934	1.63E-05	0.934	8.2E-06
1.5681	5.8E-06	0.9399	1.6E-05	0.9399	7.87E-06	1.5681	4.84E-06	0.9399	1.62E-05	0.93986	8.1E-06
1.5779	5.7E-06	0.9457	1.59E-05	0.9457	7.8E-06	1.5779	4.78E-06	0.9457	1.61E-05	0.94571	8E-06
1.5877	5.7E-06	0.9516	1.58E-05	0.9516	7.74E-06	1.5877	4.73E-06	0.9516	1.6E-05	0.95157	8E-06
1.5975	5.6E-06	0.9574	1.57E-05	0.9574	7.65E-06	1.5975	4.67E-06	0.9574	1.6E-05	0.95743	7.9E-06
1.6072	5.6E-06	0.9633	1.56E-05	0.9633	7.58E-06	1.6072	4.61E-06	0.9633	1.59E-05	0.96328	7.8E-06
1.617	5.5E-06	0.9691	1.55E-05	0.9691	7.5E-06	1.617	4.56E-06	0.9691	1.58E-05	0.96914	7.8E-06
1.6268	5.5E-06	0.975	1.54E-05	0.975	7.43E-06	1.6268	4.5E-06	0.975	1.57E-05	0.97499	7.7E-06
2.1251	3.7E-06	1.2736	1.12E-05	1.2736	4.87E-06	2.1251	2.55E-06	1.2736	1.2E-05	1.2736	5.4E-06
2.1348	3.6E-06	1.2795	1.11E-05	1.2795	4.82E-06	2.1348	2.52E-06	1.2795	1.2E-05	1.2795	5.4E-06
2.1446	3.6E-06	1.2854	1.11E-05	1.2854	4.79E-06	2.1446	2.49E-06	1.2854	1.19E-05	1.2854	5.3E-06
2.1544	3.6E-06	1.2912	1.1E-05	1.2912	4.77E-06	2.1544	2.47E-06	1.2912	1.18E-05	1.2912	5.3E-06
2.1642	3.6E-06	1.2971	1.09E-05	1.2971	4.73E-06	2.1642	2.44E-06	1.2971	1.18E-05	1.2971	5.2E-06
2.1739	3.6E-06	1.3029	1.09E-05	1.3029	4.69E-06	2.1739	2.42E-06	1.3029	1.17E-05	1.3029	5.2E-06
2.1837	3.5E-06	1.3088	1.09E-05	1.3088	4.66E-06	2.1837	2.39E-06	1.3088	1.17E-05	1.3088	5.2E-06
2.1935	3.5E-06	1.3146	1.08E-05	1.3146	4.63E-06	2.1935	2.37E-06	1.3146	1.16E-05	1.3146	5.1E-06
2.2032	3.5E-06	1.3205	1.07E-05	1.3205	4.59E-06	2.2032	2.35E-06	1.3205	1.16E-05	1.3205	5.1E-06
2.213	3.5E-06	1.3264	1.07E-05	1.3264	4.57E-06	2.213	2.32E-06	1.3264	1.15E-05	1.3264	5.1E-06
2.2228	3.5E-06	1.3322	1.06E-05	1.3322	4.55E-06	2.2228	2.3E-06	1.3322	1.15E-05	1.3322	5E-06
2.2325	3.4E-06	1.3381	1.05E-05	1.3381	4.49E-06	2.2325	2.28E-06	1.3381	1.14E-05	1.3381	5E-06
2.555	2.9E-06	1.5313	8.94E-06	1.5313	3.72E-06	2.555	1.67E-06	1.5313	9.81E-06	1.5313	4.1E-06
2.5647	2.9E-06	1.5372	8.88E-06	1.5372	3.69E-06	2.5647	1.65E-06	1.5372	9.77E-06	1.5372	4.1E-06
2.5745	2.9E-06	1.543	8.84E-06	1.543	3.68E-06	2.5745	1.64E-06	1.543	9.73E-06	1.543	4E-06
2.5843	2.9E-06	1.5489	8.82E-06	1.5489	3.68E-06	2.5843	1.62E-06	1.5489	9.68E-06	1.5489	4E-06
2.5941	2.9E-06	1.5547	8.78E-06	1.5547	3.65E-06	2.5941	1.61E-06	1.5547	9.64E-06	1.5547	4E-06
2.6038	2.9E-06	1.5606	8.72E-06	1.5606	3.63E-06	2.6038	1.6E-06	1.5606	9.6E-06	1.5606	4E-06
2.6136	2.8E-06	1.5664	8.69E-06	1.5664	3.61E-06	2.6136	1.58E-06	1.5664	9.56E-06	1.5664	3.9E-06
2.6234	2.9E-06	1.5723	8.65E-06	1.5723	3.6E-06	2.6234	1.57E-06	1.5723	9.52E-06	1.5723	3.9E-06
2.6331	2.8E-06	1.5782	8.61E-06	1.5782	3.59E-06	2.6331	1.55E-06	1.5782	9.47E-06	1.5782	3.9E-06
2.6429	2.8E-06	1.584	8.58E-06	1.584	3.57E-06	2.6429	1.54E-06	1.584	9.43E-06	1.584	3.9E-06

2.6527	2.8E-06	1.5899	8.55E-06	1.5899	3.57E-06	2.6527	1.53E-06	1.5899	9.39E-06	1.5899	3.8E-06
2.6625	2.8E-06	1.5957	8.5E-06	1.5957	3.55E-06	2.6625	1.51E-06	1.5957	9.35E-06	1.5957	3.8E-06
2.6722	2.8E-06	1.6016	8.45E-06	1.6016	3.52E-06	2.6722	1.5E-06	1.6016	9.31E-06	1.6016	3.8E-06
2.682	2.8E-06	1.6074	8.44E-06	1.6074	3.52E-06	2.682	1.49E-06	1.6074	9.27E-06	1.6074	3.8E-06
2.6918	2.8E-06	1.6133	8.4E-06	1.6133	3.51E-06	2.6918	1.47E-06	1.6133	9.23E-06	1.6133	3.8E-06
2.7015	2.8E-06	1.6192	8.35E-06	1.6192	3.48E-06	2.7015	1.46E-06	1.6192	9.19E-06	1.6192	3.7E-06
2.7113	2.8E-06	1.625	8.32E-06	1.625	3.46E-06	2.7113	1.45E-06	1.625	9.16E-06	1.625	3.7E-06
2.7211	2.7E-06	1.6309	8.29E-06	1.6309	3.45E-06	2.7211	1.44E-06	1.6309	9.12E-06	1.6309	3.7E-06
2.7309	2.8E-06	1.6367	8.23E-06	1.6367	3.44E-06	2.7309	1.42E-06	1.6367	9.08E-06	1.6367	3.7E-06
2.7406	2.7E-06	1.6426	8.2E-06	1.6426	3.41E-06	2.7406	1.41E-06	1.6426	9.04E-06	1.6426	3.6E-06
3.2096	2.4E-06	1.9237	6.86E-06	1.9237	2.88E-06	3.2096	9.63E-07	1.9237	7.44E-06	1.9237	2.8E-06
3.2194	2.4E-06	1.9295	6.83E-06	1.9295	2.9E-06	3.2194	9.56E-07	1.9295	7.41E-06	1.9295	2.8E-06
3.2292	2.4E-06	1.9354	6.81E-06	1.9354	2.88E-06	3.2292	9.49E-07	1.9354	7.39E-06	1.9354	2.7E-06
3.2389	2.4E-06	1.9412	6.79E-06	1.9412	2.84E-06	3.2389	9.42E-07	1.9412	7.36E-06	1.9412	2.7E-06
3.2487	2.4E-06	1.9471	6.77E-06	1.9471	2.85E-06	3.2487	9.35E-07	1.9471	7.33E-06	1.9471	2.7E-06
4.1574	2.2E-06	2.4917	5.3E-06	2.4917	2.43E-06	4.1574	5.06E-07	2.4917	5.23E-06	2.4917	1.7E-06
4.1671	2.2E-06	2.4976	5.28E-06	2.4976	2.41E-06	4.1671	5.03E-07	2.4976	5.22E-06	2.4976	1.7E-06
4.1769	2.2E-06	2.5034	5.27E-06	2.5034	2.41E-06	4.1769	5E-07	2.5034	5.2E-06	2.5034	1.7E-06
4.1867	2.2E-06	2.5093	5.26E-06	2.5093	2.42E-06	4.1867	4.97E-07	2.5093	5.18E-06	2.5093	1.7E-06
4.1965	2.2E-06	2.5151	5.25E-06	2.5151	2.4E-06	4.1965	4.94E-07	2.5151	5.16E-06	2.5151	1.6E-06
4.2062	2.2E-06	2.521	5.23E-06	2.521	2.41E-06	4.2062	4.91E-07	2.521	5.15E-06	2.521	1.6E-06
4.216	2.2E-06	2.5268	5.24E-06	2.5268	2.42E-06	4.216	4.88E-07	2.5268	5.13E-06	2.5268	1.6E-06
4.2258	2.2E-06	2.5327	5.2E-06	2.5327	2.41E-06	4.2258	4.86E-07	2.5327	5.11E-06	2.5327	1.6E-06
4.5287	2.1E-06	2.7142	4.88E-06	2.7142	2.37E-06	4.5287	4.08E-07	2.7142	4.61E-06	2.7142	1.4E-06
4.5384	2.1E-06	2.7201	4.86E-06	2.7201	2.36E-06	4.5384	4.06E-07	2.7201	4.6E-06	2.7201	1.4E-06
4.5482	2.1E-06	2.7259	4.88E-06	2.7259	2.37E-06	4.5482	4.04E-07	2.7259	4.58E-06	2.7259	1.4E-06
4.558	2.1E-06	2.7318	4.86E-06	2.7318	2.36E-06	4.558	4.01E-07	2.7318	4.57E-06	2.7318	1.4E-06
4.5677	2.1E-06	2.7376	4.86E-06	2.7376	2.35E-06	4.5677	3.99E-07	2.7376	4.55E-06	2.7376	1.4E-06
4.5775	2.1E-06	2.7435	4.85E-06	2.7435	2.34E-06	4.5775	3.97E-07	2.7435	4.54E-06	2.7435	1.4E-06
4.8804	2.1E-06	2.925	4.63E-06	2.925	2.31E-06	4.8804	3.38E-07	2.925	4.11E-06	2.925	1.2E-06
4.8902	2.1E-06	2.9309	4.62E-06	2.9309	2.3E-06	4.8902	3.36E-07	2.9309	4.09E-06	2.9309	1.2E-06
4.8999	2.1E-06	2.9368	4.6E-06	2.9368	2.29E-06	4.8999	3.35E-07	2.9368	4.08E-06	2.9368	1.2E-06
4.9097	2.1E-06	2.9426	4.6E-06	2.9426	2.29E-06	4.9097	3.33E-07	2.9426	4.07E-06	2.9426	1.2E-06
4.9195	2.1E-06	2.9485	4.6E-06	2.9485	2.29E-06	4.9195	3.31E-07	2.9485	4.06E-06	2.9485	1.2E-06
4.9293	2.1E-06	2.9543	4.58E-06	2.9543	2.3E-06	4.9293	3.3E-07	2.9543	4.04E-06	2.9543	1.2E-06
4.939	2.1E-06	2.9602	4.59E-06	2.9602	2.29E-06	4.939	3.28E-07	2.9602	4.03E-06	2.9602	1.1E-06
4.9586	2.1E-06	2.9719	4.58E-06	2.9719	2.3E-06	4.9586	3.25E-07	2.9719	4E-06	2.9719	1.1E-06
4.9683	2.1E-06	2.9777	4.55E-06	2.9777	2.29E-06	4.9683	3.23E-07	2.9777	3.99E-06	2.9777	1.1E-06
4.9781	2.1E-06	2.9836	4.56E-06	2.9836	2.28E-06	4.9781	3.22E-07	2.9836	3.98E-06	2.9836	1.1E-06
4.9879	2.1E-06	2.9895	4.55E-06	2.9895	2.3E-06	4.9879	3.2E-07	2.9895	3.97E-06	2.9895	1.1E-06
4.9976	2.1E-06	2.9953	4.51E-06	2.9953	2.29E-06	4.9976	3.18E-07	2.9953	3.95E-06	2.9953	1.1E-06

Table 2.6 Safranine-O -chlorine dioxide simulation data product and intermediate formation- compiled data.

TIME	CLO2-	P1	I1	P2
0.014605	2.16E-06	1.21E-09	2.15E-06	4.96E-09
0.024376	3.56E-06	1.99E-09	3.55E-06	1.37E-08
0.034146	4.93E-06	2.76E-09	4.90E-06	2.66E-08
0.043917	6.28E-06	3.51E-09	6.23E-06	4.37E-08
0.053688	7.59E-06	4.24E-09	7.52E-06	6.47E-08
0.063458	8.87E-06	4.96E-09	8.78E-06	8.97E-08
0.073229	1.01E-05	5.67E-09	1.00E-05	1.18E-07
0.083	1.14E-05	6.35E-09	1.12E-05	1.51E-07
0.09277	1.26E-05	7.03E-09	1.24E-05	1.87E-07
0.10254	1.37E-05	7.68E-09	1.35E-05	2.26E-07
0.11231	1.49E-05	8.33E-09	1.46E-05	2.69E-07
0.12208	1.60E-05	8.96E-09	1.57E-05	3.15E-07
0.63993	5.03E-05	2.89E-08	4.48E-05	5.51E-06
0.6497	5.07E-05	2.91E-08	4.50E-05	5.64E-06
0.65947	5.10E-05	2.93E-08	4.52E-05	5.76E-06
0.66924	5.13E-05	2.95E-08	4.54E-05	5.88E-06
0.67901	5.16E-05	2.97E-08	4.56E-05	6.01E-06
0.68878	5.19E-05	2.99E-08	4.58E-05	6.13E-06
0.69855	5.23E-05	3.01E-08	4.60E-05	6.26E-06
0.70832	5.26E-05	3.03E-08	4.61E-05	6.38E-06
0.71809	5.28E-05	3.05E-08	4.63E-05	6.51E-06
0.72786	5.31E-05	3.07E-08	4.65E-05	6.63E-06
0.73763	5.34E-05	3.09E-08	4.66E-05	6.76E-06
0.74741	5.37E-05	3.10E-08	4.68E-05	6.88E-06
0.75718	5.40E-05	3.12E-08	4.69E-05	7.01E-06
0.76695	5.42E-05	3.14E-08	4.71E-05	7.13E-06
0.77672	5.45E-05	3.16E-08	4.72E-05	7.26E-06
0.78649	5.47E-05	3.17E-08	4.73E-05	7.38E-06
0.79626	5.50E-05	3.19E-08	4.74E-05	7.51E-06
0.80603	5.52E-05	3.20E-08	4.76E-05	7.63E-06
0.8158	5.55E-05	3.22E-08	4.77E-05	7.76E-06
0.82557	5.57E-05	3.24E-08	4.78E-05	7.89E-06
0.83534	5.59E-05	3.25E-08	4.79E-05	8.01E-06
1.0308	5.97E-05	3.50E-08	4.92E-05	1.05E-05
1.0405	5.99E-05	3.51E-08	4.92E-05	1.06E-05
1.0503	6.00E-05	3.52E-08	4.93E-05	1.07E-05
1.0601	6.02E-05	3.54E-08	4.93E-05	1.09E-05
1.0698	6.03E-05	3.55E-08	4.93E-05	1.10E-05
1.0796	6.05E-05	3.56E-08	4.93E-05	1.11E-05
1.5681	6.52E-05	3.90E-08	4.84E-05	1.67E-05
1.5779	6.52E-05	3.91E-08	4.84E-05	1.68E-05
1.5877	6.53E-05	3.91E-08	4.83E-05	1.69E-05
1.5975	6.53E-05	3.92E-08	4.83E-05	1.70E-05
1.6072	6.54E-05	3.92E-08	4.82E-05	1.71E-05
1.617	6.54E-05	3.93E-08	4.82E-05	1.72E-05
1.6268	6.55E-05	3.93E-08	4.81E-05	1.73E-05
1.6365	6.56E-05	3.94E-08	4.81E-05	1.74E-05
1.6463	6.56E-05	3.94E-08	4.80E-05	1.75E-05
1.6561	6.57E-05	3.95E-08	4.80E-05	1.76E-05
1.6658	6.57E-05	3.95E-08	4.79E-05	1.77E-05
1.6756	6.58E-05	3.95E-08	4.79E-05	1.78E-05
1.6854	6.58E-05	3.96E-08	4.79E-05	1.79E-05
1.6952	6.59E-05	3.96E-08	4.78E-05	1.80E-05
1.7049	6.59E-05	3.97E-08	4.78E-05	1.81E-05
1.7147	6.60E-05	3.97E-08	4.77E-05	1.82E-05
1.7245	6.60E-05	3.97E-08	4.77E-05	1.83E-05
1.7342	6.61E-05	3.98E-08	4.76E-05	1.84E-05
1.744	6.61E-05	3.98E-08	4.76E-05	1.85E-05
1.7538	6.61E-05	3.99E-08	4.75E-05	1.86E-05
1.7636	6.62E-05	3.99E-08	4.74E-05	1.87E-05
1.7733	6.62E-05	3.99E-08	4.74E-05	1.88E-05
1.7831	6.63E-05	4.00E-08	4.73E-05	1.89E-05
1.7929	6.63E-05	4.00E-08	4.73E-05	1.90E-05
1.8026	6.64E-05	4.00E-08	4.72E-05	1.91E-05
1.8124	6.64E-05	4.01E-08	4.72E-05	1.92E-05
1.8222	6.64E-05	4.01E-08	4.71E-05	1.93E-05
1.8319	6.65E-05	4.01E-08	4.71E-05	1.94E-05
1.8417	6.65E-05	4.02E-08	4.70E-05	1.95E-05
1.8515	6.66E-05	4.02E-08	4.70E-05	1.95E-05
1.8613	6.66E-05	4.02E-08	4.69E-05	1.96E-05
2.8676	6.87E-05	4.23E-08	4.12E-05	2.75E-05
2.8774	6.87E-05	4.23E-08	4.11E-05	2.76E-05
2.8872	6.88E-05	4.23E-08	4.11E-05	2.77E-05
2.897	6.88E-05	4.23E-08	4.10E-05	2.77E-05
2.9067	6.88E-05	4.24E-08	4.10E-05	2.78E-05

2.9165	6.88E-05	4.24E-08	4.09E-05	2.78E-05
2.9263	6.88E-05	4.24E-08	4.08E-05	2.79E-05
2.936	6.88E-05	4.24E-08	4.08E-05	2.80E-05
2.9458	6.88E-05	4.24E-08	4.07E-05	2.80E-05
2.9556	6.88E-05	4.24E-08	4.07E-05	2.81E-05
2.9653	6.88E-05	4.24E-08	4.06E-05	2.81E-05
2.9751	6.88E-05	4.24E-08	4.06E-05	2.82E-05
2.9849	6.89E-05	4.24E-08	4.05E-05	2.83E-05
2.9947	6.89E-05	4.25E-08	4.05E-05	2.83E-05
3.0044	6.89E-05	4.25E-08	4.04E-05	2.84E-05
3.0142	6.89E-05	4.25E-08	4.04E-05	2.84E-05
3.024	6.89E-05	4.25E-08	4.03E-05	2.85E-05
3.1705	6.90E-05	4.26E-08	3.96E-05	2.94E-05
3.1803	6.90E-05	4.26E-08	3.95E-05	2.94E-05
3.1901	6.90E-05	4.26E-08	3.95E-05	2.95E-05
3.4246	6.92E-05	4.28E-08	3.84E-05	3.08E-05
3.4343	6.92E-05	4.28E-08	3.83E-05	3.08E-05
3.4441	6.92E-05	4.29E-08	3.83E-05	3.09E-05
3.4539	6.92E-05	4.29E-08	3.82E-05	3.09E-05
3.5027	6.92E-05	4.29E-08	3.80E-05	3.12E-05
3.5125	6.92E-05	4.29E-08	3.79E-05	3.12E-05
3.5223	6.92E-05	4.29E-08	3.79E-05	3.13E-05
3.532	6.92E-05	4.29E-08	3.79E-05	3.13E-05
3.5418	6.93E-05	4.29E-08	3.78E-05	3.14E-05
3.5516	6.93E-05	4.29E-08	3.78E-05	3.14E-05
3.6786	6.93E-05	4.30E-08	3.72E-05	3.21E-05
3.6884	6.93E-05	4.30E-08	3.72E-05	3.21E-05
4.0597	6.95E-05	4.32E-08	3.56E-05	3.38E-05
4.0694	6.95E-05	4.32E-08	3.56E-05	3.39E-05
4.0792	6.95E-05	4.32E-08	3.55E-05	3.39E-05
4.089	6.95E-05	4.32E-08	3.55E-05	3.39E-05
4.0987	6.95E-05	4.32E-08	3.55E-05	3.40E-05
4.1085	6.95E-05	4.32E-08	3.54E-05	3.40E-05
4.1183	6.95E-05	4.32E-08	3.54E-05	3.41E-05
4.1281	6.95E-05	4.33E-08	3.53E-05	3.41E-05
4.1378	6.95E-05	4.33E-08	3.53E-05	3.41E-05
4.1476	6.95E-05	4.33E-08	3.53E-05	3.42E-05
4.1574	6.95E-05	4.33E-08	3.52E-05	3.42E-05
4.1671	6.95E-05	4.33E-08	3.52E-05	3.43E-05
4.1769	6.95E-05	4.33E-08	3.52E-05	3.43E-05
4.1867	6.95E-05	4.33E-08	3.51E-05	3.43E-05
4.1965	6.95E-05	4.33E-08	3.51E-05	3.44E-05
4.2062	6.95E-05	4.33E-08	3.50E-05	3.44E-05
4.4016	6.96E-05	4.34E-08	3.43E-05	3.52E-05
4.4114	6.96E-05	4.34E-08	3.43E-05	3.52E-05
4.4212	6.96E-05	4.34E-08	3.42E-05	3.53E-05
4.4309	6.96E-05	4.34E-08	3.42E-05	3.53E-05
4.4407	6.96E-05	4.34E-08	3.42E-05	3.54E-05
4.4505	6.96E-05	4.34E-08	3.41E-05	3.54E-05
4.4603	6.96E-05	4.34E-08	3.41E-05	3.54E-05
4.47	6.96E-05	4.34E-08	3.41E-05	3.55E-05
4.4798	6.96E-05	4.34E-08	3.40E-05	3.55E-05
4.4896	6.96E-05	4.34E-08	3.40E-05	3.55E-05
4.4993	6.96E-05	4.34E-08	3.40E-05	3.56E-05
4.5091	6.96E-05	4.34E-08	3.39E-05	3.56E-05
4.5189	6.96E-05	4.34E-08	3.39E-05	3.57E-05
4.5287	6.96E-05	4.34E-08	3.39E-05	3.57E-05
4.5384	6.96E-05	4.34E-08	3.38E-05	3.57E-05
4.5482	6.96E-05	4.34E-08	3.38E-05	3.58E-05
4.558	6.96E-05	4.34E-08	3.38E-05	3.58E-05
4.5677	6.96E-05	4.34E-08	3.37E-05	3.58E-05
4.8804	6.97E-05	4.35E-08	3.27E-05	3.69E-05
4.8902	6.97E-05	4.35E-08	3.27E-05	3.70E-05
4.8999	6.97E-05	4.35E-08	3.26E-05	3.70E-05
4.9097	6.97E-05	4.35E-08	3.26E-05	3.70E-05
4.9195	6.97E-05	4.35E-08	3.26E-05	3.71E-05
4.9293	6.97E-05	4.35E-08	3.25E-05	3.71E-05
4.939	6.97E-05	4.35E-08	3.25E-05	3.71E-05
4.9488	6.97E-05	4.36E-08	3.25E-05	3.72E-05
4.9586	6.97E-05	4.36E-08	3.24E-05	3.72E-05
4.9683	6.97E-05	4.36E-08	3.24E-05	3.72E-05
4.9879	6.97E-05	4.36E-08	3.23E-05	3.73E-05
4.9976	6.97E-05	4.36E-08	3.23E-05	3.73E-05

Available online at www.sciencedirect.com
SCIENCE DIRECT®
Talanta 64 (2004) 18–22
Talanta
www.elsevier.com/locate/talanta

Effluent treatment using electrochemically bleached seawater—oxidative degradation of pollutants

S.B. Jonnalagadda*, S. Nadupalli

Department of Chemistry, University of Durban-Westville, P. Bag X54001, Durban 4000, South Africa

Received 12 August 2003; received in revised form 24 November 2003; accepted 27 November 2003

Available online 19 May 2004

Abstract

Use of seawater electrolytically enriched with hypochlorite and the in situ generation of hypochlorite on the high seas, stand a good chance for disinfection and decrease of bio and non-biodegradable organics in effluent before discharged into estuaries and deep oceans. Enriched seawater effectively decreased the biological oxygen demand measured over 5 days (BOD) and chemical oxygen demand (COD) levels of semi-treated wastewater. The oxidative degradation of Brilliant Blue, a triaryl industrial dye by hypochlorite and electrolytically enriched seawater are compared at pH 6.5. Both had similar magnitude second-order rate constants ($21 \pm 1\,M^{-1}\,s^{-1}$) and procedure is feasible. Increase in acid concentration enhanced the reaction rate. With 1:1 and 1:100 molar ratios of dye to hypochlorite, the COD $= 140\,mg\,L^{-1}$ of 1.0×10^{-3} M dye reduced to 100 and 30 mg L^{-1} respectively.

Keywords: Seawater; Hypochlorite; Electrochemical generation; Oxidative degradation; Chemical pollutants; Disinfection

1. Introduction

Urbanization has had significant impacts on the human health through hydrology of the environment by controlling, the nature of runoff waters and the delivery of pollutants to rivers, streams, lakes and ocean. The striking feature of the distribution of the world's population is the tendency for urbanization near vast water sources. Since the beginning of the Industrial Revolution, urban development has influenced the flow and storage of water, as well as the quality of available fresh water. Many coastal cities dispose their municipal wastewater to the sea through ocean outfall facilities, either as raw sewage or after preliminary treatment. The environmental impacts of these discharges depend strongly on the discharge location, level of treatment, if any, and on the physical, chemical and biological nature of the water body. Due to poor water quality resulting from highly polluted effluent discharges, many estuaries and sea beaches are health hazards. The impact of wastewater discharges on the marine environment is likely to worsen in the future, due to population growth, urbanization and the increase in water supply connection and sewerage levels. The growth will be most severe in developing countries, while in industrialized countries it might actually decrease as a result of water demand management and the introduction of cleaner production and water saving technologies [1].

Literature survey shows a number of oxidative methods including advanced oxidation processes involving ozone, peroxide, UV radiation and catalysts [2]. Comminellis and Pulgarin have investigated the anodic oxidation of organics on the electrode surface [3]. Rodrigo et al., have reported improved ways to treat wastewater electrochemically, using boron-duped diamond electrodes [4], while Ferro et al., have reported the efficient way generating chlorine using boron-doped diamond electrodes. Haenni et al., have reported the scope for such system in disinfecting pool water have been reported [5,6]. Chlorination through use of gas chlorination or hypochlorination has become the most common type of wastewater and water disinfection [7]. Hypochlorination of water is more economical in water treatment. Hypochlorite is a strong oxidizing agent, biocide, defouling agent and deodorizer. Normally, the hypochlorination is achieved through a chemical feed pump to inject

* Corresponding author. Tel.: +27-31-204-4325; fax: +27-31-204-4000.
E-mail addresses: jonna@pixie.udw.ac.za (S.B. Jonnalagadda), srinivas@pixie.udw.ac.za (S. Nadupalli).

0039-9140/$ – see front matter © 2004 Elsevier B.V. All rights reserved.
doi:10.1016/j.talanta.2003.11.045

a calcium or sodium hypochlorite solution. The generation of hypochlorite using seawater as the chloride source has great scope, as it leads to insitu generation of hypochlorite under verity of situations, where seawater is accessible and abundant. Another dimension the utility of bleached sea water is reported passivity in metals from corrosion through decreased dissolved oxygen levels. The solubility of oxygen in water is dramatically reduces by increased hypochlorite levels.

This manuscript covers the systematic studies showing the effect electrochemically generated hypochlorite using seawater and its scope in oxidation of organics and in disinfection to achieve hygienic, aesthetic and sustainable environment through the improved effluent quality.

2. Experimental

Natural Seawater composition of chloride ion, Cl^- is about 19,5000 ppm or 19.5 g L^{-1} and Na^+ ion is about 10.7 g L^{-1} [8]. Thus seawater with 0.53 mol L^{-1} of chloride ion, works out to be a abundant source of chloride for electrochemical generation of chlorine, and then hypochlorite, through it's disproportionation reaction [9].

For the control experiments, hypochlorite was generated by bubbling chlorine gas through cold solution of 5% sodium hydroxide. The Baird and Tatlock Electrolytic Analysis apparatus was used for electrochemical generation of hypochlorite from seawater. The equipment consists of a single compact unit containing its own low voltage direct current supply unit capable of giving an output of 0–10 A at up to 12 V. Optimum and cost effective conditions for the generation of hypochlorite from sea water were covered vessel with volume 200 ml water; electrolysis duration 45 min; temperature 20 °C; pH 6.74. Under these conditions $(12.2 \pm 0.3) \times 10^{-2}$ M of hypochlorite was obtained [9]. Arsenite method was used for the determination of the hypochlorite concentration in the sample [7,10].

The electrolysis chemistry is as follows:

$$\text{Anode} : 2Cl^-(aq) \rightarrow Cl_2(g) + 2e^-$$

$$\text{Cathode} : 2H_2O(l) + 2e^- \rightarrow H_2(g) + 2OH^-(aq)$$

$$\text{Overall} : 2H_2O(l) + 2Cl^-(aq) \rightarrow H_2(g) + Cl_2(g) + 2OH^-(aq)$$

and

$$Cl_2(g) + H_2O(l) \rightarrow 2H + (aq) + OCl^-(aq) + Cl^-(aq)$$

2.1. Bacterial sensitivity, BOD and COD tests

These tests constitute a simple and reliable technique especially applicable to routine bacteriological work. It consists of concentrating disks with known concentrations of hypochlorite, placing them on plates of a culture medium containing a bacterium and after incubation, determining the degree of sensitivity by measuring the easily visible areas of inhibition of growth produced by the diffusion of hypochlorite from the disks into the surrounding medium. biological oxygen demand measured over 5 days (BOD), chemical oxygen demand (COD), total dissolved and total suspended solids were determined using standard procedures [9].

2.2. Kinetics

The kinetics of the reaction is studied using the HITECH SF-61 DX2 Micro volume double mixing stopped flow apparatus with thermostat control and software for data capture and analysis. The reaction kinetics was monitored at (25.0 ± 0.1) °C.

3. Results and discussion

3.1. Bacterial sensitivity

The bacterial sensitivity test using the medium nutrient agar coated on petri dishes and the bacterium, *Escherichia coli* (*E. coli*) showed that the hypochlorite solution generated using seawater sample is good anti bacterial and equally efficient as the commercial bleach samples under comparable conditions in the bacterial growth inhibition, after the 24 h incubation [9].

3.2. BOD_5 and COD

The effect of the seawater sample containing hypochlorite on the BOD levels of wastewater is investigated by adding varying amounts of seawater to fixed volumes of wastewater. Wastewater samples were collected from the sewage treatment works after the primary treatment, but prior to the secondary treatment. The BOD level for the untreated samples (200 ml) was reduced from 1.3 mg L^{-1} to 0.1 mg L^{-1} upon treatment with seawater sample (6 ml). The reduction of BOD levels is expected based on the diminished bacterial oxidation of organics mater due the anti bacterial action of hypochlorite. Sample from waste water works after secondary treatment had almost zero BOD levels, which had no effect due to addition of bleached seawater [9]. The chemical oxygen demand of primarily treated Sample (100 ml) was reduced from 440 mg L^{-1} to 160 mg L^{-1} upon mixing with 50 ml to 40 mg L^{-1} with 100 ml of the bleached seawater sample. Obviously, the powerful oxidizing capacity of hypochlorite decreases the COD levels [9].

3.3. Oxidative degradation of organics

Further, the oxidative degradation kinetics of the organics normally present in the effluent is investigated in detail. The reaction of a selected representative dye, Brilliant Blue

which is used in textile and food industries, with hypochlorite is studied under controlled conditions and using the bleached seawater.

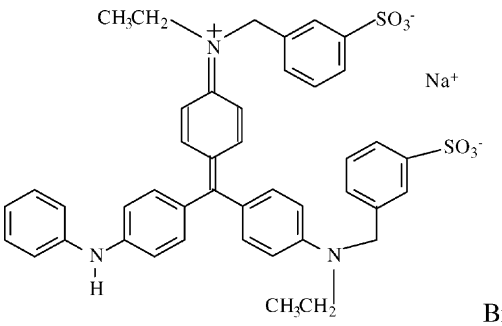

Brilliant Blue

Brilliant Blue is a triarylmethane type of dye (disodium α-(4-(*N*-ethyl-3-sulfonatobenzylamino) phenyl)-α-(4-*N*-ethyl-3-sulfonatobenzylamino, cyclohexa-2,5-dienylidene) toluene-2-sulfonate). Brilliant Blue is water soluble with λ_{MAX} at 555 nm and absorption coefficient, $\varepsilon = 2.15 \times 10^4\,dm^3\,mol^{-1}\,cm^{-1}$. Hence the kinetics was monitored at 555 nm.

All the kinetic runs were conducted with excess hypochlorite and low dye concentrations. Under such conditions experiments followed pseudo first-order kinetics, indicating reaction order with respect to the dye is one. Further the pseudo first-order rate constant, k' increased proportionally with the increase in the initial concentration of hypochlorite suggesting that reaction has first-order dependence on the concentration of the oxidant and total order is two.

All experiments were repeated with seawater containing electrochemically generated hypochlorite. Fig. 1 illustrates the kinetic profiles of depletion of Brilliant Blue in presence of seawater containing different initial amounts of hypochlorite. The reaction of dye both with control hypochlorite solution and enriched seawater too had second-order and one each with respect to both the dye and hypochlorite. Table 1 summarizes the pseudo first-order constants from the experiments, and the estimated half reaction times and second-order rate constants for both the control and seawater enriched experiments.

Further, the $\ln k'$ versus ln [hypochlorite] for the control and seawater experiments gave straight lines with ($y = 1.1572x + 4.0049$, $R^2 = 0.9954$) and ($y = 1.0891x + 4.0049$, $R^2 = 0.9885$) respectively. A perusal of the slopes shows that under both the situations, the reactions have first-order dependence on hypochlorite concentration. The second-order rate constants of the two sets of experiments are of similar magnitude and most importantly the reactions are fast. This conclusively confirms the scope of hypochlorite enriched seawater in treatment of wastewaters and industrial effluent.

At very high pH, where bulk of the hypochlorite is in the hypochlorite form and with very low concentration of HOCl, reaction is very slow suggesting the rate constant for the reaction between OCl^- and the dye is small.

As all the experiments were done at pH 6.5, the effect of acid on the reaction between Brilliant Blue and hypochlorite is further investigated with added acid under both control and seawater enriched with hypochlorite conditions and results were similar. The kinetic data obtained with seawater conditions is summarized in Table 2. With the increase in the concentration of added acid the pseudo first-order rate constant increased. To understand the reaction dynamics, a close look at the chemistry of hypochlorite is essential. HOCl with $pK_a = 7.4$ is a week acid and it's dissociation constant is 4×10^{-8} indicating that even very low concentration of acid shifts the equilibrium towards formation of HOCl [11]. The

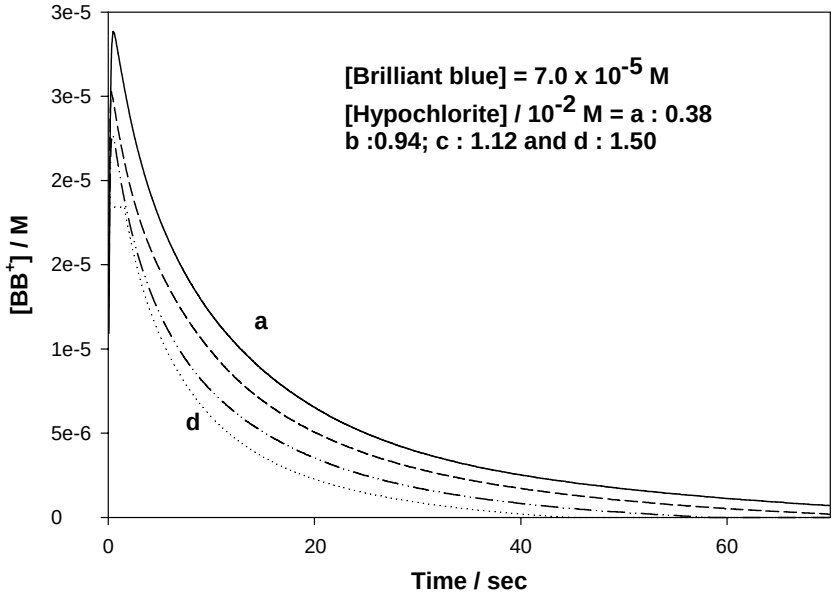

Fig. 1. Effect of Electrolyzed seawater on the depletion rate of Brilliant Blue–absorbance vs. time plots.

Table 1
Rate coefficients for the reaction between Brilliant Blue and (i) hypochlorite (control), and (ii) electrolytically bleached seawater

Hypochlorite (control)[a]				Seawater enriched with hypochlorite[a]			
OCL^- (10^{-3} M)	k' (10^{-2} s^{-1})	$t_{1/2}$ (s)	k (M^{-1} s^{-1})	OCl^- (10^{-3} M)	k' (10^{-2} s^{-1})	$t_{1/2}$ (s)	k (M^{-1} s^{-1})
1.17	2.23	31.0	19.09	3.75	7.90	8.8	21.07
2.34	5.13	13.5	21.94	7.50	15.95	4.3	21.27
3.51	7.39	9.4	21.06	9.38	19.29	3.6	20.58
4.68	10.73	6.5	22.94	11.25	24.11	2.9	21.43
5.85	13.13	5.3	22.44	15.0	33.45	2.1	22.30
Mean $k = 21.49 \pm 0.64$				Mean $k = 21.34 \pm 0.52$			

$[BB^+] = 7.5 \times 10^{-5}$ M, pH = 6.5 and temperature = 25 °C.
[a] Total hypochlorite concentration = $[OCl^-] + [HOCl]$.

preliminary experiments showed that at very high pH, above 9, when bulk of the hypochlorite is in the hypochlorite form and with very low concentration of HOCl, the reaction was very slow suggesting the rate constant for the reaction between OCl^- and the dye is small. At pH 7.4, the concentrations of hypochlorite and hypochlorous acid will be equal. With the increase in acid concentration, the HOCl concentration increases and at pH 6.5, the percentage of hypochlorous acid in the mixture reaches about 71%, suggesting the major pathway for the reaction is through of oxidation by HOCl (Table 1).

With initial concentration of hypochlorite 1.5×10^{-3} M (Table 2) to achieve pH 6.5, in the control experiment the added acid concentration is about 1.68×10^4 M and the resultant hypochlorous acid concentration is 1.166×10^4 M in both cases.

Table 2 summarizes the added initial acid and the compiled hypochlorous acid concentrations and the corresponding pseudo first order rate constants (k') obtained. The plot of the $\ln k'$ versus $\ln$ [HOCl] concentration gave a good straight line with $R^2 = 0.987$, suggesting the first-order dependence of the reaction rate on the acid concentration. The calculated second order rate constants for the over all second-order rate constants are also summarized in Table 2.

To investigate the impact of the oxidation of Brilliant Blue using hypochlorite, the BOD and COD for the reaction mixture was determined in duplicate experiments. The BOD values were very low with significant changes, for prior to and after reaction of dye with the bleached seawater. 1.0×10^3 M Brilliant Blue (1 ml) had initial COD of 140 mg L^{-1} and upon addition bleached seawater in the 1:1 and 1:100 molar ratios, the COD reduced to 100 and 30 mg L^{-1} respectively. Even with 1:100 molar ratio, the residual COD shows that the dye is oxidized, but not completely mineralized. The total oxidizable carbon (TOC) could not be determined.

To estimate scope of the bleached seawater in oxidizing the wastewater containing other dyes, the kinetics of number of dyes which are normally used in the textile and other industries or as stains with hypochlorite are studied in presence of hypochlorite and bleached seawater from the unpublished data and from the literature are compiled and summarized in Table 3.

Table 3 summarizes the second-order rate constants for the reaction of hypochlorite at pH 6.5 for variety of dyes. The magnitude of the rate coefficients clearly demonstrate that most of the dyes are easily oxidized by the hypochlorie enriched seawater. Ru(III) is observed to catalyze the oxidation by hypochlorite, hence studies are in progress to explore suitable heterogeneous catalyst to enhance the efficiency of oxidation by hypochlorite under seawater pH conditions.

Ocean outfalls can work efficiently and may be a satisfactory solution to effluent management. Under the right conditions, properly treated effluent discharged into deep ocean water with strong currents will have little or no environmental impacts.

Table 2
Effect of acid on the reaction between Brilliant Blue and seawater enriched with hypochlorite

$[H^+]$ (10^{-4} M)	[HOCl] (10^{-3} M)	k (10^{-2} s^{-1})	k (M^{-1} s^{-1})[a]
0	1.066	3.20	30.02
1.0	1.166	3.45	29.59
2.0	1.266	3.71	29.31
3.0	1.366	4.03	29.51
4.0	1.464	4.49	30.66
5.0	1.499	4.62	30.82
Mean = 29.99 ± 0.63			

$[BB^+] = 7.5 \times 10^{-5}$ M, hypochlorite 1.5×10^{-3} M, initial pH = 6.5 and temperature = 25 °C.
[a] $k = k'/[HOCl]$.

Table 3
Second-order rate coefficients for different dyes with hypochlorite

Name of dye	Category of dye	k (M^{-1} s^{-1})
Brilliant Blue[a]	Triaryl dye	21.5 ± 0.6
Indigocarmine [12][b]	Indigo dye	18.0 ± 0.1
Amaranth [13][a]	Azo dye	26.2 ± 0.5
Safranine-O [13][a]	Phenazine dye	48.4 ± 1.1
Methylene Violet [14][b]	Phenazine dye	22.1 ± 0.5
Meldola's Blue [15][b]	Phenoxazine dye	2.1 ± 0.3
Brilliant Cresyl Blue [15][b]	Phenoxazine dye	21.2 ± 0.3
Nile Blue [15][b]	Phenoxazine dye	1020 ± 120

Temperature: 25 °C, pH = 6.5.
[a] Both controlled and enriched seawater experiments.
[b] Controlled runs only.

4. Conclusions

The bleached seawater can effectively oxidize the aromatic dye, Brilliant Blue in short duration, but the residual COD values after oxidation indicate that complete mineralization does not occur for the studies conditions. The effluent treatment using the hypochlorite enriched seawater has potential to decrease the levels of toxins, bacteria, BOD, COD and organics to the acceptable levels before discharged into deep oceans, rivers or estuaries, to afford aesthetic, hygienic and sustainable environment and safe seas for future generations.

In addition to the effluent treatment, the electrolytic generation of hypochlorite in high seas has great scope in the disinfection, deodourising and defouling the deep sea platforms, ship decks and the oceanariams. The use of efficient catalysts and improved electrolyzing systems such as boronduped diamond electrodes could further enhance the economic and effective use of bleached sea water in treatment of wastewaters.

The solubility of oxygen in water is dramatically reduces by increased hypochlorite levels. Thus, bleached seawater also provides an additional advantage as anti-corrosion agent towards metals in the installations exposed to seawater.

Acknowledgements

Authors thank the National Research Foundation, Pretoria and the University of Durban-Westville, Durban for the financial support both research and participation in the conference.

References

[1] W. Viessman, M.J. Hammer, Water supply and pollution control, fifth edition, Harper Collins College publishers, New York, 1993, p. 860.
[2] R. Andreozzi, V. Caprio, A. Insola, R. Marotta, Catálisis Today 53 (1999) 51.
[3] Ch. Comminellis, S. Pulgarin, J. Appl. Electrochem. 21 (1991) 703.
[4] M.A. Rodrigo, P.A. Michaud, I. Duo, G. Cerisola, Ch. Comminellis, J. Electrochem. Soc. 148 (2001) D60–D64.
[5] S. Ferro, A. De Battisti, I. Duo, Ch. Comninellis, W. Haenni, A. Perret, J. Electrochem. Soc. 147 (2000) 2614.
[6] W. Haenni, J. Gobet, A. Perret, L. Pupunat, Ph. Rychen, Ch. Comninellis, B. Corea, in: Proceedings of the Electrochem. Soc. Meeting, San Francisco, 2001, pp. 1–8.
[7] G. Gordon, W.J. Cooper, R.G. Rice, G.E. Pacey, Disinfectant Residual measurement Methods, AWWA Research Report American Water Works Research Foundation, Denver, Colorado, 1987, and references therein.
[8] G. Bearman, Ocean Chemistry and deep-sea sediments, Pergamon, Sydney, 1989.
[9] V. Chunilall, M. Govender, S.B. Jonnalagadda, J. Environ. Sci. Health A37 (2002) 1523, and references therein..
[10] A.I. Vogel, Textbook Of Quantitative Inorganic Chemistry, third ed., Longmans Green and Co., London, 1966, p. 365.
[11] L.C. Adam, I. Fabian, K. Suzuki, G. Gordon, Inorg. Chem. 31 (1992) 3534.
[12] A. Hariram, V. Govender, S.B. Jonnalagadda, J. Environ. Sci. Health 38 (2003) 1055.
[13] S. Nadupalli, S.B. Jonnlagadda, unpublished work.
[14] L.Q. Qwabe, Kinetic-Analytical determination of Ru(III) using Oxidation of Phenoxazine dyes, M.Sc. Thesis, University of Durban-Westville, 2002.
[15] S.B. Jonnalagadda, B. Pare, M. Shezi, Int. J. Chem. Kinet., Wiley, New York, 35, 2003, 21.